SOVIET PHYSICS

JETP

A translation of the Journal of Experimental and Theoretical Physics of the USSR.

SOVIET PHYSICS JETP VOL. 34 (7), NO. 6, pp. 939 - 1170 December, 1958

SOME FEATURES OF THE PROCESS OF CHARGED π-MESON PRODUCTION ON CARBON BY 670 Mev PROTONS

L. S. AZHGIREI, I. K. VZOROV, V. P. ZRELOV, M. G. MESHCHERIAKOV and V. I. PETRUKHIN

Joint Institute for Nuclear Research

Submitted to JETP editor January 6, 1958

J. Exptl. Theoret. Phys. (U.S.S.R.) **34**, 1357-1366 (June, 1958)

The energy spectra of π^+ and π^- mesons from p + C collisions are measured at an angle of 56° to the proton beam, using a magnetic spectrometer designed especially for such types of measurements. The spectra of both π^+ and π^- mesons each had a maximum in the region $\sim$110 Mev and could still be measured up to $\sim$400 Mev. Smearing out of the spectrum on the high-energy side is thought to result from production of π mesons inside the nucleus on correlated groups of nucleons which have large relative momenta. The differential cross sections for π^+ and π^- production were $(5.1 \pm 0.8) \times 10^{-27}$ and $(1.0 \pm 0.2) \times 10^{-27}$ cm^2/sterad. The angular distributions of π^+ and π^- mesons were nearly isotropic in the c.m. system of the colliding nucleons. The measured ratio of π^+ to π^- yields was not in agreement with that predicted by the simple model in which π mesons are produced only via excitation of the nucleon to a $T = J = 3/2$ intermediate state, and indicates that inelastic collisions in the $T = 0$ state contribute substantially.

1. INTRODUCTION

In a preceding article[1] we described measurements of the energy spectra of π^+ and π^- mesons produced by 660-Mev protons on beryllium and carbon. For both elements the π^+ spectrum, observed at an angle of 24° relative to the proton beam, showed a strong maximum in the region of energies in the center of mass system of the two colliding nucleons (c.m.s.) corresponding to the maximum of the total cross section for the scattering of π mesons by nucleons. This situation can be viewed as an indication that the production of π mesons at this energy in nucleon-nucleon collisions inside the nucleus is mainly determined by the presence of resonance interaction between the π meson and one of the nucleons in a state of angular momentum $J = 3/2$ and isotopic spin $T = 3/2$ ($P_{3/2,3/2}$-state). However, for both elements the measured ratio of π^+ to π^- production turned out to be markedly lower than the ratio calculated under the assumption that the interaction of the nucleon with the nucleus can be reduced to a series of collisions of nucleon pairs, in which the production of π mesons proceeds only via the intermediate $P_{3/2,3/2}$-state.[2]

For a more detailed explanation of the character of the process of π-meson production by protons on complex nuclei, it is essential, first, to make a quantitative estimate of how the form of the energy spectra and π^+ to π^- ratio change with angle. Second, it is necessary to note the influence of the process of π-meson production in collisions of the incident proton with compact groups of strongly-interacting nucleons on the form of the spectra near to the upper energy limits. Such a process appears possible, if one takes account of the fact that collisions of protons with quasi-deuteron groups in the nuclei occur fairly often.[3]

The experiments described in this article were carried out on the six-meter synchrocyclotron of the Joint Institute for Nuclear Research with the

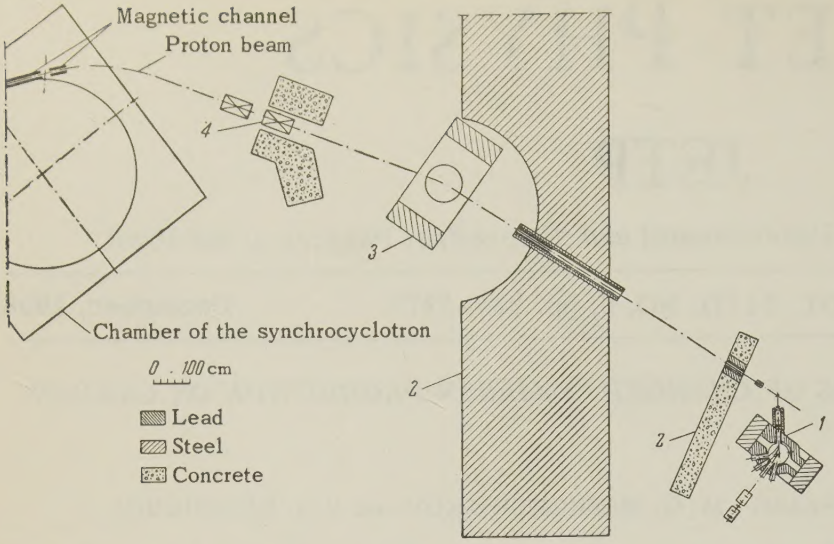

FIG. 1. Placement of the spectrometer (1), shielding wall (2), deflecting magnet (3), and focusing lens (4), shown relative to the synchrocyclotron chamber.

object of clarifying the features indicated above of charged π-meson production on carbon by 670-Mev protons.

2. EXPERIMENTAL SETUP

The energy spectra of π^+ and π^- mesons were measured with a magnetic spectrometer. Its placement relative to the vacuum chamber of the synchrocyclotron and concrete shielding is shown in Fig. 1. The extracted proton beam was focused by two quadrupole lenses, deflected through 12° by a magnet, and then led through a 2-cm diameter steel collimator, placed in a four-meter shielding wall of reinforced concrete, and directed towards the spectrometer. The intensity of the beam was controlled by an ionization chamber (He at a pressure of 0.5 atmos). At the position of the target, the mean proton energy in the beam was 670 ± 5 Mev, and the intensity of the current in the beam (cross section ~7 cm^2) was ~3×10^8 protons/cm^3 sec.

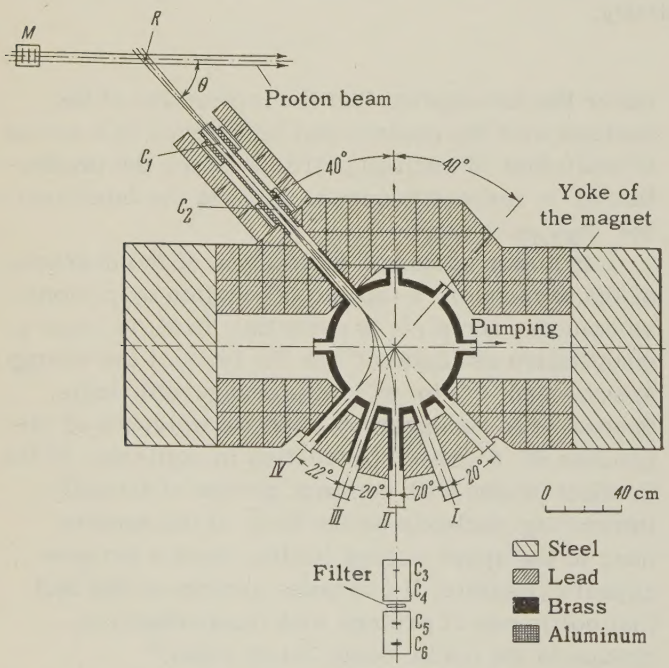

FIG. 2. Diagram of the spectrometer: M – monitor, R – target, C_1 to C_6 – scintillators.

The basic piece of experimental apparatus was an analyzing magnet which weighed 28 tons and had circular pole tips of diameter 60 cm and a gap of 6 cm. The maximum magnetic field was 20,000 oersteds. The field strength H in the gap was measured to an accuracy of 0.2% by nuclear absorption. An electronic stabilizer held the given magnetic field strength constant within 0.2%. The supply to the magnet was such that the field through the coils could be reversed, making it possible to analyze particles of either polarity. A vacuum chamber of diameter 60 cm was mounted between the poles of the magnet. In the brass rim of this chamber were ten radial openings with soldered brass tubes. The ends of the tubes were covered with copper foil 40 μ thick.

Using channels I, II, III, and IV of the spectrometer, shown in Fig. 2, π mesons with energies up to 500 Mev could be analyzed. As the charged particles pass through the channels II, III, and IV, they are focused in the horizontal plane by the homogeneous magnetic field of the spectrometer. In the experiments described, the distance from the center of the target to the edge of the poles was 144 cm. The calculated distances from the edge of the poles to the focal surface for channels II, III and IV are given in Table I, together with other spectrometer characteristics. In calculating the parameters of the spectrometer, the drop off of the field at the edge and the stray field in the gap of the magnet were taken into account. Values for

TABLE I

Channel	I	II	III	IV
Angle of deflection	20°	40°	60°	82°
Radius of curvature ρ of the mean trajectory in cm	200	97	61	42
Distance from the edge of the pole to the focal surface in cm		926	82	19

the radii of curvature of the mean trajectories were found by measurements with a thin current-carrying wire and also by calibration measurements of the position of the peaks corresponding to protons from elastic p-p scattering and π^+ mesons from the reaction $p + p \rightarrow d + \pi^+$.

The entrance telescope, consisting of the two scintillation counters C_1 and C_2 connected for two-fold coincidence, selected π mesons from the beam produced in the target. The scintillators of the counters C_1 and C_2 were placed in a branch tube connected to the chamber of the spectrometer. Particles going through the spectrometer were registered by an exit telescope composed of four scintillation counters C_3, C_4, C_5 and C_6, connected pairwise (C_3C_4, C_5C_6) for two-fold coincidence. Pulses from the two-fold coincidences were, in turn, included in a secondary two-fold coincidence circuit. In the experiments, two-fold coincidences in the entrance telescope, four-fold coincidences in the exit telescope, and six-fold coincidences in the pulses from all counters could be registered. The background of random coincidences was measured by introducing a delay line, to shift the coincidence pulse from counters C_5C_6. Standard electronic circuitry was employed for amplification, discrimination, and for the coincidence circuits. The resolving times of the coincidence schemes are given in Table II, along with the widths and heights of the scintillators, ground tolan crystals about 2.5 mm thick. The scintillators defined the dimensions of the beam traversing the spectrometer so that particles in the path did not touch the walls of the apparatus at any point. This excluded any possibility of distortion of the form of the spectrum because of scattering or slowing down of the particles. The scintillators were joined to photomultipliers of type FEU-19M. To collect the light more effectively, the scintillators were surrounded by reflectors made of aluminum foil. The photoelectric multiplier was shielded from scattered magnetic fields by multi-layer screens of soft iron. Before the measurements were begun, it was established that the counting equipment worked on a plateau of ~100 v with respect to the voltage of the photoelectric multipliers. The scintillation-counting efficiency was close to 100% in the entire range of π-meson energies studied.

In view of the high intensity of the beam in the experimental area, it was necessary to surround the entrance telescope and chamber of the spectrometer by a thick lead shield, as shown in Fig. 2. To shield the counting apparatus from the protons scattered off the end of the collimator which defined the beam, a supplementary reinforced-concrete wall, which was one meter thick and had an opening of diameter 5 cm through which the focused beam from the target passed was placed in front of the spectrometer.

Depending on the purpose of the experiment, the exit telescope was placed in one of the guiding grooves cut, coaxial with channels I to IV, in a duraluminum plate securely attached to the magnet. The analyzing magnet, together with the vacuum chamber, shielding and the equipment on which the target was fastened, could be rotated on a platform which, in turn, could be moved along a rail perpendicular to the proton beam. In this way the angle of observation of the secondary particles could be varied between 15 and 175° relative to the primary beam.

The system described here, comprising two telescopes and an analyzing magnet between them, was especially well suited for the counting of particles in a narrow range of momenta. Under the conditions of the present experiment, such particles were secondary protons, π mesons, μ mesons, and electrons. The relative content of these particles in the beam with given momentum was determined by range measurements in copper, for which copper filters were introduced just in front of the scintillator C_5.

TABLE II

Counter	Dimensions of the scintillator, cm	Resolution time of the coincidence circuit, sec		
C_1	1.3×3.1	$3\cdot10^{-8}$		$7\cdot10^{-8}$
C_2	1.2×3.1			
C_3	3.6×3.6	$3\cdot10^{-8}$	$5\cdot10^{-8}$	
C_4	2.0×4.0			
C_5	6.0×6.0	$3\cdot10^{-8}$		
C_6	6.0×6.0			

3. EXPERIMENTAL PROCEDURE AND ANALYSIS OF RESULTS

In these experiments the energy spectra of positive and negative mesons from p + C collisions were observed at an angle of 56° relative to the initial beam; this corresponded to emission of π

TABLE III

Energy of the mesons, Mev	$\frac{d^2\sigma^+}{d\omega dE}$, 10^{-29} $\frac{cm^2}{sterad\ Mev}$	$\frac{d^2\sigma^-}{d\omega dE}$, 10^{-29} $\frac{cm^2}{sterad\ Mev}$	$\left(\frac{d^2\sigma^+}{d\omega dE}\right)/\left(\frac{d^2\sigma^-}{d\omega dE}\right)$
30	1.08±0.10	0.23±0.02	4.72±0.64
47	1.66±0.09		
68	2.28±0.13	0.54±0.03	4.22±0.34
85	2.92±0.13		
109	3.08±0.08	0.59±0.02	5.23±0.27
130	2.96±0.07		
154	2.66±0.05	0.51±0.02	5.18±0.27
186	2.12±0.06		
203	1.56±0.06	0.27±0.02	5.86±0.51
226	1.06±0.05		
250	0.58±0.06	0.09±0.01	6.44±0.87
247	0.33±0.05		
300	0.18±0.02	0.022±0.006	8.13±2.43
324	0.080±0.016	0.009±0.004	8.64±4.35
348	0.068±0.009	0.003±0.004	
370	0.052±0.031	0.012±0.005	
394	0.008±0.014		

mesons at approximately 90° in the c.m.s. of the colliding nucleons. The main part of the measurements were carried out with a graphite target of height 3 cm, width 2 cm, and thickness 1.53 g/cm^2. The target impurities did not exceed 0.01% by weight. The target was so placed that the normal to its surface coincided with the axis of the telescope C_1C_2. The energy of the incident protons in the center of the target was 669 Mev. The angular divergence of the analyzed beam constituted $\sim \pm 1°$ in the horizontal plane. The exit telescope was so placed at the end of channel II that the distance from the edge of the pole to the scintillator C_4, which acted as an exit slit, was 75 cm. Under these conditions, the momentum interval selected by the scintillators of the spectrometer was constant over the whole range of momenta studied, and comprised $\Delta p \approx 0.05\,p$.

The experiments reduced to measurements, as a function of the magnetic field, of the following quantities: (a) the rate of counting of the six-fold coincidences between pulses from counters $C_1 - C_6$ with the target in the beam and without it; (b) the rate of counting of six-fold random coincidences with the target in the beam and with a delay line to shift the coincident pulse from the pair of counters C_5C_6 by 3.2×10^{-7} sec. When the range of secondary protons present in the analyzed beam became equal to the thickness of the first five scintillators, a copper filter was placed between scintillators C_5 and C_6. Its thickness was sufficient to stop secondary protons. The measurements were carried out so that the momentum intervals corresponding to the various thicknesses of filters employed overlapped; this made it possible to estimate directly the magnitude of correction needed to account for absorption of π mesons in the filter. In addition, this correction was also calculated from known data on the nuclear-interaction cross sections of π^+ and π^- mesons. In this way, corrections were introduced for absorption of π mesons in the target and in the scintillators, and also for the change in energy loss with changing energy of the π mesons. The loss of π mesons in the beam by multiple scattering in the target and in the first scintillators was found to have a negligible effect on the spread of the energy interval studied, and, therefore, no corresponding correction was introduced.

In calculating the correction for the decay of the π mesons in flight, their mean life time was taken to be $(2.55 \pm 0.11) \times 10^{-8}$ sec. Corrections for the presence of μ-mesons and electrons in the analyzed beam of π mesons of both signs were found, as already noted at the end of Sec. 2, by painstaking measurements of the range curves in copper at various energies. To minimize the possible effect of vertical defocusing in the scattered magnetic field, the analyzed beam was made of relatively small height in these experiments and the particles were made to enter and leave at right angles to the edge of the field. Comparison of the counting rate for π mesons at various field strengths and for a different height of analyzed beam showed that the distortion of the form of the spectrum due to the variation of vertical defocusing with field strength was within the limits of the statistical errors of the measurements.

Introduction of the corrections listed above into the number of registered six-fold coincidences per monitor count gave the relative yield $Q(p)$ of π mesons emitted with momentum in the interval $p - \frac{1}{2}\Delta p$ to $p + \frac{1}{2}\Delta p$. The differential cross section per unit momentum of the meson, $d^2\sigma/d\omega\,dp$, was connected with $Q(p)$ by the usual relation

$$d^2\sigma / d\omega dp = Q(p) / nN\Delta\omega\Delta p \sim Q(p) / nN\Delta\omega H\rho,$$

where n is the number of carbon nuclei per cm^2

of target surface, N is the current of primary protons incident on the target per unit monitor count, and $\Delta\omega$ is the solid angle subtended by the scintillators at the center of the target.

The transformation from momentum distribution to energy distribution was carried out by the formula

$$d^2\sigma / d\omega\, dp = v d^2\sigma / d\omega\, dE,$$

where v is the velocity of the π meson.

In view of the impossibility of defining accurately the quantity $\Delta\omega$, the absolute values of $d^2\sigma/d\omega\, dE$ were evaluated by normalizing the area under the π-meson spectrum, using the differential cross section for elastic p-p scattering. This operation reduced to comparing the areas lying under the π-meson spectrum and under the proton peak in p-p scattering, measured by the polyethylene-carbon difference method under the same conditions as the π-meson spectrum. The π-meson curves giving $d^2\sigma/d\omega\, dp$ as a function of p were extrapolated linearly from the lowest experimental point to the origin of coordinates. The differential cross section for elastic p-p scattering for 670 Mev and 56° (60° in the c.m.s. of the colliding protons) was taken to be the same as for 657 Mev, i.e., equal to $(6.70 \pm 0.26) \times 10^{-27}$ cm^2/sterad [$(3.41 \pm 0.13) \times 10^{-27}$ cm^2/sterad in the c.m.s.].[4]

4. RESULTS OF THE EXPERIMENTS AND DISCUSSION

The values of $d^2\sigma^+/d\omega\, dE$ and $d^2\sigma^-/d\omega\, dE$, in the laboratory system, are given in Table III together with the statistical errors of measurements. The spectra of the π^+ and π^- mesons, constructed from the data in Table III, are shown in Fig. 3. There the upper parts of both spectra are shown separately, with the ordinate enlarged ten-fold compared with the remaining parts of the spectra. It can be seen that the spectra of π mesons of both signs have maxima in the region $\sim$110 Mev. The mean energy of the π^+ mesons is $\sim$136 Mev, that of the π^- mesons $\sim$126 Mev. If, neglecting the motion of the nucleons inside the nucleus, we transform the spectra to the c.m.s. under the assumption that π mesons are produced by collision of the protons with individual nucleons inside the nucleus, then it turns out that in this system: (a) the mean energy of the π^+ mesons is 108 Mev, and thus does not differ appreciably from the value found previously at 24° ($\sim$45° in the c.m.s.); (b) the mean energy of the π^- mesons is 102 Mev, which is $\sim$17 Mev larger than the value found at $\sim$45°; (c) the energy interval from 30 to 200 Mev, which includes

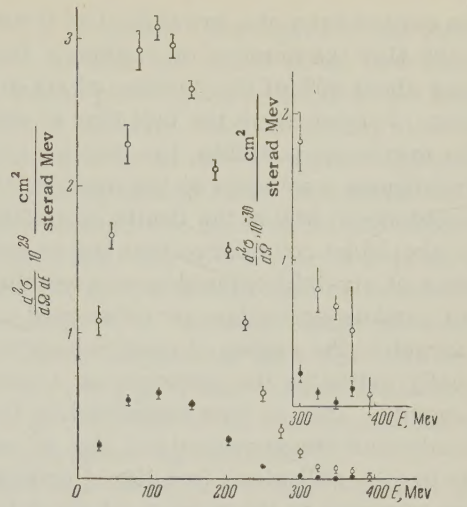

FIG. 3. Energy spectra of π^+ and π^- mesons from p + C collisions at an angle of 56° to the beam of 670- Mev protons. ○ – π^+ mesons, ● – π^- mesons.

about 90% of the π mesons, corresponds in the c.m.s. to emission angles between 110 and 88°. In this angular interval, the yields of π^+ and π^- mesons from the reactions $pn \rightarrow \pi^+ + 2n$ and $pn \rightarrow \pi^- + 2p$ should be roughly the same, because of charge invariance. From the values obtained for the mean energies of π^+ and π^- mesons, it follows that in a single act of production of a π meson, emitted at an angle of 56° to the beam, about 80% of the available energy is used up on the average.

Putting these data together with results of analogous measurements of Yuan and Lindenbaum,[5] it is seen that upon increasing the energy of the incident protons from 670 to 1000 and 2300 Mev (in the last case paired production of π mesons is dominant), the maximum of the π^+-meson spectrum is hardly shifted in the direction of higher energies. Over the whole region of energies and angles studied, the position of the maximum in the π^+ spectra closely corresponds to the resonance energy of the $P_{3/2,3/2}$-state. This is convincing proof that the interaction of the π meson with the nucleon in the $T = J = 3/2$ state plays the essential role in the production of a large part of the π^+ mesons in nucleon-nucleon collisions.

A characteristic feature of the observed π^+ and π^- spectra is the presence of a long 'tail' on the high energy side. It can be seen from Fig. 3 that the spectra of π mesons of both signs persist almost up to 400 Mev. It can not be excluded that the spectra stretch even further, right up to the maximum possible energy (470 Mev) corresponding to the reaction $p + C^{12} \rightarrow \pi^+ + C^{13}$. However, observations at such high energies would re-

quire the expenditure of a great deal of time, since even at 390 Mev the number of random coincidences comprises about 90% of the number of six-fold coincidences. Judging from the fact that at energies above the maximum possible, the number of six-fold coincidences was equal to the number of random coincidences, within the limits of statistical error, it should be considered that the excess in the number of six-fold coincidences over the background of random coincidences (observed with the carbon target in the region of energies above 320 Mev) really indicates the presence of π mesons of high energy. This is also supported by the fact that in analogous measurements of the π^+-spectrum due to p-p collisions in a liquid hydrogen target, no increase in the number of six-fold coincidences over the background of random coincidences was observed to the right of the peak corresponding to the π^+ mesons from the reaction $p + p \rightarrow d + \pi^+$.

In order for a π meson to be emitted, in a proton-proton collision, with energy 400 Mev at an angle of 56° to the beam of 669-Mev protons, the nucleon in the nucleus must move towards the incident proton with a momentum of at least* $\sim$ 350 Mev/c, which exceeds by more than $\sim$100 Mev/c the upper limit of the momentum corresponding to a degenerate Fermi gas of noninteracting nucleons. The separate nucleons in the nucleus possess high momenta because of the presence of strong, short-acting interactions between pairs of nucleons which lead to the appearance of compact two-nucleon groups[6,7] that last for only a short time. Observation of deuterons knocked out of light nuclei by 675-Mev protons[3] shows that the incoming protons sometimes undergo elastic collisions with such compact two-nucleon groups inside the nucleus. The substantial smearing out of the π-meson spectra on the high energy side means that collisions inside the nucleus between the incident protons and groups of nucleons having large relative momenta sometimes also gives rise to π meson production. Since this observation comes only from the high-energy parts of the spectra, of the π-mesons produced on compact groups of nucleons, it is hard to estimate quantitatively the contribution of this process to the total yield of the π mesons. However, it is clear that the dominant process is that of production of π mesons in the collision of the incident protons with individual nucleons. It should be noted that, owing to the Pauli principle, emission of π mesons with energies close to the maximum possible should be strongly suppressed in collisions of nucleons with compact groups of nucleons. In the case of production of π mesons by protons on two-nucleon groups the Pauli principle should have a greater effect in processes such as $p + pp \rightarrow \pi^0 + 3p$, $p + np \rightarrow \pi^- + 3p$, $p + nn \rightarrow \pi^+ + 3n$ than in processes of the type $p + pp \rightarrow \pi^+ + n + 2p$, $p + pp \rightarrow \pi^+ + p + 2n$, etc.

Integration of $d^2\sigma/d\omega\, dE$ over the energy yields the following values for the differential cross sections for the production of π mesons at angle of 56° to the proton beam in p + C collisions:

$$d\sigma^+/d\omega = (5.1 \pm 0.8)\cdot 10^{-27} \text{ cm}^2/\text{sterad};$$
$$d\sigma^-/d\omega = (1.0 \pm 0.2)\cdot 10^{-27} \text{ cm}^2/\text{sterad}.$$

The indicated errors include both the statistical errors and all uncertainties arising in determining the absolute value of $d^2\sigma/d\omega\, dE$. Corresponding values of $d\sigma/d\omega$ for π^+ and π^- mesons in the c.m.s. are $(3.3 \pm 0.7) \times 10^{-27}$ and $(0.65 \pm 0.12) \times 10^{-27}$ cm^2/sterad. From this, the differential cross section for production of π^+ mesons on one proton in the carbon atom turns out to be $\sim 0.5 \times 10^{-27}$ cm^2/sterad, whereas the differential cross section for production of π^+ mesons under the same conditions in free p-p collisions is $(0.65 \pm 0.10) \times 10^{-27}$ cm^2/sterad.

Together with measuring the spectra at 56°, we also determined the absolute values of $d^2\sigma/d\omega\, dE$ for the π-meson spectra measured earlier[1,8] at 24°. These were emitted in the bombardment of hydrogen, beryllium, and carbon by protons of roughly the same energy. It was found that at $\sim$45° in the c.m.s., the differential cross sections for production of π^+ and π^- mesons on carbon were $(3.6 \pm 1.0) \times 10^{-27}$ and $(0.52 \pm 0.13) \times 10^{-27}$ cm^2/sterad respectively. In this case the differential cross section for production of π^+ mesons on a single proton in the carbon nucleus has again a value $\sim 0.5 \times 10^{-27}$ cm^2/sterad, whereas in free p-p collisions this is $\sim 1.4 \times 10^{-27}$ cm^2.

Thus, from the results of absolute measurements of yields of charged π mesons from p + C collisions at 24° and 56° to the proton beam, one can assert the following: (1) The differential cross section for production of π^+ and π^- mesons does not depend strongly on the angle in the c.m.s. (2) When the angle is reduced from $\sim$90° to $\sim$45°, the ratio of differential cross sections for production of π^+ mesons in p-p collisions inside the carbon

*This value of the minimum momentum of a nucleon in the nucleus was obtained by considering the $p + p \rightarrow d + \pi^+$ reaction under the assumption that, in all, 30 Mev went into tearing the nucleon away, exciting the final nucleus, and into the recoil. For this, the Fermi energy of the nucleon $E \approx 24$ Mev corresponds to a maximum π-meson energy of $\sim$ 310 Mev.

nucleus to that in collisions of free protons drops from ~ 0.8 to ~ 0.3. This is caused both by the reabsorption of π mesons in the initial nuclei, the influence of which increases with decreasing angle, and by the difference in the angular distributions of the π mesons produced by protons on free protons and on those bound in a nucleus. In the former case, according to Neganov and Savchenko,[9] the angular distribution of π^+ mesons in the reaction $p + p \rightarrow \pi^+ + n + p$ has the form $0.66 + \cos^2 \vartheta$. Under the assumption that the emission of charged π mesons in $p + C$ collisions is isotropic over the entire range of angles, the total cross sections for production of π^+ and π^- mesons would be estimated to be $\sim 44 \times 10^{-27}\,cm^2$ and $\sim 7 \times 10^{-27}\,cm^2$, respectively. From this, on account of charge independence, one has the relation $\sigma^+ + \sigma^- = 2\sigma^0$ between the cross sections for the production of positive, negative, and neutral π mesons on nuclei with isotopic spin zero. For $p + C$ collisions at 670 Mev, this gives $\sigma^0 \approx 25 \times 10^{-27}\,cm^2$, which agrees well with the value $(28 \pm 3) \times 10^{-27}\,cm^2$ obtained at roughly the same energy by observing γ-rays from the decay of π^0 mesons.[10]

As can be seen from Table III, the values of the ratio $(d^2\sigma^+/d\omega\,dE)/(d^2\sigma^-/d\omega\,dE)$ increase slowly with energy, namely, from ~ 4.7 for 30 Mev to ~ 8 for 300 Mev. This result differs markedly from that obtained at 24°, where the same ratio grew from ~ 1 to ~ 15 over the energy interval 30 to 300 Mev. For 56°, the ratio of integrated yields $(d\sigma^+/d\omega)/(d\sigma^-/d\omega)$ was 5.2 ± 0.7. Approximately the same value should be obtained for the ratio σ^+/σ^- of the total cross sections for the production of π^+ and π^- mesons in hydrogen, if the conclusion about the weak dependence of $d\sigma^+/d\omega$ and $d\sigma^-/d\omega$ on angle is correct. In fact, at 24° the ratio $(d\sigma^+/d\omega)/(d\sigma^-/d\omega)$ constitutes 7.0 ± 0.8.

If it is assumed that single production of π mesons in nucleon-nucleon collisions proceeds only through the excitation of one of the colliding nucleons into an intermediate resonant $P_{3/2,3/2}$-state, then, according to the calculation of Peaslee,[2] the ratio σ^+/σ^- should be 11 in the case of protons bombarding a nucleus containing equal numbers of protons and neutrons. The sharp disagreement between this number and experiment means, first, that in collisions of protons with bound nucleons nonresonant production of π mesons in the p-n system in the state $T = 0$ proceeds together with resonant production of π mesons in p-p and p-n systems with states of $T = 1$. In order to satisfy the observed value of the ratio $(d\sigma^+/d\omega)/(d\sigma^-/d\omega)$, it is necessary to assume that production of π^- mesons in the p-n system proceeds equally in states with $T = 1$ and $T = 0$.* Peaslee's disregard of the interference between different states of the two-nucleon system, which participate in the process of production of π mesons, could evidently also lead to an erroneous value of σ^+/σ^-. This argument was recently used by Mandelstam[12] to explain the marked difference between the theoretical and experimental values of the ratio σ^+/σ^0 for p-p collisions at 660 Mev. Finally, it should also be considered that the production of π^+ mesons inside the nucleus could be partly suppressed as a result of de-excitation of the $P_{3/2,3/2}$-state without emission of a π meson in collision of the excited nucleon with one of the neighboring nucleons.[13,14]

The authors would like to express their gratitude to A. S. Kuznetsov for participation in planning and setting up the electronic gear.

[1] Meshcheriakov, Vzorov, Zrelov, Neganov, and Shabudin, J. Exptl. Theoret. Phys. (U.S.S.R.) **31**, 55 (1956), Soviet Phys. JETP **4**, 79 (1957).

[2] D. C. Peaslee, Phys. Rev. **94**, 1095 (1954); **95**, 1580 (1954).

[3] Azhgirei, Vzorov, Zrelov, Meshcheriakov, Neganov, and Shabudin, J. Exptl. Theoret. Phys. (U.S.S.R.) **33**, 1185 (1957), Soviet Phys. JETP **6**, 911 (1957).

[4] N. P. Bogachev and I. K. Vzorov, Dokl. Akad. Nauk SSSR **99**, 931 (1954).

[5] L. C. L. Yuan and S. J. Lindenbaum, Phys. Rev. **93**, 143 (1954); **103**, 404 (1956).

[6] Brueckner, Eden, and Francis, Phys. Rev. **98**, 1445 (1955).

[7] H. A. Bethe, Phys. Rev. **103**, 1353 (1956).

[8] Meshcheriakov, Zrelov, Neganov, Vzorov, and Shabudin, J. Exptl. Theoret. Phys. (U.S.S.R.) **31**, 45 (1956), Soviet Phys. JETP **4**, 60 (1957).

[9] B. S. Neganov and O. V. Savchenko, J. Exptl. Theoret. Phys. (U.S.S.R.) **32**, 1265 (1957), Soviet Phys. JETP **5**, 1033 (1957).

[10] Iu. D. Prokoshkin and A. A. Tiapkin, J. Exptl. Theoret. Phys. (U.S.S.R.) **33**, 313 (1957), Soviet Phys. JETP **6**, 245 (1958).

[11] Iu. M. Kazarinov and Iu. N. Simonov, J. Exptl. Theoret. Phys. (U.S.S.R.) **35**, 78 (1958), Soviet Phys. JETP **9** (in press).

[12] S. Mandelstam, Proc. Roy. Soc. **A244**, 491 (1958).

[13] N. Austern, Phys. Rev. **100**, 1522 (1955).

[14] R. Wilson, Phys. Rev. **104**, 218 (1956).

Translated by G. E. Brown
284

*In connection with this, it should be noted that in the data of Kazarinov and Simonov,[11] the total cross section for inelastic scattering at 590 Mev, in the $T = 0$ state of the two-nucleon system, is $(9.3 \pm 3.7) \times 10^{-27}\,cm^2$.

ENERGY LEVELS OF Dy^{161}*

S. A. BARANOV, Iu. F. RODIONOV, G. V. SHISHKIN, and L. V. CHISTIAKOV

Submitted to JETP editor March 13, 1958

J. Exptl. Theoret. Phys. (U.S.S.R.) **34**, 1367-1380 (June, 1958)

The decay of beta-active Tb^{161} was studied using a double focusing magnetic β-spectrometer, a proportional counter spectrometer and a scintillation spectrometer. The results of the investigation enable us to establish the existence of the following γ-transitions Dy^{161}: 25.6 (E1); 25.8 (E1); 27.7; 42; 48.9 (M1); 52; 57.6; 74.5 (E1); 103.8; 131.5 kev. Gamma ray transitions with E_γ = 20.4, 23.1, 46.3, 53.2, 57.0, 78.3, 84.0, 105.8 and ~275 kev were established less reliably. In studying the decay of Tb^{161}, we also observed groups of β-particles with endpoints E_{01} = 540 kev, E_{02} = 465 kev, (E_{03} = 415 kev), and $E_{04} \approx$ 215 kev. On the basis of the experimental data, a possible energy level scheme is proposed for Dy^{161}.

1. INTRODUCTION

RADIOACTIVE Tb^{161} decays by beta emission to stable Dy^{161}. The half-life of Tb^{161} is 7.2 days. Some information concerning the radiations emitted in the decay of this nucleus and about the levels of Dy^{161} has been given in several quite incomplete papers.[1-8]

In 1956, Cork et al.[9] and Smith et al.[10], using scintillation and β-spectrometers, studied the decay of Tb^{161} in more detail, and constructed different level schemes for Dy^{161}. These investigations still did not enable one to resolve certain discrepancies in the decay scheme of Dy^{161}. We therefore undertook a further more careful investigation of both the electron spectrum, including its low-energy part ($E_{conv.\,min}$ = 3 kev), and the soft γ-radiation occurring in the decay of Tb^{161}.

2. APPARATUS AND PREPARATION OF RADIOACTIVE Tb^{161} SOURCE

For our investigation of the electron spectrum of Tb^{161}, we used a magnetic β-spectrometer with $\pi\sqrt{2}$ double focusing.[11] The resolving power of the spectrometer was 0.3%, with a solid angle equal to 0.4% of 4π. The Tb^{161} source used here was deposited on a thin organic backing (thickness 10^{-5} cm) and had dimensions 1.5×25 mm^2.

To study the γ-radiation accompanying the Tb^{161} decay, we used proportional-counter spectrometers filled with mixtures of A + CH_4, Kr + CH_4, and Xe + CH_4, and a scintillation spectrometer with a NaI (Tl) crystal. These experiments were done with another Tb^{161} source, whose absolute decay rate had previously been measured with a 4π-counter[12] operating in the region of limited proportionality. The various equipments were calibrated using well-known electron and γ-ray lines of Am^{241} (references 13 and 14), Cs^{137}, and Na^{22}.

The Tb^{161} sample was obtained from the reaction: $Gd^{160}(n\gamma)\,Gd^{161} \xrightarrow[3.7\ min]{\beta^-} Tb^{161}$. The starting material was gadolinium, enriched to 99.9% in the Gd^{160} isotope. The Gd^{160} sample was irradiated with thermal neutrons in the RFT reactor for a period of seven days. The irradiated sample was dissolved in dilute HCl and then the rare earths were precipitated out as fluorides using HF. The hydroxide residue was dissolved in a minimal amount of 0.1 N HCl, and the solution was transferred to a column of Dowex-50 resin. The chromatographic separation was carried out with 0.4 N lactic acid having pH = 4.3 using the method described by Thompson et al.[15] The eluate fraction corresponding to the terbium peak on the chromatogram was dried, and the residue was heated and dissolved in HCl. The twice-normal (with respect to HCl) solution which was obtained was deposited on an organic backing. After drying, $TbCl_3$ was left on the plate.

For the β-spectrometer studies, we first deposited a small (1.5×25 mm^2) semi-transparent strip of aquadag on the organic backing. The aquadag guaranteed that the source wetted the backing and had the necessary conductivity. The Tb^{161} sample prepared in this way had a surface density of about 5 micrograms/cm^2.

Since the thickness of the film over the window of the β-detector in the β-spectrometer was ~10^{-5} cm, this together with the source just de-

*This work was reported at the eighth All-Union Conference on Nuclear Spectroscopy (Leningrad, January, 1958).

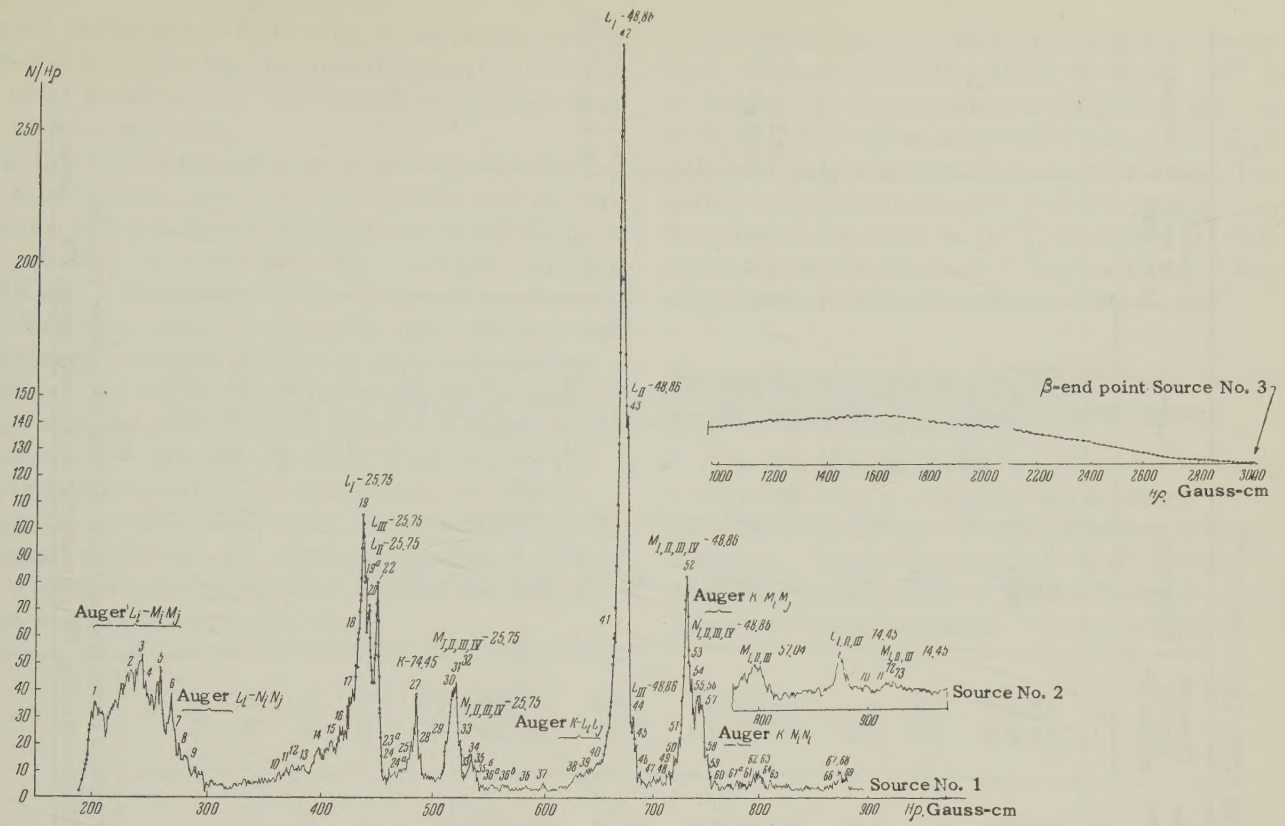

FIG. 1. Electron Spectrum of Tb^{161}.

scribed enabled us to study the electron spectrum down to very low energies.

3. EXPERIMENTAL RESULTS

(a) β-Spectrometer Measurements

Figure 1 shows a large part of the β-spectrum (source #3) and electron spectrum of Tb^{161} in the range of Hρ values from 200 to 900 Gauss-cm as obtained with the thin source (surface density 5 microgm/cm), and in the interval of Hρ values from 780 to 980 Gauss-cm, as gotten with a more intense source (#2).

The tens of electron lines observed by us, which, as we see from Fig. 1, are primarily in the low-energy part of the spectrum, and the absence of even weak high energy conversion lines would seem to justify the assumption that almost all of the energy levels of Dy^{161} are located in the energy interval from 0 to 132 kev. Analysis of individual parts of the electron spectrum enabled us to show that in this nucleus there are γ-transitions with only slightly different energies. As an example of this statement, a portion of the spectrum is shown in Fig. 2 in which there are clearly visible the L-conversion lines (19, 20, 22) of the known γ-transition with energy 25.75 kev (cf. for example Ref. 10), and the L-lines of an unknown γ-transition with E_γ = 25.6 kev (lines 18, 19a, 21). The dotted lines in the Figure are the L_{II} and L_{III} lines of E_γ = 25.75, as obtained by graphical resolution. One can apparently also assert the existence of a γ-transition with $E_\gamma \approx 23.1$ kev (cf. Table I and Fig. 1, peaks 14, 15, 16).

Table I gives the interpretation of the conversion lines corresponding to γ-transitions in Dy^{161} as well as the intensities for some of the lines. In the last column we give the multipolarities of the tran-

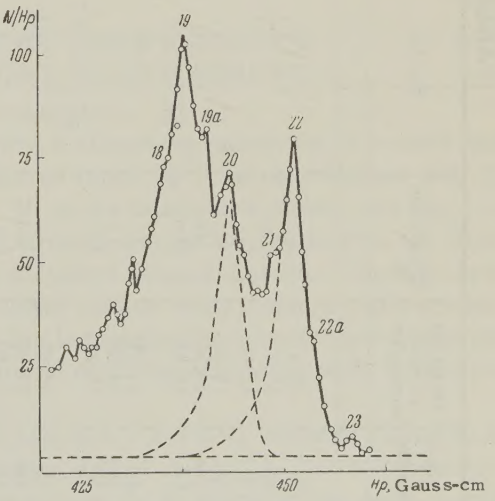

FIG. 2. Portion of the electron spectrum of Tb^{161}.

TABLE I. Interpretation of Electron Lines from Decay of Tb^{161}

Line number	Observed electron energy, kev	Conversion	E_γ, kev	Intensity in arbitrary units	Remarks
1	2	3	4	5	6
10	11.4	L_I	20.45		
11	11.8	L_{II}	20.39	0.7	
12	12.15	L_{III}	20.20		
23	18.35	M_I	20.38		
23a	18.50	M_{II}	20.35		
24	18.65	M_{III}	20.33		or $L_I - 27.7$
			av. 20.35*		
14	14.11	L_I	23.16		
15	14.55	L_{II}	23.14		
16	15.25	L_{III}	23.05		
			av. 23.12*		
18	16.55	L_I	25.60		
19a	17.00	L_{II}	25.59	19.1	
21	17.85	L_{III}	25.55		
			av. 25.58		(E 1)
19	16.80	L_I	25.85		
20	17.25	L_{II}	25.84	(23.2)	Calculated
22	17.85	L_{III}	25.65	18.00	
30	23.70	M_I	25.74	22.7	
31	23.85	M_{II}	25.70		The value of I_M is the sum
32	24.10	M_{III}	25.78	24.6	of $I_M(25.75)$
33	24.35	M_{IV}	25.69		$+ I_M(25.58)$
34	25.35	N_I	25.77		Cf. I_M or
35	25.60	N_{IV}	25.77	5.6	$M - 27.7$
			av. 25.75		E 1
24	18.65	L_I	27.70		
24a	19.15	L_{II}	27.74		
25	20.00	L_{III}	27.80		
35	25.60	M_I	27.63		
35b	25.90	M_{II}	27.75		
36a	27.10	N_I	27.52		
36b	27.45	N_{II}	27.78		
			av. 27.70		
37a	33.60	L_I	42.65		
37b	34.10	L_{II}	42.70		
37c	34.90	L_{III}	42.75		
			av. 42.70		
40	37.65	L_{II}	46.24		
41	38.25	L_{III}	46.30		
			av. 46.27		E 2 (?)
42	39.85	L_I	48.90		
43	40.30	L_{II}	48.89	177.0	
44	41.00	L_{III}	48.80		
52	46.80	M_I	48.84		
53	47.00	M_{II}	48.85	37.7	
54	47.20	M_{III}	48.88		
57	48.45	N_I	48.87		
			av. 48.86		M 1
47	43.00	L_I	52.05		
48	43.80	L_{II}	52.39		
			av. 52.22*		
49	44.6	L_{II}	53.20		
50	45.3	L_{III}	53.10		
			av. 53.15*		
55	48.00	L_I	57.05		
57	48.45	L_{II}	56.94		or $L_I - 57.55$
58	49.10	L_{III}	56.90		or $L_{II} - 57.7$
63	55.00	M_I	57.04		
64	55.30	M_{II}	57.15		
65	56.65	N_I	57.05		
			av. 57.04		
1	3.7	K	57.7		
57	48.45	L_I	57.55		or $L_I - 57.05$
58	49.10	L_{II}	57.69		or $L_{III} - 57.05$
			av. 57.64		
27	20.75	K	74.52	12.6	
67	65.45	L_I	74.50		
68	65.85	L_{II}	74.44	3.9	
69	66.35	L_{III}	74.35		
71	72.35	M_I	74.40		
72	72.65	M_{II}	74.50		
73	72.80	M_{III}	74.48		
			av. 74.45		E 1
36	30.25	K	83.9		
			av. 83.9		
60	50.0	K	103.77		
			av. 103.77		
61a	52.0	K	105.77		
			av. 105.77		
	77.7	K	131.47		
			av. 131.47**		

*Another interpretation of the electron lines is not excluded.

**Observed using Pb as converter with a very strong Tb^{161} source.

sitions, as determined from the experimental data. It should be noted that the identification of individual lines is not unique, and certain of the lines are not given in the table.

In the Kurie plot (cf. Fig. 3) constructed from the experimental data, one can resolve four partial spectra with end points respectively equal to $E_{01} = 540 \pm 5$ kev, $E_{02} = 465$ kev, $E_{03} = 410$ kev and $E_{04} = 215$ kev. The portion of the β-spectrum corresponding to β-particle energies above 500 kev was taken very carefully with three different sources. However, we did not observe the partial β-spectrum with end point 570 kev which was reported by Smith et al.[10] Since the method of resolution of a Kurie plot into individual components is very inexact, as we shall show later the possibility is not excluded that there are additional partial β-spectra with end point energies of 515 and 490 kev, as were reported in reference 10.

Summarizing the experimental data presented here, we may conclude that the decay of Tb^{161} shows a complex β-spectrum, consisting of at least 4 to 6 partial β-spectra having (except for $E_{04} \approx 215$ kev) only slightly different end points. Together with the large number of low energy γ-transitions observed in Dy^{161} (cf. Table I), this indicates the existence of a large number of energy levels close to the ground state in Dy^{161}.

(b) Measurements with the Proportional Counter Spectrometer and Gamma Spectrometer

The use of proportional counters for studying x-rays and soft γ-radiation has a variety of advantages over the use of a scintillation γ-spectrometer. This is especially true with regard to resolving power, which is the fundamental characteristic of such equipment. The investigation of

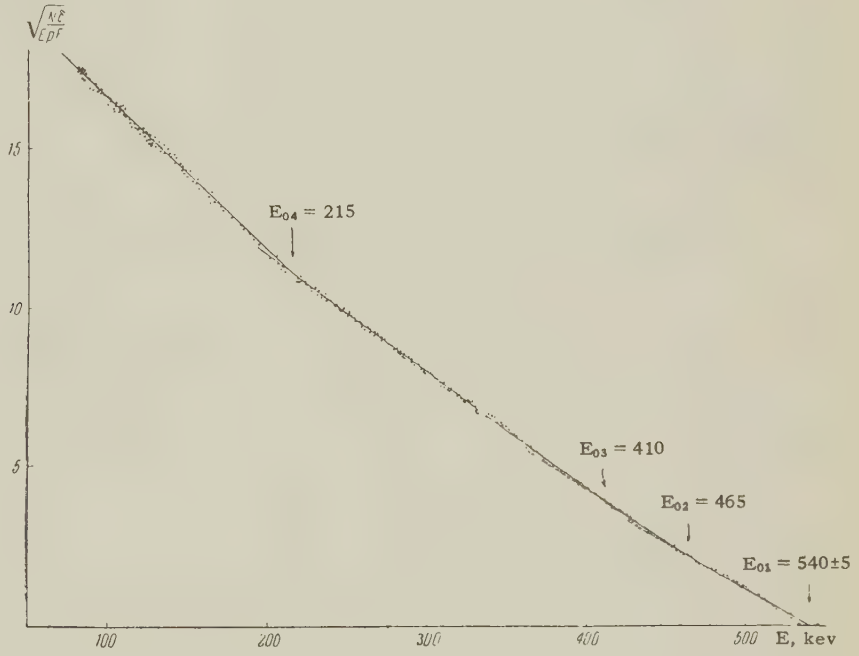

FIG. 3. Kurie plot of β-spectrum of Tb^{161}; N is the number of particles recorded, E is the total energy of the β-particles; F, p, δ are tabulated functions from β-decay theory.

the γ-spectrum in the energy interval 2 to 130 kev was therefore done only with such counters, filled with mixtures of the following gases: A + CH_4, Kr + CH_4, and Xe + CH_4. A scintillation spectrometer with a NaI (Tl) crystal was used to study the spectrum of γ-rays with $E_\gamma > 130$ kev.

Combined with these detectors we used an unsaturated linear amplifier and multi-channel pulse-amplitude differential analyzers. One of these had 150 channels, and was constructed under the direction of, and according to the design of Tsytovich.[16] The shape of the low energy spectrum of x-rays and γ-radiation was reproduced on a linear scale on one of the oscillograph tubes (diameter 300 mm) of this analyzer.

Figure 4 shows the spectrum of x-rays and soft γ-radiation from Dy^{161} in coordinates (N, $E_{x,\gamma}$), where N is the number of pulses and $E_{x,\gamma}$ is the energy of the x-ray or γ-ray in kev, for three different series of measurements. The data from which these curves were constructed were not corrected for the negligible background or for the variation of counting efficiency with γ-ray energy E_γ.

The use of a Kr + CH_4 counter filling in the first series and of Xe + CH_4 in the other two sets enables us clearly to separate the main x-ray and γ-ray lines and to eliminate the so-called satellite

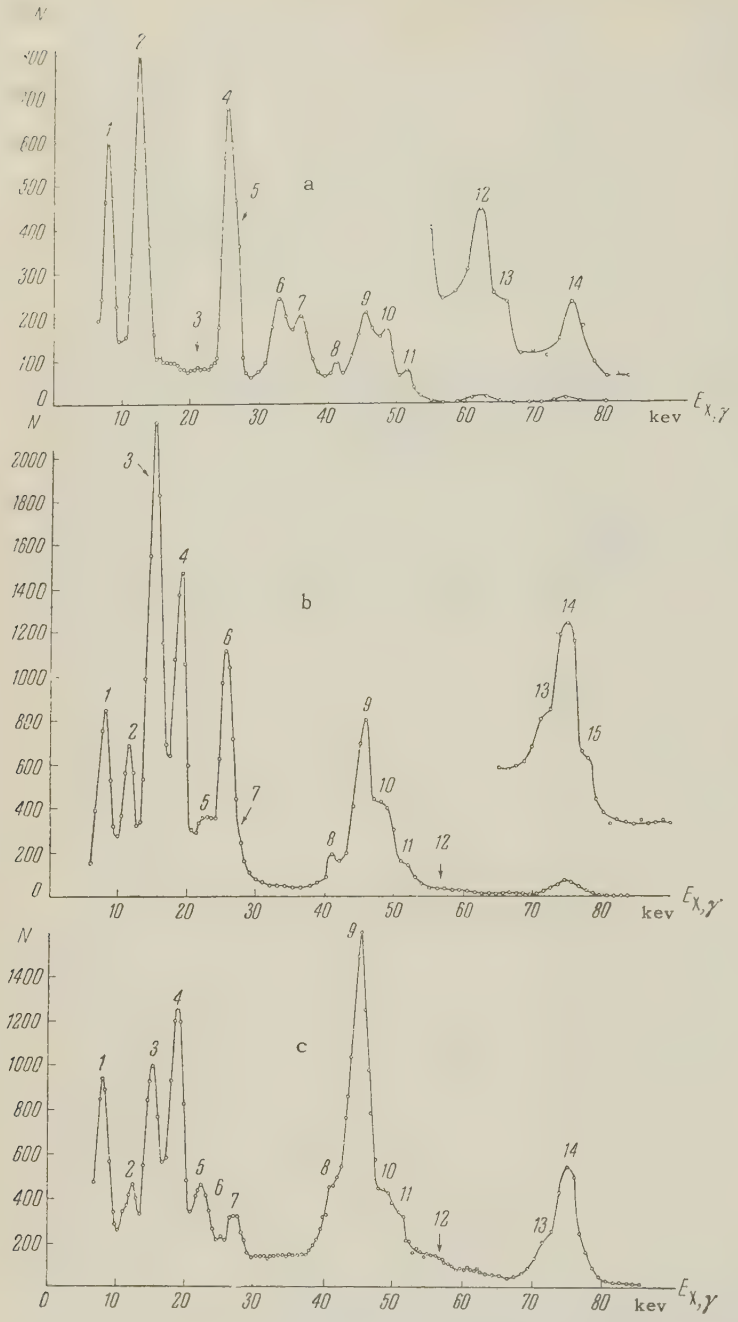

FIG. 4. X-rays and soft γ-radiation from Dy^{161}; (a) counter filled with Kr + CH_4 mixture, (b) and (c) counter filled with Xe + CH_4 mixture; (a) and (b) – 2 mm Al Absorber, (c) – 1 mm Cu absorber

peaks.* From a comparison of Figs. 4a and 4b, for example, we easily see that lines 2, 6, 7, 12, and 13 (Fig. 4a) are satellite peaks. Figure 4c shows the same spectrum with a 1 mm thick copper absorber placed between the source and the end window of the proportional counter. This experiment enabled us to establish with certainty the presence of the two seemingly doubtful satellite peaks 5 and 7. These lines have a complex shape. Consequently the possibility is not excluded that there are four γ-rays corresponding to them, with energies of approximately 52, 53, 57, and 57.6 kev. This statement is not in contradiction with the data given in Table I. A similar conclusion can apparently be drawn concerning peak 2 of Fig. 4c.

The detailed interpretation of the observed γ-ray lines shown in Figs. 4a and 4b is given in Table II. The intensities of individual γ-lines are given in percent in the last column. In this case corrections were made for background and for the effi-

*The absorption of low energy γ-quanta in a counter filled with a heavy gas occurs via the photoeffect. If the characteristic x-radiation of the gas atoms is not recorded by the counter, then in addition to the main line ($E_0 = E_\gamma$) there will appear a satellite line, having energy $E = E_\gamma - E_{K_\alpha}$. Here E_γ is the energy of the γ-quanta entering the counter, and E_{K_α} is the energy of the K_α-radiation of the atoms of the gas in the counter.

TABLE II

Line No.	Counter filling (Kr + CH_4)		Counter filling (Xe + CH_4)		
	Energy $E_{X,\gamma}$, kev	Interpretation of line	Energy $E_{X,\gamma}$, kev	Interpretation of line	Intensity in %
1	8.0 ± 0.1	E_X of counter wall material	8.0 ± 0.1	E_X of counter wall material	
2	12.6 ± 0.1	E_S^* from sum of E_γ = 25.75 and E_γ = 25.58 kev	12.0 ± 0.2	E_S of E_γ = 41.5 kev	
3	21 ± 0.2	E_γ (?)	15.5 ± 0.3	E_S of E_X = 45 kev	
4	25.5 ± 0.3	sum of E_γ= 25.75 and E_γ = 25.58 kev	19.3 ± 0.3	E_S of E_γ = 49 kev	
5	27.0 ± 0.3	E_γ	22.5 ± 0.3	E_S of $E_{X,\gamma}$ = 52 kev	
6	32.5 ± 0.3	E_S of E_X = 45 kev	25.5 ± 0.3	sum of E_γ = 25.75 and 25.58 kev	26.3 ± 3
7	36.5 ± 0.3	E_S of E_X = 49 kev	27.0 ± 0.3	sum of E_γ and E_S of E_γ = 57 kev	
8	41.5 ± 0.3	$E_\gamma + E_S$ of $E_{X,\gamma}$ = 52 kev	41.5 ± 0.3	sum of E_γ and E_S of E_γ = 72 kev	9.9 ± 1
9	45.0 ± 0.3	E_X	45 ± 0.3	sum of E_X and E_S of E_γ = 75 kev	
10	49.0 ± 0.3	E_γ	49.0 ± 0.3	sum of E_γ and E_S of E_γ = 78 kev	42 ± 4
11	52.0 ± 0.3	$E_{X,\gamma}$	52.0 ± 0.3	$E_{X,\gamma}$	
12	62.5 ± 0.4	E_S of E_γ = 75 kev	57.0 ± 0.3	E_γ	4.4 ± 0.5
13	65.0 ± 0.5	E_S of E_γ = 78 kev	72.0 ± 0.5	(E_γ and E_S) of E_γ = 102 kev?	2.6 ± 0.5
14	75.0 ± 0.5	E_γ	75.0 ± 0.5	E_γ	8.6 ± 0.9
15	78.0 ± 0.5	E_γ ?**	78.0 ± 0.5	E_γ?*	5.9 ± 0.6

*E_S denotes a satelite line.

**Part of the equipment using the proportional counter was shielded with lead, so that the 78-kev γ-ray line can be assigned to the characteristic Pb radiation.

TABLE III. Energy (in kev) of γ-transitions in Dy^{161}

This paper	Cork et al.[9]	Smith et al.[10]	This paper	Cork et al.[9]	Smith et al.[10]	Remarks
20.35			57.04		56.9±0.4	
23.12			57.64	57.3		
25.58			74.45	74.8	74.6±0.4	
25.75	25.6	25.5±0.1	78.11?	78.3		Low probability of existence
27.70	27.7		83.90			
42.70			103.77			
46.27			105.77	106.2		
48.86	48.9	48.9±0.1	131.5	132.1		
52.22			~275*			
53.15						

*These γ-rays were observed in a scintillation spectrometer with a very strong source.

ciency of recording of γ-rays of different energies by the counter filled with the Xe + CH_4 mixture.

An examination of the data of Table II shows that some of the γ-lines are masked by the satellite peaks of γ-quanta of higher energy. However, in the majority of cases, simultaneous analysis of the results of the measurements with the β-spectrometer and the proportional counters makes it possible to eliminate the uncertainty. The γ-lines corresponding to γ-ray energies of 72 and 78 kev are peculiar. These lines cannot be interpreted uniquely, and their existence remains an open question.

Table III summarizes the data concerning γ-transitions in Dy^{161}, as found in the present work and in Refs. 9, 10. These data will be used later

TABLE IV. Absolute Conversion Coefficients η for γ-rays of Dy^{161}

E_γ, kev	$\frac{E_\gamma}{m_0 c^2}$	Experimental values of η		Theoretical values of η						Multipolarity
		A_K/B	$A_{\Sigma L}/B$	$E1$		$E2$		$M1$		
				η_K	$\eta_{\Sigma L}$	η_K	$\eta_{\Sigma L}$	η_K	$\eta_{\Sigma L}$	
25.75	~0.05		0.98±0.18		1.79		85.41		17.9	$E1$
48.86	~0.10		1.72±0.30		0.261		25.96*		2.30	$M1$
					0.266*				2.14*	
74.45	~0.15	0.46±0.10		0.56	0.083	2.82	2.57	4.45	0.71	$E1$
				0.52*	0.088*	1.97*	2.41*	4.37*	0.65*	

*These are theoretical conversion coefficients calculated by Sliv, taking into account the finite size of the nucleus and screening by the atomic electrons. The remaining values of η were obtained by interpolation in Rose's tables.[17]

in the paper to construct the level scheme of Dy^{161}.

4. DETERMINATION OF MULTIPOLARITY OF GAMMA-TRANSITIONS

The measurements which were done only with the β-spectrometer enable us quite definitely to assign the multipolarity of the 25.75 kev γ-transition. For this case, $(L_{II}/L_{III})_{exp} = 0.793$. The theoretical values of this ratio for E1, E2, and M1, respectively, are 0.781, 1.424, and 7.000. Thus the 25.75 kev γ-line can be assigned to be electric dipole. From the data presented in Table I and Fig. 1, one might also conclude that the multipolarities of the γ-quanta with $E_\gamma = 48.86$ and $E_\gamma = 74.45$ kev must be M1 and E1, respectively. This conclusion is not certain, especially for the second case. We therefore chose a different way of determining the multipolarity of the γ-radiation, based on the determination of absolute conversion coefficients from the experimental data.

As we said earlier, the measurements of the γ-radiation of Dy^{161} with a proportional counter were done using a source whose absolute β-activity had been determined using a 4π counter. After introducing the appropriate corrections, this enabled us to determine the quantity B, i.e., the number of γ-quanta of the given energy accompanying a single β-emission. The results with the β-spectrometer, in turn, enabled us to determine the other essential quantity A — the number of K-, L- or M-electrons (for a given E_γ) which accompany a single β-decay. The ratio $\eta = A/B$ of these two quantities is the absolute conversion coefficient. By comparing the experimental and theoretical values, we established the multipolarities of some of the γ-transitions.

In Table IV we give the experimental values of the absolute conversion coefficients for the 25.75, 48.9 and 74.5 kev γ-rays. The right half of the table gives the theoretical values of η for various multipolarities. The assigned multipolarities of the γ-transitions are given in the last column.

It is easy to see from Table IV that the γ-radiations with energy 48.9 and 74.5 kev should be assigned respectively to magnetic and electric dipole. The disagreement between the theoretical and experimental values of η (for E1) for $E_\gamma = 25.8$ kev cannot be explained by the inaccuracy of the theoretical values or by the large experimental errors.

As we showed earlier (cf. Fig. 2 and Table I), there are two γ-transitions in Dy^{161} with almost equal energies $E_\gamma = 25.75$ and 25.58 kev. In studying the γ-spectrum with a proportional counter, it is not possible to separate these two lines. Therefore γ-line 6 in Fig. 4a (and the corresponding line 4 in Fig. 4b) is the sum of these two γ-lines. If we take account of this fact, the value of B should be somewhat lower for $E_\gamma = 25.75$ kev than the value used for the calculation of $\eta_{\Sigma L} = A_{\Sigma L}/B$. Consequently, $\eta_{exp} = A_{\Sigma L}/B$ is in this case close to the theoretical value $\eta_{\Sigma L} = 1.79$ (for E1 radiation) given in Table IV. It is not difficult to show by a simple calculation that the γ-ray with $E_\gamma = 25.56$ kev is electric dipole.

5. DISCUSSION OF RESULTS; LEVEL SCHEME FOR Dy^{161}

There are many difficulties in constructing a level scheme for Dy^{161} from the experimental data. As we said earlier, the β-spectrum of Tb^{161} is complex, and consists of 4 to 6 partial β-spectra whose end points differ very little from one another. The construction of these spectra from the Kurie plot and the estimate of their intensity is very inaccurate.

With the present accuracy of the experiment, the interpretation of certain of the conversion and γ-ray lines is not unique, which also complicates

the setting up of a level scheme for Dy^{161}. In this connection it is not without interest to remark that even the apparently definitely established γ-lines with energies 25.7 and 48.9 kev (cf. for example Ref. 10) are complex, each consisting of two components. This assertion is obvious for the case of $E_\gamma = 25.7$ kev (cf. Fig. 2). The proof of the assertion for the 48.9 kev line follows from the fact that the halfwidth $\xi_{49} = \Delta H\rho/H\rho$ of the $L_1 - 48.9$ line is somewhat greater than the halfwidth ξ_{75} of the $K - 74.5$ line.* According to our estimates, the second component E'_γ has an energy ~ 0.2 kev less than the main γ-line which is several times more intense. It should be mentioned that we are at the limit of our experimental accuracy, which reduces the rigor of this proof. However, as we shall see later, this interpretation is supported by other experimental facts.

Using the energy values for these four γ-quanta, it is easy to see that the sums $(25.75 + 48.70)$ and $(25.58 + 48.86)$ kev coincide precisely with $E_\gamma = 74.45$ kev. Consequently, the γ-rays with energies 25.75 and 25.58 kev are, respectively, in cascade with the 48.70 and 48.86 γ-quanta.

Using the data of Table I, it is not hard to show that the 74.5 kev transition, which is equal to the energy difference of two partial β-spectra $(E_{01} - E_{02})$ is a direct transition to the ground state of Dy^{161}. Thus there must also be levels at 25.8 and 48.9 kev between the ground state of this nucleus and the level at 74.5 kev.

If we make use of the experimental values of the intensities $I = N_{l_K} + N_\gamma$ of the γ-transitions, it can be shown that $I_{74.5} \approx 35$, $I_{48.9+48.7} \approx 250$, $I_{25.8} \approx 100$, and finally $I_{25.6} \approx 30$ (intensities in arbitrary units). These data show that in the β-decay of Tb^{161} there is also a β-transition to the 48.9 kev level, and possibly also to the 25.8 kev level in Dy^{161}. The end point of the first partial β-spectrum is ~ 490 kev, and that of the second ~ 514 kev. As was stated earlier (cf. Section 3a), this is not contradicted by the data of Smith et al.[10] In addition, the γ-ray at 131.5 kev, the cascade γ-rays with energies $E_\gamma = 74.5$ and 57.0 kev, and the observed partial β-spectrum with end point $E_{03} = 410$ kev indicate the existence of a level at 131.5 kev. From the data of Tables I and III it also follows that there should be levels at 103.8 and ~ 325 kev.

It is clear that we have by no means used all of the experimental data in this analysis. Apparently, in addition to those given above, there are levels of Dy^{161} which manifest themselves weakly in the β-decay of Tb^{161}.

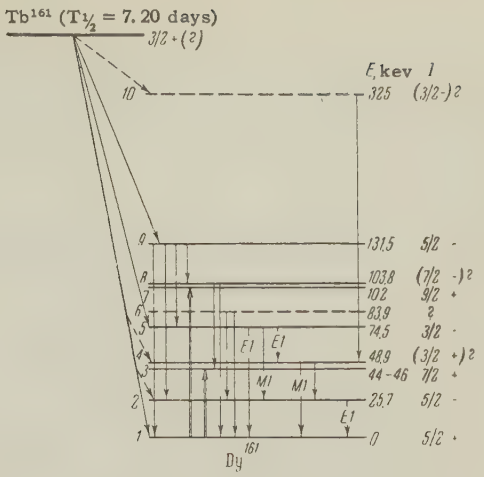

FIG. 5. Level Scheme of Dy^{161}.

There are statements in the literature that Pieper and Heydenburg[18] have repeated their experiments on Coulomb excitation of dysprosium, using enriched isotopes. Similar experiments have also been done very recently by Elbeck, Nielsen and Olsen.* According to these investigators, the first two levels of the ground rotational band of Dy^{161} are located at distances of $(46 - 44)$ and $(103 - 102)$ kev from the ground state, which has a spin $I_0 = 5/2$.[19,20]

The 44 and 102 kev levels scarcely appear in the β-decay of Tb^{161}. Some indications for the $44 - 46$ kev level can be found from our data (cf. Table I and Fig. 1). There may be a very weak L-46 conversion line in this energy range, which is masked by the K-LL Auger electrons. The 103.8 kev γ-transition mentioned earlier could also be a proof of the existence of the 102 kev level. However this is unlikely, since the observed γ-ray of energy $27.7 = (131.5 - 103.8)$ kev can hardly be assigned to be magnetic quadrupole or E3 radiation (cf. the level scheme in Fig. 5).

Summarizing our discussion, we conclude that the following energy levels of Dy^{161} are established: 25.8, $44 - 46$, 74.5, 84?, 102, 103.8, 131.5, ~ 325 kev.

In Fig. 5 we show a possible level scheme for Dy^{161} constructed from the experimental data. The spin assignments are shown at the right. The levels are designated by the numbers given on the left. Levels 3 and 7 belong to the ground rotational band, which is associated with collective motion of the

*The analysis was carried out for four series of measurements of the K-74.5 and $L_I - 48.9$ conversion lines from different sources.

*This work was done at the Institute for Theoretical Physics of Copenhagen University in 1957 (Private communication).

nucleons in the nucleus. Levels 2 and 5 are due to single particle excitation. Levels 8 and 9 are apparently terms of the rotational bands based on levels 2 and 5. Levels 4, 6 and 10 are not completely established, and their nature remains an open question.

The proposed scheme does not pretend to be conclusive. Certain similarities with this scheme can be found from the theoretical computations of Nilsson[21] and Mottelson and Nilsson.[20]

In conclusion we should mention that we have not given the log $f\tau$ values of the various γ-transitions, because these quantities cannot be determined accurately from the experimental data. The log $f\tau$ value is approximately 6 to 7. We should also mention that the half life of Tb^{161}, as determined using a 4π counter, was $T_{1/2} = (7.20 \pm 0.07)$ days. This value is in good agreement with the value of $T_{1/2}$ given in the short note of Cork et al.[9]

We are very grateful to G. Ia. Shchepkin for preparing the pure Gd^{160} isotope, and to S. N. Belenkii and R. M. Polevoi for assistance in this work.

We should like to thank P. E. Nemirovskii, A. I. Baz', V. M. Strutinskii, L. K. Peker and D. F. Zaretskii for participating in discussion of this work. We are also greatly indebted to L. A. Sliv for providing us with new values of the L-subshell conversion coefficients.

Note added in proof (May 24, 1958).
After this paper went to press, one of us (S.A.B.) received from the Institute for Theoretical Physics of Copenhagen University two preprints of papers on the levels of Dy^{161}. The experimental study of the Tb^{161} decay was done by a group of authors (P. G. Hansen, O. Nathan, O. B. Nielsen, R. K. Sheline), and the theoretical work by D. R. Bes.

The main results of these papers are in agreement with the results presented in our paper. However, there is a considerable discrepancy between the estimates of the intensity of the γ-rays with $E_\gamma = 25.7$ and 48.9 kev. This discrepancy is apparent from the following data:

Ratio of intensity of γ-transitions	Cork et al.[9]	Smith et al.[10]	Baranov et al.	Hansen et al.
I_{26}/I_{49}	2.1	0.6	0.4	1.0

The discrepancy apparently arises from inaccuracy in determining the intensity of the 25.7 kev γ-transition.

This question is of vital importance for the construction of the Dy^{161} level scheme, and requires more careful checking. Unfortunately, the experimental curves in the low-energy region of the electron spectrum are given only by Smith et al.[10] and in the present paper.

[1] Krisberg, Pool, and Hibdon, Phys. Rev. **74**, 44 (1948).

[2] F. D. S. Butement, Phys. Rev. **75**, 1276 (1949).

[3] B. H. Ketelle, Oak Ridge Report, cited in Hollander, Perlman and Seaborg, Revs. Mod. Phys. **25**, 469 (1953).

[4] Scharff-Goldhaber, der Mateosian, McKeown, and Sunyar, Phys. Rev. **78**, 325 (1950).

[5] R. E. Hein and A. F. Voigt, Phys. Rev. **79**, 783 (1950).

[6] Cork, LeBlanc, Nester, and Stumpf, Phys. Rev. **88**, 685 (1952).

[7] R. Barloutaud and R. Ballini, Compt. rend. **241**, 389 (1955).

[8] N. P. Heydenburg and G. M. Temmer, Phys. Rev. **100**, 150 (1955).

[9] Cork, Brice, Schmid, and Helmer, Bull. Am. Phys. Soc., Ser. II, **1**, 297 (1956).

[10] Smith, Hamilton, Robinson, and Langer, Phys. Rev. **104**, 1020 (1956).

[11] Baranov, Malov, and Shliagin, Приборы и техника эксперимента (Instr. and Meas. Eng.) **1**, 1 (1956).

[12] S. A. Baranov and R. M. Polevoi, Приборы и техника эксперимента (Instr. and Meas. Eng.) **3**, 32 (1957).

[13] S. A. Baranov and K. N. Shliagin, Тр. сессии АН СССР по мирному использованию атомной энергии. Отделение физ.-мат. наук. (Reports of the Session of the Academy of Sciences of the U.S.S.R. on Peaceful Uses of Atomic energy. Division of Physical and Mathematical Sciences) p. 251, 1956.

[14] Hollander, Smith, and Rasmussen, Phys. Rev. **102**, 1372 (1956).

[15] Thompson, Harvey, Choppin, and Seaborg, J. Amer. Chem. Soc. **76**, 6231 (1954).

[16] A. P. Tsytovich, Приборы и техника эксперимента (Instr. and Meas. Eng.) **5**, 118 (1957).

[17] Beta- and Gamma-Ray Spectroscopy, ed. by K. Siegbahn, Amsterdam, 1955.

[18] N. P. Heydenburg and G. F. Pieper, Phys. Rev. **107**, 1297 (1957).

[19] A. H. Cooke and J. G. Park, Proc. Phys. Soc. **A69**, 282 (1956).

[20] B. Mottelson and S. G. Nilsson, Phys. Rev. **99**, 1615 (1955).

[21] S. G. Nilsson, Kgl. Danske Videnskab. Selskab Mat.-fys. Medd. **29**, No. 16 (1955).

Translated by M. Hamermesh
285

FISSION OF URANIUM NUCLEI AND PRODUCTION OF MULTI-CHARGED FRAGMENTS ON EMULSION NUCLEI BY HIGH-ENERGY POSITIVE π MESONS

I. S. IVANOVA

Radium Institute, Academy of Sciences U.S.S.R.

Submitted to JETP editor December 7, 1957

J. Exptl. Theoret. Phys. (U.S.S.R.) 34, 1381-1388 (June, 1958)

The interaction between 280-Mev π^+ mesons and uranium nuclei, accompanied by fission, was studied by means of nuclear emulsions. It has been concluded, from an analysis of the light charged particles emitted in fission, that the absorption of π^+ mesons occurs predominantly in interactions involving a pair of nucleons (n, p). The main features of uranium fission induced by high-energy π^+ mesons are investigated. Some peculiarities of production of multi-charged ($Z \geq 4$) fragments on emulsion nuclei by high-energy positive π mesons are noted. An estimate is given for the cross section for production of such fragments on heavy emulsion nuclei (Ag, Br).

THE present work is devoted to two problems connected with the interaction between high-energy π^+ mesons and complex nuclei: the fission of uranium nuclei induced by 280-Mev π^+ mesons, and the production of multi-charged fragments on emulsion nuclei by π^+ mesons of the same energy.

The work has therefore been divided into two parts, corresponding to the above phenomena.

1. INTERACTION BETWEEN 280 Mev π^+ MESONS AND URANIUM NUCLEI ACCOMPANIED BY NUCLEAR FISSION

In the study of the properties of π mesons, which are so important for the problem of nuclear forces, attention has been mainly given to the elementary interactions of mesons with protons and deuterons. Many investigations have been carried out, and interesting qualitative and quantitative results have been obtained. A number of processes going on in the nucleus can be observed in interactions between π mesons and complex nuclei, which makes it difficult to interpret the primary interaction between mesons and the nucleons of the nucleus. Some problems, however, such as the question of whether the meson is absorbed in interaction with a pair of nucleons or with several nucleons, or whether the interaction between a π meson and the nucleons can be considered as consecutive interactions with separate nucleons, etc., can be solved only by studying the interaction with complex nuclei.

Majority of the investigations devoted to these problems have been carried out by means of nuclear emulsions and have been mainly concerned with the interaction between comparatively low-energy positive and negative π mesons ($E < 150$ Mev) and emulsion nuclei. The interaction between high-energy π mesons ($E > 150$ Mev) and nuclei of the emulsion has been studied mainly for the case of negative π mesons.[1-6] Interactions between fast mesons with Pb, C, Be, Al, and Cu nuclei have been studied mainly by means of cloud chambers[7-10] and scintillation counters.[11-13]

According to our present ideas, a high-energy meson colliding with a nucleus can, in interaction with nucleons, undergo elastic or inelastic scattering, scattering accompanied by a change of charge, or absorption. Energetic nucleons due to scattering or meson absorption, can collide with other nucleons (cascade process) in traversing the nucleus and leave the nucleus altogether (if their energy is sufficient). The excited nucleus loses energy emitting nucleons.

A certain difficulty is encountered in interpreting interactions with the emulsion nuclei due to the presence of both light and heavy nuclei in the emulsion. Besides, the result of the primary interaction between a π meson and an emulsion nucleus is strongly masked by the large number of charged particles "evaporated" from the nucleus.

There are some advantages in studying the interaction between high-energy positive π mesons with uranium nuclei. Firstly, such events can be easily identified by subsequent fission of the uranium nucleus which is bound to happen in the majority of cases. Fission serves, therefore, as an identification mark for uranium nuclei. Secondly,

TABLE I

Particle type and energy	Relativistic emulsion		Emulsion P-9	
	Mean number of charged particles per fission	Forwards/ backwards ratio	Mean number of charged particles per fission	Forwards/ backwards ratio
π^+, $E = 280$	2.1 ± 0.17	1.1 ± 0.2	1.01 ± 0.05	1.27 ± 0.17
p, $E = 350$	0.9—1.0	~ 3.4	0.60 ± 0.06	1.7 ± 0.2
p, $E = 140$	0.40 ± 0.06	4	0.25 ± 0.02	2.6 ± 0.5
Slow π^- mesons	~ 0.12		0.10 ± 0.02	

only a small number of charged particles is expected to evaporate from a uranium nucleus since, in heavy nuclei, excitation energy is dissipated mainly through the emission of neutrons. In consequence, it is easier to identify charged particles emitted as the result of interaction between a π meson and nucleons.

We have selected and studied the interaction events accompanied by fission. An analysis of the charged particles emitted in such events makes it possible to draw certain conclusions concerning the absorption of π^+ mesons. Besides, we studied the fission of U nuclei induced by high-energy positive mesons, in view of the lack of data on that subject.*

Uranium was introduced into the emulsions by soaking the plates in a 4% aqueous solution of $UO_2Na(C_2H_3O_2)_3$. In that way it was possible to introduce $\sim 10^{20}$ uranium nuclei into 1 cm^3 of emulsion. The plates were then irradiated. Positive 300-Mev mesons were produced by the synchrocyclotron of the Joint Institute for Nuclear Research. The plates were bombarded with 280-Mev mesons selected from the beam by means of a copper absorber.

Two types of special fine-grain emulsions† were used in the experiment. The first type was capable of recording relativistic particles of minimum ionization, while the second (type P-9) had a sensitivity threshold for 45 to 50-Mev protons. Both these emulsions have high sensitivity and good discrimination for particles of different charge. The relativistic emulsion made it possible to detect all charged particles accompanying the interaction and, consequently, to obtain a full picture of the event (as far as charged particles were concerned). This emulsion cannot, however, be irradiated by a large meson flux (because of the resulting background which makes scanning difficult), and the number of fission events observed in this emulsion is small. A large number of fission events has been observed and studied in the P-9 emulsion, which could be irradiated with a large meson flux. The data thus obtained augmented substantially those obtained by means of the relativistic emulsion, and made it possible to study the main features of uranium fission induced by high-energy positive mesons.

We found and studied 73 cases of fission of the U nucleus, induced by fast π^+ mesons in the relativistic emulsion, and 460 cases in the P-9 emulsion. The majority of fission events induced by high-energy π^+ mesons is accompanied by emission of charged particles.

The mean number of charged particles per fission induced by π^+ mesons ($E = 280$ Mev) for the two types of emulsion (columns 2 and 4), and the angle formed by these particles with the direction of the incident π^+ meson (columns 3 and 5), are given in Table I. Analogous data on fission induced by 350-Mev and 140-Mev protons and slow negative mesons, obtained by us earlier, are included for comparison.

It follows from the second column of the table that, in relativistic emulsion, the mean number of charged particles per fission induced by fast π^+ mesons is much larger than the mean number of charged particles emitted in fission induced by 350-Mev and 140-Mev protons. It follows from the comparison of the mean numbers of charged particles in fission induced by π^+ mesons, observed in different emulsions (columns 2 and 4), that most of these particles have a high energies, $E > 50$ Mev.

Let us consider now the angles of emission with respect to the fission producing particle, given in the third column of the table for relativistic emulsion (the ratio of the number of particles emitted in the forward direction to the number of particles emitted backwards). For the case of π^+-meson induced fission, the distribution is nearly isotropic (1.1 ± 0.2), while for fission induced by fast protons there is a strong preponderance of forward-moving particles (the forward to backward ratio

*The only data available are on uranium fission induced by slow negative mesons[14-17] and on the fission of Hg induced by 150-Mev π^- mesons.[18]

†The emulsions were prepared in the laboratory of Prof. N. A. Perfilov.

is > 3).

The above data on the mean number of charged particles and their direction do not contradict the assumption that the majority of charged particles, associated with fission induced by fast mesons, results from the primary interaction between the π^+ meson and nucleons of the nucleus. These particles may comprise both scattered protons and particles ejected by them in a cascade process, and protons produced in the absorption of the meson together with charged particles ejected by them from the nucleus in a cascade process. The number of charged particles evaporated by the uranium nucleus is small.

If the interaction in π^+ meson absorption involves a (n,p) pair, we should observe two protons emitted at 180° to each other in c.m. system. High-energy cascade particles ejected by these nucleons preserve, essentially, the directions of the primaries. If the absorbed π^+ meson interacts with several nucleons, there is no preference for large angles (> 120°) between emitted particles. We have carried out an analysis of the light charged particles, accompanying the π^+-meson induced fission in relativistic emulsion. The angles (in space) between emitted protons, and their energies, were measured in events accompanied by the emission of two or three protons. The energies of these protons were measured by the grain density method. The dependence of the spatial angle of proton pairs on the sum of the energies of these protons is shown in Fig. 1. It can be seen that the

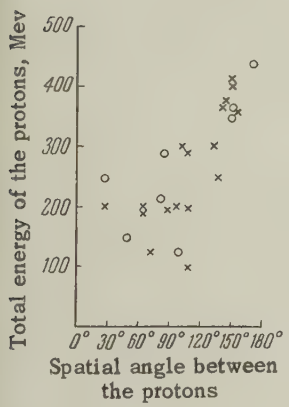

FIG. 1. Dependence of the spatial angle between protons of a pair on the total energy of the protons: ○ – for events with emission of two protons, × – for events with emission of three protons (relativistic emulsion).

angle increases with the energy of emitted protons, approaching 150° for a pair energy equal to ~400 Mev. This is in agreement with the assumption that the 280-Mev π^+ mesons are, mostly absorbed in interaction with the (n,p) pairs.

A large number of the charged particles accompanying the fission of uranium induced by π^+ mesons is, evidently, produced in a cascade process. It is possible, however, for example in emission of two protons after the absorption of a π^+ meson, that one of the protons leaves the nucleus without undergoing a collision with other nucleons in the nucleus, while the other collides first with a neutron. In the emission of three protons, it is possible that one of the two protons produced as the result of π^+ absorption leaves the nucleus without collision, while the other ejects another proton. A microphotograph of such an event is shown in Fig. 2.

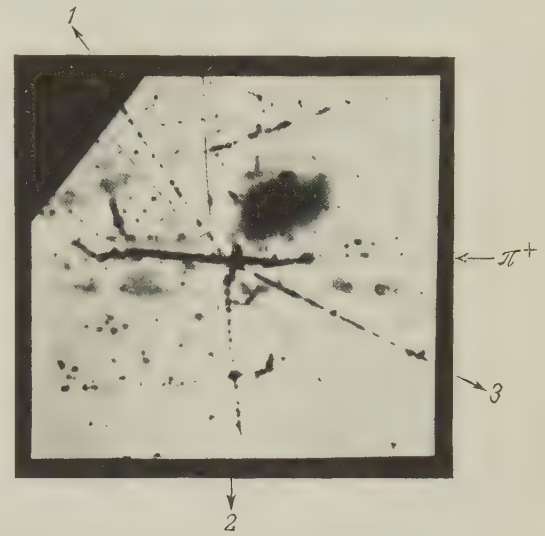

FIG. 2. Fission of a uranium nucleus induced by a 280-Mev π^+ meson. 1 – proton of ~ 220 Mev, 2 – proton of ~ 100 Mev, 3 – proton of ~ 80 Mev (Magnification 1550 ×).

The assumption that the mesons are mostly absorbed by (n,p) pairs is indirectly confirmed by data obtained by means of the P-9 emulsion. In this emulsion we measured the projection of the angles between emitted protons. The solid line in Fig. 3 illustrates the dependence of the number of proton pairs on the angle (projected)

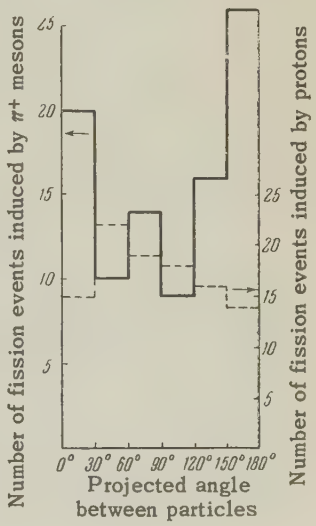

FIG. 3. Dependence of the number of emitted pairs on the projected angle between the particles of the pair: solid line – for π^+-meson induced fission, dotted line – for high-energy proton induced fission (emulsion P-9).

between the components of a pair. We note a marked increase in the number of events with large angles (> 120°). In Fig. 3 we included for comparison (dotted line) a similar dependence for protons emitted in uranium fission induced by high-energy (460 to 660 Mev) protons, investigated by us earlier in the P-9 emulsion. The histogram is constructed also for fission events accompanied by the emission of two and three particles. The charged particles recorded in the emulsion P-9 in proton-induced fission events are mainly evaporated protons. These should possess an almost isotropic distribution of the angles of emission, very different from the curve obtained for fission induced by fast π^+ mesons. This effect can be seen in Fig. 3. Consequently, the preponderance of large angles between emitted protons (in fissions induced by π^+ mesons) can be explained by the presence of cascade particles, ejected from the nucleon by the proton pair originating in the absorption of π^+ meson.

The above analysis of fission events induced by π^+ mesons in both types of emulsion, relativistic and P-9, makes it possible to conclude that, for the most part, the π^+ mesons are absorbed in interaction with the (n, p) nucleon pairs.[34] The data obtained in the present experiment do not exclude the possibility that the π^+ mesons may be absorbed in the first interaction, without previous energy loss.

All fission events detected in the relativistic emulsion were specially examined for the presence of a scattered meson emitted from the nucleus undergoing fission. In seven cases out of 73, a π^+ meson with energy greater than 45 to 50 Mev was observed in addition to light charged particles.*

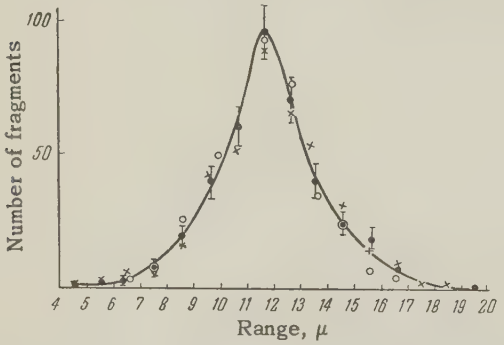

FIG. 4. Range distribution of single fragments in emulsion for fission events, induced by: ● – 280-Mev π^+ mesons ○ – 350-Mev protons, × – slow π^- mesons.

*It should be noted that only mesons with energies greater than > 45 to 50 Mev can be properly identified from the ratio of the grain density of the given particle to the grain density of a particle with minimum ionization.

This amounts to ~10% of the interaction events leading to fission.

The fission of uranium nuclei induced by positive mesons can therefore be explained as due to passage of fast nucleons through the nucleus, originating in meson absorption, and to meson scattering with large energy transfer.

We shall note the following features of uranium fission, induced by 280-Mev π^+ mesons, which were obtained in our experiment: The solid curve in Fig. 4 represents the range distribution of single fragments of uranium fission induced by 280-Mev π^+ mesons. The curve has a maximum indicating a predominantly symmetric fission. The dots in the figure represent distributions in fission induced by 350-Mev protons[19] and by slow π^- mesons.[14] It can be seen that, within the limits of errors, all the points lie on the curve. The mean total range of fragments in π^+-meson induced fission events, equal to 23.5 μ, coincides, within experimental error, with that in fission induced by 350-Mev and 140-Mev protons (23.1 μ and 23.3 μ respectively) and by slow π^- mesons (23.7 μ).

We estimated the cross-section for the fission of uranium by 280-Mev π^+ mesons. The cross-section was determined both from the experiments with the relativistic emulsion and those with the P-9 emulsion. The number of uranium nuclei in the emulsion was measured by counting the number of α-particles emitted by uranium. The meson flux in the relativistic emulsion was measured by counting the meson tracks, and was calculated for the P-9 emulsion from the irradiation time. According to our measurements, the cross-section for the fission of uranium, induced by 280-Mev π^+ mesons, is equal to $(1.0 \pm 0.2) \times 10^{-24}$ cm^2.

2. PRODUCTION OF MULTI-CHARGED ($Z \geq 4$) FRAGMENTS ON EMULSION NUCLEI IN INTERACTION WITH 280-Mev POSITIVE MESONS

The mechanism of production of multi-charged fragments accompanying the interaction between fast mesons and nuclei has not been fully explained. The production of multi-charged fragments can be observed not only in interactions of cosmic rays,[20-25] but in interactions between nuclei and nucleons with energy of the order of several hundred Mev.[26-32] An extensive study,[33] devoted to the production of multi-charged fragments on emulsion nuclei by high energy protons, has shown that the process cannot be explained by an evaporation or a cascade theory, but requires special assumptions on the interaction between fast protons and nuclei. In connection with the above, it is of interest to investi-

FIG. 5. Interaction between a π^+ meson (E = 280 Mev) and a heavy emulsion nucleus, accompanied by the emission of a multi-charged fragment (B_6^5) (Magnification 1000 ×).

TABLE II

	Relativistic emulsion		Emulsion P-9		Forwards/backwards ratio of fragments (both emulsions)
	Mean number of prongs per star	Forwards/backwards ratio of prongs	Mean number of prongs per star	Forwards/backwards ratio of prongs	
Stars with multi-charged fragments produced by 280-Mev π^+ mesons	5.4±0.2	1.3±0.3	4.9±0.2	1.1±0.1	3.2±1
Stars without multi-charged fragments, produced by 280-Mev π^+ mesons	<4.9±0.1 (~3.9)	1.2±0.1	<4.4±0.1 (~3.3)	1.15±0.08	

gate the production of such fragments by high-energy π mesons as well.*

In the experiments with the relativistic emulsion we recorded 24 interaction events between 280-Mev π^+ mesons and emulsion nuclei, accompanied by production of multi-charged ($Z \geq 4$) fragments. Sixty-five similar events were observed in the P-9 emulsion.

A microphotograph of an interaction between a π^+ meson and a heavy emulsion nucleus, accompanied by emission of B_6^5, is shown in Fig. 5 (relativistic emulsion).

Some data on stars, accompanied by emission of multi-charged fragments and unaccompanied by such an event, are given in Table II.

The mean number of prongs in stars, with and without emission of multi-charged particles is given in the first and third column of the table for the two types of emulsion. The mean number of prongs in stars unaccompanied by fragment emission should be lower than that given in the table, since such stars with zero and one charged particles are not noted in scanning, while stars with two charged particles are also partially overlooked. Approximate values of the mean number of prongs, calculated with allowance for missed stars, are given in parentheses.

The ratios of the numbers of light charged particles emitted forwards (with respect to the incident π^+ meson) to the number of charged particles emitted backwards are given in the second and fourth columns. The same ratio for the fragments, measured by means of both emulsions, is given in the last column.

The above data indicate a certain similarity between the production of multi-charged fragments in interaction between high-energy π^+ mesons and emulsion nuclei and the production of these fragments in interaction involving the emulsion nuclei and high-energy protons.[33] It follows from Table II that, for π^+ mesons, production of fragments is more probable in events with many prongs. The same has been noted for fast protons.[33]

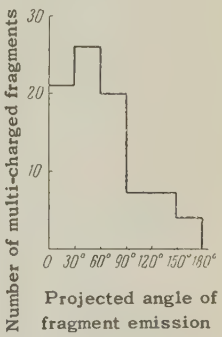

FIG. 6. Distribution of multi-charged fragments as function of the projected angle of emission relative to the π^+-meson direction.

The angular distribution of the emitted multi-charged fragments about the direction of the incident π^+ meson is of special interest. It has been found that the emitted fragments are directed predominantly forwards. This follows from the last column of Table II (forwards/backwards = 3.2) and from Fig. 6, representing the dependence of

*The presence of such fragments in interaction between 750-Mev π^- mesons and emulsion nuclei (16 cases) is mentioned in reference 2.

the number of emitted fragments on the projected angle of emission relative to the direction of the incident meson. It should be noted that a similar preponderance of multi-charged fragments emitted forwards has been observed for production of these fragments on emulsion nuclei by high-energy protons.[33] All other light charged particles produced in nuclear disintegrations induced by π^+ mesons are emitted almost isotropically (columns 2 and 4).

The cross section for the production of multi-charged fragments on heavy emulsion nuclei (Ag, Br) by 280-Mev π^+ mesons, estimated from the data obtained in the present work, equals $(0.62 \pm 0.2) \times 10^{-27}\,\mathrm{cm}^2$.

We investigated the possibility of multi-charged fragment production in events in which the incident π^+ meson is not absorbed in the nucleus, but only scattered. We studied the light charged particles emitted in addition to the fragments in stars, observed in the relativistic emulsion. The ratio of grain density of the tracks of fast particles to the grain density of tracks of particles with minimum ionization was measured. As particles with minimum ionization we chose the primary-meson background recorded in the relativistic emulsion. This made it possible to detect scattered mesons of > 45 to 50 Mev.

An emitted π meson, accompanying a multi-charged fragment, was found in five events out of the 24 stars detected in the sensitive emulsion. Four events were identified by a low value of I_{part}/I_{min}, and the fifth from the general energy balance of all emitted charged particles. It follows that the absorption of the meson is not necessary for the production of a multi-charged fragment by a fast meson.

The preliminary data given above do not contradict the assumption that the production of multi-charged fragments in the interaction between fast π^+ mesons and nuclei can be induced by fast nucleons produced in the first scattering act of the π^+ meson on a nucleon accompanied by a large energy transfer. This fact could explain to a certain extent the angular distribution of emitted fragments. It can also be maintained, however, that the angular distribution observed is not contradicted by the assumption that the fragments are produced in the nucleus in the first inelastic interaction of the meson.

In conclusion, the author wishes to express his gratitude to B. S. Neganov of the Joint Institute of Nuclear Research for his help in irradiating the plates with π^+ mesons, and to Prof. N. A. Perfilov for his constant interest in the work.

[1] M. Blau and M. Caulton, Phys. Rev. **90**, 150 (1954).

[2] M. Blau and A. Oliver, Phys. Rev. **102**, 489 (1956).

[3] W. Fry, Phys. Rev. **93**, 845 (1954).

[4] A. Morrish, Phil. Mag. **45**, 47 (1954); Phys. Rev. **90**, 974 (1954).

[5] N. A. Mitin and E. L. Grigor'iev, Dokl. Akad. Nauk SSSR **103**, 219 (1955).

[6] R. Hill, Phys. Rev. **101**, 1127 (1956).

[7] Dzhelepov, Ivanov, Kozadaev, Osipenkov, Petrov, and Rusakov, J. Exptl. Theoret. Phys. (U.S.S.R.) **31**, 923 (1956), Soviet Phys. JETP **4**, 864 (1957).

[8] G. Saphir, Phys. Rev. **104**, 525 (1956).

[9] E. Tanney and J. Tinlot, Phys. Rev. **92**, 974 (1954).

[10] J. Kessler and L. Lederman, Phys. Rev. **94**, 689 (1954).

[11] Ivanov, Osipenkov, Petrov, and Rusakov, J. Exptl. Theoret. Phys. (U.S.S.R.) **31**, 1097 (1956), Soviet Phys. JETP **4**, 922 (1957).

[12] Ignatenko, Mukhin, Ozerov, and Pontecorvo, Dokl. Akad. Nauk SSSR **103**, 395 (1955).

[13] D. Stork, Phys. Rev. **93**, 868 (1954).

[14] N. A. Perfilov and I. S. Ivanova, J. Exptl. Theoret. Phys. (U.S.S.R.) **29**, 551 (1955), Soviet Phys. JETP **2**, 433 (1956).

[15] Belovitskii, Romanova, Sukhov, and Frank, J. Exptl. Theoret. Phys. (U.S.S.R.) **29**, 537 (1955), Soviet Phys. JETP **2**, 493 (1956).

[16] S. Al-Salam, Phys. Rev. **84**, 254 (1951).

[17] W. John and W. Fry, Phys. Rev. **91**, 1234 (1953).

[18] N. Sugarman and A. Heber, Bull. Am. Phys. Soc. **28**, 13 (1953).

[19] N. S. Ivanova and I. I. P'ianov, J. Exptl. Theoret. Phys. (U.S.S.R.) **31**, 416 (1956), Soviet Phys. JETP **4**, 367 (1957).

[20] Heitler, Powell, and Fertel, Nature **144**, 283 (1939).

[21] G. Occhialini and C. Powell, Nature **159**, 93 (1947).

[22] C. Franzinetti and R. Payne, Nature **161**, 735 (1948).

[23] E. Shopper, Naturwiss. **34**, 118 (1947).

[24] P. Modgson and D. Perkins, Nature **163**, 439 (1949).

[25] A. Bonnetti and C. Dilworth, Phil. Mag. **40**, 585 (1949).

[26] S. Wright, Phys. Rev. **79**, 838 (1950).

[27] E. Titterton, Phil. Mag. **42**, 113 (1951).

[28] L. Marquez and J. Perlman, Phys. Rev. **81**, 913 (1953).

[29] D. Greenberg and J. Miller, Phys. Rev. **84**, 845 (1951).

[30] R. Batzel and G. Seaborg, Phys. Rev. **82**, 606 (1951).
[31] W. Barkas, Phys. Rev. **87**, 207 (1952).
[32] L. Marquez, Phys. Rev. **86**, 405 (1952).
[33] O. V. Lozhkin and N. A. Perfilov, J. Exptl. Theoret. Phys. (U.S.S.R.) **31**, 913 (1956), Soviet Phys. JETP **4**, 790 (1957).
[34] Bruckner, Serber, and Watson, Phys. Rev. **81**, 575 (1951).

Translated by H. Kasha
286

SOVIET PHYSICS JETP VOLUME 34 (7), NUMBER 6 DECEMBER, 1958

SURFACE IMPEDANCE OF SUPERCONDUCTING CADMIUM

M. S. KHAIKIN

Institute of Physical Problems, Academy of Sciences, U.S.S.R.

Submitted to JETP editor December 19, 1957

J. Exptl. Theoret. Phys. (U.S.S.R.) **34**, 1389-1397 (June, 1958)

The apparatus described here can be used to measure the surface impedance of a metal at a wavelength of 3.2 cm in the "super-low" temperature region of $\sim 0.1°K$. The complex surface impedance of a cadmium single crystal has been measured in the temperature interval between 0.1 and 0.6°K. The results of the measurements are analyzed. The penetration depth of the electromagnetic field in the superconducting cadmium has been determined and found to be $\delta_0 = (13 \pm 1.4) \times 10^{-6}$ cm for $T \to 0$.

THE measurement of the surface impedance of superconductors is particularly interesting in the frequency range satisfying the condition $h\nu/kT_c \gtrsim 1$, which can also be written as $\lambda T_c \gtrsim 1$ (λ = wavelength in cm, T_c critical temperature of the superconductor in °K). This condition can be satisfied by two different methods: by decreasing the wavelength λ of the applied electromagnetic radiation, and by investigating superconductors with lower critical temperatures T_c.

Until now most investigators have followed the first method[1-4] up to the present limits of radio techniques ($\lambda \sim 0.2$ cm). Only preliminary work has been carried out with the second method.[5,6] In this case, as in all work in this field, the temperature of the sample (Al) was reduced to 0.85°K by pumping off the liquid helium which cooled the whole of the apparatus under investigation.

This paper describes apparatus for the measurement of samples cooled to $\sim 0.1°K$ by the magnetic method (with ammonium iron alum used as the cooling agent). This makes possible a value $h\nu/kT_c = 0.9$ in investigations of cadmium at a wavelength of 3.2 cm, for example. This value is reached only at $\lambda = 0.46$ cm when working with tin. One of the features of the apparatus is that

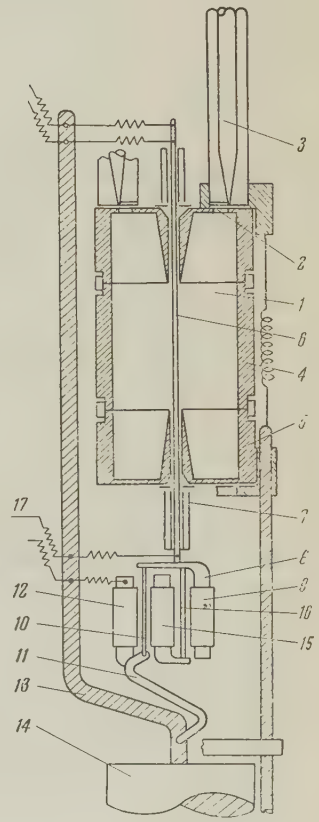

FIG. 1. Outline of the apparatus. On the right are shown some constructional details of the apparatus. The vacuum jacket is not shown.

only the sample, which serves as part of the measuring resonator, is cooled to the temperature of the alum. The remaining parts of the apparatus are at the temperature of the helium bath ($\sim 1.6°K$).

APPARATUS

The coaxial resonator (Fig. 1) with cavity 1 of diameter 1.6 cm and length 3.4 cm (somewhat larger than $\lambda = 3.2$ cm, owing to the effect of the conical ends of the internal conductor) has two symmetrical apertures 2, which are connected to the generator and to the detector by means of the coaxial lines 3. The power transfer efficiency (10^{-2} to 10^{-4} at resonance) may be regulated externally by means of a device which rotates the resonator about its axis of symmetry and displaces the two apertures relative to the coaxial lines. Cavity 1 of the resonator is formed by four conductors: cylinder 4 of length $\lambda/2$, two end flanges 5 of length $\lambda/4$, and the central part of the sample 6, which serves as the axial conductor. The electric contacts between the different parts of the resonator are not important, because all connections coincide with nodal lines of the resonance currents. The internal surfaces of the axial bores (diameter 1 mm) of flanges 5 are covered by layer of polystyrene of thickness 3 to 5 μ. This prevents electrical contact between the specimen and the flanges. The cylinder and the flanges are made of oxygen-free copper and have been electropolished internally.

The cylindrical sample 6, with a diameter of 0.9 mm, fits closely into the bores of the end flanges of the resonator and extends in length right through the resonator. The losses in high-frequency power from the resonator via the sample are smaller by 1 to 1.5 orders of magnitude than the power transferred to the detector; this is brought about by the open-circuited quarter-wave lines, which are formed by the conical parts of the resonator flanges together with the sample, and also by the quarter-wave "reflectors" 7 placed at the ends of the sample. The lower part of the sample is soldered to copper strip 8 with cadmium — the same metal as the sample. Copper strip 8 serves to conduct the heat to carbon thermometer 9, which measures the temperature of the sample. A heat conductor 10, made of the same metal as the sample but having a thermal resistance an order of magnitude higher than the sample, is also soldered to strip 8. This arrangement ensures a homogeneous temperature in the sample when heated by high frequency currents throughout the temperature range over which the measurements are made. An additional thermometer measures the temperature at the upper end of the sample, to check that this condition was fulfilled.

Heat conductor 10 is soldered to copper strip 11 ($0.1 \times 1.5 \times 15$ mm^3), at the upper end of which is located heater 12. The latter enables one to raise the temperature of the sample above that of the salt by means of the heat flow produced in strip 11 and conducted away by heat conductor 13. This conductor is a copper wire, 2 mm in diameter, whose end has been flattened into a broad strip (2 cm) and pressed into the salt 14. Heater 15 is connected to strip 8 by means of heat conductor 16 whose thermal resistance is about half that of the sample. This heater is used to determine the power dissipated in the sample by the high-frequency current. For this an equivalent direct current is made to flow through the heater and adjusted so that there is no change in the reading of thermometer 9. The thermometers were made of resistor material in the shape of thin copper-plated platelets of a conducting substance ($0.5 \times 2 \times 5$ mm^3). The copper strips of the electric and thermal conductors were also electroplated to the thermometer; the completed thermometer was soldered with Wood's metal to a thin-walled copper screen. The resistance of the thermometer changes from $\sim 50\,\Omega$ at 4.2°K to $\sim 400\,\Omega$ at 0.1°K. The heaters are fabricated like the thermometers, but are made of a material whose resistance is practically constant in the temperature range of the experiment.

The thermometers were calibrated by the magnetic temperature of the ammonium iron alum used as cooling agent. The alum permeability was determined by measuring the mutual inductance of coils surrounding the salt with an R-56 ac potentiometer at 60 cycles. The alum was cooled by helium until the start of demagnetization; the helium was then removed from the cavity of the apparatus by means of a carbon adsorption pump. The pressure of the helium used as heat exchanger was estimated from the rise in the temperature of a special carbon thermometer over that of the helium bath. The thermometer was hung inside the vacuum jacket of the apparatus with thin caprone threads (measuring current 80 μa, resistance 3 kΩ).

The electric leads to the sample for measuring its dc conductivity, to the thermometers, and to the heaters are made of constantan 30 microns in diameter. The center of each lead 17 (only a few of them are shown in Fig. 1) was brought into thermal contact with heat conductor 13.

By demagnetizing the salt from ~ 7 kilogauss at $\sim 1.6°K$ it was possible to obtain a temperature of $\sim 0.12°K$. The salt warmed up at a rate of

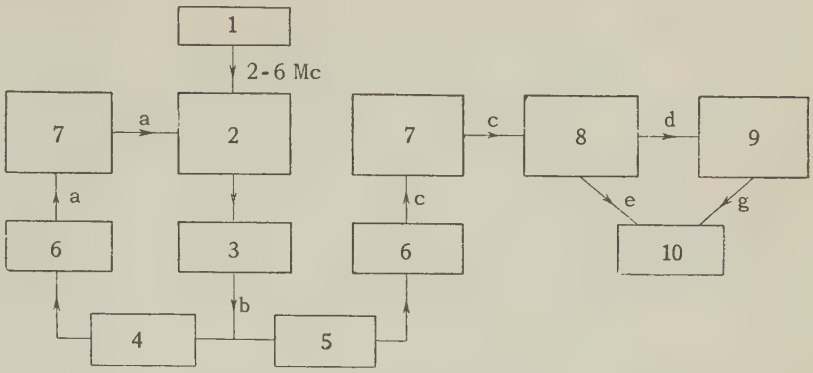

FIG. 2. Block-diagram of the electronic equipment for the continuous registration of the frequency characteristic and of the changes in the resonant frequency of the resonator. The letters represent the voltages and currents shown in Fig. 3. 1—Standard Signal Generator GSS-6; 2—Sweep Generator and Modulator of the Klystron; 3—Klystron K-20; 4—Standard resonator; 5—Resonator to be Measured; 6—Detectors; 7—Amplifiers; 8—First Differentiating Circuit; 9—Second Differentiating Circuit; 10—Six-Point Recording Potentiometer EPP-09.

$\sim 0.02°K/hr$, corresponding to a heat influx of ~ 30 erg/sec. In the absence of an hf field (< 1 erg/sec), no direct heat flux to the sample could be detected (by thermal radiation and through points of contact with the resonator).

ELECTRONIC CIRCUIT

The frequency characteristics and changes in the resonant frequency of the resonator were measured with an electronic circuit which made it possible to register these values automatically (together with the temperature of the sample) on a six-point EPP-09 recording potentiometer.

The operating principle of the circuit is as follows (Figs. 2 and 3). The modulating voltage from standard signal generator GSS-6, with a frequency F = 2 to 6 Mcs, is applied to the reflector of the klystron K-20. This produces sidebands in the klystron-output spectrum, separated from the carrier frequency by an amount F. Furthermore, the carrier frequency of the klystron is modulated, at a frequency of 25 to 50 cycles, by a saw-tooth voltage applied to the reflector from the sweep generator. There is a linear shift in the frequency spectrum of the klystron during the first half cycle of the saw tooth voltage, as shown in Fig. 3b. During the second half cycle, there is a linear shift in the opposite direction.

The limits of deviation of the carrier frequency of the klystron are determined by the resonances of the standard resonator (Fig. 3a), which occur at the instant when the carrier frequency or one of the side bands of the spectrum of the klystron are equal to the resonant frequency f_{st} (Fig. 3b). A superconducting cylindrical lead resonator with a Q on the order of 10^6 (resonance mode H_{011}) served as standard resonator. The signal from the standard resonator triggers the sweep generator and, therefore, also the direction of the shift in the carrier frequency. In this way, the magnitude of the shift in the klystron frequency is equal to the modulation frequency F from the GSS-6 standard signal generator.

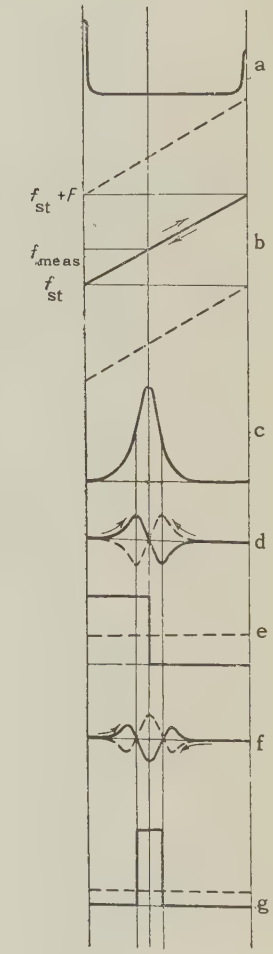

FIG. 3. Illustration of the operating principle of the electronic circuit. The time variations of the voltages and currents are shown at some points of the circuit in Fig. 2. During one half cycle of the sweep-voltage the changes take place from left to right, during the other half cycle – from right to left.

As the carrier frequency of the klystron covers the pass band of the tested resonator, a signal, which has the shape of the frequency characteristic of the resonator (Fig. 3c), reaches the detector. The first derivative of this signal (Fig. 3d) vanishes at the instant when the carrier frequency of the klystron coincides with the resonant frequency of the resonator. A pulse produced at this instant switches on or off one of the output currents of an electronic circuit (Fig. 3e) in such a way that the time average of this current (Fig. 3e, dotted line) is proportional to the difference in the frequencies of the measured and of the standard resonator

$f_{meas} - f_{st}$. This mean value of the current is recorded by the potentiometer EPP-09. In the same way, a second differentiation of the resonator signal (Fig. 3f) produces a current (Fig. 3g) whose time average is proportional to the width of the frequency band of the resonator. This current is also recorded by the potentiometer.

The electronic circuit contains about 60 vacuum tubes. A separate paper will be devoted to its description.*

THE SAMPLE

The sample investigated was an electropolished cylindrical single crystal of cadmium of purity 99.999% and a diameter of 0.9 mm. The hexagonal axis of the crystal was parallel to the axis of the cylinder to an accuracy of a few degrees. The hf currents travelled along the surface of the cylinder, so that the surface resistance of the cadmium was measured practically in the direction of its hexagonal axis. The dc conductivity of the sample at 4°K was $(22 \pm 5) \times 10^{20}$ esu, exceeding its conductivity at 300°K by a factor of $(1.5 \text{ to } 2) \times 10^4$.

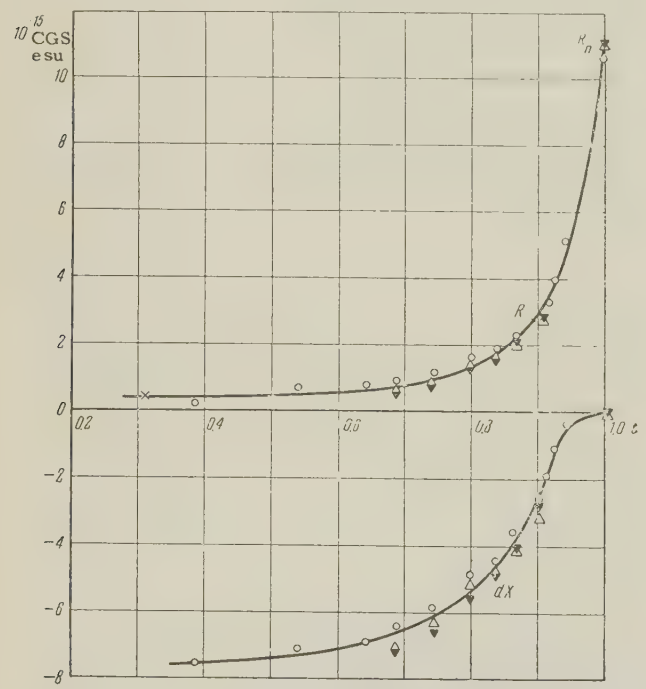

FIG. 4. The surface resistance R and the changes in the surface reactance dX of cadmium as a function of the relative temperature $t = T/T_c$ ($T_c = 0.56$°K). The three types of symbols represent three series of measurements.

THE MEASUREMENTS

The change Δf in the width of the frequency band of the resonator and the shift df in its resonant frequency were measured experimentally during the transition of the sample from the superconducting to the normal state (and back). These quantities determine the resistance R of the sample and the change dX in its reactance:

$$R = 2\pi K \Delta f; \quad dX = -4\pi K df.$$

The quantity $K = 4.7 \times 10^{-9}$ H was calculated from the dimensions of the resonator and from the type of oscillations excited in it; it was verified experimentally (to an accuracy of ~10%) by measuring the width of the frequency characteristic of the resonator at room temperature. At helium temperatures, the width of the frequency characteristic of the resonator with the cadmium sample in its normal condition was equal to 845 kc. Of these, 495 kc are due to losses in the copper walls and to losses by radiation in the coupling apertures, and 350 kc are caused by losses in the sample (accuracy ±5 kc). Figure 4 shows the results of measurements of the surface impedance of a sample of single crystal cadmium.

The "residual" resistance R_S of the superconducting sample at temperatures much below critical is quite small and its value, determined from the width of the frequency characteristic of the resonator, becomes quite inaccurate. For this reason R_S must be determined from the rf heating of the sample as mentioned above, by replacing the hf heating with the power dissipated in the heater 15. In practice, however, it is more convenient and accurate to measure the ratio of R_S to the resistance of the sample in the normal state R_n:

$$R_s / R_n = \Delta f_n W_s / \Delta f_s W_n,$$

where Δf_S and Δf_n are the widths of the resonator frequency characteristics with the superconducting and the normal sample, respectively, and W_S and W_n denote the power dissipated by the hf current in the superconducting and the normal sample. This ratio is equal to 2 ± 0.5% (Fig. 4, the cross on the R curve) for cadmium at ~0.15°K. During these measurements it is necessary to maintain constant the power from the generator (klystron) to the line that excites the resonator, and the power transfer efficiency, which should be small compared to unity.

The dc conductivity of the sample is determined during the high-frequency investigations by measurements with a tuned photoamplifier[7] at 4.64 cps. It is thus possible to check any differences in the critical temperature for transitions to the superconducting state under dc condictions and at high frequencies.[1,6] No such difference was found in the experiments described here (to an accuracy

*The circuit was developed together with I. I. Losev.

of ~0.003°K).

RESULTS

By measuring the surface resistance of a superconductor it is possible to determine the dielectric constant ϵ and the ratio of the conductivity of the normal electrons to their mean free path σ/l.[8-10] The two terms which appear in the expression

$$\varepsilon = \varepsilon_0 - c^2/\omega^2\delta^2, \qquad (1)$$

can be separated if the results of independent measurements at different frequencies ω are known, or, in particular, if the depth of penetration δ of a weak static magnetic field into the superconductor is known. After measuring ϵ at one frequency ω, one can either calculate δ, assuming $\epsilon_0 \ll c^2/\omega^2\delta^2$, or one can try to separate the terms containing ϵ_0 and δ by making use of additional considerations, e.g., the law governing the variation of δ with the temperature T.

Figure 5 shows the variation of ϵ with the relative temperature $t = T/T_c$ ($T_c = 0.56$°K is the critical temperature of cadmium), obtained from an analysis of the measurements of the complex surface impedance of cadmium in accordance with Abrikosov's equations.[9] The application of Ginzburg's[8] equations leads to practically the same results. The points lie a few percent higher but still within the possible error of the measurements.

As can be seen from Fig. 5, the variation $\epsilon(t)$ in the region $0.3 < t < 1$ can be expressed by the simple empirical law:

$$-\varepsilon = 14.4\,(1 - t^4)\cdot 10^8 \text{ CGS electrostatic units.} \qquad (2)$$

The value of δ, calculated from the equation

$$\delta = c/\omega\sqrt{-\varepsilon} \qquad (3)$$

assuming that $\epsilon_0 \ll c^2/\omega^2\delta^2$, leads to the expression

$$\delta = 13.4\,(1 - t^4)^{-1/2}\cdot 10^{-6} \text{ cm}, \qquad (4)$$

which has the form of the usually[11,12] obtained relationship

$$\delta = \text{const}\,(1 - t^4)^{-1/2}. \qquad (5)$$

The accuracy of determination of δ is about 10%.

By estimating the limiting value for δ at $T = 0$ as $\delta_0 = (13.4 \pm 1.4) \times 10^{-6}$ cm, we can calculate for cadmium the parameter κ of the theory of Ginzburg and Landau:[13]

$$\kappa = 2.16\cdot 10^7 H_c\delta_0^2 = 0.11 \pm 0.02,$$

where $H_c = 28.8$ oersteds is the critical magnetic field for cadmium.[14] The value obtained for κ is

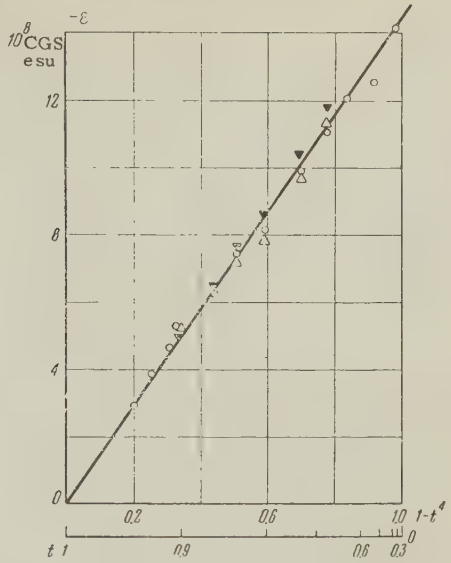

FIG. 5. Variation of the dielectric constant of superconducting cadmium with the relative temperature t. The three types of symbols represent three series of measurements.

in good agreement with theoretical considerations (for "soft" superconductors, $\kappa < 1/\sqrt{2}$).

By investigating the variation of the critical field of small cadmium spheres with their dimensions, Steele and Hein[15] obtained $\delta_0 = (9 \text{ to } 11) \times 10^{-4}$ cm. This value for δ_0 is far too high. This is particularly clear on calculating κ from it (~600!). The result of Steele and Hein is apparently incorrect, though it is difficult to show the reason for their mistake.

The ratio of the conductivity produced by normal electrons to their mean free path σ/l may be found from the complex surface impedance of the superconductor $Z = R + iX$:

$$\sigma/l = \text{const}\,(1 + \eta)\,X^3/|Z|^6, \qquad (6)$$

where the parameter $-1 \le \eta \le +3$ depends on the ratio R/X. (The surface reactance X of the superconductor is calculated from the equation $X = X_n - dX$, where dX is the experimentally-measured change in the surface reactance of the metal at the transition from the normal to the superconducting state, and the surface reactance X_n of the normal metal is determined from the relationship $X_n = R_n\sqrt{3}$, according to the theory of the anomalous skin effect.[16])

The results of the calculation of σ/l from Eq. 6 are shown in Fig. 6; the curve is drawn through the experimental points approximately. The large scatter of the points may be explained by the fact that the quantities X and R, measured to an accuracy of 3 to 5%, appear in Eq. 6 with high powers. This causes an almost tenfold increase in the

relative error in the calculation of $(\sigma/l)_S$ for the superconductor.

The value of $(\sigma/l)_0$ for the normal metal is determined to an accuracy of about 10%. Knowing $(\sigma/l)_0$ and the conductivity σ, one can estimate the mean free path in the normal metal: $l \sim 0.1$ mm.

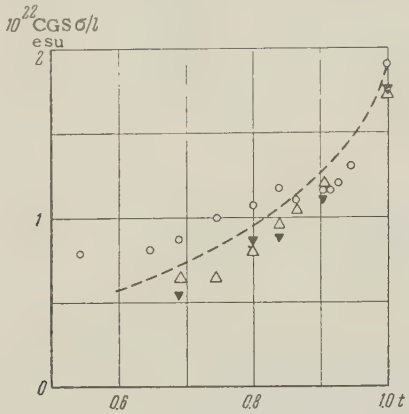

FIG. 6. Variation of the ratio of the conductivity produced by normal electrons to their mean free path with the relative temperature t. The curve has been drawn approximately through the experimental points. The three types of symbols represent three series of measurements.

The experimentally found variation of σ/l with temperature is not in disagreement (Fig. 7) with the law:

$$1 - [(\sigma/l)_s/(\sigma/l)_0] = C(1 - t^4). \qquad (7)$$

A more positive verification cannot be given because of the above-mentioned insufficient accuracy of the results. For cadmium we obtain $C = 0.85 \pm 0.2$. Analogous experiments on tin give $C = 1.0 \pm 0.2$. A formula in the form of Eq. 7 can be obtained by making the following assumptions. We assume that the equation

$$n_0 = n_n + kn_s, \qquad (8)$$

is correct, which establishes the relationship between the two electron densities: n_0 — normal electrons in the normal metal; n_n and n_s — normal and superconducting electrons in the superconductor. The coefficient k does not depend on temperature. Rewriting Eq. 8 with the use of the formulae

$$n_0 = \frac{mv_0}{e^2}(\sigma/l)_0; \quad n_s = \frac{m\omega^2}{4\pi e^2}\varepsilon,$$

and also assuming that the mean free path of normal electrons is the same in the normal metal and in the superconductor, we obtain

$$1 - \frac{(\sigma/l)_s}{(\sigma/l)_0} = \frac{kn_s}{n_0} = \frac{k\omega^2}{4\pi v_0}\frac{\varepsilon}{(\sigma/l)_0}, \qquad (9)$$

where $v_0 = (1 \text{ to } 2) \times 10^8$ cm/sec is the Fermi velocity of the normal electrons (the effective masses of the normal and of the superconducting electrons are assumed to be equal).

Substituting the experimentally found values for ϵ and $(\sigma/l)_0$ in Eq. 9 and comparing with Eq. 7 we obtain k = 5 to 10 for cadmium. For tin we obtain k = 4 to 8, which is in agreement with the known data.[11] Thus for cadmium, as well as for tin and several other sufficiently investigated metals, it is not permissible to assume k = 1 when using Eq. 8.

The surface resistance of cadmium in the normal state is $R_n = (11 \pm 1) \times 10^{-15}$ esu. This is appreciably larger than the result of Chambers,[17] who obtained for polycrystalline cadmium $R_n = (7.7 \pm 0.3) \times 10^{-15}$ esu. Because of this, the corresponding values of $(\sigma/l)_0$ calculated from Eq. 6 differ by a factor of about 3. The discrepancy may be due to a strong anisotropy of the surface resistance of cadmium. Such an assumption, however, requires experimental verification.

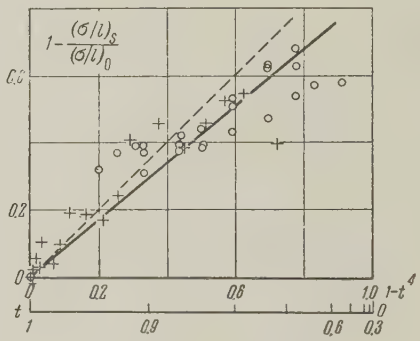

FIG. 7. The full line and the circles refer to measurements on cadmium, the dotted line and the crosses to measurements on tin.

Analyzing the measured surface resistances of different superconductors (Hg, Sn, Al, Zn, In) made at high frequencies (1200 to 36,000 Mc), Faber and Pippard[5] found that a plot of $\log(2 \times 10^5\, G_1/T_c)$ and $\log G_2$ vs. $\log(\omega/T_c)$ is a straight line of slope $\frac{2}{3}$ (reference 5, Fig. 5). These quantities characterize the slope of the curve R(T) close to T_c and far away from T_c, respectively. Evaluation of the measurements of R(T) for cadmium (Fig. 4) leads to values of $G_1 = 11 \times 10^{-5}$ and $G_2 = 30$, which lie well on the extension of the straight line in Fig. 5 of the paper by Faber and Pippard.[5] Owing to the low critical temperature of cadmium, the points of this figure, observed by investigating cadmium at a frequency of 9400 Mc, lie at higher ω/T_c values than all other measurements made in that work.[5]

CONCLUSIONS

A method has been developed for measuring the

complex surface impedance of superconductors in the temperature region down to $\sim 0.1°K$, obtainable by demagnetization of paramagnetic salts. By investigating superconductors with low critical temperatures it is possible to obtain values of the parameter $h\nu/kT_c$ several times larger than when working in the region of helium temperatures (1 to 4°K) at the same frequencies.

The complex impedance of a single crystal of superconducting cadmium has been measured. The temperature dependence has been obtained for (a) the depth of penetration of an electromagnetic field into superconducting cadmium, and (b) the ratio of the conductivity produced by normal electrons to their mean free path. In analyzing the second quantity, measurements of the surface resistance of tin have also been utilized.

The author takes the opportunity to thank P. L. Kapitza for his interest in the work, A. I. Shal'nikov for his continuous interest and valuable advice, and also G. S. Chernyshev and I. I. Losev for technical help.

[1] Blevins, Gordy, and Fairbank, Phys. Rev. **100**, 1215 (1955).

[2] E. Fawcett, Proc. Roy. Soc. **A232**, 519 (1955).

[3] Bezuglyi, Galkin, and Levin, Dokl. Akad. Nauk SSSR **105**, 683 (1955).

[4] A. A. Galkin and P. A. Bezuglyi, Dokl. Akad. Nauk SSSR **97**, 217 (1954).

[5] T. E. Faber and A. B. Pippard, Proc. Roy. Soc. **A231**, 336 (1955).

[6] Biondi, Garfunkel, and McCoubrey, Phys. Rev. **101**, 1427 (1956).

[7] Iu. V. Sharvin, J. Exptl. Theoret. Phys. (U.S.S.R.) **22**, 367 (1952).

[8] V. L. Ginzburg, J. Exptl. Theoret. Phys. (U.S.S.R.) **29**, 748 (1955). Soviet Phys. JETP **2**, 589 (1956).

[9] A. A. Abrikosov, Dokl. Akad. Nauk SSSR **86**, 43 (1952).

[10] M. S. Khaikin, Dokl. Akad. Nauk SSSR **86**, 517 (1952).

[11] D. D. Schoenberg, Superconductivity, IIL, 1955.

[12] A. B. Pippard, Proc. Roy. Soc. **A203**, 98 (1950).

[13] V. L. Ginzburg and L. D. Landau, J. Exptl. Theoret. Phys. (U.S.S.R.) **20**, 1064 (1950).

[14] B. B. Goodman and E. Mendoza, Phil. Mag. **42**, 594 (1951).

[15] M. C. Steele and R. A. Hein, Phys. Rev. **105**, 877 (1957).

[16] G. E. H. Reuter and E. H. Sondheimer, Proc. Roy. Soc. **A195**, 336 (1948).

[17] R. G. Chambers, Proc. Roy. Soc. **A215**, 481 (1952).

Translated by P. F. Schmidt
287

IONIZATION OF MOLECULAR HYDROGEN BY H^+, H_2^+, *AND* H_3^+ *IONS*

V. V. AFROSIMOV, R. N. IL'IN, and N. V. FEDORENKO

Leningrad Physico-Technical Institute, Academy of Sciences, U.S.S.R.

Submitted to JETP editor January 8, 1958

J. Exptl. Theoret. Phys. (U.S.S.R.) 34, 1398-1405 (June, 1958)

We have studied the composition of the secondary ions produced by single collisions between H_2 molecules and primary H^+, H_2^+, and H_3^+ ions with energies from 5 to 180 kev. The total cross sections were determined: σ_0, for electron capture by the primary ions, σ_-, for the formation of free electrons, and $\sigma_{H_2^+}$ and σ_{H^+}, for the formation of H_2^+ ions and protons. σ_{H^+} is considerably smaller than $\sigma_{H_2^+}$ over the entire range of energy investigated. The curves of $\sigma_{H^+}(v)$ for the primary ions H^+ and H_2^+ showed maxima at velocities of 1.7×10^8 cm/sec and 1.9×10^8 cm/sec respectively. The maximum value of σ_{H^+} was about 5×10^{-17} cm^2, approximately 100 times larger than the corresponding cross section for the case of electron bombardment.[1]

INTRODUCTION

THE cross sections for ionization and charge exchange have been calculated theoretically only for the simplest cases, including the (H^+, H) system. A number of authors[2-4] have calculated the cross section for charge exchange in this system, while the cross section for ionization has been calculated by Bates and Griffing.[5] Considerable experimental data, covering a wide range of energy,[6-10], are available on the charge-exchange cross section for the (H^+, H_2) system. However, the cross section for the ionization of hydrogen molecules by hydrogen ions has been determined only for energies below 40 kev.[7,9,11] As to the composition of the secondary ions, we have only the very limited data by Keene.[7]

The aim of the present work was to study the ionization of hydrogen by H^+, H_2^+, and H_3^+ ions, and the distribution of e/m of the secondary ions over the relatively wide energy range from 5 to 180 kev.

Secondary ions can appear during collisions between protons and H_2 molecules as a result of the usual charge exchange, ionization of the molecules to form molecular ions, and dissociation of the molecular ions so formed, resulting in one or two new protons. We shall denote the cross sections for the corresponding processes by the letter σ with the upper indices c, i, and d respectively. The lower indices 01 and 02 will indicate the formation of either one or two positively-charged secondary ions from the hydrogen molecule. In addition, we must allow for possible processes in which the primary proton captures one or two electrons, accompanied by the dissociation of the secondary molecular ion (indices cd and ccd). The process of single-electron capture plus dissociation was first studied by Lindholm,[12] who found that the cross section for this process, as in the usual types of charge exchange, depended strongly on the resonance defect ΔE. The quantity ΔE is in this case the difference between the recombination energy of the primary ion and the vertical dissociation energy of the secondary ion formed by the charge exchange.* The dissociation of H_2 molecules to form protons when bombarded with electrons and fast atomic particles should come about as the result of a transition to the ionized state in accordance with the Franck-Condon principle.

From the interaction potential-energy curves given in Massey and Burhop's monograph[13] for various electronic states of the hydrogen molecule, we have compiled a table of possible processes by which secondary ions might be formed from the (H^+, H_2) system.

The columns of the table list: (1) the serial number provisionally assigned to each process; (2) the formula for the process; (3) the notation for the cross section; (4) the excited state of the molecular ion corresponding to the given process; (5) is the recombination energy (or the energy of formation of a fast H^- ion from a proton) E_i; (6) the ver-

*By "vertical dissociation energy" we mean the energy of a transition, obeying the Franck-Condon principle, for the ground state of the molecule to the ionized state, with subsequent dissociation (See also reference 13).

1	2	3	4	5	6	7	8
№	Process			E_1, ev	E_2, ev	ΔE, ev	ΔT, ev
1	$\underline{H^+} + H_2 \rightarrow \underline{H} + H_2^+$	σ_{01}^c	$^2\Sigma g$	13.6	15.6—18	2—4.4	—
2			$^2\Sigma g$	13.6	18	4.4	0
3	$\underline{H^+} + H_2 \rightarrow \underline{H} + H + H^+$	σ_{01}^{cd}	$^2\Sigma u$	13.6	28—32.5	14.4—18.9	5—7
4	$\underline{H^+} + H_2 \rightarrow \underline{H^+} + H^+{}_2 + e$	σ_{01}^i	$^2\Sigma g$	—	15.6—18	15.6—18	—
5			$^2\Sigma g$	—	18	18	0
6	$\underline{H^+} + H_2 \rightarrow \underline{H^+} + H + H^+ + e$	σ_{01}^d	$^2\Sigma u$	—	28—32.5	28—32.5	5—7
7	$\underline{H^+} + H_2 \rightarrow \underline{H^-} + 2H^+$	σ_{02}^{ccd}	—	14.3	46—50	31.7—35.7	7.5—10
8	$\underline{H^+} + H_2 \rightarrow \underline{H} + 2H^+ + e$	σ_{02}^{cd}	—	13.6	46—50	32.4—36.4	7.5—10
9	$\underline{H^+} + H_2 \rightarrow \underline{H^+} + 2H^+ + 2e$	σ_{02}^d	—	—	46—50	46—50	7.5—10

tical dissociation energy E_2; (7) $\Delta E = E_1 - E_2$, i.e., the energy spent in carrying out the indicated process, which is equal to the resonance defect for processes 1, 2, 3, 7, and 8; (8) is the kinetic energy T acquired by the secondary proton formed during the process as the result of the dissociation of the molecular ion. The symbol for the primary particle is underlined in each formula.

When the primary particle is a molecular ion, the mechanism of secondary-particle formation from H_2 molecules must still be the same as in the case of the (H^+, H_2) system, but since there is a much larger number of possible states for the primary particle, the processes are more numerous and more complex.

1. EXPERIMENTAL PROCEDURE

The apparatus in which the experiments were performed, and the methods employed, are described in detail in our previous papers.[14,15] A beam of primary ions, uniform in composition and energy, was directed into a collision chamber where the pressure was between 1 and 1.5×10^{-4} mm Hg. This low pressure allowed only single collisions between the primary particles and the gas molecules. The pressure in other parts of the apparatus was kept below 5×10^{-6} mm Hg with the aid of differential pumps.

The secondary ions and free electrons produced in the gas were collected on the plates of a measuring capacitor located inside the collision chamber.

The total cross section σ_+ for the formation of secondary ions and the total cross section σ_- for the formation of free electrons were determined from the formulas

$$\sigma_+ = i_+ / i_1 N l, \quad (1)$$

$$\sigma_- = i_- / i_1 N l, \quad (2)$$

where i_+ and i_- are the positive and negative saturation currents at the plates of the measuring capacitor. N is the number of gas molecules per cubic centimeter in the collision chamber, l is the length of the measuring electrodes, and i_1 is the primary ion beam current. Under the conditions of the experiments, the current i_1 was 1×10^{-7} to 1×10^{-6} amp, and the currents i_+ and i_- varied between 5×10^{-10} and 2×10^{-8} amp. The currents were measured by a mirror galvanometer with an ultimate sensitivity of 1.5×10^{-10} amp/division.

In order to analyze the e/m distribution of the secondary ions, a magnetic sector mass-spectrometer was connected to the collision chamber, in a plane perpendicular to the primary beam. The slow secondary ions were accelerated at the entrance to the analyzer, by an electric field. The analyzer was used to determine the ratio

$$\sigma_{H_2^+} / \sigma_{H^+} = \alpha_{H_2^+} / \alpha_{H^+}, \quad (3)$$

where $\alpha_{H_2^+}$ and α_{H^+} are the relative intensities of the H_2^+ and H^+ lines in the secondary ion spectrum, and $\sigma_{H_2^+}$ and σ_{H^+} are the corresponding cross sections for the formation of these secondary ions. The absolute values of the cross sections were determined from the formulas

$$\sigma_{H_2^+} = \sigma_+ \alpha_{H_2^+}, \quad (4)$$

$$\sigma_{H^+} = \sigma_+ \alpha_{H^+}. \quad (5)$$

The ion currents in the analyzer were between 2×10^{-10} and 2×10^{-13} amp, and were measured by an electrometer amplifier with a sensitivity of 2×10^{-14} amp/division.

The cross sections σ_+ and σ_- can be expressed in terms of the cross sections of the individual processes in the following way:

$$\sigma_+ = (\sigma_{01}^c + \sigma_{01}^i) + (\sigma_{01}^{cd} + \sigma_{01}^d) + 2(\sigma_{02}^d + \sigma_{02}^{cd} + \sigma_{02}^{ccd}), \quad (6)$$

$$\sigma_- = \sigma_{01}^i + \sigma_{01}^d + 2\sigma_{02}^d + \sigma_{02}^{cd} + (\sigma_{12}^d + 2\sigma_{13}^d), \quad (7)$$

where the cross section σ_{12}^d accounts for the dis-

sociation of the primary molecular ion, H_2^+ or H_3^+, with emission of an electron, while the cross section σ_{13}^d account also for the dissociation of H_3^+ ion with emission of two electrons. Subtracting (7) from (6) we get

$$\sigma_+ - \sigma_- = \sigma_{01}^c + \sigma_{01}^{cd} + \sigma_{02}^{cd} + 2\sigma_{02}^{ccd} - (\sigma_{12}^d + 2\sigma_{13}^d). \quad (8)$$

The first three terms on the right-hand side of Eq. (8) comprise the total cross section for the capture of one electron by a primary ion:

$$\sigma_0 = \sigma_{01}^c + \sigma_{01}^{cd} + \sigma_{02}^{cd}. \quad (9)$$

Since, according to the data given in reference 9, $\sigma_{02}^{ccd} \ll \sigma_+ - \sigma_-$ for protons, the total capture cross section σ_0 can be determined from the data obtained by the potential method, using the approximate formula

$$\sigma_0 = \sigma_+ - \sigma_-. \quad (10)$$

We have applied Eq. (10) also to the case of H_2^+ and H_3^+ as primary molecular ions, using the analogous approximation. The corrections necessary in this case, which must increase σ_0 slightly, can be introduced only when the cross sections σ_{12}^d and σ_{13}^d can be measured independently.

The cross section for the formation of secondary H_2^+ and H^+ can be expressed in terms of the process cross sections in the following way:

$$\sigma_{H_2^+} = \sigma_{01}^c + \sigma_{01}^i, \quad (11)$$

$$\sigma_{H^+} = \sigma_{01}^{cd} + \sigma_{01}^d + 2(\sigma_{02}^{cd} + \sigma_{02}^d + \sigma_{02}^{ccd}). \quad (12)$$

All the cross sections which we obtained were calculated "per molecule" and are expressed in cm^2. The possible errors in determining the cross sections σ_+, σ_-, $\sigma_{H_2^+}$, and σ_{H^+} are estimated to be ± 12%, equally caused by errors in measuring the current (±6%) and the gas pressure in the collision chamber (±6%). If the cross sections σ_0 are small compared with the corresponding σ_+ and σ_-, their measurement errors are considerably larger.

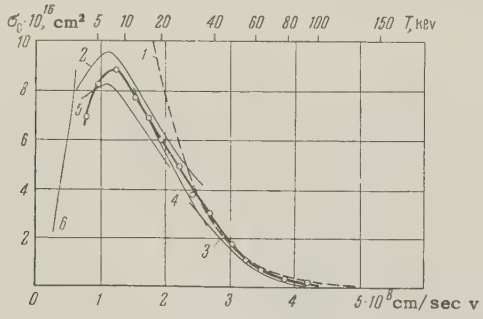

FIG. 1. Total cross section for capture of electrons by protons. o – data of this work, 1 – theoretical curve after Jackson and Schiff.[3] Remaining curves are experimental, after the following: 2 – Keene,[7] 3 – Ribe,[8], 4 – Fogel',[9] 5 and 6 – Stedeford and Hasted.[10]

2. RESULTS OF THE MEASUREMENTS AND DISCUSSION OF THE RESULTS

1. Total Capture Cross Section σ_0.

Figures 1, 2, and 3 show the dependence of σ_0 on v for H^+, H_2^+, and H_3^+ ions respectively.

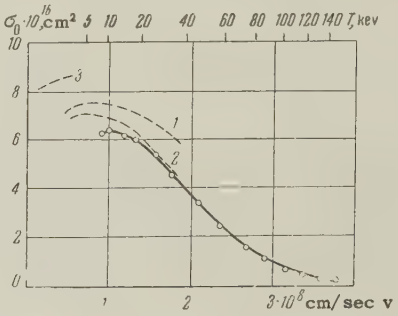

FIG. 2. Total cross section for capture of electrons by H_2^+ ions. o – data of this work. Experimental curves after the following: 1 – Keene,[7] 2 and 3 – Stedeford and Hasted.[10]

Experimental data on charge exchange of protons in molecular hydrogen have also been obtained recently by Keene,[7] Ribe,[8] Forel,[9] and Stedeford and Hasted.[10] In these experimental studies, as in our work, it was really the total capture cross section that was being measured [see Eq. (9)]. All the experimental results, including our own, agree among themselves within the limits of experimental error. The curves of $\sigma_0(v)$ have a maximum at $T \approx 8$ kev, as first observed by Bartels.[6]

Figure 1 also shows the theoretical curve for the charge exchange of protons in atomic hydrogen, from the paper by Jackson and Schiff.[3]* This curve agrees with the experimental results for the (H^+, H_2) system in the velocity range $v > e^2/\hbar$, and gives too high a cross section for $v \leq e^2/\hbar$.

For the (H_2^+, H_2) system (Fig. 2) we show also the data of Keene[7] and Stedeford and Hasted.[10] These agree, within experimental error, with the results of our work. The presence of a maximum in the $\sigma_0(v)$ curve is evidence that the (H_2^+, H_2) system does not exhibit resonance. The electron capture probably occurs in an excited state of the H_2 molecule.

Electron capture by the H_3^+ ion is a complicated process, since there is no known stable state of the H_3 molecule. Apparently the capture of an elec-

*This curve practically coincides with the curves of Bates and Dalgarno[2] and Pradhan.[4] In going from the (H+, H) system to (H+, H_2), the authors of references 2 and 3 double the corresponding cross sections, neglecting the molecular bonds.

tron by a H_3^+ ion leads to dissociation into an H_2 molecule and a hydrogen atom. The $\sigma_0(v)$ curve for H_3^+ ions has a maximum, which is difficult to interpret.

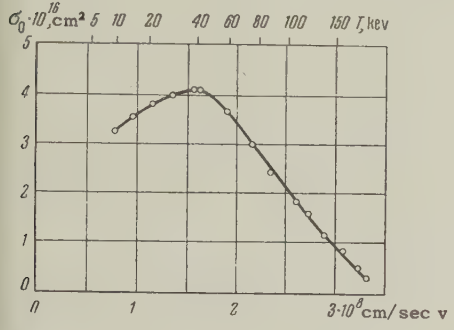

FIG. 3. Total cross section for capture of electrons by H_3^+ ions.

2. Production of Secondary H_2^+ Ions

Figure 4 shows the curves of $\sigma_{H_2}(v)$ which we have obtained by using primary H^+, H_2^+, and H_3^+ ions, and the corresponding curve for electron bombardment from reference 1. It follows from Eq. (11) that $\sigma_{H_2^+}$ is the sum of the cross sections for the usual charge exchange, σ_{01}^c, and for ionization with the emission of an electron, σ_{01}^i. A comparison of Fig. 4 with the curves in Figs. 1 to 3 shows that when the primary ion velocity is less than $e^2/\hbar$, the cross section for ordinary charge exchange is the major component of σ_{H_2}. The $\sigma_{H_2^+}(v)$ and $\sigma_0(v)$ curves are therefore similar in the region where $v < e^2/\hbar$. Conversely, if $v > e^2/\hbar$, the chief contributor to the total cross section σ_{H_2} is the ionization cross section, since $\sigma_0 < 10^{-16}$ cm² for all primary hydrogen ions even when v is as low as 3.5×10^8 cm/sec. From Fig. 4 it can also be seen that, in the region where $v > e^2/\hbar$, the more nuclei in the primary ions, the greater the cross section σ_{H_2}. By our assumption, the ionization processes take place mostly during collisions in which the electron shells of the ion and the molecule interpenetrate. In this case the magnitude of the ionization cross section must depend on the nuclear charge of the primary ion, and also on the number of nuclei if the primary ion is molecular. We have published analogous conclusions[15] concerning the ionization of inert gases by atomic ions.

3. Production of Secondary Protons

Figure 5 shows the curves of $\sigma_{H^+}(v)$ which we have obtained for primary H^+, H_2^+, and H_3^+ ions, and the corresponding curve for the case of electron bombardment from reference 1. The cross section for the production of secondary protons is considerably smaller, over the whole energy region we investigated, than the cross section for the production of H_2^+ molecular ions. For primary H^+ and H_2^+ ions, the σ_{H^+} curves have a well defined peak that reaches approximately 5×10^{-17} cm². The corresponding maximum cross section for electrons is only approximately 4×10^{-19} (reference 1).

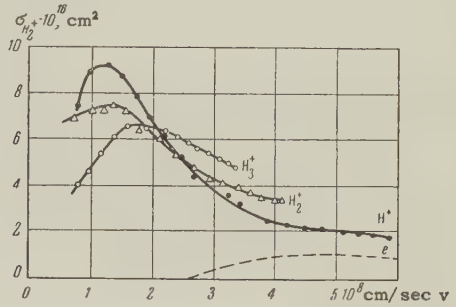

FIG. 4. Cross section for production of secondary H_2^+ ions. Corresponding primaries are marked on the curves. Dotted curve – data of reference 1.

Secondary protons can result from processes 2, 3, and 5 to 9 (cf. table). We believe that the secondary protons are due predominantly to dissociation of molecular hydrogen ions H_2^+, which have been produced by charge exchange and by ionization with electron emission (processes 2, 3, 5, and 6). This assumption is supported by the results we have obtained by studying the kinetic energies of the secondary protons. In this study we have used a special analyzer apparatus (described in an earlier paper[16]) to determine, by means of a retarding electric field, the kinetic energies of secondary ions of various charges and masses, emitted at a specified angle relative to the direction of the primary beam. For primary hydrogen-ion energy of 75 kev, it was found that most secondary protons carried energies less than 7 ev, and that only an insignificant fraction had energies from 7 to 12 ev. This indicates that the cross sections of processes 7, 8, and 9 are small compared

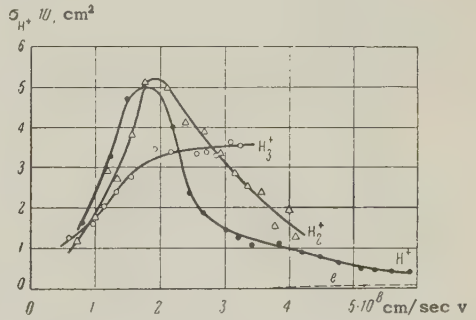

FIG. 5. Cross section for production of secondary protons. Corresponding primaries are marked on the curves. Dotted curve – data of reference 1.

with those of processes 2, 3, 5, and 6. It is interesting that the secondary-proton energy distribution is found to depend little on the angle of proton

travel. This is what can be expected if the energy is acquired by the proton not by direct transfer of momentum from the primary particle, but as a result of the dissociation of a molecular ion H_2^+.

We believe that the maximum in the $\sigma_{H^+}(v)$ curve for H^+ and H_2^+ primaries is due to the dissociation of the molecular ions produced by charge exchange (processes 2 and 3). An argument in favor of this belief is the analogy between the $\sigma_{H^+}(v)$ curves in Fig. 5 and the curves for the total capture cross section in Figs. 1 and 2. It is easy to verify that the curves of $\sigma_{H^+}(v)$ for the primary ions H^+ and H_2^+, like the curves of $\sigma_0(v)$, have maxima in nearly the same position and of approximately the same magnitude. It should be noted that the maxima of the $\sigma_{H^+}(v)$ curves for H^+ and H_2^+ primaries, like the maxima of the usual charge-exchange curves, are located in the region $v < e^2/\hbar$. When the primary ions are H_3^+, the cross section σ_{H^+} for this velocity interval like the cross section σ_0, is considerably smaller than that for the H^+ and H_2^+ ions.

In view of the fact that ΔE is larger for processes 2 and 3 than for usual charge exchange (process 1), the curve $\sigma_{01}^{cd}(v)$ can be expected to have a maximum at a higher velocity than the curve $\sigma_{01}^{c}(v)$. This assumption is confirmed, as can be seen from Figs. 1, 2, and 5.

With increasing energy of primary ions, as pointed out above, ionization with emission of one electron (process 4) begins to play the principal role in the production of secondary molecular ions H_2^+. It is natural to assume that, analogously, the production of secondary protons should become more and more dependent on ionization processes 5 and 6, and then on processes 8 and 9, which involve a relatively large energy loss.

4. Production of Free Electrons

Our analysis of secondary ions by their e/m distribution gives grounds for assuming that when primary protons pass through molecular hydrogen, the greater part of the free electrons is produced simultaneously with the H_2^+ ions. We therefore integrate the cross section σ_- in the same way as the ionization cross section σ_{01}^{i}. In the case of the (H_2^+, H_2) and (H_3^+, H_2) systems, the cross section σ_- contains also a contribution due to the electrons removed from the shells of the primary ions. Figure 6 shows the $\sigma_-(v)$ curves obtained for H^+, H_2^+, and H_3^+ ions, along with the corresponding curve for electron bombardment, taken from reference 1. The curves for H^+ and H_2^+ have a maximum somewhat above $v = e^2/\hbar$. It is easy to verify that the greater the number of protons in the given hydrogen ions, the greater the cross section σ_- (like $\sigma_{H_2^+}$). All the hydrogen ions have a large cross section σ_- even at velocities $v < e^2/\hbar$, where no ionization is observed in the case of electron bombardment.

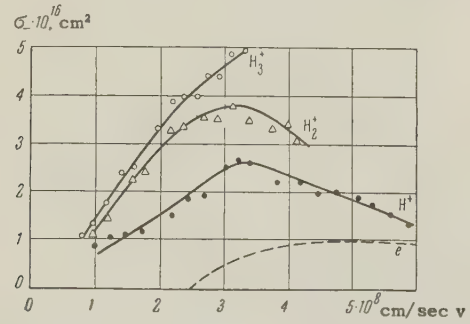

FIG. 6. Total cross section for production of free electrons. Corresponding primaries are marked on the curves. Dotted curve – data of reference 1.

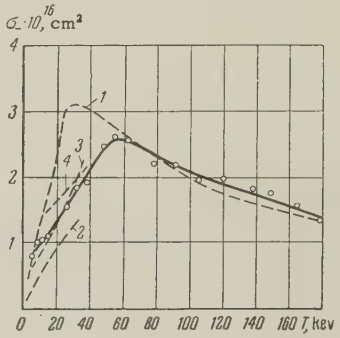

FIG. 7. Total cross section for production of free electrons by protons. o – data of this work. 1 – theoretical curve for ionization of H_2 by protons, calculated from data by Bates and Griffing.[5] Experimental curves after the following: 2 – Keene,[7] 3 – Fogel',[9] 4 – Gilbody and Hasted.[11]

The $\sigma_-(v)$ curve obtained for protons is compared in Fig. 7 with the analogous data from previous experimental investigations[7,9,11] and with the theoretical curve of Bates and Griffing.[5] These authors have calculated the cross section for the ionization of atomic and molecular hydrogen by protons, using the Born approximation. The maximum of the theoretical curve does not agree with ours. Data available from other investigations for the region in which the theoretical curve has a maximum agree better among themselves and with our data than with the theory. It must be noted, however, that the extension of the Born approximation to include the velocity region $v < e^2/\hbar$ does not lead to any discrepancy in the order of magnitude of the cross section. The theoretical curve agrees, within the limits of experimental error, with our data for the upper portion of the investigated interval.

In conclusion, the authors consider it their pleasant duty to express deep gratitude to Prof.

V. M. Dukel' skii and O. B. Firsov for discussion of the work and for useful critical comments.

[1] H. F. Newhall, Phys. Rev. **62**, 11 (1942).
[2] D. R. Bates and A. Dalgarno, Proc. Phys. Soc. **A66**, 972 (1953).
[3] J. D. Jackson and H. Schiff, Phys. Rev. **89**, 359 (1953).
[4] T. Pradhan, Phys. Rev. **105**, 1250 (1957).
[5] D. R. Bates and G. Griffing, Proc. Phys. Soc. **A66**, 961 (1953).
[6] H. Bartels, Ann. Physik **13**, 373 (1932).
[7] J. P. Keene, Phil. Mag. **40**, 369 (1949).
[8] F. L. Ribe, Phys. Rev. **83**, 1217 (1951).
[9] Fogel', Krupnik, and Safonov, J. Exptl. Theoret. Phys. (U.S.S.R.) **28**, 589 (1955), Soviet Phys. JETP **1**, 415 (1955).
[10] J. B. H. Stedeford and J. B. Hasted, Proc. Roy. Soc. **A227**, 466 (1955).
[11] H. B. Golbody and J. B. Hasted, Proc. Roy. Soc. **A240**, 382 (1957).
[12] E. Lindholm, Proc. Phys. Soc. **A66**, 1068 (1953).
[13] H. S. W. Massey and E. H. S. Burhop, Electronic and Ionic Impact Phenomena, Oxford, 1952.
[14] Fedorenko, Afrosimov, and Kaminker, J. Tech. Phys. (U.S.S.R.) **26** 1929 (1956), Soviet Phys. JTP **1**, 1861 (1956).
[15] N. V. Fedorenko and V. V. Afrosimov, J. Tech. Phys. (U.S.S.R.) **26**, 1941 (1956), Soviet Phys. JTP **1**, 1872 (1956).
[16] V. V. Afrosimov and N. V. Fedorenko, J. Tech. Phys. (U.S.S.R.) **27**, 2557 (1957), Soviet Phys. JTP **2**, 2378 (1957).

Translated by J. G. Adashko
288

SOVIET PHYSICS JETP VOLUME 34(7), NUMBER 6 DECEMBER, 1958

SOME PHOTOREACTIONS ON LIGHT NUCLEI

V. N. MAIKOV

P. N. Lebedev Physics Institute, Academy of Sciences, U.S.S.R.

Submitted to JETP editor January 8, 1958

J. Exptl. Theoret. Phys. (U.S.S.R.) **34**, 1406-1419 (June, 1958)

The reactions $C^{12}(\gamma, 3\alpha)$, $O^{16}(\gamma, 4\alpha)$; $(\gamma, p\alpha)$ on C^{12}, N^{14}, and O^{16}; and $C^{12}(\gamma, pt)2\alpha$ were investigated with photographic emulsions. The dependence of the γ-ray energy on the reaction cross section and the energy and angular characteristics of the disintegration products were obtained. The contribution of the reactions $C^{12}(\gamma, p\alpha)Li^7$ and $C^{12}(\gamma, pt)2\alpha$ to the total cross section for star production in the photon energy region from 30 to 80 Mev is estimated. Some possible mechanisms for the $(\gamma, p\alpha)$ processes are discussed.

THE interaction of photons with light nuclei, leading to the emission of three or more particles, has been little investigated in the region of γ-ray energy above 30 Mev. Yet observation of stars in photographic emulsions[1,2] shows that similar "complex" reactions give, with increased γ-ray energy a substantial contribution to the total photon-absorption cross section. Investigation of such processes can, therefore, furnish information about the interaction of γ-rays with light nuclei, which becomes substantial at high energies.

In the present work we consider several types of photonuclear reactions in C^{12}, N^{14} and O^{16}. The method of photographic emulsions we used, making it possible to register charged disintegration products. The work was carried out with type Ia-2 NIKFI plates 500 μ thick, in which tracks of singly- and multiply-charged particles could be separated without difficulty. The experimental conditions were the same in the study of all reactions. Emulsions were irradiated by a bremsstrahlung beam from the synchrotron target at maximum energies

of 150 and 250 Mev at an angle of 90° to the direction of the γ-rays. Electrons were removed from the beam by a magnetic field of strength 7000 oersteds. During irradiation, the plates were shielded from scattered radiation by carbon blocks. A graphite ionization chamber directly behind the plates measured the γ-ray beam going through the emulsions.

I. ALPHA-PARTICLE REACTIONS ON CARBON AND OXYGEN

Much work has been devoted to the study of the photodisintegration of carbon into three α-particles

$$C^{12} + \gamma \rightarrow 3He^4 - 7.28 \text{ Mev} \qquad (I)$$

and of oxygen into four α-particles

$$O^{16} + \gamma \rightarrow 4He^4 - 14.4 \text{ Mev} \qquad (II)$$

Experiments were carried out both with Li radiation and with bremsstrahlung at maximum energies ~30 and 70 Mev. At present it can be considered established that the reaction (I) goes, in the region of energy studied up to ~40 Mev, mainly through different excited intermediate states of the Be^8 nuclide. Analysis of reaction (II) is more difficult.

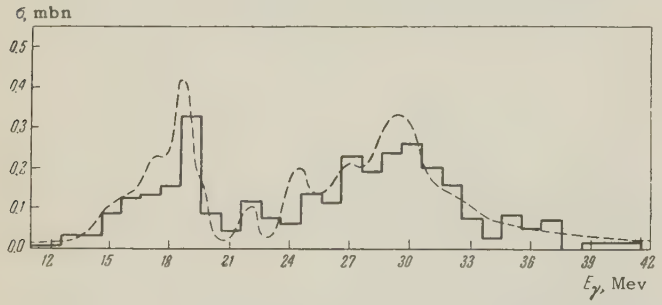

FIG. 1. Dependence of the cross section for reaction (I) on γ-ray energy. The solid line gives our data, the dashed one the data of reference 3.

However, there is reason to believe that intermediate states of C^{12} and Be^8 take part in the process.

In experiments on the synchrotron with maximum energy 70 Mev,[3,4] the reactions (I) and (II) were observed right up to photon energies ~45 Mev. Even prior to publication of these results in 1951, an attempt to observe reactions (I) and (II) at higher energies was made in our laboratory (thesis project by Iu. V. Nikol'skii). Photoemulsions were irradiated on the Physics Institute synchrotron at a maximum energy of 250 Mev. Although no noticeable yield from these reactions was observed above 45 Mev, the statistical accuracy in this experiment was not high. Somewhat later, an experiment with maximum energies 150 and 250 Mev was set up. However, as previously, the reactions $C^{12}(\gamma, 3\alpha)$ and $O^{16}(\gamma, 4\alpha)$ were observed only in the photon energy region up to ~45 Mev. The results of the experiment are given below.

In the photographic emulsions, three- and four-pronged stars were selected, all tracks of which, according to visual determination, belonged to α-particles. The laws of conservation of energy and momentum were used to distinguish between reactions (I) and (II). As criteria of the fulfilment of these laws we introduced the quantities

$$\Delta p = |\Delta \mathbf{p}| = \left| \mathbf{P}_\gamma - \sum_i \mathbf{P}_i \right|$$

and

$$(\Delta p)_{xy} = |(\Delta \mathbf{p})_{xy}| = \left| \sum_i (\mathbf{P}_i)_{xy} \right|,$$

where $\mathbf{P}_i$ is the momentum of the α-particle, determined from the relation $P_i = \sqrt{2M_iE_i}$, with the proton mass taken to be unity; $E_\gamma = \sum_i E_i + E_Q$, $P_\gamma = E_\gamma/30.6$ are the energy and momentum of the photon responsible for the disintegration; E_Q is the binding energy; $(P_i)_{xy}$ is the projection of the α-particle momentum on the xy plane, perpendicular to the direction of the γ-ray. One can show that the spread in values of Δp and $(\Delta p)_{xy}$ produced by exclusively experimental errors should follow the Maxwellian distributions $(\Delta p)^2 \times \exp\{-h^2(\Delta p)^2\}$ and $(\Delta p)_{xy} \exp\{-h^2(\Delta p)^2_{xy}\}$ respectively.

Values of Δp and $(\Delta p)_{xy}$ were calculated for each three-pronged star. Their distributions were quite close to the expected distribution law. An analogous result was obtained for four-pronged stars. In addition, each case displayed a "tail" for large values of Δp, due apparently to an admixture of extraneous reactions. The distributions were cut off at $\Delta p = 1.8$ and $(\Delta p)_{xy} = 1.3$, corresponding to 98% of the areas under the curves.

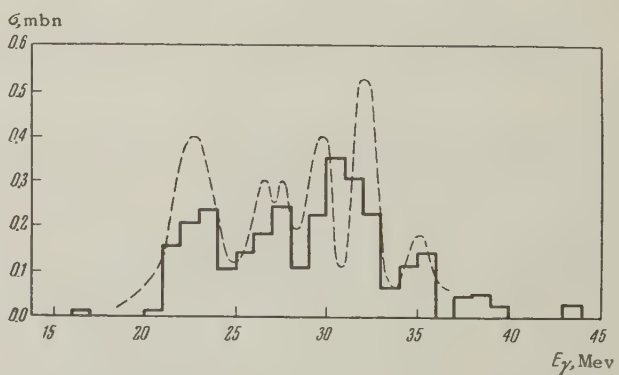

FIG. 2. Dependence of the cross section for reaction (II) on the γ-ray energy. The solid curve gives our data, the dashed one the data of reference 4.

In the analysis of the momentum balance 340 stars were employed for reaction (I) and 180 stars for reaction (II).

The cross sections for reactions (I) and (II) are given, as functions of photon energy, in Figs. 1 and 2. Experimental data obtained by irradiation at maximum energies of 150 and 250 Mev were grouped together, since no difference was observed in the cross-section behavior in these two cases. In spite of the high maximum energy of the spectrum not a single case with γ-ray energy > 50 Mev was observed. The dependence of the cross section for reactions (I) and (II) on the obtained photon energy agreed satisfactorily with the results of references 3 and 4. The sharp drop in the cross section of the studied reactions in the high-energy region is seemingly connected with the competition of various processes entailing a more complete break-up of the nucleus. Thus, the $(\gamma, p\alpha)$ reaction cross sections in carbon and oxygen, with higher thresholds, have maxima in the region ~ 35 Mev.

II. $(\gamma, p\alpha)$-REACTIONS IN C^{12}, N^{14} AND O^{16}

Another typical photonuclear reaction in C^{12}, N^{14} and O^{16} was investigated in the same emulsions:

$$C^{12} + \gamma \rightarrow H^1 + He^4 + Li^7 - 24.6 \text{ Mev}, \quad \text{(III)}$$
$$N^{14} + \gamma \rightarrow H^1 + He^4 + Be^9 - 18.3 \text{ Mev}, \quad \text{(IV)}$$
$$O^{16} + \gamma \rightarrow H^1 + He^4 + B^{11} - 23.1 \text{ Mev}. \quad \text{(V)}$$

Up to the present there has been no information about the mechanism of such a process.

1. Separation of the Reactions

A quantitative method of separating the reactions (III), (IV) and (V) was described in reference 5, where the experimental range-energy relations for Li^7, Be^9 and B^{11} nuclei in emulsion were obtained. Using these, it is possible to carry out a quantitative separation of stars with respect to reaction, using the laws of conservation of energy and momentum. In each case of disintegration, three values of Δp corresponding to the three reactions were calculated, leaving out of consideration the qualitative separation already carried out. Each of the stars was related to that reaction for which the following conditions were satisfied:

$$\left.\begin{aligned} \Delta p &\leqslant 1.8 \\ (\Delta p)_{xy} &\leqslant 1.3 \end{aligned}\right\} \text{ in the case } R_0 > 3\mu.$$

If these criteria were satisfied at the same time by two "neighboring" reactions, then the star was related to that reaction for which Δp had a minimum value. In the case where the recoil of the nucleus is $R_0 < 3\mu$, the distributions of Δp for two "neighboring" reactions begin to overlap all the more, since the distances between the range-energy curves become comparable with the errors in the measurement of the ranges. In this case, the character of the disintegration cannot be determined with sufficient reliability for all stars. The following (not quite rigorous) criteria were employed

$$\left.\begin{aligned} &\Delta p \text{ — minimal} \\ &(\Delta p)_{xy} \leqslant 1.3 \end{aligned}\right\} \text{ in the case } R_0 < 3\mu.$$

In spite of the insufficient accuracy of this condition, it may, however, be considered that reactions (III) and (V) were separated correctly in 70 to 80% of the cases (in the region $R_0 < 3\mu$) if the Gaussian character of the distribution of range errors is taken into account.

In 20% of the cases, the track of the singly charged particle went out of the emulsion. Application of the conservation laws to these stars made it possible to separate them with respect to reaction and to define the energies of these particles, assuming that the tracks were produced by protons. As a check on the correctness of the assumption, the energies of the particles going out were determined by counting grains, and the values obtained were compared with the energies determined by the conservation laws. Within the limits of experimental error, the same proton energies were obtained by these two independent means.

As a result of the analysis carried out, 1088 stars were sorted out as listed below:*

Reaction	(III)	(IV)	(V)
Number of stars	545	197	346

In the work of reference 6, the same reactions were considered and separated by an analogous method. However, the yield of reaction (V) turned out to be insignificant compared with (III) and (IV). This fact contradicts our results, and seems doubtful, since the oxygen content of Ilford emulsions is twice that of nitrogen. The small relative yield of reaction (V) was due, it would seem, to the fact that in the theoretical curves for Be and B were used to separate the reactions (IV) and (V). As already noted,[5] in the region of small energies these curves are not in agreement with experiment and their use can lead to an increase in the number of cases of reaction (IV) and a decrease in those of (V).

*A supplementary analysis of these stars showed that the possible admixture of several alternative reactions $(\gamma, d\alpha)$, (γ, pHe^3), giving stars of the same type, did not exceed ~ 5% in the case of reaction (III) and ~ 10% in the case of reactions (IV) and (V).

TABLE I. Integral cross sections for reactions (III) and (V) in mbn-Mev

E_γ, Mev	25—40	40—55	55—70	70—85
(III)	3.85±0.20	1.78±0.17	0.82±0.13	0.38±0.11
(V)	3.11±0.21	1.64±0.18	0.64±0.14	0.16±0.08

2. Experimental Results

The photographic method made it possible to determine all basic properties of the reaction products. In our experiment the energy of the particle was determined by the range, using the dependence $E = f(R)$. The error in measuring the length of short tracks (α-particles and recoil nuclei) comprised $\sim 0.5\,\mu$. In the case where the track of the proton left the emulsion, the energy of the particle was determined from the conditions of conservation of momentum in the reaction. Here the error in the energy depended to large degree on the form of the star, but did not exceed 15%. The energy of the photon in each case of disintegration was determined from the relation $E_\gamma = \sum_i E_i + E_Q$, where E_i is the kinetic energy of the particle and E_Q is the binding energy. In the case of tracks remaining in the emulsion, the error in determination of E_γ constituted ~ 1 Mev.

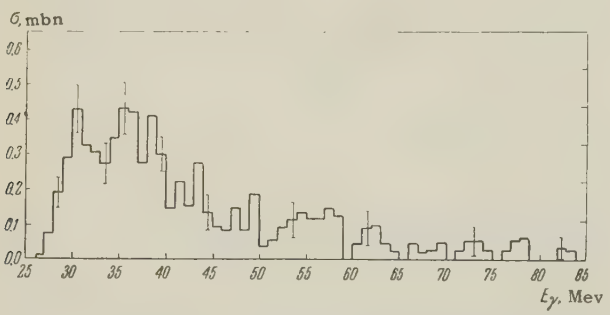

FIG. 3. Dependence of the cross section for reaction (III) on γ-ray energy.

Figure 3 shows the dependence of the cross section of process (III) on γ-ray energy. Integral cross sections for various energy ranges are given in Table I. In our work the cross section for reaction (III) in the range of photon energies from 25 to 40 Mev was found to be 2.9 times larger than in reference 6. The reasons for this large discrepancy are not clear. We note only that in our experiment the statistics were approximately 5 times larger than in the work cited.

The energy distributions of protons and α-particles are given in Fig. 4. In the proton spectrum, a high energy "tail" ($E_p > 15$ Mev, 16%) was observed. Stars in which $E_p > 15$ Mev arose

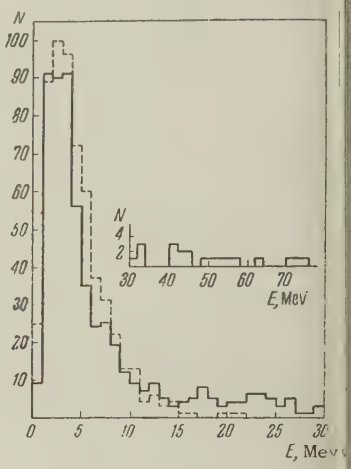

FIG. 4. Energy distributions: solid lines – protons, dashed lines – α-particles from reaction (III).

mainly (75%) from photons with energy > 45 Mev. In this case the protons carried, on the average, $\sim 75\%$ of the energy $E_0 = E_\gamma - E_Q$.

The angular distributions of protons and α-particles showed a noticeable anisotropy relative to the direction of the γ-rays in the carbon c.m. system. For protons, in addition, a displacement of the maximum into the forward hemisphere was observed.

The cross section for reaction (V) as a function of γ-ray energy is shown in Fig. 6, and the integral cross sections are listed in Table I. The energy distributions of protons, α-particles, and the nuclide B^{11} have the same character as the analogous distributions in the case of reaction (III). A great similarity is also observed in the angular characteristics.

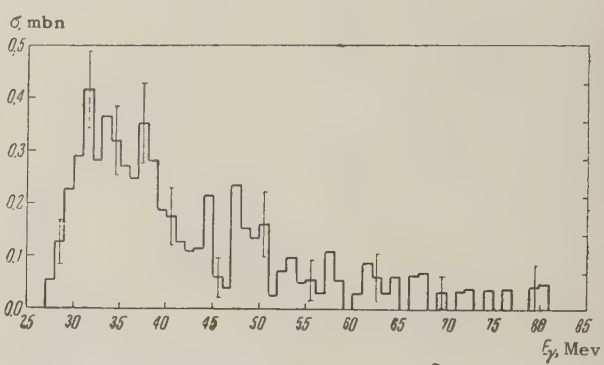

FIG. 5. Dependence of the cross section for reaction (V) on γ-ray energy.

In Fig. 5 the dependence of the yield of reaction (IV) on the γ-ray energy is given. The integral

cross section of the reaction in the region E_γ = 30 to 80 Mev was 7.35 ± 0.56 mb-Mev.

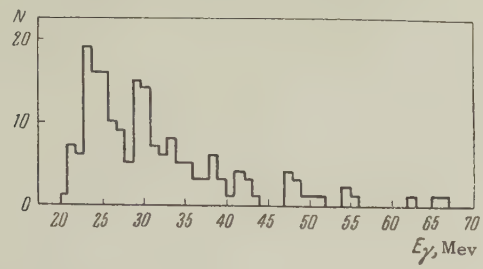

FIG. 6. Dependence of the yield for reaction (IV) on γ-ray energy.

3. Analysis of Experimental Data and Discussion of the Results

The similarity of basic characteristics of the reactions (III) and (V) noted above is apparently not accidental, since the initial nuclei have a number of common characteristics, and the reactions considered are of the same type and occur in the same region of γ-ray energy. It might be expected, therefore, that the mechanisms of interaction of the photon with the nuclei C^{12} and O^{16}, which lead respectively to reactions (III) and (V), are the same. At present, there is no concrete theoretical representation of the process of this "complete" breakup. We shall try, therefore, within the experimental framework, to clarify the most characteristic features of the process.

We consider how the energy of the photon that produces the disintegration is distributed among the products of the reaction in different intervals of the γ-ray energy. We shall compare the energy distributions of the particles with those calculated under the assumption of a symmetrical distribution of the energy among the products of the disintegration. The latter do not depend on the nature of the initial interaction. It will be assumed that there is no interaction between particles in the final state, and the distributions will be determined only by the corresponding volume in phase space. The energy distribution of the particles has in this case the form

$$P(E)\,dE \sim E^{1/2}(E_m - E)^{1/2}\,dE \qquad (1)$$

and the mean value of the energy is

$$\bar{E} = {}^1/_2 E_m, \qquad (2)$$

where $E_m = E_0(A-M)/A$ is the maximum possible energy of a particle of mass M; $E_0 = E_\gamma - E_Q$ is the energy distributed among the reaction products; A and M are the masses of the initial nucleus and studied particle, respectively. The diagram in Fig. 7 shows the mean values of the proton

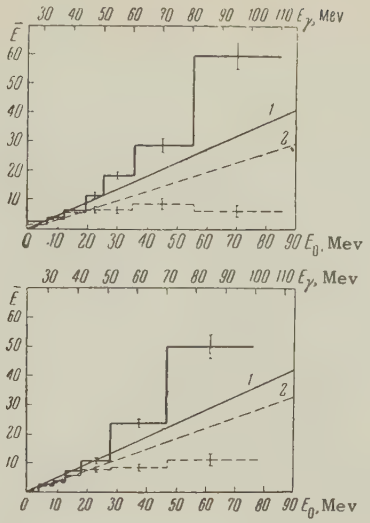

FIG. 7. Dependence of the mean energy: solid line – protons, dashed line – α-particles, plotted against energies E_0 and E_γ, in the case of reactions: (III) above and (V) below; 1 and 2 are the theoretical distributions corresponding to Eq. (2).

energies (solid line) and α-particle energies (dashed line) for different intervals in E_0 (and E_γ) for reactions (III) and (V). The experimental results are compared with the data calculated from Eq. (2). As can be seen from the figure, there is satisfactory agreement, in both cases, in the region of photon energies up to ~50 Mev. Above this energy we observe a progressive deviation from the theory. In view of the insufficient statistics, we shall consider the energetic and angular characteristics of the reaction products separately for two intervals of photon energy: $E_\gamma <$ 50 Mev and $E_\gamma >$ 50 Mev (the choice of these intervals is arbitrary).

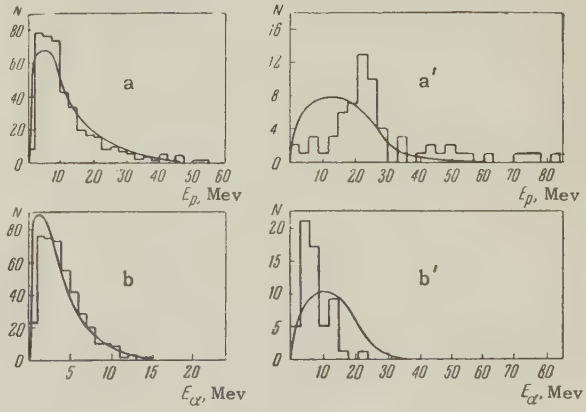

FIG. 8. Energy distributions: a, a' – protons; b, b' – α-particles from reaction (III) in two intervals of photon energy: a, b – $E_\gamma <$ 50 Mev, aand a', b' – $E_\gamma >$ 50 Mev. The smooth curve gives the distribution (1).

Figure 8 shows the energy distributions of protons and α-particles from reaction (III) for these two intervals of γ-ray energy. The smooth curve

shows the distribution (1) with account of the dependence of the particle yield on the photon energy. Although the agreement might be considered satisfactory, for cases a and b, for $E_\gamma > 50$ Mev the form of the energy spectrum differs markedly from the theoretical curve. The energy spectrum of protons from oxygen has the same character.

We consider further the experimental results from the point of view of possible interaction of the particles in final states. We introduce the relative energy of two particles T, equal to the sum of energies of these particles in their c.m. system, and relate it to the total energy E_0 distributed among all particles. Were there no interaction between the pair of particles considered, the distribution of the quantity T/E_0 would have, in our case, the form

$$P(T/E_0) \sim (T/E_0)^{1/2}(1 - T/E_0)^{1/2}. \qquad (3)$$

Equation (3) is obtained from Eq. (1) on the basis of kinematic transformations, and has the same form.

Nuclear interaction may also occur between particles in final states. The general theory of this process has been given by Watson[7] for particles of small relative momenta. Unfortunately, a quantitative comparison with the theory is not possible, at present, because of the low statistical accuracy of the results in the region of applicability of the theory. Finally, both in Eq. (3) and in the nuclear interaction, it is necessary to take into account the Coulomb interaction of the disintegration products, which may play an important role in our case of multiply charged particles. This interaction should lead, in both cases, to a decreased yield of particles with both small and large relative energies.

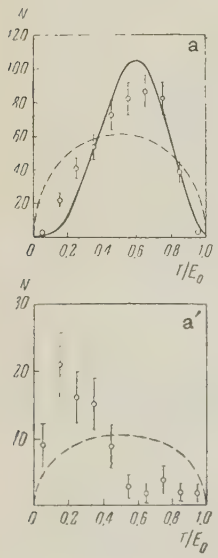

FIG. 9. Distribution of relative energy of the pair (α-particle plus recoil nucleus) in reaction (III). a – $E_\gamma < 50$ Mev; a' – $E_\gamma > 50$ Mev.

Distributions of the quantity T/E_0 for the pair (α-particle plus recoil nucleus) are given in Fig. 9 for two intervals of photon energy in reaction (III) [in the case of reaction (V), the distribution has the same character]. The same figure shows the distribution (3) for noninteracting particles (dashed curve). It can be seen from Fig. 9 that the experimental results corresponding to $E_\gamma < 50$ Mev do not completely agree with Eq. (3). However, even a rough calculation of the Coulomb interaction between all three particles (solid curve in Fig. 9) gives a fair agreement with experiment. For photon energies $E_\gamma > 50$ Mev, the analogous experimental data are in clear contradiction to the distribution of Eq. (3). Account of the Coulomb interaction in Eq. (3) would make the divergence even greater. Thus, a very characteristic peculiarity of the process is the occurrence of small relative energies of the pair (α-particle plus recoil nucleus) or the predominant emission of protons with energies near to the maximum possible.

We consider further the angular characteristics of the processes (III) and (V) in the same intervals of γ-ray energy. Figure 10 shows the angular distributions of protons from reaction (III) for $E_\gamma < 50$ Mev and $E_\gamma > 50$ Mev. The statistical errors are indicated parallel to the ordinate; ϑ is the angle between proton and direction of the γ-ray in the center-of-mass system of carbon. The angular distributions were approximated in the form

$$f(\vartheta) \sim (\alpha + \sin^2\vartheta)(1 + \beta\cos\vartheta). \qquad (4)$$

The coefficients, determined by the method of least squares, are given in Table II. In Fig. 10 the curve corresponding to Eq. (4) is drawn as the solid line. From consideration of the coefficients in Table II it can be seen that the angular distributions of protons from reactions (III) and (V) have the following general properties: the isotropic part of the angular distribution changes markedly in going from $E_\gamma < 50$ Mev to $E_\gamma > 50$ Mev, and the change in the position of the maximum of the distribution relative to 90°, if present, is not substan-

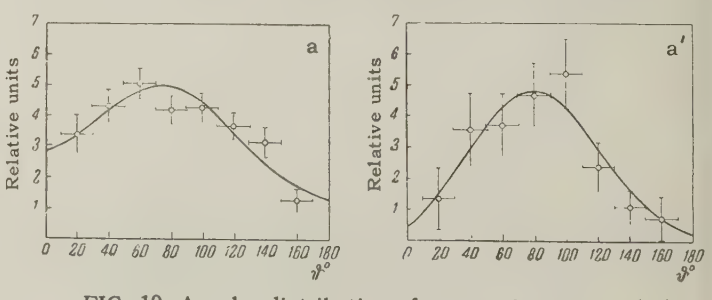

FIG. 10. Angular distribution of protons in reaction (III): a – $E_\gamma < 50$ Mev, a' – $E_\gamma > 50$ Mev.

tial, constituting ~ 10° in both cases.

An attempt was made to observe experimentally the presence of an intermediate state in the reactions considered. It is well known that various intermediate nuclei have been observed in several disintegration processes, such as $C^{12}(\gamma, 3\alpha)$, and also in several other reactions on B and Be. This has led to the idea that the disintegration does not proceed in a single act, but is a complex process of successive emission of particles with formation and decay of excited states of several intermediate nuclei. It should be noted, however, that such a character has been observed mainly in the region of comparatively low photon energies and low excitation energies. Under our conditions, such a process is not completely obvious and experimental verification is required. Let us consider, for example, the reaction (III). One could propose at least three ways in which the reaction might proceed:

$$C^{12} + \gamma \rightarrow H^1 + B^{11*}; \quad B^{11*} \rightarrow He^4 + Li^7; \qquad \text{(IIIa)}$$
$$C^{12} + \gamma \rightarrow He^4 + Be^{8*}; \quad Be^{8*} \rightarrow H^1 + Li^2; \qquad \text{(IIIb)}$$
$$C^{12} + \gamma \rightarrow Li^7 + Li^{5*}; \quad Li^{5*} \rightarrow H^1 + He^4. \qquad \text{(IIIc)}$$

In order to distinguish the paths of decay noted above, an analysis of the excitation energy E* of the intermediate nucleus was employed. The excitation energies of B^{11}, Be^8, and Li^5 were calculated for all stars relating to the reaction (III) under assumptions corresponding to the three modes of decay:

$$E^* = \sum_i^2 E_i + E_Q - E_k,$$

where E_i is the energy of the corresponding decay particle, E_Q is the binding energy of the intermediate nucleus in the decay considered, and E_k is the kinetic energy of the intermediate nucleus. If the intermediate state indicated really occurs, then an excited level of such nuclei should appear in the distribution so calculated. In our case such an analysis involved several difficulties. In fact, the expected decay should proceed through rather highly excited levels, since the threshold of disintegration is 8.5 Mev in case (IIIa) and 17.2 Mev in case (IIIb), and in this energy region the known levels of the nuclei considered are rather dense. In any case, the distance between them is not much larger than the error in determination of E*. Comparison of our experimental results with known levels of B^{11} and Be showed that the maximum in the distribution of excitation energy came in the region of those levels, with which the decay studied is most often observed.* In the region $E_\gamma < 50$ Mev, neither of the schemes (IIIa) and (IIIb) contradicted experiment, whereas for $E_\gamma > 50$ Mev the formation of the intermediate nucleus B^{11} can be considered as preferred. Because of the poor resolving power of this method, it was not possible to separate satisfactorily the intermediate nuclear states, and therefore no definite conclusions could be drawn about the occurrence of the decay scheme proposed. Our results, however, do not contradict such a mechanism.

TABLE II. Coefficients in the distribution of Eq. (4)

Reaction	$E_\gamma > 50$ Mev		$E_\gamma > 50$ Mev	
	α	β	α	β
(III)	0.98	0.32	0.17	0.41
(V)	0.76	0.41	0.04	0.45

The above analysis of the experimental data does not, at the present time, allow us to draw definite conclusions about the type of interaction between photons and light nuclei leading to the indicated reaction. We can, however, formulate several characteristic properties of the process considered, which could serve as a basis for constructing various models to represent the mechanism of the reaction:

1. The total cross sections for reactions (III) and (V) (up to $E_\gamma = 85$ Mev) are equal, respectively, to 6.8 mbn-Mev and 5.5 mbn-Mev. The dependence of the cross section on γ-ray energy has in both cases broad maxima in the region of ~ 35 Mev. The energy distributions of protons and α-particles in carbon and oxygen have the same form. The angular distributions of protons from reactions (III) and (V) coincide, within the limits of experimental error. The great similarity of all characteristics of the reactions (III) and (V) indicates that the mechanism of interaction of photons with carbon and oxygen nuclei, leading to the indicated reactions, is apparently the same and that the individual peculiarities of these nuclei are not essential in this case.

2. The distribution of photon energy among the reaction products, and also the form of the angular distribution, change with increasing γ-ray energy, so that the fraction of the photon energy transmitted to the proton is increased and the isotropic part of the angular distribution is decreased. This characteristic is possibly connected with a change in the mechanism of γ-ray absorption by the nuclei (two intervals might be conditionally

*An analogous analysis of excitation energy was made in reference 6. The experimental results are in satisfactory agreement with our data.

separated: $E_\gamma < 50$ Mev and $E_\gamma > 50$ Mev).

3. In the region $E_\gamma = 25$ to 50 Mev no one particle in the reaction is energetically distinguished from the others. Moreover, the energy of the absorbed photon is spread among the disintegration products in a symmetrical fashion, satisfying Eq. (1) if the Coulomb interaction between particles is taken into account.

The simplest way to explain the observed character of the energy distribution is to assume that the absorption of the photon by the nucleus leads to the disintegration into three particles in a single act. In this case the equally-probable position of the particles should lead to a symmetrical division of energy [Eq. (1)]. However, such a distribution of energy can also be connected with another possible mechanism of interaction between the photon with the nucleus. In particular, it does not contradict the concept of formation and subsequent decay of a compound nucleus with a high excitation energy and high density of levels. In spite of the indefiniteness of the conclusions, it is at least possible to exclude any local interaction, since it assumes a special status for some particles.

4. For $E_\gamma > 50$ Mev the protons in reactions (III) and (V) are energetically quite distinct from other particles and carry away, on the average, from 60 to 90% of the energy E_0, depending on the photon energy. Accordingly the two other particles are emitted with small relative energies.

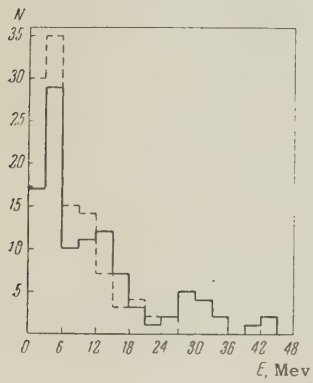

FIG. 11. Energy distributions: solid line – protons, dashed line – tritons.

Thus, the distribution of energy among the reaction products does not correspond to the concept of disintegration of the nucleus into three particles in a single act. As to the possibility of formation of the intermediate states B^{11} or N^{15}, our results, as noted above, do not contradict this concept. Several assumptions can be stated relative to the primary process of interaction of the photon with the nucleus. First, this process should be of local character. One possible process of this type is the direct photoeffect. The latter, as well known, assumes that in the interaction one of the particles is "torn loose," carrying off a large part of the photon energy and leaving the nucleus in the ground or a low excited state. In our case the remaining nucleus, if it is formed at all, should possess a comparatively high excitation, so that the decay proceeds into the particles observed. In principle such a process could, apparently, explain the results obtained in the range of photon energies above 50 Mev.

III. THE REACTION $(\gamma, pt)2\alpha$ ON CARBON*

Besides the reactions $C^{12}(\gamma, 3\alpha)$ and $C^{12}(\gamma, p\alpha)$ already considered, one more reaction involving the disintegration of carbon

$$C^{12} + \gamma \rightarrow H^1 + H^3 + He^4 + He^4 - 27 \text{ Mev} \qquad \text{(VI)}$$

was observed in the same emulsions for photon energies up to 150 Mev.

Detailed information about this reaction does not exist, at present, in the literature. The stars from reaction (VI) were identified visually as four pronged consisting of two tracks of singly-charged particles and two of multiply-charged ones. However, besides (VI), it is possible to propose several other more typical, alternate reactions giving stars of an analogous form:

$$C^{12} + \gamma \rightarrow H^1 + H^1 + He^4 + He^4 + n + n; \qquad \text{(VII)}$$
$$C^{12} + \gamma \rightarrow H^1 + H^2 + He^4 + He^4 + n; \qquad \text{(VIII)}$$
$$C^{12} + \gamma \rightarrow H^2 + H^2 + He^4 + He^4. \qquad \text{(IX)}$$

It was thus difficult to separate the reactions (VI) because the tracks of the different singly-charged particles were difficult to distinguish and the external appearance of stars produced in different reactions was similar.

We chose tentatively 200 stars by visual identification. In the first step, singly-charged particles were divided into protons and tritons according to their ability to balance the momenta of the two α-particles in the plane perpendicular to the direction of the γ-rays (plane of the emulsion). The above rough division was improved upon by measuring the separate energy losses in the emulsions (method of grain counting). Each of the stars chosen in this fashion was taken to belong to reaction (VI) and this was verified by checking conservation of energy and momentum. In the case of tracks going out of the emulsion (which, as a rule, were those of singly-charged particles) the conditions were the same as in the separation of the $(\gamma, p\alpha)$ reaction. The distribution of values of Δp

*V. I. Turovtsev took part, together with the author, in this portion of the work.

for the 200 stars studied approximated well the expected Maxwellian distribution. In the selection, as earlier, the 132 stars having the values $\Delta p \leq 1.8$ and $(\Delta p)_{xy} \leq 1.3$, were segregated as belonging to reaction (VI). In addition, for all of the particles going out of the emulsion, the energy of the particle determined from energy-momentum balance was compared with that determined from its energy loss in the emulsion (method of grain counting). In this way 20 additional stars, for which the energies of the singly-charged particles lay outside the limits of experimental errors, were excluded. It can be considered that the identification of singly-charged particles was correctly made in all of the remaining cases of stars with tracks going out of the emulsion. As a check on the reliability of identification of the tracks ending in the emulsion, grains were counted in similar remaining tracks. A satisfactory division of tracks ascribed to protons and tritons was obtained. In this fashion, 112 stars were related to reaction (VI). One can consider the reactions (VII), (VIII), and (IX) to be excluded as a result of this analysis. An added proof of this was the search for the presence of reaction (IX) in stars related to (VI). All 112 stars were considered again under the assumption that they related to reaction (IX). However, not a single case among them could really be related to this reaction.

The statistics are at present insufficient for a detailed study of reaction (VI). We give, therefore, only several of the most general characteristics of the process.

The integral cross section for the reaction, in various regions of γ-ray energy, is shown below.

E_γ, Mev	30—40	40—55	55—70	70—85
σ, mbn-Mev	0.64±0.15	1.74±0.30	1.25±0.32	0.54±0.34

Figure 11 shows the energy distributions of protons and tritons. The stars in which $E_p > E_t$ constituted ~ 70% of the total. A maximum occurred in the α-particle energy distribution at ~ 2 Mev. The yield of particles with energy greater than 15 Mev was insignificant.

The angular distribution of protons in the center-of-mass system of carbon is given for $E_\gamma < 70$ Mev in Fig. 12. The distribution was approximated by the form $(\alpha + \sin^2\vartheta)(1 + \beta\cos\vartheta)$. The coefficients, determined by the method of least squares, were: $\alpha = 0.16$, $\beta = 0.91$. Thus, the distinguishing features of the angular distribution of protons from reaction (IV) are a very small isotropic part and a displacement of the maximum relative to 90° (~ 20°).

As in the case of the $(\gamma, p\alpha)$-reaction, the distribution of the photon energy among the disintegration products was verified. A divergence from a "symmetrical" distribution of energy was observed, beginning with γ-ray energies ~ 70 Mev. The investigation of the energy and angular distributions as a function of γ-ray energies was difficult because of the small statistics. An attempt was made to consider the reaction from the point of view of the presence of intermediate states. Several different schemes for formation and subsequent decay of an excited intermediate nucleus can be imagined. We examined one of the possible chains of disintegration, i.e.,

$$C^{12} + \gamma \rightarrow H^1 + B^{11*};\ B^{11*} \rightarrow \begin{cases} H^3 + Be^{8*}; & Be^{8*} \rightarrow He^4 + He^4 \\ He^4 + Li^{7*}; & Li^{7*} \rightarrow H^3 + He^4. \end{cases}$$

Sufficiently complete information on the highly-excited levels of B^{11} does not exist. Besides this, we have already noted the difficulties connected with the analysis of the excitation energies. Our results, in any case, do not negate the possibility of formation of an intermediate state of B^{11}. A

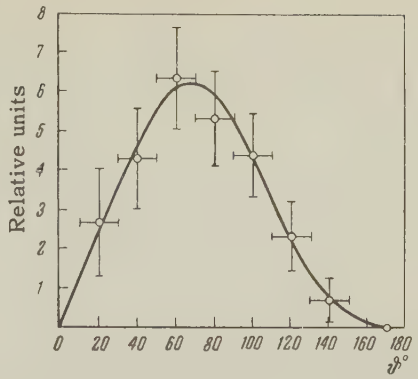

FIG. 12. Angular distribution of protons in reaction (VI) for $E_\gamma < 70$ Mev.

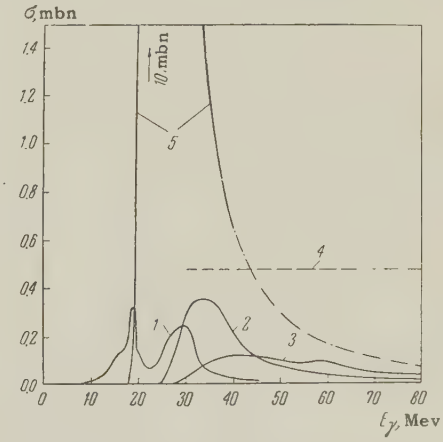

FIG. 13. Dependence of the cross sections for several reactions on the energy of the γ-ray: 1 – (I), 2 – (III), 3 – (VI), 4 – cross section for photoproduction of stars with two or more prongs in the interval E_γ = 30 to 80 Mev from reference 1, 5 – $C^{12}(\gamma, n)C^{11}$ from reference 8.

more definite conclusion can be drawn relative to the existence of Be^{8}*: the ground state and well-known 3-Mev state of Be^{8} occur in many cases of reaction (VI).

The cross sections for reactions (I), (III) and (VI) in carbon are given in Fig. 13 as functions of γ-ray energy in the region up to 80 Mev. For comparison, the form of the (γn)-reaction in carbon[8] is also shown. In the work of reference 1, the integral cross section for photoproduction of stars with two and more prongs was measured for light emulsion nuclei (C^{12}, N^{14} and O^{16}) in the interval of photon energies from 30 to 80 Mev. It comprised 80-mbn-Mev.* Then the total cross section for photoproduction of stars in carbon is approximately 23 mbn-Mev, if the total cross section is divided up in the ratio of the masses of the nuclei (some basis for this is furnished by the fact that the total cross section for absorption of photons by nuclei is proportional to A). In our experiment the integral cross section for reactions (III) and (VI), in the range of γ-ray energies from 30 to 80 Mev, was ~ 10 mbn-Mev, comprising $\sim 45\%$ of the total cross section for star photoproduction. In the interval $E_\gamma = 40$ to 80 Mev, the total cross section for the reactions studied and for (γ, n) is ~ 6.8 and 8 mbn-Mev. Thus, the reactions studied by us are processes which play an essential role in the photoproduction of stars and give, it would seem, an important contribution to the cross section for photon absorption in the region above the "giant" resonance.

*The reaction C^{12} $(\gamma, 3\alpha)$ was excluded here.

In conclusion, I should like to express my gratitude to Prof. V. I. Veksler and A. T. Varfolomeev for help in the work and discussion of the results obtained, and also to I. D. Bannikova and G. A. Prokhorova who took part in the work.

Note added in proof (23 May 1958). Calculations of the angular distributions of protons were made recently under the assumption of a direct photoeffect in the $S_{1/2}$ shells of C^{12} and O^{16}, with allowance for electric dipole and quadrupole absorption of γ-rays. A satisfactory agreement with the experimental angular distribution of protons from the reactions (III) and (V) was obtained for $E_\gamma >$ 50 Mev.

[1] R. M. Lebedev, Dissertation, Physics Institute, Academy of Sciences, U.S.S.R. (1953).

[2] S. Kikuchi, Phys. Rev. **86**, 41 (1952).

[3] E. K. Goward and J. J. Wilkins, Proc. Phys. Soc. **A65**, 671 (1952).

[4] W. K. Dawson and D. L. Livesey, Can. J. Phys. **34**, 241 (1956).

[5] V. N. Maikov, Приборы и техника эксперимента (Inst. and Meas. Eng.) (in press).

[6] D. L. Livesey, Can. J. Phys. **34**, 216 (1956).

[7] K. W. Watson, Phys. Rev. **88**, 1163 (1952).

[8] Barber, George, and Reagan, Phys. Rev. **98**, 73 (1955).

Translated by G. E. Brown
289

PHOTODISINTEGRATION OF A^{40}

I. P. IAVOR

Leningrad Physico-Technical Institute, Academy of Sciences, U.S.S.R.

Submitted to JETP editor January 10, 1958

J. Exptl. Theoret. Phys. (U.S.S.R.) **34**, 1420-1425 (June, 1958)

The photodisintegration of A^{40} induced by bremsstrahlung of 70 Mev peak energy was investigated with a cloud chamber. The relative yields of the different reactions were found, as well as the integrated cross section of the (γ, p) reaction. The angular and energy distributions of the photoprotons from argon were determined.

INTRODUCTION

OVER the last years, several papers have been published concerning the photodisintegration of A^{40}.[1-3] A^{40} is of medium atomic weight and has a high abundance (99.6%) in the natural isotopic mixture. Owing to this fact and to the circumstance that the (γ, p) threshold in A^{40} (12.44 Mev) is more than 2 Mev higher than the (γ, n) threshold (10.25 Mev) an investigation of the photoreactions in this element is of interest.

The (γ, n) and (γ, p) yields in A^{40} were studied in reference 2. It turned out that the yield of the (γ, p) process was greater than the yield of the (γ, n) process. At a γ-ray energy of 19.5 Mev, the ratio $\sigma(\gamma, p)/\sigma(\gamma, n)$ becomes > 1 and continues to increase with increasing photon energy. This is hard to explain from the point of view of the statistical theory of nuclear reactions. In reference 3, the energy and angular distributions of photoprotons were investigated by means of nuclear emulsions. While the energy spectrum of the emitted protons agrees rather well with the predictions of the statistical theory, the angular distributions obtained in reference 3 show a pronounced anisotropy that is difficult to explain.

The present work was undertaken to investigate further the photodisintegration of A^{40} and to confirm the earlier results. In our experiments we used a cloud chamber containing argon gas. This allowed us to find all cases of photodisintegration where charged particles were emitted. The cloud chamber was irradiated with bremsstrahlung of 70 Mev peak energy from the synchrotron of the Physico-Technical Institute of the Academy of Sciences, U.S.S.R.

THE CLOUD CHAMBER AND ITS FILLING

The present experiment was performed with a fast-action cloud chamber. A description of the chamber and of the auxiliary apparatus has been given earlier.[4] The working volume of the chamber has a diameter of 30 cm and a depth of 7 cm. The chamber was located in a magnetic field of strength H = 6300 oersteds. The collimated x-ray beam from the synchrotron had a diameter of 4 cm. The x-ray beam entered the cloud chamber through a thin aluminum window placed in its side wall. The tracks were photographed with a stereo camera which was used also to project the tracks during the analysis.

In the argon experiment, the cloud chamber was filled with a mixture of argon and helium (N_A = 0.69 N_{He}). The pressure of this mixture was 950 mm Hg. This mixture was chosen because of the following reasons.

(1) The construction of the chamber requires an operating pressure slightly larger above atmospheric. By adding helium to the argon, the track length of the emitted charged particles could be increased by a factor of almost two. This increase in the track lengths of the recoil nuclei is of great importance in identifying (γ, p) and (γ, pn) reactions.

(2) The helium in the chamber gas mixture was used in the present work as a monitor to obtain the irradiation dose. This was its main function.

The photoreactions on helium differ very much from those on argon (and on the oxygen and car-

Yields of the different reactions of the photodisintegration of A^{40}

Reaction	Number of cases	$\int_0^{70} \sigma dE$, Mev-bn
(γp)	474	0.35 ± 0.1
(γpn)	43	≈ 0.035
$(\gamma\alpha)$ and $(\gamma\alpha n)$ stars	102	≈ 0.07
(γn)	10	≈ 0.007
	—	0.23

bon contained in the condensing vapors of the chamber). The cross sections of the different photoreactions in helium are known and have been repeatedly checked.[5-7] Thus one can determine the absolute yields of the different reactions by relating them to the yields of reactions in helium without having to utilize auxiliary apparatus to determine the γ-radiation intensity.

YIELDS OF THE PHOTONUCLEAR REACTIONS

All possible photoprocesses involving the emission of charged particles were registered by the cloud chamber.

As a result of a (γ, n) process on argon, the recoil nuclei produce short heavily ionizing tracks. In most cases the track lengths do not exceed 1 to 2 mm. At the same time, the electrons and positrons in the chamber produce a background which makes it difficult to determine the total number of the (γ, n) reactions. The (γ, n) reaction therefore was not studied further.

The reactions (γ, p) and (γ, pn) have a characteristic appearance in the cloud chamber. They consist of a proton track of rather weak ionization with a heavy short track of the recoil nucleus at its start. Such tracks are denoted in the literature as "flags." The (γ, p) and (γ, d) reactions were not separated in the present experiment. The (γ, p) and (γ, pn) reactions were identified by kinematical considerations. In the center-of-mass system, the proton and the recoiling nucleus form an angle of 180°. In the laboratory system the reaction products have an additional forward velocity due to the momentum of the absorbed photon, and the emission angle is reduced. However, even in the most favorable case (photon energy close to the peak energy; recoil nucleus in a very highly excited state) the angle does not decrease by more than 15 to 18°. Furthermore, the proton, recoil nucleus, and the photon are obviously coplanar. In the (γ, pn) reaction the proton can be emitted in an arbitrary direction with respect to the recoil nucleus. Obviously the error in the determination of the relative yield of the (γ, pn) reaction is confined to the cases in which the neutron is emitted with very low energy relative to the proton energy, or in which the neutron is emitted almost in the same direction as the proton. It is also confined to the fraction of cases in which the recoil nucleus has such a short track, that it is difficult to determine the direction of its motion.

The reactions (γ, α) and $(\gamma, \alpha n)$ are similar to the described proton "flags". However, they can be easily identified by the considerable ionization density of the α-particle tracks, and also by the track length of the recoil nuclei. It must be noted that it is much more difficult to discriminate between the (γ, α) and $(\gamma, \alpha n)$ reactions than between the (γ, p) and (γ, pn) reactions. This is caused by the relatively small momentum carried by the neutron, compared to the momentum of the α-particle. The neutron has therefore a relatively small influence on the angle between the α-particle and the recoil nucleus.

All photodisintegrations resulting in emission of three or more charged particles were counted as "stars."

The condensing vapor consisted of a mixture of 70% ethyl alcohol and 30% water, leading also to photoprocesses on O and C. The corresponding processes on argon, oxygen, and carbon could not be distinguished in our experiment, except for a small number of (γ, p) flags which happened to be favorably oriented. In order to account for the background due to these reactions, an auxiliary experiment was performed where the cloud chamber was filled only with helium but had the same content of condensing vapors and otherwise identical conditions. The yields of the different reactions on O and C were determined in relation to the (γ, p) reaction in helium. They then were corrected for the change of the partial pressure of helium in the helium-argon mixture and used to determine the number of corresponding reactions in argon (relative to the known number of helium (γ, p) flags in the helium-argon mixture). Under the actual conditions of the experiment, the background reactions of the (γ, p) and (γ, pn) type amounted to 15% of the (γ, p) and (γ, pn) reactions in argon. The values of the relative yields of the different photoreactions on argon are given in the table.

By comparing the numbers of (γ, p) reactions in argon and in helium, the integrated cross section of the (γ, p) reaction in argon was determined in the following manner. To eliminate errors associated with vertical tracks, only those argon and helium flags were counted whose tracks did not make an angle greater than 65° with the horizontal plane. It was found that there were 67 helium (γ, p) flags and 474 argon flags of the same type (after subtracting the background flags due to the water and alcohol vapors). The value of the integrated (γ, p) cross section of helium for a photon peak energy of 70 Mev (0.034 Mev-bn) was taken from references 5 to 7. Then the integrated cross section of argon, for a photon peak energy of 70 Mev, turns out to be 0.35 Mev-bn. This does not agree with the result of reference 2,

which apparently is much too large.

It is of interest to compare the experimentally-determined total integrated photon absorption cross section with the theoretical predictions. According to Levinger and Bethe,[8] this quantity equals 0.83 Mev-bn, assuming that the fraction of exchange forces is $x = 0.5$. From the experiment we have the value 0.69 Mev-bn. This can be taken to be in good agreement with the theoretical value, since in this range of atomic numbers the experimental values of the integrated absorption cross section are in general slightly smaller than the theoretical ones calculated with $x = 0.5$.[9] The integrated cross sections of the different processes in argon are given in the table.

The integrated cross section for the (γ, n) reaction was taken from reference 10.

THE ENERGY DISTRIBUTION OF THE PHOTOPROTONS

The energies of the protons were determined in the following ways: (1) from the curvature of the tracks in the magnetic field, (2) from the track length of the recoil nucleus [for the (γ, p) reactions], (3) from the range of the proton track in the chamber for small proton energies, and (4) very crudely from the visually-determined ionization density. In practice the measurement was performed in each case with all methods applicable to the particular case, except for the fourth method, which was used only as an order-of-magnitude check.

The precision of the measurement of the track curvature is limited by the multiple scattering of protons of a few Mev in the chamber gas. This has been considered, for example, in reference 11. Furthermore, in general the curvature can be determined sufficiently well only for tracks which are so oriented as to have a visible length of 10 to 15 cm. The second method can be used only for (γ, p) reactions, where a unique correlation exists between the energy of the proton and the energy (and consequently also the range) of the recoil nucleus. One sees from Table I that the main photoproton yield comes from (γ, p) reactions, and only $\sim 10\%$ is due to the (γ, pn) reaction. Therefore, (2) was the main method used in the present experiment.

The energy spectrum of photoprotons from A^{40} was determined up to a proton energy of 15 Mev. The corresponding range of the recoil nucleus for the condition of our experiment was ~ 0.14 cm. Most photoprotons from argon have energies up to 8 or 10 Mev. The number of protons with energies > 10 Mev, i.e., with a recoil range > 0.1 cm, is relatively small. Since protons of equal energy produce much larger recoils if they are emitted from carbon and oxygen than from argon, one has to determine the contribution of the background nuclei to recoils of ranging from 0.1 to 0.15 cm. It was found in the auxiliary experiment with the pure helium filling that most photoprotons from C and O had recoil ranges > 0.1 cm (referred to the larger stopping power of the helium-argon mixture). In fact, the number of (γ, p) reactions in O and C with a recoil range up to 0.15 cm does not exceed 10% of all reactions of this kind. Since the total number of (γ, p) reactions of O and C is only $\sim 10\%$ of the argon reactions, the contribution of background protons to the high-energy tail of the protons from argon is unimportant in the 10 to 15 Mev range.

No range-energy relation for Cl^{39} ions is known in the literature. Assuming that the energy dependence of the range of Cl^{39} differs from that of A^{40} by less than the uncertainties of the present experiment, one can use the known range-energy relation for A^{40}.[12] A check on the curvatures and ranges of the corresponding protons gave a satisfactory agreement.

The recoil-nuclei ranges were approximately determined by projecting the photographs. They were more precisely determined under the microscope, taking the inclination of the track into account. To avoid errors connected with large inclinations, both the curvatures and the ranges were determined only for tracks which made an angle of not more than 45° with the horizontal plane. The accuracy of the measurement of the track lengths of the recoils was 0.1 mm.

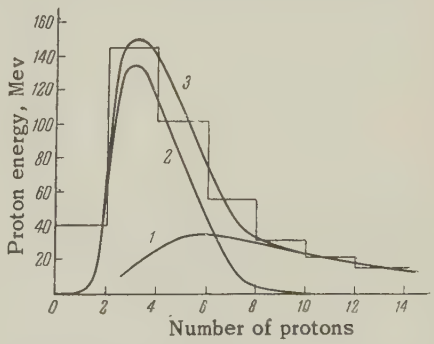

FIG. 1. Energy distribution of photoprotons from argon: 1 – distribution calculated from the theory of the direct photoeffect; 2 – distribution calculated from the statistical theory of nuclear reactions; 3 – total theoretical energy distribution of photoprotons; histogram – experimental results.

The energy distribution obtained for photoprotons from argon is given by the histogram of Fig. 1. The other curves in Fig. 1 show the spectra as given by the statistical theory of nuclear reactions

and by Courant's theory[13] of the direct photoeffect. The spectrum of evaporation photoprotons is given[14] by

$$I(\varepsilon)\,d\varepsilon = \varepsilon\sigma_c(\varepsilon)\,e^{-\varepsilon/T}d\varepsilon \int_{B_p+\varepsilon}^{E_{\gamma m}} N_\gamma(E)\,\sigma_{\gamma n}(E)\,dE.$$

The following values were assumed for the parameters entering this expression: nuclear temperature T = 1 Mev; proton binding energy in A^{40}, B_p = 12.44 Mev[2]; cross section $\sigma_{\gamma n}(E)$ for the reaction $A^{40}(\gamma, n)A^{39}$ as a function of the energy of the photons, E, was taken from reference 15; the bremsstrahlung spectrum $N_\gamma(E)$ with peak energy E = 70 Mev was taken from reference 16. The energy distributions of the "direct" photoprotons was calculated from the formula

$$I(\varepsilon)\,d\varepsilon = f(\varepsilon)\,d\varepsilon \int_{B_p+\varepsilon}^{E_{\gamma m}} N_\gamma(E)\,E^{-3}dE,$$

where $f(\epsilon)$ is the penetrability of the coulomb barrier.

The calculated energy distributions agree well with the experimental photoproton spectra if one assumes a ratio of the direct to evaporation yields of 1:1, 2. It should also be mentioned that there exist many photoprotons from the (γ, p) reaction of A^{40}, with energies between 15 and 30 Mev, which are not included in the histogram of Fig. 1.

ANGULAR DISTRIBUTIONS OF PHOTOPROTONS

The inclinations of the photon tracks to the horizontal plane and the angles θ between the proton tracks and the directions of the x-ray beam were determined by projecting the photographs. The errors of this method do not exceed 2°. Tracks with inclination angles up to 45° were used for the angular distributions. The tracks thus selected were grouped in bands 20° wide. The distribution obtained was then expressed per unit solid angle by applying appropriate angle-dependent factors which were assumed to be constant in any particular angular band. The obtained angular distribution of photoprotons from A^{40} with energies 2 to 15 Mev in the laboratory system is shown as a histogram in Fig. 2. The ordinate is in relative units. The statistical errors are also indicated. An analogous histogram from preliminary experiments was given earlier,[17] but was not reduced to yield per unit solid angle.

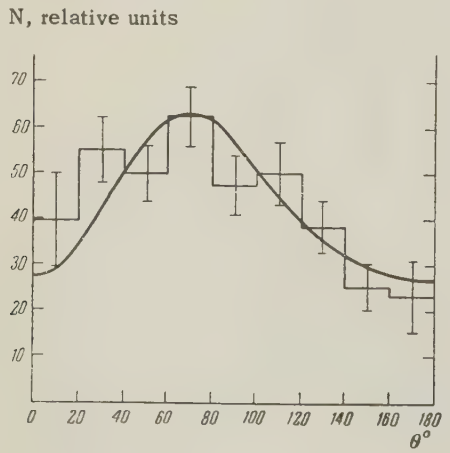

FIG. 2. Angular distribution of photoprotons, from argon with energies of 2 to 15 Mev. The histogram is the result of analysis of 406 proton tracks. The number of tracks shown has been referred to unit solid angle.

The forward shift of the maximum in the angular distribution cannot be explained by the momentum of the incoming photon, since the transformation to center-of-mass coordinates is unimportant for such a heavy nucleus as A^{40}.

The solid curve drawn in Fig. 2 has the form

$$I(\theta) = A + B(\sin\theta + p\sin\theta\cos\theta)^2,$$

with A = 27, B = 30, and p = 0.5. The parameter p is connected with the ratio of dipole to quadrupole absorption of photons, $\sigma_Q/\sigma_D = p^2/5$. Thus, in our case, the quadrupole absorption amounts to ~5% of the dipole absorption.

The angular distribution of photoprotons from argon obtained in reference 3 with bremsstrahlung with 22.5 Mev peak energy has its maximum near 70°, like our Fig. 2.

CONCLUSIONS

The experimental results on the photodisintegration of A^{40} obtained in the present work are not in disagreement with the results of most papers devoted to the investigation of the photonuclear reactions of medium weight nuclei.[14,18-20] The dipole character of the photon absorption of A^{40} nuclei is corroborated by comparing the experimental integrated absorption cross sections with the theoretical predictions, as well as by the angular distribution of the photoprotons. The anomalously large photoproton yield compared with the photoneutron yield is not as sharp as indicated by the results of reference 2. It can be explained in part by the large contribution of the direct photoprotons, which follows from the comparison of the experimental photoproton spectrum of argon with theoretical predictions. At γ-energies of up to 70 Mev essentially there occur in argon two competing reactions, (γ, p) and (γ, n), with approximately equal integrated cross sections and with a small contribution from (γ, α), $(\gamma, \alpha n)$ and (γ, pn) reactions.

In conclusion, the author expresses his thanks to Prof. A. P. Komar for his continuing interest in this work and for a number of valuable comments.

[1] D. Wilkinson and J. H. Carver, Phys. Rev. **83**, 466 (1951).
[2] McPherson, Pederson, and Katz, Can. J. Phys. **32**, 593 (1954).
[3] B. M. Spicer, Phys. Rev. **100**, 791 (1955).
[4] I. P. Iavor and A. P. Komar, J. Tech. Phys. (U.S.S.R.) **27**, 868 (1957), Soviet Phys. JTP **2**, 794 (1957).
[5] E. R. Gaerttner and M. L. Yeater, Phys. Rev. **83**, 146 (1951).
[6] E. G. Fuller, Phys. Rev. **96**, 1306 (1954).
[7] A. N. Gorbunov and V. M. Spiridonov, J. Exptl. Theoret. Phys. (U.S.S.R.) **33**, 21 (1957), Soviet Phys. JETP **6**, 16 (1958).
[8] J. S. Levinger and H. A. Bethe, Phys. Rev. **78**, 115 (1950).
[9] Montalbetti, Katz, and Goldemberg, Phys. Rev. **91**, 659 (1953).
[10] Ferguson, Halpern, Nathans, and Yergin, Phys. Rev. **95**, 776 (1954).
[11] Wright, Morrison, Reid, and Atkinson, Proc. Phys. Soc. **A69**, 77 (1956).
[12] P. M. S. Blackett and D. S. Lees, Proc. Roy. Soc. **134**, 658 (1932).
[13] E. D. Courant, Phys. Rev. **82**, 703 (1951).
[14] W. K. Dawson, Can. J. Phys. **34**, 1480 (1956).
[15] M. M. Shapiro, Phys. Rev. **90**, 171 (1953).
[16] L. I. Schiff, Phys. Rev. **83**, 252 (1951).
[17] A. P. Komar and I. P. Iavor, J. Exptl. Theoret. Phys. **31**, 531 (1956), Soviet Phys. JETP **4**, 432 (1957).
[18] B. C. Diven and G. M. Almy, Phys. Rev. **80**, 407 (1950).
[19] P. R. Byerly and W. E. Stephens, Phys. Rev. **83**, 54 (1951).
[20] Katz, Haslam, Goldemberg, and Taylor, Can. J. Phys. **32**, 580 (1954).

Translated by M. Danos
290

SOVIET PHYSICS JETP VOLUME 34 (7), NUMBER 6 DECEMBER, 1958

ENERGY SPECTRUM AND ANGULAR DISTRIBUTION OF π^+ MESONS PRODUCED ON CARBON BY 660-Mev PROTONS

A. G. MESHKOVSKII, Ia. Ia. SHALAMOV, and V. A. SHEBANOV

Submitted to JETP editor January 13, 1958

J. Exptl. Theoret. Phys. (U.S.S.R.) **34**, 1426-1433 (June, 1958)

The energy spectrum of π^+ mesons produced by 660-Mev protons on carbon was measured at five angles from 19°30′ to 65°. The absolute cross-sections $d\sigma_+/d\Omega$ were also measured. In the c.m.s. of the two colliding nucleons, the mean π^+ meson energy was found to be independent of the angle of emission, and equal to 100 Mev. Conclusions are drawn concerning the angular distribution of π^+ mesons; the total cross-section for their production on carbon by 660-Mev protons has been found to be $(46.7 \pm 5.1) \times 10^{-27}$ cm^2. The probability of π^+-meson production in p — p collisions in the carbon nucleus is half the analogous probability for free p — p collisions.

1. INTRODUCTION

THE production of charged π mesons on carbon by 660-Mev protons was investigated for various angles of observation in several experiments.[1-4] Meshcheriakov et al. measured the relative energy spectrum of π^+ and π^- mesons at 24°.[1] Energy spectra and absolute yields of π^+ mesons[2] and π^- mesons[3] were studied at 45°. Analogous information on mesons of both signs was obtained for 90° as well.

In the present work, we have studied the energy

spectra and the absolute yield of positive π mesons produced by 660-Mev protons on carbon at 19°30′, 29°, 38°, 56°, and 65° in the laboratory system. All measurements were carried out on the external proton beam of the synchrocyclotron of the Joint Institute for Nuclear Research, Laboratory of Nuclear Problems, using a π-meson spectrometer described earlier.[5]

TABLE I

19°30′		29°		38°		56°		65°	
Meson energy, Mev	$\frac{d^2\sigma_+}{d\Omega\, dE}\cdot 10^{28}$, cm² sterad⁻¹ Mev⁻¹	Meson energy, Mev	$\frac{d^2\sigma_+}{d\Omega\, dE}\cdot 10^{28}$, cm² sterad⁻¹ Mev⁻¹	Meson energy, Mev	$\frac{d^2\sigma_+}{d\Omega\, dE}\cdot 10^{28}$, cm² sterad⁻¹ Mev⁻¹	Meson energy, Mev	$\frac{d^2\sigma_+}{d\Omega\, dE}\cdot 10^{28}$, cm² sterad⁻¹ Mev⁻¹	Meson energy, Mev	$\frac{d^2\sigma_+}{d\Omega\, dE}\cdot 10^{28}$, cm² sterad⁻¹ Mev⁻¹
102	2.97±0.38	80	2.45±0.72	80	2.44±0.26	75	2.79±0.24	44	1.68±0.32
129	3.61±0.39	105	2.31±0.55	104	2.58±0.27	88	3.05±0.33	60	2.36±0.19
161	4.21±0.47	135	3.81±0.65	128	3.06±0.27	100	3.16±0.17	87	2.62±0.28
188	4.16±0.39	160	3.78±0.53	152	3.13±0.25	116	2.77±0.18	111	1.81±0.15
225	4.68±0.42	187	4.10±0.54	172	3.17±0.26	130	2.34±0.14	142	1.78±0.13
261	4.66±0.42	212	4.04±0.64	192	2.75±0.33	149	2.19±0.19	161	1.19±0.10
283	4.14±0.41	235	4.70±0.51	212	2.65±0.31	172	1.86±0.23	178	1.14±0.11
300	4.66±0.42	262	4.37±0.49	231	2.42±0.23	192	1.38±0.07	190	0.78±0.10
317	3.15±0.37	283	3.43±0.41	253	2.11±0.20	212	1.05±0.08	206	0.75±0.10
328	2.86±0.45	299	2.51±0.28	269	1.95±0.15	236	0.74±0.14	245	0.43±0.07
341	2.10±0.28	324	1.90±0.39	275	1.70±0.16	251	0.51±0.13	268	0.38±0.07
356	2.31±0.25	—	—	295	1.59±0.18	263	0.55±0.12	—	—
—	—	—	—	313	1.11±0.17	278	0.56±0.11	—	—

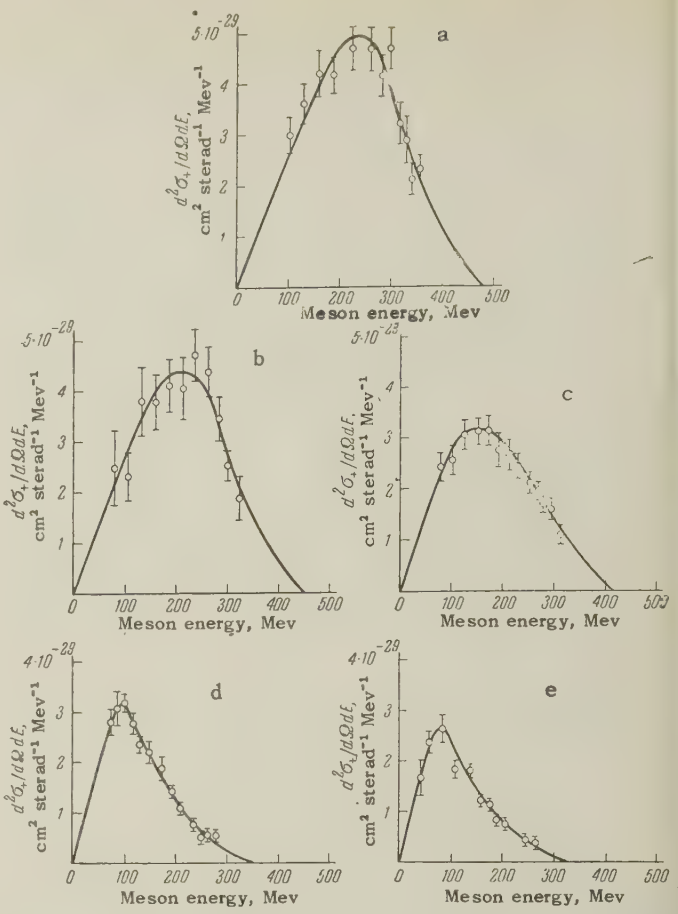

FIG. 1. Energy spectrum of π^+ mesons produced by 660-Mev protons on carbon at a – 19° 30′, b – 29°, c – 38°, d – 56°, and e – 65° in the laboratory frame.

2. RESULTS

The results of measurements of the differential cross-sections $d^2\sigma_+/d\Omega dE$ at various angles of observation are given in Table I. The errors given in the table represent the statistical errors of the measurements. The energy spectra of π^+ mesons based on the date of Table I are shown in Fig. 1. The curves are drawn to obtain best fit with experimental points. Our experimental data are insufficient to determine the shape of the spectrum in the low energy region, in view of the high energy threshold for π mesons detection in the spectrometer. In that region, the curves have been drawn under the assumption that the spectrum is almost linear near the origin of the coordinate system. This was shown experimentally[1] for carbon at 24°, and also in the study of the yield of π mesons with energies up to 40 Mev on emulsion nuclei.[6] It has been assumed that the cut-off in the high-energy region occurs at the π^+ meson energy, calculated from kinematic considerations under the assumption that the energy of nucleons in the nucleus is

TABLE II

Angle of observation, laboratory system	11°30′	29°	38°	45°	56°	65°
$d\sigma_+/d\Omega$ B cm² sterad⁻¹ × 10⁻²⁷	12.34±1.44	10.22±0.78	7.13±0.43	6.77±0.62	4.62±0.28	3.70±0.57
$d\sigma^*_+/d\Omega^*$ B cm² sterad⁻¹ × 10⁻²⁷	3.61±0.42	3.54±0.27	2.90±0.17	3.27±0.30	2.96±0.18	3.01±0.46
Mean energy $\bar{E}^*$ in c.m.s., Mev	101	103	102	103	101	106
Mean angle of emission in c.m.s., $\bar{\vartheta}^*$	36°	53°	67°	77°	93°	103°

of the order of 25 Mev. Extrapolation of the experimental curves in Fig. 1 into the high-energy region is, at all angles, in satisfactory agreement with the calculated maximum energy of π^+ mesons.

Results of integration of the spectra over the curves, i.e., the cross-sections $d\sigma_+/d\Omega$, are given in Table II. The value of $d\sigma_+/d\Omega$ for 45°, measured earlier,[2] is also given in the table. Both statistical and systematic errors, the latter ranging for the various angles, from 5 to 10% were taken into account in the integration.

It is known from experiments on the production of π mesons by protons and neutrons of various energies, that in collisions between nucleons and complex nuclei π mesons are produced essentially on single nucleons of the nucleus and not on the nucleus as a whole. In connection with the above fact, it is of interest to transform the obtained spectra into the c.m.s. of two colliding nucleons. Results of integration of the spectra in the c.m.s., i.e. the values of the cross-section $d\sigma^*_+/d^*\Omega$, as well as the average π^+-meson energy in the c.m.s. for each spectrum and the mean angle of emission $\bar{\vartheta}^*$, are given in Table II. The values of $\bar{\vartheta}^*$ represent a rough estimate, since the motion of the nucleus was neglected in their calculation.

The dependence of the cross section $d\sigma^*_+/d\Omega^*$ on the angle of emission ϑ^* in the c.m.s., based on the data of Table II, is shown in Fig. 2. The curve is drawn for best fit with the experimental points. Assuming that this experimental curve represents the angular distribution of π^+ mesons in the interval 36 to 103° in the c.m.s., we have calculated the cross-section σ^*_+ for π^+-meson production in that region. We found σ^*_+ (36 to 103°) = $(20.5 \pm 0.8) \times 10^{-27}$ cm².

3. SHAPE OF THE SPECTRUM AND MEAN POSITIVE π-MESON ENERGY

As the result of transformation of the π^+ meson spectra into the c.m.s., we find that a maximum is attained at $E^* = 100$ Mev for $\bar{\vartheta}^* = 36°$. For $\bar{\vartheta}^* = 93°$ and $\bar{\vartheta}^* = 103°$, the maxima in the c.m.s. are located between 70 and 75 Mev. The maxima of the remaining spectra are contained between 70 and 100 Mev, a shift of the position of the maximum in the c.m.s. towards higher energies being observed for smaller angles, indicating that the shape of the spectrum depends on the angle. A similar variation of the spectrum with the angle was observed earlier for free p — p collisions in the reaction $pp \rightarrow pn\pi^+$.[5,7] It is possible that the effect exists in production of π^+ mesons on bound protons as well.

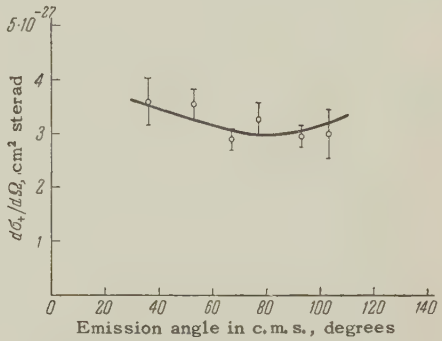

FIG. 2. Dependence of the differential cross section for the production of π^+ mesons on carbon on the angle of emission in the c.m.s.

It follows from Table I that the mean π^+-meson energy $\bar{E}^*$ in the c.m.s. hardly varies with the angle of emission and amounts to 100 Mev. The same value of mean π^+-meson energy has been obtained earlier for Be and C at 24° in the laboratory system.[1] Most remarkable is the fact that the position of the maximum and the value of the mean energy change very little at higher proton energies. This result follows from comparison of the present results and those of other experiments carried out at 660 Mev[1] with the data of Yuan and Lindenbaum,[8] who have found for Be that, at an energy of 1 Bev, the π^+-meson spectrum attains a maximum at 100 Mev for an angle of observation of 32° in c.m.s. A further energy increase to 2.3

Bev causes the maximum to shift only 30 Mev. This weak dependence of π-meson energy on the proton energy can be explained[8] by the predominant role of the isobaric $P_{-3/2\,-3/2}$ state in the π-meson production.

4. ANGULAR DISTRIBUTION OF π^+ MESONS AND CALCULATION OF THE TOTAL CROSS-SECTION

It follows from Fig. 2 that the cross-section $d\sigma_+^*/d\Omega^*$ does not vary greatly with the angle between 36° and 103°. An analogous result has been obtained for neutral π mesons produced on carbon by 660-Mev protons.[9] It follows that the π^0-meson yield in the c.m.s. varies very slowly with the angle in the interval 0° to 100°. A marked increase in the π^0 yield is observed with a further increase in angle. The π^0-meson production cross section for 180° is twice that for 0° in the c.m.s. This increase can be explained by simple qualitative considerations which follow from the optical model of the nucleus and which are connected with the absorption of protons traversing the nucleus. An analogous increase of the cross section for large angles can be observed for charged π mesons.

Prokoshkin[9] calculated the angular distribution of π^0 mesons produced by protons on carbon, using the optical model, and assuming an isotropic angular distribution of π^0 mesons in the c.m.s. in proton-nucleon collisions. The calculated curve is in good agreement with the experimental data. To calculate an analogous curve for π^+ production, it is necessary to know the angular distribution of π^+ mesons in elementary collisions. Experimental data concerning this problem are, at present, inconsistent[7,10] but, most probably, the angular distribution of π^+ mesons in $p-p$ collisions at 660 Mev does not differ appreciably from isotropic.[5] Taking the above into account, one could expect that the angular distribution of π^+ mesons produced by protons on carbon should not differ appreciably from the angular distribution of π^0 mesons.

The similarity between the angular distributions of π^+ and π^0 mesons, expected in view of the above considerations, permits us to find the total cross-section for the production of π^+ mesons on carbon by 660-Mev protons, from the data of the present work. The fraction of the total production cross section of neutral π mesons contributed by the angle interval from 36° to 103° in the c.m.s. can be calculated from experimental data,[9] and amounts to 45%. Assuming that the angular distribution of π^+ mesons is similar to that of π^0 mesons, we obtain from $\sigma_+(36°\text{ to }103°) = 20.5\times10^{-27}\,\text{cm}^2$, measured in the present experiment (Sec. 2), a value $\sigma_+ = 45.5\times10^{-27}\,\text{cm}^2$ for the total cross-section for the production of π^+ mesons on carbon.

5. PRODUCTION OF π MESONS ON CARBON AND THE PRINCIPLE OF ISOTOPIC INVARIANCE

The cross-section obtained in Sec. 4 can also be estimated from the principle of isotopic invariance. It should be noted that the isotopic spin of C^{12} is zero. The principle of isotopic invariance leads to the following relation for the production of π mesons in collisions between nucleons and nuclei of zero isotopic spin:

$$\sigma_+ + \sigma_- = 2\sigma_0, \tag{1}$$

where σ_+, σ_-, and σ_0 are the total or the differential production cross-sections for π^+, π^-, and π^0 mesons respectively.[11] Equation (1) was tested experimentally for deuterons and carbon, in π meson production by protons, at 45° in the laboratory system.[3]

Data on the cross sections for production of negative and neutral π mesons on carbon are necessary for a comparison of the results of the present work with Eq. (1). The results for π^0 mesons are known for a wide angle interval.[9] The yield of π mesons can be estimated from the ratio $d\sigma_+/d\sigma_-$ for carbon, given by several authors.

The results are collected below:

Observation angle in the lab. system	24°	45°	56°	90°
$d\sigma_+/d\sigma_-$	7.0 ± 0.8[1]	6.8 ± 1.1[3]	5.2 ± 0.6[12]	5.0 ± 0.7[4]

It can be seen that the ratio $d\sigma_+/d\sigma_-$ varies slowly with the angle and that the π^--meson yield is only 15 to 20% of the π^+-meson yield. Both facts make it possible to compare the experimental results with Eq. (1), in spite of insufficient data on π^--meson production.

On the basis of the above data, we shall assume that $\sigma_+^*/\sigma_-^* = 6\pm1$ between 37° and 103° in the c.m.s. Then, for the same angle interval, $\sigma_+^* + \sigma_-^* = (7/6)\,\sigma_+^* = (24.0\pm1.1)\times10^{-27}\,\text{cm}^2$ (using the value for $\sigma_+^*(36°\text{ to }103°)$ given in Sec. 2). Using the data of reference 9, we obtain, for the same angle interval, $2\sigma_0^* = (25.5\pm2.7)\times10^{-27}\,\text{cm}^2$. Relation (1) is therefore satisfied, as expected from the principle of isotopic invariance.

In view of the good agreement between the absolute measurements of the present work and the results obtained for π^0 mesons, Eq. (1) can be used to compute the total cross section. Assuming that

for total cross-sections we have $\sigma_- = \frac{1}{6}\sigma_+$, and taking into account that $\sigma_0 = (28 \pm 3) \times 10^{-27}\,\text{cm}^2$,[9] Eq. (1) yields $\sigma_+ = (48.0 \pm 5.3) \times 10^{-27}\,\text{cm}^2$. This result is in a good agreement with the value $\sigma_+ = 45.5 \times 10^{-27}\,\text{cm}^2$ obtained in Sec. 4 from different considerations. From the two results we obtain $\sigma_+ = (46.7 \pm 5.1) \times 10^{-27}\,\text{cm}^2$.

6. COMPARISON OF YIELDS OF π^+ MESONS PRODUCED ON FREE AND BOUND PROTONS

It is useful, for the understanding of processes that take place during the production of π mesons on complex nuclei, to estimate the relative probabilities of π-meson production on free and bound nucleons. We shall make such an estimate for positive π mesons produced on the protons of a carbon nucleus, using the results of the present experiment.

Let us write the total cross section for carbon in the form $\sigma_+ = \sigma^+_{p'} + \sigma^+_{n'}$, where $\sigma^+_{p'}$ and $\sigma^+_{n'}$ are the cross sections corresponding to π^+-meson production on the protons and on the neutrons of the carbon nucleus respectively. We shall note, furthermore, that the principle of charge symmetry requires that, for the production of π mesons on free neutrons, the cross-section for the $pn \to nn\pi^+$ reaction equal that for the $pn \to pp\pi^-$ reaction, i.e., $\sigma^+_n = \sigma^-_n$. We can assume, with an accuracy sufficient for our purposes, that an analogous relation holds for experiments with complex nuclei, i.e., that $\sigma^+_{n'} = \sigma^-_{n'}$. On the other hand, $\sigma^-_{n'}$ is the cross-section for the production of π^- mesons on carbon, i.e., equal to σ_-, since the production of π mesons on nuclei can occur in $p-n$ collisions only. We have, therefore, $\sigma_+ = \sigma^+_{p'} + \sigma^+_{n'} = \sigma^+_{p'} + \sigma^-_{n'} = \sigma^+_{p'} + \sigma_-$. Moreover, it has been shown in Sec. 5 that $\sigma_- \approx \frac{1}{6}\sigma_+$ and, consequently, $\sigma_+ = \sigma^+_{p'} + \frac{1}{6}\sigma_+$. Hence, using the value of σ_+ obtained in the present experiment, and relating the cross-section $\sigma^+_{p'}$ to one proton of the carbon nucleus, we find that the π^+-meson production cross section on a bound proton equals $(6.5 \pm 0.8) \times 10^{-27}\,\text{cm}^2$. The value of the cross section for an analogous process on a free proton is $(13 \text{ to } 14) \times 10^{-27}\,\text{cm}^2$.[5,7,10] We conclude, therefore, that the probability for π^+-meson production in $p-p$ collision in the carbon nucleus at 660 Mev is half the analogous probability for collisions of free protons. It should be noted that a similar halving of the probability has been observed in the production of π^0 mesons on carbon as well. This was found from the values of the cross sections $\sigma(pp \to \pi^0)$, $\sigma(pn \to \pi^0)$, and $\sigma(pC \to \pi^0)$, measured at 660 Mev.[9]

To explain these facts, we shall make use of the theory of Ansel'm and Shekhter,[13] who have shown that the experimental data on the production of π mesons on complex nuclei by protons can be explained by means of a model, according to which the π mesons observed are produced only on the surface of the nucleus (according to a $A^{2/3}$ law), and that deviations are due to the absorption of protons in traversing the nucleus. Let us denote by σ' the total cross section for π-meson production on the nucleus in the absence of absorption, and by σ the actually-observed cross section. We then obtain[13]

$$\frac{\sigma'}{\sigma} = (\eta R)^2 \int_0^\pi \frac{d\sigma_+}{d\Omega}(\vartheta) \sin\vartheta\, d\vartheta \Big/ \int_0^\pi \frac{d\sigma_+}{d\Omega}(\vartheta)\, F(\eta R, \vartheta) \sin\vartheta\, d\vartheta. \tag{2}$$

where $d\sigma_+/d\Omega$ is the π^+-meson production cross section in free nucleonic collisions, η the proton absorption coefficient, R the radius of the nucleus, and F a function calculated in reference 13. The value of η and the dependence of $d\sigma_+/d\Omega$ on ϑ must be known if the computations are to be according to Eq. (2). The absorption coefficient η can be found from the expression

$$\frac{\sigma_a}{\pi R^2} = 1 - \frac{1 - (1 + 2\eta R)\exp\{-2\eta R\}}{2(\eta R)^2}, \tag{3}$$

which follows from the optical model of the nucleus.[14] The cross section σ_a for the inelastic interaction between protons and nuclei can be obtained from experimental data obtained at 650 Mev[15]. The dependence of $d\sigma_+/d\Omega$ on ϑ can be approximated by the expression $a + b\cos^2\vartheta$.[7,10] It is found that the result for σ'/σ depends very little on a and b so that their value is immaterial for the calculation.

Computation carried out according to Eq. (2) showed that $\sigma'/\sigma = 1.8$, which has to be considered as good agreement with the experimental value $\sigma'/\sigma \cong 2$. One can therefore attribute the 50% decrease in the probability for π^+-meson production in $p-p$ collisions in the carbon nucleus, compared with the analogous probability for free $p-p$ collisions, to the absorption of protons in the nuclear matter, assuming that the π^+ mesons observed are produced on the surface of the nucleus.

In conclusion, the authors wish to thank Iu. D. Prokoshkin for the discussion of results.

[1] Meshcheriakov, Vzorov, Zrelov, Neganov, and Shabudin, J. Exptl. Theoret. Phys. (U.S.S.R.) **31**, 55 (1956), Soviet Phys. JETP **4**, 79 (1957).

[2] Meshkovskii, Pligin, Shalamov, and Shebanov, J. Exptl. Theoret. Phys. (U.S.S.R.) **31**, 987 (1956), Soviet Phys. JETP **4**, 842 (1957).

[3] Meshkovskii, Pligin, Shalamov, and Shebanov, J. Exptl. Theoret. Phys. (U.S.S.R.) **32**, 1328 (1957), Soviet Phys. JETP **5**, 1085 (1957).

[4] V. M. Sidorov, J. Exptl. Theoret. Phys. (U.S.S.R.) **28**, 727 (1955), Soviet Phys. JETP **1**, 600 (1955).

[5] Meshkovskii, Pligin, Shalamov, and Shebanov, J. Exptl. Theoret. Phys. (U.S.S.R.) **31**, 560 (1956), Soviet Phys. JETP **4**, 404 (1957).

[6] Alpers, Barkov, Gerasimova, Gurevich, Mishakova, Mukhin, and Nikol'skii, J. Exptl. Theoret. Phys. (U.S.S.R.) **30**, 1034 (1956), Soviet Phys. JETP **3**, 735 (1956).

[7] V. M. Sidorov, J. Exptl. Theoret. Phys. (U.S.S.R.) **31**, 178 (1956), Soviet Phys. JETP **4**, 22 (1957).

[8] L. C. L. Yuan and S. J. Lindenbaum, Phys. Rev. **103**, 404 (1956).

[9] Iu. D. Prokoshkin, Symposium CERN (1956), part II, page 385.

[10] B. S. Neganov and O. V. Savchenko, J. Exptl. Theoret. Phys. (U.S.S.R.) **32**, 1265 (1957), Soviet Phys. JETP **5**, 1033 (1957).

[11] J. M. Luttinger, Phys. Rev. **86**, 571 (1952).

[12] Azhgirei, Vzorov, Zrelov, Meshcherakov, and Petrukhin, J. Exptl. Theoret. Phys. (U.S.S.R.) **34**, 1357 (1958), Soviet Phys. JETP **7**, 939 (1958).

[13] A. A. Ansel'm and V. M. Shekhter, J. Exptl. Theoret. Phys. (U.S.S.R.) **33**, 481 (1957), Soviet Phys. JETP **6**, 1376 (1958).

[14] Fernbach, Serber, and Taylor, Phys. Rev. **75**, 1352 (1950).

[15] V. I. Moskalev and B. V. Gavrilovskii, Dokl. Akad. Nauk SSSR **110**, 972 (1956), Soviet Phys. "Doklady" **1**, 607 (1956).

Translated by H. Kasha
291

SOVIET PHYSICS JETP VOLUME 34(7), NUMBER 6 DECEMBER, 1958

ON THE EXISTENCE OF A TANGENTIAL VELOCITY DISCONTINUITY IN THE SUPERFLUID COMPONENT OF HELIUM NEAR A WALL

G. A. GAMTSEMLIDZE

Tiflis State University

Submitted to JETP editor January 20, 1958

J. Exptl. Theoret. Phys. (U.S.S.R.) **34**, 1434-1437 (June, 1958)

The question of the development of a discontinuity in the velocity of the superfluid component of helium II moving relative to a solid wall is investigated experimentally. It has been assumed that the formation of such surface discontinuities requires the application of some minimal force, which is manifested in the form of a threshold shear stress. Apparatus has been constructed which permits the threshold shear stress to be determined with great accuracy. The measurements have shown that tangential discontinuities in the velocity of the superfluid component of helium II do not arise in the vicinity of a wall.

COMPARISON of the results of measurements on the viscosity η_n of the normal component of liquid helium II carried out by means of the oscillating disk method[1,2] on the one hand, and by the method of the uniformly rotating cylinder,[3] on the other, has revealed the existence of a considerable

discrepancy in the magnitude of η_n, especially in the low-temperature region.

In this connection, Ginzburg[4] has advanced a hypothesis regarding the possible occurrence of a tangential discontinuity in the velocity of the superfluid component of helium II at the boundary between the liquid and the wall, as well as the necessity for taking into account a surface energy σ associated with this discontinuity and equal according to his estimates, to between 5×10^{-2} and 5×10^{-3} erg/cm^2.

The effect of this surface energy upon the flow of helium II should, in Ginzburg's opinion, be manifested as a minimal energy σS, required in order to set a solid body of surface area S into motion in the helium II.

The primary purpose of the present work has been to test experimentally the hypothesis outlined above.

DESCRIPTION OF THE APPARATUS

The apparatus (cf. Fig. 1) consists of a system of mica disks 1, each 50 μ thick and 32 mm in diameter. These disks, 45 in number, were arranged parallel to one another along an aluminum shaft 4 mm in diameter, and were separated by aluminum washers 8 mm in diameter and 2 mm thick.

The stack of disks thus assembled was suspended on a straightened glass rod 2 whose upper portion was fitted with a small mirror 3 and a clamp 4, by means of which it was attached to the lower end of a phosphor-bronze fiber 5, 50 μ in diameter and 12 cm long, which served as a suspension.

The upper end of the suspension was connected to a frame 6 by means of a clamp 7. The frame was in the form of a plane parallelopiped made of aluminum foil 1 mm thick; its linear dimensions were $24 \times 10 \times 30$ cm. The frame and disks were in turn suspended together on a copper strip 8 of rectangular cross section, through which current was supplied to a single-layer coil, of 10 turns per centimeter, wound upon the frame.

A spiral spring, fitted into a circular metal seat 9 attached to the cupro-nickel supports 10, served as the second conducting lead. One end of the spring was soldered to the seat, while the other end was fitted by means of a collar to the neck 11 of the clamp 7, which was in electrical contact with the coil. The spiral spring served at the same time to return the frame to its equilibrium position.

A second mirror 12 was cemented to the neck of the clamp, permitting observation of the rotation of the frame as current was passed through it.

The entire suspension system was enclosed within a glass cylinder 13, the lower end of which

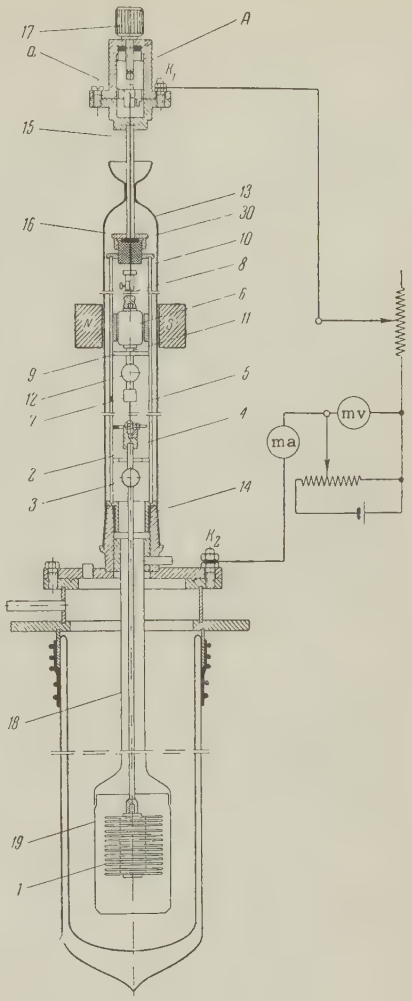

FIG. 1. Diagram of the apparatus.

was ground to fit the cone 14 and the upper to fit the tube 15 of the seal 16.

The disks and the frame were locked by rotation of knob 17 of lock A screwed to the top of the tube 15.

The lower portion of the suspension system (the glass rod and the system of disks) was surrounded by the glass tube 18 and the glass vessel 19 coupled to it, which protected the system from parasitic effects associated with the pumping of the helium vapor.

STATEMENT OF THE PROBLEM

The object of the experiment was to attempt to detect an effect analogous to that of static friction between solid surfaces. In the presence of such an effect the disks should remain stationary, at rest in the helium II, up to some definite angle of twist of the fiber.

Having determined the limiting angle of twist φ_f and knowing the elastic constant f of the fiber, one

could then use the familiar formula $f\varphi_f/2$ for the energy of deformation to determine the desired energy σS.

The disks were made of mica with the object of securing a body of large surface area $S = 720$ cm^2 and a moment of inertia I as small as 8 gm cm^2, in order to satisfy the condition

$$f\varphi^2_{min}/2 \ll \sigma S. \quad (1)$$

The experiment as undertaken made it possible to obtain for the minimum angle of twist of the fiber φ_{min} the value $\varphi_{min} = \Delta n/2L_f = 3.3 \times 10^{-4}$ radians, where L_f is the distance of the scale used for the frame from the corresponding mirror, while $\Delta n = 1$ mm is the minimum deflection of the light spot along the frame scale which could be detected under the conditions of the experiment. We obtained $f = 2.2$ dyne-cm for the torsional constant of the fiber employed, from its given linear dimensions, and $T = 12$ sec for the natural period of oscillation of the system.

The condition for an "infinite" liquid $\lambda < l$ was satisfied in the experiment. Here $\lambda = (2\eta/\rho_n\omega)$ is the penetration depth for the viscous wave and l is the least distance between the surfaces (moving, or moving and stationary) in the system. We assumed for l the minimum value, the distance between the disks, and the values for η and ρ_n were taken from the work of Andronikashvili[1,5] for the temperature of 1.46°K at which the experiment was carried out.

Inserting into the condition (1) the values for f, φ_{min}, and S we obtain $\sigma = 1.7 \times 10^{-10}$ erg/cm^2. This is the smallest value of σ which may be detected with the apparatus used, and is smaller by a factor of 3.5×10^8 than the value proposed by Ginzburg. This shows the high sensitivity of the apparatus, and makes it possible to twist the fiber over a wide range, still keeping the system of disks at rest, if the ideas of Ginzburg are correct.

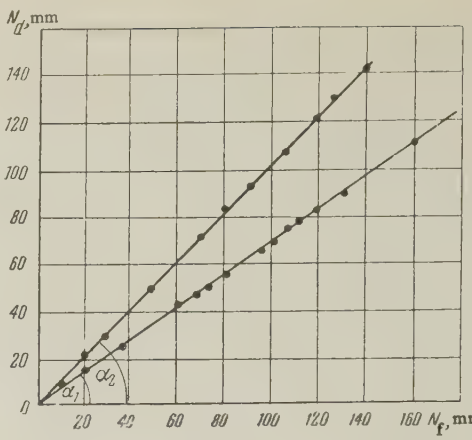

FIG. 2. Calibration curves: $\tan \alpha_1 = \Delta N_d/\Delta N_f = 0.71 \pm 0.007$; $\tan \alpha_2 = \Delta N_d/\Delta N_f = 1.03 \pm 0.01$.

RESULTS OF THE EXPERIMENT

The actual experiment was preceded by the recording of a calibration curve for the apparatus under vacuum; the dependence of the equilibrium orientation of the system of disks in vacuo upon the orientation of the frame was determined. The equilibrium points for the disk system and the frame were found from the positions N_d and N_f of the light spots along the corresponding scales.

Two such curves are given in Fig. 2. The first of these was taken with the scales at approximately equal distances, $L_d = 155 \pm 0.5$ cm and $L_f = 150 \pm 0.5$ cm, and the second when they were at different distances, $L_d = 105 \pm 0.5$ cm and $L_f = 150 \pm 0.5$ cm.

It should be noted that the equation $\Delta N_d/\Delta N_f = L_d/L_f$ is satisfied to within 1%. It can thus be concluded that the mutual orientation of the planes of the mirrors relative to one another under vacuum is maintained as the frame is rotated, and that for deflections of the spot along the scale of 140 to 150 mm the disks rotate through the same angle as the frame to an accuracy of ± 1%.

Following the recording of the calibration curve experiments were carried out in helium II.

The data from the experiments (for $L_d = 155$

Data						Data					
24/XII		18/I		1/II		24/XII		18/I		1/II	
N_f	N_d	N_f	N_d	N_f	N_d	N_f	N_d	N_f	N_d	N_f	N_d
in millimeters						in millimeters					
1	1	1	1	1.5	1	12	12	10	9	10	9.5
2	1	2	2	2.5	2	13	13	12	11	11	11
3	2	3	2	3.5	4	14	14	14	13	11	11
4	4	4	4	5	5	16	16	15	15	13.5	14
5	4	5	4	6	6	17	18	18	17	15	15
7	7	7	6	7.5	7.5	18	19	19	19	16	16
9	9	8	7	8	7.5	19	20	23	23	18	18
11	10	9	8	8.5	8	21	21	28	28	22	21

and $L_f = 150$ cm) are presented in the table; the overall distribution of the data relative to the calibration curve is shown in Fig. 3.

As is evident from Fig. 3, twisting of the fiber causes the disks to follow the rotation of the frame. This circumstance makes it possible to express the opinion that under the conditions of an "infinite" fluid the effect of static friction is not observed in helium II, and, consequently, that no surfaces of tangential discontinuity in the velocity arise at the boundary between a moving solid body and helium II.

If surfaces of discontinuity should in fact arise, then the value of their energy σ must not exceed $\sim 10^{-10}$ erg/cm^2. In this case it is necessary to note that such a value for the energy could on no account explain the existing discrepancies between the values for the viscosity as measured by various methods.[1,3]

In conclusion, the author is deeply grateful to the supervisor of this work, Professor E. L. Andronikashvili, for his valued instructions and advice, to the machinists for the liquefaction machines, I. M. Paramonov and E. I. Shalvashvili, and also to his scientific collaborator B. P. Zhvaniya.

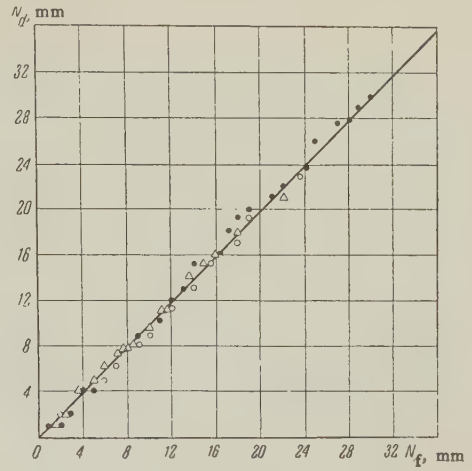

FIG. 3. Dependence of the equilibrium orientation N_d of the disk system upon the orientation N_f of the frame; i.e., the angle of twist of the fiber. Solid line – calibration curve. ● – measurements of 24 Dec., 1956; ○ – measurements of 18 Jan., 1957, Δ – measurements of 1 Feb., 1957.

[1] E. L. Andronikashvili, J. Exptl. Theoret. Phys. (U.S.S.R.) **18**, 429 (1948).

[2] A. C. Hollis-Hallett, Proc. Roy. Soc. (London) **210**, 409 (1952).

[3] A. C. Hollis-Hallett, Proc. Cambridge Phil. Soc. **49**, 717 (1953).

[4] V. L. Ginzburg, J. Exptl. Theoret. Phys. (U.S.S.R.) **29**, 244 (1955), Soviet Phys. JETP **2**, 170 (1956).

[5] E. L. Andronikashvili, J. Exptl. Theoret. Phys. (U.S.S.R.) **18**, 424 (1948).

Translated by S. D. Elliott
292

INTERACTION BETWEEN ELECTRONS AND LATTICE VIBRATIONS IN A NORMAL METAL

A. B. MIGDAL

Moscow Institute of Engineering Physics

Submitted to JETP editor July 12, 1957; resubmitted March 20, 1958

J. Exptl. Theoret. Phys. (U.S.S.R.) **34**, 1438-1446 (June, 1958)

A method is developed which enables one to obtain the electron-energy spectrum and dispersion of the lattice vibrations without assuming that the interaction between electrons and phonons is small.

1. INTRODUCTION

THE attraction between electrons due to the exchange of phonons leads in superconductors to the formation of a bound state of two electrons with opposite momenta. In the ground state of a superconductor a condensed component consisting of these bound electrons is formed and a gap results in the energy spectrum.[1]

In papers on the theory of superconductivity[1] the interaction between electrons and lattice vibrations has been assumed to be small, although we know that this condition is not fulfilled for all superconductors. It is therefore of interest to construct a theory which is not limited in this way.

In the present paper we develop a method which enables one to consider the interaction between electrons and lattice vibrations in a normal metal without assuming that the interaction is small. The method is based on the use of quantum field-theoretical equations.

The application of field theory to superconductors involves certain difficulties. The state which contains the "condensate" of bound electrons cannot be obtained from the ground state of noninteracting particles by applying the interaction adiabatically. The necessary condition for the use of ordinary field-theoretical methods is thus violated. The method developed below for a normal metal, where this difficulty does not occur, can therefore be extended to a superconductor only through a separate investigation.

The interaction between electrons and lattice vibrations in a normal metal is certainly of interest in itself. Fröhlich[2] used perturbation theory to investigate this interaction. He considered an isotropic model of a metal described by the Hamiltonian

$$H = H_0 + H_1,\ H_0 = \sum_{\mathbf{p}} \varepsilon_{\mathbf{p}}^0 a_{\mathbf{p}}^+ a_{\mathbf{p}} + \sum_{q<q_m} \omega_{\mathbf{q}}^0 b_{\mathbf{q}}^+ b_{\mathbf{q}},$$
$$H_1 = \sum_{\mathbf{p},\, q<q_m} \alpha_{\mathbf{q}} a_{\mathbf{p}+\mathbf{q}}^+ a_{\mathbf{p}} (b_{\mathbf{q}} + b_{-\mathbf{q}}^+), \qquad (1)$$

where $a_{\mathbf{p}}$, $a_{\mathbf{p}}^+$ and $b_{\mathbf{q}}$, $b_{\mathbf{q}}^+$ are the annihilation and creation operators of electrons and phonons and q_m is the maximum phonon momentum. We know that $\alpha_{\mathbf{q}}^2$, which determines the interaction between electrons and phonons, is given for small q (in atomic units) by

$$\alpha_q^2 = (\lambda_0 \pi^2 / p_0)\, \omega_q^0,\ \omega_q^0 = c_0 q, \qquad (2)$$

where c_0 is the unrenormalized velocity of sound, $c_0 \sim M^{-1/2}$, M is the mass of an ion and λ_0 is a dimensionless parameter, introduced by Fröhlich,[2] which does not contain the ion mass; $\lambda_0 \lesssim 1$.

It will be shown below that the energy spectrum of the Hamiltonian (1) cannot be obtained by perturbation theory, despite the smallness of the parameter $M^{-1/2}$ in $\alpha_{\mathbf{q}}^2$. The criterion for the applicability of perturbation theory is the smallness of λ_0, which does not contain the ion mass. Field theoretical methods[3] enable us to obtain the energy spectrum, without assuming that λ_0 is small, as a power series in $M^{-1/2}$.

2. METHOD OF SOLUTION

We introduce the electron and phonon propagation functions G and D:

$$G = i \langle T\Psi(1)\, \Psi^+(2) \rangle,\ D = i \langle T\varphi(1)\, \varphi(2) \rangle, \qquad (3)$$

where the averaging is performed over the ground state of the system

$$\varphi = e^{iHt} \sum_{q<q_m} (b_{\mathbf{q}} + b_{-\mathbf{q}}^+)\, e^{i\mathbf{q}\mathbf{r}} \alpha_{\mathbf{q}} e^{-iHt},$$
$$\Psi = e^{iHt} \sum_{\mathbf{p}} a_{\mathbf{p}} e^{i\mathbf{p}\mathbf{r}} e^{-iHt}.$$

Dyson's equations relate D and G to the vertex

part Γ, which is defined by the following set of diagrams:

(4)

Here $q = (\mathbf{q}, \omega)$ and $p = (\mathbf{p}, \epsilon)$. The interaction energy in (1) can be written in the form

$$H_1 = \sum_{\substack{\mathbf{p} \\ q<q_m}} \Psi^+_{\mathbf{p}+\mathbf{q}} \Psi_{\mathbf{p}} \varphi_{\mathbf{q}},$$

where $\Psi_{\mathbf{p}}$ and $\varphi_{\mathbf{q}}$ are spatial Fourier components of the operators in the Green's functions. Therefore the first diagram in (4) corresponds to $\Gamma = \Gamma_0 = 1$. It will be shown below that the following terms in (4) are of the order of $M^{-1/2}$. Therefore Γ can be replaced by 1 in Dyson's equations, after which a closed system of equations is obtained for D and G. In the momentum representation Dyson's equations are

$$\begin{aligned} G(p) &= G_0(p) + G_0(p)\,\Sigma(p)\,G(p), \\ \Sigma(p) &= \frac{1}{i}\int G(p-q)\,D(q)\,\Gamma\left(p-\frac{q}{2}, q\right) d^4q, \\ D(q) &= D_0(q) + D_0(q)\,\Pi(q)\,D(q), \\ \Pi(q) &= \frac{1}{i}\int G\left(p+\frac{q}{2}\right) G\left(p-\frac{q}{2}\right)\Gamma(p,q)\,d^4p, \end{aligned} \tag{5}$$

where

$$d^4p = d\mathbf{p}\,d\varepsilon/(2\pi)^4, \quad d^4q = d\mathbf{q}\,d\omega/(2\pi)^4,$$

Σ and Π are the irreducible parts of the electron and phonon self energies, and D_0 and G_0 are the electron and phonon Green's functions in the absence of interaction:[2]

$$\begin{aligned} G_0(p) &= \frac{1}{\varepsilon^0_{\mathbf{p}} - \varepsilon - i\Delta(p)}, \\ D_0(q) &= \alpha_q^2\left\{\frac{1}{\omega_q^0 - \omega - i\delta} + \frac{1}{\omega_q^0 + \omega - i\delta}\right\}, \end{aligned} \tag{6}$$

where

$$\Delta(p) \to \begin{cases} +0 & p > p_0, \\ -0 & p < p_0 \end{cases}, \quad \delta \to +0.$$

Assuming $\Gamma = 1$ in (5), we obtain G and D. As was shown in reference 3, the energy spectrum is determined by the poles of the analytic continuation of $G(\mathbf{p}, \epsilon)$ and $D(\mathbf{q}, \omega)$ in the complex plane.

3. THE VERTEX PART

We shall show that the vertex part differs from $\Gamma_0 = 1$ by a quantity of the order of $M^{-1/2}$. Let us consider a first-order perturbation correction to Γ.

We shall assume that

$$p \sim p_0, \ \varepsilon \sim \mu_0, \ \omega \lesssim \omega_q|_{q=2p_0} = \omega_0,$$

since for our further calculations this is the important range of values of p and ω. From our definition of G and D each internal line of the diagrams corresponds to a Green's function divided by i. We obtain

$$\Gamma_1(p, q) = i\int D_0(p - p_1)\, G_0\left(p_1 + \frac{q}{2}\right) G_0\left(p_1 - \frac{q}{2}\right) dp_1. \tag{7}$$

In accordance with (6), the function $D_0(\mathbf{p} - \mathbf{p}_1, \epsilon - \epsilon_1)$ possesses the following properties:

When $|\mathbf{p} - \mathbf{p}_1| \sim p_0$ and $\epsilon - \epsilon_1 \ll \omega_0$, D_0 can be replaced by

$$D_0 = 2\pi^2\lambda_0/p_0.$$

When $\epsilon - \epsilon_1 \gg \omega_0$, D_0 diminishes as $(\epsilon - \epsilon_1)^{-2}$. For $|\mathbf{p}_1 - \mathbf{p}| > q_m$, $D_0 = 0$. Using these properties of D_0, we obtain for Γ_1:

$$\Gamma_1 \sim \frac{\lambda_0 i}{8\pi^2 p_0} \int_{\varepsilon-\omega_0/2}^{\varepsilon+\omega_0/2} d\varepsilon_1 \int_{|\mathbf{p}-\mathbf{p}_1|<q_m} G_0\left(\mathbf{p}_1 + \frac{\mathbf{q}}{2}, \varepsilon_1 + \frac{\omega}{2}\right) \times G_0\left(\mathbf{p}_1 - \frac{\mathbf{q}}{2}, \varepsilon_1 - \frac{\omega}{2}\right) d\mathbf{p}_1. \tag{8}$$

Integration with respect to ϵ_1 gives the factor $\omega_0 \sim M^{-1/2}$ and leads to

$$\Gamma_1 \sim \lambda_0\omega_0/p_0^2 \sim \lambda_0/\sqrt{M},$$

if integration over p_1 does not introduce factors $\sim 1/\omega_0$. Such factors result only for small $q \lesssim \omega_0/p_0$ and $\omega < \omega_0$, when the two poles of the integrand approach each other. Then the integrand has a maximum near $p_1 = g$, where g is given by $\epsilon^0_g = \epsilon_1 \simeq \epsilon$ and thus $g \sim p_0$. Integration over regions far from this maximum does not introduce factors $\sim 1/\omega_0$. We can therefore limit ourselves to consideration of the integral over p_1 in the region $(p_1 - g)/g \ll 1$. Using (6) and the notation $\epsilon^0_{p_1} - \epsilon = E$, we obtain from (8)

$$\Gamma_1 \sim i\lambda_0 p_0 \int_{\varepsilon-\omega_0/2}^{\varepsilon+\omega_0/2} d\varepsilon_1 \int_{-1}^{1} dx \int_{-\infty}^{\infty} dE \Big/ \left[E + \frac{v_g q x}{2} - \frac{\omega}{2} - i\Delta\left(\varepsilon_1 + \frac{\omega}{2}\right)\right]\left[E - \frac{v_g q x}{2} + \frac{\omega}{2} - i\Delta\left(\varepsilon_1 - \frac{\omega}{2}\right)\right].$$

For simplicity it is assumed here that $q_m > p + g$, and the condition $|\mathbf{p}-\mathbf{p}_1| < q_m$ imposes no limitation on integration near $p_1 = g$.

Integration with respect to E gives

$$\Gamma_1 \sim \lambda_0 p_0 \int_{\varepsilon-\omega_0/2}^{\varepsilon+\omega_0/2} d\varepsilon_1 \int_{-1}^{1} dx \frac{\theta(\varepsilon_1-\mu_0+\omega/2)-\theta(\varepsilon_1-\mu_0-\omega/2)}{v_g q x-\omega+i\delta\omega/|\omega|},$$

where

$$\theta(y)=\begin{cases}1 & y\geqslant 0\\ 0 & y<0\end{cases}, \qquad v_g=\frac{\partial\varepsilon_g^0}{\partial g}.$$

Integrating with respect to x, we obtain

$$\Gamma_1 \sim \frac{\lambda_0}{p_0 q}\left[\ln\left|\frac{v_g q+\omega}{v_g q-\omega}\right| - i\pi\theta(v_g q-|\omega|)\right] \times \int_{\varepsilon-\mu_0-\omega_0/2}^{\varepsilon+\omega_0/2-\mu_0}\left[\theta\left(t+\frac{\omega}{2}\right)-\theta\left(t-\frac{\omega}{2}\right)\right]dt. \qquad (9)$$

The last integral differs from zero in the region $|\epsilon-\mu_0| \lesssim \omega_0$ and is of the order of ω_1, where ω_1 is the smaller of the numbers ω_0 and ω. It follows from (9) that the largest value $\Gamma_1 \sim \lambda_0$ is reached for $\omega \sim \omega_0$ and $q \sim \omega_0/p_0$. These values of q and ω play no part in our subsequent calculations. Indeed, for the calculation of $\Sigma(p)$ according to (5) the essential values are $q \sim p_0$ and $\omega \sim \omega_0$, for which it follows from (8) that $\Gamma_1 \sim M^{-1/2}$. For obtaining $\Pi(q)$ the essential values are $\omega \sim \omega_q \sim qp_0/\sqrt{M} \ll p_0 q$ (ω_q is the frequency of a phonon of momentum q). From (9) we obtain

$$\Gamma_1 \sim \lambda_0 \frac{\omega}{p_0 q}\left[\frac{\omega}{2v_g q}-i\pi\right] \sim \frac{\lambda_0}{M}+i\frac{\lambda_0}{\sqrt{M}}.$$

We thus have $\Gamma = 1 + O(M^{-1/2})$. It can be shown that this estimate is not changed when diagrams of a higher order are taken into account.

4. THE PHONON GREEN'S FUNCTION

As will be seen from our subsequent calculations, $G(\mathbf{p}, \epsilon)$ differs essentially from $G_0(\mathbf{p}, \epsilon)$ only in a narrow range of values of p and ϵ: $|\mathbf{p}-\mathbf{p}_0| \sim \omega_0/p_0$; $\epsilon - \epsilon_0^0 \sim \omega_0$. In the calculation of $\Pi(q, \omega)$ according to (5) the integration is performed over a wide range of the variables, which permits us to replace G by G_0 accurately to terms $\sim M^{-1/2}$. For $\Pi(\mathbf{q}, \omega)$ we obtain from (5)

$$\Pi(\mathbf{q},\omega) \approx \frac{1}{i}\int G_0\left(p+\frac{q}{2}\right)G_0\left(p-\frac{q}{2}\right)d^4p. \qquad (10)$$

Integration of (10) with respect to ϵ gives

$$\Pi(\mathbf{q},\omega)=\frac{1}{(2\pi)^3}\int\frac{n(\mathbf{p}-\mathbf{q}/2)-n(\mathbf{p}+\mathbf{q}/2)}{\varepsilon^0_{\mathbf{p}+\mathbf{q}/2}-\varepsilon^0_{\mathbf{p}-\mathbf{q}/2}-\omega-i\delta\omega/|\omega|}d^3p, \qquad (11)$$

where

$$n(p)=\begin{cases}1 & p>p_0\\ 0 & p<p_0.\end{cases}$$

We see from (10) and (11) that $\Pi(\mathbf{q}, \omega)$ is an even function of ω. For subsequent calculations the important values of $\Pi(\mathbf{q}, \omega)$ are obtained for

$$\omega \sim \omega_q \sim p_0 q/\sqrt{M} \ll p_0 q.$$

With these values of ω we have from (11)

$$\Pi(\mathbf{q},\omega)=\frac{p_0}{(2\pi)^2}\left[g\left(\frac{q}{2p_0}\right)+\pi i\frac{|\omega|}{2p_0 q}\right], \qquad (12)$$

where

$$g(x)=\frac{1}{2}\left[1+\frac{1-x^2}{2x}\ln\left|\frac{1+x}{1-x}\right|\right]. \qquad (13)$$

g(x) can be represented in the interval $0 < x < 1$ with sufficient accuracy by

$$g(x)\approx 1-x^2/2. \qquad (13')$$

From (2), (5) and (12) we obtain

$$D(\mathbf{q},\omega)=\frac{1}{D_0^{-1}(q,\omega)-\Pi(\mathbf{q},\omega)} = \frac{2\omega_q^0\alpha_q^2}{\left[(\omega_q^0)^2-\omega^2-(\omega_q^0)^2\lambda_0\left(g\left(\frac{q}{2p_0}\right)+i\pi\frac{|\omega|}{2p_0 q}\right)\right]}.$$

The real part of the pole of $D(\mathbf{q}, \omega)$ gives the renormalized phonon frequency

$$\omega_q^2=(\omega_q^0)^2\left[1-\lambda_0 g\left(\frac{q}{2p_0}\right)\right]\approx(\omega_q^0)^2\left(1-\lambda_0+\lambda_0\frac{q^2}{8p_0^2}\right). \qquad (14)$$

Eq. (13′) was used in the derivation of this last equation. The imaginary part of the pole gives the phonon attenuation

$$\delta_1(q)=1/4\pi\lambda_0(\omega_q^0)^2/p_0 q. \qquad (15)$$

The relative attenuation is given by

$$\delta_1(q)/\omega_q=\lambda_0(\omega_q^0)^2\pi/4p_0 q\omega_q \sim \lambda_0/\sqrt{M} \ll 1.$$

From (14) and (15)

$$D(\mathbf{q},\omega)=\alpha_q^2\frac{\omega_q^0}{\omega_q}\left(\frac{1}{\omega_q-\omega-i\delta_1(q)\omega/|\omega|} + \frac{1}{\omega_q+\omega-i\delta_1(q)\omega/|\omega|}\right). \qquad (16)$$

Thus the phonon Green's function D, which was obtained by taking the interaction with electrons into account, differs from D_0 through replacement of the frequencies ω_q^0 by $\omega_q - i\delta_1(q)$ and the occurrence of the renormalizing factor ω_q^0/ω_q.

5. THE ELECTRON GREEN'S FUNCTION

From (5) we have

$$G = 1/[\varepsilon_p^0 - \varepsilon - \Sigma(\mathbf{p},\varepsilon)], \tag{17}$$

$$\Sigma(\mathbf{p},\varepsilon) = \frac{1}{i(2\pi)^4} \int\limits_{|\mathbf{p}-\mathbf{p}_1|<q_m} D(\mathbf{p}-\mathbf{p}_1, \varepsilon-\varepsilon_1)\, d\mathbf{p}_1\, d\varepsilon_1 / [\varepsilon_{p_1}^0 - \varepsilon_1 - \Sigma(\mathbf{p}_1, \varepsilon_1)]. \tag{18}$$

G will now be obtained by solving the integral equation (18).

It is easily seen that $\Sigma(\mathbf{p}, \epsilon) \sim \omega_0$, so that G differs essentially from G_0 only for $|\epsilon_p^0 - \epsilon| \sim \omega_0$. The relative change of the excitation energy is large only for $\epsilon_p^0 - \mu_0 \sim \omega_0$. Thus the electron excitation spectrum varies appreciably only close to the Fermi surface in the range $p - p_0 \sim \omega_0/p_0$.

We introduce the notation

$$(\varepsilon_p^0 - \mu_0)/\omega_0 = \xi, \quad (\varepsilon - \mu)/\omega_0 = \eta,$$
$$\Sigma(\xi, \eta) = \Sigma(0, 0) + \omega_0 f(\xi, \eta), \tag{19}$$

where

$$\mu = \mu_0 + \Sigma(0,0),$$
$$\omega_0 = \omega_q|_{q=2p_0} = \omega_{2p_0}^0\left(1 - \frac{\lambda_0}{2}\right). \tag{19'}$$

As was shown in reference 3, the imaginary part of $\Sigma(\xi, \eta)$ must vanish for any value of ξ when ϵ equals the chemical potential.

As will be shown below $\Sigma(0, 0)$ is real. Therefore

$$\operatorname{Im}\Sigma(0, \eta) = \omega_0 \operatorname{Im} f(0, \eta);$$

since according to (19)

$$f(0, \eta)|_{\eta=0} = 0$$

and thus Im Σ vanishes for $\epsilon = \mu$ (μ is the chemical potential).

In the notation of (19) and (19') G becomes

$$G(\xi, \eta) = \frac{1}{\omega_0} \frac{1}{\xi - \eta + f(\xi, \eta)}. \tag{20}$$

From the foregoing discussion we are interested in ξ and $\eta \sim 1$.

In (19) we pass from integration over the angles of the vector $\mathbf{p}_1$ to integration over $q = |\mathbf{p} - \mathbf{p}_1|$: $q\,dq = pp_1\,dx$, where x is the cosine of the angle between $\mathbf{p}$ and $\mathbf{p}_1$. We have

$$\Sigma(\mathbf{p},\varepsilon) = \frac{1}{i(2\pi)^3 p} \int\limits_{-\infty}^{\infty} d\omega \int\limits_{|p-p_1|<q<p+p_1;\ q<q_m} q\,dq\,p_1\,dp_1$$
$$\times D(q,\omega)/[\varepsilon_{p_1}^0 - \varepsilon - \omega - \Sigma(p_1, \varepsilon+\omega)], \tag{21}$$

or

$$\Sigma(p, \varepsilon) = \frac{1}{(2\pi)^3\, ip} \int\limits_{-\infty}^{\infty} d\omega \int\limits_{0}^{q_m} q\,dq D(q, \omega)$$
$$\times \int\limits_{|p-q|}^{p+q} p_1\,dp_1/[\varepsilon_{p_1}^0 - \varepsilon - \omega - \Sigma(p_1, \varepsilon+\omega)]. \tag{21'}$$

As mentioned previously, values of p close to p_0 are of interest, so that $(p - p_0)/p_0 \sim 1/\sqrt{M}$. Therefore in the right-hand side of (21) p can be replaced by p_0 accurately to within $M^{-1/2}$. We divide the integration over p_1 into two regions defined by

$$1)\ |\xi_1| = |\varepsilon_{p_1}^0 - \mu_0|/\omega_0 \leqslant \gamma \text{ and } 2)\ |\xi_1| > \gamma,$$

where γ lies between the following limits:

$$1 \ll \gamma \ll 1/\nu, \quad \nu = \omega_0/p_0 \sim 1/\sqrt{M}. \tag{22}$$

In the integral over region 1 $\Sigma(p, \epsilon)$ in the integrand can be replaced by $\Sigma(p_0, \epsilon+\omega)$ accurately to within $\sim M^{-1/2}$.

We note that for $q_m > 2p_0$ region 1 exists only for $q < 2p_0$. Therefore for the integration over p_1 in (21), in the term corresponding to region 1 the integration over q is carried as far as the smaller of the quantities q_m and $2p_0$.

Since $D(q, \omega)$ for $\omega \gg \omega_0$ vanishes as ω^{-2}, in the integral of (21) the essential result is found for $\omega \sim \omega_0$, and for integration in region 2 we can neglect $\epsilon - \mu_0$ and $\Sigma(p_1, \epsilon+\omega)$ in the denominator of the integrand compared with $\epsilon_{p_1}^0 - \mu_0$, with accuracy $\sim 1/\gamma$. Therefore integration over the region $|\xi_1| > \gamma$ introduces into Σ a term which is independent of p and ϵ. This term is $\Sigma(0, 0) = \mu - \mu_0$, since integration over the region $|\xi_1| < \gamma$ yields an expression which vanishes for $\eta = 0$.

Therefore the change of the chemical potential is given by

$$\mu - \mu_0 = \Sigma(0, 0)$$
$$= \frac{1}{ip(2\pi)^3} \int\limits_{-\infty}^{\infty} d\omega \int\limits_{0}^{q_m} q\,dq D(q,\omega) \int\limits_{|p_0-q|}^{p_0+q} \frac{p_1\,dp_1}{\varepsilon_{p_1}^0 - \mu_0}. \tag{23}$$

The integral over p_1 in (23) is taken in the sense of the principal value, which corresponds to dropping of the region $|\xi_1| < \gamma$, which is small compared with the essential region of integration.

Subtracting $\Sigma(0, 0)$ from the left and right members of (21) and dividing by ω_0, we obtain an integral equation for $f(0, \eta) = f(\eta)$:

$$f(\eta) = \frac{1}{ip(2\pi)^3} \int\limits_{-\infty}^{\infty} d\eta' \int\limits_{-\gamma}^{\gamma} d\xi_1 \int\limits_{0}^{q_1} \frac{D(q, \omega_0\eta')\, q\,dq}{\xi_1 - \eta - \eta' - f(\eta+\eta')}, \tag{24}$$

where q_1 is the smaller of the numbers q_m and $2p_0$. Here terms $\nu\xi, \nu\xi_1 \ll 1$ have been dropped.

Since the essential values in (24) are $\eta' \ll \gamma$ the limits with respect to ξ_1 can be replaced by $\pm\infty$.

Integration over ξ_1 gives

$$\lim_{\gamma\to\infty}\int_{-\gamma}^{\gamma}\frac{d\xi_1}{\xi_1-\varphi(\eta,\eta')}=\pi i\,\mathrm{Sgn}\,\mathrm{Im}\,\varphi(\eta,\eta')=\pi i\,\mathrm{Sgn}\,f_1(\eta+\eta'),$$

where f_1 denotes the imaginary part of f. As was shown in reference 2, the imaginary part of the Green's function, and thus $f_1(\eta)$, reverses its sign for $\eta = 0$; moreover, $f_1(\eta) > 0$ for $\eta > 0$. Therefore

$$\mathrm{Sgn}\,f_1(\eta)=\mathrm{Sgn}\,\eta.$$

Inserting these results in (24), we obtain

$$f(\eta)=\frac{1}{8\pi^2p_0}\int_0^{q_1}q\,dq\int_0^{\infty}\mathrm{Sgn}(\eta+\eta')\,D(q,\omega_0\eta')\,d\eta'$$
$$=\frac{1}{8\pi^2p_0}\int_0^{q_1}q\,dq\int_{-\eta}^{\eta}D(q,\omega_0\eta')\,d\eta'.$$

We use the notation

$$f(\eta)=f_0(\eta)+if_1(\eta).$$

For f_0 and f_1 we obtain

$$f_0=\frac{\alpha_q^2}{8\pi^2p_0\omega_q^0}\int_0^{q_1}q\,dq\int_{-\eta}^{\eta}(\omega_q^0)^2\,\frac{2}{\omega_q^2-\omega_0^2\eta'^2}\,d\eta', \quad (25a)$$

$$f_1=\frac{\alpha_q^2}{8\pi^2p_0\omega_q^0}\,2\pi\int_0^{q_1}(\omega_q^0)^2\,q\,dq\int_{-\eta}^{\eta}\frac{2\delta_1(q)\,|\eta'|\,\omega_0}{(\omega_q^2-\omega_0^2\eta'^2)^2+4\delta_1^2\omega_0^2\eta'^2}\,\frac{d\eta'}{\pi}. \quad (25b)$$

It is easily seen that for $\eta \gg 1/\sqrt{M}$ the integrand with respect to η' in (25b) can be replaced by $\delta(\omega_q - \omega_0\eta')$. Using the notation $x = q/2p_0$ and integrating over η', we obtain

$$f_0=\lambda_0\int_0^{x_1}x\,dx\,\frac{(\omega_q^0)^2}{\omega_0\omega_q}\ln\left|\frac{\eta+\omega_q/\omega_0}{\eta-\omega_q/\omega_0}\right|,$$
$$f_1=\pi\lambda_0\int_0^{y}x\,dx\,\frac{(\omega_q^0)^2}{\omega_0\omega_q}. \quad (26)$$

Here $x_1 = q_1/2p_0$, $y = g/2p_0$, where g is given by the condition $\omega_g = \omega_0\eta$ for $|\eta| < 1$ and $y = x_1$ for $|\eta| > 1$.

We introduce the variable $t = \omega_q/\omega_0$. According to (14) and (19′), t is related to x by

$$t^2=\frac{1}{1-\lambda_0/2}x^2\left(1-\lambda_0+\frac{\lambda_0}{2}x^2\right).$$

For f_0 we obtain

$$f_0=\int_0^1 dt\,\ln\left|\frac{t+\eta}{t-\eta}\right|\left(1-\frac{a}{\sqrt{a^2+t^2}}\right),\quad a^2=\frac{(1-\lambda_0)^2}{\lambda_0(2-\lambda_0)}, \quad (27)$$

For $\eta \ll 1$ we have

$$f_0(\eta)=2\eta\ln\frac{1-\lambda_0/2}{1-\lambda_0}=\lambda\eta. \quad (28)$$

The imaginary part, $f_1(\eta)$, is

$$f_1(\eta)=\pi\int_0^{t_1}\left[1-\frac{a}{\sqrt{a^2+t^2}}\right]dt=\pi\left\{t_1-a\ln\frac{t_1+\sqrt{a^2+t_1^2}}{a}\right\}, \quad (29)$$

where $t_1 = \eta$ for $|\eta| < 1$ and $t_1 = 1$ for $|\eta| > 1$; for $M^{-1/2} \ll \eta \ll 1$ we obtain

$$f_1(\eta)=\frac{\pi\eta^3}{6a^2}=\frac{\pi\lambda_0(2-\lambda_0)}{6(1-\lambda_0)^2}\eta^3. \quad (30)$$

For $\eta \ll 1/\sqrt{M}$ in the denominator of the integrand of (25b) η' can be neglected. This gives

$$f_1=\lambda_0^2\frac{\omega_0}{4p_0^2}\int_0^{x_1}\frac{dx}{[1-\lambda_0 g(x)]^2}\,\eta\,|\eta|. \quad (31)$$

The attenuation of the electron excitations given by (30) results from the emission of phonons. When the energy of a quasi-particle is very close to the Fermi surface ($\eta \ll M^{-1/2}$), a different attenuation mechanism is more important; this is attenuation due to the interaction between electrons, which results from phonon exchange. As mentioned above, interelectronic interaction leads to attenuation which is proportional to the square of the short distance from the Fermi surface, as follows from (31).

The electron energy spectrum is determined by the poles of G, that is, by the condition

$$\eta+f(\eta)=\xi. \quad (32)$$

For small η we have

$$\eta(\xi)\approx\xi/(1+\lambda).$$

Returning to the usual notation and subtracting the energy of a hole, we obtain for the excitation energy

$$E_{p_1p_2}=\varepsilon_{p_2}-\varepsilon_{p_1}=(\varepsilon_{p_2}^0-\varepsilon_{p_1}^0)/(1+\lambda)$$
$$=v_0^0(p_2-p_1)/(1+\lambda)=v_0(p_2-p_1), \quad (33)$$

where $p_2 > p_0$, $p_1 < p_0$ and v_0^0 is the unrenormalized velocity on the Fermi surface. Renormalization of the velocity on the Fermi surface is given by

$$v_0=\frac{v_0^0}{1+\lambda};\quad \lambda=2\ln\frac{1-\lambda_0/2}{1-\lambda_0}. \quad (34)$$

For $\lambda_0 \ll 1$ we obtain from (34)

$$v_0=v_0^0(1-\lambda_0).$$

This equation agrees with the result that Fröhlich obtained by using perturbation theory.

Equation (34) shows that $v_0 > 0$ for all values of λ, and the rearrangement of the Fermi distribution which Fröhlich predicted does not occur.

It follows from (30) that for $\lambda_0 \sim 1$ the excitation attenuation equals the excitation energy in order of magnitude for $\eta \sim 1$, i.e., for the excitation energy

$$E_{p_1 p_2} \sim \omega_0.$$

With further increase of the excitation energy, the attenuation ceases to increase and becomes smaller than the excitation energy. Thus for $\lambda_0 \sim 1$ electron excitations in the region $E_{p_1 p_2} \sim \omega_0$ cannot be described by means of quasi-particles.

[1] L. N. Cooper, Phys. Rev. **104**, 1189 (1956); Bardeen, Cooper and Schrieffer, Phys. Rev. **106**, 162 (1957); N. N. Bogoliubov, J. Exptl. Theoret. Phys. (U.S.S.R.) **34**, 58 (1958), Soviet Phys. JETP **7**, 41 (1958); L. P. Gor'kov, J. Exptl. Theoret. Phys. (U.S.S.R.) **34**, 735 (1958), Soviet Phys. JETP **7**, 505 (1958).

[2] H. Fröhlich, Phys. Rev. **79**, 845 (1950).

[3] V. M. Galitskii and A. B. Migdal, J. Exptl. Theoret. Phys. (U.S.S.R.) **34**, 139 (1958), Soviet Phys. JETP **7**, 96 (1958).

Translated by I. Emin
293

SOVIET PHYSICS JETP VOLUME 34 (7), NUMBER 6 DECEMBER, 1958

COOLING OF AIR BY RADIATION
II. STRONG COOLING WAVE

Ia. B. ZEL'DOVICH, A. S. KOMPANEETS, and Iu. P. RAIZER

Institute of Chemical Physics, Academy of Sciences, U.S.S.R.

Submitted to JETP editor December 20, 1957

J. Exptl. Theoret. Phys. (U.S.S.R.) **34**, 1447-1454 (June, 1958)

Radiation-cooling wave of air accompanied by a large temperature drop, is considered. It is shown that, the radiation is always from the lower edge of the wave, regardless of the value of the upper temperature, and that the radiation transfer inside a strong wave has the character of radiant heat conduction. The strong-wave mode with adiabatic cooling is considered.

In the first part of this work (reference 1)* we have described qualitatively the cooling of a large volume of hot air by radiation. We have found in this case that a unique temperature profile is developed in the air in the form of a step or a cooling wave (CW) propagating towards the hotter air. The air in the wave cools down from a high temperature T_1 to a lower temperature T_2. At the lower temperature T_2 the air becomes transparent, i.e., stops absorbing and emitting radiation.

In reference 1 we have considered the limiting case of a weak CW, in which the upper and lower temperatures T_1 and T_2 are not greatly different, and consequently the flux from the CW is close enough to either σT_1^4 or to σT_2^4. In this article we present the theory of a strong CW, in which the upper temperature can be unlimited. The fundamental problem consists obviously of determining the radiation flux from the front of the CW to infinity. Another problem is to find the temperature distribution in the front of the CW.

*Henceforth, when referring to the formulas of the first part of this article, we shall precede the number of the formula by I [e.g. (I.4), (I.10)].

1. DETERMINATION OF THE RADIATION FLUX FROM THE FRONT OF THE COOLING WAVE

It was indicated in reference 1 that to find the stationary mode of the CW it is necessary to employ one of two procedures. In the first we introduce a constant adiabatic-cooling term into the energy equation. In the second we determine at the very outset the transparency temperature T_2, using formula (I.4). We then assume that when

$T < T_2$ the air is absolutely transparent ($l = \infty$), thereby excluding from consideration the region of air already cooled by the radiation, which absorbs the light rather weakly.

The first procedure gives a more complete picture of the temperature distribution, since it permits an investigation of the course of the temperature in the cooled air and accounts for the absorption of light in this air. It leads, however, to excessive mathematical complications in the analysis of the temperature profile inside the CW (i.e., at temperatures above the transparency temperature) and in the determination of the flux from the front of the CW. Meanwhile, adiabatic cooling plays a very insignificant role inside the CW. It is therefore preferable to consider the internal structure of the CW by using the second procedure. Here the energy equation (I.6) becomes

$$u\rho_1 c_p \frac{dT}{dx} + \frac{dS}{dx} = 0 \quad \text{or} \quad u\rho_1 c_p \frac{dT}{d\tau} + \frac{dS}{d\tau} = 0, \tag{1}$$

and its integral becomes

$$u\rho_1 c_p (T_1 - T) = S. \tag{2}$$

Referring (2) to the lower edge of the CW, we obtain an equation for the energy balance in the CW

$$u\rho_1 c_p (T_1 - T_2) = S_2. \tag{3}$$

The most general considerations show that the flux S_2 from the front of the CW can be bounded both from above and from below.

Let us consider the lower edge of the CW, where the temperatures are close to T_2. According to the condition assumed by us, the air is not cooled at any point of the wave to a temperature below T_2, for it stops absorbing and radiating light when $T < T_2$. Consequently, once it reaches a temperature T_2, the air cannot be cooled further, so that T_2 is the lowest of all possible temperatures in the wave. Therefore, $dT/d\tau \geq 0$ at the edge of the CW, and from (1) we have $dS/d\tau \leq 0$. It follows from (I.11) that the radiation density at the edge of the CW is less than the equilibrium value, $U_{eq2} = 4\sigma T_2^4/c$. Therefore, in the diffusion approximation, the effective temperature of the radiation going to "infinity" from the boundary of the CW is determined by the formula

$$S_2 = \sigma T_{\text{eff}}^4 \tag{4}$$

and cannot be lower than the lowest temperature T_2 in the CW. Consequently, the flux S_2 and the effective temperature T_{eff} remain within very narrow limits:

$$\sigma T_2^4 < S_2 < 2\sigma T_2^4; \tag{5}$$

$$T_2 < T_{\text{eff}} < \sqrt[4]{2}\, T_2. \tag{6}$$

Thus, regardless of the amplitude of the CW, which can be characterized by the ratio T_1/T_2, no matter how high the upper temperature, it is always the lower edge of the CW that radiates. This conclusion follows from the stationary nature of the profile of the CW.

The radiation from the surface of a heated body bordering on a transparent region is generated in a surface layer of optical thickness τ on the order of several units, since the quanta produced in the deeper layers are almost all absorbed in the outer layer. The effective radiation temperature T_{eff} is obviously equal to a certain mean temperature of the radiating layer. It follows from formula (6) that the temperature cannot vary much in a radiating layer with an optical thickness on the order of several units. This is the condition for the existence of a local thermodynamic equilibrium between the radiation and matter, or for the existence of radiant heat conduction. The greater the amplitude of the CW, i.e., the closer U_2 is to U_{eq2} and the closer S_2 is to $2\sigma T_2^4$, the better is this condition satisfied.

In fact, if the change in temperature in the radiating layer is of the order T_2, then the change in flux in this layer, according to (2), is $|\Delta| \sim u\rho_1 c_p T_2$. However, in a strong wave, according to (3), $S_2 \sim u\rho_1 c_p T_1$, since $T_2 \ll T_1$. It is then possible, with the aid of (I.11) and (5), to estimate also the relative deviation of the radiation density U from the equilibrium value U_{eq}

$$\left(\frac{U_{eq} - U}{U_{eq}}\right)_2 = -\frac{1}{cU_{eq2}}\left(\frac{dS}{d\tau}\right)_2.$$

Since $\tau \sim 1$, in the radiating layer, the derivative $(dS/d\tau)_2$ is on the order of $|\Delta S|$ and

$$\left(\frac{U_{eq} - U}{U_{eq}}\right)_2 \sim \frac{|\Delta S|}{cU_{eq2}} \sim \frac{S_2}{cU_{eq2}} \frac{T_2}{T_1} \sim \frac{T_2}{T_1}.$$

Inasmuch as the flux in the radiating layer of a strong CW is almost constant, $|\Delta S|/S_2 \sim T_2/T_1 \ll 1$, the situation on the lower edge of a strong CW is quite analogous to the situation in photospheres of stationary stars. The problem of determining the connection between the flux S_2 with the transparency temperature T_2 in an exact calculation of the angular distribution of the radiation is equivalent, in the limit of the strong CW, to the well-known Milne problem,[2] the exact solution of which

$$S_2 = \frac{4}{\sqrt{3}}\sigma T_2^4 \tag{7}$$

differs only little from the diffusion solution adopted by us

$$S_2 = 2\sigma T_2^4. \tag{8}$$

2. TEMPERATURE DISTRIBUTION IN THE COOLING WAVE

It was shown above that the radiation density is quite close to equilibrium at the lower edge of a strong CW. It is natural to assume that the local equilibrium extends over the entire wave, and to put $U \approx U_{eq}$ in Eq. (I.12):

$$S = \frac{c}{3}\frac{dU_{eq}}{d\tau} = \frac{16\sigma T^3}{3}\frac{dT}{d\tau}. \tag{9}$$

Inserting the flux (9) into the energy integral (2), we obtain an equation for the temperature

$$dT/d\tau = 3u\rho_1 c_p (T_1 - T)/16\sigma T^3, \tag{10}$$

from which it is seen that, the derivative $dT/d\tau$ and, consequently, the deviation from the condition of local equilibrium, diminish monotonically with increasing temperature as the distance from the lower edge of the CW increases. Thus, the energy transferred by radiation in a strong CW has the character of radiant heat conduction. This indeed proves the correctness of the method we have used to average the free path over the spectrum[2] inside the CW (see reference 1).

Equation (10) is integrated by quadratures and gives the temperature profile in the CW

$$t = 1 - (1 - t_2)\exp[-\tau/\tau_e + q(t)], \tag{11}$$

where

$$q(t) = (t - t_2)[1 + \tfrac{1}{2}(t + t_2) + \tfrac{1}{3}(t^2 + tt_2 + t_2^2)];$$
$$\tau_e = 8(1 - t_2)/3t_2^4, \quad t = T/T_1, \quad t_2 = T_2/T_1. \tag{11'}$$

Near the lower edge $T \sim T_2$, so that $T \ll T_1$ in a strong CW. The numerator of the right half of (10) can then be replaced with the aid of (3) and (8), yielding the approximate solution at the lower edge of the wave

$$T^4 = T_2^4\left(1 + \frac{3}{2}\tau\right). \tag{12}$$

This expression, naturally, coincides with the diffusion solution of the Milne problem.

The asymptotic form of the profile for $\tau \gg \tau_e$ can be obtained by putting $q(t) \approx q(1)$ in formula (11). When $t_2 \ll 1$, this quantity is $^{11}/_6$. From the formula obtained thereby it follows that τ_e is the effective optical thickness of the CW.

If we extrapolate the approximate formula (12) all the way to the upper temperature T_1, the optical thickness of the CW becomes approximately four times smaller than τ_e. According to (11') the optical thickness of the CW increases very rapidly with increasing amplitude of the CW [as $(T_1/T_2)^4$]. Figure 1 shows the distribution of $t(\tau)$ for $t_2 = 0.2$.

Let us find now the temperature distribution along the geometric coordinate x. We place the origin of coordinates at the lower edge of the wave, where $T = T_2$ and $\tau = 0$. Rewriting Eq. (I.10) in terms of a new variable temperature instead of the optical thickness τ, and substituting $dT/d\tau$ according to formula (10), we obtain with the aid of expressions (3) and (8)

$$-x = \int_0^\tau l(T)\,d\tau = \frac{8(T_1 - T_2)}{3T_2^4}\int_{T_2}^{T}\frac{l(T)\,T^3 dT}{T_1 - T}. \tag{13}$$

At temperatures not too close to the upper temperature T_1, it is possible to put in (13) approximately $T_1 - T \approx T_1 - T_2$. Inserting into (13) the free path obtained from formula (I.3),* we obtain

$$-\frac{x}{l_2} = \frac{8}{3}z_2^7\int_z^{z_2} e^{z-z_2}\frac{dz}{z^8}, \quad z = \frac{I}{kT}, \quad z_2 = \frac{I}{kT_2}; \quad l_2 = l(T_2). \tag{14}$$

Formula (14) confirms the premise of reference 1, that the temperature in the CW has a sharp step on the high-temperature side. Figure 2 shows the distribution of $T(x)$ on the lower edge, as given by (14).

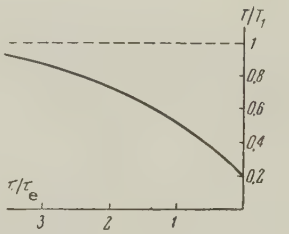

FIG. 1. $T_2/T_1 = 1/5$; $\tau_e = 1670$

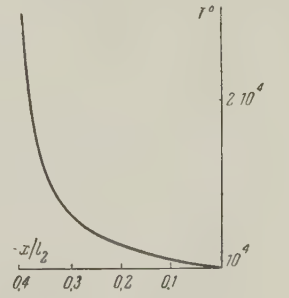

FIG. 2. $T_1 = 10{,}000°$

*According to (I.3), $l \sim (T^2/\rho)\exp[I/kT]$. As a consequence of the constant pressure in the CW (see reference 1), we have $\rho \sim T^{-1}$ and $l \sim T^3 \exp[I/kT]$.

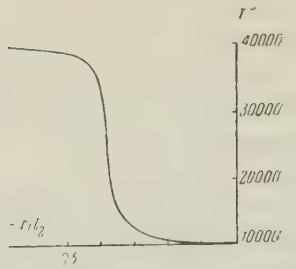

FIG. 3. $T_1 = 40{,}000°$, $T_2 = 10{,}000°$.

The exponential dependence of $l(T)$, which results in a sharp step in CW, is valid actually only in the temperature range where the first ionization alone is significant, i.e., up to ~ 30,000 to 40,000°. At higher temperatures, l goes through a minimum and then increases (relatively slowly). Therefore, the upper edge of a sufficiently strong wave with $T_1 > 50{,}000$ to 100,000° is quite spread out, more so than $T(\tau)$ of formula (11). [Were l constant in the high-temperature region, the profile of $T(x)$ would coincide exactly in this region with the profile of $T(\tau)$]. An approximate profile of the temperature over the entire wave is shown in Fig. 3.

To estimate the accuracy of the radiant heat-conduction approximation in which the temperature profile has been determined, and to define thereby the concept of a "strong" wave, we can determine the correction to the value of the flux $S_2 = 2\sigma T_2^4$, necessitated by the deviation from local equilibrium. Obviously, this correction gives the accuracy of the approximate solution of the equation for the CW, since the greatest deviation from local equilibrium occurs precisely on the lower boundary of the wave. Calculation of the above correction by the method of successive approximation yields: $1 - S_2/2\sigma T_2^4 = 0.18$ for $T_1/T_2 = 1.5$. Its value becomes 0.1 for $T_1/T_2 = 3$. Thus, the accuracy of the radiant heat-conduction approximation increases rapidly with increasing amplitude of the CW, and a wave with $T_1/T_2 = 3$ can be considered strong to within 5%.

3. LOWEST EDGE OF COOLING WAVE AND TRANSITION TO THE TRANSPARENT ZONE OF THE COOLED AIR

We have considered above the structure of the CW front, i.e., of that layer in which the air cools by radiation from an initial temperature T_1 to the transparency temperature T_2. We have used from the very outset the general condition (I.2) to determine the transparency temperature, and have assumed that when $T_1 < T_2$ the air is absolutely transparent. Actually, the absorption of light by air cooled below temperature T_2, although small, is nevertheless finite.

What happens to the radiation from the front of the CW, and how does the temperature behave in the zone of the cooled air?

The process in this region is essentially nonstationary and depends on the actual conditions, such as dimensions, hydrodynamic motion, or additional mechanisms of light absorption which take place at low temperatures (see reference 1). We shall consider here the important case when the air pressure has not yet dropped to atmospheric and the radiation-cooled air continues to cool adiabatically. Owing to the exceedingly strong dependence of l on T, the air is adiabatically cooled quite rapidly to a temperature, at which the absorption becomes so small that this region of air no longer exerts any influence whatever on the mode of the CW.

Little is changed by the adiabatic cooling in that layer of air, which still can influence the general distribution of the temperature, and in which the temperature drops to 1,000 or 2,000° below the transparency temperature. A process with adiabatic cooling is therefore quasi-stationary over the entire region of interest.

Let us trace the successive changes in the state of an air particle that enters a strong CW or, what is the same, let us move in the positive direction of the x axis at a constant velocity u. Let the particle enter the CW with a high initial temperature T_1. It will start to cool rapidly by radiation. The radiation density in the particle remains in this case at all times below equilibrium, since the energy absorbed per unit time is less than the radiated energy; the radiation flux increases in the particle. The speed of adiabatic cooling is first considerably below the speed of radiant cooling. This continues until the particle cools down to such a low temperature, that the speed of adiabatic cooling exceeds the speed of radiant heat exchange. As a consequence of the exceedingly sharp drop in absorption (and radiation) with diminishing temperature, even slight adiabatic cooling makes the particle almost transparent after that instant, and the radiant heat exchange soon ceases.

Now the radiation density, which is determined by the flux generated in the hotter layers and passing through the particle, remains almost constant. On the other hand, the equilibrium radiation density, proportional to T^4, diminishes rapidly. The radiation density in the "transparent" region becomes greater than equilibrium, unlike the "nontransparent" one (the energy absorbed per unit

time becomes greater than the radiated energy). The air then becomes somewhat heated by the radiation, and the flux diminishes. Consequently, there exists on the x axis such a point $x = x_2$ (with corresponding optical thickness and temperature τ_2 and T_2 respectively), which separates the regions of the "nontransparent" air, which is intensely cooled by radiation, from the almost-transparent air, which is slightly heated by the radiation. The radiation density at this point is exactly equal to the corresponding equilibrium value $U_2 = U_{eq2}$, and the flux S_2 in it is a maximum.

Obviously, the point at which the cooling of the air by radiation ceases should indeed be considered the lower boundary of the CW, and the temperature in this point should be considered the transparency temperature for a given value of adiabatic cooling A. The flux S_0 that goes to infinity is somewhat less than the flux S_2 from the surface of the CW front, owing to absorption in the "transparent" zone. This absorption turns out to be small: the optical thickness of the "transparent" zone, as estimated in the Appendix, is approximately $\tau_2 \approx 0.16$, so that S_0 is only little less than S_2,

The temperature and flux profiles T(x) and S(x), corresponding to the above qualitative description of the process, are shown schematically in Figs. 4 and 5. At low temperatures the curve

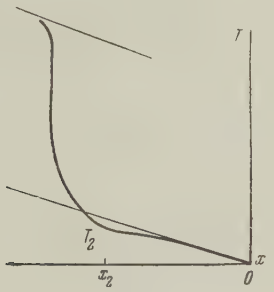

FIG. 4.

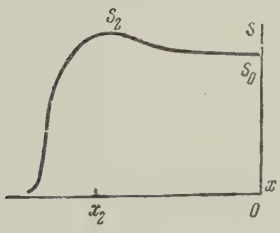

FIG. 5.

T(x) follows very closely the lower straight line corresponding to the constant adiabatic cooling A and to the flux S_0 going to infinity. The curve approaches this line from below, since the air in this region is heated by radiation. On the high temperature side, the T(x) curve deviates greatly from the upper straight line corresponding to adiabatic cooling A and zero flux. On the lower edge of the CW, where the flux is a maximum, the downward deviation of the temperature from the lower straight line is also a maximum, as can be seen from the energy equation (I.6).

As shown in the Appendix, the transparency temperature depends only logarithmically on the value of the adiabatic cooling and on the amplitude of the CW.

We are grateful to Academician N. N. Semenov for stimulating discussions.

APPENDIX

We consider the stationary mode of a strong CW with adiabatic cooling A. The integration constant of the energy integral (I.17), like that in the case of a weak CW, equals the flux that goes to infinity.

$$u\rho_1 c_p T + S = -Ax + S_0. \tag{15}$$

On the low-temperature side, when the flux S tends to S_0, the temperature curve approximates the lower straight line

$$u\rho_1 c_p T = -Ax, \tag{16}$$

and on the high-temperature side, as $S \to 0$, the temperature is asymptotic to the upper line*

$$u\rho_1 c_p T = -Ax + S_0. \tag{17}$$

In the "transparent" region $|x| > |x_2|$, where the adiabatic cooling can be neglected, the solution of the equations coincides with the solution obtained in Sec. 2. One need merely write, in lieu of the particular integral (11) passing through the point $\tau = 0$, $T = T_2$, the general integral passing through the still arbitrary point (τ_2, T_2). By extrapolating this solution to the transparency temperature T_2, we obtain the previous connection between the flux and the temperature T_2, namely $S_2 = 2\sigma T_2^4$.

In the "transparent" region $|x| < |x_2|$, the radiating ability is very small at low temperatures, the flux becomes unilateral: all the quanta move only "forward" and leave the region of sufficiently high

*In a mode without adiabatic cooling, the condition $S \to 0$ on the high-temperature side is equivalent to the condition $T \to T_1 = \text{const}$. On the other hand, there the temperature gradient is not only different from zero, but tends to a constant value at high temperatures. To satisfy the condition $S \to 0$ at $T \to \infty$, and for the mode to exist, it is essential that $l \to 0$ sufficiently rapidly at $T \to \infty$. In the problem of the weak CW, this condition was automatically satisfied through the use of the approximation formula (I.23).

temperature. The integral expressions (I.13) and (I.14) now become

$$S = cU/2 = S_0 e^{2\tau}. \tag{18}$$

Extrapolation of this solution, which is valid for $U_{eq} \ll U$, to the point x_2 where $U_2 = U_{eq2}$ also yields a flux $S_2 = 2\sigma T_2^4$.

By definition, the transparency temperature corresponds to the place in the wave, where the speed of radiant heat exchange dS/dx changes sign, i.e., vanishes. It is clear, however, that near this temperature the rate of radiant cooling of the particle drops to a value on the order of the rate of adiabatic cooling. In fact, as already mentioned above, owing to the sharp temperature dependence of the coefficient of absorption, to which the rate of radiant cooling is proportional, even a small adiabatic temperature drop reduces sharply the rate of radiant heat exchange. The transparency temperature T_2 can therefore be determined from the condition that the rate of radiant cooling, obtained from the extrapolated solution in the "nontransparent" region, must be equal to the rate of adiabatic cooling A.

We calculate the rate of radiant cooling at a point with temperature T_2 with the aid of formulas (1), (3), (8), (9) and (I.10):

$$\left(\frac{dS}{dx}\right)_2 = -u\rho_1 c_p \left(\frac{dT}{dx}\right)_2 = u\rho_1 c_p \frac{3S_2}{16\sigma T_2^3 l(T_2)}$$

$$= \frac{3}{8}\frac{u\rho_1 c_p T_2}{l(T_2)} = \frac{3}{4}\frac{\sigma T_2^4}{l(T_2)(T_1/T_2 - 1)}. \tag{19}$$

We thus arrive at a transcendental equation for the transparency temperature in terms of the velocity of the CW or in terms of the upper temperature T_1 of the CW:

$$\frac{8}{3}\frac{Al(T_2)}{u\rho_1 c_p T_2} = \frac{4}{3}\frac{Al(T_2)(T_1/T_2 - 1)}{\sigma T_2^4} = 1. \tag{20}$$

Thanks to the exponential dependence of l on T, the transparency temperature depends only logarithmically on the amplitude of the CW, an amplitude characterized by the velocity or upper temperature of the wave, and on the adiabatic cooling.

It is clear that the temperature defined by Eq. (20) is equal, within logarithmic accuracy, to the "true" transparency temperature, which is defined by the condition that the radiant heat exchange vanish. This has made the above approximation possible. Geometrically, condition (20) signifies that we extrapolate the solution from the "nontransparent" side until the slope of the temperature curve dT/dx coincides with the slope of the line (16), which the temperature curve approaches from below in the "transparent" region (see Fig. 4).

We must still determine the position of the lower edge of the CW, i.e., the coordinates x_2 and τ_2. For this purpose we determine approximately the optical thickness τ corresponding to some point x in the "transparent" region. Noting that in the low-temperature limit the absorption of the flux is negligible ($S \approx S_0$) and the temperature curve T(x) almost coincides with the lower straight line (17), we obtain

$$\tau = -\int_0^x \frac{dx}{l(T)} = -\int_0^T \frac{dx}{dT}\frac{dT}{l(T)} \approx \frac{u\rho_1 c_p}{A}\int_0^T \frac{dT}{l(T)}. \tag{21}$$

Here we bear in mind the "exact" Kramers formula for the free path instead of approximation (I.23), by which $l = \infty$ when $T = 0$. Inserting the free path given by (I.3) into (21) and recalling that at low temperatures an exponential law is much stronger than a power law, we obtain by approximate integration

$$\tau \approx \frac{u\rho_1 c_p T}{Al(T)}\frac{kT}{I} = \frac{|x|}{l(T)}\frac{kT}{I}. \tag{22}$$

By the very nature of its derivation, this formula is valid when $\tau \ll 1$. If it is referred to the lower edge of the CW, i.e., to the point where $T = T_2$, we obtain with the aid of (20)

$$\tau_2 \approx 8kT_2/3I. \tag{23}$$

Since $I = 14$ ev and $T_2 \approx 10{,}000°$ in air, $\tau_2 \approx 0.164$ turns out to be rather small, and (23) can be considered as the optical thickness of the lower edge of the CW.

The geometric coordinate of the lower edge of the CW, which equals, according to (22) and (23),

$$|x_2| = u\rho_1 c_p T_2/A = {}^8/_3 l(T_2), \tag{24}$$

represents in this case the distance, at which the temperature is reduced by adiabatic cooling from T_2 to 0.

As expected, the free path corresponding to the transparency temperature is exactly of the same order as determined from the value of the adiabatic cooling and its time of action.

[1] Zel'dovich, Kompaneets, and Raizer, J. Exptl. Theoret. Phys. (U.S.S.R.) **34**, 1278 (1958); Soviet Phys. JETP **7**, 000 (1958).

[2] A. Unsold, Physik der Sternatmosphären Berlin, 1955.

Translated by J. G. Adashko
294

SCATTERING OF NEUTRONS FROM NONSPHERICAL NUCLEI

E. V. INOPIN

Physico-Technical Institute, Academy of Sciences, Ukrainian S.S.R.

Submitted to JETP editor June 19, 1957; resubmitted March 22, 1958

J. Exptl. Theoret. Phys. (U.S.S.R.) **34**, 1455-1464 (June, 1958)

A method for calculating the scattering of neutrons from semi-transparent nonspherical nuclei, based on the use of the exact solutions of the wave equation in spheroidal coordinates, is described.

1. INTRODUCTION

THE scattering of neutrons from nonspherical nuclei was discussed in papers by Drozdov[1] and the author.[2] In these papers it was assumed that (1) the nucleus may be considered at rest during the course of the interaction ("adiabatic approximation"), and (2) the condition $kR \gg 1$ holds (k is the wave vector of the neutron, R the nuclear radius). The papers of Zaretzkii and Shut'ko[3] and Brink[4] discuss the same question using perturbation theory, which is evidently valid only for very small deformations of the nucleus.

For comparison with experiment, the case of interest is that of arbitrary deformations and small energies of the incoming neutron. Here the condition $dR \gg 1$ will not be fulfilled, but the adiabatic approximation remains in force if the energy of the incoming neutron E_n is not too small. The criterion for the applicability of the adiabatic approximation follows from the comparison of the time of flight R/v of the neutron through the nucleus and the characteristic period of the nucleus $\omega^{-1} \approx \hbar/\epsilon$, where ϵ is the energy of the first excited rotational state ($\epsilon \approx 0.1$ Mev). Thus we obtain

$$\varepsilon kR / E_n \ll 1. \qquad (1)$$

This condition is well satisfied for heavy nuclei and neutron energies of a few Mev. A more rigorous examination shows that condition (1) is valid if the probability for exciting the second rotational level is sufficiently small. This will be the case for small deformations of the nucleus, i.e., $\Delta R/R \ll 1$.

In the present paper we compute the scattering of neutrons from a semi-transparent nonspherical even-even nucleus (the spin of the nucleus is zero) represented by a rotation ellipsoid with arbitrary eccentricity. To be specific, we consider a prolate spheroid; the results obtained can be easily used for an oblate spheroid. As in reference 1 and 2, we use the adiabatic approximation. However, we calculate the scattering amplitude not in the quasiclassical approximation, but exactly, using the known particular solutions of the wave equation in spheroidal coordinates.

2. PARTICULAR SOLUTIONS OF THE WAVE EQUATION IN SPHEROIDAL COORDINATES

To solve our problem we must first determine the scattering from a nucleus with fixed orientation. We then have to average this scattering amplitude over the orientations.[1]

We introduce the coordinate system K, with a z axis in the direction of motion of the incoming neutron, and the system K', whose z' axis is aligned with the symmetry axis of the nucleus. The semi-axes of the ellipsoid are a and b ($a > b$). The orientation of the nucleus is specified by the unit vector ω directed along the z' axis.

We introduce the spheroidal coordinates μ, θ, φ, which, for the case of a prolate spheroid, are defined by the relations

$$x' = \frac{d}{2} \sinh \mu \sin\theta \cos\varphi, \quad y' = \frac{d}{2} \sinh \mu \sin\theta \sin\varphi,$$

$$z' = \frac{d}{2} \cosh \mu \cos\theta; \qquad (2)$$

d is the distance between the foci of the spheroid. The coordinate surfaces $\mu = \text{const}$ are confocal spheroids, going into spheres for large distances from the center. The surfaces $\theta = \text{const}$ are rotation hyperboloids, going into cones for large distances from the center (i.e. θ goes over into the ordinary polar angle for large distances). φ is the ordinary azimuthal angle. We also introduce the symbols $\eta = \cos\theta$, $\xi = \cosh\mu$ ($-1 \leq y \leq 1$, $1 \leq \xi \leq \infty$).

Let ξ_0 be the value of the coordinate ξ defin-

ing the nuclear boundary $[\xi_0 = (1 - b^2/a^2)^{-1/2}]$. With Feshbach, Porter, and Weisskopf[5] we shall assume that the neutron moves in the field

$$V(\xi) = \begin{cases} -V_0 - iW_0, & \xi < \xi_0 \\ 0, & \xi > \xi_0. \end{cases} \tag{3}$$

To find the wave function of the scattered neutron we have to solve the wave equation

$$(\Delta + k^2)\psi = 0 \text{ for } \xi > \xi_0, \quad (\Delta + \varkappa^2)\psi = 0 \text{ for } \xi < \xi_0, \tag{4}$$
$$\varkappa = k\sqrt{1 + V_0/E_n + iW_0/E_n}.$$

These solutions must then be "joined" at $\xi = \xi_0$.

The solutions of the wave equation in spheroidal coordinates have been investigated in detail in reference 6. With the notation somewhat changed,* these results lead essentially to the following.

The wave equation has a set of particular solutions each characterized by the quantum numbers l and m. These numbers can take on the same values as the quantum numbers of the orbital angular momentum and its projection. The particular solution ψ_{lm} has the form

$$\psi_{lm} = R_{lm}(c, \xi) J_{lm}(c, \mathbf{n}), \quad c = \tfrac{1}{2}kd = \sqrt{1 - (b/a)^2}\,(a/b)^{1/3}kR \tag{5}$$

(R is the radius of a spherical nucleus with the same volume, n is a unit vector specified by the "angle" θ and the angle φ).

The "angular" part of the solution is defined thus:

$$J_{lm}(c, \mathbf{n}) = \sum_n s^l_{nm}(c)\, Y_{nm}(\mathbf{n}),$$
$$s^l_{nm}(c) = \Big[\sum_n |b^l_{nm}|^2\Big]^{-1/2} b^l_{nm}(c), \tag{6}$$
$$b^l_{nm}(c) = \left[\frac{2n+1}{2}\cdot\frac{(n-|m|)!}{(n+|m|)!}\right]^{-1/2} d^l_{n-|m|}(c),$$
$$s^l_{nm}(0) = \delta_{nl}.$$

The functions $J_{lm}(\mathbf{c}, \mathbf{n})$ are orthonormal, therefore

$$\sum_n s^{l'*}_{nm}(c)\, s^l_{nm}(c) = \delta_{ll'}. \tag{7}$$

The quantities d:: which appear in the expression for the coefficients s^l_{nm} have been determined in reference 6, where they are tabulated for $l < 3$. The summation in (6) goes only over either even or odd indices, and starts with a value n equal to m or m + 1, depending on whether l is even or odd.

*In particular, the number l used here, and the number l used in reference 6, are related by $l_{[6]} = l - |m|$.

The "radial" functions R_{lm} are of two kinds: (1) the regular function $R^{(1)}_{lm}$, which for large ξ has the form

$$R^{(1)}_{lm}(c,\xi) \approx \frac{\sin(c\xi - l\pi/2)}{c\xi} \approx \frac{\sin(kr - l\pi/2)}{kr} \tag{8}$$

[here we use the fact that $c\xi = kr$ for large r, as is easily seen from (2)]; (2) the function is irregular at $\xi = 1$, having for large distances the form

$$R^{(2)}_{lm}(c,\xi) \approx -\frac{\cos(c\xi - l\pi/2)}{c\xi} \approx -\frac{\cos(kr - l\pi/2)}{kr}. \tag{9}$$

Reference 6 gives a method for developing these functions as expansions in Bessel functions.

We expand the plane wave in terms of these solutions:

$$e^{i\mathbf{k}\cdot\mathbf{r}} = \exp\{ic[\cosh\mu\cos\theta\cos\theta' + \sinh\mu\sin\theta\sin\theta'\cos(\varphi - \varphi')]\} \tag{10}$$
$$= \sum_{lm} A_{lm} J^*_{lm}(c,\mathbf{q})\, J_{lm}(c,\mathbf{n})\, R^{(1)}_{lm}(c,\cosh\mu),$$

where $\mathbf{q} = \mathbf{k}/k$, and θ', φ' are the angles of vector q in the K′ system. It is immediately seen from symmetry considerations that the expansion coefficients (10) contain the quantities $J^*_{lm}(c, \mathbf{q})$. The coefficients A_{lm} can be obtained by observing that for large distances $\sinh\mu \approx \cosh\mu = \xi$, hence

$$e^{i\mathbf{k}\cdot\mathbf{r}} \approx \exp\{ic\xi[\cos\theta\cos\theta' + \sin\theta\sin\theta'\cos(\varphi - \varphi')]\} = e^{ic\xi\mathbf{q}\cdot\mathbf{n}}$$
$$\approx \sum_{lm} 4\pi i^l \frac{\sin(c\xi - l\pi/2)}{c\xi} Y^*_{lm}(\mathbf{q})\, Y_{lm}(\mathbf{n}). \tag{11}$$

Equating (11) and (10) for large ξ, multiplying both sides by $J^*_{lm}(c, \mathbf{n})\, J_{lm}(c, \mathbf{q})$, and integrating over the solid angles corresponding to q and n, we obtain $A_{lm} = 4\pi i^l$

3. SCATTERING AMPLITUDE

The general solution of the wave equation (4) in the exterior region ($\xi > \xi_0$) can be written in the form

$$\psi^{(e)} = \sum_{lm} B_{lm} J_{lm}(c,\mathbf{n})\, R_{lm}(c,\xi), \tag{12}$$

where B_{lm} is a coefficient depending on q, and R_{lm} has the form

$$R_{lm}(c,\xi) = \cos\delta_{lm} R^{(1)}_{lm}(c,\xi) - \sin\delta_{lm} R^{(2)}_{lm}(c,\xi). \tag{13}$$

Imposing the usual requirement

$$\psi^{(e)} \approx e^{i\mathbf{k}\cdot\mathbf{r}} + f(\mathbf{q},\mathbf{n})\, e^{ikr}/r \text{ for } r \to \infty, \tag{14}$$

we find

$$B_{lm} = 4\pi i^l e^{i\delta_{lm}} J^*_{lm}(c,\mathbf{q}); \quad (15)$$

the scattering amplitude is

$$f(\mathbf{q},\mathbf{n}) = \frac{2\pi}{ik}\sum_{lm} J^*_{lm}(c,\mathbf{q})\,[e^{2i\delta_{lm}} - 1]\,J_{lm}(c,\mathbf{n}). \quad (16)$$

To find the scattering phase δ_{lm} it is necessary to investigate the solution of (4) in the interior region ($\xi < \xi_0$). In this case the general solution will contain only the regular functions $R^{(1)}_{lm}$, and it will be of the form

$$\psi^{(i)} = \sum_{lm} C_{lm} J_{lm}(p,\ \mathbf{n})\, R^{(1)}_{lm}(p,\ \xi), \quad (17)$$

where $p = \kappa d/2$. This solution has to be "joined" with the solution (12) at $\xi = \xi_0$. This "joining" is complicated by the fact that the functions $J_{lm}(p, \mathbf{n})$ and $J_{lm}(c, \mathbf{n})$ represent two different complete systems of functions. They can be reduced to one system by expanding, say, $J_{lm}(c, \mathbf{n})$ in terms of $J_{lm}(p, \mathbf{n})$:

$$J_{l'm}(c,\ \mathbf{n}) = \sum_{l} u^m_{ll'}(c,\ p)\, J_{lm}(p,\ \mathbf{n}), \quad (18)$$

where

$$u^m_{ll'}(c,\ p) = \int J^*_{lm}(p,\ \mathbf{n})\, J_{l'm}(c,\ \mathbf{n})\, d\mathbf{n} = \sum_n s^{l*}_{nm}(p)\, s^{l'}_{nm}(c). \quad (19)$$

Evidently $u^m_{ll'} = 0$ if the numbers l and l' have opposite parity.

Now

$$\psi^{(e)} = \sum_{lm} J_{lm}(p,\ \mathbf{n}) \sum_{l'} B_{l'm} u^m_{ll'}(c,\ p)\, R_{l'm}(c,\xi). \quad (20)$$

Equating the functions $\psi^{(i)}$ and $\psi^{(e)}$ and their derivatives at $\xi = \xi_0$, we obtain a system of equations for the phases

$$C_{lm} R^{(1)}_{lm}(p,\ \xi_0) = \sum_{l'} B_{l'm} u^m_{ll'}(c,\ p)\, R_{l'm}(c,\ \xi_0),$$

$$C_{lm} R^{(1)\prime}_{lm}(p,\ \xi_0) = \sum_{l'} B_{l'm} u^m_{ll'}(c,\ p)\, R'_{l'm}(c,\ \xi_0); \quad (21)$$

$$(l = 0,\ 1,\ 2,\ \ldots).$$

Here the prime denotes the derivative with respect to ξ_0. Dividing the second equation by the first and using

$$x_{lm} = \frac{1}{2}(1 - e^{2i\delta_{lm}})\, J^*_{lm}(c,\ \mathbf{q}),$$

$$T_{lm} = R^{(1)\prime}_{lm}(p,\ \xi_0) / R^{(1)}_{lm}(p,\ \xi_0),$$

we obtain

$$\sum_{l'} M^m_{ll'} x_{l'm} = N_{lm},\ (l = 0,\ 1,\ 2,\ \ldots), \quad (22)$$

where

$$M^m_{ll'} = i^{l'} u^m_{ll'}\,[R^{(1)\prime}_{l'm}(c,\ \xi_0) + iR^{(2)\prime}_{l'm}(c,\ \xi_0) - T_{lm}(R^{(1)}_{l'm}(c,\ \xi_0) + iR^{(2)}_{l'm}(c,\ \xi_0))], \quad (23)$$

$$N_{lm} = \sum_{l'} i^{l'} u^m_{ll'}\,[R^{(1)\prime}_{l'm}(c,\ \xi_0) - T_{lm} R^{(1)}_{l'm}(c,\ \xi_0)]\, J^*_{l'm}(c,\ \mathbf{q}). \quad (24)$$

The system (22) can be solved in the following manner. We set $x_{lm} = 0$ for $l \geq l_0$, where l_0 is a sufficiently large number. Then the system becomes finite, and the number of equations will be equal to the number of variables. We denote the solutions of this system by $x^{(0)}_{lm}$. The next step is to set $x_{lm} = 0$ for $l \geq l_0 + 2$, and obtain the next approximation, the solutions $x^{(2)}_{lm}$. A detailed analysis shows that, for small neutron energies and small deformations of the nucleus ($\Delta R/R \ll 1$), such a process converges very rapidly. In practice, for small deformations, one can set equal to zero all the phases that are sufficiently small for the spherical nucleus. For small neutron energies this leads to a solution of a system with two or three unknowns. Thus, for example, for heavy nuclei and $E_n \approx 1$ Mev the phases with $l = 4$ are already very small. In this case we obtain for x_{00} and x_{20} the system

$$M^0_{00}x_{00} + M^0_{02}x_{20} = N_{00},\ M^0_{20}x_{00} + M^0_{22}x_{20} = N_{20}. \quad (25)$$

Analogous systems are obtained for the quantities x_{10}, x_{30} and x_{11}, x_{31}, and the quantities x_{21}, x_{22}, x_{32}, x_{33} are determined by first-degree equations. Thus, in particular,

$$x_{21} = N_{21} / M^1_{22}. \quad (26)$$

In the resulting solution of system (22) the quantities x_{lm} will, of course, be expressed in the form

$$x_{lm} = \sum_{\lambda} x^{\lambda}_{lm} J^*_{\lambda m}(c,\ \mathbf{q}). \quad (27)$$

Here λ runs through values of the same parity as that of l. For $E_n \sim 1$ Mev and $\Delta R/R \ll 1$ these sums will contain only one or two terms.

Now the scattering amplitude takes the form

$$f(\mathbf{q},\ \mathbf{n}) = \frac{4\pi i}{k}\sum_{lm\lambda} x^{\lambda}_{lm} J^*_{\lambda m}(c,\ \mathbf{q})\, J_{lm}(c,\ \mathbf{n}) \quad (28)$$

4. CROSS SECTIONS

We proceed to calculate the various cross sections connected with the scattering of neutrons from nonspherical nuclei

The integral cross section σ_s (the cross section for the excitation of all rotational levels, including the elastic scattering) is given by the expression (cf. reference 1):

$$\sigma_s = \frac{1}{4\pi}\int d\omega \int d\mathbf{n}\,|f(\mathbf{q},\ \mathbf{n})|^2. \tag{29}$$

Integration over $\mathbf{n}$ gives

$$\int d\mathbf{n}\,|f(\mathbf{q},\ \mathbf{n})|^2 = \frac{16\pi^2}{k^2}\sum_{lm\lambda\lambda'} x^{\lambda}_{lm}(x^{\lambda'}_{lm})^* J^*_{\lambda m}(c,\ \mathbf{q})\,J_{\lambda' m}(c,\ \mathbf{q}). \tag{30}$$

Since the azimuthal angle of vector $\mathbf{q}$ drops out, one can change the integration over ω in (29) to an integration over $\mathbf{q}$, i.e. instead of averaging over the orientations of the nucleus we average over the directions of the incoming neutron. The result is

$$\sigma_s = \frac{4\pi}{k^2}\sum_{lm\lambda} |\,x^{\lambda}_{lm}\,|^2. \tag{31}$$

The total cross section σ_t for all processes is expressed by the imaginary part of the scattering amplitude in the forward direction, averaged over the orientations of the nucleus:

$$\sigma_t = \frac{1}{k}\,\mathrm{Im}\int d\omega f(\mathbf{q},\ \mathbf{q}). \tag{32}$$

From this we obtain

$$\sigma_t = \frac{4\pi}{k^2}\sum_{lm}\mathrm{Re}\,(x^{l}_{lm}). \tag{33}$$

The capture cross section σ_c is equal to the difference of σ_t and σ_s:

$$\sigma_c = \frac{4\pi}{k^2}\sum_{lm\lambda}[\mathrm{Re}\,(x^{\lambda}_{lm}\delta_{l\lambda}) - |\,x^{\lambda}_{lm}\,|^2]. \tag{34}$$

In the calculation of the differential cross sections it is necessary to go from the system K′ to the system K. We note that the symbol $Y_{lm}(\mathbf{a})$ has a definite meaning only if we define a definite coordinate system to which the unit vector $\mathbf{a}$ is referred. The vector $\mathbf{a}$ will carry a prime if it is referred to the system K′, and will be without prime if referred to system K.

The cross section for the process in which the neutron is inelastically scattered into the direction $\mathbf{n}$, and the nucleus goes from the ground state ($I = 0$) into the rotational state with angular momentum I and momentum projection M, is defined by the expression

$$\sigma_{IM}(\mathbf{n}) = \frac{1}{4\pi}\left|\int Y^*_{IM}(\omega)\,f(\mathbf{q}',\ \mathbf{n}')\,d\omega\right|^2. \tag{35}$$

On substituting (28) for the amplitude, the computation of the integral in this expression reduces to the calculation of the integrals

$$Q^{IM}_{nn'm} = (-1)^m\int d\omega Y^*_{IM}(\omega)\,Y^*_{nm}(\mathbf{q}')\,Y^*_{n'-m}(\mathbf{n}'). \tag{36}$$

In going from the system K to the system K′ for an arbitrary vector $\mathbf{a}$ we obtain

$$Y_{lm}(\mathbf{a}) = \sum_{m'} D^{(l)}_{mm'}(\omega)\,Y_{lm'}(\mathbf{a}'), \tag{37}$$

where $D^{(l)}_{mm'}$ is an element of the irreducible representation of the rotation group of order $2l+1$. For the inverse transformation we have, owing to the unitarity of the matrices $D^{(l)}$,

$$Y_{lm}(\mathbf{a}') = \sum_{m'} D^{(l)*}_{m'm}(\omega)\,Y_{lm'}(\mathbf{a}). \tag{38}$$

Applying this formula to the vectors $\mathbf{q}$ and $\mathbf{n}$, and noting that $Y^*_{nm'}(\mathbf{q}) = \sqrt{(2n+1)/4\pi}\,\delta_{m'0}$, we obtain

$$Q^{IM}_{nn'm} = (-1)^m\sqrt{\frac{2n+1}{4\pi}} \times\sum_{\mu} Y^*_{n'\mu}(\mathbf{n})\int d\omega Y^*_{IM}(\omega)\,D^{(n)}_{0m}(\omega)\,D^{(n')}_{\mu-m}(\omega). \tag{39}$$

Using the well-known Wigner theorem,[7] we have

$$D^{(n)}_{0m}D^{(n')}_{\mu-m} = \sum_{L}(nn'0\mu\,|\,nn'L\mu)\,(nn'm-m|\,nn'L0)\,D^{(L)}_{\mu 0}, \tag{40}$$

where $(nn'0\mu\,|\,nn'L\mu)$ and $(nn'm-m\,|\,nn'L0)$ are Clebsch-Gordan coefficients. Moreover, we have

$$D^{(L)}_{\mu 0}(\omega) = \sqrt{\frac{4\pi}{2L+1}}\,Y_{L\mu}(\omega). \tag{41}$$

Substituting (40) into (39) and using (41), we obtain finally

$$\sigma_{IM}(\mathbf{n}) = \frac{1}{2I+1}\frac{4\pi}{k^2}\Big|\sum_{lm\lambda nn'}(-1)^m\sqrt{2n+1}\,(nn'0M\,|\,nn'IM) \times(nn'm-m\,|\,nn'I0)\,s^{\lambda}_{nm}s^{l}_{n'm}x^{\lambda}_{lm}Y_{n'M}(\mathbf{n})\Big|^2. \tag{42}$$

The cross section (42) is obviously independent of the azimuthal angle.

It is easily shown that for $c \to 0$ i.e., in going to a spherical nucleus, formula (42) gives for $I = 0$ the usual formula for the elastic scattering from a spherically symmetric field, while the cross sections go to zero for $I \neq 0$. Indeed, for $c = 0$, $s^{\lambda}_{nm} = \delta_{n\lambda}$, $s^{l}_{n'm} = \delta_{n'l}$, $x^{\lambda}_{lm} = x_l\delta_{l\lambda}$. For the proof we must also make use of the relation

$$\sum_m(-1)^m(lLm-m\,|\,lL0) = [(l00\,|\,l00)]^{-1}\delta_{l0}. \tag{43}$$

It is also easily seen that σ_{IM} vanishes for odd I. Indeed, since the numbers n and n' in

(42) are of the same parity (the parity of l), we have for all m and odd I

$$(nn'm - m \mid nn'I0) + (nn' - mm \mid nn'I0) = 0. \quad (44)$$

This relation is obtained by expanding the product $Y_{n,m}Y_{n',-m}$ into a Clebsch-Gordan series, and by requiring that this expansion have no odd harmonics. Using (44) and the obvious relation $x^{\lambda}_{lm} = x^{\lambda}_{1-m}$, we have the required proof. Even-even nuclei do not have states with odd I, therefore this last property allows us to sum over the complete system of spherical functions used in the derivation of (29).

Integrating (42) over the angles and summing over M, we obtain, using the orthogonality of the Clebsch-Gordan coefficients, the integral cross section for the excitation of the I-th rotational level

$$\sigma_I = \frac{4\pi}{k^2} \sum_{nn'} \Big| \sum_{l\lambda m} (-1)^m (nn'm - m \mid nn'I0)\, s^{\lambda}_{nm} s^{l}_{n'm} x^{\lambda}_{lm} \Big|^2. \quad (45)$$

The summation over I in this formula leads back to (31), if we use (7).

We have mentioned in the beginning that perturbation theory is applicable only for very small deformations of the nucleus. Indeed, the case of a spherical nucleus is obtained for $c \to 0$ and $p \to 0$, i.e., we should use as small parameters the quantities

$$c = \sqrt{1 - (b/a)^2}\,(a/b)^{2/3} kR$$

and $$p = \sqrt{1 - (b/a)^2}\,(a/b)^{2/3} \varkappa R.$$

From the results of Stratton et al.[6] it follows that the parameter in the spheroidal functions may be considered small if it does not exceed unity. For the applicability of perturbation theory it is therefore necessary that $|p| < 1$ (the limitation of c does not come into play, since $c < |p|$), or

$$\frac{a^2 - b^2}{a^2} |\varkappa R| < \frac{1}{|\varkappa R|}, \quad \text{i.e.} \quad \frac{\Delta R}{R} |\varkappa R| \ll 1, \quad (46)$$

since $|\kappa R| \approx 10$ for heavy nuclei. It is therefore clear that perturbation theory is of no practical use in our case.

It also follows from the foregoing that we can set $s^{\lambda}_{nm} = \delta_{n\lambda}$, $s^{l}_{n'm} = \delta_{n'l}$ in (42) and (45), if the energies and deformations are small, and $c < 1$. Then the formulas assume the simple form:

$$\sigma_{IM} = \frac{4\pi}{2I+1} \frac{1}{k^2} \Big| \sum_{lm\lambda} (-1)^m \sqrt{2\lambda + 1}\, (\lambda l 0 M \mid \lambda l I M) \times (\lambda lm - m \mid \lambda l I 0) x^{\lambda}_{lm} Y_{lM}(\mathbf{n}) \Big|^2; \quad (47)$$

$$\sigma_I = \frac{4\pi}{k^2} \sum_{l\lambda} \Big| \sum_{m} (-1)^m (\lambda lm - m \mid \lambda l I 0)\, x^{\lambda}_{lm} \Big|^2. \quad (48)$$

5. NUMERICAL CALCULATIONS AND COMPARISON WITH EXPERIMENT

In order to estimate the magnitude and the character of the effects of the nonsphericity of the nucleus, we made several computations of the scattering.

In constructing the "radial" functions and their derivatives inside the nucleus, i.e. in the numerical calculation of the quantities T_{lm}, we found it convenient not to use the method of reference 6, which is of little practical use for $p \gg 1$, but to use a method described briefly below.

The equation for the radial function $R_{lm}(p, \xi)$ will be:[6]

$$(1 - \xi^2) \frac{d^2 R_{lm}}{d\xi^2} - 2\xi \frac{dR_{lm}}{d\xi} + \left(\lambda_{lm} - \frac{m^2}{1 - \xi^2} - p^2 \xi^2 \right) R_{lm} = 0, \quad (49)$$

where λ_{lm} is a separation constant which represents an eigenvalue arising from the requirement of regularity of the solutions of the wave equation. For $p \gg 1$, we find λ_{lm} with the help of an asymptotic formula obtained by Meixner:[8]

$$\begin{aligned} \lambda_{lm}(p) = {} & pq + m^2 - \tfrac{1}{8}[q^2 + 5] - \tfrac{q}{64p}[q^2 + 11 - 32\, m^2] \\ & - \tfrac{1}{1024p^2}[5(q^4 + 26q^2 + 21) - 384m^2(q^2 + 1)] \\ & - \tfrac{1}{p^3}\Big[\tfrac{1}{128 \cdot 128}(33q^5 + 1594q^3 + 5621q) \\ & - \tfrac{m^2}{128}(37q^3 + 167q) + \tfrac{m^4}{8} q\Big] + O(p^{-4}), \end{aligned} \quad (50)$$

where $q = 2l + 1$.

It is easily seen that, for $p \gg 1$ and not too large nonsphericity ($\Delta R/R \approx 0.2 - 0.3$), the motion described by Eq. (49) is quasi-classical in the neighborhood of the nuclear boundary. Therefore, applying the usual quasi-classical method, we obtain for the logarithmic derivative of the "radial" function the following expression:

$$\begin{aligned} T_{lm} = \frac{R^{(1)'}_{ml}(p, \xi_0)}{R^{(1)}_{ml}(p, \xi_0)} = {} & -\frac{\xi_0}{4} \frac{2\xi_0^2 - 1 - \alpha}{(\xi_0^2 - \alpha)(\xi_0^2 - 1)} \\ & + p \sqrt{\frac{\xi_0^2 - \alpha}{\xi_0^2 - 1}} \cot \Phi(\xi_0), \end{aligned} \quad (51)$$

$$\alpha = \frac{\lambda_{lm}}{p^2}, \quad \Phi(\xi_0) = p \left\{ \frac{\sqrt{\xi_0^2 - \alpha}}{\xi_0} \sqrt{\xi_0^2 - 1} - (1 - \alpha) F\left(\arcsin \frac{1}{\xi_0}, \sqrt{\alpha} \right) + E\left(\arcsin \frac{1}{\xi_0}, \sqrt{\alpha} \right) \right\} - \frac{l\pi}{2},$$

F and E are the elliptic integrals of first and second kind.

In our calculations we made the following choice of parameters:

$$E_n = 1\,\text{Mev},\quad A = 178,$$

$$R = 1.4\ A^{1/3}\cdot 10^{-13}\,\text{cm},\quad V_0 = 42\,\text{Mev},$$

$W_0/V_0 = 0.03$, $a/b = 1.25$. This choice of parameters corresponds to the Hf nucleus (in particular, the deformation parameters are chosen to agree approximately with the results of Mottelson and Nilsson[9] and with the experimental evidence on scattering gathered by Barschall and Walt[10]). Figure 1 gives the angular distribution obtained in reference 10, as well as the summary angular distribution calculated with a nonspherical nucleus and the distribution calculated with a spherical nucleus. We see that the angular distributions for the spherical and the nonspherical nucleus differ little in the region of small angles, but are distinctly different for large angles. Here the behavior of the angular distribution for the nonspherical nucleus is visibly in better agreement with the experimental evidence that that of the angular distribution for the spherical nucleus. In the table we compare the values of σ_t, σ_c and σ_s (these are given in barns). We see that the model of a nonspherical nucleus explains the values of σ_t and, in particular, of σ_c better than the model of a spherical nucleus. However, for σ_s the value obtained with a spherical nucleus is somewhat closer to the experimental value.

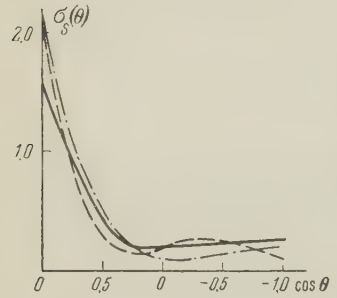

FIG. 1. Angular distribution (in barns per sterad) of neutrons scattered by the Hf nucleus. Solid curve: experiment; dash-dotted curve: a/b = 1.25; dashed curve: a/b = 1.00

The example considered shows therefore that the nonsphericity has a noticeable influence on the scattering. However, for a more definite choice we need additional experiments and more detailed calculations. In particular, it is necessary to consider the contribution from scattering accompanied by formation of the compound nucleus.

We clearly get a more immediate comparison of theory and experiment if we take account of the excitation of rotational levels by the neutrons. We see from the table that $\sigma_2/\sigma_s \approx 0.1$, i.e., the cross section for inelastic scattering with the excitation of the first rotational level is as large as 10% of the elastic scattering cross section. Moreover, it is seen from Fig. 2 that the inelastic scattering goes mainly into large angles, whereas the elastic scattering is concentrated into the small angles. Therefore, for large angles the probability for inelastic scattering is only 2 to 3 times smaller than the probability for elastic scattering into the same angle. For large angles we have thus favorable conditions under which to explore experimentally the excitation of rotational levels by neutrons. Unfortunately, the corresponding experiments have so far not been made. A calculation using for the deformation parameter the value $a/b = 1.1$ gave $\sigma_2/\sigma_s \approx 0.03$, i.e., the cross section for the excitation of the first rotational level increases approximately linearly with the deformation.

	σ_t	σ_c	σ_s	σ_2
Spherical nucleus	5.85	1.06	4.79	—
Non-spherical nucleus	6.70	2.47	4.23	0.42
Experiment	7.20	2.10	5.10	—

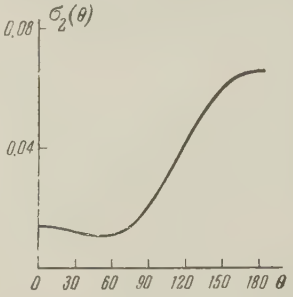

FIG. 2. Angular distribution (in barns per sterad) of neutrons scattered inelastically by the Hf nucleus with the simultaneous excitation of the first rotational level.

The author expresses his gratitude to V. N. Gribov for a valuable discussion, and to Z. V. Gerasimenko for help in the numerical calculations.

[1] S. I. Drozdov, J. Exptl. Theoret. Phys. (U.S.S.R.) **28**, 734 (1955); Soviet Phys. JETP **1**, 591 (1955).

[2] E. V. Inopin, J. Exptl. Theoret. Phys. (U.S.S.R.) **30**, 210 (1956); Soviet Phys. JETP **3**, 134 (1956).

[3] D. F. Zaretskii and A. V. Shut'ko, J. Exptl. Theoret. Phys. (U.S.S.R.) **30**, 141 (1956); Soviet Phys. JETP **3**, 98 (1956).

[4] D. M. Brink, Proc. Phys. Soc. (London) **A68**, 994 (1955).

[5] Feshbach, Porter, and Weisskopf, Phys. Rev. **96**, 448 (1954).

[6] Stratton, Morse, Chu, and Hutner, Elliptic Cylinder and Spheroidal Wave Functions, MIT, 1941.

[7] E. P. Wigner, Gruppentheorie und ihre Anwendung auf die Quantenmechanik der Atomspektren, Braunschweig, 1931.

[8] J. Meixner, Z. angew. Math. Mech. **28**, 304 (1948).

[9] B. R. Mottelson and S. G. Nilsson, Phys. Rev. **99**, 1615 (1955); Проблемы современной физики (Prob. of Mod. Phys.) **1**, 186 (1956).

[10] M. Walt and H. H. Barschall, Phys. Rev. **93**, 1062 (1954).

Translated by R. Lipperheide
295

SOVIET PHYSICS JETP VOLUME 34(7), NUMBER 6 DECEMBER, 1958

PARAMAGNETIC LATTICE RELAXATION IN HYDRATED SALTS OF DIVALENT COPPER

Sh. Sh. BASHKIROV

Kazan' State University

Submitted to JETP editor April 27, 1957; resubmitted February 27, 1958

J. Exptl. Theoret. Phys. (U.S.S.R.) **34**, 1465-1469 (June, 1958)

A theoretical calculation of the spin-lattice relaxation time in hydrated salts of divalent copper is carried out. The anisotropy of the relaxation time experimentally observed in $CuSO_4 \cdot 5H_2O$ crystals can be explained by taking into account the anisotropy of the spin-orbit interaction in the Cu^{++} ion due to partially covalent nature of the copper ion bonds in the crystal.

1. INTRODUCTION

HYDRATED salts of divalent copper form a group of paramagnets whose magnetic properties are comparatively well known: detailed examinations of the static susceptibility and paramagnetic resonance spectra have been carried out for a number of these salts, and experimental data on the spin-lattice relaxation are on hand. We shall dwell below on those results that have been utilized for our calculations.

In the crystals of hydrated copper salts the water molecules that surround a magnetic ion form, at the point where the magnetic ion is located, an electric field of cubic symmetry on which is superimposed a comparatively weak field of lower symmetry (tetragonal, trigonal, or rhombic). We shall now examine the Tutton's copper salts and the hydrated copper sulfate $CuSO_4 \cdot 5H_2O$. The unit cells of the crystals of the above salts contain two Cu^{++} ions each. The internal field is of tetragonal, almost cubic, symmetry. The angle between the tetragonal axes is 82° for two magnetic ions of a unit cell of the crystal.[1,2]

The basic state of the Cu^{++} ion is the ^2D state. The ground orbital level of the Cu^{++} ion is split up into a triplet and a doublet by the cubical field, the doublet lying lower. The orbital doublet is split up into two single levels by the tetragonal field. Since the spin is $S = \frac{1}{2}$, the lower level is a Kramer doublet whose degeneracy is removed by the external magnetic field (see diagram). Optical examinations have shown that the magnitude Δ of the splitting due by the cubical component of the field is 12,300 cm^{-1} (references 1, 3, 4). Reliable data on the magnitude δ of the splitting due to the tetragonal component of the field are lacking. Following Owen's[4] calculations, we assume δ = 1400 cm^{-1}. In accordance with the diagram, we shall designate the two possible spin orientations in an external magnetic field H by + and − signs.

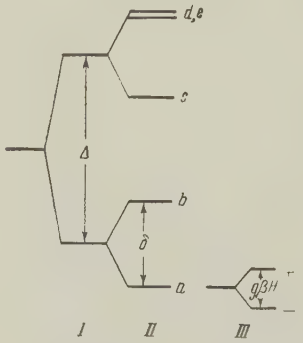

Scheme of the successive splitting of the ground level of a Cu^{++} ion under the influence of: I – an electric field of cubic symmetry; II – tetragonal symmetry; III – levels of the electron spin in the external magnetic field.

The paramagnetic-resonance spectra observed in crystals of Tutton's salts have been interpreted with g-factor values $g_\parallel = 2.4$ and $g_\perp = 2.1$ (Ref. 1).* Here $g_\parallel$ and $g_\perp$ characterize the

*More exact values of the g-factor for different Tutton's salts are given in the paper by Bleany et al.[5]

splitting of the lower Kramer doublet by a magnetic field directed, respectively, parallel and perpendicular to the axis of symmetry of the internal crystal field. It follows from the theory of electron magnetic resonance spectra that a deviation of the g-factor value from the pure spin value is caused by the residual orbital magnetism of the lower orbital singlet of order $\lambda\beta/\Delta$, where λ is the spin-orbit interaction constant. However, calculations of corrections to the g-factor of the λ/Δ type have led to values of $g_\parallel$ and $g_\perp$ which differ from the measured ones. It was therefore assumed that the value of the constant λ in the crystals of Tutton's salts differs from its value for the free Cu^{++} ion ($\lambda = -829\ cm^{-1}$) and equals $-695\ cm^{-1}$ (reference 1).

The measured g-factor values for the Cu^{++} ion in $CuSO_4 \cdot 5H_2O$ crystals are $g_\parallel = 2.47$ and $g_\perp = 2.06$. To explain the experimentally-obtained g-factor values it is necessary to assume the intensities of the tetragonal or rhombic components of the internal crystal field to be very great (of the same order as the cubical one)[2], an assumption not confirmed by the results of the optical investigations. Abe and Ono[3] offer another explanation. They assume that in the $CuSO_4 \cdot 5H_2O$ crystals the constant λ of the spin-orbit bond is an anisotropic quantity with components $\lambda_\parallel = -700\ cm^{-1}$ and $\lambda_\perp = -370\ cm^{-1}$.

The difference between the value of λ in crystals and its value for the free Cu^{++} ion, and the anisotropic character of this value in $CuSO_4 \cdot 5H_2O$ crystals, can be attributed to the partially covalent character of the Cu^{++} ion bond with the nearest atoms of oxygen. A detailed analysis of the influence of covalent bonds in a crystal on the magnitude of the g-factor can be found in the works of Owen[4] and Stevens.[6]

It was established by Kronig[7] and Van Vleck[8] that in the hydrated salts of ions of the iron group the spin-lattice interaction is brought about chiefly by modulation of the internal crystal field by the thermal vibrations of the crystal lattice. Only the orbital motions of the electrons are directly influenced by the electric field. The interaction of the spin with the electric field is effected through the coupling of the spin with the orbit. The dependence of the spin-lattice relaxation time on the orientation of the crystal in the external magnetic field, found by Volokhova[9] in $CuSO_4 \cdot 5H_2O$ crystals, is therefore not unexpected. The anisotropic character of the constant λ is expected to entail an anisotropy of the relaxation time.

We have calculated the spin-lattice relaxation time ρ and determined that the anisotropy of ρ detected in $CuSO_4 \cdot 5H_2O$ crystals can be explained by anisotropy of the constant λ. The expression obtained by us for ρ can also be applied to other salts of the Cu^{++} ion by assuming $\lambda_\parallel = \lambda_\perp$.

2. CALCULATION OF THE RELAXATION TIME

A system of orbital levels of the Cu^{++} ion in the electric field of the crystal with the above mentioned symmetry can be characterized by the following wave functions:[1,10]

$$\Psi_a = (\psi_2 + \psi_{-2})/\sqrt{2},\ \Psi_b = \psi_0,\ \Psi_c = i(\psi_2 - \psi_{-2})/\sqrt{2},$$
$$\Psi_d = i(\psi_1 + \psi_{-1})/\sqrt{2},\ \Psi_e = (\psi_1 - \psi_{-1})/\sqrt{2}. \quad (1)$$

The indices a, b, c, d, e correspond to the diagram.

For a Hamiltonian that takes into account the interaction of the paramagnetic ion with the lattice vibrations we use the expression of Kronig,[7] which is the linear term of a series expansion of the electric potential of the crystal in terms of normal lattice vibrations. For the sake of convenience, we shall write it in a somewhat modified form and with different symbols:

$$\mathcal{H}^{(1)} = f[(3z^2 - r^2)f_1 + 2(x^2 - y^2)f_2 - 2xyf_3 - 2xzf_4 - 2yzf_5], \quad (2)$$
$$f = 8e\mu a^{-5} q\Phi, \qquad f_1 = u_z\lambda_z - {}^2/_3 u_x\lambda_x - {}^2/_3 u_y\lambda_y,$$
$$f_2 = u_x\lambda_x - u_y\lambda_y, \qquad f_3 = u_y\lambda_x + u_x\lambda_y,$$
$$f_4 = u_z\lambda_x + u_x\lambda_z, \qquad f_5 = u_z\lambda_y + u_y\lambda_z.$$

Here u_x, u_y, u_z and λ_x, λ_y, λ_z are cosines determining the directions of polarization and the velocities of elastic-wave propagation, respectively; q is the normal coordinate, μ is the effective dipole moment of the water molecule, $\phi = 2\pi a\nu/c$, c is the velocity of sound, a is the lattice constant; and e is the electron charge.

With the aid of the eigenfunctions (1) for matrix elements $\mathcal{H}^{(1)}$, we obtain the following expressions:

$$\langle a|b\rangle = 4\sqrt{3}\alpha\bar{r}^2 f f_2,$$
$$\langle b|c\rangle = 2\sqrt{3}\alpha\bar{r}^2 f f_3,\ \langle a|c\rangle = 0,$$
$$\langle a|d\rangle = -\sqrt{3}\langle b|d\rangle = -3\alpha\bar{r}^2 f f_5, \quad (3)$$
$$\langle a|e\rangle = \sqrt{3}\langle b|e\rangle = -3\alpha\bar{r}^2 f f_4,$$

where $\alpha = {}^2/_{21}$ and $\bar{r}^2$ is the mean square of the distance of the 3d-electron from the nucleus.

Choosing the direction of the magnetic field H as the axis of quantization of the electron spin, we write the operator of the spin-orbit coupling in the following form:

$$\mathcal{H}_{s0} = \sum_{x'=x',y',z'} [\lambda_\perp (L_x l_{xx'} s_{x'} + L_y l_{yx'} s_{x'}) + \lambda_\parallel L_z l_{zx'} s_{x'}]. \quad (4)$$

Here $l_{xx'}$, $l_{xy'}$ . . . are the cosines of the angles between the axes xyz and x'y'z', where xyz is the coordinate system connected with the symmetry axes of the internal crystal field, and the z' axis is parallel to H.

Let us determine the matrix elements of $\mathcal{H}_{s0}$ needed for the subsequent computations:

$$\begin{aligned} &\langle a|b\rangle = \langle b|c\rangle = 0, \\ &\langle a|c\rangle = 2i\lambda_{\parallel}(l_{zz'}s_{z'} + l_{zy'}s_{y'} + l_{zx'}s_{x'}), \\ &\langle b|d\rangle = \sqrt{3}\langle a|d\rangle \\ &= i\sqrt{3}\lambda_{\perp}(l_{xz'}s_{z'} + l_{xy'}s_{y'} + l_{xx'}s_{x'}), \\ &\langle b|e\rangle = -\sqrt{3}\langle a|e\rangle \\ &= i\sqrt{3}\lambda_{\perp}(l_{yz'}s_{z'} + l_{yy'}s_{y'} + l_{yx'}s_{x'}). \end{aligned} \tag{5}$$

Let us examine the relaxation that results from the Raman scattering of phonons. This case is decisive even at comparatively low temperatures.

Since the splitting factors Δ and δ are sufficiently large ($\Delta, \delta \gg kT$), relaxation will take place only because of transitions between the two lower spin levels. To determine the probability of transition a, $+ \rightarrow$ a, $-$ due to Raman scattering of phonons, it is necessary to obtain for the perturbation energy a matrix element of the type $\mathcal{H}$(a, +, n, n'; a, $-$, n $-$ 1, n' + 1) where n and n' are quantum numbers pertaining to the absorbed and emitted quanta of the elastic vibrations repectively. The latter may be obtained in the third approximation with the aid of expressions (2) and (4), which we will regard as a perturbation. It is necessary to take into consideration that $\Delta \gg \delta$ and for this reason we must choose from among all the terms of $\mathcal{H}'$ those in which the next nearest orbital level b is used as one of the intermediate states.

Taking this into account we obtain:

$$\mathcal{H}' = \sum_{\alpha=c,d,e}\left[\frac{P^{+}(n,n',\alpha) - P^{-}(n',n,\alpha)}{(-\Delta)(-\delta+h\nu)} + \frac{P^{-}(n',n,\alpha) - P^{+}(n,n',\alpha)}{(-\Delta)(-\delta-h\nu')}\right] + \frac{F^{+}(n,n',\alpha) - F^{-}(n',n,\alpha)}{(-\Delta+h\nu)(-\delta+h\nu)} + \frac{F^{-}(n',n,\alpha) - F^{+}(n,n',\alpha)}{(-\Delta-h\nu')(-\delta-h\nu')},$$

$$P^{\pm}_{(n,n',\alpha)} = \langle a, +|\mathcal{H}_{s0}|\alpha,-\rangle\langle\alpha, n|\mathcal{H}^{(1)}|b, n\mp1\rangle\langle b, n'|\mathcal{H}^{(1)}|a,n'\pm1\rangle, \tag{6}$$

$$F^{\pm}_{(n,n',\alpha)} = \langle a, n|\mathcal{H}^{(1)}|b, n\mp1\rangle\langle b, +|\mathcal{H}_{s0}|\alpha, -\rangle\langle\alpha, n'|\mathcal{H}^{(1)}|a, n'\pm1\rangle.$$

We next take it into account that $h\nu \ll \delta$ and consider the frequencies ν and ν' of the emitted and absorbed phonons to be equal (this is permissible if $g\beta H \ll kT$).

The following expression is then obtained in the usual way[8] for the probability of relaxation:

$$\begin{aligned} &A_{+-} = {}^1/_2 AI_8[\lambda_{\parallel}^2 + \lambda_{\perp}^2 - (\lambda_{\parallel}^2 - \lambda_{\perp}^2)l_{zz'}^2], \\ &A = 3.5\cdot10^3\pi^4(h/D\Delta\delta^2)^2(e\mu\bar{r}^2/a^4)^4\left(c_l^{-5} + \frac{3}{2}c_t^{-5}\right)^2, \\ &I_8 = \int_0^{k\Theta/h}\frac{\nu^8 e^{h\nu/kT}}{(e^{h\nu/kT}-1)^2}d\nu. \end{aligned} \tag{7}$$

Here D is the crystal density, c_l and c_t the propagation velocities of longitudinal and transverse elastic waves and Θ the characteristic Debye temperature.

According to the Casimir and Du Pre thermodynamic theory of paramagnetic relaxation,[11] the relaxation time is $\rho = 2\pi C_H/\alpha$, where C_H is the heat capacity of the spin system in the presence of a constant magnetic field H, while α is the coefficient of thermal conductivity between the spin system and the lattice. Using for C_H and α the relations given by Al' tshuler[12] and averaging over the internal magnetic fields with account of the anisotropy of the g-factor, we obtain:

$$\rho = \frac{2\pi}{AI_8}\frac{g_0^2H_0^2 + g_i^2H_i^2/2}{[\lambda_{\parallel}^2 + \lambda_{\perp}^2 - (\lambda_{\parallel}^2 - \lambda_{\perp}^2)\cos^2\varphi]\,g_0^2H_0^2 + {}^2/_3(\lambda_{\parallel}^2 + 2\lambda_{\perp}^2)\,g_i^2H_i^2},$$

$$g_0^2 = g_{\parallel}^2\cos^2\varphi + g_{\perp}^2\sin^2\varphi, \quad g_i^2 = {}^1/_3(g_{\parallel}^2 + 2g_{\perp}^2), \tag{8}$$

where H_i is the effective internal magnetic field, H_0 the intensity of the external magnetic field, and φ the angle between H_0 and the symmetry axis of the electric field of the crystal z.

To illustrate the obtained angle dependence, we shall determine the numerical value of ρ for a $CuSO_4 \cdot 5H_2O$ crystal.

Let us evaluate the constants in (8). The values of Δ, δ, $\lambda_{\parallel}$, $\lambda_{\perp}$ have been given in the first part of this paper. Assuming $\mu = 2 \times 10^{-18}$ cgs esu and using the formula[4] $\Delta = 25e\mu\bar{r}^4/3a^6$, we obtain $a = 2.1 \times 10^{-8}$ cm. We then assume $c_l = c_t = 2.5 \times 10^5$ cm/sec and $\Theta = 100°$K.

Let us determine the values of ρ for the directions of the external magnetic field that correspond to the angles $\varphi_\alpha = 41°$, $\varphi_\beta = 49°$ and $\varphi_\gamma = 90°$ (principal magnetic axes of the crystal) at T = 290°K. In strong magnetic fields ($H_0^2 \gg H_i^2$) we have*

*Considering that the values of the constants are only approximately known, it is sensible to speak only of the order of magnitude of ρ. Exact values of ρ are given as illustration of the angle dependences obtained.

$\rho_\alpha = 0.5 \cdot 10^{-8}$, $\rho_\beta = 0.45 \cdot 10^{-8}$, $\rho_\gamma = 0.34 \cdot 10^{-8}$ sec.

In weak fields ($H_0^2 \ll H_i^2$) we get $\rho = 0.2 \cdot 10^{-8}$ sec. For a polycrystalline specimen

$$\rho = {}^1/_3 (\rho_\alpha + \rho_\beta + \rho_\gamma).$$

The resulting dependence of the relaxation time on the orientation of the $CuSO_4 \cdot 5H_2O$ crystal in an external magnetic field H_0 agrees very well with the experimental results obtained by Volokhova.[9] With a certain approximation the dependence of ρ on the absolute value of H_0 also agrees with the results obtained by Volokhova. The temperature dependence of ρ is determined by the integral I_8.

If the constant λ is isotropic, then the probability of the relaxation transition $A_{+-}(7)$ will also be isotropic. The anisotropy of ρ will be determined in this case by the anisotropy of the g-factor only. With $g_\parallel = 2.4$ and $g_\perp = 2.1$ the computed values of ρ for H_0 directed along the three magnetic axes of the crystal differ by no more than 4%, i.e., it is difficult to attribute to the anisotropy of the g-factor even a comparatively small (10 to 20%) anisotropy of ρ as observed in the crystals of Tutton's copper salts.[9] It may be presumed that the constant λ of the spin-orbit coupling is also anisotropic here, the more so since these salts are similar to $CuSO_4 \cdot 5H_2O$ in their crystalline structure.

In conclusion, the author wishes to thank S. A. Al' tshuler for suggesting this work and for valuable advice.

[1] A. Abraham, and M. H. Pryce, Proc. Roy. Soc. **A206**, 164 (1951).
[2] D. Bagguley and J. Griffits, Proc. Roy. Soc. **A201**, 366 (1950).
[3] H. Abe and K. Ono, J. Phys. Soc. Japan **11**, 947 (1956).
[4] J. Owen, Proc. Roy. Soc. **A227**, 183 (1955).
[5] Bleaney, Bowers and Ingram, Proc. Roy. Soc. **A228**, 147 (1955).
[6] K. W. H. Stevens, Proc. Roy. Soc. **A219**, 542 (1953).
[7] R. L. Kronig, Physica **6**, 33 (1939).
[8] J. H. Van Vleck, Phys. Rev. **57**, 462 (1940).
[9] T. I. Volkhova, J. Exptl. Theoret. Phys. (U.S.S.R.) **33**, 856 (1957), Soviet Phys. JETP **6**, 661 (1958).
[10] D. Polder, Physica **9**, 709 (1942).
[11] H. B. Casimir and K. F. Du Pre, Physica **5**, 507 (1938).
[12] S. A. Alt' shuler, J. Exptl. Theoret. Phys. (U.S.S.R.) **24**, 681 (1953).

Translated by P. F. Schmidt
296

SOVIET PHYSICS JETP VOLUME 34(7), NUMBER 6 DECEMBER, 1958

KINETIC THEORY OF THE FLOW OF A GAS THROUGH A CYLINDRICAL TUBE

O. GHERMAN

Bucharest, Romania

Submitted to JETP editor May 17, 1957; resubmitted January 30, 1958

J. Exptl. Theoret. Phys. (U.S.S.R.) **34**, 1470-1474 (June, 1958)

By introducing a certain "anisotropy function" a good description of the flow of a gas can be obtained, even at pressures at which only empirical formulas have been used hitherto. Furthermore, the term corresponding to the slipping of the gas relative to the walls is obtained automatically, without any additional hypotheses; the same is true of the minimum rate of flow at intermediate pressures. Our final formula is qualitatively correct at all pressures, including intermediate ones.

IT is well known that hydrodynamics cannot provide the solution of the problem of the flow of gases at low pressures. Knudsen[1] succeeded in establishing the correct laws of flow at such pressures by using kinetic theory. In an intermediate range of pressures, however, neither hydrodynamics nor

the kinetic theory as developed by Knudsen can give correct results.

To obtain the laws of flow at arbitrary pressures one must resort to interpolation, as was done by Knudsen. None of these formulas, however, gives an explanation of the laws of flow at intermediate pressures.

Pollard and Present[2] developed a theory for small pressures, in which they took account not only of collisions of the molecules with the walls but also of collisions between molecules. These authors assume that out of the $(n\bar{v}/\lambda)\,d$ molecules that collide during unit time in the volume $d\tau$, the number that leave the volume element in the solid angle $d\omega$ is independent of its orientation relative to the axis of the tube and is given by

$$(n\bar{v}/\lambda)\,d\tau\,d\omega/4\pi. \qquad (1)$$

Consequently the method of Pollard and Present amounts essentially to a kinetic theory of diffusion in tubes. Their results for the diffusion of gases at low pressures are in better agreement with experimental data than the results of the ordinary kinetic theory of gases.

Hiby and Pahl[3-5] have shown that the collision process in a flowing gas gives rise to an anisotropy in the distribution of the molecules that have had collisions. The result is an additional current due to this anisotropy. They have given a purely kinetic formulation of the problem of gas flow. In this formulation, however, the calculations are extraordinarily complicated, so that these authors have in fact had to confine themselves to obtaining a second-order correction to the calculations of Pollard and Present. The predictions of the theory of Hiby and Pahl are in good agreement with the results of experiments at low pressures.

We attempt below to give a unified phenomenological approach to the problem of gaseous flow, which leads to good results at both low and ordinary pressures. The basis of our arguments is the method of Pollard and Present, to which we add certain plausible physical assumptions.

Let us consider a very long cylindrical tube, between the ends of which there is a pressure drop that is extremely small in comparison with the average pressure in the tube. Our hypothesis is that the number of molecules leaving the volume element $d\tau$ in the tube in the solid angle $d\omega$ per unit time is given by

$$\frac{n(x)+f_a}{\lambda}\bar{v}\,d\tau\,\frac{d\omega}{4\pi},$$

where $\lambda^{-1}n(x)\bar{v}\,d\tau\,d\omega/4\pi$ is the isotropic contribution and f_a is a function that characterizes the anisotropy and depends on: (a) the density $n(x)$ of the gas in $d\tau$, (b) the gradient of the density along the axis of the tube, dn/dx, (c) the distance r between $d\tau$ and the axis of the tube, (d) the angle ψ between the axis of the solid angle $d\omega$ and the axis of the tube, and (e) a specific molecular quantity s_p (see Fig. 1).

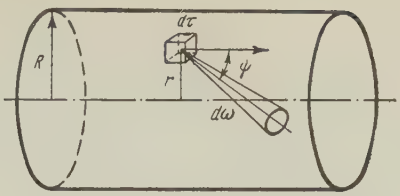

FIG. 1

The expression given above can be written in the form

$$\bar{v}\,d\tau\,\frac{d\omega}{4\pi}\left[n(x)+f_a\left(r, R, \frac{dn}{dx}, \psi, n, s_p\right)\right]/\lambda. \qquad (2)$$

In order to obtain the explicit form of the function f_a we make use of the characteristic data of our problem. Since there is a small difference of pressure between the ends of the tube, f_a can be expanded in a power series in dn/dx, in which we keep only the first two terms. If there is no density gradient, the anisotropy function is zero and the first term in the expansion is zero. Thus we have

$$f_a = \frac{dn}{dx} f(r,\ \psi,\ n,\ s_p).$$

If we assume that the molecules are diffusely reflected by the walls, then we can suppose that the anisotropy function is zero or close to zero at $r = R$. The maximum anisotropy is attained at the axis of the tube, so that if we expand $f(r, \psi, n, s_p)$ in powers of r we get the following form:

$$f = {}^1/_2\,(r^2 - R^2)\,f_1(\psi,\ n,\ s_p).$$

We shall assume that the dependence of f on ψ is such that a larger number of molecules leaves $d\tau$ in the direction of flow of the gas than in the opposite direction. This means that f is positive for values of ψ which correspond to the direction of the flow and is negative for the opposite direction. In relation to the molecules that emerge after colliding, the flowing gas acts like a semitransparent mirror which makes the majority of these molecules leave the volume element in the direction of the flow. We shall assume that in the perpendicular direction the distribution remains unchanged as compared with the isotropic case. From the multitude of angular functions that satisfy the requirements given above, we choose the simplest:

$$f_1(\psi,\ n,\ s_p) = f_2(n,\ s_p)\cos\psi.$$

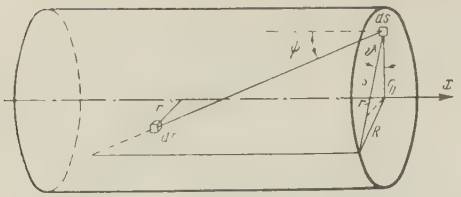

FIG. 2

(It is obvious that in a rigorous treatment one would have to use Fourier series, but for our purpose the approximation just made is satisfactory.)

With a correct choice of $f_2(n, s_p)$, the anisotropy function increases with increasing pressure. (It is obvious that at very small pressures the anisotropy vanishes, and that it increases as the pressure is raised.) We set

$$f_2(n,\ s_p) = k/\lambda$$

and shall show that this choice leads to results in agreement with the experimental data. Let us consider the tube shown in Fig. 2. The number of molecules that traverse the element of area dA of a cross-section in unit time is given by the expression of Pollard and Present with an added anisotropic term:

$$dN = dN_{1s} + kdA\frac{\bar{v}}{4\pi}\int_{\tau}\frac{(r^2 - R^2)\cos^2\psi e^{-\rho/\lambda}}{2\lambda^2\rho^2}\,d\tau\,\frac{dn}{dx}. \qquad (3)$$

Choosing spherical coordinates with the center at the point dA and remembering that for very long tubes dn/dx is practically constant, we get

$$dN = dN_{1s} \cdot$$

$$+ kdA\frac{dn}{dx}\frac{\bar{v}}{4\pi}\int_0^{2\pi} d\varphi\int_0^{\pi} d\psi\cos^2\psi\sin\psi\int_0^{s/\sin\psi}\frac{r^2 - R^2}{\lambda^2}\,e^{-\rho/\lambda}d\rho. \qquad (4)$$

Using the notations of Fig. 2 we have

$$r^2 = r_0^2 + \rho^2\sin^2\psi - 2r_0\rho\sin\psi\cos\vartheta,$$
$$R^2 = r_0^2 + s^2 - 2r_0 s\cos\vartheta.$$

Substituting this into Eq. (4) and integrating with respect to φ, we get

$$dN = dN_{1s} + kdA\frac{dn}{dx}\frac{\bar{v}}{4}\int_0^{\pi} d\psi\cos^2\psi\sin\psi\times$$
$$\times\int_0^{s/\sin\psi}(r_0^2 - R^2 + \rho^2\sin^2\psi - 2r_0\rho\sin\psi\cos\vartheta)\lambda^{-2}e^{-\rho/\lambda}d\rho. \qquad (5)$$

In the case of a small pressure drop along the tube we can regard the mean free path as approximately constant, so that in Eq. (5) we may carry out the integration with respect to ρ:

$$N = N_{1s}$$
$$+\frac{k\bar{v}}{4}\iint dA\int_0^{\pi}\cos^2\psi\sin\psi\left\{\left(\frac{r_0^2 - R^2}{\lambda} - 2r_0\sin\psi\cos\vartheta + 2\lambda\sin^2\psi\right)\right.$$
$$\left. + (2r_0\sin\psi\cos\vartheta - 2s\sin\psi - 2\lambda\sin^2\psi)\,e^{-s/\lambda\sin\psi}\right\}d\psi. \qquad (6)$$

At large pressures, for which $R \gg \lambda$, we keep only the first term in Eq. (6). Then

$$N \approx \frac{k\bar{v}}{4}\frac{dn}{dx}\iint dA\int_0^{\pi}\frac{r_0^2 - R^2}{\lambda}\cos^2\psi\sin\psi\,d\psi = \frac{R^4\pi k\bar{v}}{12\lambda}\frac{dn}{dx}.$$

If we take $k \approx {}^3/_2(\overline{v^2}/\bar{v}^2) \approx {}^3/_2$, then this formula reduces to Poiseuille's law; this shows that the choice of the anisotropy function was correctly made. With this value of k we have in the general case

$$N = N_{1s}$$
$$+\frac{3}{8}\frac{dn}{dx}\bar{v}\iint dA\int_0^{\pi}\cos^2\psi\sin\psi\,d\psi\left[\left(\frac{r_0^2 - R^2}{\lambda} - 2r_0\sin\psi\cos\vartheta\right.\right.$$
$$\left.\left. + 2\lambda\sin^2\psi\right) + (2r_0\sin\psi\cos\vartheta - 2s\sin\psi - 2\lambda\sin^2\psi)\,e^{-s/\lambda\sin\psi}\right].$$

To perform the integration we choose a coordinate system in the transverse section in the way shown in Fig. 3. We have here

$$A = \int_0^{\pi} d\alpha\int_0^{2R\sin\alpha} sds;\quad r\cos\vartheta = s - R\sin\alpha$$

and for N we now have

$$N = N_{1s} - \left[\frac{\pi R^4\bar{v}}{8\lambda} + \frac{\pi R^3\bar{v}}{12} - \frac{\lambda\pi R^2\bar{v}}{5}\right]\frac{dn}{dx}$$
$$+\frac{3}{8}\frac{dn}{dx}\bar{v}\iint dA\int_0^{\pi}\cos^2\psi\sin\psi\,(-2R\sin\psi\sin\alpha - 2\lambda\sin^2\psi)$$
$$\times\exp(-s/\lambda\sin\psi)\,d\psi.$$

Changing the order of the integrations, we bring the last term into the form

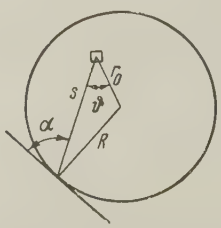

FIG. 3

$$\frac{3}{8}\frac{dn}{dx}\bar{v}\int_0^{\pi} d\alpha \int_0^{\pi} \cos^2\psi \sin\psi\,(-2R\sin\alpha\sin\psi - 2\lambda\sin^2\psi)\int_0^{2R\sin\alpha} se^{-s/\lambda\sin\psi}ds.$$

Integrating over ds, we reduce the problem to the evaluation of a double integral, which can only be done numerically.

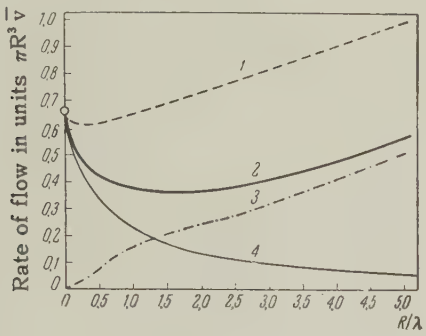

FIG. 4. 1 – observed rate of flow as function of total pressure gradient (Knudsen); 2 – our results; 3 – the anisotropic part of the rate of flow; 4 – rate of flow obtained by Pollard and Present.

At densities such that $\lambda/2 \geq R$, a good approximation to the integral is obtained by expanding the exponential function in power series and integrating numerically over the range $\pi/10 \leq \psi \leq \pi - \pi/10$. In this case we get for the "anisotropic part" of the rate of flow the values shown by the dotted curve. If we add to it the values given by the isotropic term, we get a rate of flow in good qualitative agreement with Knudsen's data,[1] which are shown by the dashed curve.

Thus we have obtained a law which automatically leads to the presence of slip (smaller than the Maxwellian slip) and of a minimum rate of flow, and which is in good agreement with experimental data.

[1] M. Knudsen, Ann. Physik **28**, 75, 999 (1909).
[2] W. G. Pollard and R. D. Present, Phys. Rev. **73**, 762 (1948).
[3] J. W. Hiby and M. Pahl, Z. Naturforsch. **7A**, 533, 542 (1952).
[4] J. W. Hiby and M. Pahl, Z. Physik **129**, 517 (1951).
[5] J. W. Hiby and M. Pahl, Z. Physik **130**, 348 (1951).

Translated by W. H. Furry
297

SOVIET PHYSICS JETP VOLUME 34 (7), NUMBER 6, DECEMBER, 1958

PROPAGATION OF AN ELECTROMAGNETIC FIELD IN A MEDIUM WITH SPATIAL DISPERSION

V. D. SHAFRANOV

Submitted to JETP editor January 7, 1958

J. Exptl. Theoret. Phys. (U.S.S.R.) **34**, 1475-1489 (June, 1958)

General formulas are obtained for the propagation of an electromagnetic field in a semi-infinite, homogeneous, anisotropic medium with spatial dispersion. The propagation of a transverse wave along a magnetic field in a plasma is investigated, taking account of the thermal motion of the electrons. Strong absorption of the field is found in the region for which Cerenkov radiation is possible in the plasma.

IN the present paper we consider the penetration of an electromagnetic field into a semi-infinite, homogeneous, anisotropic medium with spatial dispersion. This problem is an extension of the second part of the well-known paper by Landau[1] in which the penetration of a longitudinal electric field into an isotropic plasma was treated.

In Sec. 1 we obtain general formulas which, in

conjunction with appropriate boundary conditions, can be used to determine the penetration of the longitudinal and the transverse fields.* These formulas are suitable, for example, for analysis of the anomalous skin effect. In Sec. 2 we solve the specific problem involving a plasma, located in a homogeneous magnetic field, in which a transverse wave propagates along the direction of the field.

1. GENERAL FORMULAS

1. We consider a monochromatic field with time dependence of the form $e^{-i\omega t}$. The field propagates from vacuum into a medium which fills the semispace $z > 0$. Because of spatial dispersion there is a functional relation between the electric displacement vector $\mathbf{D}$ and the electric field $\mathbf{E}$:

$$D_\alpha(\mathbf{r}) = \int K_{\alpha\beta}(\mathbf{r}, \mathbf{r}') E_\beta(\mathbf{r}')\, d\mathbf{r}'. \qquad (1)$$

If the spatial dispersion is neglected (in a plasma this procedure corresponds to neglecting the thermal motion of the electrons[2]), we have $K_{\alpha\beta}(\mathbf{r}, \mathbf{r}') = \epsilon_{\alpha\beta}\delta(\mathbf{r}-\mathbf{r}')$ and the local relation between $\mathbf{D}$ and $\mathbf{E}$ is obtained.

In a uniform field the function $K_{\alpha\beta}(\mathbf{r}, \mathbf{r}')$, which is determined by the law of motion of the charges, depends on the vectors $\mathbf{r}$ and $\mathbf{r}'$ only through their difference $\mathbf{R} = \mathbf{r} - \mathbf{r}'$. In a semi-infinite medium the dependence on $\mathbf{r}$ and $\mathbf{r}'$ is affected by the boundary. It will be assumed that the reflection of the charges at the boundary is specular. Under these conditions, the charge distribution functions are not distorted at the boundary and the above dependence on R still applies: $K_{\alpha\beta}(\mathbf{r}, \mathbf{r}') = K_{\alpha\beta}(\mathbf{R})$.

In the general case, the electromagnetic field is determined from the integro-differential equation

$$\operatorname{curl}\operatorname{curl}\mathbf{E} - \frac{\omega^2}{c^2}\mathbf{D} = i\frac{4\pi\omega}{c^2}\mathbf{j}_{\text{trans}}. \qquad (2)$$

As boundary conditions we require that the tangential components of the electric and magnetic fields be continuous across the vacuum-medium interface and that the normal component of the electric induction vector be continuous:

$$[\mathbf{n}\times\mathbf{E}_e] = [\mathbf{n}\times\mathbf{E}^0],\ [\mathbf{n}\times\mathbf{H}_e] = [\mathbf{n}\times\mathbf{H}^0],\ (\mathbf{n}\cdot\mathbf{E}_e) = (\mathbf{n}\cdot\mathbf{D}). \qquad (3)$$

The subscript "e" refers to the total field, made up of the incident and reflected wave, while the superscript "0" refers to the penetrating wave; $\mathbf{n} = \{0, 0, 1\}$ is a unit vector normal to the boundary surface.

The integro-differential equation (1) is solved most conveniently by expanding all quantities in plane waves. For this purpose we transform the problem from that of finding the penetration of a field from vacuum into a semi-infinite medium $z > 0$ into the problem of finding the field in an infinite medium $-\infty < z < \infty$ excited by surface currents and charges concentrated in the plane $z = 0$. It is easy to show that the tangential component of the magnetic field, $\mathbf{H}_t = \mathbf{n}\times\mathbf{H}$, and the normal component of the electric displacement vector $D_n = \mathbf{n}\cdot\mathbf{D}$ are odd functions of z and are discontinuous at the surface $z = 0$. The discontinuities in H_t and D_n correspond to surface currents and charges. The appropriate volume charge density, which yields the proper boundary conditions for H_t and D_n in the plasma, can be written

$$\mathbf{j}_{\text{trans}} = \frac{c}{2\pi}\left\{[\mathbf{n}\times\mathbf{H}^0]\,\delta(z) + i\frac{\omega}{4\pi}(\mathbf{n}\cdot\mathbf{E}_e)\,\mathbf{n}\,\operatorname{Sgn} z\right\}. \qquad (4)$$

Expanding all quantities in plane waves

$$\mathbf{E}(z) = \int \mathbf{E}(\mathbf{k})\, e^{i\mathbf{k}\cdot\mathbf{r}}\, d\mathbf{k}, \quad \delta(z) = \frac{1}{2\pi}\int e^{i\mathbf{k}\cdot\mathbf{r}}\,\delta(\mathbf{k}_\perp)\, d\mathbf{k}, \qquad (5)$$

$$K_{\alpha\beta}(\mathbf{r}) = \frac{1}{(2\pi)^3}\int \varepsilon_{\alpha\beta}(\mathbf{k})\, e^{i\mathbf{k}\cdot\mathbf{r}}\, d\mathbf{k},$$

$$\operatorname{Sgn} z = -\int\left[\delta(k_z) - \frac{1}{i\pi k_z}\right] e^{i\mathbf{k}\cdot\mathbf{r}}\,\delta(\mathbf{k}_\perp)\, d\mathbf{k},$$

$$\mathbf{k}_\perp = \{k_x, k_y, 0\},$$

we find the Fourier components of Eq. (2):

$$-k_\alpha k_\beta E_\beta(\mathbf{k}) + k^2 E_\alpha(\mathbf{k}) - \frac{\omega^2}{c^2}\varepsilon_{\alpha\beta}(\mathbf{k})\,E_\beta(\mathbf{k}) = i\frac{\omega}{\pi c}[\mathbf{n}\times\mathbf{H}^0]_\alpha\delta(\mathbf{k}_\perp) + \frac{\omega^2}{c^2}(\mathbf{n}\cdot\mathbf{E}_e)\,\mathbf{n}_\alpha\left[\delta(k_z) - \frac{1}{i\pi k_z}\right]\delta(\mathbf{k}_\perp). \qquad (6)$$

Taking account of the δ-function in $\mathbf{k}_\perp$ on the right-hand side of this equation, we have on the left-hand side $k_x = k_y = 0$. We also introduce the notation $k_z = N\omega/c$. In component form, the equations become

$$\begin{aligned} N^2E_x - \varepsilon_{x\alpha}(N)E_\alpha &= -i\frac{c}{\pi\omega}H_y^0\delta(\mathbf{k}_\perp),\\ N^2E_y - \varepsilon_{y\alpha}(N)E_\alpha &= i\frac{c}{\pi\omega}H_x^0\delta(\mathbf{k}_\perp),\\ -\varepsilon_{z\alpha}(N)E_\alpha &= -\frac{c}{\omega}E_{ez}\left[\delta(N) - \frac{1}{i\pi N}\right]\delta(\mathbf{k}_\perp). \end{aligned} \qquad (6')$$

*The terms "longitudinal" and "transverse" refer to the method of exciting the field in the anisotropic medium. Thus, if the field propagates from vacuum into the medium these terms, refer to the field in vacuum. As is well known, however, the field which penetrates into the anisotropic medium cannot, in general, be divided into a purely transverse part and a purely longitudinal part.

2. We now consider the longitudinal field. Setting $H_x^0 = H_y^0 = 0$, we introduce the quantities

$$\eta_{xx} = \varepsilon_{xx} - \varepsilon_{xz}\varepsilon_{zx}/\varepsilon_{zz};\ \eta_{yy} = \varepsilon_{yy} - \varepsilon_{yz}\varepsilon_{zy}/\varepsilon_{zz},$$
$$\eta_{xy} = \varepsilon_{xy} - \varepsilon_{xz}\varepsilon_{zy}/\varepsilon_{zz};\ \eta_{yx} = \varepsilon_{yx} - \varepsilon_{yz}\varepsilon_{zx}/\varepsilon_{zz}. \tag{7}$$

Using the first two equations in (6) to eliminate E_x and E_y we have

$$E_z = -\frac{c}{\omega}\frac{E_{ez}}{\varepsilon_{zz}(N)}\frac{(N^2-\varepsilon_1^0)(N^2-\varepsilon_2^0)}{(N^2-\varepsilon_1)(N^2-\varepsilon_2)}\left[\delta(N) - \frac{1}{i\pi N}\right]\delta(\mathbf{k}_\perp). \tag{8}$$

Here we have introduced the notation

$$\begin{aligned} &N^4 - N^2(\eta_{xx}+\eta_{yy}) + \eta_{xx}\eta_{yy} \\ &-\eta_{xy}\eta_{yx} \equiv (N^2-\varepsilon_1)(N^2-\varepsilon_2), \\ &N^4 - N^2(\varepsilon_{xx}+\varepsilon_{yy}) \\ &+\varepsilon_{xx}\varepsilon_{yy} - \varepsilon_{xy}\varepsilon_{yx} \equiv (N^2-\varepsilon_1^0)(N^2-\varepsilon_2^0). \end{aligned} \tag{9}$$

The expression for the field in the medium assumes the form

$$E_z(z) = -E_{ez}\int_{-\infty}^{+\infty}\frac{(N^2-\varepsilon_1^0)(N^2-\varepsilon_2^0)}{(N^2-\varepsilon_1)(N^2-\varepsilon_2)}\frac{e^{i\omega Nz/c}}{\varepsilon_{zz}(N)}\left[\delta(N) - \frac{1}{i\pi N}\right]dN. \tag{10}$$

In an isotropic plasma $\epsilon_1^0 = \epsilon_1$, $\epsilon_2^0 = \epsilon_2$ and Eq. (10) coincides with Landau's expression for the longitudinal field. The function K_k which appears in reference 1 is related to $\epsilon_{zz}(N)$ by the expression $\epsilon_{zz}(N) = 1 - K_k$ so that $K_0 = 1 - \epsilon_{zz}(0)$.

In the absence of spatial dispersion (i.e., when $\epsilon_{\alpha\beta}$ is independent of N) the integral in Eq. (10) is computed easily:

$$E_z(z) = \frac{E_{ez}}{\varepsilon_{zz}}\left\{\frac{\varepsilon_1^0\varepsilon_2^0}{\varepsilon_1\varepsilon_2} + \frac{(\varepsilon_1-\varepsilon_1^0)(\varepsilon_1-\varepsilon_2^0)}{\varepsilon_1(\varepsilon_1-\varepsilon_2)}\exp\left\{i\frac{\omega}{c}\sqrt{\varepsilon_1}z\right\}\right.$$
$$\left. + \frac{(\varepsilon_2-\varepsilon_2^0)(\varepsilon_2-\varepsilon_1^0)}{\varepsilon_2(\varepsilon_2-\varepsilon_1)}\exp\left\{i\frac{\omega}{c}\sqrt{\varepsilon_2}z\right\}\right\}. \tag{11}$$

3. We next consider the penetration of the transverse field. Let $E_{ez} = 0$. From the last equation in (6′) we find

$$E_z(z) = -(\varepsilon_{zx}E_x + \varepsilon_{zy}E_y)/\varepsilon_{zz}. \tag{12}$$

Substituting this expression in the first two equations we obtain

$$\begin{aligned} (N^2-\eta_{xx})E_x - \eta_{xy}E_y &= -i\frac{c}{\omega\pi}H_y^0\delta(\mathbf{k}_\perp), \\ -\eta_{yx}E_x + (N^2-\eta_{yy})E_y &= i\frac{c}{\omega\pi}H_x^0\delta(\mathbf{k}_\perp). \end{aligned} \tag{13}$$

We introduce the notation

$$\begin{aligned} E &= E_x + \lambda E_y, \\ H^0 &= H_y^0 - \lambda H_x^0, \end{aligned} \tag{14}$$

and determine the values $\lambda = \lambda_1$ and $\lambda = \lambda_2$ and $\epsilon = \epsilon_1$ and $\epsilon = \epsilon_2$ from the relation

$$\varepsilon = \eta_{xx} + \lambda\eta_{yx} = \eta_{yy} + \eta_{xy}/\lambda. \tag{15}$$

Then we obtain in place of Eq. (13) two equations of the form

$$(N^2-\varepsilon)E = -i\frac{c}{\omega\pi}H^0\delta(\mathbf{k}_\perp). \tag{16}$$

The roots $\lambda_{1,2}$ of Eq. (15) determine the ratio of the x-th and y-th field components of the normal ordinary and extraordinary waves.

The corresponding functions $\epsilon(N) = \epsilon_1(N)$ and $\epsilon(N) = \epsilon_2(N)$ are determined through the tensor $\epsilon_{\alpha\beta}(\mathbf{k})$ in the same way as the squares of the refractive indices for the ordinary and extraorinary waves in the absence of spatial dispersion. It is easily shown that

$$\lambda_1\lambda_2 = -\frac{\eta_{xy}}{\eta_{yx}};\quad \lambda_1+\lambda_2 = \frac{\eta_{yy}-\eta_{xx}}{\eta_{yx}} \tag{17}$$

and

$$\varepsilon_1+\varepsilon_2 = \eta_{xx}+\eta_{yy};\ \varepsilon_1\varepsilon_2 = \eta_{xx}\eta_{yy} - \eta_{xy}\eta_{yx}. \tag{18}$$

It is apparent from Eqs. (18) and (9) that both definitions of $\epsilon_{1,2}$ (9) and (15) are the same. In accordance with Eqs. (5) and (16), the expression for the electric field can be written in the form

$$E_{1,2}(z) = -\frac{i}{\pi}\int_{-\infty}^{+\infty}\frac{H_{1,2}^0 e^{i\omega Nz/c}}{N^2-\varepsilon_{1,2}(N)}dN. \tag{19}$$

If there is no spatial dispersion, we obtain by the method of residues

$$E_{1,2}(z) = \frac{H_{1,2}^0}{\sqrt{\varepsilon_{1,2}}}\exp\{i\sqrt{\varepsilon_{1,2}}z\}. \tag{20}$$

Using the boundary conditions given in (3), it is easy to determine from Eq. (19) all components of an electromagnetic field that propagates in an anisotropic medium with spatial dispersion.

Formulas (10) and (19) are of interest in connection with the penetration of a field into a plasma located in a magnetic field. It is important to note that the functions $\epsilon_{\alpha\beta}(\mathbf{k})$ and, thus, $\epsilon_{1,2}(N)$ are not analytic when thermal motion of the electrons in the plasma is taken into account. Thus, for example, the integral in (19) cannot be computed by residues and the field in the plasma cannot be expressed by a simple formula such as (20).

2. TRANSVERSE ELECTROMAGNETIC FIELD PROPAGATING IN A PLASMA ALONG THE MAGNETIC FIELD

1. In a plasma which is located in a homogeneous magnetic field H_0, the tensor $\epsilon_{\alpha\beta}(\mathbf{k})$ is given by the equation

$$\varepsilon_{\alpha\beta}(\mathbf{k}) = \delta_{\alpha\beta} + i\frac{4\pi e^2 n_0}{\omega T}\left\langle \int_0^\infty v_\alpha(t)\, v_\beta(0) \exp\left\{ i\left(\omega t - \mathbf{k}\int_0^t \mathbf{v}(\xi)\, d\xi\right) - \nu t\right\} dt\right\rangle. \tag{21}$$

Here n_0 is the electron density in the plasma and $\mathbf{v}(t)$ describes the motion of an electron in the homogeneous magnetic field; if the magnetic field is along the z axis,

$$v_x = v_\perp(0)\cos(\omega_H t + \varphi);\ v_y = v_\perp(0)\sin(\omega_H t + \varphi),$$
$$v_z = v_z(0); \tan\varphi = v_{y0}/v_{x0};\ \omega_H = |e|H_0/mc\sqrt{1-(v/c)^2}. \tag{22}$$

The triangular brackets denote averages taken over a Maxwellian velocity distribution, T is the temperature of the plasma, expressed in energy units, and ν is the frequency of collisions between electrons and heavy particles in the plasma.

Equation (21) is an inversion of the correlation function for microcurrents.[3] It can be shown that this formula is the same as the expression for $\epsilon_{\alpha\beta}(\mathbf{k})$ obtained in references 4 to 6.

If the wave is propagated in the z direction (along the magnetic field) and $T \ll mc^2$, the tensor $\epsilon_{\alpha\beta}$ assumes the form

$$\varepsilon_{\alpha\beta} = \delta_{\alpha\beta} - \frac{\omega_0^2}{\omega^2}\frac{1}{\beta\sqrt{\pi}N}\left\{ \frac{1}{2} W\left(\frac{\omega - \omega_H + i\nu}{\omega\beta N}\right)\begin{pmatrix} 1 & -i & 0 \\ i & 1 & 0 \\ 0 & 0 & 0 \end{pmatrix} + \frac{1}{2} W\left(\frac{\omega + \omega_H + i\nu}{\omega\beta N}\right)\begin{pmatrix} 1 & i & 0 \\ -i & 1 & 0 \\ 0 & 0 & 0 \end{pmatrix} + W_1\left(\frac{\omega + i\nu}{\omega\beta N}\right)\begin{pmatrix} 0 & 0 & 0 \\ 0 & 0 & 0 \\ 0 & 0 & 1 \end{pmatrix}\right\}. \tag{23}$$

Here $\omega_0^2 = 4\pi e^2 n_0/m$; $\beta^2 = 2T/mc^2$ and

$$W(u) = \int_{-\infty}^{+\infty} \frac{e^{-t^2}}{u - t}\, dt = -i\pi e^{-u^2}\left\{ \operatorname{Sgn}\operatorname{Im} u + \frac{2i}{\sqrt{\pi}}\int_0^u e^{t^2} dt\right\},$$
$$W_1(u) = \int_{-\infty}^{+\infty} \frac{2t^2 e^{-t^2}}{u - t}\, dt = 2u^2 W(u) - 2\sqrt{\pi}u. \tag{24}$$

According to Eqs. (7), (15), and (23), $\lambda^2 = \epsilon_{xy}/\epsilon_{yx} = -1$. The values $\lambda = \pm i$ correspond to a field $E = E_x \pm iE_y$ which is circularly polarized. The function $\epsilon(N) = \epsilon_{1,2}(N)$, which appears in Eq. (19), is found to be $\epsilon = \epsilon_{xx} \pm i\epsilon_{yx}$; in view of Eqs. (23) and (24),

$$\varepsilon = 1 + i\frac{\sqrt{\pi}}{\beta}\frac{\omega_0^2}{\omega^2 N} e^{-(x/N)^2}\left(\operatorname{Sgn} N + \frac{2i}{\sqrt{\pi}}\int_0^{x/N} e^{t^2} dt\right),$$
$$x = (\omega \pm \omega_H + i\nu)/\omega\beta. \tag{25}$$

2. The electric field in the plasma is expressed by Eq. (19), where $H^0_{1,2} = H^0_x \mp iH^0_y$. For the ordinary wave $x = (\omega + \omega_H + i\nu)/\omega\beta \gg 1$ and the spatial dispersion is unimportant since, when $x/N \gg 1$, the expression for ϵ assumes the form

$$\varepsilon = 1 - \omega_0^2/\beta\omega^2 x = 1 - \omega_0^2/\omega(\omega + \omega_H + i\nu).$$

We next consider the penetration of the extraordinary wave, setting $\nu = 0$. The situation here is similar to that which obtains in the oscillations of a plasma in an external electric field. The integral in (19) can be computed approximately by transforming to the complex plane. In order to carry out this procedure, we introduce in place of $\epsilon(N)$ (25) the analytic functions $\epsilon^{(1)}(N)$ and $\epsilon^{(2)}(N)$ which coincide with $\epsilon(N)$ for $N < 0$ and $N > 0$ respectively:

$$\varepsilon^{(1)}(N) = 1 - i\frac{\sqrt{\pi}}{\beta}\frac{\omega_0^2}{\omega^2 N} e^{-(X/N)^2}\left(1 - \frac{2i}{\sqrt{\pi}}\int_0^{X/N} e^{t^2} dt\right);$$
$$\varepsilon^{(2)}(N) = 1 + i\frac{\sqrt{\pi}}{\beta}\frac{\omega_0^2}{\omega^2 N} e^{-(X/N)^2}\left(1 + \frac{2i}{\sqrt{\pi}}\int_0^{X/N} e^{t^2} dt\right). \tag{26}$$

Hereinafter $X \equiv (\omega - \omega_H)/\omega\beta$.

As N approaches zero, both functions tend to the limiting value ϵ_0, which equals the square of the refractive index for the extraordinary wave if thermal motion is disregarded

$$\varepsilon_0 = 1 - \omega_0^2/\omega(\omega - \omega_H);\ (\omega \neq \omega_H). \tag{27}$$

In the upper half of the complex variable N, the same limiting value is obtained for $\epsilon^{(1)}(N)$ as N approaches zero by any path which does not pass through the sector $\pi/4 < \arg N < 3\pi/4$ when $\omega < \omega_H$. The same holds for $\epsilon^{(2)}(N)$ if the path which does not pass through this sector when $\omega > \omega_H$.

In accordance with Eqs. (19) and (26), the electric field can be written in the form*

*The first expression for the field of a transverse wave propagating along a magnetic field was derived by Silin.[7] In his paper, however, no account was taken of the difference in the sign of Im K ± (k) for $k > 0$ and $k < 0$. In our case this difference leads to the difference in the functions $\varepsilon^{(1)}(N)$ and $\varepsilon^{(2)}(N)$ [Sgn N in Eq. (25)!]. The function $\varepsilon^{(1)}(N)$, which differs from $\varepsilon^{(2)}(N)$, appears because of the necessity for introducing advanced potentials as well as retarded potentials in the boundary value problem.

$$E(z) = -\frac{1}{\pi} H^0 \left\{ \int_{-\infty}^{0} \frac{e^{i\omega Nz/c}}{N^2 - \varepsilon^{(1)}(N)} dN + \int_{0}^{\infty} \frac{e^{i\omega Nz/c}}{N^2 - \varepsilon^{(2)}(N)} dN \right\} \quad (28)$$

or, going over to integration in the complex plane

$$E(z) = -\frac{i}{\pi} H^0 \left\{ \oint_{C_1} \frac{e^{i\omega Nz/c}}{N^2 - \varepsilon^{(1)}(N)} dN + \oint_{C_2} \frac{e^{i\omega Nz/c}}{N^2 - \varepsilon^{(2)}(N)} + \frac{2i\sqrt{\pi}}{\beta} \frac{\omega_0^2}{\omega^2} \int_{OA} \frac{\exp\{-X^2/N^2 + i\omega Nz/c\}}{N[N^2 - \varepsilon^{(1)}(N)][N^2 - \varepsilon^{(2)}(N)]} dN \right\}. \quad (29)$$

The contours C_1, C_2 and the path of integration OA for the frequencies $\omega < \omega_H$ and $\omega > \omega_H$, are chosen as shown in Fig. 1. The curve OA passes

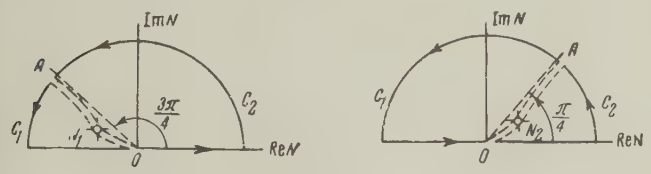

a FIG. 1 b

through the saddle point of the integrand in the third term in Eq. (29). The first and second integrals in Eq. (29) are computed by the method of residues. If N_0 is a root of the equation $N^2 - \epsilon^{(\alpha)}(N) = 0$ ($\alpha = 1, 2$), the corresponding integral makes the following contribution to the field:

$$E_1(z) = \frac{H^0}{N_0} \frac{e^{i\omega N_0 z/c}}{1 - (1/2N_0)\, d\varepsilon^{(\alpha)}(N_0)/dN_0}. \quad (30)$$

This part of the field propagates as a damped wave in the plasma. The asymptote for large values of z in the last integral can be obtained by the method of steepest descent. We first exclude the resonance region. Then the saddle points are

$$N_1 = (2cX^2/\omega z)^{1/3} e^{i5\pi/6} \quad \text{for } \omega < \omega_H;$$
$$N_2 = (2cX^2/\omega z)^{1/3} e^{i\pi/6} \quad \text{for } \omega > \omega_H.$$

At large values of z, $N_{1,2}$ is small so that we can write in the denominator of the integrand $N^2 - \epsilon^{(1)}(N) = N^2 - \epsilon^{(2)}(N) = -\epsilon_0$. A simple calculation of the last term in the field expression (29) yields

$$E_2(z) = \frac{2H^0}{\sqrt{3}\beta} \frac{\omega_0^2}{\omega^2 \varepsilon_0^2} \left[\frac{2\beta c}{z(\omega_H - \omega)}\right]^{1/3} \exp\left\{-\frac{3}{2}\left(\frac{z(\omega_H - \omega)}{2\beta c}\right)^{2/3} + i\left[\frac{3\sqrt{3}}{2}\left(\frac{z(\omega_H - \omega)}{2\beta c}\right)^{2/3} + \frac{\pi}{6}\right]\right\}; \quad (\omega < \omega_H), \quad (31)$$

$$E_2(z) = \frac{2H^0}{\sqrt{3}\beta} \frac{\omega_0^2}{\omega^2 \varepsilon_0^2} \left[\frac{2\beta c}{z(\omega - \omega_H)}\right]^{1/3} \exp\left\{-\frac{3}{2}\left(\frac{z(\omega - \omega_H)}{2\beta c}\right)^{2/3} - i\left[\frac{3\sqrt{3}}{2}\left(\frac{z(\omega - \omega_H)}{2\beta c}\right)^{2/3} - \frac{5\pi}{6}\right]\right\}; \quad (\omega > \omega_H).$$

When $\beta = 0$ the field $E_2(z)$ vanishes and, in accordance with Eqs. (29) and (30), we are left with the simple wave $E(z) = (H^0/\sqrt{\epsilon_0}) \exp\{i\omega\sqrt{\epsilon_0}\, z/c\}$. When $\epsilon_0 > 0$ this expression is obtained from a second term in Eq. (29); when $\epsilon_0 < 0$ it is obtained from the first. If $\beta \neq 0$, the chief contribution is associated with the field $E_2(z)$.

3. We consider Eqs. (29) to (31) in three frequency regions, assuming at the outset that $\omega_0^2 \gg \omega_H^2\beta$ (high electron density).

(a) $\omega < \omega_H$. In this region the equation $N^2 - \epsilon^{(1)}(N) = 0$ has no roots in the contour C_1 and the first integral in Eq. (29) vanishes. The equation $N^2 - \epsilon^{(2)}(N) = 0$ has a root $N_0 = n + iq$, which is determined at resonance by the expressions

$$q^3 + q/4 = \sqrt{\pi}\omega_0^2/8\beta\omega_H^2; \quad n^2 = 1 + 3q^2 \quad (32)$$

and far from resonance, $n \gg q$, by the approximation formulas:

$$n^2 = 1 + \frac{2}{3}\frac{\omega_0^2}{\omega^2 n} \exp\{-(X/n)^2\} \int_0^{-X/n} e^{t^3} dt \approx 1 + \frac{\omega_0^2}{\omega(\omega_H - \omega)},$$

$$q = \frac{\sqrt{\pi}}{2\beta} \frac{\omega_0^2}{\omega^2 n^2} \exp\{-(X/n)^2\}. \quad (33)$$

These formulas define the absorption line shape for a linear oscillator (in this case the electron in the magnetic field) when the Doppler effect is taken into account. It is easy to show that when $\beta = 0$ in the plasma the square of the refractive index has the following form [in place of (27)]:

$$\varepsilon = 1 - \frac{\omega_0^2}{\omega(\omega - \omega_H)} + i\pi \frac{\omega_0^2}{\omega} \delta(\omega - \omega_H);$$

the δ-function in the imaginary part of ϵ means that the electrons absorb energy at the resonance frequency. If there is a spread in the electron velocities v_z the absorption line is broadened as a consequence of the Doppler effect and Eq. (33) is obtained.

Equation (33) differs from the well-known expression for the Doppler-broadened absorption of an oscillator in that the phase velocity is c/n rather than the free-space velocity. As a result E_1 [Eq. (30)] falls off rapidly (is absorbed) over a relatively wide range of frequencies (greater than $\omega_H\beta$) when the electron density is high. Absorption is especially important when $\omega_0^2/\omega_H^2 \geq 1/\beta^2$ or $H_0^2/8\pi \leq n_0 T$. Thus, for example, when $\omega_0^2/\omega_H^2 = 1/\beta^2$, the absorption factor is $q = 0.27\beta$ at a frequency which is one-fifth of the resonance frequency ($\omega = \frac{1}{5}\omega_H$).

At high values of z the electric field is given by Eq. (31); this expression also shows strong attenuation of the field amplitude.

(b) $\omega_H \leq \omega < \omega_1$, $\omega_1 = \omega_H/2 + \sqrt{\omega_H^2/4 + \omega_0^2}$. In this region $\epsilon_0 < 0$, and propagation does not

take place if thermal motion is not taken into account. When $\omega \geq \omega_H$, the equation $N^2 - \epsilon^{(1)}(N) = 0$ has one pure imaginary root in the upper half of the plane, $N_0 = iq$ where q is determined from the equation

$$q^2 + 1 = \frac{\sqrt{\pi}}{\beta} \frac{\omega_0^2}{\omega^2 q} \exp\{(X/q)^2\} \left(1 - \frac{2}{\sqrt{\pi}} \int_0^{X/q} e^{-t^2} dt\right). \quad (34)$$

The quantity q falls off monotonically from $\omega = \omega_H$ to a value $\omega = \omega_1$ at which it vanishes. As $q \to 0$, using the asymptotic value of the error integral which appears in (34) we have

$$q^2 = \omega_0^2/\omega^2\beta X^4 - 1 = \omega_0^2/\omega(\omega - \omega_H) - 1 = -\varepsilon_0$$

and the limiting frequency, at which $q = 0$, is ω_1. The corresponding field E_2 is attenuated, just as in the case in which the thermal motion is not considered.

Outside the sector $\pi/4 < \arg N < 3\pi/4$, the equation $N^2 - \epsilon^{(2)}(N) = 0$ has a root with an imaginary part which approaches infinity as $\beta \to 0$. The corresponding field is not of interest because it is so small.

At large values of z, the most important contribution is due to $E_2(z)$ which propagates in the plasma and is absorbed in exponential fashion (the exponent is $z^{2/3}$). The existence of an absorbed wave means that if $\beta \neq 0$ the electromagnetic wave is not completely reflected in the region where $\epsilon_0 < 0$.

(c) $\omega > \omega_1$. In this region the second and third terms in Eq. (29) assume major importance. The equation $N^2 - \epsilon^{(2)}(N) = 0$ has the root $N_0 = n + iq$ where $q \ll n$, thus Eqs. (33) hold

$$n^2 = \varepsilon_0 = 1 - \omega_0^2/\omega(\omega - \omega_H),$$
$$q = \frac{\sqrt{\pi}}{2} \frac{\omega_0^2}{\omega^2 \beta \varepsilon_0} \exp\{-(X/\varepsilon_0)^2\}. \quad (35)$$

In contrast to Eq. (33), here $n^2 = \epsilon_0$ is less than unity and absorption is not important, It should be kept in mind that in obtaining the tensor $\epsilon_{\alpha\beta}(\mathbf{k})$ use has been made of a nonrelativistic Maxwellian electron distribution ($mc^2 \gg T$) so that the terms which contain the factor $e^{-\beta^{-2}}$ in the formulas should be considered precisely zero. Thus, when $\omega \gg \omega_H$, q vanishes and an unattenuated wave $E = (H^0/\sqrt{\epsilon_0}) \exp\{i\omega\sqrt{\epsilon_0}\, z/c\}$ propagates in the plasma.

4. We now consider the case in which ϵ is slightly different from unity $\omega_0^2/\omega_H^2\beta < 1$ (low electron density $n_0 < 0.9 \times 10^5 \beta H_0^2$).

In this case the equation $N^2 - \epsilon^{(2)}(N) = 0$ has the solution

$$N_0^2 = 1 - \frac{2\omega_0^2}{\omega^2\beta} \exp\{-X^2\} \int_0^X e^{t^2} dt + i \frac{\sqrt{\pi}}{\beta} \frac{\omega_0^2}{\omega^2} \exp\{-X^2\} \quad (36)$$

where $\mathrm{Re}\, N_0 \gg \mathrm{Im}\, N_0 > 0$ for all frequencies. The solution of the equation $N^2 - \epsilon^{(1)}(N) = 0$ differs in the sign of the imaginary part. Thus when it is slightly different from unity, the refractive index is calculated from usual dispersion equations (5) and (6), where the integrals of the type in (24) are taken along a path which goes around the pole $t = u$ from below (corresponding to the condition $\mathrm{Sgn}\, \mathrm{Im}\, u = 1$). It is apparent from Eq. (36) that, with the exception of the narrow resonance region, $\mathrm{Im}\, N_0 \ll 1$ everywhere. The amplitude of the propagating part $E_1(z)$ thus turns out to be considerably larger than that of the nonpropagating part $E_2(z)$. The analysis of the penetration of the electromagnetic wave is thus reduced to the usual problem involving the dispersion equation in (36).

5. If the magnetic field is at some arbitrary angle $\theta \neq 0$ with respect to the direction of propagation of the wave (z axis), all the formulas become much more complicated. In this case the tensor $\epsilon_{\alpha\beta}(\mathbf{k})$ contains all nine components. Resonances appear at frequencies which are multiples of ω_H.[5] The additional terms in $\epsilon_{\alpha\beta}(\mathbf{k})$ however, are proportional to different powers of β and when $\beta \ll 1$ these terms are unimportant. Hence, a first approximation to $\epsilon_{\alpha\beta}(\mathbf{k})$, with thermal motion taken into account, is given by Eq. (23). From this formula it is apparent that the tensor $\epsilon_{\alpha\beta}(\mathbf{k})$ is the same as the tensor $\epsilon_{\alpha\beta}$ computed for the case in which $\beta = 0$ (ref. 9) if

$$\text{(a)}\ (\omega - \omega_H)/\omega\beta N \cos\theta \gg 1 \quad \text{(b)}\ 1/\beta N \gg 1.$$

The first condition means that the imaginary parts of the components of the dielectric permittivity tensor ϵ_{xx}, ϵ_{yy}, $i\epsilon_{xy}$ must be small. The second means that the imaginary part of ϵ_{zz} must be small. These conditions are not satisfied in two regions: (a) close to the resonance frequency, and (b) at frequencies for which the index of refraction calculated with the usual formulas, with $\beta = 0$, is large. The violation of the first condition is associated with magnetic radiation at a frequency ω_H and a corresponding resonance absorption. The violation of the second condition is due to coherent Cerenkov radiation and the radiation absorption associated with this effect (this question is considered in detail in the Appendix). The width of the absorption band, as can be seen from the example involving longitudinal propagation, may be very large.

CONCLUSIONS

1. At a given frequency ω a transverse electromagnetic wave in a medium with spatial dispersion cannot, in general, be represented in the form of a wave $e^{i(\omega N_0 z/c-\omega t)}$ as is the case in the absence of dispersion. If a solution is sought in this form in the case of a wave which propagates along a magnetic field in a plasma, the following dispersion equation is obtained:

$$N^2 = 1 + i\frac{\sqrt{\pi}}{\beta}\frac{\omega_0^2}{\omega^2 N}\exp\left\{-\left(\frac{\omega-\omega_H}{\omega\beta N}\right)^2\right\}$$

$$\times\left\{\operatorname{Sgn}\operatorname{Im}\left(\frac{\omega-\omega_H}{\omega\beta N}\right)+\frac{2i}{\sqrt{\pi}}\int_0^{(\omega-\omega_H)/\omega\beta N} e^{t^2}dt\right\}.$$

This expression contains the nonanalytic function $\operatorname{Sgn}\operatorname{Im}(\omega-\omega_H)\omega\beta N$ and leads to an incorrect solution when $\omega > \omega_H$, where this equation has no roots at all.

The electromagnetic field must be determined in each individual case, taking account of the boundary conditions. This is the procedure used in analyzing the field in oscillations of a plasma in an external longitudinal electric field.[1]

2. Analysis of the propagation of an electromagnetic field in a plasma in a magnetic field indicates that this field consists of two parts. One part of the field is characterized by a phase velocity which depends on the z coordinate ($v_{phase} \sim z^{1/3}$) and decays exponentially (exponent $z^{2/3}$). The other part of the field is the usual wave.

At high values of electron density, $n_0 \gg 0.9 \times 10^5\ \beta H_0^2$, the refractive index for this wave is determined from the equation $N^2 - \epsilon^{(2)}(N) = 0$ in the region $\epsilon_0 > 0$ and from the equation $N^2 - \epsilon^{(1)}(N) = 0$ in the region $\epsilon_0 < 0$ [cf. Eq. (26)].

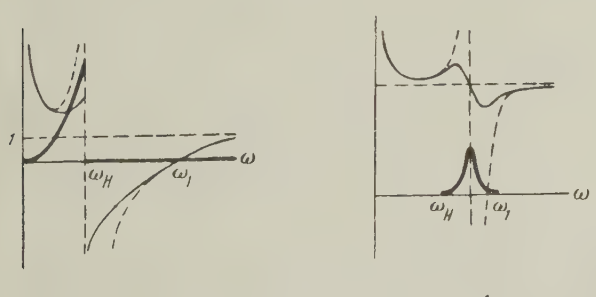

FIG. 2. The square of the refractive index N_0^2 for an extraordinary wave which propagates along the magnetic field: a – for $\omega_0^2 \gg \omega_H^2\beta$, b – for $\omega_0^2 < \omega_H^2\beta$. The thin lines are $\operatorname{Re} N_0^2 \equiv n^2 - q^2$, the heavy lines are $\operatorname{Im} N_0^2 \equiv 2nq$, and the dashed lines $N_0^2 = \varepsilon_0 \equiv 1 - \omega_0^2/\omega(\omega-\omega_H)$ (thermal motion is neglected); $\omega_H = |e|H_0/mc$; $\omega_0^2 = 4\pi e^2 n_0/m$; $\omega_1 = \omega_H/2 + \sqrt{\omega_H^2/4 + \omega_0^2}$.

In the region in which ϵ_0 (the square of the refractive index) is much greater than unity when the thermal motion is not taken into account, there is strong absorption of the wave. The approximate behavior of the real and imaginary parts of the square of the refractive index for the extraordinary wave in longitudinal propagation is shown in Fig. 2a.

At low values of the electron density, $n_0 < 0.9 \times 10^5\ \beta H_0^2$, the refractive index is determined from the equation $N^2 - \epsilon^{(2)}(N) = 0$ and has the same form as that for a simple resonator in which the Doppler effect is taken into account[8] (Fig. 2b).

In conclusion we wish to express our gratitude to Academician M. A. Leontovich for suggesting this work and for help in its execution.

APPENDIX

Cerenkov Radiation

1. If the medium contains electrons with thermal velocities greater than the phase velocity of an electromagnetic wave at some given frequency, the electrons radiate at this frequency. In accordance with Kirchhoff's Law, these electrons will also absorb electromagnetic waves at the same frequency (Cerenkov absorption). This can be seen directly in the case of a weakly-absorbing medium in which the radiancy of the medium η_ω is related to the absorption α_ω by the expression

$$\eta_\omega = \alpha_\omega I_\omega, \qquad (1)$$

where I_ω is the equilibrium radiation intensity.

As an example we may consider the following model. A gas of free electrons, with a Maxwellian velocity distribution, is located in a transparent dielectric, the refractive index of which satisfies the condition $n > 1$ in the absence of the electron gas. In this example it is most fruitful to consider methods of calculating the Cerenkov absorption and the mechanism responsible for this absorption.

The absorption coefficient is determined by calculating the dielectric permittivity of the medium, taking account of the thermal motion of the electrons. The value of the dielectric permittivity, ϵ, which determines the propagation of a plane wave, can be obtained from Eq. (21) of Sec. 2. For nonrelativistic electron velocities

$$\varepsilon = n^2 - \frac{4\pi e^2 n_0}{m\omega}\int\left\{\frac{1}{\omega - \mathbf{kv}} - i\pi\delta(\omega - \mathbf{kv})\right\} f_0(\mathbf{v})\,d\mathbf{v}, \qquad (2)$$

$$f_0(\mathbf{v}) = (m/2\pi T)^{3/2}\exp(-mv^2/2T),$$

where m and n_0 are the electron mass and electron density respectively, k is the wave vector, and T is the temperature expressed in energy units. We assume that the electron density is

small, $4\pi e^2 n_0/m\omega^2 \ll 1$, so that the real part of the integral can be neglected as compared with n^2 and we can write $|k| = n\omega/c$. The square of the total index of refraction is found to be

$$N^2 = \varepsilon = n^2 + i\,\frac{4\pi e^2 n_0}{m\omega^2}\,\frac{c\pi}{n}\left(\frac{m}{2\pi T}\right)^{1/2} e^{-mc^2/2Tn^2} \qquad (3)$$

while the absorption coefficient is

$$\alpha = \frac{\omega}{c}\,\frac{\operatorname{Im} N^2}{n} = \frac{\omega_0^2}{\omega c}\,\frac{\pi^{1/2}}{3n^2}\,e^{-1/\beta^2 n^2}, \qquad (4)$$

$$\omega_0^2 = 4\pi e^2 n_0/m;\ \beta^2 = 2T/mc^2.$$

As is apparent from Eq. (2), the imaginary part of ϵ, which is responsible for absorption, is nonvanishing when the electron velocities satisfy the Cerenkov condition $\omega = \mathbf{k}\cdot\mathbf{v}$ or

$$v\cos\theta = c/n, \qquad (5)$$

where θ is the angle between the vectors $\mathbf{k}$ and $\mathbf{v}$.

Inasmuch as the electron velocity cannot exceed the velocity of light $v < c$, this condition means in general that there is a sharp boundary (in terms of ω), for the absorption band. If the relativistic electron velocity distribution is used, this boundary is taken into account automatically. In this case the absorption coefficient assumes the form [in place of Eq. (4)]:

$$\alpha = \frac{2\pi^2\omega_0^2}{\omega c n^2}\,C\,\frac{e^{-b}}{b}\left(1+\frac{1}{b}\right),\ b = \frac{mc^2}{T\,(1-1/n^2)^{1/2}},\ n > 1; \qquad (6)$$

$$\alpha = 0,\ n \leqslant 1.$$

Here

$$C = (4\pi)^{-1}\left[\frac{T}{mc^2}\,K_0\left(\frac{mc^2}{T}\right) + 2\left(\frac{T}{mc^2}\right)^2 K_1\left(\frac{mc^2}{T}\right)\right]$$

is the normalization constant in the Maxwell distribution.[10] When $mc^2T \gg 1$

$$C \approx (mc)^3\,(2\pi mT)^{-3/2} e^{mc^2/T}.$$

As follows from Eq. (6), the approximate formula (4) applies if $n^2 \gg 1$ and $(1-1/n^2)^{1/2} = 1 - 1/2n^2$.

To demonstrate that the absorption in question is actually related to Cernekov radiation we compute the absorption coefficient using Kirchhoff's law (1). In order to carry out this procedure, it is first necessary to compute the radiancy η_ω. An electron moving with a velocity v in a medium of refractive index n radiates the following energy per unit time and frequency interval ω:[3]

$$\mathcal{E}_\omega = \frac{e^2\omega}{c^2}\left(1 - \frac{c^2}{n^2v^2}\right)v. \qquad (7)$$

Averaging this expression over a Maxwellian velocity distribution, we find in the nonrelativistic approximation

$$\eta_\omega = \int n_0\,\mathcal{E}_\omega\,f_0(\mathbf{v})\,d\mathbf{v} = \frac{2e^2\omega n_0}{V\pi c}\,\beta e^{-1/\beta^2 n^2}. \qquad (8)$$

Substituting the equilibrium intensity of the radiation obtained by the Rayleigh-Jeans Law for a medium of refractive index n, $I_\omega = (\omega^2 T/\pi^2 c^2)\,n^2$, and the value of η_ω of (8) into Eq. (1), we obtain, in complete agreement with (4)

$$\alpha_\omega = \frac{\omega_0^2}{\omega c}\,\pi^{1/2}\,\frac{1}{3n^2}\,e^{-1/\beta^2 n^2}.$$

To explain the mechanism of Cerenkov absorption, we introduce a coordinate system which moves with a velocity $\mathbf{v}$ at an angle θ to the wave vector $\mathbf{k}$. If the velocity v and the angle θ are chosen in accordance with Eq. (5) the field in this coordinate system is independent of time [$\omega' = \omega(1 - vn\cos\theta/c)/\sqrt{1-\beta^2} = 0$]. As can be shown easily by the usual transformation formulas, in this coordinate system the nonvanishing component of the electric field E′ lies in the plane defined by the vectors $\mathbf{k}$ and $\mathbf{v}$. The amplitude of this field is related to the amplitude of the laboratory field component E, which lies in the plane of the vectors $\mathbf{k}$ and $\mathbf{v}$ (cf. Fig. 3), by the relation

$$E' = E\,\frac{v\sqrt{n^2-1}}{c\sqrt{1-v^2/c^2}}\sin\theta. \qquad (9)$$

An electron which moves in the laboratory coordinate system with a velocity $\mathbf{v}$ which satisfies (5) is at rest in the moving system. Consequently, this electron is acted on by a force $f = eE'$ which is constant in time. The continuous acquisition of energy by electrons under the influence of this force results in a reduction in the energy flux of the electromagnetic field, i.e. absorption.

2. Cerenkov absorption can play an important role in a plasma in a magnetic field. The magnetic field causes an increase in the refractive index in certain frequency regions. The resulting retardation of the wave causes marked broadening of the absorption band in the region of the cyclotron resonance; moreover, the increased refractive index means that the plasma electrons can become "faster-than-light" electrons, i.e. electrons with velocities greater than the velocity of light in the "medium". Both of these effects become especially important when $nT \approx H^2/8\pi$ (i.e., when the pres-

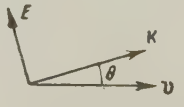

FIG. 3

sure associated with the electron plasma component becomes comparable with the magnetic pressure) because under these conditions the phase velocity in the low frequency region is smaller than the mean thermal velocity of the electrons.

Cerenkov radiation arises in a plasma as a consequence of free motion of electrons along the strong magnetic field lines. The possibility of this radiation has been indicated by Veksler.[11] The radiation due to a charge moving with uniform motion along a magnetic field has been calculated by Kolomenskii.[12] If $nT \approx H^2/8\pi$, the energy radiated per unit time by an electron which moves with velocity v along the field is approximately $d\mathcal{E}/dt \approx e^2\omega_H^2 v/c^2$ where $\omega_H = eH/mc$. This energy is approximately c/v times greater than the energy radiated by an electron which moves with the same velocity, but in a circle in a plane perpendicular to the magnetic field! The large amount of energy radiated by an isolated electron obviously does not mean that the plasma loses enormous amounts of energy by radiation (since the maximum loss, in accordance with the laws of thermal radiation, cannot depend on the nature of the radiator). The foregoing is merely an indication of the correspondingly strong absorption of this type of radiation in the plasma.

Since the refractive index is approximately unity at high frequencies, the Cerenkov absorption is important only at relatively low frequencies $\omega \leq \omega_H$. If $T \ll mc^2$, as has been shown in Sec. 2, we need not consider in the dielectric permittivity tensor ϵ_{ik} terms associated with higher resonances $\omega = 2\omega_H$, $\omega = 3\omega_H$, . . . , except in the case in which propagation takes place across the magnetic field. Under these conditions the tensor components are the same when thermal motion is neglected (magnetic field parallel to the axis)

$$\varepsilon_{ik} = \begin{pmatrix} \varepsilon & ig & 0 \\ -ig & \varepsilon & 0 \\ 0 & 0 & \eta \end{pmatrix}, \qquad (10)$$

where

$$\varepsilon = 1 - \frac{\omega_0^2}{2\omega}\langle -i\pi\delta_+(\omega - \omega_H - kv\cos\theta) - i\pi\delta_+(\omega + \omega_H - kv\cos\theta)\rangle;$$

$$g = \frac{\omega_0^2}{2\omega}\langle -i\pi\delta_+(\omega - \omega_H - kv\cos\theta) + i\pi\delta_+(\omega + \omega_H - kv\cos\theta)\rangle; \qquad (11)$$

$$\eta = 1 - \frac{\omega_0^2}{\omega}\langle -i\pi\delta_+(\omega - kv\cos\theta)\rangle; \quad \delta_+(x) = \delta(x) + i/\pi x.$$

The triangular brackets denote averages over the distribution function $f_0(v)\,dv = (m/2\pi T)^{1/2} \times e^{-mv^2/2T}\,dv$, θ is the angle between the direction of propagation and the magnetic field, and v is the electron velocity along the z axis.

The imaginary parts of ϵ and g, which contain δ-functions with argument $\omega \pm \omega_H - kv\cos\theta$, describe the radiation or absorption at the resonance frequency ω_H, and take account of the Doppler effect which arises as a consequence of the free motion of the charges along the magnetic field lines.

The Cerenkov radiation or absorption lies in the imaginary part of the tensor component $\epsilon_{zz} = \eta$ which contains the δ-function with argument $\omega - kv\cos\theta$. If the absorption is small, we can write as an approximation $k = n\omega/c$ where n is the real part of the refractive index, $N = n + iq$, and the condition $\omega - kv\cos\theta = 0$ reduces to (5). It is apparent that the Cerenkov radiation obtains for waves which propagate at an angle θ, for which the imaginary part of the refractive index q depends on η, while the real part meets the requirement $n > 1$. In longitudinal propagation ($\theta = 0$) we have $N^2 = \epsilon \pm g$ and there is no Cerenkov absorption. This result is clear from an examination of Eq. (9): when $\theta = 0$, we have $E' = 0$. In transverse propagation ($\theta = \pi/2$) we have $N^2 = (\epsilon^2 - g^2)/\epsilon$ for the extraordinary wave; the absence of Cerenkov absorption is due in this case to the fact that, in accordance with (5), the electron velocity would have to be infinite when $\theta = \pi/2$. The number of such electrons is zero. For the ordinary wave $N^2 = \eta$; since $\mathrm{Re}\,\eta = 1 - (\omega_0/\omega)^2 < 1$, there is no absorption. This case is the same as for propagation in the absence of a magnetic field. Thus, Cerenkov absorption takes place only in oblique propagation ($\theta \neq 0$, $\theta \neq \pi/2$).

The general expression for the square of the refractive index is:

$$N^2 = A/B$$

$$A = (\varepsilon^2 - g^2 - \varepsilon\eta)\sin^2\theta + 2\varepsilon\eta \pm \sqrt{(\varepsilon^2 - g^2 - \varepsilon\eta)^2\sin^4\theta + 4\eta^2 g^2\cos^2\theta}, \qquad (12)$$

$$B = 2(\varepsilon\sin^2\theta + \eta\cos^2\theta).$$

It is of interest to determine the boundary of the absorption band in which $\mathrm{Im}\,N^2 \ll \mathrm{Re}\,N^2$. In this frequency region the tensor components ϵ_{ik} can be written in the form

$$\varepsilon = \varepsilon_0 + i\varepsilon_1, \quad g = g_0 + ig_1; \quad \eta = \eta_0 + i\eta_1, \qquad (13)$$

where ϵ_0, g_0 and η_0 are the values of ϵ, g, and η when thermal motion is not taken into account and ϵ_1, g_1 and η_1 are small corrections which

take account of the absorption. In the approximation which is linear in ϵ_1, g_1 and η_1

$$N^2 = n^2(1 + ia/A_0 - ib/B_0), \tag{14}$$

where n^2 is the square of the refractive index when thermal motion is not taken into account, A_0 and B_0 are the values of A and B under the same conditions,

$$a = [2(\varepsilon_0\varepsilon_1 - g_0g_1) - \varepsilon_0\eta_1 - \eta_0\varepsilon_1]\sin^2\theta + 2(\eta_0\varepsilon_1 + \varepsilon_0\eta_1)$$

$$\pm \frac{(\varepsilon_0^2 - g_0^2 - \varepsilon_0\eta_0)(2\varepsilon_0\varepsilon_1 - 2g_0g_1 - \varepsilon_0\eta_1 - \varepsilon_1\eta_0)\sin^4\theta + 4(\eta_0^2 g_1g_1 + \eta_0 g_0^2\eta_1)\cos^2\theta}{[(\varepsilon_0^2 - g_0^2 - \varepsilon_0\eta_0)^2\sin^4\theta + 4\eta_0^2 g_0^2\cos^2\theta]^{1/2}}, \quad b = 2(\varepsilon_1\sin^2\theta + \eta_1\cos^2\theta), \tag{15}$$

and in the expressions for $\epsilon_1(k)$, $g_1(k)$ and $\eta_1(k)$ we take $k = n\omega/c$.

The Cerenkov absorption is most important when:

$$\text{(a) } \omega_0^2/\omega_H^2 \gg 1, \quad \text{(b) } \omega \ll \omega_H. \tag{16}$$

Let us consider this case in greater detail. If the first condition is satisfied, $n^2 \sim \omega_0^2/\omega_H^2 \gg 1$; in particular, if $nT \sim H^2/8\pi$, $n^2 \sim \beta^{-2}$ and the majority of the plasma electrons are "faster-than-light" electrons. This condition simplifies the calculation considerably because when $\omega_0^2/\omega_H^2 \gg 1$, for values of θ for which the following condition is satisfied:

$$\sin^4\theta/\cos^2\theta \ll 4\omega_0^4/\omega^2\omega_H^2, \tag{17}$$

we have the case of so-called "quasi-longitudinal propagation,"[9] in which the square of the refractive index is, disregarding thermal motion,

$$n^2 = -\omega_0^2/\omega(\omega \pm \omega_H\cos\theta). \tag{18}$$

The refractive index for the extraordinary wave exceeds unity (minus sign in the denominator) at frequencies ω which satisfy the condition $0 < \omega < \omega_H\cos\theta$. Near the right-hand boundary of this frequency region, as follows from the results of Sec. 2, we have resonance absorption when $\omega_0^2/\omega_H^2 \gg 1$. If the second condition in (16) is satisfied, however, resonance absorption no longer plays a role and in the expressions for ϵ and g we can omit the imaginary parts and deal only with the pure Cerenkov absorption. Thus, the Cerenkov absorption determines the shape of the total absorption band on the low-frequency side.

Under the assumptions indicated in (16), the components of the tensor ϵ_{ik} (10) assume the form:

$$\varepsilon = \varepsilon_0 = \omega_0^2/(\omega_H^2 - \omega^2); \quad g = g_0 = \varepsilon_0\omega_H/\omega;$$

$$\eta = \eta_0 + i\eta_1 = -\frac{\omega_0^2}{\omega^2} + i\sqrt{\pi}\frac{2\omega_0^2}{\omega^2(\beta n\cos\theta)^3}\exp\left\{-\frac{1}{\beta^2 n^2\cos^2\theta}\right\}. \tag{19}$$

Substituting these values in Eqs. (14) and (15) we have

$$N^2 = \frac{\omega_0^2}{\omega(\omega_H\cos\theta - \omega)}\left\{1 + i\sqrt{\pi}\frac{\omega^{5/2}(\omega_H\cos\theta - \omega)^{1/2}}{\omega_0^3} \times \frac{\sin^2\theta}{(\beta\cos\theta)^3}\exp\left[-\frac{\omega(\omega_H\cos\theta - \omega)}{\omega_0^2\beta^2\cos^2\theta}\right]\right\}. \tag{20}$$

The absorption coefficient is

$$\alpha = \frac{\omega}{c}\frac{\operatorname{Im} N^2}{n} = \sqrt{\pi}\frac{\omega}{c}\frac{\omega^2}{\omega_0^2}\frac{\sin^2\theta}{(\beta\cos\theta)^3}\exp\left[-\frac{\omega(\omega_H\cos\theta - \omega)}{\beta^2\omega_0^2\cos^2\theta}\right]. \tag{21}$$

These formulas apply when $\omega \ll \omega_H$ and for values of θ which satisfy the condition given in (17); from Eq. (16) $\omega_0^2 \gg \omega_H^2$ so that it follows from Eq. (17) that Eqs. (20) and (21) are valid over the entire region of variation of θ with the exception of the narrow cone close to $\theta = \pi/2$, defined by the condition

$$|\pi/2 - \theta| < \omega|\omega_H|/2\omega_0^2.$$

[1] L. D. Landau, J. Exptl. Theoret. Phys. (U.S.S.R.) **16**, 574 (1946).

[2] M. E. Gertsenshtein, J. Exptl. Theoret. Phys. (U.S.S.R.) **22**, 303 (1952).

[3] L. D. Landau and E. M. Lifshitz, Электродинамика сплошных сред (Electrodynamics of Continuous Media) GITTL (1957).

[4] M. E. Gertsenshtein, J. Exptl. Theoret. Phys. (U.S.S.R.) **27**, 180 (1954).

[5] B. N. Gershman, J. Exptl. Theoret. Phys. (U.S.S.R.) **24**, 659 (1953).

[6] Sitenko and Stepanov, J. Exptl. Theoret. Phys. (U.S.S.R.) **31**, 642 (1956); Soviet Phys. JETP **4**, 512 (1957).

[7] V. P. Silin, Тр. Физич. ин-та АН СССР (Trans. Phys. Inst. Acad. Sci. U.S.S.R.) Vol. VI, p. 251, 1955.

[8] M. Born, Optique (Russ. Transl.) DNTVU 1937.

[9] V. L. Ginzburg, Теория распространения радиоволн в ионосфере (Theory of Propagation of

Radiowaves in the Ionosphere) Moscow — Leningrad, (1949).

[10] L. D. Landau and E. M. Lifshitz, Статистическая физика (Statistical Physics) GITTL (1951).

[11] V. I. Veksler, Атомная энергия (Atomic Energy) 5, 427 (1957).

[12] A. A. Kolomenskii, Dokl. Akad. Nauk SSSR 106, 982 (1956), Soviet Phys. "Doklady" 1, 133 (1956).

Translated by H. Lashinsky
298

SOVIET PHYSICS JETP VOLUME 34 (7), NUMBER 6 DECEMBER, 1958

*VELOCITY AND TEMPERATURE DISCONTINUITIES NEAR THE WALLS OF A BODY AROUND WHICH RAREFIED GASES FLOW WITH TRANSONIC VELOCITIES**

M. F. SHIROKOV

Moscow Aviation Institute

Submitted to JETP editor November 20, 1957

J. Exptl. Theoret. Phys. (U.S.S.R.) **34**, 1490-1495 (June, 1958)

New and more general formulas are derived for velocity and temperature discontinuities on a gas-wall surface for rarefied gas flows of arbitrary Mach number. The equation for the velocity discontinuity is practically the same as that for $M \ll 1$; on the other hand, the relation for the temperature discontinuity differs markedly from the well-known Maxwell formula for a gas at rest near a wall.

IN previous investigations, even in the most detailed,[1] the effects of the slipping of rarefied gases along the walls and the temperature discontinuities on the gas-wall boundary have been studied only in cases corresponding to $M \ll 1$. Here M is a dimensionless quantity, equal to the ratio of the speed of flow far from the wall to the speed of sound (the Mach number). Furthermore, there is a great need to know the laws governing these effects for flows with arbitrary values of M, since the gas dynamics of rarefied gases are of considerable interest at the present time, principally in connection with the problem of the flight of rocket missiles and apparatus at the upper levels of the atmosphere.

The work below had as its aim the solutions of these problems.

1. INITIAL ASSUMPTIONS; THE VELOCITY DISTRIBUTION FUNCTION f

As is well known,[2] the equations of gas dynamics preserve their usual form in relation to the expression for the heat flow q_μ and the stress tensor $\tau_{\mu\nu}$ if

$$Ml/L = M^2/R < 1, \tag{1.1}$$

where l is the length of the molecular mean free path, L a characteristic linear dimension of the object (or channel) in the flow, and R the Reynolds number. q_μ and $\tau_{\mu\nu}$ are in this case expansions in powers of the parameter Ml/L, with factors in the form of first, second and higher derivatives, with respect to the coordinates x_α, of the mean velocity $\bar{u}_\mu$ and of the temperature T.

We assume condition (1.1). Then

$$\rho\bar{u}_\nu = \rho v_\nu, \quad \overline{\rho u_\mu u_\nu} = p\delta_{\mu\nu} - \tau_{\mu\nu} + \rho v_\mu v_\nu,$$
$$\rho\left(\frac{1}{2}\overline{u^2 u_\nu} + \varepsilon\bar{u}_\nu\right) = pv_\nu + q_\nu - \tau_{\mu\nu}v_\mu + \rho v_\nu\left(\frac{v^2}{2} + c_v T\right), \tag{1.2}$$

where v_μ is the mean velocity of the macroscopic motion of the medium, ϵ is the internal energy of the molecule of the gas, and c_V is the specific heat at constant volume.

The laws of conservation of mass, momentum, and energy at the gas-wall boundary can be written in the following form, if we denote the unit normal vector by n_ν:

$$\rho\bar{u}_\nu n_\nu = (\rho\bar{u}_\nu)^* n_\nu, \quad \overline{\rho u_\mu u_\nu} n_\nu = \rho\,\overline{(u_\mu u_\nu)^*} n_\nu,$$
$$\rho\left(\frac{1}{2}\overline{u_\mu u_\mu u_\nu} + \overline{\varepsilon u_\nu}\right) n_\nu = \rho\left(\frac{1}{2}\overline{u_\mu u_\mu u_\nu} + \overline{\varepsilon u}\right)^* n_\nu. \tag{1.3}$$

*This work was completed in 1950.

In these equations, the asterisk denotes quantities produced by the flow of molecules incident on the wall and reflected from it, while the quantities without the asterisk refer to the layer of gas infinitesimally close to the wall.

The velocity distribution function, which is a solution of the Boltzmann equation for the given problem, should have the form

$$f = f_M(1 + \psi), \quad \psi \ll 1, \tag{1.4}$$

$$f_M = (h/\pi)^{3/2} \exp\{-h(u_\mu - v_\mu)(u_\mu - v_\mu)\}, \tag{1.5}$$

where f_M is the well-known Maxwell distribution function,

$$\psi = A + B(u_\mu - v_\mu)(u_\mu - v_\mu) + C\tau_{\alpha\beta}(u_\alpha - v_\alpha)(u_\beta - v_\beta) + [D + E(u_\alpha - v_\alpha)(u_\alpha - v_\alpha)](u_\beta - v_\beta)q_\beta. \tag{1.6}$$

Furthermore, the conditions of thermodynamic equilibrium should be satisfied for f and ψ at each point of the medium and at each instant of time:

$$\int f\,du_1du_2du_3 = \int f d\omega = \int f_M d\omega = 1,$$
$$\int f u_\alpha d\omega = \int f_M u_\alpha d\omega = v_\alpha, \tag{1.7}$$
$$\int \xi_\alpha\xi_\beta d\omega = \int (u_\alpha - v_\alpha)(u_\alpha - v_\alpha)d\omega = \int a^2 f d\omega = \int a^2 f_M d\omega.$$

The constants A, B, C, D, and E should be chosen to satisfy conditions (1.7) and (1.2). This leads to a system of equations for the constants:

$$\int [A + Ba^2 + C(\tau_{11}\xi_1^2 + \tau_{22}\xi_2^2 + \tau_{33}\xi_3^2)] f_M d\omega = 0,$$
$$\int \xi_\alpha\xi_\beta f_M (D + Ea^2) d\omega = 0, \tag{1.7a}$$

$$\int [A + Ba^2 + C(\tau_{11}\xi_1^2 + \tau_{22}\xi_2^2 + \tau_{33}\xi_3^2)] a^2 f_M d\omega = 0;$$
$$\rho \int (A + Ba^2 + C\tau_{\alpha\beta}\xi_\alpha\xi_\beta) f_M \xi_\mu\xi_\nu d\omega = -\tau_{\mu\nu}, \tag{1.2a}$$
$$\frac{\rho}{2}\int (D + Ea^2) a^2\xi_\mu^2 d\omega = 1.$$

In these expressions, the quantities ξ_μ and a^2 are determined by means of (1.7), while we denote by ξ_μ^2 simply the square of the component ξ_μ, and the sum of squares of ξ_α is written, as usual, in the form $\xi_\alpha\xi_\alpha = a^2$.

In order that the quantities A, B, C, . . . be independent of $\tau_{\mu\nu}$ and q_μ, it is necessary to employ the Stokes hypothesis:

$$\tau_{11} + \tau_{22} + \tau_{33} = 0, \tag{1.8}$$

satisfaction of which is implied in the choice of the distribution function in the form (1.6).

Carrying out integration in Eqs. (1.7a) and (1.2a), and solving the resultant set of equations, we find

$$A = B = 0, \quad C = -2h^2/\rho; \quad D = -4h^2 q; \quad E = 1.6\,h^3/\rho. \tag{1.9}$$

2. VELOCITY AND TEMPERATURE DISCONTINUITIES ON THE GAS-WALL INTERFACE

We assume that a part s of the molecules is reflected diffusely from the wall with a Maxwellian velocity distribution f'_M, corresponding to a certain effective temperature T', connected with the wall temperature T_w by the Knudsen accomodation coefficient:

$$T' - T = \alpha(T_w - T). \tag{2.1}$$

Further, we let the remaining faction of the molecules (1 − s) be reflected specularly from the wall. Then the first of equations (1.3) can be written in the form

$$s\left(\int_{-\infty}^{+\infty}\int_{0}^{+\infty}\int_{-\infty}^{+\infty} u_2 f'_M d\omega + \int_{-\infty}^{+\infty}\int_{-\infty}^{0}\int_{-\infty}^{+\infty} f u_2\, d\omega\right)$$
$$+(1-s)\int_{-\infty}^{+\infty}\int_{-\infty}^{+\infty}\int_{-\infty}^{+\infty} f u_2 d\omega = 0,$$

regarding the normal n to be directed along the x_2 axis, inside the gas. Or, taking it into account that the latter integral is equal to zero, we shall have, leaving in what follows, for brevity, one integral with the designation of the limits of integration with respect to the variable x_2:

$$\int_0^\infty u_2 f'_M d\omega + \int_{-\infty}^0 u_2 f\, d\omega = 0. \tag{2.2}$$

Further, in accord with the second equation of (1.3), and considering that

$$\int_0^\infty f'_M u_\alpha u_2 d\omega = 0 \text{ for } \alpha \neq 2,$$

we obtain

$$\int_0^\infty f u_\alpha u_2 d\omega - (1-s)\int_0^{-\infty} f u_\alpha u_2 d\omega = 0, \tag{2.3}$$

$$\int_0^\infty f u_2^2 d\omega = s\int_0^\infty f'_M u_2^2 d\omega + (1-s)\int_0^{-\infty} f u_2^2 d\omega. \tag{2.4}$$

Finally, the last equation of (1.3) yields:

$$2[-v_\alpha\tau_{\alpha 2} + q_2] = \rho s\left\{\int_0^\infty f'_M u_2(u^2 + 2\varepsilon) d\omega + \int_{-\infty}^0 f(u^2 + 2\varepsilon) u_2 d\omega\right\}. \tag{2.5}$$

Equations (2.2) to (2.5) express the boundary conditions for the gas dynamic flow of rarefied gases. For their formulation in concrete form, however, it is necessary to calculate the integrals involved, making use of the distribution function f found above; in this case we assume for molecules reflected with accomodation

$$f'_{\text{M}} = A(1 + b_1 a^2 + b_2 a^4 + b_3 a^6)\, e^{-h u_\alpha u_\alpha}. \qquad (2.6)$$

The coefficients A, b_1, b_2, . . . are determined from the normalization condition $\int f'_{\text{M}}\, d\omega = 1$ and fulfilment of Eq. (2.2) and two other relations which shall be used later:

$$\int_0^\infty f'_{\text{M}} u_2 \left(\frac{u^2}{2} + \varepsilon\right) d\omega = \alpha \int_0^\infty f^w_{\text{M}} u_2 \left(\frac{u^2}{2} + \varepsilon^w\right) d\omega$$

$$- (1 - \alpha) \int_{-\infty}^0 f u_2 \left(\frac{u^2}{2} + \varepsilon\right) d\omega, \qquad (2.7)$$

$$\int_0^{-\infty} f'_{\text{M}} u_2 d\omega = \alpha \int_0^\infty f^w_{\text{M}}\, u_2\, d\omega - (1 - \alpha) \int_{-\infty}^0 f u_2 d\omega. \qquad (2.8)$$

Substituting Eq. (1.4) for f in (2.3), we get

$$\int_{-\infty}^{\infty+} f_{\text{M}} (\xi_\alpha \xi_2 + v_\alpha \xi_2 + \psi^\xi_\alpha \xi_2 + \psi v_\alpha \xi_2)\, d\omega$$

$$+ s \int_0^{-\infty} f_{\text{M}} (\xi_\alpha \xi_2 + v_\alpha \xi_2 + \psi^\xi_\alpha \xi_2 + \psi v_\alpha \xi_2)\, d\omega = 0.$$

Multiplying this relation by ρ and computing the corresponding integrals with the help of (1.5) to (1.9), we get

$$-\tau_{\alpha 2} + \rho v_\alpha \bar{\xi}_2 s + \frac{s}{2} \tau_{\alpha 2} + 0.2\, s \left(\frac{h}{\pi}\right)^{1/2} q_\alpha - \frac{s \tau_{22} h^{1/2}}{2\pi^{3/2}} v_\alpha = 0, \qquad (2.9)$$

where

$$\bar{\xi}_2 = -\int_{-\infty}^0 \xi_2 f_{\text{M}} d\omega = 1/2 \sqrt{h\pi} = \bar{a}/4, \qquad (2.10)$$

Here $\bar{a}$ is the mean velocity of the random thermal motion of the molecules entering, according to the molecular kinetic theory, into the expression for the viscosity η.

As is well known,

$$h = 1/2\,(c_p - c_v)\, T = \gamma / 2 c_p (\gamma - 1)\, T. \qquad (2.11)$$

Furthermore, we have for the heat-flow vector and for the tensor of viscous forces

$$q_\alpha = -\lambda \frac{\partial T}{\partial x_\alpha};\quad \tau_{\mu\nu} = \eta \left(\frac{\partial u_\mu}{\partial x_\nu} + \frac{\partial u_\nu}{\partial x_\mu} - \frac{2}{3} \delta_{\mu\nu} \frac{\partial u_\alpha}{\partial x_\alpha}\right). \qquad (2.12)$$

Finally, we introduce the dimensionless number

$$\text{Pr} = \eta c_p / \lambda. \qquad (2.13)$$

Substituting the values of the corresponding quantities λ, q_α, etc. from (2.10) to (2.13) in Eq. (2.9), and taking it into account that in flow over the wall we can always set $\tau_{22} = 0$, we get

$$v_\alpha = \frac{\eta}{\beta} \frac{\partial v_\alpha}{\partial x_2} + \frac{0.2}{(\gamma - 1)\,\text{Pr}} \frac{\eta}{\rho T} \frac{\partial T}{\partial x_\alpha}, \qquad (2.14)$$

where

$$\eta/\beta = (2/s - 1)\,(2\eta/\rho\bar{a}). \qquad (2.15)$$

In these relations, β is the coefficient of external friction and η/β is the slipping coefficient.

There are several theoretical formulas for the viscosity coefficient. Apparently, the best of these is the Chapman formula:[2]

$$\eta = 0.499\, \rho \bar{a} l. \qquad (2.16)$$

Substitution of this value of η in (2.15) gives

$$\eta/\beta = 0.998\,(2/s - 1)\, l. \qquad (2.17)$$

According to experimental data, $s \approx 0.8$ to 1 for various surfaces and gases; therefore, $h/\beta \approx l$.

Equations (2.14) to (2.17) for the velocity discontinuity do not contain anything new in comparison with the expressions obtained earlier in molecular-kinetic theory. Their derivation, given above, only furnishes a basis for the possibility of using the ordinary formulas for the velocity discontinuity at a wall at arbitrary values of the Mach number M.

The formulas obtained for the temperature discontinuity are essentially new, however. With the help of Eq. (2.8), we can transform Eq. (2.2) to the form:

$$\int_0^\infty f^w_{\text{M}} u_2\, d\omega + \int_{-\infty}^0 f u_2\, d\omega = 0.$$

Then, in accord with Eq. (2.10),

$$\int_0^\infty f^w_{\text{M}} u_2\, d\omega = -\int_{-\infty}^0 f u_2\, d\omega = -\int_{-\infty}^0 f_{\text{M}} u_2\, d\omega = \frac{\bar{a}}{4}. \qquad (2.18)$$

From (2.5) and (2.6) we obtain

$$2\,(q_2 - v_a \tau_{\alpha 2}) = \rho s \alpha \left\{ \int_0^\infty f^w_{\text{M}} u_2\, (u^2 + 2\varepsilon^w)\, d\omega \right.$$

$$\left. + \int_{-\infty}^0 f u_2\, (u^2 + \varepsilon)\, d\omega \right\}.$$

In correspondence with Eq. (1.4), we can transform this equation, considering that $v_2 = 0$, to the form

$$q_2 - v_x\tau_{x2} = {}^1/_2\, s\alpha\rho\,(M_1 + M_2 + M_3), \qquad (2.19)$$

where

$$M_1 = \int_0^\infty f_M^w u_2\,(u^2 + 2\varepsilon^w)\,d\omega, \qquad (2.20)$$

$$M_2 = \int_{-\infty}^0 f_M u_2\,(u^2 + 2\varepsilon)\,d\omega, \qquad (2.21)$$

$$M_3 = \int_{-\infty}^0 f_M\psi\,\{\xi_\alpha\xi_\alpha\xi_2 + 2\bar{\xi}_\alpha\xi_2 v_\alpha + v_\alpha v_\alpha\xi_2\}\,d\omega. \qquad (2.22)$$

Calculation of these integrals, making use of (2.11) and (2.18), gives

$$M_1 = \bar{a}\,\{c_pT\,(\gamma - 1)/\gamma + \varepsilon^w/2\}, \qquad (2.20a)$$

$$M_2 = -\bar{a}\,\{c_pT\,(\gamma - 1)/\gamma + \varepsilon/2 + v^2/4), \qquad (2.22a)$$

$$M_3 = \frac{1}{\rho}\left(q_2 - v_\alpha\tau_{\alpha 2} - 0.8\,\frac{q_\alpha v_\alpha}{\bar{a}}\right)$$

$$+ \tau_{22}C\int_{-\infty}^0 (\xi_2^3 - \xi_3^2\xi_2)\,(1 + a^2)\,f_M\,d\omega. \qquad (2.21a)$$

Substituting the values of M in (2.19) and taking $\tau_{22} = 0$ as before, we get

$$(q_2 - v_\nu\tau_{\nu 2})\left(1 - \frac{s\alpha}{2}\right) + \frac{0.4\,s\alpha}{\pi}\,q_\nu\,\frac{v_\nu}{\bar{a}}$$

$$= \frac{s\alpha\rho\bar{a}}{4}\left\{\frac{2c_p\,(\gamma - 1)}{\gamma}\,(T_w - T) + (\varepsilon^w - \varepsilon) - \frac{v^2}{2}\right\}.$$

From molecular-kinetic theory,

$$\varepsilon^w - \varepsilon = \left(c_v - \frac{3}{2}\,c_p\,\frac{\gamma - 1}{\gamma}\right)(T_w - T) = -\,\Delta T c_p\,\frac{5 - 3\gamma}{2\gamma} \qquad (2.23)$$

With the help of this relation, the preceding equation is transformed to the form

$$(-v_\alpha\tau_{\alpha 2} + q_2)\left(\frac{2}{s\alpha} - 1\right) + \frac{0.8}{\pi}\,\frac{q_\alpha v_\alpha}{\bar{a}} = -\,\frac{s\bar{a}}{4}\,\mu c_p\left(\Delta T + \frac{v^2}{c_p\mu}\right), \qquad (2.24)$$

where

$$\mu = (\gamma + 1)/\gamma. \qquad (2.25)$$

Equation (2.24) determines the value of the temperature discontinuity between the gas and the wall for flow past it at Mach numbers $M \gtrsim 1$. In contrast with the formula for the velocity discontinuity (2.14), it differs essentially from the well-known Maxwell formula, which corresponds to the case of gas at rest near a wall ($M = 0$) and which can be obtained by putting $v_\alpha = 0$ in (2.24).

In the simpler case of two-dimensional flow in the x_1, x_2 plane (which will occur, for example, for a plane Prandtl boundary layer), we can transform Eq. (2.24) [by making use of Eqs. (2.12) and (2.13)] to the form

$$\Delta T + \frac{v^2}{\mu c_p} = g\,\frac{\partial}{\partial x_2}\left(T + \Pr\frac{v_1^2}{c_p}\right) + g_1\,\frac{\partial T}{\partial x_1}, \qquad (2.26)$$

where

$$g = (2/s\alpha - 1)\,(4\eta/\Pr\mu\bar{a}s), \qquad (2.27)$$

$$g_1 = (3.2\,\eta/\pi\mu\rho\bar{a}\,\Pr)\,(v_1/a), \qquad (2.28)$$

or, if we use the Chapman formula (2.16) for the viscosity,

$$g = (2/s\alpha - 1)\,(1.996\,l/\mu\,\Pr), \qquad (2.27a)$$

$$g_1 = 0.359\,v_1 l/\pi\mu\,\Pr\,\bar{a}. \qquad (2.28a)$$

For computational purposes, it is useful to note that with use of boundary-layer theory, we can neglect in the formulas for velocity and temperature discontinuities, (2.14) and (2.16), the terms containing the derivative $\partial T/\partial x$, if x_1 is directed along the flow in the immediate vicinity of the wall. In addition, we can, with accuracy sufficient for practical purposes, consider $\mu \approx 2$ and $\Pr = 1$. Then Eq. (2.26) takes the form

$$\Delta\Theta = g\partial\Theta/\partial x_2, \qquad (2.26b)$$

which coincides with the known Maxwell formula if we replace the ordinary temperature T in it by the "throttling" temperature used in gas dynamics:

$$\Theta = T + v^2/2c_p. \qquad (2.29)$$

Once more, it should be noted that by setting $v_1 = 0$ and $s = 1$, (2.26) and (2.27) reduce to the known Maxwell expressions for the temperature discontinuity on the gas-wall interface [if the gas is at rest relative to the wall ($M = 0$)].

In conclusion, we point out that instead of (2.26) and (2.14) one can easily obtain if necessary more general formulas for velocity and temperature discontinuities by substituting in Eqs. (2.9) and (2.24) the expressions for heat flow and the stress tensor,[2] taking into account terms of higher order in M^2/R with higher derivatives. The relations obtained by such a method are, however, too cumbersome to cite here.

[1] P. S. Epstein, Phys. Rev. **23**, 710 (1924).

[2] S. Chapman, Phil. Trans. Roy. Soc. (London) **A216**, 279 (1915).

[3] D. Burnett, Proc. Lond. Math. Soc. **40**, 382 (1935).

Translated by R. T. Beyer
299

THE MECHANICS OF FORMATION OF STRIATIONS IN THE POSITIVE COLUMN OF A GAS DISCHARGE

I. M. CHAPNIK

Moscow State University

Submitted to JETP editor November 27, 1957

J. Exptl. Theoret. Phys. (U.S.S.R.) **34**, 1496-1503 (June, 1958)

It is shown that the appearance of striations in the positive column cannot be explained by the instability of a uniform column. With the assumption that the variation in density of charged particles along the column can be neglected, a nonlinear equation for the electron temperature and potential gradient has been derived from the equation of conservation of the particles. This equation admits of periodic solutions. Whether the column is uniform or striated depends upon the boundary conditions at the cathode end.

UNDER certain conditions, the uniform luminosity of the positive column in a discharge is broken up. Instead of a continuous luminosity distribution, of bright stripes or striations appear along the axis of the column. These can be either stationary or shift rapidly along the column (running striations).[1] The presence of striations is accompanied by periodic variations of the energy of the charged particles, of the potential gradient, and of other quantities along the column axis.

In attempting to explain this phenomenon it is natural to assume first that the breakdown of the uniform column when striations are present is due to instability in the uniform column.[2]

However, a test of column stability, carried out by the method of small perturbations,[3] using the system of equations recently developed by us,[4] does not support this hypothesis. In studying the stability of the column, we took the following into account: A stationary striation represents a steady-state phenomenon. For a transition to occur place from a uniform to a striated column, the small perturbations must be chosen of the form*

$$\varepsilon = \bar{\varepsilon} e^{ikx+\omega t};\ \nu = \bar{\nu} e^{ikx+\omega t} \text{ etc.}, \qquad (1)$$

where $k = 2\pi/\lambda$ and ω is a real number.

Substituting $n_e = n_c(1+\nu)$, $U_e = U_{ec}(1+\epsilon)$ and so on, into our system of equations [reference 4, Eq. (9)], and using the definitions in (1), we obtain the following equation with respect to k and ω:

$$\frac{3}{4}\left(U_{ec}k^2 + \frac{\omega}{b_p}\right)\frac{1}{b_e}\frac{\partial H_1}{\partial U_{ec}} + E_x^2\frac{\mu^2}{a^2}U_e\left(\frac{U_i}{U_{ec}} - 1\right) = 0, \qquad (2)$$

where

$$H_1 = \frac{4}{3}\sqrt{2e/\pi m}\,(\varkappa/\lambda_e)\,U_{ec}^{3/2},$$

and the dependence of the electron energy loss by collision, κ, on the mean electron energy U_{ec} for different gases in given in Engel' and Shtenbek's book.[5] Since $U_i/U_{ec} - 1 > 0$ and, for gases in which striations occur, $\partial H_i/\partial U_{ec} > 0$, it follows that Eq. (2) can be satisfied only by negative values of ω, i.e., our model of the positive column has no instability.

The purpose of the present work is to establish the following mechanism for the formation of striations. In the discharge regions adjacent to the ends of the positive column (e.g. the Faraday dark space) the mean electron energy, potential gradients etc. may have values different from those which must exist in the positive column under the given conditions (i.e., for the given value of pa). On the other hand, the equations which describe the electron-ion plasma possess, in addition to a solution independent of the x coordinate, another solution which is the sum of the x-independent solution and a certain oscillating function

$$U_e(pa, x) = U_{ec}(pa) + \varepsilon(pa, x)\,U_{ec}(pa).$$

Since our system of equations has a unique solution for the given boundary conditions, any other boundary condition involving a discontinuous change in the parameters at the boundary can be satisfied only by the periodic solution $U_{ec} + \epsilon U_{ec}$ (which corresponds to the presence of striations in the column). At the same time, boundary conditions without discontinuities can be satisfied only by the solution U_{ec} (in which case there are no striations). In some cases, because of fluctuations in

*The notation of our previous paper[4] will be used throughout this article.

the parameters, the discontinuity at the boundary of the positive column may vary periodically with time. Such oscillating boundary conditions are satisfied by a solution corresponding to a shifting of the periodic structure along the axis of the column (running striations)*.

Measurements[5,7] show that, in fact, there is a discontinuous change in electron temperature potential gradient and other parameters at the cathode end of the positive column. Shottky[8] developed a system of equations by which he was able to calculate, for different discharge conditions (different pa), values of electron temperature, potential gradient, and the radial distribution of electron density which were well confirmed by experiment. The system of equations which we have used appears to be a natural extension of Shottky's equations to the case of a non-uniform plasma.

In the system of equations used here (as in Shottky's) we disregard electron capture by gas molecules, ionization by collision, and recombination in the gas space.

A simple calculation shows that under the usual conditions (if there are no vapors of water, alcohol, or fatty acids in the tube[4b] (and if the current is not too large) the corresponding terms in the equations are small in comparison with the other terms, and may be neglected. For the last two processes one can reach the same conclusion even without any calculation, since the positive column, and hence also the striations in it, obey the similarity law very exactly.[9] These processes, which represent violations of the similarity law, can therefore not play an important part. We have taken the electron temperature to be constant along any radius of the tube, but variable along the axis. The electron and ion densities may vary with the radius, but are constant along the tube axis.†

Taking $n_e = n_p = N$ to be independent of the x coordinate, we have two continuity equations for the electrons and the ions (see reference 4):

$$\partial N/\partial t + \operatorname{div}(\mathbf{u}_e N) - ZN = 0, \tag{3}$$

$$\partial N/\partial t + \operatorname{div}(\mathbf{u}_p N) - ZN = 0, \tag{4}$$

$$u_{ex} = -b_e(E_x + \gamma_e \partial U_e/\partial x), \tag{5}$$

$$u_{px} = b_p(E_x - \gamma_p \partial U_p/\partial x), \tag{6}$$

$$u_{pr} = -\frac{D_a}{N}\frac{\partial N}{\partial r}, \quad Z = \beta e^{-U_i/U_e}. \tag{7}$$

Here γ_e and γ_p are the thermal diffusion coefficients for the electrons and ions.[10]

For the stationary case (fixed striations), after substituting (5), (6), and the first equation of (7) into (3) and (4), and dividing by N, we obtain

$$-b_e\frac{\partial E_x}{\partial x} - \gamma_e b_e\frac{\partial^2 U_e}{\partial x^2} - \frac{D_a}{N}\frac{1}{r}\frac{\partial}{\partial r}\left(r\frac{\partial N}{\partial r}\right) - Z = 0,$$

$$b_p\frac{\partial E_x}{\partial x} - \gamma_p b_p\frac{\partial^2 U_p}{\partial x^2} - \frac{D_a}{N}\frac{1}{r}\frac{\partial}{\partial r}\left(r\frac{\partial N}{\partial r}\right) - Z = 0. \tag{8}$$

Separating the variables in the usual way, we obtain an equation for the electron and ion densities

$$\frac{1}{r}\frac{\partial}{\partial r}\left(r\frac{\partial N_r}{\partial r}\right) + \frac{\lambda^2}{b_p}N_r = 0, \tag{9}$$

whose solution (under the conditions of Shottky's limiting case) have the form

$$N_r = N_{r0} I_0(\lambda r/\sqrt{b_p}), \quad \lambda^2 = (\mu/a)^2 b_p.$$

This is the well-known Shottky solution for the distribution of charged particles along the radius of a discharge tube.

For the energies of the electrons and ions in this case, we obtain from (8) the following two equations:

$$-b_e\frac{\partial E_x}{\partial x} - \gamma_e b_e\frac{\partial^2 U_e}{\partial x^2} + \frac{\mu^2}{a^2}b_p U_e - Z = 0,$$

$$b_p\frac{\partial E_x}{\partial x} - \gamma_p b_p\frac{\partial^2 U_p}{\partial x^2} + \frac{\mu^2}{a^2}b_p U_e - Z = 0. \tag{10}$$

In the case of a uniform column ($\partial E_x/\partial x = \partial^2 U_e/\partial x^2 = \partial^2 U_p/\partial x^2 = 0$) these equations reduce to the Shottky equation for the electron temperature as a function of the discharge parameters:

$$(\mu/a)^2 b_p U_{ec} - Z_c = 0. \tag{11}$$

The term $(\mu/a)^2 b_p U_{ec}$ in Eqs. (10) and (11) describes the depletion of charged particles due to ambipolar diffusion.*

We now find a solution of the system of equations (10) in the form:

$$U_e(pa, x) = U_{ec}(pa) + \varepsilon(pa, x)\,U_{ec}(pa),$$
$$U_p(pa, x) = U_{pc}(pa) + \varepsilon_1(pa, x)\,U_{pc}(pa). \tag{12}$$

Substituting (12) into the system (10), using the relations (7) and (11), and dividing the first of these equations by $b_e U_{ec}$ and the second by $b_p U_{ec}$, we obtain

*The part played by the stability of processes at the ends of the column is indicated in reference 6.

†The physical conditions under which these assumptions are realized are dealt with at the end of this paper.

*In references 11 and 12 this term is omitted without justification. If this term is included, it is easy to see that there is no periodic solution at all under these author's assumption that the electron temperature is constant along the axis.

$$-\frac{1}{U_{ec}}\frac{\partial E_x}{\partial x}-\gamma_e\frac{\partial^2\varepsilon}{\partial x^2}-\frac{\mu^2}{a^2}\frac{b_p}{b_e}\left(\exp\left\{\frac{U_i\varepsilon}{U_e(1+\varepsilon)}\right\}-1-\varepsilon\right)=0;$$

$$\frac{1}{U_{ec}}\frac{\partial E_x}{\partial x}-\gamma_p\frac{\partial^2\varepsilon_1}{\partial x^2}\frac{U_{pc}}{U_{ec}}-\frac{\mu^2}{a^2}\left(\exp\left\{\frac{U_i\varepsilon}{U_e(1+\varepsilon)}\right\}-1-\varepsilon\right)=0. \quad (13)$$

Comparing these two equations, and noting that γ_e and γ_p are of the order of unity[10] while $U_{pc}/U_{ec} \ll 1$ and $b_p/b_e \ll 1$, we obtain (after dividing through by γ_e) a nonlinear equation describing the variation of ϵ along the axis of the positive column:

$$\frac{d^2\varepsilon}{dx^2}+\frac{\mu^2}{a^2}\left(\exp\left\{\frac{U_i\varepsilon}{U_e(1+\varepsilon)}\right\}-1-\varepsilon\right)=0. \quad (14)$$

If the deviation from a uniform distribution is very small, so that $\epsilon U_i/U_e \ll 1$, then (14) can be approximated by the linear equation

$$\frac{d^2\varepsilon}{dx^2}+\frac{1}{\gamma_e}\frac{\mu^2}{a^2}\left(\frac{U_i}{U_e}-1\right)\varepsilon=0, \quad (15)$$

whose solutions are harmonic functions with the period

$$l_{1in}\approx(2\pi a/\mu)(\gamma_e U_i/U_e)^{1/2}. \quad (16)$$

This is the result we obtained previously.[4]* Experiment shows, however, that the amplitudes of the electron-temperature deviations are not small, and may amount,[7,13,14] for example, to $\epsilon \approx 0.5$. Since $U_i/U_e \approx 10$, then $\epsilon U_i/U_e \approx 5$, i.e., the use of Eqs. (15) and (16) is not rigorously correct. We are forced to consider the nonlinear equation (14). Equations of this type have been thoroughly studied in the theory of nonlinear oscillations.[15] These are the so-called oscillation equations of a system with a nonlinear restoring force, from which Eq. (14) differs only in the definitions of the variables. For convenience, we shall use the terminology of oscillation theory in the following discussion.

We shall write equation (14) in the form $d^2\epsilon/dx^2 + f(\epsilon) = 0$, where

$$f(\varepsilon)=\frac{1}{\gamma}\frac{\mu^2}{a^2}\left(\exp\left\{\frac{U_i\varepsilon}{U_e(1+\varepsilon)}\right\}-1-\varepsilon\right)$$

is the "restoring force". We then calculate the "potential energy" of the system, reckoning the ordinate from the point at which $\epsilon = 0$:

$$F(\varepsilon)-F(0)=\int_0^\varepsilon f(\varepsilon)\,d\varepsilon=\int_0^\varepsilon\frac{\mu^2}{\gamma a^2}\left(\exp\left\{\frac{U_i\varepsilon}{U_e(1+\varepsilon)}\right\}-1-\varepsilon\right)d\varepsilon$$

$$=\frac{\mu^2}{\gamma a^2}\left\{-\left(1+\varepsilon+\frac{1}{2}\varepsilon^2\right)+(1+\varepsilon)\exp\left\{\frac{U_i\varepsilon}{U_e(1+\varepsilon)}\right\}\cdot\right.$$
$$\left.-\frac{U_i}{U_e}e^{U_i/U_e}\left[-\mathrm{Ei}\left(\frac{-U_i}{U_e(1+\varepsilon)}\right)+\mathrm{Ei}\left(\frac{-U_i}{U_e}\right)\right]\right\}, \quad (17)$$

$$-\mathrm{Ei}(-x)=\int_x^\infty e^{-t}dt/t.$$

Figure 1 shows the calculated "restoring force" and "potential energy" of our system (the constant factor $\mu^2/\gamma a^2$, which is not essential here, has been dropped). Beneath this are shown the energy curves determined by the equation

$$\dot{\varepsilon}^2-\dot{\varepsilon}_0^2=2[F(\varepsilon)-F(0)], \quad (18)$$

where $[F(\epsilon) - F(0)]$ is determined from Eq. (17).

It is evident from Fig. 1 that the restoring force is strong for positive deviations of the electron energy and weak for negative deviations. The shapes of the "potential energy" and "energy" curves provide a clue to the nature of the solution. At the point $\epsilon = 0$ there is a minimum in the "potential energy". The origin is a singular point. In the absence of an initial deflection (i.e., no discontinuity at the end of the column) the most stable state is that of equilibrium (a uniform distribution of electron temperatures — no striations). If there is an initial deflection of not too large a magnitude, there is a stable periodic solution (striations) in which the amplitude of the electron-temperature fluctua-

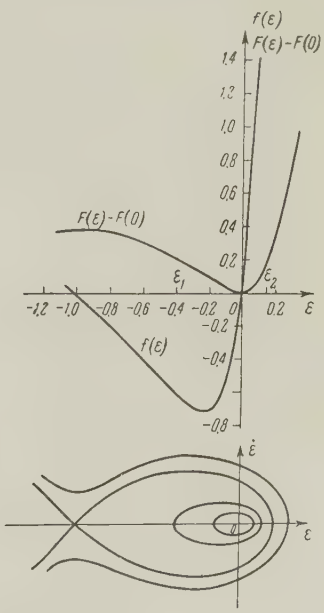

FIG. 1

*Objections have been raised in reference 12 to the fact that $l \approx \sqrt{\gamma_e}$, i.e., $l = 0$ when $\gamma_e = 0$. The quantity γ_e is equal to zero only if $1/\lambda_e \approx c_e$, but no gas is known with this property. For inert gases $1/\lambda_e \approx (e_e - c_0)$, but in this case $\gamma_e \neq 0$.

tions is determined by the size of the discontinuity at the boundary.

The curve of electron energy variation along the column axis can be obtained (by numerical integration, in our case) from the first integral of (14), which has the form:[15]

$$x = \int_0^{\varepsilon} \left\{ \dot{\varepsilon}_0^2 + \frac{2\mu^2}{\gamma a^2} \left[\left(1 + \varepsilon + \frac{1}{2}\varepsilon^2\right) - (1+\varepsilon) \times \exp\left\{\frac{U_i \varepsilon}{U_e(1+\varepsilon)}\right\} + \frac{U_i}{U_e} e^{U_i/U_e} \times \left\{ -\mathrm{Ei}\left(\frac{-U_i}{U_e(1+\varepsilon)}\right) + \mathrm{Ei}\left(\frac{-U_i}{U_e}\right)\right\}\right]\right\}^{-1/2} d\varepsilon. \quad (19)$$

However, the shape of the curve can also be studied by considering the "potential energy" curve and Eq. (14) as it stands. This curve differs markedly from the sinusoidal one determined by the linear equation (15). Let us take the value of the maximum negative excursion to be $\epsilon_1 = -0.5$ (corresponding to the usual values of ϵ_i for striations). From the "potential energy" curve we find the corresponding positive excursion to be $\epsilon_2 = 0.15$. Since the period of a system with a strong restoring force is less than the period of a weak force,[15] then the period (length of one striation) corresponding to a low electron temperature is longer than the period corresponding to a higher electron temperature. Furthermore, we can calculate from (14) the radius of curvature of the $\epsilon(x)$ curve at the minimum and maximum points (where $d\epsilon/dx = 0$). Taking $U_i/U_e = 10$, $a = 1.5$ cm, $\mu = 2.4$, and $\gamma = 1$, we get

$$R_{\varepsilon_1=-0.5} = |(d^2\varepsilon/dx^2)^{-1}_{\varepsilon=-0.5}| \approx 0.8 \text{ cm}.$$

Similarly, we obtain

$$R_{\varepsilon_2=0.15} \approx 0.13 \text{ cm}.$$

The $U_e = f_1(x)$ is shown in Fig. 2 (cf. reference 13).

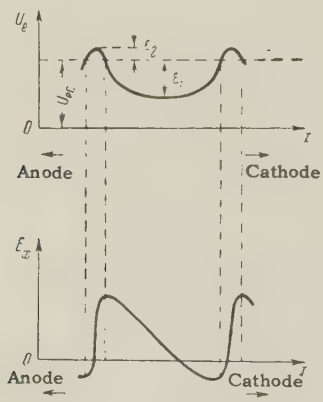

FIG. 2

The curve $E_x = f_2(x)$ can be obtained from the curve $U_e = f_1(x)$ and the first equation of (13) which, considering that $b_p \ll b_e$, can be written:

$$\frac{dE_x}{dx} \approx -\gamma_e U_{ec} \frac{d^2\varepsilon}{dx^2} = -\gamma_e \frac{d^2 U_e}{dx^2}. \quad (20)$$

The curve $E_x = f_2(x)$ is also shown in Fig. 2. It is characterized by a very sharp rise of field intensity within the narrow luminous portion of the striation. The maximum field does not coincide with the maximum electron temperature (or luminosity), but is slightly displaced toward the cathode, while at the same time the minimum lies on the anode side of the luminous portion of the striation.

The period (i.e., the spacing of the striations) can be calculated from the formula:[15]

$$l = l_1 + l_2 = 2\int_0^{\varepsilon_1} \frac{d\varepsilon}{\sqrt{2[F(\varepsilon_1) - F(\varepsilon)]}} + 2\int_0^{\varepsilon_2} \frac{d\varepsilon}{\sqrt{2[F(\varepsilon_2) - F(\varepsilon)]}}, \quad (21)$$

where l_1 and l_2 are the lengths of the low-temperature and high-temperature portions of the striation respectively.

Inserting (17) into (21) we find for l_1

$$l_1 = \frac{a}{\mu}\sqrt{2\gamma}\int_0^{\varepsilon_1} \left\{(\varepsilon - \varepsilon_1) + \frac{1}{2}(\varepsilon^2 - \varepsilon_1^2) - \left[(1+\varepsilon_1)\exp\left\{\frac{U_i\varepsilon_1}{U_e(1+\varepsilon_1)}\right\}\right.\right. \quad (22)$$
$$\left.\left. - (1+\varepsilon)\exp\left\{\frac{U_i\varepsilon}{U_e(1+\varepsilon)}\right\} + \frac{U_i}{U_e}e^{U_i/U_e}\left\{-\mathrm{Ei}\left(\frac{-U_i}{U_e(1+\varepsilon_1)}\right) + \mathrm{Ei}\left(\frac{-U_i}{U_e(1+\varepsilon)}\right)\right\}\right]\right\}^{-1/2} d\varepsilon.$$

There is an analogous expression for l_2. The integral (22) apparently cannot be expressed in terms of elementary functions, but can be evaluated graphically or by numerical methods.

It is essential to ascertain whether the period calculated from (21) differs seriously from the value calculated from (16), which is based on a linear approximation. If in (22) we apply the Lagrange theorem to the terms in the square and curly brackets, we readily obtain the following estimates for l_1 and l_2:

$$l_{1\min} \approx l_{2\max} \approx \frac{1}{2} l_{1\text{in}},$$
$$l_{1\max} \approx \frac{2a}{\mu}\sqrt{2\gamma}\sqrt{\frac{-\varepsilon_1}{1-\varepsilon_1}}, \quad (23)$$
$$l_{2\min} \approx \frac{2a}{\mu}\left[2\gamma\frac{U_i}{U_e}\exp\left\{\frac{-U_i\varepsilon_2}{U_e(1+\varepsilon_2)}\right\}\right]^{1/2}.$$

If $\epsilon_1 = 0.5$ and $\epsilon_2 = 0.15$ (which are typical for striated discharges) (23) gives

$$l_{1\max} \approx 1.5\, l_{1in},\quad l_{2\min} \approx {}^1/_3\, l_{1in}. \qquad (24)$$

From (23) it follows that the period calculated from (21) can never be less than $\frac{1}{2} l_{1in}$ or greater than $2l_{1in}$, and if $\epsilon_1 > -0.5$ it is approximately equal to l_{1in}.

Before we turn to an experimental verification of the theory, let us return to the mechanical analogy of our system, which illustrates our conclusions so graphically. If we consider the variable ϵ in (14) as a displacement from the equilibrium position and the variable x as the time, this equation describes, for example, the motion of a mass suspended by a spring which is "strong" under tension and "weak" under compression. If the displacement and velocity are zero at the initial instant, there will be no oscillations; but if there is an initial velocity, oscillations will result. If there is a constant dissipative force, the vibrations will die out; if the dissipative forces act for only a short period of time, for instance during a half cycle, then after they cease to act the vibrations will continue with reduced amplitude, or cease altogether. Conversely, a short-lived injection of energy will lead to an increased amplitude. Returning now to the positive column, we note that here the "velocity" corresponds to the electron temperature gradient $\partial U_e/\partial x$.

Figure 3 shows the variation of U_e near the heat of the column.[7] It is immediately evident from the figure that in narrow region x_0x_1 at the head of the column there is an abrupt change in electron temperature from its value in the Faraday dark space to a value corresponding to the positive column (according to Schottky).

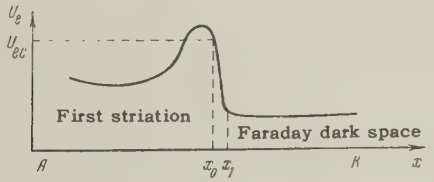

FIG. 3

This creates an initial gradient ("velocity") which in turn leads to stratification ("oscillations") that extends from the cathode end of the column right up to the anode. The conditions near the anode apparently do not affect the production of striations. Kliarfel' d[14] and Zaitsev[16] found that when the anode was moved or the gas pressure varied, the striations merely peeled off the anode. In a few cases the striations arising from the electron temperature gradient at the head of the column rapidly died out, whereupon the column became uniform.[14]*

By analogy with the mechanical system described above, it should be possible to affect the positive column, for instance to remove or add striations, by introducing charged probes into the corresponding portions of the striations.[14] The fact that it is possible by this method to suppress the striations in the region between the probe and the anode supports our conclusions about the stability of the positive column. Striations can also be removed or excited by transverse discharges of direct or high-frequency current (locally increasing U_e) or by local magnetic fields (lowering U_e).[14] For instance, if the electron temperature is raised in the dark portion of the striation, this must result in a weakening or destruction of the striations on the anode side of the disturbance. Conversely, a corresponding lowering of the electron temperature by a local magnetic field must lead to stronger stratification.

Such a conversion of the positive column from one type to another may be useful, for instance, when measuring U_{ec}, knowledge of which is indispensable for a comparison of the experimental and theoretical variations of the electron temperature. The mechanism with which we propose to explain the running striations can be verified by artificially creating an electron-temperature discontinuity within a discharge containing running striations. Such a discontinuity can be produced with the aid of an auxiliary transverse[14] or local high-frequency discharge, and must be greater than the value of the oscillation discontinuity. Instead of running striations we should then have standing ones. Apparently it is possible to create running striations in a uniform column by means of auxiliary transverse alternating-current discharges.

The assumption of an "incompressible" electron-ion plasma leads to a system of striations which do not decay. Taking account of the "compressibility" leads to the appearance in Eq. (14) of a supplementary term $(d\epsilon/dx)(d\nu/dx)$, describing the decay or build-up of the striations ("self-oscillation").†

In order to compare the theoretical and measured values of U_e and E_x and of the phase difference between them, it is necessary to produce striations with zero decay in the discharge. To

*The effect of the atomic properties of the gas on the decay of the striations and the "compressibility" of the electron plasma will be considered in a separate paper.

†See preceding footnote.

accomplish this in a gas where the striations normally decay, it is possible, for instance, to mix with it a gas in which the striations build up (hydrogen), in the proper proportion to reduce the decay rate to zero.

Thus, Kliarfel' d[14] found that the addition of approximately 30% of hydrogen to neon reduced the decay to zero. It would seem to be possible to use corresponding mixtures of other gases as well, for instance, mixtures of two molecular gases.

In conclusion, I consider it a pleasure to express my thanks to Academician N. M. Bogoliubov for supervising this work, and to Prof. V. L. Granovskii, Prof. Ia. P. Terletskii, and A. A. Zaitsev for their encouragement and for discussion of the results.

[1] N. A. Kaptsov, Электрические явления в газах и вакууме (Electrical Phenomena in Gases in Vacuum), 1950.

[2] H. Robertson, Phys. Rev. **105**, 368 (1957).

[3] M. J. Druyvestein, Physica **1**, 273 (1934).

[4] I. M. Chapnik, Dokl. Akad. Nauk SSSR **107**, 529 (1956), Soviet Phys. "Doklady" **1**, 199 (1956); J. Tech. Phys. (U.S.S.R.) **27**, 978 (1957), Soviet Phys. JTP **2**, 894 (1957).

[5] A. von Engel and M. Steenbeck, Elektrische Gasentladungen, part II, (Russ. Transl.) 1936.

[6] A. A. Zaitsev and Kh. A. Dzherpetov, J. Exptl. Theoret. Phys. (U.S.S.R.) **24**, 516 (1953).

[7] D. Oettingen, Ann. Physik, **19**, 513 (1934).

[8] H. Schottky, Physik. Z. **25**, 342 (1924).

[9] H. Holm, Wiss. Veröff. a. d. Siemens-Konzern. **3**, 159 and 188 (1923).

[10] V. L. Granovskii, Электрический ток в газе (Electric Currents in Gases), 1952.

[11] S. Watanabe and W. Oleson, Phys. Rev. **99**, 1701 (1955).

[12] O. L. Prudkovskaia and M. F. Shirokov, Dokl. Akad. Nauk SSSR **112**, 1023 (1957), Soviet Phys. "Doklady" **2**, 96 (1957).

[13] H. Paul, Zeits. f. Phys. **97**, 330 (1935).

[14] B. H. Kliarfel' d, J. Exptl. Theoret. Phys. (U.S.S.R.) **22**, 66 (1952).

[15] J. Stoker, Nonlinear Vibrations in Mechanical and Electrical Systems, Interscience, N. Y., 1950.

[16] A. A. Zaitsev, Вестник МГУ (Bull. Moscow State Univ.) No. 9, 55 (1950).

Translated by D. C. West
300

ON THE SOLUTION OF THE KINETIC EQUATIONS OF TRANSPORT OF NEUTRONS OR γ-RAY QUANTA BY THE METHOD OF PARTIAL PROBABILITIES

I. G. DIAD' KIN

Volga-Ural Branch, All-Union Geophysical Scientific-Research Institute

Submitted to JETP editor December 12, 1957

J. Exptl. Theoret. Phys. (U.S.S.R.) **34**, 1504-1517 (June, 1958)

The problem of solving the kinetic equations for the slowing down and diffusion of neutrons and for the propagation of γ-ray quanta is reduced to a less complicated problem of multiple integration. An exact solution of the kinetic equation (stationary and also nonstationary) is found in the form of a sum, in which the κ-th term is an approximately 3κ-fold integral, which has as its meaning the probability for the transition of a particle from one point of its phase space to another after κ collisions. In the particular case of the slowing down and diffusion of neutrons with constant mean free path, it is shown that this exact solution, which depends on all six variables (the three space coordinates and the three components of the momentum) reduces to simple quadratures and sums.

1. STATEMENT OF THE PROBLEM

THE stationary kinetic equation for the slowing down of neutrons is (cf. reference 1):

$$[l(u)\,\Omega\,\mathrm{grad}+1]\,\Psi(\mathbf{r},\Omega,u)=\int_0^u du_1\int d^2\Omega_1\Psi(\mathbf{r},\Omega_1 u_1)$$

$$\times f(\Omega\cdot\Omega_1,\,u-u_1)\,h(u_1)+Q(\mathbf{r},\Omega,u). \qquad (1)$$

Here $\Psi(\mathbf{r}, \Omega, u)$ is the number of collisions per unit volume of the phase space at the element $d^3\mathbf{r}d^2\Omega du$; $u = \ln(E/E_0)$, with E the energy of the neutron and E_0 a certain energy taken as a unit; Ω is the unit vector of the direction of the momentum; $h(u) = l(u)/l_S(u)$, with l the mean free path and l_S the mean free path against scattering; $f(\Omega\cdot\Omega_1, u)$ is the scattering function, which in the case of symmetry about the center of mass is given by

$$\sum_M C_M\frac{M+1}{8\pi M}e^{-u}\delta\left\{\Omega\cdot\Omega_1-\left[\frac{M+1}{2}e^{-u/2}-\frac{M-1}{2}e^{u/2}\right]\right\},$$

where M is the mass of the nucleus in units of the neutron mass; l_{SM} is the free path against scattering by the element of mass M.

It is required to find the Green's function G of this equation, i.e., a function such that

$$\Psi(\mathbf{r},\Omega,u)=\int d^3\mathbf{r}_1d^2\Omega_1du_1G(\mathbf{r}_1,\mathbf{r},\Omega_1,\Omega,u_1,u)\,Q(\mathbf{r}_1,\Omega_1,u_1). \qquad (2)$$

The integration is taken over the entire six-dimensional phase space. Substituting Eq. (2) into Eq. (1), one verifies without difficulty that G satisfies the following equation:

$$[l\Omega\,\mathrm{grad}+1]\,G(\mathbf{r}_1,\mathbf{r},\Omega_1,\Omega,u_1,u)$$

$$=\int_0^u du_2\int d^2\Omega_2G(\mathbf{r}_1,\mathbf{r},\Omega_1,\Omega_2,u_1,u_2) \qquad (3)$$

$$\times f(\Omega\cdot\Omega_2,\,u-u_2)+\delta(\mathbf{r}_1-\mathbf{r})\,\delta(\Omega_1-\Omega)\,\delta(u_1-u).$$

In obtaining this equation one must change the order of integration of the variables with indices 1 and 2.

Equation (3) is an integro-differential equation. It can be transformed into the purely integral equation

$$G(\mathbf{r}_1,\mathbf{r},\Omega_1,\Omega,u_1,u)=G_0(\mathbf{r}_1,\mathbf{r},\Omega_1,\Omega,u_1,u)$$

$$+\int du_2\int_0^{u_2}du_3\int d^2\Omega_2\int d^2\Omega_3\int d^3\mathbf{r}_2G_0(\mathbf{r}_2,\mathbf{r},\Omega_2,\Omega,u_2,u) \qquad (4)$$

$$\times G(\mathbf{r}_1,\mathbf{r}_2,\Omega_1,\Omega_3,u_1,u_3)\,f(\Omega_2\cdot\Omega_3,\,u_2-u_3)\,h(u_3),$$

where $G_0(\mathbf{r}_1, \mathbf{r}, \Omega_1, \Omega, u_1, u)$ satisfies Eq. (3) without the integral term in the right member

$$(l\Omega\,\mathrm{grad}+1)\,G_0(\mathbf{r}_1,\mathbf{r},\Omega_1,\Omega,u_1,u)$$

$$=\delta(\mathbf{r}_1-\mathbf{r})\,\delta(\Omega_1-\Omega)\,\delta(u_1-u). \qquad (5)$$

For the proof one must substitute the expression for G in the right member of Eq. (4) into the left member of Eq. (3) and note that the gradient operator acts only on the coordinates without indices.

Equations (5) and (4) can be given a simple physical interpretation. The quantity G_0 is proportional to the probability of transition of a neutron with the momentum direction Ω_1 and energy corresponding to u_1 from the point $\mathbf{r}_1$ to the point $\mathbf{r}$, with its momentum direction changed to Ω and its energy variable to u, without collisions. Stated more simply: the neutron has passed from point $\vec{1}$ of phase space to point $\vec{0}$ without scattering or absorption $[G_0(\vec{1}, \vec{0})]$.

The quantity $G(\vec{1}, \vec{0})$ is proportional to the probability (hereafter we shall simply say is the probability) of transition of the neutron from the point $\vec{1}$ to the point $\vec{0}$ with the occurrence of any number of collisions. According to Eq. (4) this probability is equal to the sum of the probabilities of the following events: 1. The neutron has passed from $\vec{1}$ to $\vec{0}$ without having any collisions (the first term G_0), 2. The neutron, having come from $\vec{1}$, and after having any number of collisions, was at the point $\mathbf{r}_2$ with momentum direction Ω_3 and energy variable u_3 [factor $G(\mathbf{r}_1, \mathbf{r}_2, \Omega_1, \Omega_3, u_1, u_3)$]. At this point it was scattered or absorbed, with transition to the point $\vec{2}$ [factor $h(u_3) f(\Omega_2\Omega_3, u_2 - u_3)$]. After this it has passed without collisions from the point $\vec{2}$ to $\vec{0}$ [factor $G_0(\vec{2}, \vec{0})$]. The integration is taken over all the intermediate-state variables $\mathbf{r}_2$, Ω_2, Ω_3, u_2, u_3. The function f assures that the laws governing the scattering are satisfied.

Equation (4) is thus a recussion formula that relates the probability distribution after each κ-th collision with the $(\kappa+1)$-th one.

2. THE EXPRESSION FOR THE GREEN'S FUNCTION OF THE KINETIC EQUATION IN TERMS OF MULTIPLE INTEGRALS

To solve the integral equation (4) we shall employ the usual method of successive approximations. This makes it possible to find successively the pictures after 0, 1, 2, . . . κ collisions (functions G_0, G_1, . . . , G_K, respectively). Each subsequent G_{K+1} is found by integrating the product of the preceding function by the kernel G_0. G_K can be called a partial probability, since it plays the same role for the kinetic equation that a partial wave does for the wave equation.

Let us first find G_0 from Eq. (5). Inserting $\delta(\mathbf{r}_1 - \mathbf{r})$ in the form

$$\delta(\mathbf{r}_1 - \mathbf{r}) = \frac{1}{8\pi^3}\int d^3\mathbf{k} \exp(-i\mathbf{k}(\mathbf{r}_1 - \mathbf{r})),$$

and dividing by the operator $(l\Omega \operatorname{grad} + 1)$, we get

$$G_0(\vec{1}, \vec{0}) = \delta(\Omega_1 - \Omega)\,\delta(u_1 - u)\,\frac{1}{8\pi^3}\int \frac{\exp(-i\mathbf{k}(\mathbf{r}_1 - \mathbf{r}))}{1 + il\mathbf{k}\cdot\Omega} d^3\mathbf{k}. \tag{6}$$

Performing the integration with respect to one of the components of the vector $\mathbf{k}$ (for example, k_x) by means of the theory of residues, we get

$$G_0(\vec{1}, \vec{0}) = \frac{1}{l(u)}\delta(\Omega_1 - \Omega)\,\delta(u_1 - u)\,\frac{\gamma[(r_{1x} - r_x)/\Omega_x]}{|\Omega_x|} \times \exp\left(-\frac{r_{1x} - r_x}{l\Omega_x}\right)\delta\left(\Omega_y\frac{r_{1x} - r_x}{\Omega_x} - r_{1y} + r_y\right) \times \delta\left(\Omega_z\frac{r_{1x} - r_x}{\Omega_x} - r_{1z} + r_z\right); \tag{7}$$

$$\gamma(\alpha) = \begin{cases} 1 & \text{for } \alpha > 0, \\ 0 & \text{for } \alpha < 0. \end{cases}$$

From this it can be seen that G_0 has a singularity on the straight line

$$\frac{r_{1x} - r_x}{\Omega_x} = \frac{r_{1y} - r_y}{\Omega_y} = \frac{r_{1z} - r_z}{\Omega_z} = \text{const} = s > 0. \tag{8}$$

According to Eq. (8) the vectors $(\mathbf{r} - \mathbf{r}_1)$ and Ω are strictly parallel. Since $|\Omega| = 1$, this means that

$$s = |\mathbf{r}_1 - \mathbf{r}|. \tag{9}$$

Equation (7) can then be rewritten in the form

$$G_0(\vec{1}, \vec{0}) = \frac{\exp(l^{-1}|\mathbf{r}_1 - \mathbf{r}|)}{l|\mathbf{r}_1 - \mathbf{r}|^2}\,\delta(\Omega_1 - \Omega) \times \delta(u_1 - u)\,\delta\left(\Omega - \frac{\mathbf{r} - \mathbf{r}_1}{|\mathbf{r}_1 - \mathbf{r}|}\right). \tag{10}$$

In these transformations repeated use has been made of the property of the δ function,

$$\delta[f(x)] = \sum_s f(x - x_s)/f'(x_s); \quad f(x_s) = 0. \tag{11}$$

It can be seen from Eq. (10) that G_0 contains a dependence of the form $R^{-2}\exp(R/l)$, which is characteristic of a transmitted beam, as was naturally to be expected.

It must be remembered that a δ function of unit vectors factors into only two δ functions, corresponding to the number of independent components. For example,

$$\delta(\Omega - \Omega_1) = \delta(\mu - \mu_1)\,\delta(\varphi - \varphi_1),$$

where μ, μ_1 are the cosines of the polar angles and φ, φ_1 are the azimuthal angles.

To solve Eq. (4) it is more convenient to insert in it the function G_0 in the form (6), not in the form (10). We obtain:

$$G(\vec{1}, \vec{0}) = G_0(\vec{1}, \vec{0}) + \frac{1}{8\pi^3}\int_0^u du_3 \int d^2\Omega_3 \int d^3\mathbf{r}_2 h(u_3)\; G(\mathbf{r}_1, \mathbf{r}_2, \Omega_1, \Omega_3, u_1, u_3) f(\Omega\cdot\Omega_3, u - u_3) \int d^3\mathbf{k}\, \frac{\exp[-i\mathbf{k}(\mathbf{r}_2 - \mathbf{r})]}{1 + il\mathbf{k}\cdot\Omega}. \quad (12)$$

Carrying out a straightforward calculation, we find:

$$G_1 = \frac{1}{8\pi^3}\int d^3\mathbf{k}\, \frac{f(\Omega\cdot\Omega_1, u - u_1)\exp[-i\mathbf{k}(\mathbf{r}_1 - \mathbf{r})]\, h(u_1)}{(1 + il\mathbf{k}\cdot\Omega)(1 + il_1\mathbf{k}\cdot\Omega_1)}.$$

Here and in what follows use is made of the fact that the integration with respect to $\mathbf{r}_2$ can be performed at once and gives $\delta(\mathbf{k}_1 - \mathbf{k})$, so that the integral with respect to $\mathbf{k}$ will still remain a triple integral. Furthermore, we have written as a simplification

$$l_n = l(u_n);\; l = l(u).$$

Continuing the process of calculating the "partial probabilities," we find

$$G_2 = \frac{1}{8\pi^3}\int d^3\mathbf{k} \int_0^u du_2 \int d^2\Omega_1\, \frac{\exp[-i\mathbf{k}(\mathbf{r}_1 - \mathbf{r})]\, h(u_1)\, h(u_2)}{(1 + il\mathbf{k}\cdot\Omega)(1 + il_1\mathbf{k}\cdot\Omega_1)(1 + il_2\mathbf{k}\cdot\Omega_2)}$$

$$\times f(\Omega_2\cdot\Omega_1, u_2 - u_1) f(\Omega\cdot\Omega_2, u - u_2);$$

$$G_\varkappa = \frac{1}{8\pi^3}\int d^3\mathbf{k} \int_0^u du_2 \int d^2\Omega_2 \int_0^{u_2} du_3 \int d^2\Omega_3 \ldots \int_0^{u_{\varkappa-1}} du_\varkappa \int d^2\Omega_\varkappa$$

$$\times \exp[-i\mathbf{k}(\mathbf{r}_1 - \mathbf{r})] \frac{h(u_1) f(\Omega\cdot\Omega_2, u - u_2) f(\Omega_\varkappa\cdot\Omega_1, u_\varkappa - u_1)}{(1 + il\mathbf{k}\cdot\Omega)(1 + il_1\mathbf{k}\cdot\Omega_1)}$$

$$\times \prod_{\alpha=2}^{\varkappa} \frac{h(u_\alpha)}{1 + il_\varkappa\mathbf{k}\cdot\Omega_\alpha} \prod_{\omega=2}^{\omega=\varkappa-1} f(\Omega_\omega\cdot\Omega_{\omega+1},\; u_\omega - u_{\omega+1}),$$

$$G(\vec{1}, \vec{0}) = \sum_{\varkappa=0}^{\infty} G_\varkappa(\vec{1}, \vec{0}). \quad (13)$$

This is indeed the final form for the Green's function of the stationary kinetic equation. We note that nowhere in the above calculations has use been made of the concrete form of the function $f(\Omega\cdot\Omega_1,\; u - u_1)$, nor of its dependence on any combination of its arguments. Therefore the formulas (13) are also valid when $f \equiv f(\Omega, \Omega_1, u, u_1)$.

Each term of G is positive, according to its physical meaning, so that the series (13) is a series of positive terms. Thus the problem of solving the kinetic equation has been reduced to a problem of multiple integration. Well developed procedures of approximate integration exist for the calculation of multiple integrals. We once again emphasize the fact that Eq. (13) provides an exact solution of the kinetic equation, valid for arbitrary energies and distances from the source, and for any form of the function f.

3. GENERALIZATION TO THE CASE OF THE NONSTATIONARY KINETIC EQUATION

In this case the operator $(l\Omega\,\mathrm{grad} + 1)$ in Eq. (1) is replaced by

$$\left(\frac{l(u)}{v}\frac{\partial}{\partial t} + l(u)\,\Omega\,\mathrm{grad} + 1\right).$$

The integral equation for the Green's function takes the form

$$G(t_1 - t, \vec{1}, \vec{0}) = G_0(t_1 - t, \vec{1}, \vec{0}) + \int du_2 \int_0^{u_2} du_3 \int d^2\Omega_2 \int d^2\Omega_3$$

$$\times \int dt_2 \int d^3\mathbf{r}_2 G_0(t_2 - t, \vec{2}, \vec{0}) G(t_1 - t_2, \mathbf{r}_1, \mathbf{r}_2, \Omega_1, \Omega_3, u_1, u_3)$$

$$\times f(\Omega_2\cdot\Omega_3, u_2 - u_3)\, h(u_3), \quad (14)$$

where G_0 satisfies the equation

$$\left(\frac{l}{v}\frac{\partial}{\partial t} + l\Omega\,\mathrm{grad} + 1\right) G_0(t_1 - t, \vec{1}, \vec{0}) = \delta(t_1 - t)\,\delta(\mathbf{r}_1 - \mathbf{r})\,\delta(\Omega_1 - \Omega)\,\delta(u_1 - u). \quad (15)$$

Representing δ functions as Fourier integrals, we get

$$G_0(t_1 - t, \vec{1}, \vec{0}) = \frac{1}{16\pi^4}\delta(\Omega_1 - \Omega)\;\delta(u_1 - u)\int d^3\mathbf{k}\, d\sigma \times \frac{\exp[-i\sigma(t_1 - t) - i\mathbf{k}(\mathbf{r}_1 - \mathbf{r})]}{1 + il\sigma\tau + il\mathbf{k}\cdot\Omega} = \frac{1}{l\tau}\delta(\Omega_1 - \Omega)\,\delta(u_1 - u)$$

$$\times \delta\left(\mathbf{r}_1 - \mathbf{r} - \frac{t_1 - t}{\tau}\Omega\right)\exp\left(-\frac{|t_1 - t|}{l\tau}\right), \quad (16)$$

$$\tau = l(u)/v.$$

Equation (16) expresses the physically obvious fact that G_0 is different from zero only on a segment of a straight line for which the equations are

$$\frac{r_{1x} - r_x}{\Omega_x} = \frac{r_{1y} - r_y}{\Omega_y} = \frac{r_{1z} - r_z}{\Omega_z} = |\mathbf{r}_1 - \mathbf{r}| = \frac{|t_1 - t|}{\tau}.$$

As before, the vector Ω is parallel to the vector $\mathbf{r}_1 - \mathbf{r}$, but the length of the segment depends on the time.

The method of successive approximations gives at once

$$G_\varkappa = \frac{1}{16\pi^4}\int d^3\mathbf{k}\, d\sigma \int_0^u du_2 \int d^2\Omega_2 \int_0^{u_2} du_3 \int d^2\Omega_3 \ldots \int_0^{u_{\varkappa-1}} du_\varkappa \int d^2\Omega_\varkappa\, \frac{\exp[-i\sigma(t_1 - t) - i\mathbf{k}(\mathbf{r}_1 - \mathbf{r})]\, h(u_1) f(\Omega\cdot\Omega_2, u - u_2) f(\Omega_\varkappa\cdot\Omega_1, u_\varkappa - u_1)}{(1 + il\sigma\tau + il\mathbf{k}\cdot\Omega)(1 + il_1\sigma\tau_1 + il_1\mathbf{k}\cdot\Omega_1)}$$

$$\times \prod_{\alpha=2}^{\varkappa} \frac{h(u_\alpha)}{1 + il_\alpha\sigma\tau_\alpha + il_\alpha\mathbf{k}\cdot\Omega_\alpha} \prod_{\omega=2}^{\varkappa=1} f(\Omega_\omega\cdot\Omega_{\omega+1},\; u_\omega - u_{\omega-1});$$

$$G(t_1 - t, \vec{1}, \vec{0}) = \sum_{\varkappa=0}^{\infty} G_\varkappa(t_1 - t, \vec{1}, \vec{0}). \quad (17)$$

4. SOLUTION OF THE KINETIC EQUATION FOR THE PROPAGATION OF GAMMA-RAY QUANTA AND THE DIFFUSION OF THERMAL NEUTRONS

The transport equation for γ-ray quanta is

$$(l_k \Omega \operatorname{grad} + 1)\,\Psi(\mathbf{r}, \Omega, E) = \int_E^{E_0} dE_1 \int d^2\Omega_1 h(E_1)$$

$$\times\, M(\Omega\cdot\Omega_1, E, E_1)\,\Psi(\mathbf{r}, \Omega_1, E_1) + Q(\mathbf{r}, \Omega, E), \qquad (18)$$

where $\Psi(\mathbf{r}, \Omega, E)/l_c$ is the number of quanta at the phase point $\vec{0}(\mathbf{r}, \Omega, E)$. The energy is expressed in units of the rest mass of the electron. l_c is the mean free path against Compton scattering, l_p is that against the photoelectric effect,

$$h = l_p l_c/(l_c + l_p),$$

and $M(\Omega\cdot\Omega_1, E, E_1)$ is the Klein-Nishina differential cross section for scattering of a quantum from the state Ω_1, E_1 into the state Ω, E.

The analogy between Eq. (18) and Eq. (1) is almost complete. Therefore the Green's function of Eq. (18) is given by Eqs. (10) and (13), if one makes in them the replacements

$$l \to l_c;\ u = 0 \to E_0;\ u \to E;\ f \to M;\ \int_0^{u_\alpha} \to \int_{E_\alpha}^{E_0}. \qquad (19)$$

It is also easy to write down the Green's function for the diffusion of thermal neutrons. In this case the kinetic equation does not contain the energy (cf. reference 2). Therefore in the formulas (13) one must omit all the integrations over u_α, so that, for example,

$$G_\varkappa^{\text{dif}}(\vec{1}, \vec{0}) = \frac{1}{8\pi^3}\int d^3\mathbf{k} \int d^2\Omega_2 \int d^2\Omega_3 \ldots \int d^2\Omega_\varkappa$$

$$\times \frac{h^\varkappa f(\Omega\cdot\Omega_2) f(\Omega_\varkappa\cdot\Omega_1)}{(1 + il\mathbf{k}\cdot\Omega)(1 + il\mathbf{k}\cdot\Omega_1)(1 + il\mathbf{k}\cdot\Omega_\varkappa)} \prod_{\alpha=2}^{\varkappa-1} \frac{f(\Omega_\alpha\cdot\Omega_{\alpha+1})}{1 + il\mathbf{k}\cdot\Omega_\alpha}. \qquad (20)$$

5. CASE OF SLOWING DOWN AND DIFFUSION OF NEUTRONS IN A MEDIUM IN WHICH THE MEAN FREE PATH IS CONSTANT

The method of solving the kinetic equation by means of partial probabilities, which has been explained and applied to all the equations of transport of neutrons and γ-ray quanta in Secs. 1 to 4, has reduced the problem of obtaining the solutions of these equations to problems of multiple integration. For these latter problems there exists well-developed procedures for both exact and approximate solution.

As an example, in the present section we shall find the exact spatial and energetic distribution of neutrons slowed down in a medium in which the mean free path is constant, and in which the nuclei scatter the neutrons symmetrically in the center-of-mass system. The case of the diffusion of thermal neutrons is obtained as a special case of this one. As is well known, no method hitherto presented has made it possible to find the exact solution of the kinetic equation for this case. In performing the multiple integrations we shall employ the usual operator method and expansion in series of Legendre polynomials.

We expand all the scattering functions in series of Legendre polynomials

$$f(\Omega\cdot\Omega_1, u - u_1) = \sum A_a(u - u_1) P_a(\Omega\cdot\Omega_1) \qquad (21)$$

$$= \sum_{a=0}^{\infty} \sum_{m=0}^{a} \varepsilon_m \frac{(a-m)!}{(a+m)!} A_a(u - u_1) P_a^m(\mu) P_a^m(\mu_1) \cos m(\varphi - \varphi_1);$$

$$\varepsilon_m = \begin{cases} 1 & \text{for } m = 0, \\ 2 & \text{for } m \neq 0; \end{cases}$$

$P_a^m(\mu)$ are the associated Legendre polynomials; $\mu_\alpha = \mathbf{k}_0\cdot\Omega_\alpha$ is the cosine of the angle between the vectors Ω_α and $\mathbf{k}$; $\mathbf{k}_0 = \mathbf{k}/|\mathbf{k}|$; φ is the azimuthal angle of Ω_α in the plane perpendicular to $\mathbf{k}$.

This expansion at once makes it possible to simplify the multiple integration with respect to the logarithmic energy variables in the case in which l does not depend on u and either there is no capture of the fast neutrons [$h(u) \equiv 1$], or else $h(u) = \text{const}$.

In fact, we write

$$W = \int_0^u du_2 \int_0^{u_2} du_3 \ldots \int_0^{u_{\varkappa-1}} du_\varkappa A_a(u - u_2) A_b(u_2 - u_3) \ldots$$

$$\ldots A_g(u_{\varkappa-1} - u_\varkappa) A_h(u_\varkappa - u_1). \qquad (22)$$

We perform the Laplace transformation

$$W(p) = \int_0^\infty e^{-pu} W du.$$

Changing the order of integration over u and u_2, we get

$$W(p) = \int_0^\infty du_2 \int_{u_2}^\infty du e^{-pu} \int_0^{u_2} du_3 \ldots$$

$$\int_0^{u_{\varkappa-1}} du_\varkappa A_a(u - u_2) \ldots A_h(u_\varkappa - u_1)$$

$$= \int_0^\infty A_a(t_2) e^{-pt_2} dt_2 \int_0^\infty du_2 e^{-pu_2} \int_0^u du_3 \ldots \int_0^{u_{\varkappa-1}} du_\varkappa$$

$$\times A_b(u_2 - u_3) \ldots A_h(u_\varkappa - u_1).$$

Continuing this process in the same way and writing

$$A_a(p) = \int_0^\infty e^{-pu} A_a(u)\, du, \tag{23}$$

we get

$$W(p) = A_a(p)\, A_b(p) \ldots A_g(p) \int_0^\infty e^{-pu_\varkappa} A_h(u_\varkappa - u_1)\, du_\varkappa$$

$$= A_a(p)\, A_b(p) \ldots A_g(p)\, e^{-pu_1} A_h(p). \tag{24}$$

Thus instead of the multiple integrals with respect to the u_α we have a single integration:

$$W = L^{-1}(p, u - u_1)\, A_a(p)\, A_b(p) \ldots A_g(p)\, A_h(p),$$

$$L^{-1}(p, u) = \frac{1}{2\pi i} \int_{c-i\infty}^{c+i\infty} e^{pu} dp, \tag{25}$$

where, as usual, the straight line $\mathrm{Re}(p) = c$ is drawn to the right of the singular points.

To avoid misunderstanding we remark that just as in the kinetic equations, the integration over u starts at zero in Eq. (23), too. This means that the maximum energy of the neutrons from the sources is taken to correspond to zero (in the opposite case the integration would be taken from $-\infty$). Therefore we always have

$$A_a(u) \equiv 0 \text{ for } u < 0.$$

We now go on to the integration over the solid angles. After the series expansion and the Laplace transformation, there remain integrals and sums of the form

$$\sum_{g,h=0}^{\infty} \sum_{m=0}^{g} \sum_{n=0}^{h} \varepsilon_m \varepsilon_n A_g^m(p)\, A_h^n(p) \int_0^{2\pi} d\varphi_\varkappa \int_{-1}^{+1} d\mu_\varkappa \cos m(\varphi_{\varkappa-1} - \varphi_\varkappa) \cos n(\varphi_\varkappa - \varphi_1) \frac{P_g^m(\mu_{\varkappa-1}) P_g^m(\mu_\varkappa)\, P_h^m(\mu_\varkappa)\, P_h^m(\mu_1)}{1 + ilk\mu_\varkappa}$$

$$= \sum_{g,h=0}^{\infty} \sum_{m=0}^{\min(g,h)} \frac{4\pi i}{lk} \varepsilon_m A_g^m(p)\, A_h^m(p)\, P_g^m(\mu_{\varkappa-1})\, D_{gh}^m\left(\frac{i}{kl}\right) P_h^m(\mu_1) \cos m(\varphi_{\varkappa-1} - \varphi_1); \tag{26}$$

where the quantities

$$D_{gh}^m(y) = D_{hg}^m(y) = \begin{cases} P_g^m(y)\, Q_h^m(y) & \text{for } g \leqslant h, \\ Q_g^m(y)\, P_h^m(y) & \text{for } g \geqslant h \end{cases}$$

are calculated in the Appendix. Here we have written

$$A_g^m(p) = A_g(p)\,(g-m)!\,/\,(g+m)! \tag{27}$$

Carrying out successively the integrations over μ_{K-1}, μ_{K-2}, $\ldots$ μ_2, we get:

$$G_\varkappa(\vec{1}, \vec{0}) = \frac{1}{8\pi^3} \sum_{a,b,\ldots,h=0}^{\infty} \sum_{m=0}^{\min(a,b,\ldots,h)} L^{-1}(p, u - u_1) \int d^3\mathbf{k} \exp[-i\mathbf{k}(\mathbf{r}_1 - \mathbf{r})]\, \varepsilon_m A_a^m(p)\, A_b^m(p) \ldots A_g^m(p)\, A_h^m(p)$$

$$\times \left(\frac{4\pi i}{lk}\right)^{\varkappa-1} \frac{P_a^m(\mathbf{k}_0\cdot\Omega) D_{ab}^m D_{bc}^m \ldots D_{gh}^m (i/lk)\, P_h^m(\mathbf{k}_0\cdot\Omega_1)}{(1 + il\mathbf{k}\cdot\Omega)(1 + il\mathbf{k}\cdot\Omega_1)} \cos m(\varphi - \varphi_1) \tag{28}$$

It must be remembered that the angles φ and φ_1 are measured in the plane perpendicular to $\mathbf{k}$, so that $\varphi - \varphi_1$ is the angle between $\mathbf{k}\times\Omega$ and $\mathbf{k}\times\Omega_1$.

The expression (28) can be considerably simplified if we expand the fractional quantities depending on Ω and Ω_1 in series of $P_c(\mathbf{k}_0\cdot\Omega)$ and $P_d(\mathbf{k}_0\cdot\Omega_1)$, interchange the summations over the upper and lower indices, and introduce the matrix notation:

$\| AD^m \|$ — is the matrix of the quantities $\sqrt{A_a^m(p)\, A_b^m(p)}\, D_{ab}^m(i/kl)$.

Then

$$G_\varkappa(\vec{1}, \vec{0}) = \sum_{m=0}^{\infty} \sum_{a=m}^{\infty} \sum_{b=m}^{\infty} \frac{\varepsilon_m}{4(2\pi)^5} L^{-1}(p, u - u_1) \int d^3\mathbf{k} \exp[-i\mathbf{k}(\mathbf{r}_1 - \mathbf{r})] \frac{(2a+1)(2b+1)}{\sqrt{A_a^m(p)\, A_b^m(p)}} P_a^m(\mathbf{k}_0\cdot\Omega)\, P_b^{-m}(\mathbf{k}_0\cdot\Omega_1)$$

$$\times \left(\frac{4\pi i}{lk}\right)^{\varkappa+1} (\| AD^m \|^{\varkappa+1})_{ab} \cos m(\varphi_1 - \varphi). \tag{29}$$

Summing all the G_K and using the property of the geometric progression, we get

$$G(\vec{1},\vec{0}) = \sum_{\varkappa=0}^{\infty} G_\varkappa = \sum_{m=0}^{\infty}\sum_{a,b=m}^{\infty} \frac{i\varepsilon_m (2a+1)(2b+1)}{2(2\pi)^4} L^{-1}(p, u-u_1)$$

$$\times \int d^3\mathbf{k} \exp[-i\mathbf{k}(\mathbf{r}_1-\mathbf{r})] \frac{\Phi^m_{ab}(p,k,l)\, P^m_a(\mathbf{k}_0\cdot\Omega)\, P_b^{-m}(\mathbf{k}_0\cdot\Omega_1)\cos m(\varphi-\varphi_1)}{lk\,(A^m_a(p)\,A^m_b(p))^{1/2}}; \tag{30}$$

$$\Phi^m_{ab}(p,\ k,\ l) = \left(\| AD^m \| / \left(1 - \frac{4\pi i}{lk} \| AD^m \|\right)\right)_{ab}. \tag{31}$$

Here the matrix of the fraction must be understood in the sense of a series expansion. In addition we have used the fact that Eq. (29) is also valid for $\kappa = 0$. To prove this one expands the expression for G_0 obtained from Eq. (16) in a Laplace integral and Legendre series.

We now recall that in the particular case of scattering symmetrical in the center-of-mass system one has the formulas (cf. reference 1)

$$A_0(p) = \sum_M C_M \frac{(M+1)^2}{16\pi M} \frac{1-\exp[-(p+1)u_M]}{p+1};$$

$$A_1(p) = \sum_M C_M \frac{3(M+1)^2}{4\pi M}$$

$$\times \frac{2p+2-M+(2p+2+M)\exp[-(p+1)u_M]}{(2p+1)(2p+3)}; \ldots;$$

$$A_a(p) = \sum_M C_M \frac{(2a+1)(M+1)^2}{16\pi M} \int_0^{u_M} e^{-(p+1)u} P_a(X_M(u))\, du;$$

$$X_M(u) = \frac{M+1}{2} e^{-u/2} - \frac{M-1}{2} e^{u/2}; \qquad u_M = 2\ln\frac{M+1}{M-1}.$$

Thus Eqs. (30) and (31) give the Green's function of the kinetic equation for the slowing down of neutrons. They are of simple structure and are written in vector form. We note that the functions G_K given by Eq. (29) are interesting in themselves, since they are the probabilities for κ collisions. In particular, it will be shown below that in the case of atoms of a single kind

$$G_\varkappa \equiv 0 \text{ for } \varkappa < (u-u_1)/u_M.$$

It is also easy to write down the Green's function for the diffusion of thermal neutrons. Using the recipe from Sec. 4, we quickly obtain

$$G_{\text{dif}}(\vec{1},\vec{0})$$

$$= \sum_{m=0}^{\infty}\sum_{a,b=m}^{\infty} \frac{\varepsilon_m(2a+1)(2b+1)}{2(2\pi)^4} \int d^3\mathbf{k} \exp[-i\mathbf{k}(\mathbf{r}_1-\mathbf{r})]$$

$$\times \frac{i}{lk} \Phi^m_{ab}(k,l)\, P^m_a(\mathbf{k}_0\cdot\Omega)\, P_b^{-m}(\mathbf{k}_0\cdot\Omega_1) \frac{\cos m(\varphi-\varphi_1)}{\sqrt{A^m_a A^m_b}},$$

$$\Phi^m_{ab}(k,l) = \left(\| AD^m \| / \left(1 - \frac{4\pi i h}{lk} \| AD^m \|\right)\right)_{ab}. \tag{32}$$

Suppose that in an infinite homogeneous medium there are sources $S(\mathbf{r}, \Omega, u)$. Then the solution of the kinetic equation for slowing down is written in the form

$$\Psi(\mathbf{r},\Omega,u) = \sum_{m=0}^{\infty}\sum_{a,b=m}^{\infty} \frac{\varepsilon_m(2a+1)(2b+1)}{4\pi} \int_{c-i\infty}^{c+i\infty}\int d^3\mathbf{k}$$

$$\times \frac{\exp(pu+i\mathbf{kr})}{\sqrt{A^m_a(p)}\, lk} \Phi^m_{ab}(p,k,l)\, P^m_a(\mathbf{k}_0\cdot\Omega)\, S^m_b(p,\mathbf{k},\varphi); \tag{33}$$

$$S^m_b(p,\mathbf{k},\varphi) = \frac{1}{2\pi^4}\int_0^\infty du_1 \int d^3\mathbf{r}_1 \int d^2\Omega_1 S(\mathbf{r}_1,\Omega_1,u_1)$$

$$\times \frac{\exp[-pu_1 - i\mathbf{kr}_1]}{\sqrt{A^m_b(p)}} P_b^{-m}(\mathbf{k}_0\cdot\Omega_1)\cos m(\varphi-\varphi_1).$$

In the particular case of a point source which is isotropic and monochromatic and is located at the point $\mathbf{r}_u$,

$$S = \delta(\mathbf{r}-\mathbf{r}_u)\,\delta(u),$$

by expanding $\exp i\mathbf{k}(\mathbf{r}-\mathbf{r}_u)$ in a series of products of Legendre polynomials and Bessel functions (cf. reference 3) and integrating over the surface of a sphere of radius k we get:

$$\Psi(\mathbf{r},\Omega,u) = \sum_{a=0}^{\infty} \frac{(2a+1)\,i}{2\pi^2 l}$$

$$\times L^{-1}(p,u) \int_0^\infty \sqrt{k}\, dk \left[\frac{\pi}{|\mathbf{r}_u-\mathbf{r}|\, A_a(p)\, A_0(p)}\right]^{1/2} \tag{34}$$

$$\times \Phi_{a0}(p,k,l)\, P_a\left(\Omega\frac{\mathbf{r}_u-\mathbf{r}}{|\mathbf{r}_u-\mathbf{r}|}\right) J_{a+1/2}(k|\mathbf{r}_u-\mathbf{r}|).$$

The arguments of the Legendre polynomials and Bessel functions correspond to the fact that Ψ depends only on the angle between the momentum and the radius vector drawn from the source, and on the magnitude of this vector. The term a = 0 gives the part of Ψ that does not depend on the direction of the momentum:

$$\Psi_0 = \frac{i\sqrt{2}}{2\pi^2 l} L^{-1}(p,u) \int_0^\infty dk \frac{\sin k|\mathbf{r}_u-\mathbf{r}|}{|\mathbf{r}_u-\mathbf{r}|\, A_0(p)} \Phi_{00}(p,k,l). \tag{35}$$

6. EXAMINATION OF THE SOLUTION AND SPECIAL CASES

The function Ψ_0 given by Eq. (35) is a sum in which the κ-th term is of the form

$$\Psi_{0\varkappa} = \frac{i\sqrt{2}}{2\pi^2 l} L^{-1}(p,u) \int_0^\infty \frac{\sin k\,|\mathbf{r}-\mathbf{r}_u|}{A_0(p)\,|\mathbf{r}_u-\mathbf{r}|} \left(\frac{4\pi i}{lk}\right)^\varkappa (\|AD\|^{\varkappa+1})_{00}\,dk = \frac{i\sqrt{2}}{2\pi^2 l} L^{-1}(p) \int_0^\infty \frac{\sin k\,|\mathbf{r}-\mathbf{r}_u|}{A_0(p)\,|\mathbf{r}_u-\mathbf{r}|} \left(\frac{4\pi i}{lk}\right)^\varkappa \left\{ \left[A_0(p)\,Q_0\left(\frac{i}{lk}\right)\right]^{\varkappa+1} \right.$$

$$+ \varkappa [A_0(p)]^\varkappa A_1(p) \left[Q_0\left(\frac{i}{kl}\right)\right]^{\varkappa-1} \left[Q_1\left(\frac{i}{kl}\right)\right]^2 + \frac{(\varkappa-2)(\varkappa-3)}{2} [A_0(p)]^{\varkappa-2} [A_1(p)]^2 \tag{36}$$

$$\left. \times \left[Q_0\left(\frac{i}{kl}\right)\right]^{\varkappa-3} \left[Q_1\left(\frac{i}{kl}\right)\right]^4 + \varkappa [A_0(p)]^{\varkappa+1} A_2(p) \left[Q_0\left(\frac{i}{kl}\right)\right]^{\varkappa-1} \left[Q_2\left(\frac{i}{kl}\right)\right]^2 + \ldots \right\} dk.$$

Here we have written out several terms of the matrix element, arranged in the order of decreasing size near $k = 0$. The integrands can easily be summed:

$$\Psi_0 = \sum_{\varkappa=0}^\infty \Psi_{0\varkappa} = \frac{i\sqrt{2}}{2\pi^2 l} L^{-1}(p) \int_0^\infty \frac{\sin k\,|\mathbf{r}_u-\mathbf{r}|\,dk}{|\mathbf{r}_u-\mathbf{r}|} \left\{ \frac{Q_0(i/lk)}{1-(4\pi i/lk)\,A_0(p)\,Q_0(i/lk)} - \frac{4\pi i}{lk} \frac{A_1(p)\,[Q_1(i/lk)]^2}{[1-(4\pi i/lk)\,A_0(p)\,Q_0(i/kl)]^2} \right.$$

$$\left. + \left(\frac{4\pi i}{lk}\right)^2 \frac{A_0(p)\,[A_1(p)]^2\,[Q_1(i/lk)]^4}{[1-(4\pi i/lk)\,A_0(p)\,Q_0(i/kl)]^3} - \frac{4\pi i}{lk} \frac{A_2(p)\,[Q_2(i/kl)]^2}{[1-(4\pi i/lk)\,A_0(p)\,Q_0(i/lk)]^2} + \ldots \right\}. \tag{37}$$

The first term in Eq. (37) is the only one in the case of scattering that is symmetrical in the laboratory reference system. It agrees with the solution of Placzek and Volkoff given in reference 1 (single-velocity approximation), as one verifies without difficulty by carrying out the integration in the complex plane. The result consists of the residues at singularities given by the equation

$$1 - \frac{4\pi i}{lk} A_0(p) \frac{\tan^{-1} kl}{kl} = 0$$

and the integral around the cut $(i/l, i\infty)$. This procedure will be carried out below in general form for the partial probabilities. If we suppose that only $A_0(p)$ and $A_1(p)$ are different from zero, then all the terms containing $A_1(p)$ can also be summed easily. It can be seen from Eqs. (36) and (37), however, that the term containing $[A_1(p)]^2$ is already of the same order as the term in $A_2(p)$.

The procedure of operating with matrices in the partial probabilities makes it possible to avoid cumbersome calculations with infinite determinants, such as occur, for example, in Wick's method (cf. references 1 and 4).

It is preferable, however, to use not the expressions (37), which are relatively complicated, but the partial probabilities (36), after first transformed them to a more convenient form. For this purpose we convert the integral over k into a complex Fourier integral. It is easy to do this if we note that

$$(\|AD(i/kl)\|^{\varkappa+1})_{00} = (-1)^{\varkappa+1} \|AD(-i/kl)\|_{00}^{\varkappa+1},$$

in view of the fact that

$$P_a(i/kl)\,Q_b(i/kl) = -P_a(-i/kl)\,Q_b(-i/kl)\,e^{-(a-b)\pi i}$$

and the circumstance that the matrix elements contain sums of terms of the form $D_{0a}D_{ab}D_{bc}\ldots D_{h0}$.

After this, noting that the points $k = \pm i/l$ are branch points and there are no other singularities, we transform the integral along the real axis into an integral along the cut $(i/l, i\infty)$ and introduce the new variable $x = i/kl$. The result is

$$\Psi_{0\varkappa} = \frac{i\sqrt{2}}{4\pi^2 l} L^{-1}(p,u) \int_0^1 dx \frac{(4\pi x)^\varkappa \exp(-|\mathbf{r}_u-\mathbf{r}|/lx)}{x^2 A_0(p)\,|\mathbf{r}_u-\mathbf{r}|}$$

$$\times \{\|AD(x-i0)\|^{\varkappa+1} - \|AD(x+i0)\|^{\varkappa+1}\}_{00} = \frac{\sqrt{2}}{2\pi^2 l} \int_0^1 dx$$

$$\times \frac{\exp(-|\mathbf{r}_u-\mathbf{r}|/lx)\,(4\pi x)^\varkappa}{x^2\,|\mathbf{r}_u-\mathbf{r}|} \left\{ L^{-1}(p,u)\,[A_0(p)]^\varkappa\,[B(x)]^{\varkappa+1} \right.$$

$$\times U_{\varkappa+1}\left(\frac{Q_0(x)}{B(x)}\right) \tag{38}$$

$$+ L^{-1}(p,u)\,[A_0(p)]^{\varkappa-1} A_1(p)\,[B(x)]^{\varkappa-1} \left[x^2\,[B(x)]^2 \right.$$

$$\times U_{\varkappa+1}\left(\frac{Q_0(x)}{B(x)}\right) - 2xB(x)\,U_\varkappa\left(\frac{Q_0(x)}{B(x)}\right)$$

$$\left. \left. + U_{\varkappa-1}\left(\frac{Q_0(x)}{B(x)}\right)\right] + \ldots \right\},$$

where $U_K(x) = \sin(\kappa \cos^{-1} x)$ are Chebyshev polynomials of the second kind and

$$D_{ab}(x \pm i0) = P_a(x)\left[Q_b \mp \frac{\pi i}{2} P_b(x)\right] \text{ for } a \leqslant b;$$

$$B(x) = \sqrt{Q_{0a}^2(x) + \pi^2/4}.$$

It is easily shown that the integrand has a sharp maximum at $x = 1$. The maximum is due not only to the presence of the exponential, but also to the logarithmic singularity at this point, $B(1) = \infty$. It is easy to see that the first term dominates the others, since near $x = 1$ it is larger than the others by at least a factor $(\ln \infty)^2$.

As for the inverse transformation of the coefficients that depend on p, this is easy to do by using the appropriate formulas given in reference 5. For example, in the case of a single element

$$A_0(u, \varkappa) = L^{-1}(p, u)[A_0(p)]^{\varkappa} = \frac{(M+1)^{2\varkappa}e^{-u}}{(16\pi M)^{\varkappa}(\varkappa-1)!}$$

$$\times \sum_{n=0}^{\varkappa} \binom{\varkappa}{n} (-1)^n (u - nu_M)^{\varkappa-1} \gamma(u - nu_M);$$

$$L^{-1}(p, u)[A_0(p)]^{\varkappa-1} A_1(p) = \int_{u-u_M}^{u} A_0(u_1, \varkappa) A_1(u - u_1)\, du_1.$$

The first of these formulas agrees with the well known relation (cf. reference 1) for the energy distribution after a given number of collisions. Marshak's review article also gives the extension to the case of a mixture of elements, and asymptotic values of the function $A_0(u, x)$, which has a sharp maximum at $\kappa = u/2u_M$. It is not hard to show by the method of mathematical induction that for $\kappa < u/u_M$, i.e., when the summation in Eq. (39) is not broken off, $A_0(u, \kappa) \equiv 0$; this is physically obvious.

Thus Eqs. (37) or (38) and (39) give expressions in quadratures for Ψ_0 and Ψ_{0K}. It is clear that for the value of κ equal to the average number of collisions needed for slowing down to a given energy one will find a maximum of Ψ_{0K}. Therefore it is sufficient to include a small number of the Ψ_0 which are in the neighborhood of this average κ. Owing to the rapid decrease of the integrand (particularly for large κ) the integration does not involve much labor.

From the structure of the formula (36) one can see how the results are to be extended to the case of a nonconstant mean free path. In first approximation it is obvious that we are to make the replacement

$$\left(AD\left(\frac{i}{kl}\right) \right\|^{\varkappa+1} \Big)_{00} \to \left(\prod_{\alpha=0}^{\varkappa} \left\| AD\left(i/k\left[l(0) + \alpha \frac{l(u) - l(0)}{\varkappa}\right]\right) \right\| \right)_{00}.$$

7. COMPARISON OF EXISTING METHODS; SUMMARY

In methods existing hitherto simplifying approximations have been introduced directly into the equation. Wick's method[1,4] is based on expanding the functions f and Ψ in series and obtaining an infinite system of equations. One then determines approximately the zeros of the infinite determinant in the denominator of the integrand. In the one-velocity method[1] and in the considerably better developed method of Temkin[6] only the scattering function is expanded in series (which is broken off after a certain term). In reference 6 the main part of the solution is found, corresponding to spherical symmetry of the scattering, and then a perturbation method is given for finding corrections.

The main shortcomings of these methods lie in the fact that their formalism (1) is not related to the physical peculiarities of the phenomenon, and (2) does not make it possible to write down an exact solution in the form of combinations of known functions and operators.

The advantage of the method of partial probabilities lies in the fact that it introduces explicitly a new physical variable — the number of collisions of a particle with nuclei of the medium. The formalism has a clear physical meaning, connects the entire problem with the theory of probability, and reduces it to a problem of multiple integration. The method deals with the actual physical picture of successive transfers of neutrons or γ-ray quanta. It makes it possible to write down in a compact form the exact solution of the kinetic equation as a function of all six variables, and then, by the use of the available apparatus of multiple integration, to bring it into a simple form convenient for calculation.

The entire method set forth above is in principle capable of being applied also to boundary-value problems. For this purpose it is necessary to choose the zeroth-order partial probability in such a way that it satisfies the boundary conditions.

APPENDIX

We shall show that

$$D^m_{ab}(y) = \frac{1}{2}\int_{-1}^{+1} \frac{P^m_a(x) P^m_b(x)}{y - x}\, dx = \begin{cases} P^m_a(x) Q^m_b(x) & a \leqslant b \\ Q^m_a(x) P^m_b(x) & a \geqslant b. \end{cases} \tag{A.1}$$

where y is not on the segment $(-1, +1)$ and

$$Q^m_a(y) = (y^2 - 1)^{m/2} d^m Q_a(y)/dy^m$$

are associated Legendre functions of the second kind (cf. reference 7).

To obtain the proof we first calculate

$$D^m_{ma}(y) = \frac{1}{2}\int_{-1}^{+1} \frac{P^m_a(x) P^m_m(x)}{y - x}\, dx. \tag{A.2}$$

Integrating by parts and differentiating with respect to y, we get:

$$\frac{d}{dy} D^m_{ma}(y) = \frac{2m-1}{2}(a+m)(a-m+1) D^{m-1}_{m-1,a}(y). \tag{A.3}$$

We use the relation

$$\frac{d}{dx}[(1-x^2)^{m/2} P^m_a(x)]$$
$$= (2m-1)(a+m)(a-m+1)(1-x^2)^{(m-1)/2} P^{m-1}_a(x),$$

and the obvious fact that for any value of m

$$D^m_{ma}(\infty) = 0. \qquad \text{(A.4)}$$

Equation (A.3) at once gives

$$\frac{d^m}{dy^m} D^m_{ma}(y) = \frac{(2m-1)!!}{2} \frac{(a+m)!}{(a-m)!} D^0_{0a}$$

$$= (2m-1)!! \frac{(a+m)!}{(a-m)!} Q_a(y). \qquad \text{(A.5)}$$

Integrating Eq. (A.5) with the supplementary condition (A.4), we get

$$D^m_{ma}(y) = (2m-1)!! \frac{(a+m)!}{(a-m)!} \int_y^\infty \int_y^\infty \dots \int_y^\infty Q_a(y)\, d^m y$$

$$= (2m-1)!! \frac{(a+m)!}{(a-m)!} Q_a^{-m}(y)\,(y^2-1)^{m/2} = P^m_m(y)\, Q^m_a(y).$$

We next take the case, with a $\geq$ m + 1:

$$D^m_{m+1,a}(y) = \frac{1}{2} \int_{-1}^{+1} \frac{P^m_{m+1}(x)\, P^m_a(x)}{y-x}\, dx$$

$$= \frac{2m+1}{2} \int_{-1}^{+1} \frac{x P^m_m(x)\, P^m_a(x)}{y-x}\, dx$$

$$= \frac{2m+1}{2}\, y \int_{-1}^{+1} \frac{P^m_m(x)\, P^m_a(x)}{y-x}\, dx = P^m_{m+1}(y)\, Q^m_a(y).$$

Here we have used the orthogonality of the associated Legendre polynomials. Thus the theorem (A.1) is proved for b = m and b = m + 1. It is now easy to prove it for arbitrary a and b by the method of mathematical induction, by using the recurrence relation

$$P^m_{a+1}(x) = \frac{2a+1}{a-m+1} x P^m_a(x) - \frac{a+m}{a-m+1} P^m_{a-1}(x).$$

[1] R. Marshak, Revs. Mod. Phys. **19**, 185 (1947).

[2] S. Glasstone and M. Edlund, The Elements of Nuclear Reactor Theory, Van Nostrand, 1952.

[3] G. N. Watson, A Treatise on the Theory of Bessel Functions, Chapter 4, Cambridge, 1945.

[4] G. Wick, Phys. Rev. **75**, 738 (1949).

[5] Ditkin and P. Kuznetsov, Справочник по операционному исчислению (Handbook of Operational Calculus), GITTL 1951.

[6] A. S. Temkin, Прикладная геофизика (Applied Geophysics) 17, Gostoptekhizdat 1957.

[7] E. W. Hobson, Theory of Spherical and Ellipsoidal Harmonics.

Translated by W. H. Furry.
301

MULTIMAGNON PROCESSES IN THE SCATTERING OF SLOW NEUTRONS IN FERROMAGNETS

S. V. MALEEV

Leningrad Physico-Technical Institute, Academy of Sciences, U.S.S.R.

Submitted to JETP editor December 21, 1957

J. Exptl. Theoret. Phys. (U.S.S.R.) **34**, 1518-1525 (June, 1958)

We calculate the cross section for the inelastic scattering of neutrons in ferromagnets, accompanied by the absorption of one magnon and the emission of another. It is shown that this cross section is small compared to that for scattering with absorption or emission of a single magnon. It is also shown that the role of scattering processes in which more than two magnons participate is negligible.

In a preceding paper of the author[1] it was shown that there are two types of multimagnon processes of scattering of slow neutrons in ferromagnets: two-magnon scattering, in which one magnon is absorbed and another emitted, and three-magnon scattering, in which two magnons are absorbed and one is emitted.

This result was based on spin wave theory in the form given by Dyson.[2,3] In Dyson's papers all types of interactions between atomic spins were neglected except for exchange interaction (which can be done only for ferromagnets with a high Curie point), and it was assumed that the magnetic atoms (or ions) form a simple Bravais lattice. Therefore the conclusion in reference 1 concerning possible multimagnon scattering processes is also valid only with respect to such ferromagnets.

We shall calculate the cross section for two-magnon scattering, limiting ourselves for simplicity to a scatterer with a cubic lattice. Using Eqs. (I.5d) and (I.6), we find the following expression for the two-magnon scattering cross section*

$$d\sigma^{\tau}_{+1,-1}/d\Omega = r_0^2\gamma^2F^2(q)\,\frac{v_0}{(2\pi)^3}\,\frac{p'}{p}\,e^{-2W_q} \times\left[1-\left(\frac{\mathbf{q}\cdot\mathbf{m}}{q}\right)^2\right] n(\mu)\,[n(\rho)+1]\,\delta(\mathbf{q}+\boldsymbol{\mu}-\boldsymbol{\rho}+\boldsymbol{\tau})\,d\boldsymbol{\rho}\,d\boldsymbol{\mu}, \tag{1}$$

where, from conservation of energy,

$$p'^2 = p^2 + \alpha(\mu^2-\rho^2), \text{ and } \alpha \gg 1.$$

From here on, as in reference 1, we replace $\mathbf{q}$ by $\boldsymbol{\tau}$ everywhere except in the argument of the δ-function, and then integrate with respect to $\boldsymbol{\rho}$. The result is:

$$d\sigma^{\tau}_{+1,-1}/d\Omega = r_0^2\gamma^2F^2(\tau)\,e^{-2W_\tau}\,\frac{v_0}{(2\pi)^3}\left[1-\left(\frac{\mathbf{m}\cdot\boldsymbol{\tau}}{\tau}\right)^2\right] \times\frac{(p'_+)^2[n(\rho_+)+1]+(p'_-)^2[n(\rho_-)+1]}{\alpha K p\,[\cos^2\zeta-\alpha^{-1}(\alpha+1)(1-Q^2\alpha^{-1}K^{-2})]^{1/2}}, \tag{2}$$

where

$$\mathbf{K} = \mathbf{P}+\boldsymbol{\mu},$$

$$\rho_\pm^2 = \alpha^{-1}(Q^2 - p'^2_\pm),$$

$$p'_\pm = \alpha K(\alpha+1)^{-1} \times\{\cos^2\zeta \pm [\cos^2\zeta-\alpha^{-1}(\alpha+1)(1-Q^2\alpha^{-1}K^{-2})]^{1/2}\}, \tag{3}$$

and ζ is the angle between $\mathbf{K}$ and $\mathbf{p}'$.

We can now easily integrate (2) over $d\Omega$, choosing the z axis along the vector $\mathbf{K}$. (The fact that this integration can be done relatively simply is the reason why the total cross section is easier to calculate than the differential cross section, since integrating (2) with respect to μ is very complicated.) We have to treat two cases:

$$1)\ \alpha K^2 > Q^2, \qquad 2)\ \alpha K^2 < Q^2. \tag{4}$$

In the first case

$$1 \geqslant \cos\zeta \geqslant \cos\zeta_0 = \{(\alpha+1)\alpha^{-1}[1-Q^2(\alpha K^2)^{-1}]\}^{1/2},$$

while in the second,* $\cos\zeta$ varies from 1 to -1; also, in the second case $p'_- < 0$ and we need keep only terms containing p'_+ in (2). In both cases the integration over $d\Omega$ reduces to an integration over $d\rho_\pm^2$. The integral is easily done and the final result is the same for both cases:

*We use the notation of reference 1, which we cite as I.

*One can show that the condition $q \approx \tau$ is not violated for any angle ζ.

$$d\sigma^{\tau}_{+1,-1}/d\Omega = r_0^2\gamma^2F^2(\tau)\,e^{-2W_\tau}\frac{v_0}{(2\pi)^3}\left[1-\left(\frac{\mathbf{m}\cdot\boldsymbol{\tau}}{\tau}\right)^2\right]\frac{\pi}{Kp}\,n(\mu)$$

$$\times\left\{\frac{2\nu T}{T_c}\ln\frac{1-\exp(-T_c\delta^2R_-^2/2\nu T)}{1-\exp(-T_c\delta^2R_+^2/2\nu T)}+R_-^2-R_+^2\right\},\quad(5)$$

where

$$R_\pm^2=(\alpha+1)^{-2}\left[\sqrt{(\alpha+1)Q^2-\alpha K^2}\mp K\right]^2=\left(\frac{\alpha}{\alpha+1}\right)^2\quad(6)$$

$$\times\left\{\sqrt{(\mu-\alpha^{-1}\mathbf{P})^2+\frac{\alpha+1}{\alpha^2}(p^2-P^2)}\mp\alpha^{-1}|\mathbf{P}+\mu|\right\}^2.$$

We still have to integrate (5) with respect to μ. The integration over the direction of μ can be changed to an integration over the length of the vector $\mathbf{K}=\mathbf{P}+\mu$, so we must find the limits of variation of K. But it is obvious, on the one hand, that

$$|P-\mu|<K<P+\mu,\quad(7)$$

and, on the other hand, we have from (6) that

$$K<(1+1/\alpha)^{1/2}Q.\quad(8)$$

The simultaneous inequalities (7) and (8) give the following results:

(1) If $p > P$, K varies between the limits (7) for all μ.

(2) If

$$P>p>\sqrt{\alpha/(\alpha+1)}P,$$

K varies between the limits (7) for all μ except those lying in the interval

$$\alpha^{-1}\left[P-\sqrt{(\alpha+1)(P^2-p^2)}\right]\leqslant\mu\leqslant\alpha^{-1}\left[P+\sqrt{(\alpha+1)(P^2-p^2)}\right],\quad(9)$$

while for these values of μ, K varies in the interval

$$|P-\mu|\ll K\leqslant\sqrt{1+1/\alpha}\,Q.\quad(10)$$

(3) If

$$p<\sqrt{\alpha/(\alpha+1)}\,P,$$

then for

$$\mu<\mu_1\leqslant\alpha^{-1}\left[-P+\sqrt{(\alpha+1)(P^2-p^2)}\right]\quad(11)$$

no scattering can occur; for values of μ in the range

$$\mu_1<\mu<\alpha^{-1}\left[P+\sqrt{(\alpha+1)(P^2-p^2)}\right],\quad(12)$$

the limits for K are given by (10), while for larger μ they are given by (7).

The shape of the region of integration over K and μ changes when $P = p$ and $P = p\sqrt{(\alpha+1)/\alpha}$. Considered as a function of P, the total cross section $\sigma^{\tau}_{+1,-1}(p, P)$ therefore has a kink at these values of P. One can show, moreover, that for $P = p \pm 0$

$$\partial\sigma^{\tau}_{+1,-1}(p,P)/\partial P=\mp\infty,$$

and consequently the cross section is a maximum for $P = p$. This is related to the fact that, for $P = p$ and $\mu = 0$, both $n(\mu)$ and the logarithm in Eq. (5) become infinite (the latter because $R_+^2 = 0$ when $P = p$ and $\mu = 0$).

From now on we shall assume that

$$P/\alpha\ll\beta,\quad(|p^2-P^2|/\alpha)^{1/2}\ll\beta,\qquad\beta=\delta^{-1}\sqrt{2\nu T/T_c}.\quad(13)$$

Since $\alpha \gg 1$, these inequalities are valid over a very wide range of values of $\mathbf{p}$ and τ.

When (13) is satisfied, expression (5) simplifies considerably. In fact, when $\mu \gtrsim \beta$, $R_\pm \approx \mu \mp K/\alpha$, and the logarithm in (5) becomes

$$(4\mu/\alpha\beta^2)Kn(\mu)+O(\alpha^{-2}),\quad(14)$$

while, if $\mu \ll \beta$, the expression in the logarithm in (5) can be replaced by $R_-^2R_+^2$, since in this case $R_\pm^2 \ll \beta^2$.

After such a simplification, it is easy to determine the dependence of the total cross section on α. First, it is clear from (14) that the contribution to the cross section from large values of $\mu(\mu \gtrsim \beta)$ is proportional to α^{-1}.

In the region of small μ, so long as $\alpha R_+ > K$,

$$\ln(R_-^2R_+^{-2})\approx 4K(\alpha R_+)^{-1},$$

i.e., the contribution to the total cross section is also proportional to α^{-1} in this case. The condition $\alpha R_+ > K$ is violated if

$$\mu^2<\alpha^{-1}(2P\mu+P^2-p^2)+O(\alpha^{-2}),$$

but the equation $R_+^2(\mu) = 0$ has roots for just these values of μ, so that in this case (5) has a logarithmic singularity and the contribution to the cross section from this region of values of μ is in order of magnitude no greater than $\Delta(a \ln \Delta + b)$, where Δ gives the dimensions of the region and a and b do not depend on Δ. Obviously, if

$$P/\alpha>\sqrt{\alpha^{-1}|p^2-P^2|},$$

then $\Delta \sim \alpha^{-1}$, and the contribution to the cross section is of order

$$\alpha^{-1}(a'\ln\alpha+b'),\quad(15)$$

where a′ and b′ do not depend on α. But if $\alpha^{-1}P < \sqrt{|p^2-P^2|/\alpha}$, then from (11),

$$\Delta=\sqrt{\alpha^{-1}|P^2-p^2|}+O(\alpha^{-1})-\mu_1=O(\alpha^{-1})$$

and the contribution to the cross section has the same form (15), but with different values of a′ and b′. Finally, the contribution to the total cross section from the difference $R_-^2 - R_+^2$ which appears

in (5) is also proportional to $1/\alpha$, so that the total cross section has the form $(A \ln \alpha + B)/\alpha$.

As already mentioned, for given values of p and τ the cross section is a maximum when $P = p$. The cross section in this case is calculated in the Appendix, where the following result is obtained:

$$\sigma^{\tau}_{+1,-1}(p, p) = 16\pi^2 r_0^2 \gamma^2 F^2(\tau) \frac{v_0}{(2\pi)^3} e^{-2W_\tau} \times \left[1 - \left(\frac{\bar{\tau}\cdot\mathbf{m}}{\tau}\right)^2\right] \frac{1}{\delta^4 \alpha p} \left(\frac{2vT}{T_c}\right)^2 \left[\ln\left(\frac{\alpha}{p\delta}\sqrt{\frac{2vT}{T_c}}\right) + 2\right] + O(\alpha^{-2}). \quad (16)$$

One can also show that for the case of long-wave neutrons ($p \ll \tau$) and for temperatures which are not very low ($\tau\alpha^{-1/2} \ll \beta^{1/2}$), the total cross section for two-magnon scattering is given by

$$\sigma^{\tau}_{+1,-1}(p, \tau) = 16\pi^2 r_0^2 \gamma^2 F^2(\tau) \frac{v_0}{(2\pi)^3} e^{-2W_\tau} \left[1 - \left(\frac{\tau\cdot\mathbf{m}}{\tau}\right)^2\right] \times \frac{1}{\delta^4 \alpha p} \left(\frac{2vT}{T_c}\right)^2 \left[\ln\left(\frac{1}{\tau\delta}\sqrt{\frac{2vT\alpha}{T_c}}\right) + C\right] + O(\alpha^{-3/2}), \quad (17)$$

where $C = 1/2 + \ln 2 - \pi^2/12 \approx 0.37$.

For comparison, we give the expressions for one-magnon scattering in the two cases which we have treated. Using (I.23) and (I.35), we find for $P = p$:

$$\sigma^{\tau}_{1}(p, p) = \sigma^{\tau}_{-1}(p, p) + \sigma^{\tau}_{+1}(p, p) = 2\pi S \gamma^2 r_0^2 \times F^2(\tau) e^{-2W_\tau} \left[1 + \left(\frac{\mathbf{m}\cdot\tau}{\tau}\right)^2\right] \frac{1}{(p\delta)^2} \frac{2vT}{T_c} \left[\ln \frac{p\delta N^{1/3}}{\alpha\pi} + O(\alpha^{-2})\right], \quad (18)$$

while for $p \ll \tau$ and $\tau\alpha^{-1/2} \ll \beta^{1/2}$, we find, using (I.24):

$$\sigma^{\tau}_{1}(p, \tau) = \sigma^{\tau}_{-1}(p, \tau) = 2\pi S r_0^2 \gamma^2 F^2(\tau) e^{-2W_\tau} \left[1 + \left(\frac{\mathbf{m}\cdot\tau}{\tau}\right)^2\right] \frac{1}{\tau p \delta^2} \frac{2vT}{T_c} [\alpha^{-1/2} + O(\alpha^{-3/2})]. \quad (19)$$

Comparing (16) with (18) and (17) with (19), we see that

$$\sigma^{\tau}_{+1,-1}(p, p) \ll \sigma^{\tau}_{1}(p, p); \quad \sigma^{\tau}_{+1,-1}(p, \tau) \ll \sigma^{\tau}_{-1}(p, \tau). \quad (20)$$

It is obvious that in general two-magnon scattering is small compared to one-magnon scattering. When condition (13) is satisfied, this follows from the fact that in this case $\sigma^{T}_{+1,-1}$ is proportional to α^{-1}.

Let us now estimate the magnitude of the three-magnon scattering. Using (I.5d) and (I.5c), it is easy to show that*

$$\sigma^{\tau}_{-1,-2}(p, P) = \frac{v_0}{2S(2\pi)^3} \int d\mu\, n(\mu) \frac{Q}{p} \sigma^{\tau}_{+1,-1}(Q, |\mathbf{P} + \boldsymbol{\mu}|), \quad (21)$$

where, in general, the region of integration over μ may be smaller than an elementary cell of the reciprocal lattice. Furthermore, it is obvious that

$$\sigma^{\tau}_{+1,-1}(Q \mid P + \mu|) \leqslant \sigma^{\tau}_{+1,-1}(Q, Q),$$

while it follows from (16) that

$$\sigma^{\tau}_{+1,-1}(Q, Q) < \frac{p}{Q} \sigma^{\tau}_{+1,-1}(p, p),$$

since $p < Q$, and therefore

$$\sigma^{\tau}_{-1,-2}(p, P) < \sigma^{\tau}_{+1,-1}(p, p) \frac{v_0}{2S(2\pi)^3} \int d\mu\, n(\mu).$$

Extending the μ integration over the whole space, we obtain finally

$$\sigma^{\tau}_{+1,-2}(p, P) < \varkappa \sigma^{\tau}_{+1,-1}(p, p)/2S, \quad (22)$$

where

$$\varkappa = 1/8\, \zeta(3/2)(v_0/\delta^3\pi^{3/2})(2vT/T_c)^{3/2} \ll 1. \quad (23)$$

Thus we see that the three-magnon scattering is small compared to one-magnon scattering.

As was stated at the beginning of the paper, all the possible multi-magnon scattering processes are included in the two we have treated if we can neglect all types of interaction of the atomic spins except the exchange interaction, and if the magnetic atoms form a simple Bravais lattice.

In the general case one can assert[4] only that the principal multi-magnon processes will be those in which the total number of spin waves changes by no more than unity. This follows from the fact that the projection of the total spin of the ferromagnet on the direction of magnetization is at least approximately an integral of the motion. In fact, the scattering amplitude depends linearly on the operators S_l^+, S_l^- and S_l^z. But it was shown in reference 1 that if the projection of the total spin of the system is conserved, the matrix elements of the operator S_l^z are different from zero only for transitions involving no change in the projection of the total spin, while the operators $S_l^{\pm}$ give non-zero matrix elements only for transitions in which the projection of the total spin changes by ± 1. It follows that the operators S_l^z are responsible for the scattering without change in the total number of magnons, and the operators $S_l^{\pm}$ for the scattering in which this number changes by ± 1.

If, however, we take account of the fact that the projection of the total spin of the ferromagnet is not an exact integral of the motion, then obviously scattering processes are possible in which the change in the total number of magnons is greater than unity. The simplest processes of this type are scattering with absorption of two magnons and scattering with emission of two magnons. Let us assume, as before, that the energy of a magnon is a quadratic function of its momentum and that α is a large number. Then, just as in the case of $\sigma^{T}_{+1,-1}$, we can show that $\sigma^{T}_{2,0}$ and $\sigma^{T}_{0,-2}$ are pro-

*For simplicity we assume the scatterer to be unmagnetized.

portional to α^{-1} (provided, of course, that condition (13) is satisfied), and consequently $\sigma^{\tau}_{2,0}$, $\sigma^{\tau}_{0,-2} \ll \sigma^{\tau}_{+1,-1}$.

We now show that if there is scattering with emission of two magnons and absorption of one magnon, this cross section is small compared to $\sigma^{\tau}_{+1,-1}$. In fact, as in the derivation of (22), we can write

$$\sigma^{\tau}_{+2,-1}(p,\ P) \leqslant \tilde{\sigma}^{\tau}_{+2,0}(p,\ p)\frac{v_0}{(2\pi)^3}\int d\nu n(\nu) = \varkappa\tilde{\sigma}^{\tau}_{+2,0}(p,\ p), \tag{24}$$

where $\tilde{\sigma}^{\tau}_{+2,0}$ is the total cross section which would be gotten from (1) by replacing $n(\mu)$ with $n(\mu)+1$ in (1), and changing the sign of μ^2 in the expression for p'.* The actual cross section for scattering with emission of two magnons, if it occurs, differs from $\tilde{\sigma}^{\tau}_{+2,0}$ by a factor which is small compared to unity. As we stated above, $\tilde{\sigma}^{\tau}_{+2,0}$ is proportional to $1/\alpha$, and consequently $\tilde{\sigma}^{\tau}_{+2,0} \lesssim \tilde{\sigma}^{\tau}_{+1,-1}$, so that $\sigma^{\tau}_{+2,-1} \ll \sigma^{\tau}_{+1,-1}$. In this same way we can show that the cross section for any other multimagnon scattering process is small compared to $\sigma^{\tau}_{+1,-1}(p, P)$.

We have thus found the following result.

If the energy of a magnon is a quadratic function of its momentum, the cross sections for all possible multi-magnon scattering processes are small compared with $\sigma^{\tau}_{+1,-1}(p, P)$. On the other hand, $\sigma^{\tau}_{+1,-1}(p, P)$ in turn is small compared with the cross section for one-magnon scattering (at least, for large α). Therefore multi-magnon scattering processes play a minor role in the inelastic scattering of slow neutrons in ferromagnets, and in particular they cannot be used to explain the observed[5,6] large value of the total cross section for inelastic magnetic scattering in ferromagnets at high temperatures.

APPENDIX

In this appendix, we shall calculate the cross section for two-magnon scattering to terms of order α^{-2}, for the case where $P = p$.

When condition (13) is satisfied, we easily obtain from (5) the expression:

$$\sigma^{\tau}_{+1,-1}(p,\ p) = 2\pi^2 r_0^2\gamma^2 F^2(\tau)\, e^{-2W_\tau}\frac{v_0}{(2\pi)^3}\left[1-\left(\frac{m\cdot\tau}{\tau}\right)^2\right]p^{-2}(J_1+J_2+J_3); \tag{A.1}$$

$$J_1 = \frac{4}{3}\alpha^{-3}\int_0^{\infty} d\mu\cdot n(\mu)\left[|p+\alpha\mu|^3 - |p-\alpha\mu|^3\right]; \tag{A.2}$$

$$J_2 = \beta\int_0^{\zeta\beta^{1/2}} d\mu\cdot\mu n(\mu)\left\{(p+\mu)\ln\left(\frac{|p-\alpha\mu|+p+\mu}{|p-\alpha\mu|-p-\mu}\right)^2 - |p-\mu|\ln\left(\frac{p+\alpha\mu+|p-\mu|}{p+\alpha\mu-|p-\mu|}\right)^2 + Q\ln\left[\frac{(|p-\alpha\mu|-Q)(p+\alpha\mu+Q)}{(|p-\alpha\mu|+Q)(p+\alpha\mu-Q)}\right]^2\right\}; \tag{A.3}$$

$$J_3 = \frac{8}{\alpha}p\int_{\zeta\beta^{1/2}}^{\infty} d\mu\cdot\mu^3 n(\mu), \tag{A.4}$$

where ζ is a number such that $\zeta \ll 1$, $\zeta\beta^{1/2} \gg p/\alpha$.

Since $p/\alpha \ll \beta^{1/2}$, we get

$$J_1 = \frac{4p}{\alpha}\beta^2\int_0^{\infty}\frac{x\,dx}{e^x-1} + O(\alpha^{-3}) \approx \frac{2}{3\alpha}\pi^2\beta^2 p. \tag{A.5}$$

It is convenient to split J_2 into two parts, in the first of which we integrate from zero to p/α, and in the second from p/α to $\zeta\beta^{1/2}$. We note that if $p < \beta^{1/2}$, we can, without violating the assumptions made about ζ, choose ζ so that p is greater than $\zeta\beta^{1/2}$, and can therefore assume that in J_2, p is greater than μ. If we replace $n(\mu)$ by $\beta\mu^{-2}$ in J_2, and introduce the new integration variable $x = \mu/p$, we get:

$$J_2 = p\beta^2(I_1+I_2); \tag{A.6}$$

$$I_1 = \int_1^{1/\alpha}\frac{dx}{x}\left\{\ln\left[\frac{2-(\alpha-1)x}{2+(\alpha-1)x}\right]^2 + x\ln\left[\frac{4-(\alpha-1)^2x^2}{(\alpha+1)^2x^2}\right]^2 + \sqrt{1+\alpha x^2}\ln\left[\frac{(\alpha+1)x+2\sqrt{1+\alpha x^2}}{(\alpha+1)x-2\sqrt{1+\alpha x^2}}\right]^2\right\}; \tag{A.7}$$

$$I_2 = \int_{1/\alpha}^{\zeta\beta^{1/2}/p}\frac{dx}{x}\left\{\ln\left[\frac{(\alpha+1)^2x^2}{4-(\alpha-1)^2x^2}\right]^2 + x\ln\left[\frac{2+(\alpha-1)x}{2-(\alpha-1)x}\right]^2 + \sqrt{1+\alpha x^2}\ln\left[\frac{\alpha^2x^2-(1+\sqrt{1+\alpha x^2})^2}{\alpha^2x^2-(1-\sqrt{1+\alpha x^2})^2}\right]^2\right\}. \tag{A.8}$$

If we make the substitution $x = t/\alpha$ in I_1 and then expand in powers of $1/\alpha$, we get

$$I_1 = \frac{6}{\alpha}\left(1+\frac{3}{4}\ln 3\right) + O(\alpha^{-2}). \tag{A.9}$$

The integral of the second term in I_2 is easily done and gives

$$I_2' = \frac{8}{\alpha}\left[\left(1-\frac{3}{4}\ln 3\right) + \ln\frac{\alpha\zeta_1\beta^{1/2}}{p}\right] + O\left(\frac{p}{\alpha^2\zeta_1\beta^{1/2}}\right). \tag{A.10}$$

In deriving this expression we used the fact that $\zeta\beta^{1/2} \gg p\alpha^{-1}$.

The remaining part of integral I_2 can be split into two terms:

*$\tilde{\sigma}^{\tau}_{+2,0}(p, P)$ and $\tilde{\sigma}^{\tau}_{0,-2}(p, P)$ are maximum at $P = p$ for the same reasons that were given for $\sigma^{\tau}_{+1,-1}(p, P)$.

$$I_2'' = I_2 - I_2' = I_+ + I_-;$$

$$I_\pm = 2\int_{(1+\alpha^{-1})^{1/2}}^{(1+\alpha\zeta^2\beta p^{-2})^{1/2}} dy\cdot y(y^2-1)^{-1}\left\{\ln\frac{\alpha+1}{\alpha-1} \mp (y\pm 1)\ln\left|1\pm\frac{2}{(\alpha-1)(y\pm 1)}\right|\right\} \quad (A.11)$$

We easily find for I_+ :

$$I_+ = \int_{(1+\alpha^{-1})^{1/2}}^{(1+\alpha\zeta^2\beta p^{-2})^{1/2}} dy^2\,(y^2-1)^{-1}\left\{-\frac{2}{\alpha^2}+\frac{4}{\alpha^2(y+1)}+O(\alpha^{-3})\right\}.$$

But this expression is smaller in absolute value than $4\alpha^{-2}\ln(\alpha\zeta\beta^{1/2}p^{-2})$, and can therefore be neglected. After substituting $t = 2[(\alpha-1)(y-1)]^{-1}$, we get for I_- :

$$I_- = \frac{2}{\alpha-1}\int_{t_1}^{t_2}\frac{dt}{t^2}\{1+[1+(\alpha-1)t]^{-1}\}$$

$$\times\left\{\ln|1-t|+\frac{1}{2}(\alpha-1)t\ln\frac{\alpha+1}{\alpha-1}\right\}; \quad (A.12)$$

$$t_1 = 2[(\alpha-1)(\sqrt{1+\alpha\zeta^2\beta p^{-2}}-1)]^{-1} \ll 1,$$
$$t_2 = 2[(\alpha-1)(\sqrt{1+\alpha^{-1}}-1)]^{-1} \approx 4+O(\alpha^{-1}). \quad (A.13)$$

From (A.12) and (A.13) we easily get

$$I_2'' = 2\alpha^{-1}\left(\frac{3}{4}\ln 3-1\right)+O\left(\alpha^{-2}\ln\alpha\right). \quad (A.14)$$

We have only J_3 left to consider. But from (A.4) we get:

$$J_3 = \frac{4}{\alpha}p\beta^2\int_{\zeta^2}^{\infty} x\,dx\,\frac{1}{(e^x-1)^2} = \frac{4}{\alpha}p\beta^2\{-\ln(1-e^{-\zeta^2})$$
$$+\int_0^{\infty}dx\,\frac{1}{e^x-1}\left(\frac{x}{e^x-1}-1\right)-\int_0^{\zeta^2}\frac{dx}{e^x-1}\left(\frac{x}{e^x-1}-1\right)\}.$$

and, since $\zeta \ll 1$, we have finally

$$J_3 = \frac{8}{\alpha}p\beta^2\left(-\ln\zeta+\frac{1}{2}-\frac{\pi^2}{12}\right). \quad (A.15)$$

Using these formulas, it is easy to get (16).

[1] S. V. Maleev, J. Exptl. Theoret. Phys. (U.S.S.R.) **33**, 1010 (1957), Soviet Phys. JETP **6**, 776 (1958).
[2] F. J. Dyson, Phys. Rev. **102**, 1217 (1956).
[3] F. J. Dyson, Phys. Rev. **102**, 1230 (1956).
[4] Elliott, Lowde, and Marshall, Proc. Phys. Soc. (London) **A69**, 939 (1956).
[5] R. D. Lowde, Proc. Roy. Soc. (London) **235**, 305 (1950).
[6] H. Palevsky and D. J. Hughes, Phys. Rev. **92**, 202 (1953).

Translated by M. Hamermesh
302

ENTROPY CHANGE DURING RELAXATION OF A GAS BEHIND A SHOCK WAVE

Iu. P. LUN' KIN

Leningrad Physico-Technical Institute, Academy of Sciences, U.S.S.R.

Submitted to JETP editor December 25, 1957

J. Exptl. Theoret. Phys. (U.S.S.R.) **34**, 1526-1530 (June, 1958)

We have investigated entropy changes which take place in shock waves as translational, rotational and vibrational degrees of freedom are successively excited and as dissociation is induced. It is shown that the largest entropy change takes place when the translational degrees of freedom are excited; excitation of other degrees of freedom involves smaller entropy variations.

1. INTRODUCTION

IN a previous paper,[1] the author set forth a method of consideration of nonequilibrium processes in a shock wave, making use of the introduction of zones of "quasi-equilibrium." The process of transition is as follows: a sudden throttling of the gas over several mean free path lengths produces an increase of temperature of the translational degrees of freedom, the remaining degrees of freedom remaining "frozen" because of their large relaxation times. Further, an additional retardation of the gas takes place and there is a transfer of energy from the translational degrees of freedom to the rotational; the vibration are "frozen" in this case. Then the vibrations are excited, and later there is dissociation of the gas.

Let us denote by the index 1 parameters of the inflowing current; by the indices 2, 3, and 4 the parameters in zones where the translational, rotational and vibrational degrees of freedom are completely excited; and by the index 5 the parameters in the zone of equilibrium dissociation. In what follows, we limit ourselves to diatomic gases. The introduction of zone 2 is strictly valid only for hydrogen and deuterium; in the heavier gases, the relaxation times of the translational and rotational degrees of freedom differ less.

In zones 2, 3:

$$\frac{p_k}{p_1} = \frac{2\gamma_k M_1^2}{\gamma_k + 1}\frac{\gamma_1}{\gamma_k} - \frac{\gamma_k - 1}{\gamma_k + 1}, \tag{1}$$

$$\frac{\rho_k}{\rho_1} = \left(\frac{\gamma_k + 1}{\gamma_k - 1}\frac{p_k}{p_1} + 1\right) \Big/ \left(\frac{\gamma_k + 1}{\gamma_k - 1} + \frac{p_k}{p_1}\right), \tag{2}$$

$$T_k/T_1 = p_k\rho_1/p_1\rho_k. \tag{3}$$

In zones 4, 5 (cf. reference 1):

$$\frac{p_k}{p_1} = \frac{\gamma_1 M_1^2 + 1}{\gamma_k' + 1} + \left[\left(\frac{\gamma_1 M_1^2 + 1}{\gamma_k' + 1}\right)^2 - \left(\frac{2\gamma_1 M_1^2}{\gamma_1' - 1} - 1\right)\frac{\gamma_k' - 1}{\gamma_k' + 1}\right]^{1/2}. \tag{4}$$

$$\frac{\rho_k}{\rho_1} = \left(\frac{\gamma_k' + 1}{\gamma_k' - 1}\frac{p_k}{p_1} + 1\right) \Big/ \left(\frac{\gamma_1' + 1}{\gamma_1' - 1} + \frac{p_k}{p_1}\right), \tag{5}$$

$$T_k/T_1 = (p_k\rho_1/p_1\rho_k)/(1 + \varkappa), \tag{6}$$

$$\gamma_k'/(\gamma_k' - 1) = H_k/(1 + \varkappa)RT_k; \tag{7}$$

$H_k = H_k(p_k, T_k)$ is the enthalpy, referred to one mole μ of the inflowing gas, and κ is the degree of dissociation.

Making use of the method outlined above, we obtain the entropy change of the gas in transition from zone to zone.

2. GENERAL RELATIONS

In the absence of dissociation, the entropy change per mole of gas is equal to

$$dS = c_p\, dT/T - R\, dp/p; \tag{8}$$

whence

$$\frac{S_2 - S_1}{R} = \frac{5}{2}\ln\frac{T_2}{T_1} - \ln\frac{p_2}{p_1}, \tag{9}$$

$$\frac{S_3 - S_2}{R} = \frac{5}{2}\ln\frac{T_3}{T_2} + \ln\frac{T_3}{T_1} - \ln\frac{p_3}{p_2}. \tag{10}$$

$$\frac{S_4 - S_3}{R} = \frac{7}{2}\ln\frac{T_4}{T_3} + \frac{e^{T_c/T_4}(T_c/T_4)}{e^{T_c/T_4} - 1} - \frac{e^{T_c/T_1}(T_c/T_1)}{e^{T_c/T_1} - 1} - \ln\frac{e^{T_c/T_4} - 1}{e^{T_c/T_1} - 1} - \ln\frac{p_4}{p_3}, \tag{11}$$

T_c is the characteristic vibration temperature.

When $T_1 \gg T_c$, i.e., the vibrations are already excited in the flow, we have

$$\frac{S_4 - S_3}{R} = \frac{7}{2}\ln\frac{T_4}{T_3} + \ln\frac{T_4}{T_1} - \ln\frac{p_4}{p_3}. \tag{12}$$

If $T_1 \ll T_c \ll T_4$, which is the case in strong shocks,

$$\frac{S_4 - S_3}{R} = \frac{7}{2}\ln\frac{T_4}{T_1} + 1 + \frac{T_c}{T_4} + \ln\frac{T_4}{T_c} - \ln\frac{p_4}{p_3}. \quad (13)$$

In the presence of dissociation,

$$dS = (1-\varkappa)\,c_{p2}\frac{dT}{T} + 2\varkappa c_{p1}\frac{dT}{T} + D(T)\frac{d\varkappa}{T} - (1+\varkappa)\,R\frac{dp}{p}. \quad (14)$$

We can set the energy of dissociation D(T) equal to the energy of dissociation at absolute zero D_0.

To compute $S_5 - S_4$, we need to know the dependence of κ on T on p in the nonequilibrium region between zones 4 and 5. We make use of the conservation equations and the equation of state

$$\rho u = \alpha,\ p + \rho u^2 = \beta,\ H + \mu u^2/2 = \varepsilon; \quad (15)$$

$$p/\rho = RT(1+\varkappa)/\mu \quad (16)$$

α, β, ϵ are expressed in terms of the boundary conditions;

$$H = (1-\varkappa)\int_0^T c_{p2}\,dT + 2\varkappa\int_0^T c_{p1}\,dT + \varkappa D_0. \quad (17)$$

The four equations in (15) and (16) contain five unknowns, ρ, u, p, T and κ. We can therefore express κ as a function of p or T alone. The exact evaluation of such functions is difficult; therefore, we make use of approximate relationships.

We set

$$c_{p2} = a + Tb,\ c_{p1} = c + Td; \quad (18)$$

a, b, c, and d are certain constants. From Eqs. (15) and (16) we have

$$u \approx (1+\varkappa)\,\alpha RT/\beta\mu;\ u^2 \approx (1+2\varkappa)\,(\alpha RT/\beta\mu)^2. \quad (19)$$

Substitution of (18) and (19) in (15) yields

$$\varkappa = \frac{\varepsilon - aT - (e+b)T^2/2}{D_0 + mT + (2e+n)T^2/2} \equiv \frac{1}{X(T)}\left[\varepsilon - aT - \frac{1}{2}(e+b)T^2\right], \quad (20)$$

where $e = \mu(\alpha R/\beta\mu)^2$, $m = 2c - a$, $n = 2d - b$. In a similar fashion, we find

$$\varkappa = (2D_0)^{-1}\left\{\varepsilon - D_0 - \left(\frac{\beta}{p} - 1\right)\frac{mR}{e} + \left\{\left[\varepsilon - D_0 - \left(\frac{\beta}{p} - 1\right)\frac{mR}{e}\right]^2 + 4D_0\left[\varepsilon - \left(\frac{\beta}{p} - 1\right)\frac{aR}{e}\right]\right\}^{1/2}\right\} = (2D_0)^{-1}\left[F - m\beta R/ep + \sqrt{(m\beta R/ep)^2 + Gm\beta R/ep + H}\right] = (2D_0)^{-1}\left[F - m\beta R/ep + \sqrt{Q(p)}\right]. \quad (21)$$

In the integration of Eq. (14) over p, we introduce the variable $x = m\beta R/ep$. Then

$$\frac{S_5 - S_4}{R} = L_1(T_4 - T_5) + L_2\ln\frac{X(T_4)}{X(T_5)} - \frac{L_3(T_5)}{X(T_5)} + \frac{L_3(T_4)}{X(T_4)} + L_4[J(T_4) - J(T_5)] + \left(1 + \frac{\sqrt{H} + F}{2D_0}\right)\ln\frac{p_4}{p_5} - \frac{1}{2D_0}\left\{\frac{m\beta R}{e}\left(\frac{1}{p_5} - \frac{1}{p_4}\right)\right. \quad (22)$$

$$\left. - \sqrt{Q(p_5)} + \sqrt{Q(p_4)} + \sqrt{H}\ln\frac{H + m\beta GR/2\,ep_5 + \sqrt{HQ(p_5)}}{H + m\beta GR/2\,ep_4 + \sqrt{HQ(p_4)}} - G\ln\frac{\sqrt{Q(p_5)} + m\beta R/ep_5 + G/2}{\sqrt{Q(p_4)} + m\beta R/ep_4 + G/2}\right\},$$

where the following notation has been introduced:

$$L_1R = \frac{e(n-2b)}{2e+n};\ L_2R = \frac{2an + m(e+b)}{2(2e+n)} - \frac{mn(e+b)}{(2e+n)^2} - \frac{a}{2};$$

$$L_3R = aD_0 + \varepsilon m + \frac{1}{2}[D_0(e+b) + \varepsilon(2e+n)]\,T = q_1 + q_2T;$$

$$L_4R = q_2 + mL_2 + \left[\varepsilon + \frac{D_0(e+b)}{2e+n}\right], \quad (23)$$

$$J = \frac{2}{\sqrt{2D_0(2e+n) - m^2}}\tan^{-1}\frac{m + (2e+n)T}{\sqrt{2D_0(2e+n) - m^2}}.$$

In order to obtain the explicit dependence of the entropy change in every region of M_1 and γ_1, we consider the limiting cases of weak and strong shocks.

3. SHOCK WAVES OF WEAK INTENSITY

In this case the specific heat of the gas can be considered constant; we need consider only $S_2 - S_1$, $S_3 - S_2$, $S_4 - S_3$:

$$\frac{p_k}{p_1} = 1 + \Delta,\ \Delta = \frac{2\gamma_k}{\gamma_k + 1}\left(M_1^2\frac{\gamma_1}{\gamma_k} - 1\right) \ll 1. \quad (24)$$

We employ a power series expansion in Δ, whence

$$\frac{S_k - S_1}{R} = \frac{2\gamma_k}{3(\gamma_k+1)^2}\left(M_1^2\frac{\gamma_1}{\gamma_k} - 1\right)^3, \quad (25)$$

$$\gamma_2 = {}^5/_3,\ \gamma_3 = {}^7/_5,\ {}^7/_5 > \gamma_4 > {}^9/_7.$$

Obviously, for given γ_k and M_1, the entropy change is the greater the larger the value of γ_1; it has a maximum value for monatomic gases. For given γ_1 and M_1, the entropy increases with decrease in γ_k, i.e., successive excitation of the degrees of freedom of the molecules is accompanied by an increase in the entropy.

From Eq. (25) we have

$$\frac{S_2 - S_1}{R} = \frac{5}{32}\left(\frac{3}{5}\gamma_1M_1^2 - 1\right)^3, \quad (26)$$

$$\frac{S_3 - S_2}{R} = \frac{35}{216}\left(\frac{5}{7}\gamma_1M_1^2 - 1\right)^3 - \frac{5}{32}\left(\frac{3}{5}\gamma_1M_1^2 - 1\right)^3 < \frac{S_2 - S_1}{R}, \quad (27)$$

$$\frac{S_4-S_3}{R}=\frac{2\gamma_4}{3(\gamma_4+1)^2}\left(\frac{\gamma_1}{\gamma_4}M_1^2-1\right)^3$$
$$-\frac{35}{216}\left(\frac{5}{7}\gamma_1M_1^2-1\right)^3<\frac{S_3-S_2}{R}. \quad (28)$$

For $^7/_5 > M_1^2 > 1$, the excitation of the translational and rotational degrees of freedom takes place without entropy change, and only the subsequent excitation of vibrations leads to its increase. This phenomenon is known as the Kantrowitz effect[2] for supersonic velocities. No sharp front of the shock wave will be observed, but rather a gradual change of the parameters over distances of several tens of mean free path lengths.

4. STRONG SHOCK WAVES

In this case, considering $M_1 > 10$, Eqs. (1) to (6) are written in the form

$$\frac{p_k}{p_1}=\frac{2\gamma_1M_1^2}{\gamma_k'+1},\quad \frac{\rho_k}{\rho_1}=\frac{\gamma_k'+1}{\gamma_k'-1},\quad \frac{T_k}{T_1}=\frac{2\gamma_1M_1^2}{(\gamma_k'+1)^2}\frac{\gamma_k'-1}{1+\varkappa}, \quad (29)$$

where $\gamma_2' = {}^5/_3$, $\gamma_3' = {}^7/_5$, $\gamma_4' \geq {}^9/_7$; in accord with Refs. 3, 4, and 5, $\gamma_5' = 1.2$. Making use of Eqs. (9), (10), (12), (13), and (29) we obtain

$$(S_2-S_1)/R=3\ln M_1+\frac{3}{2}\ln\gamma_1-3.897, \quad (30)$$

$$(S_3-S_2)/R=2\ln M_1+\ln\gamma_1-2.829<(S_2-S_1)/R, \quad (31)$$

$$(S_4-S_3)/R|_{T_1\gg T_C}=2\ln M_1+\ln\gamma_1-3.098<(S_3-S_2)/R. \quad (32)$$

For most practical problems, $T_C/T_1 \leqq 10$; therefore,

$$(S_4-S_3)/R_{T_1\ll T_C\ll T_4}=2\ln M_1+\ln\gamma_1+91.43/\gamma_1M_1^2$$
$$-4.401<(S_4-S_3)/R|_{T_1\gg T_C}. \quad (33)$$

It follows from Eqs. (32) and (33) that in a gas in which the vibrations are already appreciably excited in the flow, the entropy change, for the same values of M_1, is larger than in a gas with the vibrations unexcited.

The expression for $S_5 - S_4$ is rather complicated. We shall simplify it, in order to estimate the dependence of the entropy change in dissociation upon M_1, γ_1, and D_0. Tabulated data give $a \approx 4R$, $c \approx 2R$, $m \approx R$, $b \approx d \approx 3$ to $6 \times 10^{-2}R/T_1$, $n \approx b$; moreover, $D_0 \approx 2 \times 10^2RT_1 \approx \gamma_1M_1^2RT_1$. Making use of these values, we obtain

$$(S_5-S_4)/R\approx(A+B\gamma_1M_1^2RT_1/D_0)\cdot10^{-2}$$
$$<(S_4-S_3)/R|_{T_1\ll T_C\ll T_4}; \quad (34)$$

A and B are constants on the order of unity. It is clear that the entropy change depends more strongly on M_1 in the dissociation of a gas than ΔS does in the excitation of arbitrary degrees of freedom of the molecules. For a given M_1 this change increases with diminishing energy of dissociation.

On the basis of Eqs. (26) to (28) and (30) to (34), it can be verified that the maximum entropy change takes place in the excitation of the successive degrees of freedom. For subsequent excitation of rotation, vibration and dissociation of the gas, the increase in entropy is lessened. This is explained by the fact that in an isolated system tending toward equilibrium, an increase in the total entropy can be accompanied by a decrease in the entropy of its separate parts; for a gas these will be the different degrees of freedom of the molecules. As is easily seen, in the successive excitation of the degrees of freedom of the gas, less of it is throttled, and a smaller fraction of the directed motion is transformed into heat energy. Such an excitation takes place therefore more and more at the expense of the redistribution of the already excited degrees of freedom.

[1] Iu. P. Lun'kin, J. Tech. Phys. (U.S.S.R.) **27**, 1276 (1957); Soviet Phys. JTP **2**, 1169 (1957).

[2] A. Kantrowitz, J. Chem. Phys. **10**, 145 (1942); **14**, 150 (1946).

[3] Ia. B. Zel'dovich, J. Exptl. Theoret. Phys. (U.S.S.R.) **32**, 1126 (1957); Soviet Phys. JETP **5**, 919 (1957).

[4] L. Lamb and Shao-Chi Lin, J. Appl. Phys. **28**, 754 (1957).

[5] W. Deal, J. Appl. Phys. **28**, 782 (1957).

Translated by R. T. Beyer
303

DISPERSION RELATIONS AND THE DERIVATION OF THE EQUATIONS FOR K-MESON SCATTERING

A. M. BRODSKII

Moscow State University

Submitted to JETP editor December 27, 1957

J. Exptl. Theoret. Phys. (U.S.S.R.) **34**, 1531-1538 (June, 1958)

A study is made of the scattering of K mesons by nucleons, with inclusion of effects of the possible formation of Ξ particles. In addition to the other propositions of the standard theory, special use is made of the conditions of causality and of the unitary nature of the S matrix. These conditions, together with the additional hypothesis that the interaction is invariant with respect to rotations in four-dimensional isotopic spin space, enable us to obtain equations which are valid at not too high energies and are of the type of Low's equations[1,2] in the theory of π-meson scattering. The form of the interaction is involved in the equations through the inhomogeneous term. These equations are at the same time a generalization of the dispersion relations for scattering at arbitrary angles. Analogous equations for π-meson scattering have been obtained in reference 2, where, however, use was made of a special spectral representation of the scattering matrix.[3-5] This spectral representation is not used in the present paper.

THE fact that it is not a trivial problem to go from the scattering of π mesons to a treatment of K-meson scattering is mainly due to the special nature of the behavior of the K mesons with respect to transformations in ordinary space and isotopic spin space, and also to the fact that in the case of the K mesons it turns out to be necessary from the very beginning to take into account the interactions with particles that do not play any direct part in the scattering, in particular Σ and Λ particles, and also π mesons. In addition, one must give more careful attention to relativistic effects. The interactions are here taken to be the renormalized ones; effects of weak interactions are neglected. This last condition is formulated as the requirement that all interactions be invariant with respect to rotations in the four-dimensional isotopic space.[6] In this space nucleons, Ξ particles, and K mesons form the four-dimensional isotopic spinors:

$$\Psi_N = \begin{vmatrix} \psi_p \\ \psi_n \\ \psi_{\Xi^0} \\ \psi_{\Xi^-} \end{vmatrix} \text{ and } K = \begin{vmatrix} K^+ \\ K^0 \\ \tilde{K}^0 \\ K^- \end{vmatrix} = \| K^i \|, \quad (i = 1, 2, 3, 4); \tag{1}$$

The following representation is chosen for the isotopic matrices:*

$$\gamma_i^i = \begin{vmatrix} 0 & \tau_i \\ -\tau_i & 0 \end{vmatrix} \ (i = 1, 2, 3); \quad \gamma_0^i = \begin{vmatrix} 0 & E_2 \\ E_2 & 0 \end{vmatrix};$$
$$\gamma_5^i = \begin{vmatrix} iE_2 & 0 \\ 0 & -iE_2 \end{vmatrix}. \tag{2}$$

This way of writing makes it possible to give a unified description of the dynamical behavior of all K mesons, and furthermore the "hypercharge" Y^6 of the heavy fermions is given apart from a factor i by the eigenvalue of the matrix γ_5^i. Unlike the convention of reference 6, we regard the isotopic space as pseudo-Euclidean, since only in this kind of a space can an isotopic spinor K that does not vanish identically be taken to be self-conjugate:

$$K = -i\gamma_2^i K^*. \tag{3}$$

It is necessary, however, to impose the invariant requirement that K be self-conjugate, owing to the existence of only four different K mesons. In connection with the experimental facts that are interpreted in terms of the presence of different parities of K mesons, one can assume* that an

*Hereafter, where no special stipulation is made, the notations of reference 7 are used.

*One can try to give this fact a general explanation through the idea of a fusion of the ordinary and isotopic spaces.[8] We note also that the definition of the hypercharge is here an obvious four-dimensional way of writing the isotopic fermion number of d'Espagnat and Prendtki. The reflections in this four-dimensional isotopic space for the K mesons are analogous to the Pauli transformations[9] for spinor particles.

ordinary reflection results in multiplying each isotopic spinor by γ_5^i. To shorten the writing we shall also use the formal concept of the baryon space,[6]* in which Ψ_N and the real isotopic vector $\Psi_\Sigma(\Lambda_0, \Sigma_1 + i\Sigma_2, \Sigma_1 - i\Sigma_2, \Sigma_3)$ are represented as a two-component quantity $\Psi_B = \begin{vmatrix}\Psi_N\\ \Psi_\Sigma\end{vmatrix}$, on which the Pauli matrices ν_i act. After these remarks we can write the amplitude for the scattering of K mesons by nuclei in a form analogous to the amplitude for the scattering of π mesons:[7,10]

$$\delta(p'+q'-p-q)\,f(\mathbf{p}'s', \mathbf{q}'j;\ \mathbf{p}s, \mathbf{q}i) = \frac{\pi}{(2\pi)^3 i}\int dx dy e^{-i(qx-q'y)}\,\langle \mathbf{p}'s'\left|\frac{\delta^2 S}{\delta K_j^*(y)\,\delta K_i(x)} S^+\right|\mathbf{p}s\rangle. \tag{4}$$

Here s′ and s are spinor and isotopic indices, including the value of the hypercharge, which is equal to +1 for the incident nucleon and ±1 for the scattered nucleon. The functional derivative $\delta/\delta K_j^*(y)$ appearing in Eq. (4) can be replaced, in virtue of the condition (3), by

$$\delta/\delta(i\gamma_2^i K^*)_j = (-1)^{\max(j,5-j)}\delta/\delta K_{5-j}(y).$$

From this it follows that the amplitude for the scattering of K mesons is invariant with respect to the substitution

$$q \leftrightarrow -q' = -(p+q-p'),\qquad i \leftrightarrow 5-j \tag{5}$$

if one at the same time multiplies by the sign factor $a(ij) = (-1)^{\max(i,5-i)}\cdot(-1)^{\max(j,5-j)}$. This result is equivalent to a well known theorem of Gell-Mann and Goldberger on symmetry in the scattering of π mesons.[10] We further introduce, in analogy with reference 7, the K-meson current operator $j_i(x)$:

$$j_i(x) = i\frac{\delta S}{\delta K_i(x)}S^+ = -iS\frac{\delta S^+}{\delta K_i(x)}, \tag{6}$$

which, in virtue of the causality condition and the unitary property of the S matrix, satisfies the conditions

$$j_i^+(x) = (-1)^{\max(i,5-i)} j_{5-i}(x),$$
$$\delta j_i(x)/\delta K_j(y) = 0 \qquad \text{for } y_0 < x_0, \tag{7}$$
$$\delta j_i(x)/\delta K_j(y) = 0 \text{ and } [j_i(x),\ j_j(y)] = 0 \text{ for } (x-y)^2 \leqslant 0.$$

Using these conditions, we can rewrite the scattering amplitude in the form

$$\delta(p+q-p'-q')\,f(\mathbf{p}'s', \mathbf{q}'j;\ \mathbf{p}s, \mathbf{q}i) = \frac{\pi}{(2\pi)^3 i}(-1)^{\max(j,5-j)}\int dx dy e^{-i(qx-q'y)} \times \langle \mathbf{p}'s'|\,T(j_{5-j}(y)\,j_i(x)) + \Lambda_{5-j,i}\left(x, \frac{\partial}{\partial x}\right)\delta(x-y)\,|\mathbf{p}s\rangle. \tag{8}$$

*In reference 6 this space is called the nucleonic space.

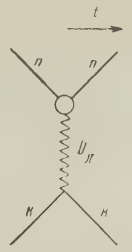

FIG. 1

To begin with let us consider separately the last term, which corresponds to the simultaneous production of the final K meson and annihilation of the initial K meson. Omitting effects of weak interactions, we find that this term is described by the diagram shown in Fig. 1, and is given by

$$\frac{1}{(2\pi)^5}\tilde{g}_{n\pi n}\tilde{g}_{K\pi K}\bar{v}^+(\mathbf{p}'s')\int dx\,dx'dy\,dy'd\xi\,d\xi' e^{i(q'y'+p'x'-px-qy)} \times \Gamma_{B\pi B}(x, x'; \xi)\,D_\pi(\xi, \xi')\,\Gamma^0_{K\pi K}(y, y'; \xi')\,v^-(\mathbf{p}s). \tag{9}$$

Here and in what follows Γ denotes as usual the total vertex part, Γ^0 denotes the vertex part in the first approximation of perturbation theory, determined by the form of the interaction in L_{int}, and D_π is the total propagation function of the π meson. Furthermore Γ^0 is proportional to the δ functions $\delta(y-y')\,\delta(y-\xi)$ or to finite derivatives of these functions; in virtue of the conservation of hypercharge or, what is equivalent, the conservation of strangeness, $\Gamma_{B\pi B}$ does not contain transitions from nucleons to χ particles. For an analogous reason, and also on account of the transformation properties of K and π mesons under reflections, in the case of parity conservation $\Gamma_{K\pi K} = 0$ and in the framework of the standard theory the entire term (9) must be set equal to zero. If, however, we require only invariance with respect to products of ordinary reflections and isotopic reflections (in particular charge conservation), and not with respect to the separate reflections,* $\Gamma_{K\pi K} \neq 0$ for $(i-j) \leq 2$.

Omitting the term (9) that has already been considered, after the usual transformations of the theory of dispersion relations,[1,7] we get from Eq. (8)

$$f(\mathbf{p}'s', \mathbf{q}'j;\ \mathbf{p}s, \mathbf{q}i) = (-1)^{\max(j,5-j)}(2\pi)^5/2 \times \int d\mathbf{k}\left\{\sum_n\left[\frac{\langle \mathbf{p}'s'|\,j_{5-i}(0)\,|n, \mathbf{k}\rangle\langle n, \mathbf{k}|\,j_j(0)\,|\mathbf{p}s\rangle}{p_0+q_0-E_n(\mathbf{k})-i\varepsilon}\delta(\mathbf{p}+\mathbf{q}-\mathbf{k}) + \frac{\langle \mathbf{p}'s'|\,j_i(0)\,|n, \mathbf{k}\rangle\langle n, \mathbf{k}|\,j_{5-j}(0)\,|\mathbf{p}s\rangle}{p_0'-q_0-E_n(\mathbf{k})+i\varepsilon}\delta(\mathbf{p}'-\mathbf{q}-\mathbf{k})\right]\right\}. \tag{10}$$

We have further in the real case

$$p_0+q_0 = p_0'+q_0',\quad p_0 \geqslant m_n \text{ and } q_0, q_0' \geqslant m_K > 0. \tag{11}$$

*This condition can be interpreted as the existence of rotations only in the combined space (ordinary × isotopic).

This last condition has allowed us to change the sign of $i\epsilon$ in the denominator of the second term of Eq. (10), since this denominator does not pass through zero. We now introduce the Hermitian and anti-Hermitian parts of the scattering amplitude:

$$D(\mathbf{p}'s', \mathbf{q}'j; \mathbf{p}s, \mathbf{q}i) = \frac{1}{2}[f(\mathbf{p}'s', \mathbf{q}'j; \mathbf{p}s, \mathbf{q}i) + f^*(\mathbf{p}s, \mathbf{q}i; \mathbf{p}'s', \mathbf{q}'j)],$$
$$A(\mathbf{p}'s', \mathbf{q}'j; \mathbf{p}s, \mathbf{q}i) = \frac{1}{2i}[f(\mathbf{p}'s', \mathbf{q}'j; \mathbf{p}s, \mathbf{q}i) - f^*(\mathbf{p}s, \mathbf{q}i; \mathbf{p}'s', \mathbf{q}'j)], \quad (12)$$

In virtue of the unitary property of the S matrix,

$$A|_{p+q=p'+q'} = -\frac{1}{2}\sum_n f^*(n, \mathbf{p}+\mathbf{q}; \mathbf{p}'s', \mathbf{q}'j) f(n, \mathbf{p}+\mathbf{q}; \mathbf{p}s, \mathbf{q}i)\,\delta(E_n - p_0 - q_0), \quad (13)$$

where $f(n, \mathbf{p}+\mathbf{q}; \mathbf{p}s, \mathbf{q}i)$ are the scattering amplitudes into states n with momentum $\mathbf{p}+\mathbf{q}$ and energy $E_n(\mathbf{p}+\mathbf{q}) > 0$. Here, as is usual in the theory of the dispersion relations, the system of states n is identified with a system of particles and complexes with the experimental values of the parameters at infinity, and is taken to be a complete set. On the other hand, from Eq. (10) with use of Eqs. (7) and (11) it follows that

$$A|_{p+q=p'+q'} = \pi\frac{(2\pi)^5}{2}(-1)^{\max(j,5-j)}\sum_n \langle \mathbf{p}'s'|j_{5-j}(0)|n, \mathbf{p}+\mathbf{q}\rangle\langle n, \mathbf{p}+\mathbf{q}|j_i(0)|\mathbf{p}s\rangle\,\delta(E_n(\mathbf{p}+\mathbf{q}) - p_0 - q_0). \quad (14)$$

It is essential that Eq. (14) is valid not only in the region $p_0 \geq m_n$, $q_0 \geq m_K$, but also in the region* $p_0 \geq m_n$, $q_0 > m - m_\Sigma$. We now consider the connection between D and A, following mainly the work of reference 7. For this purpose we introduce the function $f(z)$ of a complex variable z, obtained by replacing $q_0 - i\epsilon$ by z in Eq. (10). As follows from an examination of Eq. (10), when one takes into account the conservation laws the function $f(z)$ is analytic everywhere for $\mathrm{Im}\, z \neq 0$ and for prescribed p and p', at any rate on the segment of the real axis

$$-\sqrt{m_\Lambda^2 + (\mathbf{p}-\mathbf{q})^2} + p_0' < z < \sqrt{m_\Lambda^2 + (\mathbf{p}+\mathbf{q})^2} - p_0,$$
$$\mathrm{Im}\, z = 0.$$

We postulate further that $f(z)$ falls off at infinity† faster than z^{-1}. Using Eq. (7), one easily gets from Eq. (10) and (12) (for brevity the arguments other than q_0 are not written out):

$$D(q_0) = \frac{1}{2}\left[\lim_{z\to q_0 - i\varepsilon} f(z) + \lim_{z\to q_0 + i\varepsilon} f(z)\right];$$
$$A(q_0) = \frac{1}{2i}\left[\lim_{z\to q_0 - i\varepsilon} f(z) - \lim_{z\to q_0 + i\varepsilon} f(z)\right]. \quad (15)$$

Using the properties of the function $f(z)$ and applying the Cauchy integral theorem, taking the contours of integration shown in Fig. 2, one easily finds that

$$f(q_0 + i\varepsilon) = \frac{1}{2\pi i}\int_{-\infty}^{\infty} d\tilde{q}_0 \frac{f(\tilde{q}_0 + i\varepsilon/2)}{\tilde{q}_0 - q_0 - i\varepsilon/2};$$
$$f(q_0 - i\varepsilon) = \frac{1}{2\pi i}\int_{+\infty}^{-\infty} d\tilde{q}_0 \frac{f(\tilde{q}_0 - i\varepsilon/2)}{\tilde{q}_0 - q_0 + i\varepsilon/2}. \quad (16)$$

Thereupon, taking the average of the expressions (16) and letting ϵ go to zero, we find that

$$D(q_0) = \frac{1}{2\pi}\int_{-\infty}^{\infty} d\tilde{q}_0 \frac{(\tilde{q}_0 - q_0)A(\tilde{q}_0)}{(\tilde{q}_0 - q_0)^2 + \varepsilon^2/4} = \frac{1}{\pi}\int_{-\infty}^{\infty} A(\tilde{q}_0)\,\mathrm{P}\frac{d\tilde{q}_0}{\tilde{q}_0 - q_0}. \quad (17)$$

*In using Eq. (13) in the region $|q_0| < m_K$ one must proceed in all the intermediate manipulations as is done in reference 7, replacing m_K^2 by a fictitious quantity $\tau < q_0^2$, $q_0'^2$, with respect to which the scattering amplitude is an analytic function, and continue the result to the value $\tau = m_K^2$.

†If the stated hypothesis does not hold and $f(z)$ behaves at infinity like z^n (evidently in reality $n = 0$), one could consider instead of $f(z)$ the quantity $f(z)/(z - z_0)^{n+1}$ in the usual way, with corresponding modifications of all subsequent relations. The standard way of solving the Low equations has meaning, however, only provided that intermediate states with large numbers of particles and high energies do not for any reason make an important contribution to the scattering, since only if this is true is it possible to justify dropping out the higher amplitudes in the infinite system of coupled equations. In this case one can also confirm the assumed decrease of $f(z)$ with increasing z, by arguing as follows from Eq. (10). Neglecting, for large z, all terms except z in the denominator of Eq. (10), by representing the δ functions as Fourier series one can carry out the summation over the intermediate states. After this the numerator of the integrand will be proportional to the matrix element of the commutator $[j_i(0, y), j_{s\ j}(0)]$, which is zero in virtue of the causality condition. We emphasize that a complete treatment of this question is in general impossible in the framework of the existing theory, and that one must only hope that, as in the case of π-meson scattering, these last considerations are in some sense justified, at least for not too high energies of the scattered particles.

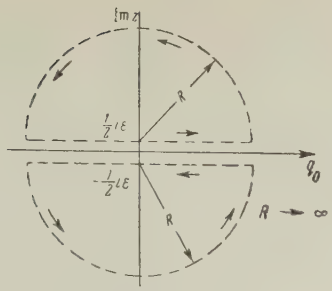

FIG. 2

It follows from Eq. (17) that for given $\mathbf{p}s$, $\mathbf{p}'s'$

$$f(\mathbf{p}'s', \mathbf{q}'j; \mathbf{p}s, \mathbf{q}i) = f_{ji}\left(q_0', \mathbf{n}' = \frac{\mathbf{q}'}{|\mathbf{q}'|}; \; q_0, \mathbf{n} = \frac{\mathbf{q}}{|\mathbf{q}|}\right)$$

$$= \frac{1}{\pi}\int_{-\infty}^{\infty} \frac{A(p_0 - p_0' + \tilde{q}_0, \mathbf{n}', j; \tilde{q}_0, \mathbf{n}, i)}{\tilde{q}_0 - q_0 - i\varepsilon}\, d\tilde{q}_0. \qquad (18)$$

In Eq. (18) we carry out the change to observable quantities, recalling that A is expressed in terms of the scattering amplitude by Eq. (13) only for $q_0', q_0 \geq m_K$; $p_0, p_0' \geq m_N$. For this purpose we go over to Salam's reference system, in which $\mathbf{p} + \mathbf{p}' = 0$. In this system[7]

$$q_0 = q_0' = \sqrt{m_K^2 + p^2 + \lambda^2}; \quad p_0 = p_0', \; \mathbf{q} = -\mathbf{p} + \lambda\mathbf{e},$$
$$\mathbf{q}' = \mathbf{p}' + \lambda\mathbf{e}, \quad \mathbf{e}^2 = 1, \; \mathbf{ep} = 0 \qquad (19)$$

and the substitution (5) takes the form

$$i \leftrightarrow j; \; q_0 \leftrightarrow -q_0; \; \mathbf{e} \leftrightarrow -\mathbf{e}. \qquad (5')$$

In view of what has been said we can write, dropping from the list of arguments the prescribed values $\mathbf{p}s$, $\mathbf{p}'s'$,

$$f_{ji}(q_0, \mathbf{e}) = \frac{1}{\pi}\int_0^{\infty}\left[\frac{A_{ij}(\tilde{q}_0, \mathbf{e})}{\tilde{q}_0 - q_0 - i\varepsilon} - a(i,j)\frac{A_{ij}(\tilde{q}_0, -\mathbf{e})}{\tilde{q}_0 + q_0 + i\varepsilon}\right] d\tilde{q}_0. \qquad (20)$$

The region of integration in Eq. (20) can be divided into two parts: from zero to E_1 (the so-called unphysical part), and from E_1 to infinity, where in the chosen system of reference $E_1 = (m_K^2 + p^2)^{1/2}$. In the second region the expression (13) can be used for A_{ji}. We see, however, that owing to the presence in Eqs. (13) and (14) of δ functions of the energy, and in virtue of the conservation laws, if we have just the condition

$$p^2 < p_1^2 = \frac{{}^1/_4\left[(m_\Sigma + 2m_\pi)^2 - m_n^2 - m_K^2\right]^2 - m_n^2 m_K^2}{m_n^2 + m_K^2 + \left[(m_\Sigma + 2m_\pi)^2 - m_n^2 - m_K^2\right]} > 0,$$

and if we assume that the amplitude $f_{hi}(q_0, \mathbf{e})$ is itself determined by the corresponding relations for all $q_0 > 0$, then the contribution in the unphysical region will be given only by states with a single intermediate Σ particle, or also with a Σ particle and a π meson (in the case of an intermediate Λ particle the presence of two π mesons is possible). Therefore in Eq. (13) and (14) we break up the sum over the intermediate states into two parts

$$\sum_n = \sum_n' + \sum_n'', \qquad (21)$$

where $\sum_n''$ denotes the sum over the positive-energy intermediate states that can give a contribution in the unphysical region, except states with one nucleon and one K meson. We shall make a direct evaluation of the contribution to A corresponding to $\sum''$. From what has been said it follows that in the first place there will occur in the sum $\sum_n''$ the anti-hermitian component $A_{ji}^{(a)}$ of the part of the scattering amplitude given by the diagram shown in Fig. 3. The corresponding quantity can be determined in complete analogy with the theory of π-meson scattering in the following way:*

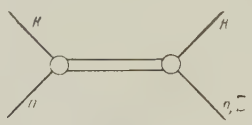

FIG. 3

$$A_{ji}^{(a)}\delta(p + q - p' - q') = -\frac{\tilde{g}_{BKB}\,\delta(-1)^{\max(j,5-j)}}{2i\cdot 2(2\pi)^5}$$

$$\times\left\{\bar{v}^+(p's')\int_0^{\infty} dp_0''\int d\mathbf{p}''\,\Gamma_{BK_{5-j}B}(p', p''; -q')\right.$$

$$\left.\times G_\Sigma(p'')\,\Gamma_{BK_iB}(p'', p'; q)\,v^-(p, s) - [\quad]\right\}. \qquad (22)$$

The second term in the curly brackets, indicated by square brackets, is obtained from the first term by the interchange $\mathbf{p}' \longleftrightarrow \mathbf{p}$, $\mathbf{q} \longleftrightarrow \mathbf{q}'$, $i \longleftrightarrow j$ and complex conjugation. Here Γ_{BKB} are vertex parts defined in the standard way:

$$\tilde{g}_{BKB}\,\Gamma_{BK_iB}(x, x'; \xi) = -\frac{\delta G_B(x, x')}{\delta\langle K_i(\xi)\rangle_0}$$

*To give to Eq. (22) an explicitly invariant form with respect to transformations in the four-dimensional isotopic space, one would have to replace $\bar{v}^+$ by $\bar{v}^+\gamma_0^i$ and make a corresponding change in the definition of G_B. To shorten the presentation we have not done this, but this circumstance must be kept in mind in examining Eq. (25) and in many other cases in which it is not sufficient to consider only invariance with respect to three-dimensional isotopic transformations.

and G_B is the total propagation function of the baryons

$$G_B = \left| \begin{matrix} G_N \\ G_\Sigma \end{matrix} \right|. \qquad (23)$$

Here, for example, $G_\Sigma = i\langle T(\bar{\psi}_\Sigma \psi_\Sigma)\rangle_0$ has the form[7]

$$G_\Sigma(p) = \frac{\gamma p s_1(p^2) + m_\Sigma s_2(p^2)}{m_\Sigma^2 - p^2 - i\varepsilon}, \qquad s_1(m_\Sigma^2) = s_2(m_\Sigma^2) = 1, \qquad (24)$$

where m_Σ is the experimental mass of the Σ particle.

By using the relation (7.15) of reference 7, the equation

$$\gamma_0 \Gamma^+_{BK_iB}(p', p''; -q')\gamma_0 = (-1)^{\max(i,5-i)} \Gamma_{BK_{5-i}B}(p'', p'; q') \qquad (25)$$

which follows from the definition of Γ_{BKB} (see also the preceding note), and Eq. (24), we get from Eq. (24), the results

$$A^{(a)}_{ji}\delta(p+q-p'-q') = -\frac{\tilde{g}^2_{BKB}}{4(2\pi)^4}(-1)^{\max(j,5-i)}\bar{v}^+(p's')\int_0^\infty dp_0''\int d\mathbf{p}$$
$$\times \Gamma_{BK_{5-j}B}(p', p''; -q')(\gamma p'' + m_\Sigma)\delta(m_\Sigma^2 - p''^2)\Gamma_{BK_iB}(p'', p'; q)v^-(ps)$$
$$= -\frac{\tilde{g}^2_{BKB}}{4(2\pi)^4}\delta(p'+q'-p-q)\int dp''\frac{\delta(p_0'' - \sqrt{\mathbf{p}''^2 + m_\Sigma^2})}{2\sqrt{\mathbf{p}''^2 + m_\Sigma^2}}\delta(p''-p-q)$$
$$\times \bar{v}^+(p's')\Gamma_{BK_{5-j}B}(p'; p'-p'')(\gamma p'' + m_\Sigma)\Gamma_{BK_iB}(p''; p''-p)v^-(\mathbf{p}, s), \qquad (26)$$

where $\Gamma(p'', p''-p)\delta(p''-p-q) = \Gamma(p'', p; q)$.

As can be seen from Eq. (26), the vertex parts $\Gamma_{BKB}(p', p''; q)$ occur only with values of the momenta that satisfy the free-particle equations with the experimental masses; using the arbitrariness in the prescription of $\tilde{g}_{BKB}$, we can define the renormalized coupling constants of the interaction of baryons with K mesons by means of the condition

$$\tilde{g}_{BKB}\Gamma_{BKB}(m_B^2, m_B^2; m_K^2) = g_{BKB}\Gamma^0_{BKB}(1 + O(q^2)), \qquad (27)$$

where $O(0) = 0$ and Γ^0_{BKB} is the interaction corresponding to the first approximation of perturbation theory for the special L_{int} with the experimental parameters.* Inserting the expression (26) as the part A in Eq. (20) and performing the integration over $\tilde{q}_0$, we verify that $A^{(a)}$ gives two terms in the scattering amplitude. In the low-energy limit these terms agree respectively with the total term of the first approximation of perturbation theory for the diagram of Fig. 3 and with the term for the diagram obtained from Fig. 3 by the substitutions (5), for the experimental values of the parameters. We note that in consequence of the conservation of hypercharge one of these terms is always equal to zero. As has already been mentioned, besides the diagram of Fig. 3 there will also be contributions $A^{(b)}$ to $\sum_n''$ from diagrams in which at some stage in the intermediate states there are π mesons present as well as Σ particles. Even at low energies, however, the anti-Hermitian part $A^{(b)}$ constructed in the same way as Eq. (26) will be determined not only by the form of the interaction and the experimental parameters (masses and coupling constants) but also, in general, by the unknown functions $s_1(p^2)$, $s_2(p^2)$ of Eq. (24), and also by the analogous functions occurring in G_n and D_π. These functions must be further determined, either by a rigorous or approximate solution of the field equations, or by the study of other experiments.

Substituting Eqs. (13) and (21) into Eq. (20) and including the term (9), we finally obtain, in the reference system $\mathbf{p} + \mathbf{p}' = 0$ [Eq. (19)] for prescribed $\mathbf{p}$s, s' and $\mathbf{p}^2 < \mathbf{p}_1^2$,

$$f_{ji}(q_0, e) = (1 + \mathrm{Int})\left\{O_{ji}(1) + \frac{1}{2\pi}\sum_n{}' \frac{f^*(n, \lambda_n' e; -ps', p + \lambda_n' ej) f(n, \lambda_n' e; ps, -p + \lambda_n' ei)}{q_0 + p_0 - E_n - i\varepsilon}\right\}. \qquad (28)$$

Here Int means the substitution (5) with multiplication by $a(ij)$; λ_n' is defined by the relation $\lambda_n'^2 = (E_n(\lambda') - p_0)^2 - \mathbf{p}^2 - m_K^2 > 0$; and $0_{ji}(1)$ denotes terms calculated on the stated basis in the first approximation of perturbation theory, with the experimental parameters, from the diagrams

*For brevity we do not display distinctions between the interaction constants between K mesons and various baryons. These constants ($g_{\Sigma KN}$, g_{NKN}, etc.) can be introduced independently of each other, by considering separately the various processes of K-meson scattering.

of Figs. 1 and 3 and diagrams with a Σ particle and a π meson, possibly with inclusion of additional experimental information.

The equation that has been obtained is the first member of an infinite system of coupled equations for the scattering amplitudes, of the type of relativistic Low equations. In the first approximation, in which one usually solves the Low equations, all the higher amplitudes are omitted, and at sufficiently low energies we arrive at a closed integral equation.* As follows from our result (28), this equation is simply the corresponding dispersion relation, with the form of the interaction entering through the inhomogeneous term. A special property of the K mesons is the fact that a study of their scattering by means of equations of the type of the Low equations can provide a basis for important conclusions about the structure of the isotopic space. Moreover, qualitative conclusions already offer a possibility, by analogy with the π-meson scattering, of settling in which state the scattering will be largest.

In conclusion the writer expresses his gratitude to Professor D. D. Ivanenko for his interest in this work and to M. K. Polivanov for comments.

*By this approximate equation $f_{ij}(q_0, e)$ is determined not only in the physical region, but also for $0 < q_0 < (m_K^2 + p^2)^{1/2}$.

[1] F. E. Low, Phys. Rev. **97**, 1392 (1955).
[2] A. M. Brodskii, J. Exptl. Theoret. Phys. (U.S.S.R.) **32**, 616 (1957), Soviet Phys. JETP **5**, 509 (1957).
[3] Y. Nambu, Phys. Rev. **100**, 394 (1955).
[4] A. Brodskii, Dokl. Akad. Nauk SSSR **111**, 787 (1956), Soviet Phys. "Doklady" **1**, 701 (1956).
[5] Проблемы современной физики (Problems of Contemporary Physics) No. 2, (1957), Introductory Article. 1957.
[6] J. Schwinger, Theorie des particules elementaires, l'Universite de Paris, 1957.
[7] N. N. Bogoliubov and D. B. Shirokov, Введение в теорию квантованных полей (Introduction to the Theory of Quantized Fields), GITTL, Moscow, 1957.
[8] D. Ivanenko and H. Sokolik, Nuovo cimento **6**, 226 (1957).
[9] G. Lüders, Nuovo cimento **7**, No. 2, 171 (1957).
[10] A. Klein, Phys. Rev. **99**, 998 (1955).

Translated by W. H. Furry
304

SOVIET PHYSICS JETP VOLUME 34 (7), NUMBER 6 DECEMBER, 1958

ONE POSSIBLE MODE OF DEVELOPMENT OF EXTENSIVE AIR SHOWERS

N. L. GRIGOROV and V. Ia. SHESTOPEROV

Moscow State University

Submitted to JETP editor December 30, 1957

J. Exptl. Theoret. Phys. (U.S.S.R.) **34**, 1539-1547 (June, 1958)

The development of extensive air showers is studied under the assumption that the fraction of energy lost in interaction of ultra-high energy particles with light nuclei is subject to strong fluctuations. It is shown that the main features of extensive air showers can be explained without recourse to the hypothesis that the nuclear component plays an important role in the development of showers in the depth of the atmosphere.

1. INTRODUCTION

IT is well known that extensive air showers (EAS) consisting of 10^4 to 10^5 particles possess a lateral distribution which is independent of the altitude of observation (within the limits of 1000 to 640 g/cm^2 atmospheric depth) and that the number of such showers varies in the atmosphere exponentially, with an absorption coefficient $1/\mu$ = 130 to 140 g/cm^2. These facts have been explained by several authors[1-3] who have assumed that the development of EAS is determined by the development of nuclear cascade. In that theory, the slow absorption of showers in the atmosphere is explained

by the weak absorption of nuclear active particles. The invariance of lateral distribution is attributed to the fact that high-energy nuclear-active particles carry a large amount of energy into the lower atmosphere and, transferring it to the soft component, counteract the aging of the shower, i.e., the change in the lateral distribution of shower particles.

We have already mentioned[4] that the above features as well as other properties of EAS, can be explained without recourse to the hypothesis that the shower development is influenced materially by the nuclear cascade. It is known that particles of up to $\sim 10^{12}$ ev have an absorption mean free path in the atmosphere equal to ~ 120 g/cm^2.[5] We shall assume therefore that the absorption mean free path is $L_a = 120$ g/cm^2 also for the particles of higher energies ($E_0 \sim 10^{13}$ to 10^{14} ev) which are responsible for shower productions (it is possible that L_p decreases with increasing energy). Without contradicting known experimental facts, we shall assume that the interaction of high-energy particles is characterized by larger fluctuations of the fraction of energy lost. In order to simplify the calculations, we shall assume that interactions of ultrahigh energy particles can be divided into two groups, one with small energy losses, and another with large energy losses, close to 100%. We shall neglect the contribution of weak interactions to shower development, assuming that a shower is produced when a particle loses a large fraction of its energy, close to 100%.

We shall consider two simplified schemes of large energy loss: (a) the total energy lost is transferred to a single photon with energy E_0 (E_0 is the energy of the primary nuclear-active particle) and the shower develops then as a pure electron-photon cascade, without nuclear-active particles; (b) the collision involving the 100% energy loss corresponds to the process studied by Landau[6] and the shower develops with contribution of nuclear-active particles.

We shall assume, furthermore, that the energy-spectrum of primary nuclear-active particles is known and is given by the expression $F(E)dE = B\,dE/E^2$.[7]

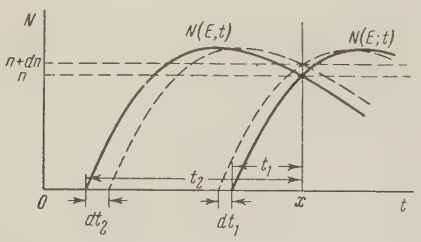

FIG. 1. Illustration for calculation of the number of showers with a given number of particles from n to n + dn at the depth x, produced by primary particles with energy E.

The problem consists of calculating those average features of EAS which have been observed in experiments on the basis of the above assumptions (for the two schemes a and b) and to determine if they depend on the presence of high-energy nuclear-active particles in the shower.

2. ALTITUDE DEPENDENCE OF THE NUMBER OF SHOWERS WITH A GIVEN NUMBER OF PARTICLES AND THE NUMBER SPECTRUM

Under the above assumptions, the development of EAS is as follows: If a particle with energy E interacts with an nitrogen or oxygen atom in the atmosphere at the point t_0, and loses in that interaction its total energy, then a shower will start developing from that point (according to either of the two schemes). Let $N(E, t)$ be the function giving the number of particles in the shower at a distance t g/cm^2 from the point of initiation (t_0) when the shower is caused by a primary of energy E. [Obviously, the choice of the scheme of development will determine the function $N(E, t)$.] At the point of observation, at atmospheric depth x g/cm^2, we shall record a shower consisting of $n = N(E, x - t_0)$ particles.

If we require that at the observation level y the shower contain between n and n + dn particles and that it be initiated by a nuclear-active primary with energy E, then it is necessary that that particle interact with large energy loss either in the layer dt_1 at the distance t_1 or in the layer dt_2 at the distance t_2 from observation level (Fig. 1), where t_1 and t_2 are the roots of the equation

$$N(E,\ t_{1,2}) = n, \tag{2.1}$$

and dt_1 and dt_2 are determined from the equations:

$$dt_1 = dn \Big/ \frac{\partial N}{\partial t}\Big|_{t=t_1}; \qquad dt_2 = dn \Big/ -\frac{\partial N}{\partial t}\Big|_{t=t_2}. \tag{2.2}$$

If $F(E)dE$ primary particles are incident on the top of the atmosphere, with energy between E and E + dE, then $F(E)' \exp\{-(x - t_1)/L_a\}\,dE$ particles with energy E will arrive at the level t_1 and $F(E)\exp\{-(x - t_2)/L_a\}\,dE$ at the level T_2. A fraction $\alpha\,dt_1/L_i$ of the particles that arrive at the level $x - t_1$ will interact with a large energy loss in the layer dt_1. Similarly, $\alpha\,dt_2/L_i$ of the primary particles that arrive at the level $x - t_2$ will interact in the layer dt_2. α is the probability of strong interaction with a large ($\sim 100\%$) energy

loss, and L_i is the interaction mean free path. The number of showers produced by nuclear-active particles with energy between E and E + dE and containing between n and n + dn particles at observation level will be, therefore, equal to

$$\frac{\alpha}{L_i} dt_1 F(E) \exp\{-(x-t_1)/L_a\}\, dE + \frac{\alpha}{L_i} dt_2 F(E) \exp\{-(x-t_2)/L_a\}\, dE = \frac{\alpha}{L_i} e^{-x/L_a} dn \cdot F(E)\, dE \times \left\{ \frac{\exp\{t_1(E, n)/L_a\}}{(\partial N/\partial t)|_{t_1}} + \frac{\exp\{t_2(E, n)/L_a\}}{-(\partial N/\partial t)|_{t_2}} \right\}. \quad (2.3)$$

Showers with a given number of particles can, however, be originated by primaries of various energies. The total number of showers $N_S(n, x)\,dn$ with number of particles between n and n + dn at the atmospheric depth x is therefore

$$N_S(x, n)\, dn = \frac{\alpha\, dn}{L_i} e^{-x/L_a} \left\{ \int_{E_{min}}^{\infty} \frac{\exp[t_1(E, n)/L_a]}{(\partial N/\partial t)|_{t_1}} F(E)\, dE + \int_{E_{min}}^{E_{max}} \frac{\exp[t_2(E, n)/L_a]}{-(\partial N/\partial t)|_{t_2}} F(E)\, dE \right\}, \quad (2.4)$$

where E_{min} and E_{max} satisfy the following equations:

$$N(E_{min};\ t_{max}) = n, \quad (2.5)$$

$$N(E_{max},\ x) = n, \quad (2.6)$$

under the additional condition $t_{max} < x$ (t_{max} is the distance from the origin, which corresponds to the maximum number of particles in the shower).

Cascade curves (near the maximum) can be approximated, with an accuracy sufficient for the calculations, by the expression

$$N(E,\ \xi) = AE \exp(-a\xi^2 + b\xi^3), \quad \xi = t - t_{max}. \quad (2.7)$$

The values of t_1 and t_2 are determined from the equations

$$t_1 = t_{max} + \xi_1, \qquad t_2 = t_{max} + \xi_2,$$

The values ξ_1 and ξ_2 are determined from the equation $N(E, \xi_{1,2}) = n$.

If we consider scheme (a), then, for the energy of primaries initiating showers having 10^4 to 10^6 particles at sea-level or at mountain altitudes, we obtain $A = 1.2 \times 10^{-9}\,ev^{-1}$ and the coefficients a and b in Eq. (2.8) are equal to 0.025 and 0.0008 respectively. $t_{max} = \ln(E/\beta)$, where β is the critical energy in air, equal to 7.2×10^7 ev.

If we denote $\ln(E/E_{min}) = z$, then, to a sufficient degree of accuracy, we can put

$$\xi_1 = -\left(\frac{z/a}{1 + (b/a)\sqrt{z/a}}\right)^{1/2}, \quad \xi_2 = \left(\frac{z/a}{1 - (b/a)\sqrt{z/a}}\right)^{1/2}. \quad (2.8)$$

The values of ξ_1, and ξ_2 obtained from Eq. (2.8) differ from the true values by less than 5% for $0 \le z \le 3.2$. It should be noted that the primary spectrum is $F(E)\,dE = B\,dE/E^{\gamma}$. The number of showers having between n and n + dn particles at the observation level is

$$N_s(n,\ x)\, dn = \frac{C\, dn}{n^{\gamma - 1 - 1/L_a}} e^{-x/L_a} \left[\int_0^{\infty} \varphi_1(z)\, dz + \int_0^{z_{max}} \varphi_2(z)\, dz \right], \quad (2.9)$$

where

$$\varphi_1(z) = \frac{\exp\{\xi_1/L_a - z(\gamma - 1 - 1/L_a)\}}{-a\xi_1(2 - 3b\xi_1/a)};$$

$$\varphi_2(z) = \frac{\exp\{\xi_2/L_a - z(\gamma - 1 - 1/L_a)\}}{a\xi_2(2 - 3b\xi_2/a)};$$

$$z_{max} = \ln(E_{max}/E_{min}) = z_{max}(n,\ x);$$

$$C = (\alpha B/L_i) A^{\gamma - 1 - 1/L_a} \beta^{-1/L_a}.$$

In the case of a nuclear cascade [scheme (b)] the function N(E, t) has been determined from curves given by Sarycheva,[7] calculated under the assumption that the primary interaction and all secondary interactions of the nuclear-active particles correspond to the Fermi-Landau[6] theory. In that case, too, the function N(E, t) can be represented in a form analogous to Eq. (2.7):

$$N(E,\ t) = AE \exp\{-a\xi^2 + b\xi^3 - c\xi^4\}$$

($a = 3.9 \times 10^{-2}$, $b = 2.8 \times 10^{-3}$ and $c = 8 \times 10^{-5}$). In this scheme, $A = 10^{-9}\,ev^{-1}$, and the coefficient β which determines $t_{max} = m(E/\beta)$ does not represent the critical energy, and is equal to 7.6×10^9 ev.

Since $z_{max} = z_{max}(n, x)$, then, as it can be seen from Eq. (2.9),

$$N_s(n,\ x)\, dn = \frac{C\, dn}{n^{\gamma - 1 - 1/L_a}} e^{-x/L_a} f(n,\ x). \quad (2.10)$$

Values of the function f(n, x) for the two schemes (a) and (b) for $\gamma = 2.7$ are given in Table I.

In calculation of the altitude dependence of the number of EAS one can use the expression (2.10) for the differential size spectrum at various observation levels. This dependence is shown for the electron-photon cascade [scheme (a)] in Fig. 2 and for the electron-nuclear cascade [scheme (b)] in Fig. 3. The x axis represents the atmospheric depth in t units, and the y axis represents the

TABLE I

Observation level g/cm²	Electron-nuclear cascade			Electron-photon cascade		
	$n = 10^4$	$n = 10^5$	$n = 10^6$	$n = 10^4$	$n = 10^5$	$n = 10^6$
640	15.5	13.4	10.1	15.2	12.1	8.8
815	19.1	17.8	16.0	22.2	18.2	14.1
1000	20.6	19.7	18.7	25.3	21.9	18.7

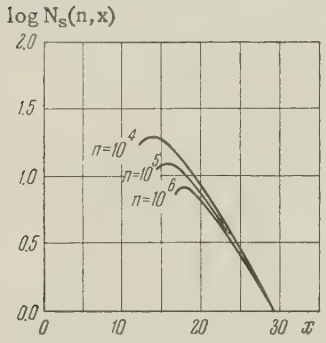

FIG. 2. Dependence of the number of showers $N_s(n, x)$ with a given number of particles n on the atmospheric depth x (in t units). Calculated according to scheme (a).

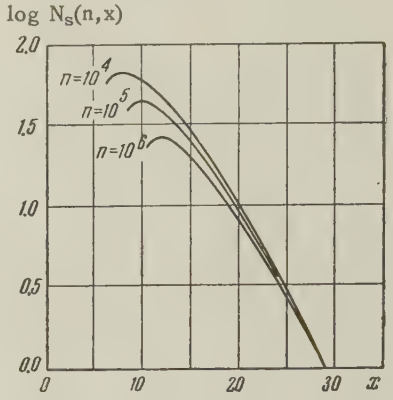

FIG. 3. Dependence of the number of showers $N_s(n, x)$ with a given number of particles n on the atmospheric depth x (in t units). Calculated according to scheme (b).

relative intensity of EAS with a given number of particles.

Information on the variation of the number of showers of given n with the atmospheric depth, for depths greater than 1000 g/cm², can be obtained from the zenith-angle dependence of showers at sea-level. Experimental data of Bassi et al.[8] and results of calculations of the zenith angle distribution of showers at sea-level for scheme a are given in Fig. 4.

In the altitude interval from mountain elevations to sea-level, the dependence of the number of EAS on x, expressed in g/cm², can be written in the form

$$N_s(n, x) = N_s(n, 1000)\, e^{\mu (1000 - x)}. \qquad (2.11)$$

Values of $1/\mu$ for altitudes from 640 to 1000 g/cm² are given in Table II for the cases of electron-photon and electron-nuclear cascades. Let us mention that the calculated values of the shower absorption coefficient do not contradict the experimental value $1/\mu = 130$ to 150 g/cm² for showers with $n = 10^4$ to 10^5.

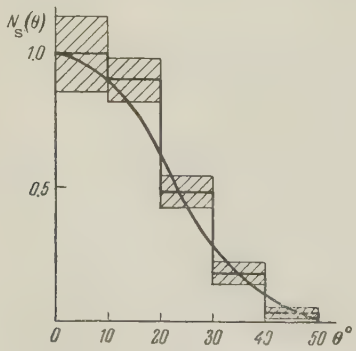

FIG. 4. Zenith angle dependence of the number of EAS $N_s(\theta)$. The curve is calculated according to the scheme a. The histogram represents experimental data.[8]

It should be noted that the fluctuation mechanism of development of EAS yields, for showers of a given n, an absorption mean free path much larger than the absorption mean free path of the shower-producing primaries. It follows that at a depth of 700 to 1000 g/cm², no equilibrium is reached yet between the electronic component and the nuclear-active particles.

For a given x and a small region of n, we can represent the differential size spectrum by a power law

$$N_s(n, x)\, dn = k dn / n^{\varkappa + 1}. \qquad (2.12)$$

comparing the right hand sides of Eqs. (2.10) and (2.12) we obtain

$$\varkappa + 1 = \gamma - 1/L_a - \partial \ln f(n, x)/\partial \ln n. \qquad (2.13)$$

Values of $\kappa + 1$, calculated according to Eq. (2.13)

TABLE II

n	1/μ, g/cm²	
	Electron-nuclear cascade	Electron-photon cascade
10^4	131	143
10^5	137	150
10^6	150	157

TABLE III

Observation level g/cm²	$\varkappa + 1$					
	Electron-nuclear cascade			Electro-photon cascade		
	$n = 10^4$	$n = 10^5$	$n = 10^6$	$n = 10^4$	$n = 10^5$	$n = 10^6$
640	2.47	2.49	2.52	2.58	2.61	2.64
1000	2.43	2.44	2.45	2.46	2.47	2.48

for $\gamma = 2.70$ for two observation levels ($x = 640$ g/cm² and $x = 1000$ g/cm²), are given in Table III.

Table III shows that the fact that κ is independent of the altitude of observation level cannot serve as an argument for the decisive role of the nuclear-active particles in the development of showers in the depth of the atmosphere.

3. BAROMETRIC EFFECT OF EXTENSIVE AIR SHOWERS

If fluctuations of the energy lost by the primary particle in interaction with air atoms represent the main factor in the development of EAS, then the value of the barometric coefficient for showers with a given n is determined, essentially, by the absorption mean free path of ultra-high-energy particles.

In fact, the barometric coefficient b is defined as [we make use of Eq. (2.10)]

$$b = -\partial N_s(n, x)/\partial x = 1/L_a - \partial \ln f(n, x)/\partial x. \quad (3.1)$$

TABLE IV

Electron-nuclear cascade			Electron-photon cascade		
$n = 10^4$	$n = 10^5$	$n = 10^6$	$n = 10^4$	$n = 10^5$	$n = 10^6$
0.016	0.020	0.030	0.026	0.037	0.056

Values of $\partial \ln f(n, x)/\partial x$ at sea-level for showers with various n are given in Table IV for both development schemes.

Calculations show that the increase in γ with n causes a slow decrease of $\partial \ln f(n, x)/\partial x$ which contributes only about 10% to the barometric coefficient.

Experimental data[9] indicate that the barometric coefficient increases with n. It follows from Eq. (3.1) that the increase in b is due, mainly, to the

TABLE V

Observation level g/cm²	$\bar{E}(n, x)$, ev					
	Electron-nuclear cascade			Electron-photon cascade		
	$n = 10^4$	$n = 10^5$	$n = 10^6$	$n = 10^4$	$n = 10^5$	$n = 10^6$
640	$1.3 \cdot 10^{13}$	$1.2 \cdot 10^{14}$	$1.2 \cdot 10^{15}$	$4.2 \cdot 10^{13}$	$3.4 \cdot 10^{14}$	$2.5 \cdot 10^{15}$
1000	$3.9 \cdot 10^{13}$	$2.7 \cdot 10^{14}$	$2.2 \cdot 10^{15}$	$1.2 \cdot 10^{14}$	$9.2 \cdot 10^{14}$	$7.2 \cdot 10^{15}$

FIG. 5. Energy distribution of primary particles producing showers with 10^5 particles at the atmospheric depth $x = 640$ g/cm². Solid line calculated according to scheme (a), the dashed according to scheme (b)

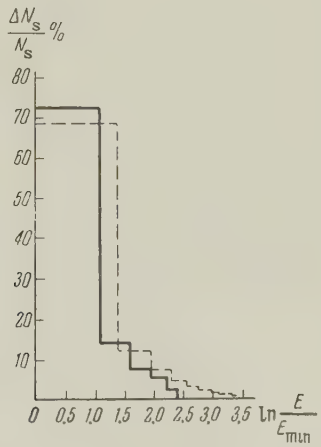

FIG. 6. Energy distribution of primary particles producing showers with 10^5 particles at the atmospheric depth $x = 1000$ g/cm². Solid line – scheme (a), dashed – scheme b.

decrease in L_a. The absorption mean free path L_a decreases, therefore monotonously with increasing energy of the primary particle. The decrease may be due either to an increase in the value of the interaction cross-section, or to increased inelasticity, or to both effects.

4. ENERGY SPECTRUM OF PRIMARY PARTICLES PRODUCING EAS WITH A GIVEN NUMBER OF PARTICLES

The number of EAS containing between n and n + dn particles at the observation level and produced by primary particles with energies between E_1 and E_2 is given by the expression

$$\Delta N_s(n, x)\, dn = \frac{C dn}{n^{\gamma-1} L_a} e^{-x/L_a} \int_{z_1}^{z_2} [\varphi_1(z) + \varphi_2(z)]\, dz,$$
$$z_{1,2} = \ln(E_{1,2}/E_{\min}). \qquad (4.1)$$

Since the total number of showers with n to n + dn particles at the observation level is given by Eq. (2.9), then the relative number of cases when a shower with a given n is produced by a nuclear-active particle with energy between E_1 and E_2 will be

$$\frac{\Delta N_s(n, x)}{N_s(n, x)} = \int_{z_1}^{z_2} [\varphi_1(z) + \varphi_2(z)]\, dz \Big/ \left[\int_0^{\infty} \varphi_1(z)\, dz + \int_0^{z_{\max}} \varphi_2(z)\, dz \right]. \qquad (4.2)$$

Using Eq. (4.2), one can compute the energy spectrum of particles producing showers containing n particles at a given level.

Energy distributions of the primaries producing showers, containing 10^5 particles at two observation levels, are shown in Figs. 5 and 6 for electron-photon (solid line) and electron-nuclear (dashed) cascades. The x axis represents the logarithm of the energy of nuclear-active particles in units of E_{min}, and the y axis the relative number of showers produced by particles of the corresponding energy interval.

The mean energy of primary particles that produce showers containing n to n + dn particles at the observation level is given by

$$\frac{\bar{E}(n, x)}{E_{\min}} = \left\{ \int_0^{\infty} e^z \varphi_1(z)\, dz + \int_0^{z_{\max}} e^z \varphi_2(z)\, dz \right\} \Big/ \left\{ \int_0^{\infty} \varphi_1(z)\, dz + \int_0^{z_{\max}} \varphi_2(z)\, dz \right\}. \qquad (4.3)$$

The values of $\bar{E}(n, x)$ calculated according to Eq. (4.3) are given in Table V.

It can be seen from Figs. 5 and 6 that if the fluctuation mechanism of development of EAS takes place in the reality, then EAS observed at sea-level with $n = 10^4$ to 10^6 are produced by primaries of a wide energy range. In connection with this, a study of the intensity distribution of the Cerenkov radiation of EAS with a given number of particles n can give information about the role of energy-loss fluctuations in the formation of EAS,[10] and a measurement of the absolute pulse size may indicate which of the considered development schemes (a) and (b) is closer to reality.

5. LATERAL DISTRIBUTION OF PARTICLES IN EAS

If we assume that EAS are produced by a single high-energy electron (photon) [scheme (a)] then the lateral distribution of shower particles at the observation level will be determined in a unique way by the value of the cascade parameter s. In scheme (a), the mean value $\bar{s}$ can be calculated as a function of n and x.

TABLE VI

Observation level g /cm²	$\bar{s}$	
	$n = 10^4$	$n = 10^5$
640	1.11	1.04
1000	1.27	1.14

It is evident that, within the framework of the development scheme used, a shower produced by a particle with energy E, at an atmospheric depth x − t, is characterized at the observation level by the value s = s(E, t). The function s(E, t) is approximated by an empirical formula which is in a good agreement (within a few percent), for primary energies of $\sim 10^{13}$ to 10^{16} ev and for $0.6 \leq s \leq 1.4$, with the values of s obtained from cascade curves:

$$s = 1 + \frac{0.63}{t_{\max}} \xi - 10^{-(t_{\max}/13.7+2)} \xi^2, \quad \xi = t - t_{\max},$$
$$\text{and } t_{\max} = \ln(E/\beta). \qquad (5.1)$$

The mean parameter $\bar{s}(n, x)$, which characterizes showers containing n to n + dn particles at the observation level x, has been calculated using Eq. (5.1). The calculations were carried out for sea-level (x = 1000 g/cm²) and mountain altitudes (x = 640 g/cm²), for showers consisting of 10^4 to 10^5 particles. The results are given in Table VI. It can be seen that in the presence of large fluctuations in the primary interaction process, even a purely electromagnetic development of the shower, without participation of nuclear-active particles, can cause showers with a given number of particles, observed at two different altitudes, to have a prac-

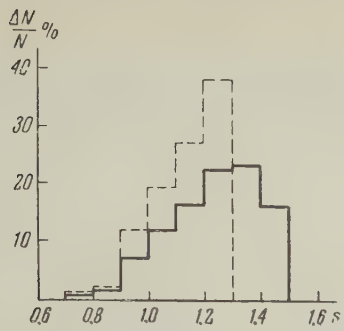

FIG. 7. Age distribution of EAS with 10^4 particles, solid line – at observation level $x = 1000$ g/cm², dashed – at $x = 640$ g/cm².

tically identical "age," i.e. the same mean $\bar{s}$.

The distribution of showers with 10^4 particles is given in Fig. 7 for two observation levels, $x = 640$ g/cm² (dashed line) and $x = 1000$ g/cm² (solid line). The x axis represents the age parameter s, and the y axis the relative number of showers with s in the corresponding interval.

Experimental study of the age distribution of EAS with given n might also throw some light upon the role of fluctuations in the development of EAS.

6. CONCLUSION

As can be seen from the above calculations, in the presence of large fluctuations in the energy loss of ultra-high-energy particles interacting with atomic nuclei, such parameters of EAS as the absorption mean free path $1/\mu$, the mean age $\bar{s}$, and the shower spectrum exponent κ are practically independent of the fact whether high-energy nuclear-active particles are present in the EAS, or whether the shower develops as an electron-photon cascade without a marked "feeding" of the shower in the depth of the atmosphere by nuclear-active particles.

We think therefore that it is highly probable that interactions of primary particles corresponding to large energy losses, and which possibly represent the main contribution to EAS production, may belong to several types. Moreover, properties of the interactions may vary within wide limits, from the case of energy transfer to one or several γ-quanta to the case of production of a large number of secondary particles with a large degree of degradation of the primary-particle energy.

We should like to stress again that the purpose of the present calculation is not to choose the most probable mode of development of EAS (according to our view, the present experimental data are not sufficient for such a decision) but to show that such experimental characteristics as the shower absorption coefficient and the independence of $\bar{s}$ and κ from the altitude of the observation level are by far insufficient to conclude about the large role of nuclear-active particles in the development of showers in the depth of the atmosphere and, even less so, to determine more precisely the number of these particles determining this development, as it has been done by several authors.[11-12] It seems to us that so long as the role of energy loss fluctuations in the production of EAS is not explained, conclusions concerning the mechanism of interactions of ultra-high-energy particles based upon such average characteristics of EAS as $1/\mu$, $\bar{s}$, and κ must be regarded as tentative.

[1] Dobrotin, Zatsepin, Rozental', Sarycheva, Khristiansen, and Eidus, Usp. Fiz. Nauk **49**, 185 (1953).

[2] O. I. Dovzhenko and S. I. Nikol'skii, Dokl. Akad. Nauk SSSR **102**, 241 (1955).

[3] V. V. Guzhavin and G. T. Zatsepin, J. Exptl. Theoret. Phys. (U.S.S.R.) **32**, 365 (1957), Soviet Phys. JETP **5**, 312 (1957).

[4] Grigorov, Shestoperov, Sobiniakov, and Podgurskaia, J. Exptl. Theoret. Phys. (U.S.S.R.) **33**, 1099 (1957), Soviet Phys. JETP **6**, 848 (1958).

[5] K. P. Ryzhkova and L. I. Sarycheva, J. Exptl. Theoret. Phys. (U.S.S.R.) **28**, 618 (1955), Soviet Phys. JETP **1**, 572 (1955).

[6] L. D. Landau, Izv. Akad. Nauk SSSR, Ser. Fiz. **17**, 51 (1953).

[7] L. I. Sarycheva, Dissertation, Phys. Inst. Acad. Sci., 1953.

[8] Bassi, Clark, and Rossi, Phys. Rev. **92**, 441 (1953).

[9] Cranshaw, Galbraith, Porter, de Beer, and Hillas, Phys. Rev. (preprint, Varenna 21 – 26 June 1957).

[10] A. E. Chudakov, Paper presented at the Varenna Conference on Cosmic Rays, 1957. Nuovo cimento (in press).

[11] G. T. Zatsepin, Oxford Conference on Extensive Air Showers, p. 8, Oxford, 1956.

[12] Dobrovol'skii, Nikol'skii, Tukish, and Iakovlev, J. Exptl. Theoret. Phys. (U.S.S.R.) **31**, 939 (1956), Soviet Phys. JETP **4**, 799 (1958).

Translated by H. Kasha
305

THEORY OF THE DEVELOPMENT OF A SPARK CHANNEL

S. I. BRAGINSKII

Submitted to JETP editor January 2, 1958

J. Exptl. Theoret. Phys. (U.S.S.R.) **34**, 1548-1557 (June, 1958)

The principal processes taking place in a spark channel at moderate currents are examined. Solutions are obtained for the motion of the gas outside the channel. A new type of hydrodynamic jump is considered — a strong discontinuity with external supply of heat. Certain solutions are found which describe the state of the gas inside the channel, and expressions are obtained for the characteristic parameters of the channel (radius, temperature, etc.).

1. INTRODUCTION

In the present paper we consider the development of a spark channel under comparatively high pressures and moderate currents. This process has been studied in detail by Mandel' shtam and his coworkers.[1-6] In reference 1, on the basis of experimental results, the idea was expressed that the rapid development of a spark channel is accounted for by the excitation of a shock wave. In subsequent papers, this phenomenon was studied in detail, both experimentally and theoretically. The theory of the development process was given by Drabkina; the results of her calculations are in good agreement with experiment. However, the theory advanced by Drabkina is not complete; the electrical conductivity and the temperature in the channel are not computed in this theory, so that it does not permit us to calculate the parameters of the spark directly, by starting from the law of current growth. Rather, it only relates the velocity of its growth with the energy released in the channel; this latter energy must be determined experimentally.

In the present research, an attempt is made to consider a specific mechanism of the discharge and to construct a step-by-step theory of the development of the channel, with account of the electrical conductivity and the thermal conductivity of the ionized gas in the channel.

In accord with the results of references 1 to 6, the picture of the development of the spark channel can be represented in the following form. A comparatively narrow current-carrying channel is formed in the gas, with high temperature and ionization. Joule heat is released in this channel, which then leads to an increase in the pressure and a thickening of the channel. The thickened channel acts like a piston on the remaining gas and, since the expansion takes place with supersonic speed, it produces a shock in the gas; this shock is propagated in front of the original "piston." The temperature in the vicinity of the shock (between the wave front and the "piston") is much higher than in the gas at rest, and the temperature in the channel itself is still many times higher than in the shock wave. Consequently, the density of the gas in the channel is very low, and the major part of the mass of the moving gas is displaced from it, which also makes it possible to consider the boundary of the channel as a piston.

The very fact of the formation of the narrow channel can evidently be understood by starting from the following considerations. After the gas sparks over and becomes conducting, Joule heat is released at points of flow. As is well known, the electrical conductivity of the gas increases rapidly with temperature. Thus, at a high degree of ionization, when the collisions of electrons with ions are important, the electrical conductivity is proportional to $T^{3/2}$, while at low ionization this dependence is even stronger, (because of the fact that the degree of ionization increases rapidly with temperature). As a consequence, a tendency appears toward a concentration of current in a comparatively narrow channel, so that at the places where the temperature is higher, the conductivity is also great, a large current exists there, and a large amount of heat is liberated, which leads to more heating, etc. The physical processes which determine the breadth of the channel and limit the concentration of current are the leakage of heat from the channel and the broadening of the heated region under the action of the pressure.

With some indefiniteness, we can consider as the channel the region from the axis to the point where the temperature becomes so low that ionization begins to fall off appreciably. In the channel, we can neglect the inertia of the gas, but it is necessary to take into consideration the release and transfer of heat. In the shock wave region,

the inertia must be considered, but we can neglect the electrical and thermal conductivities. These two regions as separated by a transition layer, the "shell" of the channel. Heating and ionization of the gas that enters the channel take place in the shell.

2. FUNDAMENTAL EQUATIONS

The fundamental equations of the problem under consideration are the equation of continuity, the equation of motion, and the equation of energy transfer:

$$\frac{\partial \rho}{\partial t} + v\frac{\partial \rho}{\partial r} + \rho\frac{\partial (rv)}{r\partial r} = 0; \tag{2.1a}$$

$$\rho\left(\frac{\partial v}{\partial t} + v\frac{\partial v}{\partial r}\right) + \frac{\partial p}{\partial r} = 0; \tag{2.1b}$$

$$\frac{\partial}{\partial t}\left(\rho\varepsilon + \frac{\rho v^2}{2}\right) + \frac{1}{r}\frac{\partial}{\partial r}\left\{r\rho v\left(\varepsilon + \frac{p}{\rho} + \frac{v^2}{2}\right)\right\} + \frac{\partial (rq)}{r\partial r} = jE. \tag{2.1c}$$

Here ρ is the density, v the velocity, p the pressure, ϵ the internal energy per unit mass of gas, q the heat flow, f the current density, and E the electric field.

We shall write the equation of state in the form

$$p = (n_e + n_i)T = (Z+1)\rho T/m_a, \tag{2.2}$$

where m_a is the average atomic mass, n_e and n_i the number of electrons and ions per unit volume, Z the average ionic charge, and $n_e = An_i$. The temperature is expressed in energy units.

We shall assume that the ionization in the channel can be computed by Sach's formula. This problem is considered in detail in reference 6.

The internal energy of the gas in the channel is expressed in the form

$$\varepsilon = \frac{3}{2}\frac{p}{\rho} + \frac{I}{m_a} = \frac{p}{\rho}\left[\frac{3}{2} + \frac{I}{(Z+1)T}\right], \tag{2.3}$$

where I is the total energy of ionization plus the energy of dissociation, referred to a single atom. It is appropriate to apply Eq. (2.3) in the case of complete ionization, for example, for hydrogen, Z = 1, I = 15.74 ev. For incomplete ionization, the energy of ionization increases with increasing temperature. According to Sach's formula, the ratio I/T depends rather weakly on the density and temperature; therefore, for a not too wide an interval of change of these parameters, the expression in the square brackets can be considered to be approximately constant. In this case it is more suitable to take the expression for the energy in the form

$$\varepsilon = \frac{1}{\gamma - 1}\frac{p}{\rho}, \tag{2.3a}$$

as was done by Drabkina.[2] Here γ is the effective ratio of specific heats. The value of γ is somewhat different for the gas in the channel and in the shock wave. According to reference 2, $\gamma = 1.25$ for hydrogen and 1.22 for air.

Transfer coefficients. The electrical conductivity σ and the thermal conductivity κ differ strongly for the ionized gas (see, for example, reference 7):

$$\sigma = \sigma_1(Z)T^{3/2} = 3\sigma'(Z)T^{3/2}/4e^2\sqrt{2\pi m}\lambda; \tag{2.4}$$

$$\varkappa = \varkappa_1(Z)T^{5/2}. \tag{2.5}$$

Here e and m are the charge and mass of the electron, $\lambda = \ln(3T^{3/2}/ze^3\sqrt{4\pi n_e})$, and $\sigma'(Z)$ is a dimensionless coefficient. For Z = 1, 2, 3, and 4 we have, respectively, $\sigma' = 1.95$, 1.135, 0.840, and 0.667. The value of $\kappa e^2/\sigma T$, according to the Wiedemann-Franz law, is of the order of unity. For Z = 1, 2, 3, and 4 this combination is equal to 1.62, 2.16, 2.40, and 2.60 respectively. The "Coulomb logarithm" λ is only slightly sensitive to the values of the quantities entering into it. For $\lambda = 5$, for example, we have $\sigma_1(1) = 3.4 \times 10^{-13}$ $\sec^{-1}\,ev^{-3/2}$, and $\kappa_1(1) = 3.9 \times 10^{20}\,cm^{-1}\sec^{-1}ev^{-5/2}$.

We note that the electrical conductivity of air increases with the temperature more slowly than $T^{3/2}$, because of the increase of Z as a consequence of ionization. At a temperature on the order of several electron volts, it changes approximately as $T^{1/2}$ and is equal to $2 \times 10^{14}\,\sec^{-1}$ for $T \approx 3$ to 4 ev.

Radiation. A simple estimate, taking experimental data[3-5] into account, shows that if the radiation from the channel were black body radiation, it would carry several tenfold more energy than is actually released in the channel. In fact, the radiation is nonequilibrium and flows freely from the channel. For open radiation, div $q = Q'_R$, where Q'_R is the energy radiated per unit volume. The fundamental mechanism of open radiation is the retardation radiation

$$Q'_{ret} = 1.5\cdot 10^{-25} n_i n_e Z^2 T_{ev}^{1/2}\ (\text{erg-cm}^{-3}\text{sec}^{-1}) \tag{2.6}$$

(see reference 8) and recombination radiation. For hydrogenlike atoms, the latter can be computed from the approximate formula

$$Q'_{rec} = 5\cdot 10^{-24} n_i n_e Z^4 T_{ev}^{-1/2}\ (\text{erg-cm}^{-3}\text{sec}^{-1}). \tag{2.7}$$

Equation (2.7) was obtained by V. I. Kogan, using the cross section of recombination at the different levels given in reference 9.

For partially-ionized atoms of the different elements, which cannot be considered hydrogenlike, one must expect that the radiation of Z charged ions is greater than calculated by the "hydrogenlike" formulas, because of the incomplete screen-

ing. This circumstance can be taken into consideration if we use the effective change $Z_{eff} = Z + \Delta$ in place of the actual charge of the ion Z. According to Unsöld,[10] we can take as a sort of mean value (as a rough approximation, with great uncertainty) $\Delta = 1.5$.

Radiation in the discrete spectrum as a result of resonance absorption is forbidden for many lines and is close to the equilibrium (Planckian) in intensity. The presence of such radiation increases the thermal conductivity of the plasma. In the present research, however, we shall not consider this radiation thermal conductivity, since its calculation is a complicated independent problem which requires a detailed knowledge of the spectrum and the line widths.

Skin effect and the magnetic field. The penetration depth δ of the field after a time t can be estimated by the formula $\delta^2 \sim c^2 t/2\pi\sigma$. According to Abramson and Gegechkori,[3,4] $\sigma = 2 \times 10^{14}\,\text{sec}^{-1}$. At the instant $t = 10^{-6}$ sec, the radius of the channel becomes $a \sim 1$ mm, which yields $\delta^2/a^2 \sim 10^2$. Thus we can consider the electric field to be constant over the cross section and use the expression $j = \sigma E$ for the current density.

We now estimate the role of magnetic forces, for which we compare the magnetic pressure $H^2/8\pi$ with the gas-kinetic pressure. The latter has the same order of magnitude as the kinetic energy per unit volume. If an appreciable amount of the liberated Joule heat remains in the form of the kinetic energy of particles in the channel, then the pressure can be estimated as

$$p \sim \frac{1}{\pi a^2}\frac{J^2 t}{\pi a^2 \sigma} \sim \frac{H^2}{8\pi}\frac{\delta^2}{a^2}. \tag{2.8}$$

It is then evident that we can regard the magnetic forces as inconsequential when we can neglect the skin effect.

The magnetic field begins to have a strong effect on the kinetics of the electrons (on the electrical conductivity and especially on the thermal conductivity) when the frequency of their rotation in the magnetic field $\omega = eH/mc$ is comparable with the collision frequency $1/\tau$. For typical values of the magnetic field and density in the channel, Mandel'shtam and his coworkers obtained in their experiments $\omega\tau \sim 0.1$.

We shall neglect both the magnetic forces and the effect of the magnetic field on the kinetics of the electrons.

The shell of the channel. Ionization jump. Since we are dealing with entirely different simplications in the channel region and the shock-wave region, it is necessary to establish the condition of joining the solutions on the boundary between the two regions. Physically, the joining takes place in the transition region, in the shell of the channel, where a transition occurs from a strongly ionized gas to a weakly ionized one, and where an intense ionization process is taking place. We shall not investigate the behavior of the quantities in the transition layer, but shall consider them (approximately) as discontinuities, as is usually done for discontinuities in hydrodynamics. We shall assume here that the transition region is not very wide.

We shall denote by $\dot{a}$ the velocity of motion of the discontinuity, and use the index 1 for quantities on the outside and the index 2 for quantities on the inside (the channel side). The laws of conservation of mass and momentum take the form

$$\rho_1 (v_1 - \dot{a}) = \rho_2 (v_2 - \dot{a}) \equiv g; \tag{2.9a}$$

$$p_1 + \rho_1 (v_1 - \dot{a})^2 = p_2 + \rho_2 (v_2 - \dot{a})^2. \tag{2.9b}$$

The density in the channel is very low, $\rho_2 \ll \rho_1$; therefore, the first condition yields $v_1 = \dot{a}$. The pressure jump is expressed in the form $\Delta p = p_1 - p_2 = g^2 (\rho_2^{-1} - \rho_1^{-1})$. Considering $\rho_2 \ll \rho_1$, $g \sim \rho_2 \dot{a}$, $p \sim \rho_1 a^2$, we find that the pressure jump is small:

$$\Delta p/p \sim \rho_2/\rho_1 \ll 1. \tag{2.10}$$

We shall assume that the pressure does not undergo a jump. Then, neglecting the heat flow on the side of the cold dense gas, we obtain the condition

$$g (\varepsilon_2 + p/\rho_2) + q_2 = 0. \tag{2.11}$$

from the conservation of energy.

3. QUASI-SELF-SIMILAR SOLUTION

As is well known (see reference 11), the motion described by two dimensional parameters is self-similar. In our case, the motion as a whole depends on a large number of parameters; however, we can find an approximate solution which is self-similar separately in the region of discharge and in the region of the shock wave. Curves representing the dependence of different quantities on the radius remain, in each of the regions, the same with passage of time, but their scales change in each region according to its own law.

Shock wave. The motion of the gas outside the channel is completely determined if the time dependence of the radius of the channel is given. The boundary of this channel plays the role of a piston which displaces the gas. If this dependence has a simple power form

$$a(t) = At^h \tag{3.1}$$

and if the pressure in the wave is so large that the

pressure of the undisturbed gas can be neglected, then the motion in the region of the shock is determined by the two dimensional parameters A, ρ_0 and is self-similar.

In place of the variables t, r in Eqs. (2.1), we introduce the variables t, $x = r/a_c(t)$, where a_c is the radius of the wave front. We introduce also the new dependent variables:

$$\rho'(x) = \rho/\rho_0, \qquad v'(x) = v/\dot{a}_c,$$
$$p'(x) = p/\rho_0\dot{a}_c^2. \tag{3.2}$$

Neglecting the heat released and transferred, we can rewrite Eq. (2.1) in the form

$$(v'-x)\frac{d\rho'}{dx} + \rho'\frac{dxv'}{xdx} = 0;$$
$$\left(1-\frac{1}{k}\right)v' + (v'-x)\frac{dv'}{dx} + \frac{1}{\rho'}\frac{dp'}{dx} = 0; \tag{3.3}$$
$$2\left(1-\frac{1}{k}\right)p' + (v'-x)\frac{dp'}{dx} + \gamma p'\frac{dxv'}{xdx} = 0.$$

The boundary conditions in a strong shock wave for $x = 1$ have the form

$$\rho' = (\gamma+1)(\gamma-1)^{-1}, \quad v' = 2(\gamma-1)^{-1},$$
$$p' = 2(\gamma-1)^{-1}. \tag{3.4}$$

Equations (3.3) with boundary conditions (3.4) were integrated numerically on an electronic computing machine for the values $k = 1, \frac{3}{4}, \frac{3}{5}$ and $\gamma = \frac{5}{3}, \frac{7}{5}, \frac{9}{7}$. The results of the integration are shown in Fig. 1. The position of the piston is determined by the point where $v' = x$. The pressure at the piston p_k can be obtained from the velocity of the piston

$$p_k = K_p\rho_0\dot{a}^2, \tag{3.5}$$

where the coefficient of resistance K_p will be considered as approximately equal to 0.9 (see Fig. 1, $K_p = p'(s)\,a^2/a_c^2$).

The Channel. Let us consider the case in which we can neglect radiation. Then

$$q = -\varkappa dT/dr. \tag{3.6}$$

We shall assume that the temperature in the channel is appreciably higher than is necessary for complete ionization. Then, on the boundary of the channel, where the ionization is beginning to fall off, the temperature will be much less than at the center, and we can set (approximately) $T = 0$ for $r = a$.

We transform from the variables t, r to the variables t, $s = r^2/a^2(t)$, and also introduce the new dependent variables

$$\vartheta(s) = \frac{T}{T_0}, \quad u = \frac{1}{\vartheta}\frac{r}{2a}\left(\frac{r}{a} - \frac{v}{\dot{a}}\right),$$
$$y = \frac{r}{2a}\left\{\frac{q}{p\dot{a}} + \frac{5}{2}\left(\frac{v}{a} - \frac{r}{a}\right)\right\}. \tag{3.7}$$

Here T_0 is the temperature on the axis. We shall regard the pressure as constant over the cross section of the channel. Equations (2.1a), (2.1c), (3.6) take the form

$$\frac{du}{ds} = \frac{1-(1/2k)}{\vartheta}, \qquad \frac{dy}{ds} = \frac{\alpha\beta}{4}\vartheta^{3/2} - \left(2-\frac{3}{4k}\right),$$
$$\frac{d\vartheta}{ds} = -\frac{y + {}^5/_2\, u\vartheta}{\alpha s\vartheta^{5/2}}, \tag{3.8}$$

where

$$\alpha = \varkappa(T_0)\,T_0/p\dot{a}a, \tag{3.9}$$
$$\beta = \sigma(T_0)\,E^2a^2/\varkappa(T_0)\,T_0. \tag{3.10}$$

The condition (2.11) becomes $y(1)/u(1) = I/(Z+1)T_0$. It is then evident that for self-similarity the temperature ought not to depend on the time. The same applies to the quantities α, β. Making use of (3.5), (3.10), we obtain the result that $a \sim t^{3/4}$, $E \sim t^{-3/4}$. The electric field is connected with the current by the relation

$$J = \langle\sigma\rangle\pi a^2E, \tag{3.11}$$

where the angular brackets denote an averaging over the cross section of the channel. Thus, the self-similar mode is obtained only in the case of a definite law of current increase: $J \sim t^{3/4}$. Actually, the current changes sinusoidally, but for the first quarter period of the sine wave we can use approximately the results obtained from the self-similar mode.

Equations (3.8) have been integrated numerically for $k = \frac{3}{4}$ with the boundary conditions

$$\text{for } s = 0 \quad u = 0, \quad y = 0, \quad \vartheta = 1,$$
$$\text{for } s = 1 \quad y/u = I/(Z+1)T_0, \quad \vartheta = 0\,(\vartheta \ll 1).$$

In the actual integration, the parameter α was

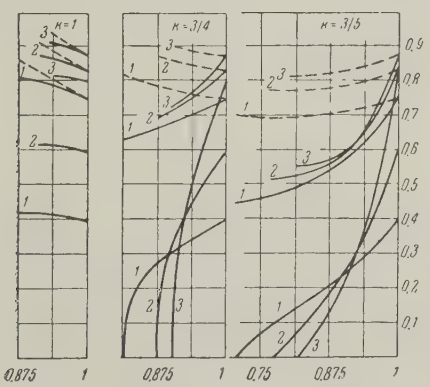

FIG. 1. Distribution of the velocity v′ (dashed lines), pressure p′ and density ρ′ behind the front of the shock wave as a function of $x = r/a_c$ for various values of k. The curves 1 correspond to $\gamma = 5/3$, 2 to $\gamma = 7/5$, and 3 to $\gamma = 9/7$.

assigned and β was so chosen that the quantity $\vartheta(1)$ was as small as possible. The exact value of $\vartheta(1)$ is rather unimportant, since the curves hardly depend on it over the major part of the interval. The characteristic curves are shown in

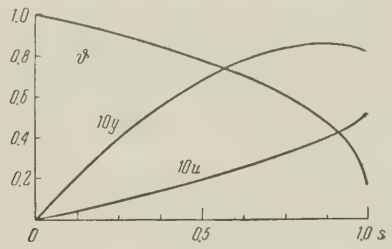

FIG. 2

Fig. 2. The values of $I/(Z+1)T_0 = 5.95$, 2.0, 1.56, 0.9, and 0.25 correspond to $\alpha = 16$, 8, 6.90, 5.33, and 4 and $\beta = 1.48$, 1.56, 1.60, 1.68, and 1.80. The coefficients $K_\sigma = \langle T^{3/2}/T^{3/2}\rangle$ and $K_\rho = \langle T_0/T\rangle$ change in this case from 0.661 to 0.632 and from 1.49 to 1.69, respectively. We shall henceforth take approximately $\beta = 1.6$, $K_\sigma = 0.655$, and $K_\rho = 1.55$. Knowing the dependence of α and β on the temperature, it is possible to find all the parameters of the channel. However, it is more suitable to use Eq. (4.4), in which we must replace σ by $\langle\sigma\rangle = \sigma_1\langle T^{3/2}\rangle$. In accord with (2.3), it is necessary to replace in Eq. (4.4′) $(\gamma-1)^{-1}$ by $3/2 + K_\rho I/(Z+1)T_0$. For the temperatures of interest, the single-term approximation $\xi \approx 3\sqrt{I/(1+Z)T_0}$ is valid with sufficient accuracy. Using Eqs. (3.10), (3.11), (4.4) and the values of the coefficients that have been obtained, we get the radius of the channel, the temperature, and the electric field. For hydrogen, we have:

$$a = 1.53\rho_0^{-5/28}(Jt^{-3/4})^{2/7}t^{3/4}; \qquad (3.12)$$

$$T_k = 3.5\rho_0^{1/14}(Jt^{-3/4})^{2/7}; \qquad (3.13)$$

$$E = 50\rho_0^{1/4}t^{-3/4}. \qquad (3.14)$$

For the temperature in the channel, the condition $T_k = (\langle T^{3/2}\rangle)^{2/3}$ is assumed. Here we have expressed T_k in ev, a in mm, E in v/cm, J in kiloamperes, t in μsec, while the density unit is 0.9×10^{-4} g/cm^3. In reference 4, for a 15-kv discharge, a 2 μhy self inductance and a 0.25 μf capacitance, the measured values for the radius of the channel (for hydrogen at atmospheric pressure, $\rho_0 = 1$) were 1.00, 1.55 and 2.60 mm for 0.3, 0.5 and 1.0 μsec, respectively. The corresponding values computed according to (3.12) are 1.00, 1.50, and 2.45. The agreement is rather good. Experimental data for the quantities in (3.13) and (3.14) are unfortunately lacking. The existence of such data would have made it possible to verify Eq. (2.5) for the thermal conductivity of the plasma, since the radiation does not play an important role in the given case.

4. HOMOGENEOUS MODEL OF A CHANNEL WITH A DENSE SHELL

If the removal of heat from the channel is brought about by transparent radiation, while the thermal conductivity can be neglected, then we can demonstrate a simple self-similar solution for the region of the channel: the pressure, temperature and density are constant over the cross section, while the velocity is proportional to the radius. The entire temperature drop is concentrated in the shell. The radiation is absorbed there, and the ionization of the gas entering the channel takes place in that region. If we consider the shell to be thin, we can obtain a set of equations for the basic parameters of the channel. In the general case, use can be made of these equations as a mathematical model describing, however roughly, the basic processes in the channel. In this case we can also take the thermal conductivity into consideration (approximately).

The equations for the energy balance in the channel and the shell have the form

$$\frac{dW}{dt} + p\frac{d\pi a^2}{dt} = Q_J; \qquad (4.1)$$

$$\left(\varepsilon + \frac{p}{\rho}\right)\frac{dM}{dt} = Q_T + Q_R, \qquad (4.2)$$

where M and W are the mass and energy of the gas in the channel. Equation (4.1) is obtained by integration of (2.1c) over the cross section of the channel (including the shell) without any assumption on the form of the distribution of the quantities over the cross section. For the homogeneous model, we set $W = M\epsilon$, $M = \pi a^2\rho$. Equation (4.2) is obtained from (2.11). The expressions for the release of Joule heat Q_J and for the heat loss by radiation Q_R and by thermal conduction Q_T can be written in the form

$$Q_J = J^2/\pi a^2\sigma, \quad Q_R = \pi a^2 Q_R'(p, T),$$
$$Q_T = 1.3\cdot 2\pi\varkappa T. \qquad (4.3)$$

In order of magnitude, $Q_T \sim \kappa(T/a)2\pi a$, while the coefficient in (4.3) is chosen in correspondence with the results of the previous section Eq. (3.10) wherein $T_k = (\langle T^{3/2}\rangle)^{2/3}$ was assumed for the characteristic temperature in the channel. Approximately, it can be obtained from (3.5) for a weak shock, or it can be considered equal to the pressure of the undisturbed gas, when the wave becomes weak and undergoes a transition to the acoustic type.

Making use of (3.5) and (2.3), we can rewrite (4.1) in the form

$$\rho_0 2\pi^2 a^3 \dot{a}^3 \xi = J^2/\sigma, \tag{4.4}$$

$$\xi = K_p\left[1 + (\gamma - 1)^{-1} 2^{-1} \dot{a}^{-2} \frac{d^2a^2}{dt^2}\right] = K_p[1 + (\gamma - 1)^{-1}(2 - k^{-1})]. \tag{4.4'}$$

Here $k = \dot{a}t/a$. Comparing (4.1) and (4.2), we obtain

$$Q_T + Q_R = \eta Q_J, \tag{4.5}$$

where η is a coefficient on the order of unity. If, for example, we can neglect the change in temperature with time, then

$$\eta = \gamma\left[1 + (\gamma - 1)\, 2\, \dot{a}^2 \left(\frac{d^2a^2}{dt^2}\right)^{-1}\right]^{-1}. \tag{4.5'}$$

For a weak shock, when the pressure in the channel can be considered equal to the pressure of the undisturbed gas p_0, we get from (2.3) instead of (4.4)

$$p_0 2\pi^2 a^3 \dot{a}\gamma/(\gamma - 1) = J^2/\sigma. \tag{4.6}$$

Equation (4.5) retains its form, but the coefficient η will be different. For example, if we neglect the change in temperature with time, then we have simply $\eta = 1$ in place of (4.5). Equations (4.4), (4.5), together with (4.3) and (3.5), (3.11) allow us to find all the parameters of the channel.

Let us consider the channel in air. The conductivity $\sigma(T)$ for air in the temperature range of interest to us changes comparatively slowly (see Sec. 3) and, by (2.4), can be taken to be approximately $\sigma = 2 \times 10^{14}\,\text{sec}^{-1}$. This is supported by the experimental data. If, making use of references 3 and 4, we take the electrical conductivity into account, then it is shown that within wide limits of change of the parameters of the discharge, σ does not depart appreciably from this value. Assuming $K_p = 0.9$, $\gamma = 1.2$ and $J \sim t$, we get $\xi = 4.5$. For these values of σ and ξ, we get for the channel radius (from Eq. (4.4)

$$a = 0.93\, \rho_0^{-1/8} J^{1/2} t^{1/8}. \tag{4.7}$$

Here a is in mm, J in kiloamperes, t in μsec, and we take as the density unit the density of the air at atmospheric pressure, $1.29 \times 10^{-3}\,\text{g/cm}^3$.

The experimental values of the radius[4] for a discharge voltage of 15 kv and capacitance $C = 0.15\,\mu\text{f}$, at 0.3, 0.5 and 1.0 μsec, are the following: for a coil inductance of $L = 2\,\mu\text{hy}$ (which corresponds to $\dot{J} = V/L = 7.5 \times 10^9\,\text{amp/sec}$): 0.65, 0.95, and 1.55 mm, respectively; for $L = 12$ ($\dot{J} = 1.25 \times 10^9$), 0.33, 0.50 and 0.80 mm, respectively; for $L = 64$ ($\dot{J} = 2.4 \times 10^8$), 0.18, 0.25 and 0.40 respectively. The corresponding values computed from (4.7) are 0.67, 1.0 and 1.62 (for $L = 2$); 0.35, 0.57 and 0.99 (for $L = 12$), 0.21, 0.32, and 0.58 (for $L = 64$). The agreement is excellent. A certain saturation at larger self inductances and values of the time is explained by the fact that (4.4) does not take the initial pressure into account. If this were done in (4.1), for example, by means of the interpolation $p = K_p\rho_0 a^2 + p_0$, then the agreement with experiment would be improved.

The spark discharge in air has also been investigated experimentally by Norinder and Karsten.[12] The values of the radius computed by (4.7) agree satisfactorily with their experimental data.

The temperature in the channel can be calculated by (4.5) and (4.3). However, this computation is difficult in practice because of the absence of reliable data on the radiation of air. We shall only put down some estimates. The coefficient η is on the order of unity. For the same discharge which was considered previously,[3] at $t = 1\,\mu$sec, the Joule heat (for $L = 2$, 12 and 64 μhy) is $Q_J = 1.7 \times 10^{13}$, 3×10^{12}, $4.2 \times 10^{11}\,\text{erg/cm-sec}$, respectively. For $L = 64$, using (4.5), we obtain $T = 3.7$ ev, while all the heat is transferred by the electronic conductivity; we can neglect radiation ($Q_R \sim 10^{10}\,\text{erg/cm-sec}$). For $L = 12$, the thermal conductivity and radiation have the same order of magnitude, but for $L = 2$, the heat is primarily conveyed by radiation. In the second case, the radiation is much greater than in the first, because of the high density of the plasma, but also because of the large value of the cross section of the channel. Taking $T = 4$ ev, we get, making use of (2.2) and (3.5), $n_i = 3.3 \times 10^{17}$, in the first case and $n_i = 9 \times 10^{17}$ in the second. These quantities greatly exceed the experimental value of 10^{17} obtained by Dolgov and Mandel'shtam.[5] According to their experimental data, $T \approx 4$ ev and $Z \approx 2$. Substituting these values in (2.5) and (4.3) we get $Q_T = 0.6 \times 10^{12}\,\text{erg/cm-sec}$. We estimate the radiation crudely by using (2.7) with an effective charge equal to $Z + 1.5 = 3.5$. This gives $Q_R = 1.6 \times 10^{12}$ for $L = 12$ and $Q_R = 4.4 \times 10^{13}$ for $L = 2$. These results correspond in order of magnitude to the experimental values of Q_J; however, the accuracy of the estimates is not very great because of the very approximate method employed in considering the radiation of air. Therefore, the role of other possible mechanisms of heat transfer, for example, radiant thermal conductivity, is not completely clear.

In conclusion, let us consider the limits of ap-

plicability of the theory developed above.

The lower limit is determined by the fact that for appreciable ionization, the temperature in the channel ought to be larger than (approximately) one electron volt. For this, the current ought to be not too small and should increase after a rather short time. The corresponding estimate can be obtained from (3.13) for hydrogen and from (4.3) and (4.4) for air. Neglecting the weak dependence on the density, and disregarding radiation, we obtain a condition for both cases, which is very rough:

$$J \gg 10^{-2} t^{3/4}. \tag{4.8}$$

The upper limit is determined by the requirement of smallness of the magnetic pressure $H^2/8\pi = J^2/2\pi a^2 c^2$ in comparison with the gas-dynamic pressure. Using (3.5) and (4.4), we get

$$H^2/8\pi p = (J/J_0)^{2/5},\ J_0 = (2^{7/2} K_p^{3/2}/\xi\pi^{1/2})(c^3\rho_0^{1/2}/\sigma), \tag{4.9}$$

where J_0 is the current at which the magnetic forces begin to be appreciable. For hydrogen, setting $\sigma = \sigma_1 T^{3/2}$, $\xi = (53/T)^{1/2}$, and using (2.4), we get

$$J_0(H_2) = 50\rho_0^{2/5} j^{-1/5}. \tag{4.10a}$$

For air, substituting a fixed value of the conductivity $\sigma = 2 \times 10^{14}$, and $\xi = 4.5$, we get

$$J_0\ (\text{air}) = 250\,\rho_0^{1/5}. \tag{4.10b}$$

The current is expressed in kiloamperes, the time in μsec, and the density in units of 0.9×10^{-4} for hydrogen and 1.29×10^{-3} for air, both in g/cm^3.

Both criteria are well satisfied for typical cases of lightning in the atmosphere. For example, let the current of the lightning be 30 kiloamperes and the time of current flow 200 μsec; then we get $0.55 \ll 30 \ll 250$. The form of the lightning current is not linear, so that the coefficient in (4.7) must be changed, but if (4.7) is used for a rough estimate, then we get, in the case considered, for the radius of the lightning channel $a \approx 4$ cm.

In conclusion, I express my deep gratitude to M. A. Leontovich, V. I. Kogan, D. A. Frank-Kamenetskii and S. L. Mandel'shtam for useful discussions, and to Z. D. Dobrokhotov and G. A. Mikhaĭlov for help in setting up the program for machine computation and for carrying out the computations.

[1] Abramson, Gegechkori, Drabkina, and Mandel'shtam, J. Exptl. Theoret. Phys. (U.S.S.R.) **17**, 862 (1947).

[2] S. I. Drabkina, J. Exptl. Theoret. Phys. (U.S.S.R.) **21**, 473 (1951).

[3] I. S. Abramson and N. M. Gegechkori, J. Exptl. Theoret. Phys. (U.S.S.R.) **21**, 484 (1951).

[4] N. M. Gegechkori, J. Exptl. Theoret. Phys. (U.S.S.R.) **21**, 493 (1951).

[5] G. G. Dolgov and S. L. Mandel'shtam, J. Exptl. Theoret. Phys. (U.S.S.R.) **24**, 691 (1953).

[6] S. L. Mandel'shtam and N. K. Sukhodrev, J. Exptl. Theoret. Phys. (U.S.S.R.) **24**, 701 (1953).

[7] S. I. Braginskii, J. Exptl. Theoret. Phys. (U.S.S.R.) **33**, 459 (1957), Soviet Phys. JETP **6**, 358 (1958).

[8] W. Heitler, The Quantum Theory of Radiation, (Oxford, 1954).

[9] H. Wessel, Ann. Physik **5**, 611 (1930).

[10] A. Unsöld, Physik der Sternatmosphären (Berlin, 1955), Ch. VI.

[11] L. I. Sedov, Методы подобия и размерности в механике (Methods of Similitude and Dimensionality in Mechanics) (GITTL, Moscow) 1954.

[12] H. Norinder and O. Karsten, Arkiv för Mat., Astr. Fys. **A36**, No. 16 (1949).

Translated by R. T. Beyer
306

ENERGY DIFFUSION OF FAST IONS IN AN EQUILIBRIUM PLASMA*

V. S. KUDRIAVTSEV

Academy of Sciences, U.S.S.R.

Submitted to JETP editor January 2, 1958

J. Exptl. Theoret. Phys. (U.S.S.R.) 34, 1558-1565 (June, 1958)

The problem of the energy diffusion of fast ions injected into an equilibrium plasma is considered. The energy distribution of the injected ions is initially monochromatic, with the energy exceeding the mean thermal energy in the plasma. It is assumed in this case that the distribution of velocity directions is isotropic. The extent to which the distribution approaches a Maxwellian one is determined. For an arbitrary initial distribution, the result can be obtained by the principle of superposition, since the equations are linear.

1. DERIVATION OF THE EQUATION

THE kinetic equation for a fully ionized plasma in the absence of external fields has the form[1]

$$\partial f / \partial t = -\operatorname{div}_{\mathbf{v}} \mathbf{j},$$

$$j_i = \frac{\pi e^2 L}{m} \sum e'^2 \int \left(f \frac{\partial f'}{m' \partial v'_k} - f' \frac{\partial f}{m \partial v_k} \right) \frac{u^2 \delta_{ik} - u_i u_k}{u^3} d\mathbf{v}'. \quad (1)$$

Here $f = f(t, \mathbf{v})$ is the distribution function, $\mathbf{j}$ is the flux density of particles in velocity space, $L = \ln [n^{-1} (\bar{\epsilon}/e^2)^3]$ is the Coulomb logarithm, m, e are the mass and charge of particles, $u_i = v_i - v'_i$ is the component of relative velocity.

Integration over $d\mathbf{v}'$ is taken over the whole velocity space. The primed variables are summed over all types of particles that collide with the given particles.

In our case the distribution function for each kind of particle is isotropic with respect to the velocity direction. We can therefore integrate in (1) over the directions of the vector $\mathbf{v}'$. Taking into account the equalities

$$\frac{\partial f}{\partial v_k} = \frac{v_k}{v} \frac{\partial f}{\partial v}, \qquad u_k (u^2 \delta_{ik} - u_i u_k) \equiv 0,$$

we obtain

$$j_i = \frac{\pi e^2 L}{m} \sum e'^2 \times \int\int \left(f \frac{\partial f'}{m' v' \partial v'} - f' \frac{\partial f}{m v \partial v} \right) v_k \frac{u^2 \delta_{ik} - u_i u_k}{u^3} v'^2 \, dv' \, d\Omega_{\mathbf{v}'}. \quad (2)$$

The integral over the angles of $\mathbf{v}'$ has the form:

$$\int \frac{u^2 \delta_{ik} - u_i u_k}{u^3} d\Omega_{\mathbf{v}'} = \frac{\partial^2}{\partial v_i \partial v_k} \int u \, d\Omega_{\mathbf{v}'}.$$

Evaluation of the last integral gives

$$\int u \, d\Omega_{\mathbf{v}'} = \frac{2\pi}{3vv'} \{ (v + v')^3 - |v - v'|^3 \}.$$

After differentiating twice and substituting into (2) we obtain for the flux in velocity space

$$j_i = \frac{\pi e^2 L}{m} \sum e'^2 \times \int \left(f \frac{\partial f'}{m' v' \partial v'} - f' \frac{\partial f}{m v \partial v} \right) \frac{8\pi}{3} v_i v'^3 \frac{8}{(v + v' + |v - v'|)^3} v' \, dv'. \quad (3)$$

This flux is directed along the vector $\mathbf{v}$, and its divergence is

$$\operatorname{div}_{\mathbf{v}} \mathbf{j} = \frac{1}{v^2} \frac{\partial}{\partial v} (v^2 j), \quad (4)$$

where j is the absolute value of the flux.

We assume that a small number of ions of definite energy, with a spherically symmetric distribution of velocity directions, is injected into an equilibrium fully-ionized plasma. Then the role played by the collisions of these particles with each other will not be great, and the change in time of the distribution function f of these particles will be determined by the collisions with the ions and the electrons of the equilibrium plasma having Maxwellian distributions:

$$f'_i = n (M/2\pi T)^{3/2} e^{-mv'^2/2T}, \quad (5)$$

$$f'_e = n (m/2\pi T)^{3/2} e^{-mv'^2/2T}, \quad (6)$$

where n is the ion or electron density, M, m are the ion and electron masses, T is the ion and electron temperature in energy units.

The distributions are normalized so that $\int f' 4\pi v'^2 \, dv' = n$. Thus the flux of injected particles in velocity space is equal to:

$$j = \frac{\pi e^4 L}{M} \int \left(f \frac{\partial f'_i}{M v' \partial v'} - f'_i \frac{\partial f}{M v \partial v} \right) \frac{8\pi}{3} v v'^3 \frac{8}{(v + v' + |v - v'|)^3} v' dv' + \frac{\pi e^4 L}{m} \int \left(f \frac{\partial f'_e}{m v' \partial v'} - f'_e \frac{\partial f}{M v \partial v} \right) \frac{8\pi}{3} v v'^3 \frac{8}{(v + v' + |v - v'|)^3} v' dv'. \quad (7)$$

*Work carried out in 1952.

Substituting for f_i' and f_e' their values from (5) and (6), and integrating over dv', we shall obtain the final expression for the flux of particles in velocity space:

$$j = -\frac{2^{5/2} e^4 L n T^{1/2}}{3\pi^{1/2} M^{5/2} v}\left\{\left[\frac{3}{4v}\sqrt{\frac{2\pi T}{M}}\,\Phi\left(\sqrt{\frac{M}{2T}}\,v\right) - \frac{3}{2}\,e^{-Mv^2/2T}\right]\right. \tag{8}$$
$$\left. + \sqrt{\frac{M}{m}}\left[\frac{3}{4v}\sqrt{\frac{2\pi T}{m}}\,\Phi\left(\sqrt{\frac{m}{2T}}\,v\right) - \frac{3}{2}\,e^{-mv^2/2T}\right]\right\}\left(\frac{f}{T} + \frac{\partial f}{Mv\partial v}\right),$$

where $\Phi(z) = \frac{2}{\sqrt{\pi}}\int_0^z e^{-t^2}\,dt$ is Kramp's function.

The kinetic equation for the injected ions, in accordance with (1) and (4) has the form

$$\frac{\partial f}{\partial t} = -\frac{1}{v^2}\frac{\partial}{\partial v}(v^2 j). \tag{9}$$

Substituting into this the expression for j from (8) we obtain:

$$\frac{\partial f}{\partial \tau} = \frac{1}{\sqrt{x}}\frac{\partial}{\partial x}\left[\sqrt{x}\,\Gamma(x)\left(f + \frac{\partial f}{\partial x}\right)\right], \tag{10}$$

with

$$x = Mv^2/2T, \quad \tau = 2^{3/2} e^4 L n t/3\pi^{1/2} M^{1/2} T^{3/2},$$
$$\Gamma(x) = \frac{3}{4}\sqrt{\pi}\,\frac{\Phi(\sqrt{x})}{\sqrt{x}} - \frac{3}{2}\,e^{-x} \tag{11}$$
$$+ \sqrt{\frac{M}{m}}\left[\frac{{}^3/_4\sqrt{\pi}\,\Phi(\sqrt{mx/M})}{\sqrt{mx/M}} - \frac{3}{2}\,e^{-mx/M}\right].$$

We shall normalize the function f by the condition

$$\int_0^\infty f\sqrt{x}\,dx = 1. \tag{12}$$

In going over from the distribution function f in velocity space to the distribution density with respect to energy $\rho = f\sqrt{x}$, we obtain from (10) the following equation for ρ:

$$\frac{\partial \rho}{\partial \tau} = \frac{\partial}{\partial x}\left[\Gamma(x)\left(\rho - \frac{\rho}{2x} + \frac{\partial \rho}{\partial x}\right)\right], \tag{13}$$

with

$$\int_0^\infty \rho\,dx = 1. \tag{14}$$

2. SOLUTION OF THE EQUATION

The initial condition for the distribution density with respect to energy of the injected ions ρ is a monochromatic distribution with the energy equal to x_0. In future we shall assume that x_0 exceeds unity. Thus

$$\rho(x, 0) = \delta(x - x_0). \tag{15}$$

With time this distribution will be smeared out by diffusion and will approach the stationary distribution which is obtained from (13) when $d\rho/d\tau = 0$ and which is, as it ought to be, Maxwellian

$$\rho(x, \infty) = 2e^{-x}\sqrt{x/\pi}. \tag{16}$$

Our problem is to find the time variation of the distribution, particularly for large times and for energies exceeding x_0.

We solve (13) by using Laplace transforms. To do this we multiply both sides of equation (13) by $e^{-\lambda\tau}$ and integrate over $d\tau$ between the limits 0 and ∞. Integrating by parts on the left-hand side and denoting

$$\rho_\lambda(x) = \int_0^\infty \rho(x, \tau)\,e^{-\lambda\tau}\,d\tau, \tag{17}$$

we obtain from (13), after taking (15) into account,

$$\lambda\rho_\lambda - \delta(x - x_0) = \frac{d}{dx}\left[\Gamma(x)\left(\rho_\lambda - \frac{\rho_\lambda}{2x} + \frac{d\rho_\lambda}{dx}\right)\right]. \tag{18}$$

The transition from $\rho_\lambda(x)$ to $\rho(x, \tau)$ is accomplished with the aid of the formula for the inverse transformation

$$\rho(x, \tau) = \frac{1}{2\pi i}\int_{\sigma - i\infty}^{\sigma + i\infty} \rho_\lambda(x)\,e^{\lambda\tau}\,d\lambda. \tag{19}$$

Here the integration over $d\lambda$ is taken in the complex λ plane along a line lying in the right-hand half-plane to the right of the singularities of $\rho_\lambda(x)$.

Let us put Eq. (18) into a more convenient form. For this we first eliminate the first derivative by the substitution

$$\rho_\lambda = x^{1/4} e^{-x/2}\,\Gamma^{-1/2} g_\lambda. \tag{20}$$

We then replace the function g_λ and the independent variable[2] x

$$F_\lambda = \Gamma^{-1/4} g_\lambda, \tag{21}$$

$$\xi = \int_0^x [\Gamma(x)]^{-1/2}\,dx, \quad \xi_0 = \int_0^{x_0} [\Gamma(x)]^{-1/2}\,dx. \tag{22}$$

As a result we obtain

$$\frac{d^2 F_\lambda}{d\xi^2} - (\lambda - u(\xi))\,F_\lambda = -x_0^{-1/4} e^{x_0/2}\,[\Gamma(x_0)]^{-1/2}\,\delta(\xi - \xi_0), \tag{23}$$

where

$$u(\xi) = \frac{d^2\,(x^{1/4} e^{-x/2}\,[\Gamma(x)]^{1/4})\,/\,d\xi^2}{x^{1/4} e^{-x/2}\,[\Gamma(x)]^{1/4}}. \tag{24}$$

Equation (23) with $\Gamma(x)$ as given by formula (11) does not have a solution in finite analytic form (except for the case $\lambda = 0$). However, one can obtain, with sufficient degree of accuracy, an approximate solution by making use of the specific form of the function $u(\xi)$. A graph of the function $u(\xi)$ for the value $m/M = 1/3600$ (deuterium plasma) is given in Fig. 1.

In the range of values of ξ from 5 to 30 (while

x varies from 4 to 25) the function $u(\xi)$ maintains an approximately constant value equal to 0.14, as can be seen from the graph. We denote this value by a. (The remaining values of the function $u(\xi)$ in the region $\xi > 30$, which are of no practical interest, increase monotonically and go through a maximum (on the order of M/m) at ξ, and then asymptotically approach zero for still greater values of ξ.

For an an approximate solution of (23), we shall choose such an expression for $\Gamma(x)$ [which we shall denote by $\gamma(x)$], as to make $u(\xi)$ a constant equal to a, i.e., in accordance with (24)

$$\frac{d^2\left(x^{1/4}e^{-x/2}[\gamma(x)]^{1/4}\right)/d\zeta^2}{x^{1/4}e^{-x/2}[\gamma(x)]^{1/4}} = a. \tag{25}$$

With such a value of γ, Eq. (23) can be solved in finite analytic form. We have denoted by ζ the quantity ξ corresponding to the new function $\gamma(x)$. Such an approximation allows us to obtain, with a sufficient degree of accuracy, the distribution function in the range of values of ξ from 5 to 30. On solving Eq. (25) for the function $x^{1/4}e^{-x/2}[\gamma(x)]^{1/4}$ we find

$$x^{1/4}e^{-x/2}[\gamma(x)]^{1/4} = C\exp(-\sqrt{a}\zeta) + C_1\exp(\sqrt{a}\zeta), \tag{26}$$

where C and C_1 are constants, which for the time being are arbitrary and will be determined later. The dependence of ζ on x is now given instead of (22) by the formula:

$$\zeta = \int_0^x [\gamma(x)]^{-1/2}dx, \quad \zeta_0 = \int_0^{x_0} [\gamma(x)]^{-1/2}dx. \tag{27}$$

Equation (23), without its right-hand side, has for $\lambda = 0$ a solution which falls off as $\xi \to \infty$, or, what is the same, for $x \to \infty$. This solution has, according to (24), the form

$$F_\lambda = \text{const}\, x^{1/4}e^{-x/2}[\Gamma(x)]^{1/4}.$$

A solution of (23) (for $\lambda = 0$) which falls off at infinity, must have for $u(\xi) = a$ the form

$$F_\lambda = \text{const}\, x^{1/4}e^{-x/2}[\gamma(x)]^{1/4}. \tag{28}$$

Comparing (28) with (26) we find that $C_1 = 0$, and thus

$$x^{1/4}e^{-x/2}[\gamma(x)]^{1/4} = C\exp(-\sqrt{a}\zeta). \tag{29}$$

The constant C is determined from the normalization condition and turns out to be equal to

$$C = (\pi a)^{1/4}. \tag{30}$$

Now we can find from (27), (29) and (30) the dependence of γ and ζ on x. We obtain

$$\zeta = -\frac{1}{2\sqrt{a}}\ln\left[1 - \Phi(\sqrt{x}) + 2\sqrt{\frac{x}{\pi}}e^{-x}\right]; \tag{31}$$

$$\gamma = \pi a\left[\frac{1-\Phi(\sqrt{x})}{\sqrt{x}e^{-x}} + \frac{2}{\sqrt{\pi}}\right]^2. \tag{32}$$

Equation (23) assumes the form

$$\frac{d^2F_\lambda}{d\zeta^2} + (a+\lambda)F_\lambda = x_0^{1/4}e^{x_0/2}[\gamma(x_0)]^{-1/4}\delta(\zeta-\zeta_0), \tag{33}$$

while ρ_λ and F_λ are related by the expression

$$\rho_\lambda = x^{1/4}e^{-x/2}[\gamma(x)]^{-1/4}F_\lambda. \tag{34}$$

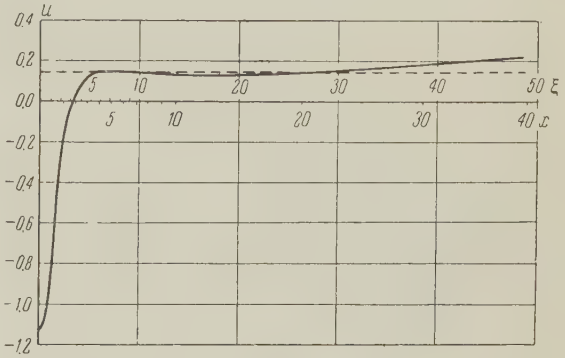

FIG. 1

Let us determine the boundary conditions for Eq. (33). Integrating (13) with respect to x between the limits 0 and ∞, and noting that it follows from (14) that $\frac{\partial}{\partial\tau}\int_0^\infty \rho dx = 0$, we obtain

$$\left\{\gamma(x)\left(\rho - \frac{\rho}{2x} + \frac{\partial\rho}{\partial x}\right)\right\}\Big|_0^\infty = 0. \tag{35}$$

As $x \to \infty$ both $\rho(x,\tau)$ and $\partial\rho/\partial x$ should tend to zero, and since at the same time $\gamma(x)$ remains finite, it must follow that

$$(\rho - \rho/2x + \partial\rho/\partial x)_{x\to\infty} = 0, \tag{36}$$

$$\{\gamma(x)(\rho - \rho/2x + \partial\rho/\partial x)\}_{x\to 0} = 0. \tag{37}$$

Upon applying the Laplace transformation to the last two equations, we shall have the same conditions also for $\rho_\lambda(x)$; obviously $(\rho_\lambda)_{x\to\infty} = 0$. From the condition $(\rho_\lambda)_{x\to\infty} = 0$, from the specific forms of the functions $\zeta(x)$ and $\gamma(x)$ given by (31) and (32) for $x \to \infty$, and from the relation (34), we obtain the boundary condition for F_λ as $x \to \infty$ ($\zeta \to \infty$)

$$(F_\lambda)_{\substack{x\to\infty \\ \lambda>0}} = 0. \tag{38}$$

Similarly we obtain the boundary condition

$$\left(\frac{1}{F_\lambda}\frac{dF_\lambda}{d\zeta}\right)_{\zeta\to 0} = -\sqrt{a}. \tag{39}$$

In addition to satisfying conditions (38) and (39), the function $F_\lambda(\xi)$ must be continuous in the whole region from zero to ∞, while at the point $\xi = \xi_0$ the derivative $dF_\lambda/d\xi$ must have a discon-

tinuity whose magnitude is found by integrating (23) over a small interval which contains the point $\zeta = \zeta_0$:

$$\left.\frac{dF_\lambda}{d\zeta}\right|_{\zeta_0}^{\zeta_0+0} = x_0^{1/4} e^{\gamma_0/2} [\gamma(x_0)]^{-1/4} = (\pi a)^{1/4} e^{-\sqrt{a}\zeta_0}. \qquad (40)$$

Conditions (38), (39), (40) and the requirement of continuity completely determine $F_\lambda(x)$ for $x > 0$. The function F_λ which satisfies all the above requirements has the form:

$$F_\lambda = \begin{cases} \dfrac{\exp\{\sqrt{a}\zeta_0 - \sqrt{a+\lambda}\,\zeta_0\}}{2(\pi a)^{1/4}\sqrt{a+\lambda}(\sqrt{a+\lambda}-\sqrt{a})}[(\sqrt{a+\lambda}-\sqrt{a})\exp(\sqrt{a+\lambda}\,\zeta) \\ \qquad + (\sqrt{a+\lambda}+\sqrt{a})\exp(-\sqrt{a+\lambda}\,\zeta)], \quad \zeta < \zeta_0 \\ \dfrac{\exp\{\sqrt{a}\zeta_0 - \sqrt{a+\lambda}\,\zeta\}}{2(\pi a)^{1/4}\sqrt{a+\lambda}(\sqrt{a+\lambda}-\sqrt{a})}[(\sqrt{a+\lambda}-\sqrt{a})\exp(\sqrt{a+\lambda}\,\zeta_0) \\ \qquad + (\sqrt{a+\lambda}+\sqrt{a})\exp(-\sqrt{a+\lambda}\,\zeta_0)], \quad \zeta > \zeta_0. \end{cases} \qquad (41)$$

The function $F_\lambda(\zeta)$ is defined for complex values of λ, including also negative values of λ, by means of analytic continuation with respect to λ, starting with positive values of λ.

According to (17) and (34) the desired distribution $\rho(x, \tau)$ is equal to

$$\rho = x^{1/4} e^{-x/2} \gamma^{-1/4} \frac{1}{2\pi i} \int_{\sigma-i\infty}^{\sigma+i\infty} F_\lambda e^{\lambda\tau} d\lambda$$
$$= \frac{(\pi a)^{1/4} e^{-\sqrt{a}\zeta}}{\gamma^{1/2}} \frac{1}{2\pi i} \int_{\sigma-i\infty}^{\sigma+i\infty} F_\lambda e^{\lambda\tau} d\lambda. \qquad (42)$$

The path of integration in the complex λ plane may be deformed in the following manner. The integrand $F_\lambda e^{\lambda\tau}$ has singularities at $\lambda = 0$ and $\lambda = -a$; in particular, the point $\lambda = 0$ is a pole with a residue equal to $2(a/\pi)^{1/4} e^{-\sqrt{a}\,\zeta}$, while the point $\lambda = -a$ is a branch point of the first order. After making a cut along the negative part of the real axis from $\lambda = -a$ to $\lambda = -\infty$, we take the path of integration along the edges of the cut in the form of a loop surrounding the point $\lambda = -a$. Then the integral in formula (42) will reduce to an integral over this loop and an integral over a circle surrounding the point $\lambda = 0$, as shown in Fig. 2. Both functions F_λ in formula (41) give, on integration, the same result for $\rho(x, \tau)$. On carrying out the integration we obtain:

$$\rho = \frac{2\sqrt{a}}{\gamma^{1/2}} \exp(-2\sqrt{a}\zeta) + \frac{e^{-a\tau}}{2\pi\gamma^{1/2}} \exp\{-\sqrt{a}(\zeta - \zeta_0)\}$$
$$\times \int_0^\infty \frac{d\mu e^{-\mu\tau}}{\sqrt{\mu}} \left[\cos\sqrt{\mu}(\zeta - \zeta_0) + \frac{\mu - a}{\mu + a}\cos\sqrt{\mu}(\zeta_0 + \zeta) - \frac{2\sqrt{\mu a}}{\mu + a}\sin\sqrt{\mu}(\zeta_0 + \zeta)\right]. \qquad (43)$$

The first term in (43) represents the integral over the circle, while the second term represents the integral over the loop. On carrying out the necessary integrations in the second term, we obtain the final expression for the distribution $\rho(x, \tau)$:

$$\rho = \gamma^{-1/2}\sqrt{a}\exp\{-2\sqrt{a}\zeta\}\left[1 + \Phi\left(\sqrt{a\tau} + \frac{\zeta + \zeta_0}{2\sqrt{\tau}}\right)\right] \qquad (44)$$
$$+ \gamma^{-1/2}\exp\{-\sqrt{a}(\zeta - \zeta_0)\}\frac{e^{-(\zeta-\zeta_0)^2/4\tau} + e^{-(\zeta+\zeta_0)^2/4\tau}}{2\sqrt{\pi\tau}} \cdot e^{-a\tau},$$

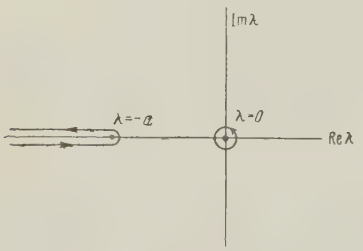

FIG. 2

where ζ and ζ_0 are determined by formula (27), while $\gamma(x)$ is determined by formula (32). As $\tau \to 0$ we obtain from (44) $\rho = \delta(x - x_0)$, while for $\tau \to \infty$, $\rho = 2e^{-x}\sqrt{x/\pi}$, as it should be.

3. RESULTS

Expression (44) obtained above for the distribution density with respect to energy $\rho(x, \tau)$ will describe, to a sufficient degree of approximation, the energy distribution of ions injected into plasma in the range of values of ξ and ξ_0 from 5 to 30. The range of the corresponding values of ζ and ζ_0 is approximately the same, while x and x_0 vary between 4 and 25. In order to describe the manner in which the distribution function approaches the stationary Maxwellian distribution

$$\rho_M = 2\gamma^{-1/2}\sqrt{a}\,e^{-2\sqrt{a}\zeta}$$

it is convenient to introduce the ratio ρ/ρ_M which

is equal to

$$\frac{\rho}{\rho_M}=\frac{1}{2}\left[1+\Phi\left(\sqrt{a\tau}-\frac{\zeta+\zeta_0}{2\sqrt{\tau}}\right)\right]$$
$$+\frac{\exp\{-a\tau+\sqrt{a}(\zeta+\zeta_0)\}}{4\sqrt{\pi a\tau}}\left[e^{-(\zeta-\zeta_0)^2/4\tau}+e^{-(\zeta+\zeta_0)^2/4\tau}\right]. \quad (45)$$

The variables ζ and ζ_0 occur in ρ/ρ_M in a symmetric way.

For given values of ζ and ζ_0 ($\zeta \neq \zeta_0$) lying within the region in which the solution is applicable the quantity ρ/ρ_M regarded as a function of time increases from zero (at $\tau = 0$) to a maximum value greater than unity (for $\tau = \tau^*$) and then decreases asymptotically approaching unity from above. For small values of the time

$$\tau \ll (\zeta+\zeta_0)/2\sqrt{a} < \zeta\zeta_0$$

ρ/ρ_M has the form:

$$\frac{\rho}{\rho_M}=\frac{1}{4\sqrt{\pi a\tau}}\exp\left\{-\left(\frac{\zeta+\zeta_0}{2\sqrt{\tau}}-\sqrt{a\tau}\right)^2\right\}(1+e^{\zeta\zeta_0/\tau}). \quad (46)$$

For large values of the time

$$\tau \gg \zeta\zeta_0 > (\zeta+\zeta_0)/2\sqrt{a}$$

we have:

$$\frac{\rho}{\rho_M}=1+\frac{1}{4\sqrt{\pi a}\tau^{3/2}}$$
$$\times\exp\left\{-\left(\sqrt{a\tau}-\frac{\zeta+\zeta_0}{2\sqrt{\tau}}\right)^2\right\}\left(\zeta-\frac{1}{\sqrt{a}}\right)\left(\zeta_0-\frac{1}{\sqrt{a}}\right). \quad (47)$$

The time $\tau = \tau^*$ at which ρ/ρ_M has a maximum is found from the condition $\partial(\rho/\rho_M)/\partial\tau = 0$ which, in accordance with (45), assumes the form:

$$e^{\zeta\zeta_0/\tau^*}=\frac{[\sqrt{a\tau^*}+(\zeta+\zeta_0)/2\sqrt{\tau^*}]^2-1/2}{a\tau^*-(\zeta-\zeta_0)^2/4\tau^*+1/2}. \quad (48)$$

Assuming that the quantity $\zeta\zeta_0/\tau^*$ is large compared with unity (this condition is fulfilled as may be seen from the result (49) obtained above for our range of ζ and ζ_0) we obtain τ^* by equating to zero the denominator of the right-hand side of (48)

$$\tau^*=\frac{\sqrt{1+4a(\zeta-\zeta_0)^2}-1}{4a}. \quad (49)$$

In conclusion, I express my gratitude to A. B. Migdal for suggesting the problem.

[1] L. Landau, J. Exptl. Theoret. Phys. (U.S.S.R.) 7, 203 (1937).

[2] R. Courant and D. Hilbert, Methoden der Mathematischen Physik, vol. 1 (Russian translation) 1951, p. 251 [Berlin, 1931; Interscience 1943].

Translated by G. Volkoff
307

ENERGY SPECTRUM OF A HIGH DENSITY ELECTRON GAS

CHEN CHUN-SIAN and CHOW SHIH-HSUN

Moscow State University

Submitted to JETP editor January 6, 1958

J. Exptl. Theoret. Phys. (U.S.S.R.) 34, 1566-1573 (June, 1958)

The procedure of approximate second quantization is used to sum the special class of diagrams corresponding to the divergent terms in the standard perturbation theory expansion for a system with coulomb interaction (infrared divergence). An energy spectrum for a high density electron gas is derived, which contains both individual excitations (quasi-particles obeying Fermi statistics) and collective excitations of the plasma type. The correction to the specific heat due to the self energy of the elementary excitations is computed. The results are compared with those of Gell-Mann and Brueckner. To a certain extent, the results can be considered to be a justification of the independent particle model in the electron theory of metals.

1. INTRODUCTION

SOME of the ideas of quantum field theory, in particular the method of graphical analysis of matrix elements, prove to be very fruitful in quantum statistics. In papers of Gell-Mann and Brueckner[1] and Sawada,[2] for the case of a high density electron gas, a partial summation is carried out over the specially selected diagrams corresponding to the most strongly divergent terms in the perturbation expansion, thus eliminating the well known "infrared catastrophe" which is related to the long range character of the coulomb interaction. Hugenholtz[3] has developed in detail a technique for constructing diagrams for a system of interacting particles obeying Fermi statistics, and has investigated the dependence of various matrix elements on the volume of the system.

In the present paper, we apply the method of approximate second quantization to a high density electron gas, and obtain the energy spectrum of the elementary excitations corresponding to both collective motion of the system and to individual excitations.

In reference 1 it was shown that for a system of Fermi particles at high density (large Fermi momentum), only those matrix elements of the Coulomb interaction are important which correspond to transitions near the Fermi surface. The electrons and holes then form bound pairs. Thus the Gell-Mann — Brueckner partial summation of diagrams in which electron and hole lines form irreducible complexes is equivalent to treating a model dynamical system with a Hamiltonian which is obtained from the exact Hamiltonian by dropping all terms which do not correspond to electron-hole pairs. It was also shown in reference 1 that the matrix elements corresponding to the exchange of an excited pair give a contribution of higher order, and can therefore be dropped. In the present paper the authors start from the results of a paper* of Bogoliubov, Tiablikov, and Tolmachev, in which the idea of partial summation of diagrams is combined with the well developed technique of computation in the method of approximate second quantization. These ideas are proving to be very fruitful and, as is well known, are very sucessful in the theory of superconductivity.[4] Thanks to the convenient form of writing diagonal matrix elements, we obtain in the present paper, in very much simpler fashion, not only the results of Gell-Mann and Brueckner,[1,5] but also explicit expressions for the energy of elementary excitations, which they were unable to get.

2. GENERAL FORMALISM

Let us proceed to formulate the problem mathematically and obtain the general relations from which it is easy to find the spectrum of elementary excitations in which we are interested. We start from the exact Hamiltonian of a system of N particles (electrons) contained in volume Ω:

*This work was reported at the seminar of the Theoretical Physics Division of the Steklov Mathematical Institute of the Academy of Sciences, USSR, in September, 1957.

$$H = \sum_{p\sigma} \varepsilon(p)\, a^*_{p\sigma} a_{p\sigma} + \sum_q \frac{\nu(q)}{2\Omega} \sum_{\substack{pp' \\ \sigma\sigma'}} a^*_{p+q\sigma} a^*_{p'-q\sigma'} a_{p'\sigma'} a_{p\sigma}; \qquad (1)$$

$a^*_{p\sigma}$ and $a_{p\sigma}$ are the creation and annihilation operators for an electron with momentum p and spin σ. We shall omit the spin indices from now on. As usual, we assume the presence of a uniformly distributed positive charge, which is necessary to maintain the neutrality and equilibrium of the system. All energies are measured in Rydbergs, and momenta in units of the Fermi momentum. Thus the expressions for the kinetic energy of the electron and the Fourier transform of the Coulomb interaction are:

$$\varepsilon(p) = (p^2 p_F^2/2m)/(e^4 m/2\hbar^2) = p^2/(r_s\alpha)^2,$$
$$\nu(q) = (4\pi\hbar^2 e^2/q^2 p_F^2)/(e^4 m/2\hbar^2) = 8\pi/k_F^3 r_s \alpha q^2, \qquad (2)$$

where $r_s = r_0/a$ is a dimensionless parameter, m and e are the mass and charge of the electron, $a = \hbar^2/me^2$, $4\pi r_0^3/3 = \Omega/N$, $p_F = \hbar k_F$ is the Fermi momentum, and $\alpha = (4/9\pi)^{1/2}$. Since r_3 is proportional to e^2, the expansion in powers of r_s is the usual perturbation series; r_s will be small if the density is sufficiently high.

If we choose as the "vacuum," with respect to which we define the electron and hole, the state Φ_G in which all individual states within a certain region (G) in momentum space are filled with electrons while all other states (H) are empty, the creation and annihilation operators for the electron and hole will be, respectively:

$$c^*_p = (1 - \varkappa(p))\, a^*_p, \quad b^*_p = \varkappa(p)\, a_p, \qquad \varkappa(p) = \begin{cases} 1 & \text{for } p \in G \\ 0 & \text{for } p \in H. \end{cases}$$
$$c_p = (1 - \varkappa(p))\, a_p, \quad b_p = \varkappa(p)\, a^*_p.$$

Then

$$a_p = c_p + b^*_p, \quad a^*_p = c^*_p + b_p. \qquad (3)$$

Using the ideas in the cited papers of Bogoliubov, Tiablikov, and Tolmachev, we show that the operation of summation of contributions from diagrams of a selected class, corresponding to the most strongly divergent terms in each order of the infinite perturbation series,[1,5] can be replaced by the simpler and well developed method of approximate second quantization. In fact, if we retain in the exact Hamiltonian only terms that can be uniquely associated with fundamental elements (irreducible complexes and vertex parts) of the diagrams of this particular class, it is clear that the exact solution of the problem for the model dynamical system with this simplified Hamiltonian is completely equivalent to the operation of summation of the infinite perturbation series which we described above. In our case, the irreducible complexes in the diagrams to be summed are the electron-hole pair lines, while the vertex parts correspond to scattering of an electron by the hole of a given pair. It is not hard to see that such irreducible complexes correspond to combinations of the type $c^*_{p+q} b^*_p$ and $b_p c_{p+q}$ in the interaction Hamiltonian, and that just these terms should be kept to get the model Hamiltonian.

It should be mentioned that a similar idea was essentially already used by Sawada,[2] but since he did not write the expression for the self energy of the pair explicitly, he did not succeed in representing the complete simplified Hamiltonian as a quadratic form to which the diagonalization method could be applied; to solve the problem he had to use more complicated mathematical methods. In doing this, he omitted the contribution from excitations of the plasma type, so that his results are not entirely correct. These deficiencies are eliminated in the present paper, and new results are obtained.

Substituting (3) in the Hamiltonian (1) and keeping only terms corresponding to irreducible electron-hole complexes, and also dropping exchange terms (an important point here is that we express the diagonal part in terms of the energy $\omega(p, q)$ of a free pair), we get the model Hamiltonian in the form

$$\tilde{H} = E(\Phi_G) - \sum_{pq} \varkappa(p)(1 - \varkappa(p+q)) \frac{\nu(q)}{2\Omega} + \sum_{pq} \omega(p, q)\, \eta^{q*}_p \eta^q_p$$
$$+ \sum_q \frac{\nu(q)}{2\Omega} \sum_{pp'} [\eta^q_p \eta^{-q}_{p'} + \eta^{q*}_p \eta^{q*}_{p'} + 2\eta^{q*}_p \eta^q_{p'}], \qquad (4)$$
$$\omega(p, q) = \varepsilon(p+q) - \varepsilon(p),$$

where $\eta^{q*}_p = c^*_{p+q} b^*_p$, $\eta^q_p = b_p c_{p+q}$ are the creation and annihilation operators for an electron-hole pair, defined with respect to the state Φ_G; they satisfy complicated commutation relations, which are different from those for both fermions and bosons. The basic idea of approximate second quantization just consists of the fact that when we treat the state Φ_G and there no particles outside the region G, these operators can be regarded as Bose operators, i.e., when applied to the state Φ_G they satisfy the same commutation relations as the usual Bose amplitudes.

The Hamiltonian (4), which is a quadratic form in η^{q*}_p, η^q_p, can be diagonalized using the familiar method of Tiablikov.[6] To do this, we make a canonical transformation to new Fermi amplitudes

$$\xi_\alpha = \sum_{pq} [u_p^{q*}(\alpha)\,\eta_p^q - v_p^{q*}(\alpha)\,\eta_p^{q*}],$$

$$\sum_{pq} \varkappa(p)(1-\varkappa(p+q))[|u_p^q|^2 - |v_p^q|^2] = 1, \qquad (5)$$

$$\xi_\alpha^* = \sum_{pq} [u_p^q(\alpha)\,\eta_p^{q*} - v_p^q(\alpha)\,\eta_p^q]; \qquad [\xi_\alpha,\ \xi_{\alpha'}^*] = \delta_{\alpha\alpha'}.$$

If u and v satisfy the equations

$$\begin{aligned} E_\alpha u_p^q(\alpha) &= \omega(p,q)\,u_p^q(\alpha) \\ &+ \frac{\nu(q)}{\Omega}\sum_{p'}\varkappa(p')[(1-\varkappa(p'+q))\,u_{p'}^q(\alpha) \\ &+ (1-\varkappa(p'-q))\,v_{p'}^{-q}(\alpha)], \\ -E_\alpha v_p^q(\alpha) &= \omega(p,q)\,v_p^q(\alpha) \\ &+ \frac{\nu(q)}{\Omega}\sum_{p'}\varkappa(p')[(1-\varkappa(p'-q))\,u_{p'}^{-q}(\alpha) \\ &+ (1-\varkappa(p'+q))\,v_{p'}^q(\alpha)], \end{aligned} \qquad (6)$$

the Hamiltonian, when expressed in terms of ξ_α^* and ξ_α takes on the diagonal form

$$\begin{aligned} \tilde{H} = E(\Phi_G) &- \sum_{\alpha,p,q} E_\alpha |v_p^q(\alpha)|^2 \varkappa(p)(1-\varkappa(p+q)) \\ &- \sum_{pq}\varkappa(p)(1-\varkappa(p+q))\frac{\nu(q)}{2\Omega} + \sum_\alpha E_\alpha \xi_\alpha^*\xi_\alpha. \end{aligned} \qquad (7)$$

Here the E_α are the energies of the elementary excitations, which are given by the zeros of the function

$$\Psi(z,q) = 1 - \frac{\nu(q)}{\Omega}\sum_{p'}\varkappa(p')(1-\varkappa(p'+q))\frac{2\omega(p',q)}{z^2-\omega^2(p',q)}. \qquad (8)$$

The part of the Hamiltonian $\tilde{H}$ which does not contain operators [without $E(\Phi_G)$]

$$\begin{aligned} \Delta E(\Phi_G) = &-\sum_\alpha E_\alpha \sum_{p,q}\frac{\varkappa(p)(1-\varkappa(p+q))}{(E_\alpha+\omega(p,q))^2} \\ &\times\left\{\sum_{p'}\left[\frac{\varkappa(p')(1-\varkappa(p'+q))}{(E_\alpha-\omega(p',q))^2}\right.\right. \qquad (9) \\ &\left.\left.-\frac{\varkappa(p')(1-\varkappa(p'+q))}{(E_\alpha+\omega(p',q))^2}\right]\right\}^{-1} - \sum_{pq}\varkappa(p)(1-\varkappa(p+q))\frac{\nu(q)}{2\Omega} \end{aligned}$$

determines the change in energy of the ground state due to dynamical correlation between electrons.*

3. GROUND STATE ENERGY

The true lowest state corresponds to a completely filled Fermi sphere (Fermi vacuum Φ_V). Substituting in (9)

$$\varkappa(p) = \theta(p),\ \theta(p) = \begin{cases} 1, & \text{for } |p|<1, \\ 0, & \text{for } |p|>1, \end{cases} \qquad (10)$$

and using (8) and the residue theorem, we easily get the expression for the correlation energy in the form*

$$\begin{aligned} \Delta E(\Phi_V) = &-\sum_q \frac{1}{4\pi i} \\ &\times\int_\Gamma\left\{\ln\left[1-\frac{\nu(q)}{\Omega}\sum_p\theta(p)(1-\theta(p+q))\frac{2\omega(p,q)}{z^2-\omega^2(p,q)}\right]\right. \\ &\left.+\frac{\nu(q)}{\Omega}\sum_p\theta(p)(1-\theta(p+q))\frac{2\omega(p,q)}{z^2-\omega^2(p,q)}\right\}dz. \end{aligned} \qquad (11)$$

The contour Γ runs clockwise around the positive real axis. If we deform Γ to run along the imaginary axis from $-\infty$ to $+\infty$, Eq. (11) coincides exactly with the result obtained in reference 1 by partial summation of the divergent perturbation series.

As is well known, the branch of collective excitations of the density-fluctuation type (plasma waves) is very important in the spectrum of a dense charged gas. As already mentioned, excitations of this type contribute to the correlation energy. From the physical point of view, the plasma oscillations are important because they show the effect of the long-range correlation between electrons, which results in the screening of the Coulomb interaction and the cutting off of integrals over virtual momenta at a lowest momentum k_c which is proportional to $r_s^{1/2}$. This is why the idea of summation of divergent diagrams is completely justified mathematically, and is the essential physical reason for the elimination of the infrared divergence, which is the basis of all the investigations discussed in the present paper. Let us show that in our formalism the plasma oscillations are included in the energy spectrum of the system. For $\Omega \to \infty$, we have the asymptotic expression:

$$\begin{aligned} \Psi(z;q) = 1 + \frac{2r_s\alpha}{\pi q^2}&\left[1-\frac{z'}{4q}\ln\frac{(z'+2q)^2-q^4}{(z'-2q)^2-q^4}\right. \qquad (12) \\ &\left.+\frac{1}{2}\left(\frac{1}{q}-\frac{q}{4}-\frac{z'^2}{4q^3}\right)\ln\frac{z'^2-(2q+q^2)^2}{z'^2-(2q-q^2)^2}\right], \qquad z' = (r_s\alpha)^2 z. \end{aligned}$$

The isolated zero of the function $\Psi(z,q)$ determines the frequency of collective ordered oscillation of the system. For $q \ll 1$ it reduces to the familiar dispersion relation for plasma waves:

$$\omega^2(q) \equiv z^2 \approx \left(\frac{4\pi e^2 n}{m} + \frac{3}{5}\frac{p_F^2}{m^2}q^2 + \cdots\right)\Big/\left(\frac{e^4 m}{2\hbar^2}\right)^2, \quad n = \frac{N}{\Omega}. \qquad (13)$$

*The second-order exchange correction is not included in expression (9) for the correlation energy.

*This formula for the case of the Fermi vacuum was obtained in the paper of Bogoliubov, Tiablikov, and Tolmachev which we cited earlier.

Aside from the plasma solution, we find from (8) only the trivial result $E_\alpha = \omega(\mathbf{p}, \mathbf{q})$ for the spectrum of elementary excitations. Thus, in our approximation the excitation energy of a pair is not changed by the interaction, or, in the language of quantum field theory, the excitation has no self energy. This is entirely natural since the matrix elements of the interaction potential corresponding to diagrams with external lines, which are the ones which would give rise to a self energy of the elementary excitations, were dropped in getting the model Hamiltonian.

We also note that η^* and η are not Bose amplitudes with respect to the excited state, since the occupation number of the excited state cannot at all be assumed to be zero. Consequently our model Hamiltonian is not suitable for investigating the spectrum of elementary excitations if we use the Fermi vacuum as the initial state.

4. ENERGY OF EXCITED STATES

This difficulty can be overcome as follows. We shall consider the model Hamiltonian (7), in which the initial state Φ_G represents the Fermi vacuum plus an electron-hole pair with momenta $\mathbf{p}_0 + \mathbf{q}_0$ and $\mathbf{p}_0$. Then all the preceding formulas remain valid except that, instead of (10), we have to substitute

$$\varkappa(\mathbf{p}) = \vartheta(\mathbf{p}) - \Delta(\mathbf{p} - \mathbf{p}_0) + \Delta(\mathbf{p} - \mathbf{p}_0 - \mathbf{q}_0),$$
$$\Delta(\mathbf{p}) = \begin{cases} 1, & \text{if } p = 0 \\ 0, & \text{if } p \neq 0. \end{cases} \tag{14}$$

The interaction Hamiltonian, consisting of operators η^* and η defined with respect to Φ_G, already contains processes of scattering of an electron (or hole) with absorption or emission of a pair with respect to the Fermi vacuum Φ_V. Thus the treatment of the new model Hamiltonian is equivalent to summation of diagrams of the type shown in Fig. 1 (except for the ground-state diagrams). Then the energy of excitation of a pair is given by the obvious relation:

$$\bar{E}(\mathbf{p}_0 + \mathbf{q}_0, \mathbf{p}_0) = E(\mathbf{p}_0 + \mathbf{q}_0, \mathbf{p}_0) - E_0 \tag{15}$$
$$= \omega(\mathbf{p}_0, \mathbf{q}_0) + W_x(\mathbf{p}_0, \mathbf{q}_0) + \Delta E(\Phi_G) - \Delta E(\Phi_V),$$

where $\bar{E}(\mathbf{p}_0 + \mathbf{q}_0, \mathbf{p}_0)$ is the excitation energy of a pair; $E(\mathbf{p}_0 + \mathbf{q}_0, \mathbf{p}_0)$ is the energy of the excited state containing one pair, and E_0 is the energy of the ground state. $W_X(\mathbf{p}_0, \mathbf{q}_0) = W_X(\mathbf{p}_0 + \mathbf{q}_0) - W_X(\mathbf{p}_0)$ is the exchange correction to the excitation energy of the pair. The expression for $W_X(\mathbf{p})$ is well known:

$$W_x(\mathbf{p}) = -\frac{1}{\pi \alpha r_s}\left[2 + \frac{1-p^2}{p}\ln\frac{1+p}{1-p}\right].$$

Substituting expression (11) for $\Delta E(\Phi_V)$ and $\Delta E(\Phi_G)$ in (15), using (10) and (14), and dropping all terms which vanish as $\Omega \to \infty$, we get the expression for the excitation energy of a pair

$$\bar{E}(\mathbf{p}_0 + \mathbf{q}_0, \mathbf{p}_0)$$
$$= \omega(\mathbf{p}_0, \mathbf{q}_0) + W_x(\mathbf{p}_0, \mathbf{q}_0) + G(\mathbf{p}_0 + \mathbf{q}_0) - G(\mathbf{p}_0),$$

$$G(\mathbf{p}_0) = -\frac{2}{\pi^3}\frac{1}{2\pi i} \tag{16}$$
$$\times\left[\int\limits_{|\mathbf{p}_0+\mathbf{q}|>1}\frac{d^3q}{q^2}\int_\Gamma \frac{\left(1 - z\tanh^{-1}\frac{1}{z}\right)2\omega(\mathbf{p}_0, \mathbf{q})\,dz}{\left[q^2 + \frac{4r_s\alpha}{\pi}\left(1 - z\tanh^{-1}\frac{1}{z}\right)\right](z^2 - \omega^2(\mathbf{p}_0, \mathbf{q}))}\right.$$
$$\left. + \int\limits_{|\mathbf{p}_0-\mathbf{q}|<1}\frac{d^3q}{q^2}\int_\Gamma \frac{\left(1 - z\tanh^{-1}\frac{1}{z}\right)2\omega(-\mathbf{p}_0, \mathbf{q})\,dz}{\left[q^2 + \frac{4r_s\alpha}{\pi}\left(1 - z\tanh^{-1}\frac{1}{z}\right)\right](z^2 - \omega^2(-\mathbf{p}_0, \mathbf{q}))}\right].$$

Using the obvious symmetry property $\bar{E}(-\mathbf{q}_0 - \mathbf{p}_0, -\mathbf{p}_0) = \bar{E}(\mathbf{p}_0 + \mathbf{q}_0, \mathbf{p}_0)$, we can change (16)* to the more convenient form:

$$G(\mathbf{p}_0) = -\frac{2}{\pi^4}\int\frac{d^3q}{q^2}$$
$$\times\int\limits_{-\infty}^{\infty}\frac{\left(1 - u\tan^{-1}\frac{1}{u}\right)\omega(\mathbf{p}_0, \mathbf{q})\,du}{\left[q^2 + \frac{4r_s\alpha}{\pi}\left(1 - u\tan^{-1}\frac{1}{u}\right)\right](u^2 + \omega^2(\mathbf{p}_0, \mathbf{q}))}. \tag{17}$$

From (17) we see that $G(\mathbf{p}_0)$ is independent of the volume of the system, which should have been anticipated from physical considerations, since this quantity represents the correlation correction to the energies of the elementary excitations, and these quantities are intensive quantities as $\Omega \to \infty$. The explicit form of $G(\mathbf{p}_0)$ can be obtained by numerical integration of (17).

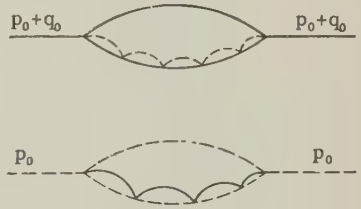

FIG. 1. We use diagrams of type considered in reference 3. The solid line shows the electron, the dotted line – the hole.

5. SPECIFIC-HEAT CORRECTION

From (16), we can easily find the correction to the specific heat in the Gell-Mann approximation.[5] For this purpose we need to know the derivative of $G(\mathbf{p}_0)$ at $|\mathbf{p}_0| = 1$ (from now on, we assume that $p_0 \gg 1$). Since the divergence in the perturbation series for the derivative of $G(\mathbf{p}_0)$ at $|\mathbf{p}_0| = 1$ appears one order earlier than for $G(\mathbf{p}_0)$, we need only include terms proportional to r_s^{-1} and $r_s^{-1}\ln r_s$.[5] In calculating the derivative of $G(\mathbf{p}_0)$

*In (16) and subsequent formulas, $\omega(\mathbf{p}_0, \mathbf{q}) = \mathbf{q}\cdot(2\mathbf{p}_0 + \mathbf{q})/2q$.

in this approximation, it is sufficient to differentiate (16) only with respect to the limit of the q integration, since the other terms give contributions of higher order in r_s. For the z integration it is convenient to choose the contour Γ as shown in Fig. 2. The integrals over Γ_1 and Γ_3 give no contribution, since the subsequent q integration goes only over the surface of the unit sphere $|q - p_0| = 1$ ($|p_0| = 1$), on which $\omega(p_0, q) = 0$. Thus we have

$$\frac{dG(p_0)}{dp_0}\Big|_{p_0=1} = \frac{-4}{\pi^3}\int \frac{d^3q}{q^2}\,\mathrm{res}\left[\frac{\left(1 - z\tanh^{-1}\frac{1}{z}\right)2\omega(p_0, q)\,(p_0, p_0 + q)}{\left[q^2 + \frac{4r_s\alpha}{\pi}\left(1 - z\tanh^{-1}\frac{1}{z}\right)\right](z^2 - \omega^2(p_0, q))}\right]$$

$$\times\,\delta(1 - |p_0 + q|) = \frac{-4}{\pi^3}\int \frac{d^3q}{q^2}\left[\frac{\left(1 - z\tanh^{-1}\frac{1}{z}\right)(p_0, p_0 + q)}{q^2 + \frac{4r_s\alpha}{\pi}\left(1 - z\tanh^{-1}\frac{1}{z}\right)}\right]_{z=\omega(p_0,q)} \delta(1 - |p_0 + q|)$$

(res denotes the residue at the point $z = \omega(p_0, q)$). Noting that $\omega(p_0, q) = 0$ on the surface $|q + p_0| = 1$ ($|p_0| = 1$), and also that $\lim_{z\to 0} z\tanh^{-1}(1/z) = 0$, we have

$$\frac{dG(p_0)}{dp_0}\Big|_{p_0=1} = \frac{-4}{\pi^3}\int \frac{d^3q\,(p_0, p_0 + q)}{q^4(1 + 4r_s\alpha/\pi q^2)}\,\delta(1 - |p_0 + q|)$$

$$= \frac{-2}{\pi^3}\int_{-1}^{+1} \frac{x\,dx}{(1 - x)^2(1 + 2r_s\alpha/\pi\,(1 - x))}. \qquad (18)$$

Here we have changed the integral over q to a surface integral over a sphere with center at p_0, and $x = p_0 \cdot (p_0 + q)$. Expression (18) diverges logarithmically. When we add to it the derivative of $W_X(p_0)$ at $p_0 = 1$, the logarithmic divergences cancel and we get an expression which is identical with Gell-Mann's[5] result:

$$\frac{\partial\bar{E}(p_0)}{\partial p_0}\Big|_{p_0=1} \approx \frac{2}{\alpha^2 r_s^2} + \frac{1}{\pi r_s\alpha}\int_{-1}^{+1}\frac{x\,dx}{(1-x)}\left[1 + \frac{2\alpha r_s}{\pi}\frac{1}{(1-x)}\right]^{-1}.$$

For the specific heat, we find the expression

$$c/c_F = \left(1 + \frac{\alpha r_s}{2\pi}[-\ln r_s + \ln[\pi/2] - 2] + \cdots\right)^{-1}, \qquad (19)$$

where c and c_F are the specific heats of the electron gas in the presence and absence of interaction, respectively.

6. DISCUSSION OF RESULTS

From the results of Secs. 3 and 4 it follows that in an electron gas there are two types of elementary excitations: excitations of individual pairs and excitations of the collective type (plasma oscillations). In investigating the physical properties of the electron gas in a metal at ordinary temperatures, excitations of the individual type are of primary interest, since we know that the plasma oscillations are not thermally excited. The essential point is that, even when we take account quite precisely of the dynamical correlations between electrons, the main role in these phenomena is played by the independent elementary excitations: the electron-hole pairs (quasi-particles, satisfying Fermi statistics). The divergences in the usual perturbation theory expansion for a system with Coulomb interaction prove to be ephemeral, and after appropriate formal manipulation give finite contributions to the energy of the ground state and the elementary excitations. These ideas are realized in a very simple way in the present paper by using the method of approximate second quantization. We have obtained finite expressions for the self energy of the elementary excitations. Therefore, to a certain extent our results can be regarded as a justification of the independent particle model in the electron theory of metals, which has been applied with great success to treat a variety of metallic properties despite the fact that this model completely neglects correlation effects. This problem has been repeatedly discussed by various authors (cf. for example, reference 7). The treatment of a more realistic model, in which the effect of the periodic field of the crystal lattice is included right from the start, will be the subject of a separate investigation.

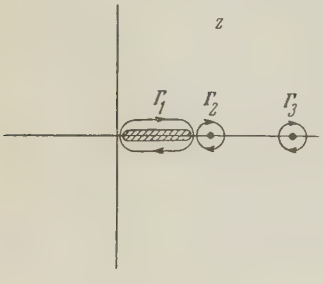

FIG. 2. The countour Γ is split into Γ_1, Γ_2, Γ_3. Γ_1 circles the cut from the origin to the point $z = 1$. Γ_2 and Γ_3 encircle the poles $z = \omega(p_0, q)$ and $z = \omega_p(q)$, respectively.

The authors take this opportunity to express their deep gratitude to Acad. N. N. Bogoliubov and V V. Tolmachev, under whose direction and constant interest this work was completed.

[1] M. Gell-Mann and K. A. Brueckner, Phys. Rev. **106**, 364 (1957).

[2] K. Sawada, Phys. Rev. **106**, 372 (1957).

[3] N. M. Hugenholtz, Physica **23**, 481 (1957).

[4] N. N. Bogoliubov, J. Exptl. Theoret. Phys. (U.S.S.R) **34**, 58, 73 (1958), Soviet Phys. JETP **7**, 41, 51 (1958); V. V. Tolmachev and S. V. Tiablikov, J. Exptl. Theoret. Phys. (U.S.S.R.) **34**, 66 (1958), Soviet Phys. JETP **7**, 46 (1958).

[5] M. Gell-Mann, Phys. Rev. **106**, 369 (1957).

[6] N. N. Bogoliubov, Лекции по квантовой статистике (Lectures on Quantum Statistics), Kiev, 1949.

[7] J. Bardeen and D. Pines, Phys. Rev. **99**, 1140 (1957).

Translated by M. Hamermesh
308

SOVIET PHYSICS JETP VOLUME 34 (7), NUMBER 6 DECEMBER, 1958

ON THE THEORY OF HIGH-SPIN PARTICLES

L. A. SHELEPIN

P. N. Lebedev Physics Institute, Academy of Sciences, U.S.S.R.

Submitted to JETP editor January 8, 1958

J. Exptl. Theoret. Phys. (U.S.S.R.) **34**, 1574-1586 (June, 1958)

An algebraic method is suggested for treating the relativistically invariant equations of high-spin particles. The direct product of generalized Dirac algebras underlies the analysis. This method can be used to obtain explicit expressions for the infinitesimal rotation matrix, the spin operator, the metric and reflection operator, as well as to limit the number of representations taken into account. The equations can be treated directly either in tensor or in spin-tensor form. The commutation relations are automatically obtained in parametric form.

1. INTRODUCTION

We consider relativistically invariant equations of the form

$$\alpha_k \partial_k \psi + \varkappa \psi = 0, \tag{1}$$

where ψ is a particle wave function with a finite number of components which transforms according to some finite-dimensional representation of the Lorentz group. Equation (1) shall be called relativistically invariant if under the Lorentz transformation $x'_i = l_{ik} x_k$ together with the transformation $\psi' = S\psi$ it remains formally invariant, in other words if

$$\alpha_i = l_{ij} S \alpha_j S^{-1}. \tag{2}$$

Now the conditions of (2) are fulfilled if

$$[I_{ik}, I_{jl}] = -\delta_{ij} I_{kl} + \delta_{il} I_{kj} + \delta_{kj} I_{il} - \delta_{kl} I_{ij}, \tag{3}$$

$$[\alpha_i, I_{jk}] = \delta_{ij} \alpha_k - \delta_{ik} \alpha_j, \tag{4}$$

where the I_{ij} are the infinitesimal-rotation matrices, defined by

$$\psi' = \psi + {}^1/_2 \varepsilon_{ik} I_{kl} \psi.$$

We shall consider here the problem of finding all relativistically-invariant equations (1) that satisfy the additional requirements that they be invariant under reflection, that there exist a nondegenerate real Lagrangian, that the energy density be positive definite for particles with integral spin or the charge be positive definite for particles with half-integral spin, and that the equations be irreducible.

This problem has been treated in general form by Gel'fand and Iaglom.[1] Their method can be used, in principle, to obtain all possible equations for high-spin particles. In actually obtaining the equations, however, certain difficulties arise. Among these are, in particular, the analysis of irreducibility, the transition to spin-tensor (or tensor) form, and the determination of the algebra of the α_k matrices. Further, there is no way to tell whether all of the equations belonging to a given maximum spin have been found.

While Gel'fand and Iaglom base their considerations on explicit expressions for the infinitesimal operators, Harish-Chandra[2,3] develops an algebraic method based on the study of an algebra designated $U(\alpha)$. This is the α-matrix algebra of the forms

$$G = c^k\alpha_k + c^{kl}\alpha_k\alpha_l + c^{klm}\alpha_k\alpha_l\alpha_m + \cdots,$$

where the $c^{k\cdots}$ are numerical coefficients. Harish-Chandra has shown that the I_{ij} matrices, the reflection matrix T, the metric matrix η (used in the definition of the bilinear invariant Hermitian form $\psi^+\eta\psi$), and the matrix S corresponding to the Lorentz transformation all belong to $U(\alpha)$. He has also shown that the α_k matrices must satisfy commutation relations which uniquely define $U(\alpha)$. He did not, however, give any concrete method for finding the matrices I_{ij}, T, η, and S, or the commutation relations of $U(\alpha)$. The present article (Sec. 2) gives such a method. It is based on a consideration of the direct product of generalized Dirac algebras $U(\Gamma)$

$$U(\alpha) = U(\Gamma)\times U(\Gamma')\times U(\Gamma'')\times\ldots$$

whose matrices Γ_i satisfy the commutation relations of Eq. (9). This method can be used to obtain and analyze equations both invariant and not invariant under reflection (these latter being of interest in connection with the nonconservation of parity in weak interactions). We shall obtain general expressions for I_{ij}, T, η, and α_k in terms of algebraic parameters. The method can be used to arrive at conclusions concerning the irreducibility of the equations, as well as to restrict the number of linked representations. In particular, we shall demonstrate (in Sec. 2) the reducibility* of the many-mass equations for spin-$\frac{1}{2}$, treated by Ulehla.[7] In our method the commutation relations for the α_k matrices are automatically obtained in parametric form. In Sec. 3 we obtain the commutation relation which Harish-Chandra[3] and Petras[5,6] found by selection. This method can be used to establish beforehand all of the equations belonging to a given maximum spin, without separate investigations of all possible methods of composition, among which many are equivalent. All of the analysis (the determination of the mass and spin states, the positive definite conditions) may be performed in spin-tensor (or tensor) form using a single standard method.

Section 2 is a general discussion, while the advantages of the method are shown in Sec. 3 by a concrete analysis of the equations for spin 1 and $\frac{3}{2}$.

2. GENERAL METHOD

We first make some general remarks. Let the $u_p(\alpha)$ (with $p = 1, \ldots, n$) form a linearly independent basis for the algebra $U(\alpha)$. Now $u_p(l\alpha)$ is also an element of $U(\alpha)$, and can therefore be expressed linearly in terms of the basis in the form

$$u_p(l\alpha) = \sum_q L_p^q u_q(\alpha). \tag{5}$$

Thus to each transformation l in α-space there corresponds a transformation L in U-space. The set of all L is a representation of the Lorentz group.[2] Using Eqs. (2) and (5), we immediately obtain the relation between this representation L and the representation S which transforms the ψ function. This relation is

$$\sum_q L_p^q u_q(\alpha) = u_p(S\alpha S^{-1}) = Su_p(\alpha)S^{-1}. \tag{6}$$

It is easily shown that this implies that if S can be written as the direct product of the representations which transform the wave functions ψ' and ψ'' that satisfy the equations

$$\alpha'_k\partial_k\psi' + \varkappa\psi' = 0,\ \alpha''_k\partial_k\psi'' + \varkappa\psi'' = 0,$$

then the algebra $U(\alpha)$ can be written in the form

$$U(\alpha) = U(\alpha')\times U(\alpha''). \tag{7}$$

The converse is also true. We recall that the direct product of an algebra with a decomposable algebra is also a decomposable algebra, from which we obtain the criterion for the reducibility of the equations.

Note that the equations given by Ulehla[7] for a spin-$\frac{1}{2}$ particle with several different mass states are reducible. Indeed, Ulehla's $U(\alpha)$ algebra corresponds to the representation (using Cartan's notation)

$$S = D(\tfrac{1}{2}, \tfrac{3}{2}) + D(\tfrac{3}{2}, \tfrac{1}{2}) + mD(0, \tfrac{1}{2}) + mD(\tfrac{1}{2}, 0),\ m \geqslant 2.$$

But this can be written as the direct product of the representations

$$[D(\tfrac{1}{2}, \tfrac{1}{2}) + (m-1)D(0,0)] \text{ or } [D(0, \tfrac{1}{2}) + D(\tfrac{1}{2}, 0)].$$

It is easily shown that any α_k matrix belonging to the first of these two representations is reducible unless m = 2. Thus all of Ulehla's equations are decomposable, except that for a single mass. This will be seen to follow automatically, furthermore, from the theory developed below.

All the finite-dimensional representations of the Lorentz group, which transform some wave function ψ, can be written as the direct sums of quantities D(m, n), where m and n are positive integers or half integers, including zero. Every such sum can be obtained by forming products of the form $\prod_i [k_i D(0, \tfrac{1}{2}) + l_i D(\tfrac{1}{2}, 0)]$. Using the crite-

*Ulehla's single-mass equation for spin-1/2 is irreducible.

rion for reducibility, we see immediately that the most general case involves direct products of representations of the form

$$D(0, {}^1/_2) + D({}^1/_2, 0). \tag{8}$$

All irreducible equations can be obtained by treating n algebras $U(\Gamma)$ corresponding to Eq. (8). An algebra $U(\Gamma)$ is a generalized Dirac algebra, for which the commutation relations hold:

$$\Gamma_k\Gamma_i + \Gamma_i\Gamma_k = 2p\delta_{ik} \tag{9}$$

(where p is any complex number). The matrix Γ_k can be written

$$\Gamma_k = \begin{pmatrix} 0 & a\sigma_k \\ b\sigma_k & 0 \end{pmatrix}, \quad p = ab,$$

while the ordinary Dirac matrices are

$$\gamma_k = \begin{pmatrix} 0 & i\sigma_k \\ -i\sigma_k & 0 \end{pmatrix}.$$

Let us thus consider the direct product of n of these algebras, or

$$U(\alpha) = U(\Gamma)\times U(\Gamma')\times U(\Gamma'')\times \ldots . \tag{10}$$

We first find the matrices I_{kj} and α_k of the algebra $U(\alpha)$. To do this, we note that α_k and $I_{kj} = -I_{jk}$ must be covariant in the indices k and kj with respect to Lorentz transformations. For the direct product of two $U(\Gamma)$ algebras we obtain in the most general case, using Eq. (9),

$$\begin{aligned} \alpha_k &= \Gamma_k(b_0 + b_1\Gamma_l\Gamma'_l + b_2\Gamma_l\Gamma_m\Gamma'_l\Gamma'_m + b_3\Gamma_l\Gamma_m\Gamma_n\Gamma'_l\Gamma'_m\Gamma'_n + b_4\Gamma_l\Gamma_m\Gamma_n\Gamma_r\Gamma'_l\Gamma'_m\Gamma'_n\Gamma'_r) \\ &+ \Gamma'_k(c_0 + c_1\Gamma_l\Gamma'_l + c_2\Gamma_l\Gamma_m\Gamma'_l\Gamma'_m + c_3\Gamma_l\Gamma_m\Gamma_n\Gamma'_l\Gamma'_m\Gamma'_n + c_4\Gamma_l\Gamma_m\Gamma_n\Gamma_r\Gamma'_l\Gamma'_m\Gamma'_n\Gamma'_r), \\ I_{kj} &= (\Gamma_k\Gamma_j + \Gamma_j\Gamma_k)(g_0 + g_1\Gamma_l\Gamma'_l + g_2\Gamma_l\Gamma_m\Gamma'_l\Gamma'_m + g_3\Gamma_l\Gamma_m\Gamma_n\Gamma'_l\Gamma'_m\Gamma'_n \\ &+ g_4\Gamma_l\Gamma_m\Gamma_n\Gamma_r\Gamma'_l\Gamma'_m\Gamma'_n\Gamma'_r) + (\Gamma'_k\Gamma'_j - \Gamma'_j\Gamma'_k)(g'_0 + g'_1\Gamma_l\Gamma'_l + \cdots) \\ &+ (\Gamma_k\Gamma'_j - \Gamma'_j\Gamma_k)(g''_0 + g''_1\Gamma_l\Gamma'_l + \cdots). \end{aligned} \tag{11}$$

For the direct product of a large number of algebras we obtain much more complicated expressions. However, relations (3) and (4) must be satisfied if the equations are to be relativistically invariant and the I_{kj} are to be infinitesimal rotation operators. This places some restrictions on the coefficients b_i, c_i, and g_i. We now insert equations such as (11) into (3) and (4), and after very cumbersome, though algebraically simple calculations, we find that for the most general case of products of 1, 2, . . . , or n algebras $U(\Gamma)$, the I_{ij} are given by

$$\begin{aligned} I_{ij} &= g_1(\Gamma_i\Gamma_j - \Gamma_j\Gamma_i), \\ I_{ij} &= g_1(\Gamma_i\Gamma'_j - \Gamma_j\Gamma_i) + g_2(\Gamma'_i\Gamma'_j - \Gamma'_j\Gamma'_i), \\ I_{ij} &= \sum_{k=1}^{n} g_k(\Gamma_i^{(k)}\Gamma_j^{(k)} - \Gamma_j^{(k)}\Gamma_i^{(k)}). \end{aligned} \tag{12}$$

Here the coefficients g_k satisfy the conditions $g_k(4p_kg_k - 1) = 0$ (no summation over k).

From these expressions we automatically obtain the minimal equations

$$\begin{aligned} &I_{ij}^2 + \tfrac{1}{4} = 0; \quad I_{ij}(I_{ij}^2 + 1) = 0; \\ &\left(I_{ij}^2 + \tfrac{1}{4}\right)\left(I_{ij}^2 + \tfrac{9}{4}\right) = 0 \text{ etc.} \end{aligned} \tag{13}$$

for the squares of the infinitesimal-rotation operators. The I_{ij} corresponding to space rotations are spin-component matrices. Equations (3) and (4) place only one restriction on the α_k. This is that the number of algebras in the direct product of (10) is uniquely determined by the maximum spin for the particle. Thus all relativistically-invariant irreducible equations with maximum spin 1 can be obtained by considering the direct product of two $U(\Gamma)$ algebras. Those with maximum spin $^3/_2$ are obtained by considering the direct product of three $U(\Gamma)$ algebras, etc.

For the equations to be invariant under reflection in space, the reflection matrix must satisfy the relations[1]

$$T^2 = E, \text{ where E is the unit matrix} \tag{14}$$

$$[T, I_{jk}]_- = 0, \quad j \neq 0, \quad k \neq 0;$$

$$[T, I_{jk}]_+ = 0, \quad j = 0, \text{ or } k = 0, \tag{15}$$

$$[T, \alpha_k]_+ = 0, \quad k = 1, 2, 3; \quad [T, \alpha_0]_- = 0. \tag{16}$$

According to (15), T must be of the form

$$T = \Gamma_0 \times \Gamma'_0 \times \Gamma''_0 \times \ldots .$$

If (14) is true, then in the most general case for a single algebra we have

$$\alpha_k = \cos\varphi\,\gamma_k + i\sin\varphi\,\gamma_5\gamma_k.$$

All the values of the parameter φ are equivalent, and we can thus always choose $\alpha_k = \gamma_k$ and $T = \gamma_0$. In the general case, however, we must treat two kinds of direct products, namely

$$U(\gamma_k)\times U(\gamma'_k)\times \ldots \text{and } U(i\gamma_5\gamma_k)\times U(i\gamma'_5\gamma'_k)\times \ldots .$$

For the direct product of two algebras, T has the two nonequivalent definitions

$$T = \gamma_0\gamma_0', \quad T = -\gamma_5\gamma_5'\gamma_0\gamma_0', \tag{17}$$

corresponding to the tensor and pseudotensor theories. For three algebras there are also two nonequivalent reflection laws, namely

$$T = \gamma_0\gamma_0'\gamma_0'', \quad T = -\gamma_0\gamma_5'\gamma_0'\gamma_5''\gamma_0'', \tag{18}$$

corresponding to the spinor and the pseudospinor theories, etc. In general when treating equations invariant under reflection, it is necessary and sufficient to consider the direct product of ordinary Dirac algebras together with the two different possible reflection laws indicated in (17) and (18).

The existence of an invariant real Lagrangian for Eq. (1) requires the existence of a bilinear invariant Hermitian form $\psi_1^+\eta\psi_2$, where η is the metric matrix. If this is to be a Lorentz invariant, reflection invariant, and Hermitian form, and if the Lagrangian for the equation is to be real, then we must have

$$\left.\begin{aligned} &[\eta, I_{jk}]_- = 0, \ j \neq 0, \ k \neq 0; \ [\eta, I_{jk}]_+ = 0, \ j = 0 \ \text{ or } \ k = 0; \\ &T\eta T = \eta; \qquad \eta = \eta^+; \end{aligned}\right\} \tag{19}$$

$$(\eta\alpha_k)^+ = -\eta\alpha_k, \ k = 1, 2, 3; \ (\eta\alpha_0)^+ = \eta\alpha_0. \tag{20}$$

It is easily shown that conditions (19) imply that in our representation T and η are represented by matrices which are equivalent up to a constant factor. On going to another representation, however, T and η in general transform differently. The allowable transformations R under which the theory is invariant are of the form[8]

$$\begin{aligned} &\psi \to \psi' = R^{-1}\psi, \quad \eta \to \eta' = R^+\eta R; \\ &\alpha_k \to \alpha_k' = R^{-1}\alpha_k R, \quad T \to T' = R^{-1}TR. \end{aligned} \tag{21}$$

In any representation, therefore, we may write

$$\eta = \Lambda T, \tag{22}$$

where Λ is a scalar matrix (see also Harish-Chandra[3]). Relations (20) restrict the coefficients in the expression for the α_k.

These coefficients are restricted also by the requirements that there exist mass and spin eigenstates and that either the charge or energy be positive definite. We proceed with the first of these requirements. Consider the spin operator Z. As is known, $Z^2 = Z_x^2 + Z_y^2 + Z_z^2$. But the infinitesimal space rotation operators are just the spin-component operators. Therefore

$$Z^2 = I_{12}^2 + I_{23}^2 + I_{31}^2. \tag{23}$$

We find the eigenfunction belonging to a given value of the total spin by solving

$$Z^2\psi_\xi = \xi(\xi + 1)\psi_\xi. \tag{24}$$

We now apply the mass operator α_0 to each of the eigenfunctions ψ_ξ, obtaining

$$\alpha_0\psi_\xi = \lambda\psi_\xi. \tag{25}$$

In this way we find the eigenvalues λ and eigenfunctions $\psi_{\xi\lambda}$ of α_0, and hence the mass states.

At this point the analysis can be brought directly into algebraic form. To find states with positive definite energy density, we then must require that

$$\eta\alpha_0^{f(n)+2} \geqslant 0, \tag{26}$$

whereas if the charge is to be definite, we require

$$\eta\alpha_0^{f(n)+1} \geqslant 0, \tag{27}$$

where the inequality means that the eigenvalues of the matrix are greater than or equal to zero.[3] Here $f(n) = n$ when n is even, $f(n) = n - 1$ when n is odd, and n is the lowest power in the minimal polynomial $\alpha_0^n(\alpha_0^2 - 1)\ldots(\alpha_0^2 - m^2)$.

The analysis can be cast in spin-tensor (or tensor) form, and the transition to this form is elementary. Then for each simultaneous eigenfunction $\psi_{\xi\lambda}$ of the spin and mass, we must require that

$$\psi_{\xi\lambda}^+\eta\alpha_0\psi_{\xi\lambda} \geqslant 0, \tag{28}$$

or

$$\psi_{\xi\lambda}^+\eta_i\psi_{\xi\lambda} \geqslant 0 \tag{29}$$

for half integral or integral spin, respectively.

As an example, we apply this method in the next section to the equations with maximum spin 1 in algebraic form, and to those with maximum spin $\frac{3}{2}$ in spin-tensor form. The commutation relations are then automatically obtained in parametric form.

3. SPECIFIC EXAMPLES

The case of maximum spin $\frac{1}{2}$ is trivial. There is only one irreducible equation which satisfies the necessary physical requirements, namely the Dirac equation, for which

$$\begin{aligned} &\alpha_k = \gamma_k; \ T = \eta = \gamma_0; \ \eta\alpha_0 = 1 > 0, \ I_{ij} = \tfrac{1}{4}(\gamma_i\gamma_j - \gamma_j\gamma_i), \\ &\gamma_i\gamma_j + \gamma_j\gamma_i = 2\delta_{ij}. \end{aligned} \tag{30}$$

As mentioned in the previous section, we shall treat maximum spin 1 algebraically. The most general form of the α_k for an equation which is relativistically invariant and invariant under reflection is

$$\begin{aligned} \alpha_k = {} & \gamma_k(b_0 + b_1J + b_2J^2 + b_3Js + b_4s) \\ & + \gamma_k'(c_0 + c_1J + c_2J^2 + c_3Js + c_4s), \\ & J = \gamma_l\gamma_l', \ s = \gamma_5\gamma_5'. \end{aligned} \tag{31}$$

Inserting α_0 and $\eta = \gamma_0\gamma_0'$ into (20), we find that the conditions for the existence of an invariant La-

grangian are

$$\begin{aligned} &\operatorname{Im} c_0 = \operatorname{Im}(b_1 - 2c_2),\ \operatorname{Re} c_1 = 2b_2,\ \operatorname{Re} c_4 = b_3,\\ &\operatorname{Im} b_0 = \operatorname{Im}(c_1 - 2b_2),\ \operatorname{Re} b_1 = 2c_2,\ \operatorname{Re} b_4 = c_3,\\ &\operatorname{Im} c_1 = \operatorname{Im} c_3 = \operatorname{Im} b_2 = \operatorname{Im} b_3 = 0. \end{aligned} \tag{32}$$

Let us perform an equivalence transformation (21) of the form

$$R = a_0 + a_1 J + a_2 J^2 + a_3 Js + a_4 s. \tag{33}$$

We have at our disposal four arbitrary constants. In the transformed matrix we can choose $b_1 = b_4 = 0$. Then, according to (32), $a_3 = b_2 = c_3 = c_2 = 0$, and b_0 and c_0 are real. Thus, if an invariant Lagrangian exists, we may restrict our considerations to $\alpha_k = b_0\gamma_k + c_0\gamma'_k$.

If the energy density is to be positive definite, then

$$\eta\alpha_0^2 \geqslant 0. \tag{34}$$

Since $\eta\alpha_0^2 = (b_0^2 + c_0^2)\gamma_0\gamma'_0 + 2b_0c_0$ and $\gamma_0\gamma'_0$ have eigenvalues ± 1, we may write (34) in the form

$$b_0^2 + c_0^2 \leqslant 2b_0c_0,$$

which can happen only if $b_0 = c_0$. If $b = 1/2$, the minimal equation for α_0 is

$$\alpha_0(\alpha_0^2 - 1) = 0. \tag{35}$$

Thus the α_k are given by

$$\alpha_k = {}^1/_2(\gamma_k + \gamma'_k). \tag{36}$$

This leads simply to the Duffin-Kemmer commutation relations

$$\alpha_k\alpha_i\alpha_l + \alpha_l\alpha_i\alpha_k = \delta_{li}\alpha_k + \delta_{ki}\alpha_l. \tag{37}$$

On going to tensor form, the direct product of two bispinors decomposes into a scalar C, a pseudoscalar $\tilde{C}$, a vector A^m, a pseudovector $\tilde{A}^m$, and a second-rank tensor H^{nm}. Here the symbol $\sim$ denotes the pseudo-quantity. In tensor form Eq. (1) is

$$\begin{aligned} &\partial_k A^k + \varkappa C = 0,\ (\partial_n\tilde{A}^m - \partial_m\tilde{A}^n) + \varkappa\tilde{H}^{mn} = 0,\\ &\partial_m C + \varkappa A^m = 0,\ \partial_n\tilde{H}^{mn} + \varkappa\tilde{A}^m = 0. \end{aligned} \tag{38}$$

In the other theory, which corresponds to $T = \eta = -\gamma_5\gamma'_5\gamma_0\gamma'_0$, we have

$$\begin{aligned} &\partial_k\tilde{A}^k + \varkappa\tilde{C} = 0, \qquad (\partial_n A^m - \partial_m A^n) + \varkappa H^{mn} = 0,\\ &\partial_m\tilde{C} + \varkappa\tilde{A}^m = 0, \qquad \partial_n H^{mn} + \varkappa A^m = 0. \end{aligned} \tag{39}$$

As is seen, the algebra of the α_k matrices is decomposable. The α_k matrices can be written in the form

$$\alpha_k = \begin{pmatrix} 0 & 0 & 0 \\ 0 & \beta_k & 0 \\ 0 & 0 & \hat{\beta}_k \end{pmatrix}.$$

The algebra formed by these matrices contains 126 independent matrices. It decomposes into a homogeneous algebra containing only the known matrix, a five-dimensional algebra $U(\beta)$, and a ten-dimensional algebra $U(\hat{\beta})$. From the explicit form

$$(\beta_k)_{nm} = \begin{pmatrix} 0 & \delta_{km} \\ \delta_{nk} & 0 \end{pmatrix},\ (\hat{\beta}_k)_{\substack{rsm\\ r's'm'}} = \begin{pmatrix} 0 & \delta_{rk}\delta_{sm'} - \delta_{sk}\delta_{rm'} \\ \delta_{kr'}\delta_{ms'} - \delta_{ns}\delta_{mr'} & 0 \end{pmatrix} \tag{40}$$

of the matrices, we obtain the commutation relations for the algebras $U(\beta)$ and $U(\hat{\beta})$, namely

$$\begin{aligned} &\beta_i\beta_k\beta_l + \beta_l\beta_k\beta_i = \delta_{ik}\beta_l + \delta_{kl}\beta_i\\ &\beta_i\beta_k\beta_l = 0, \quad \text{if} \quad i \neq k,\ l \neq k,\\ &\beta_\alpha^2\beta_l = \beta_{\alpha'}^2\beta_l,\ \alpha \neq \alpha' \neq l,\\ &B^2 = 5B - 4E, \text{ where } B = \sum_\alpha \beta_\alpha^2. \end{aligned} \tag{41}$$

These four relations uniquely define a $U(\beta)$ algebra with 25 independent matrices.

The algebra $U(\hat{\beta})$ is uniquely defined by the commutation relations

$$\begin{aligned} &\hat{\beta}_i\hat{\beta}_k\hat{\beta}_l + \hat{\beta}_l\hat{\beta}_k\hat{\beta}_i = \delta_{lk}\hat{\beta}_i + \delta_{ik}\hat{\beta}_l.\\ &B^2 = 5B - 6E. \end{aligned} \tag{42}$$

This contains 100 independent matrices, corresponding to the ten-dimensional representation.

We note that (41) and (42) are very important results. For instance, Petras[6] obtained parametric commutation relations in which β was a parameter, but which did not include all of Eq. (41) (the third relation was missing). His expressions cannot be used alone to obtain the complete commutation relations explicitly. A similar remark can be made about the work of Harish-Chandra.[3]

By finding the eigenvalues of the spin operator, we can show that the five-dimensional representation corresponds to a particle with spin 0, and that the ten-dimensional representation corresponds to one with spin 1. Thus there exist only four irreducible equations satisfying the physical requirements. Their matrices satisfy the commutation relations (41) and (42), namely

$$\begin{aligned} &\text{in the } U(\beta) \text{ algebra } I_{ij} = \beta_i\beta_j - \beta_j\beta_i,\ T = \eta = 2\beta_0^2 - 1;\\ &\text{in the } U(\hat{\beta}) \text{ algebra } I_{ij} = \hat{\beta}_i\hat{\beta}_j - \hat{\beta}_j\hat{\beta}_i,\ T = \eta = 2\beta_0^2 - 1. \end{aligned} \tag{43}$$

Here we have $T\psi = +\psi$ or $T\psi = -\psi$ depending on whether we are using the tensor or pseudotensor theory.

For the case of maximum spin $3/2$, all allowable α_k matrices are contained in the direct product of three Dirac algebras. We are interested, however, only in those equations for which there exists an invariant Lagrangian. It is known[1] that α_k cannot correspond to an equation for which there exists an invariant Lagrangian if $D(m, n)$ and $D(n, m)$

are not both contained in the representation according to which ψ transforms, or in other words if this representation is not symmetric. Multiplication again by $D(0, \frac{1}{2}) + D(\frac{1}{2}, 0)$ would give an asymmetric expression. In that case the resulting direct product would be one for which no invariant Lagrangian exists. We need therefore consider the direct product only of those algebras for which there is an invariant Lagrangian. Then the α_k matrices of a direct product of two Dirac algebras can always be written in the form $(\gamma_i + \gamma_i')/2$. But the algebra $U[(\gamma_i + \gamma_i')/2]$ is decomposable. Therefore all of the desired irreducible equations with maximum spin $\frac{3}{2}$ can be obtained by considering the direct products

$$U(\gamma_i) \times U(\beta_i), \tag{44}$$

$$U(\gamma_i) \times U(\hat{\beta}_i) \tag{45}$$

(including both the spinor and pseudospinor theories).

In order to exhibit the possibilities of our method, let us consider the algebra indicated in (44) in spinor form. The most general form of the α_k for this direct product is

$$\alpha_k = b_1\gamma_k + b_2\gamma_k\gamma_l\beta_l + b_3\gamma_k\beta_l\beta_l + b_4\gamma_l\beta_k\beta_l + b_5\gamma_l\beta_l\beta_k + b_6\beta_k + b_7\beta_k\beta_l\beta_l + b_8\gamma_k\gamma_l\gamma_m\beta_l\beta_m + b_9\gamma_k\gamma_l\beta_m\beta_m\beta_l. \tag{46}$$

Equation (1) with the α_k given by (46) can be written in the spin-tensor form

$$\begin{aligned} a_{11}\gamma_k\partial_k\psi_1 + a_{12}\gamma_k\partial_k\psi_2 + a_{13}\partial_k F_k + \varkappa\psi_1 = 0,\\ a_{21}\gamma_k\partial_k\psi_1 + a_{22}\gamma_k\partial_k\psi_2 + a_{23}\partial_k F_k + \varkappa\psi_2 = 0,\\ a_{31}\hat{R}_n\psi_1 + a_{32}\hat{R}_n\psi_2 + a_{33}Q_{ns}F_s + \varkappa F_n = 0. \end{aligned} \tag{47}$$

Here $\hat{R}_n = \partial_n - \frac{1}{4}\gamma_n\gamma_k\partial_k$, $Q_{ns} = \delta_{ns}\gamma_k\partial_k - \frac{1}{2}\gamma_n\partial_s$, $\begin{pmatrix}\psi_1\\ \psi_2\\ F_n\end{pmatrix}$ is the wave function of the system, ψ_1 and ψ_2 are bispinors, and the spin tensor F_n satisfies the equation $\gamma_n F_n = 0$. The a_{ij} are related to the b_i by

$$\begin{aligned} a_{11} = b_1 + 4b_3 + b_4 + b_5 - 2b_8,\ a_{12} = 2b_2 + b_6 + b_7 + 16b_9,\\ a_{22} = -\tfrac{1}{2}b_1 - \tfrac{1}{2}b_3 + b_4 + b_5 + 4b_8,\\ a_{21} = -\tfrac{1}{2}b_2 + \tfrac{1}{4}b_6 + b_7 - \tfrac{1}{2}b_9,\\ a_{33} = b_1 + b_3,\quad a_{13} = b_6 + b_7,\\ a_{32} = 2b_1 + 2b_3 + 4b_4,\quad a_{31} = 2b_2 + b_6 + 4b_7 + 2b_9,\\ a_{23} = \tfrac{1}{2}b_1 + \tfrac{1}{2}b_3 + b_5. \end{aligned} \tag{48}$$

To find the spin and mass states, we note that according to (12) and (43) the infinitesimal rotation operator can be written

$$I_{ij} = \tfrac{1}{4}(\gamma_i\gamma_j - \gamma_j\gamma_i) + \beta_i\beta_j - \beta_j\beta_i. \tag{49}$$

The squares of the I_{ij} satisfy

$$(I_{ij}^2 + \tfrac{1}{4})(I_{ij}^2 + \tfrac{9}{4}) = 0.$$

To separate the states with spin $\frac{1}{2}$ from those with spin $\frac{3}{2}$, we shall write out the spin operator Z^2. According to (23) and (49), the result of operating on ψ with Z^2 is

$$\begin{aligned} &\tfrac{3}{4}\psi_1\\ &\tfrac{3}{4}\psi_2\\ &2(\delta_{n1}F_1 + \delta_{n2}F_2 + \delta_{n3}F_3) - [(\delta_{n2}\gamma_2 + \delta_{n3}\gamma_3)\gamma_1 F_1 + (\delta_{n3}\gamma_3\\ &+ \delta_{n1}\gamma_1)\gamma_2 F_2 + (\delta_{n1}\gamma_1 + \delta_{n2}\gamma_2)\gamma_3 F_3] + \tfrac{3}{4}F_n. \end{aligned} \tag{50}$$

Setting $\xi = \frac{1}{2}$ in (24), we obtain the spin-$\frac{1}{2}$ eigenfunction. This is the wave function in which ψ_1, ψ_2, and F_0 are arbitrary, but $-\gamma_1F_1 = -\gamma_2F_2 = -\gamma_3F_3 = (\frac{1}{3})\gamma_0F_0$ (twelve independent quantities). We now set $\xi = \frac{3}{2}$, obtaining $F_0 = \psi_1 = \psi_2 = 0$, and $\gamma_1F_1 + \gamma_2F_2 + \gamma_3F_3 = 0$ (only eight independent quantities).

The eigenvalues and eigenfunctions of the mass operator α_0 are determined by the equations

spin 3/2:
$$\begin{aligned} a_{33}\gamma_0F_i = \lambda F_i;\\ a_{11}\gamma_0\psi_1 + a_{12}\gamma_0\psi_2 + a_{13}F_0 = \lambda\psi_1, \end{aligned} \tag{51}$$

spin 1/2:
$$\begin{aligned} a_{21}\gamma_0\psi_1 + a_{22}\gamma_0\psi_2 + a_{23}F_0 = \lambda\psi_2,\\ \tfrac{3}{4}a_{31}\gamma_0\psi_1 + \tfrac{3}{4}a_{32}\gamma_0\psi_2 + \tfrac{1}{2}a_{33}F_0 = \lambda\gamma_0F_0. \end{aligned} \tag{52}$$

Using the explicit expression for γ_0, it can be shown that the eigenfunctions of γ_0 belonging to the eigenvalues ± 1 are not linked. Thus to every positive root $+\lambda$ there corresponds a negative root $-\lambda$ (see also Gel'fand and Iaglom[4]). For the state with spin $\frac{3}{2}$ we have $\lambda = a_{33}$.

It is easily seen from (52) that if at least one state with spin $\frac{1}{2}$ is to exist, we must have

$$\begin{aligned} \tfrac{3}{4}a_{13}a_{31} = -\frac{a_{11}^2(a_{22} + a_{33}/2)}{a_{22} - a_{11}};\\ \tfrac{3}{4}a_{23}a_{32} = \frac{a_{22}^2(a_{11} + a_{33}/2)}{a_{22} - a_{11}}. \end{aligned} \tag{53}$$

In this case

$$\lambda_{1,2} = \pm(a_{11} + a_{22} + \tfrac{1}{2}a_{33}),\ \lambda_{3,4} = \lambda_{5,6} = 0.$$

Since we have restricted our considerations to (44), there are three inequivalent possibilities for the matrix η. These are

$$\eta = \gamma_0(\gamma_0'\gamma_0''),\ \eta = \gamma_0(i\gamma_5'\gamma_0'\cdot i\gamma_5''\gamma_0''),$$
$$\eta = i\gamma_5\gamma_0\cdot(i\gamma_5'\gamma_0'\cdot\gamma_0'').$$

In the algebra given by (44) these correspond to

$$T = \eta = \gamma_0(2\beta_0^2 - 1), \tag{54}$$

$$T = \eta = \gamma_0(2\beta_0^2 - 1) - \tfrac{1}{2}\gamma_l\gamma_0\gamma_m\beta_l\beta_m, \tag{55}$$

$$T = \eta = \gamma_0(2\beta_0^2 + \tfrac{2}{3} - \tfrac{5}{3}\beta_l^2) - \tfrac{1}{2}\gamma_l\gamma_0\gamma_m\beta_l\beta_m. \tag{56}$$

Inserting (54) and α_0 into the quadratic form $\psi^+\eta\alpha_0\psi$, we have

$$\psi^+\eta\alpha_0\psi = a_{11}\psi_1^+\psi_1 + a_{13}\psi_1^+\gamma_0 F_0 + a_{22}\psi_2^+\psi_2 + a_{23}\psi_2^+\gamma_0 F_0 + a_{31}F_0^+\gamma_0\psi_1 + a_{32}F_0^+\gamma_0\psi_2 + a_{33}F_0^+F_0 - a_{33}F_n^+F_n.$$

It is seen from this that a necessary condition for the existence of an invariant real Lagrangian is that

$$\bar{a}_{11} = a_{11},\ \bar{a}_{22} = a_{22},\ \bar{a}_{33} = a_{33},\ a_{13} = \bar{a}_{31},\ a_{23} = \bar{a}_{32}. \quad (57)$$

We now investigate the conditions under which the charge density is positive definite, using (28). It can be shown that if two or three mass states with spin $\frac{1}{2}$ exist, the conditions on the a_{ik} are necessarily contradictory. If there is only one mass state with spin $\frac{1}{2}$, we have

$$-a_{33}F_n^+F_n > 0,\ \frac{(a_{11}+a_{22}+a_{33}/2)^2}{(a_{11}+a_{33}/2)(a_{22}+a_{33}/2)}F_0^+F_0 \geqslant 0. \quad (58)$$

Conditions (53), (57), and (58) are contradictory, i.e., it is impossible to introduce a positive definite charge density in the case given by (54).

Similar considerations hold for equations (55) and (56). If there exists only one state with spin $\frac{1}{2}$, a definite charge density can be introduced. If

$$T = \eta = \gamma_0(2\beta_0^2 - 1) - \tfrac{1}{2}\gamma_l\gamma_0\gamma_m\beta_l\beta_m$$

(pseudospinor theory) the conditions for the existence of a Lagrangian are

$$\bar{a}_{11} = a_{11},\ \bar{a}_{22} = a_{22},\ \bar{a}_{33} = a_{33},\ 2\bar{a}_{13} = a_{31},\ -\bar{a}_{23} = a_{32}, \quad (59)$$

and those for a definite charge are

$$a_{33} > 0,\ a_{11} > a_{22},\ a_{11} < -a_{33}/2. \quad (60)$$

If

$$T = \eta = \gamma_0(2\beta_0^2 + \tfrac{2}{3} - \tfrac{5}{3}\beta_l^2) - \tfrac{1}{2}\gamma_l\gamma_0\gamma_m\beta_l\beta_m$$

(spinor theory) the conditions for the existence of a Lagrangian are

$$\bar{a}_{11} = a_{11},\ \bar{a}_{22} = a_{22},\ \bar{a}_{33} = a_{33},\ -3\bar{a}_{13} = a_{31},\ -\bar{a}_{23} = a_{32}, \quad (61)$$

and those for a definite charge are

$$a_{33} > 0,\ a_{11} > -(a_{22} + a_{33}/2),\ a_{22} < -a_{33}/2. \quad (62)$$

The spin-$\frac{1}{2}$ equations with a single mass state must satisfy the subsidiary conditions

$$(a_{31}/a_{11}^2)\psi_1 + (a_{32}/a_{22}^2)\psi_2 = 0,$$
$$(\tfrac{3}{4}M + \gamma_\nu\partial_\nu)(a_{31}\psi_1 + a_{32}\psi_2) + \tfrac{3}{8}a_{33}M\left(\frac{a_{31}}{a_{11}}\psi_1 + \frac{a_{32}}{a_{12}}\psi_2\right) + a_{33}(\tfrac{1}{2}\partial_\nu F_\nu - \gamma_0\gamma_\nu\partial_\nu F_0) - \varkappa\gamma_0 F_0 = 0;\ \nu = 1,2,3;\ M = \varkappa(a_{11} + a_{22} + \tfrac{1}{2}a_{33})^{-1}. \quad (63)$$

With the aid of (48), we obtain commutation relations for the α_k in the parametric form

$$\alpha_k = (a_{33} - b_3)\gamma_k + b_3\gamma_k\beta_l\beta_l + (\tfrac{1}{4}a_{32} - \tfrac{1}{2}a_{33})\gamma_l\beta_k\beta_l + (a_{23} - \tfrac{1}{2}a_{33})\gamma_l\beta_l\beta_k + b_8\gamma_k\gamma_l\gamma_m\beta_l\beta_m + \tfrac{1}{12}\{(4a_{31} + a_{13})\gamma_k\gamma_l\beta_l + 2(-a_{31} + 8a_{13})\beta_k + 2(a_{31} - 2a_{13})\beta_k\beta_l\beta_l - (a_{31} + a_{13})\gamma_k\gamma_l\beta_m\beta_m\beta_l\}; \quad (64)$$
$$b_8 = \tfrac{1}{4}(a_{22} + \tfrac{3}{2}a_{33} - a_{23} - \tfrac{1}{4}a_{32});\ b_3 = \tfrac{1}{3}(a_{11} + \tfrac{1}{2}a_{22} + \tfrac{3}{4}a_{33} - \tfrac{3}{2}a_{23} - \tfrac{3}{8}a_{32}).$$

Here the commutation relations between the γ matrices are given by (30), while those between the β matrices are given by (41). The values of the constants a_{13}, a_{31}, a_{32}, and a_{23} depend on the choice of theory.

Thus we see that physical requirements lead to definite restrictions on the coefficients a_{ij}. If we specify the mass states we can write the equations for special cases. Then the values of a_{11}, a_{22}, and a_{33} will be fixed. Inserting these into the appropriate formulas, we obtain the positive definite conditions, the subsidiary conditions, and the algebra of the α_k matrices without performing any further calculations. There exist only four types of equations (with spinor and pseudospinor versions). These are the following.

1. The Ginzburg equation, with $a_{33} = 1$. This equation was obtained by Ginzburg[9] in 1943 in spin-tensor form. In 1952 Bhabha[8] dealt with it in spinor form, and it has been treated in detail by Fainberg,[10] It describes a particle which can be found in two states with spin $\frac{3}{2}$ and $\frac{1}{2}$. If $a_{22} = -a_{33}/2$ or $a_{11} = -a_{33}/2$, it breaks up into the Dirac equation and the Pauli-Fierz equation. We remark that the positive-energy equation given algebraically by Harish-Chandra[3] is a special case of the Ginzburg equation.

2. The Fradkin equation with $a_{33} = 1$, $a_{22} = -(a_{11} + \frac{1}{2})$. The existence of this equation was pointed out by Fradkin in 1950.[11] It contains no mass state with spin $\frac{1}{2}$, and involves only the single constant a_{11}. When $a_{11} = 0$, it becomes the Pauli-Fierz equation. In the absence of an external field, the equation together with its subsidiary conditions is identical with the Pauli-Fierz equation. When, however, one introduces a gauge-invariant interaction with the electromagnetic field, these equations differ. The Fradkin equation describes a particle with spin $\frac{3}{2}$ and an anomalous magnetic moment.

3. The Ulehla-Petras equation with $a_{33} = 0$ and

$a_{22} = 1$. This equation was obtained algebraically by Petras and investigated by Ulehla.[7] It contains no state with spin $3/2$ and involves the single arbitrary constant a_{11}. In the free state it coincides with the Dirac equation. When the interaction with an electromagnetic field is included, it describes a particle with spin $1/2$ and anomalous magnetic moment.

4. The Pauli-Fierz equation. This equation was obtained by Fierz[12] and has been treated in spin-tensor form by Ginzburg.[13] If $a_{22} = -a_{33}/2$, terms with an even number of β matrices remain in Eq. (64). Using the explicit form of β given by (40), we find that the product $\beta_k\beta_l$ can be written in the form $\begin{pmatrix} \delta_{kl} & 0 \\ 0 & B^{kl} \end{pmatrix}$, where the B^{kl} satisfy the relations

$$B^{kl}B^{mn} = \delta_{lm}B^{kn}. \tag{65}$$

This equation can therefore be written in the form (setting $a_{11} = 0$)

$$\alpha_k = \gamma_k + \left(\frac{1}{\sqrt{3}} - 1/2\right)\gamma_l B^{lk} + \left(-\frac{1}{4\sqrt{3}} - 1/2\right)\gamma_l B^{kl} + 1/4\left(1 - \frac{\sqrt{3}}{4}\right)\gamma_l\gamma_k\gamma_m B^{lm}. \tag{66}$$

Equations (66), (65), and (30) determine the commutation relations of the algebra, and the minimal polynomial of α_0 is $\alpha_0^2(\alpha_0^2 - 1)$. The reflection matrix is $T = \eta = \gamma_0(2B_{00} - 1) - (1/2)\gamma_l\gamma_0\gamma_m B^{lm}$, and the infinitesimal rotation matrices are given by $I_{ij} = (1/4)(\gamma_i\gamma_j - \gamma_j\gamma_i) + B^{ij} - B^{ji}$. Petras[5] obtained the Pauli-Fierz equation by selection in the somewhat different form in which

$$\alpha_k = \gamma_k + \gamma_l(B^{lk} - B^{kl})/\sqrt{3}. \tag{67}$$

It is easily shown that the equivalence transformation

$$R = E + (\sqrt{3}/8)\gamma^l\gamma^m B^{lm} \tag{68}$$

will bring (67) into the form given by (66). This exhausts all of the irreducible equations in the direct product of (44). By performing a similar analysis for (45), we can write down all of the desired irreducible equations for particles with maximum spin $3/2$. We are at present in the process of analyzing (45) and obtaining an explicit expression for the algebra given by (44). The method of the present article can be standardized for particles of higher spins $(2, 5/2, \ldots)$ and has certain definite advantages over other existing methods.

In conclusion I express my sincere gratitude to Professor V. L. Ginzburg, V. Ia. Fainberg, and E. S. Fradkin for attention to the work and for very valuable discussions.

[1] I. M. Gel'fand and A. M. Iaglom, J. Exptl. Theoret. Phys. (U.S.S.R.) **18**, 703 (1948).
[2] Harish-Chandra, Phys. Rev. **71**, 793 (1947).
[3] Harish-Chandra, Proc. Roy. Soc. (London) **192**, 195 (1948).
[4] I. M. Gel'fand and A. M. Iaglom, J. Exptl. Theoret. Phys. (U.S.S.R.) **18**, 1096 (1948).
[5] M. Petraš, Č. S. fysik. Časopis **5**, 160 (1955).
[6] M. Petraš, Č. S. fysik. Časopis **5**, 418 (1955).
[7] I. M. Ulehla, J. Exptl. Theoret. Phys. (U.S.S.R.) **33**, 473 (1957), Soviet Phys. JETP **6**, 369 (1958).
[8] Bhabha, Phil. Mag. **43**, 33 (1952).
[9] V. L. Ginzburg, J. Exptl. Theoret. Phys. (U.S.S.R.) **13**, 93 (1943).
[10] V. Ia. Fainberg, Труды ИФАН (Trans. Phys. Inst. Acad. Sci.) **6**, 269 (1955).
[11] E. S. Fradkin, J. Exptl. Theoret. Phys. (U.S.S.R.) **20**, 27 (1950).
[12] M. Fierz and W. Pauli, Proc. Roy. Soc. (London) **173A**, 211 (1939).
[13] V. L. Ginzburg, J. Exptl. Theoret. Phys. (U.S.S.R.) **12**, 425 (1942).

Translated by E. J. Saletan
309

PERIODIC SOLUTIONS OF THE NONLINEAR GENERALIZED DIRAC EQUATION

D. F. KURDGELAIDZE

Moscow State University

Submitted to JETP editor January 15, 1958

J. Exptl. Theoret. Phys. (U.S.S.R.) 34, 1587-1592 (June, 1958)

The nonlinear Dirac equation is considered, and a method for its solution is given. Periodic solutions are obtained in general form. A relation is established between the nonlinear Dirac equation and the Klein-Gordon equation.

As has been pointed out repeatedly in the literature, it is possible that an important part in the solution of problems of the theory of elementary particles will be played by nonlinear generalized equations, and in particular by the nonlinear generalized Dirac equation.

In the present paper we do not consider the question of the derivation of nonlinear generalized field equations. Taking the equations as given, we examine the possibility of solving them analytically. Furthermore, on the basis of physical considerations we seek solutions that are periodic functions; under certain restrictions we are able to obtain these solutions in a closed analytic form.

1. THE GENERAL FORM OF THE NONLINEAR GENERALIZED DIRAC EQUATION

Let us consider the nonlinear Dirac equation in its general form,* which has as special cases the generalization of the basic Dirac equation by the addition of terms $\lambda(\bar{\psi}\psi)\psi$ or $\lambda(\bar{\psi}\gamma_5\psi)\gamma_5\psi$, first suggested by Ivanenko[1,2] and by Ivanenko and Mirianashvili,[3] or in the case of vanishing rest mass by Heisenberg:[4]

$$\left\{-\frac{\partial}{i\partial t}-\frac{1}{i}\alpha\nabla-\rho_3 A(\psi^*,\psi)\right\}\psi=0 \tag{1.1}$$

and its complex conjugate equation:

$$\psi^*\left\{\frac{\partial}{i\partial t}+\frac{1}{i}\alpha\nabla+\overline{A^*(\psi^*,\psi)}\rho_3\right\}=0, \tag{1.2}$$

where

$$\psi^*\overline{A^*(\psi^*,\psi)}\rho_3=(\rho_3 A(\psi^*,\psi)\psi)^*. \tag{1.3}$$

We introduce the usual notation[5]

$$\gamma_n=-i\rho_3\alpha_n,\ \gamma_4=\rho_3,\ \psi^+=-i\psi^*\gamma_4,\qquad x_4=it,\ x_\mu(x_n,x_4). \tag{1.4}$$

*The notations are the same as in reference 1 ($\hbar=c=1$).

Then Eqs. (1.1) and (1.2) are written in the forms

$$\{\gamma_\mu\partial/\partial x_\mu+A(\psi^*,\psi)\}\psi=0, \tag{1.5}$$

$$\psi^+\{\gamma_\mu\partial/\partial x_\mu+\gamma_4\overline{A^*(\psi^*,\psi)}\gamma_4\}=0. \tag{1.6}$$

The nonlinearity of Eq. (1.1) is contained in $A(\psi^*,\psi)$, which does not depend on derivatives and is a function of ψ^*,ψ only. By considerations of invariance, $A(\psi^*,\psi)$ must have the form[6]

$$A(\psi^*,\psi)=A((\psi^*\Gamma^{(1)}_{l_1}\psi)T^{(1)}_{\nu_1}(\psi^*\Gamma^{(2)}_{l_2}\psi)T^{(2)}_{\nu_2}\dots(\psi^*\Gamma^{(n)}_{l_n}\psi)T^{(n)}_{\nu_n}),$$

where

$$\Gamma^{(1)}_{l_1},\Gamma^{(2)}_{l_2}\dots\Gamma^{(n)}_{l_n};\ T^{(1)}_{\nu_1}T^{(2)}_{\nu_2}\dots T^{(n)}_{\nu_n}, \tag{1.7}$$

are, generally speaking, matrices. In addition, the invariance of the expression requires that the indices $l_i\nu_i$ not include any free indices.

The limitation that we impose here on $A(\psi^*,\psi)$ is that we consider only the case

$$A(\psi^*,\psi)=A((\psi^*\Gamma^{(1)}_{l_1}\psi)(\psi^*\Gamma^{(2)}_{l_2}\psi)\dots(\psi^*\Gamma^{(n)}_{l_n}\psi)). \tag{1.8}$$

As is well known, the solution of Eqs. (1.5), (1.6) depends not only on x_μ, but also on the spin coordinate s.

We assume that the solutions of the equation allow the separation of the spin and (four-dimensional) space coordinates. We shall try to find these solutions in the form

$$\psi=\chi(s)\varphi(x_\mu),\ \psi^*=\chi^*(s)\varphi^*(x_\mu) \tag{1.9}$$

with the condition $\chi^*(s)\chi(s)=1$.

We now introduce the notation

$$\rho(x_\mu)=\varphi(x_\mu)\varphi^*(x_\mu)=\rho^*(x_\mu). \tag{1.10}$$

Then Eq. (1.8) takes the form

$$A(\psi^*,\psi)=A((\chi^*\Gamma^{(1)}_{l_1}\chi)\dots(\chi^*\Gamma^{(n)}_{l_n}\chi)\rho^n(x_\mu))=A(\rho), \tag{1.11}$$

where we have used the fact that, $(\chi^*\Gamma^{(1)}_{l}\chi)\dots(\chi^*\Gamma^{(n)}_{l_n}\chi)$, is a numerical quantity which can be included in the constant coefficient of the function $\rho^n(x_\mu)$. Thus we get

$$\gamma_4\overline{A^*(\psi^*,\psi)}\,\gamma_4=\gamma_4\overline{A^*(\rho)}\,\gamma_4=\gamma_4A^*(\rho)\gamma_4=A^*(\rho). \quad (1.12)$$

Then Eqs. (1.5) and (1.6) take the forms

$$\{\gamma_\mu\partial/\partial x_\mu+A(\rho)\}\chi(s)\varphi(x_\mu)=0; \quad (1.13)$$

$$\chi^+(s)\{\gamma_\mu\partial/\partial x_\mu-A^*(\rho)\}\varphi^*(x_\mu)=0. \quad (1.14)$$

2. SOLUTION OF THE NONLINEAR DIRAC EQUATION

On the basis of physical considerations we shall look for solutions of Eqs. (1.13), (1.14) in the class of periodic functions:

$$\varphi(x_\mu)=\varphi(\sigma),\ \sigma=k_\mu x_\mu,\ k_\mu(k_n,k_4),\ k_4=i\omega. \quad (2.1)$$

Then we have

$$\{\gamma_\mu k_\mu d/d\sigma+A(\rho)\}\chi(s)\varphi(\sigma)=0, \quad (2.2)$$

$$\chi^+(s)\{\gamma_\mu k_\mu d/d\sigma-A^*(\rho)\}\varphi^*(\sigma)=0. \quad (2.3)$$

Let us consider the system of equations

$$d\varphi/d\sigma=-A(\rho)\varphi/i\lambda,\ d\varphi^*/d\sigma=A^*(\rho)\varphi^*/i\lambda. \quad (2.4)$$

As we see, if φ and φ^* are solutions of (2.4), then Eqs. (2.2) and (2.3) reduce to a system of equations for the spin factor of the solution

$$(i\gamma_\mu k_\mu+\lambda)\chi(s)=0,\ \chi^+(s)(i\gamma_\mu k_\mu+\lambda)=0. \quad (2.5)$$

We supplement Eq. (2.5) with the following two equations for the spin*

$$(ks-\sigma_s\mathbf{k})\chi(s)=0,\ \chi^+(s)(ks-\sigma_s\mathbf{k})=0. \quad (2.6)$$

The solutions of the system of equations (2.5) and (2.6) are well known.[1]

Let us now return to the solution of the system of equations (2.4). We write the functions $A(\rho)$ and $A^*(\rho)$ in the form†

$$A(\rho)=a(\rho)+ib(\rho),\ A^*(\rho)=a(\rho)-ib(\rho). \quad (2.7)$$

Then Eq. (2.4) gives

$$\frac{d\rho}{d\sigma}=-\frac{2}{\lambda}b(\rho)\rho;\quad \int\frac{d\rho}{\rho b(\rho)}=-\frac{2\sigma}{\lambda}+c_1. \quad (2.8)$$

We denote the solution of Eq. (2.8) by $\rho=f(\sigma)$,

*As is well known, in the linear theory one introduces for the spin the operator $\sigma\nabla/ik$. The necessity of this is basically due to the existence of a superposition principle for the linear equations. In a nonlinear theory the introduction of a differential operator leads to serious difficulties, but because of the absence of a superposition principle it is also not necessary. We here use the single term $\sigma_s k$.

†In $A(\psi^*,\psi)$ the function of $i=(-1)^{1/2}$, which changes the sign of the term with $b(\rho)$ when one goes from the equation to its complex conjugate, can be performed by γ_5. In such a case, however, one must remove the restriction (1.8) and replace λ by $\lambda_1+\gamma_5\lambda_2$ in Eq. (2.5).

and substituting it into Eq. (2.4) we get

$$d\varphi/\varphi=-A(\sigma)d\sigma/i\lambda,\quad d\varphi^*/\varphi^*=A^*(\sigma)d\sigma/i\lambda. \quad (2.9)$$

The solutions of these equations have the form

$$\frac{\varphi}{\varphi_0}=\exp\left\{\frac{i}{\lambda}\int A(\sigma)d\sigma\right\} \quad (2.10)$$

$$=\exp\left\{-\frac{1}{\lambda}\int b(\sigma)d\sigma+\frac{i}{\lambda}\int a(\sigma)d\sigma\right\},$$

$$\frac{\varphi^*}{\varphi_0^*}=\exp\left\{-\frac{i}{\lambda}\int A^*(\sigma)d\sigma\right\} \quad (2.11)$$

$$=\exp\left\{-\frac{1}{\lambda}\int b(\sigma)d(\sigma)-\frac{i}{\lambda}\int a(\sigma)d\sigma\right\},$$

$$\frac{\rho}{\rho_0}=\exp\left\{-\frac{2}{\lambda}\int b(\sigma)d\sigma\right\}. \quad (2.12)$$

As we see, the density is determined by $b(\rho)$ only. From this it follows in particular that for $b(\rho)=0$ the nonlinear Dirac equation has no other complex solution besides

$$\rho=\rho_0=\text{const},\ \varphi=\varphi_0e^{ik_\mu x_\mu},\ \varphi^*=\varphi_0^*e^{-ik_\mu x_\mu},$$
$$k_\mu^2=-\lambda^2=-a^2(\rho_0), \quad (2.13)$$

and in the case $a(\rho_0)=k_0$ we arrive at an ordinary solution of the linear Dirac equation.

The real solutions of the equations (2.9) can be obtained directly from the solutions (2.10) and (2.11). In fact, for $a(\rho)=0$ we have

$$\frac{\varphi}{\varphi_0}=\frac{\varphi^*}{\varphi_0^*}=\exp\left\{-\frac{1}{\lambda}\int b(\sigma)d\sigma\right\}. \quad (2.14)$$

For $b(\rho)=0$, if we replace $(i\lambda)$ by $-\lambda'$ with $\lambda'^2>0$, Eqs. (2.9) and (2.5) become[7]

$$d\varphi/d\sigma=d\varphi^*/d\sigma=a(\rho)\varphi/\lambda'=a(\rho)\varphi^*/\lambda', \quad (2.15)$$

$$(i\gamma_\mu k_\mu+(i\lambda'))\chi(s)=0,\ \chi^+(s)(i\gamma_\mu k_\mu+(i\lambda')^*)=0, \quad (2.16)$$

and the solutions for the spin factors are given by[1]

$$\chi(s)=\Omega B(s,\varepsilon,(i\lambda')),\ \chi^*=B^*(s,\varepsilon,(i\lambda')^*)\Omega^*,$$
$$B^*(s,\varepsilon,(i\lambda)^*)=\frac{1}{2c_0}(\sqrt{1+s}f^*(\varepsilon), \quad (2.17)$$

$$\sqrt{1-s}f^*(\varepsilon),\ \varepsilon\sqrt{1+s}f^*(\varepsilon),\quad -\varepsilon\sqrt{1-s}f^*(-\varepsilon)),$$

$$f^*(\varepsilon)=\sqrt{1+(i\lambda')^{*2}/K^2},\quad k_\mu^2=k^2-K^2=\lambda'^2,\quad K=\mp\omega,$$
$$c_0=\sqrt{1+\lambda'^2/K^2}=|k|/K.$$

It must be noted that, just as in the linear theory, one can choose in the nonlinear theory also two of the four amplitudes arbitrarily and determine the other two from (2.5). The expressions for the amplitudes will be just the same as in the linear theory, except that the mass k_0 is replaced by λ.

In the Newtonian approximation $K\gg\lambda$, just as

in the linear theory, two of the amplitudes can be neglected in comparison with the other two.[8]

3. THE RELATION BETWEEN THE NONLINEAR DIRAC AND KLEIN-GORDON EQUATIONS

Let us consider the Dirac equation (1.5). Applying to it the operator $\gamma_\nu \partial/\partial x_\nu$, we get

$$\frac{\partial^2\psi}{\partial x_\nu^2} + \left(\gamma_\nu \frac{\partial}{\partial x_\nu} A(\psi^*, \psi)\right)\psi + \gamma_\nu A(\psi^*, \psi)\frac{\partial\psi}{\partial x_\nu} = 0. \quad (3.1)$$

Under the restrictions imposed on our present problem we have

$$\gamma_\nu A(\psi^*, \psi)\frac{\partial\psi}{\partial x_\nu} = A(\rho)\gamma_\nu \frac{\partial\psi}{\partial x_\nu} = -A^2(\rho)\psi, \quad (3.2)$$

$$\left(\gamma_\nu \frac{\partial}{\partial x_\nu} A(\psi^*, \psi)\right)\psi = \frac{dA(\rho)}{d\rho}\frac{d\rho}{d\sigma}\gamma_\nu k_\nu \psi \quad (3.3)$$

$$= -2i\rho b(\rho)\frac{dA(\rho)}{d\sigma},$$

where we have used Eqs. (2.9) and (2.5). Substituting Eqs. (3.2) and (3.3) into Eq. (3.1), we arrive at the equation

$$\partial^2\psi/\partial x_\mu^2 - B(\rho)\psi = 0, \quad (3.4)$$

where

$$B(\rho) = A^2(\rho) + i2\rho b(\rho)\frac{dA}{d\rho} \quad (3.5)$$

$$= a^2 - \frac{d}{d\rho}(\rho b^2(\rho)) + i2b(\rho)\frac{d}{d\rho}(\rho a(\rho)).$$

We also get an analogous relation for the complex conjugate function.

We arrive at the same result if we apply the operator $d/d\sigma$ to Eq. (2.4) and use Eqs. (2.8) and (2.1).

We now suppose that we are given a nonlinear Klein-Gordon equation of the form (3.4) and its complex conjugate equation. It is required to find the corresponding Dirac equation. The problem reduces to the determination of $A(\rho)$ and $A^*(\rho)$ in terms of $B(\rho)$ and $B^*(\rho)$. Equation (3.5) and its complex conjugate give a system of nonlinear differential equations to determine $a(\rho)$ and $b(\rho)$ in terms of the given values of $B(\rho)$ and $B^*(\rho)$.

If we introduce the notations

$$\tau = -1/\rho,\ \xi = \rho a(\rho) = -\frac{1}{\tau}a(\tau),$$

$$\eta = \sqrt{\rho}\, b(\rho) = b(\tau)/\sqrt{-\tau}, \quad (3.6)$$

$$f_1(\tau) = -\tau^{-2}B_1(\tau),\quad f_2(\tau) = \frac{1}{2}(-\tau)^{-5/2}B_2(\tau),$$

where

$$B_1(\tau) = (B(\tau) + B^*(\tau))/2, \quad (3.7)$$

$$B_2(\tau) = (B(\tau) - B^*(\tau))/2i,$$

then Eq. (3.5) and its complex conjugate can be written in the form

$$\eta\, d\xi/d\tau = f_2(\tau), \quad (3.8)$$

$$d\eta^2/d\tau - \xi^2 = f_1(\tau). \quad (3.9)$$

In the particular case in which $f_2(\tau) = 0$ ($B_2(\tau) = 0$), the system of equations (3.8), (3.9) is easily solved, and we find:

a) $\eta = 0$, $\xi = \sqrt{-f_1(\tau)}$; $b(\rho) = 0$ $a(\rho) = \sqrt{B_1(\rho)}$,

b) $\eta \neq 0$, $\xi = \xi_0$, $\eta = \{\int (f_1(\tau) + \xi_0^2)\, d\tau\}^{1/2}$, (3.10)

that is,

$$a(\rho) = \frac{C_1}{\rho},$$

$$b(\rho) = \left\{\left(C_2 - \frac{C_1^2}{\rho} - \int B_1(\rho)\, d\rho\right)/\rho\right\}^{1/2}. \quad (3.11)$$

If, on the other hand, $f_2(\tau) \neq 0$, then the system of equations (3.8) and (3.9) can be put in the form

$$\xi'' - (f_2'/f_2)\xi' + (1/2f_2^2)(\xi^2 - f_1)\xi'^3 = 0, \quad (3.12)$$

$$\eta = \left(\int \{f_1(\tau) + \xi^2\}\, d\tau\right)^{1/2}. \quad (3.13)$$

In view of the complexity of these equations, however, it is difficult to find their solution in general form.

As we see, in the nonlinear theory A and B are related through (ordinary) differential equations, unlike the linear theory, in which this connection is purely algebraic.

On this account, for given B and B* the functions A and A* are determined only to within two arbitrary constants if $f_2(\tau) = 0$ and three arbitrary constants if $f_2(\tau) \neq 0$. A unique connection between B and A can be secured in the usual way, by adjoining supplementary conditions to the differential equation.[7]

In cases in which one is able to reduce the nonlinear Klein-Gordon equation (3.4), (3.5) to a nonlinear Dirac equation, the solution can be found as indicated above.

I regard it as my obligation to express my deep gratitude to Professor D. D. Ivanenko for his constant interest in this work.

[1] A. A. Sokolov and D. D. Ivanenko, Квантовая теория поля (Quantum Field Theory), GITTL, 1952.

[2] D. D. Ivanenko, J. Exptl. Theoret. Phys. (U.S.S.R.) 8, 260 (1938).

[3] D. D. Ivanenko and M. Mirianashvili, Dokl. Acad. Nauk SSSR 106, 413 (1956), Soviet Phys. "Doklady" 1, 41 (1956).

[4] W. Heisenberg, Revs. Mod. Phys. **29**, 269 (1957); Gött. Nachr. No. 8, 111, (1953).
[5] G. Wentzel, Quantentheorie der Wellenfelder, Edwards Bros., Ann Arbor, 1946.
[6] D. D. Ivanenko and A. M. Brodskii, J. Exptl. Theoret. Phys. (U.S.S.R.) **24**, 383 (1953).
[7] D. F. Kurdgelaidze, J. Exptl. Theoret. Phys. (U.S.S.R.) **32**, 1156 (1957), Soviet Phys. JETP **5**, 941 (1957).
[8] L. de Broglie, L'Electron Magnetique, Paris, 1934.

Translated by W. H. Furry
310

SOVIET PHYSICS JETP VOLUME 34(7), NUMBER 6 DECEMBER, 1958

ELECTROMAGNETIC WAVES IN ISOTROPIC AND CRYSTALLINE MEDIA CHARACTERIZED BY DIELECTRIC PERMITTIVITY WITH SPATIAL DISPERSION

V. L. GINZBURG

P. N. Lebedev Physics Institute, Academy of Sciences, U.S.S.R.

Submitted to JETP editor January 6, 1958

J. Exptl. Theoret. Phys. (U.S.S.R.) **34**, 1593-1604 (June, 1958)

The dielectric permittivity tensor ϵ_{ik} is usually taken to be a function of frequency alone, i.e. one neglects spatial dispersion — the dependence of ϵ_{ik} on the wavelength. However, even in non-gyrotropic media spatial dispersion must be considered in cases of weak absorption, when the refractive index increases rapidly and becomes infinite if dispersion and absorption are not taken into account. Spatial dispersion is also important in the analysis of longitudinal (plasma) waves which propagate in an isotropic medium or along the principal dielectric axes in crystals. It is also shown that spatial dispersion leads to a weak optical anisotropy in cubic crystals. In addition to the above, an analysis is made of the collective (discrete) energy losses in solids.

1. INTRODUCTION

In analyzing the propagation of light and electromagnetic waves of longer wavelengths in a medium, one usually uses the local relation

$$D_l = \varepsilon_{lk}(\omega) E_k, \qquad (1.1)$$

where $\mathbf{D}$ and $\mathbf{E}$ are taken at ω, the frequency of the Fourier components of the electric induction and field intensity at the point $\mathbf{r}$. If there is absorption, the tensor ϵ_{ik} becomes complex and $\mathbf{D}$ must be replaced by $\mathbf{D} - i(4\pi/\omega)\mathbf{j}$ where $\mathbf{j}$ is the density of the conduction current. In order to simplify the analysis this substitution is implied below, but not carried out explicitly.

The relation in (1.1) does not reflect the nature of the field variation in space, that is to say, it applies only if we neglect spatial dispersion — the dependence of the tensor ϵ_{ik} on the wavelength. The spatial dispersion can be characterized by the parameter $a/\lambda = an/\lambda_0$, where a is a characteristic length for a given medium (molecular dimensions, lattice constants, Debye radius, etc.), $\lambda_0 = 2\pi c/\omega$ is the wavelength in vacuum, $\lambda = \lambda_0/n$ is the wavelength in the medium and n is the index of refraction. In condensed media in the optical region usually $a/\lambda_0 \sim 1$ to 3×10^{-3} so that spatial dispersion is negligibly small in most cases.* This, however, is not the case if we are interested in effects associated with spatial inhomogeneities of the field. A well-known example of this type is natural optical activity — an effect which is of order a/λ. It will be shown below that taking terms of order $(a/\lambda)^2$ into account leads to an additional effect — weak optical anisotropy in cubic crystals.

*The time dispersion, which leads to a dependence of ε_{ik} on ω may be large under these same conditions because it is characterized by the parameter ω/ω_j, where ω_j is a characteristic frequency of the medium.

It is also necessary to go beyond the local relation (1.1), as is well-known, when one considers longitudinal (plasma) waves in a medium (ionized gas, solids). Finally, in cases of weak absorption, it is necessary to take account of terms of order $(a/\lambda)^2$ at frequencies close to characteristic frequencies of the medium, i.e., in regions in which the refractive index n becomes very large. This situation is completely understandable because when $n \to \infty$, the parameter an/λ_0 also increases without limit. This case has been already considered in an analysis of waves in a magneto-active plasma close to resonance[1] and in absorption of light by excitons in crystals.[2] Although calculations involving spatial dispersion have already been carried out in individual cases, it would appear that there are still a number of points which are not entirely clear. For this reason certain aspects of this problem are considered below.

If small, the effect of spatial dispersion can be taken into account by writing the relation between **D** and **E** in the form

$$D_i = \varepsilon_{ik}(\omega) E_k + \gamma_{ikl}(\omega) \frac{\partial E_k}{\partial x_l} + \delta_{iklm}(\omega) \frac{\partial^2 E_k}{\partial x_l \partial x_m}. \quad (1.2)$$

The term containing γ_{ikl} is responsible for optical activity (cf. reference 3, §83) and vanishes if there is a center of aymmetry in the body. Below we shall assume with one important exception, that $\gamma_{ikl} = 0$. Considering plane waves, for which the field is proportional to the factor $\exp\{i(\omega t - \mathbf{k}\cdot\mathbf{r}\} = \exp\{i(\omega t - \omega \hat{n}\mathbf{s}\cdot\mathbf{r}/c)\}$ we write (1.2) in the form (we consider only plane waves for which the planes of constant phase coincide with planes of constant amplitude):

$$D_i = \hat{\varepsilon}_{ik} E_k, \quad \hat{\varepsilon}_{ik} = \varepsilon_{ik} - \alpha_{iklm} s_l s_m \hat{n}^2, \quad \alpha_{iklm} = (\omega/c)^2 \delta_{iklm}, \quad (1.3)$$

where **s** is the unit vector normal to the wave, $\hat{n} = n - i\kappa$ is the complex refractive index (n is the index of refraction, κ is the absorption factor). The coefficient δ is of the order of the square of the characteristic length a and $|\alpha_{iklm}| \sim (a/\lambda_0)^2$. It is apparent that the tensor α_{iklm} can always be assumed symmetric with respect to the indices l and m. Using the principal of symmetry for the kinetic coefficients it can be shown (reference 3, §83) that the tensor α_{iklm} is also symmetric with respect to the indices i and k (it is assumed that there is no external field). In the absence of absorption, this tensor is real. Further simplification of the tensor derives from the symmetry of the medium.

The expansion given in (1.2) and (1.3) is not always possible. For example, if one of the components ϵ_{ab} of the tensor ϵ_{ik} tends toward infinity, terms of order $(a/\lambda_0)^2 n^2$ can always be neglected as compared with it. On the other hand, the quantity $1/\epsilon_{ab}$ becomes small and the last term may become important in the expansion

$$1/\hat{\varepsilon}_{ab} = 1/\varepsilon_{ab} + \beta_{ablm} s_l s_m \hat{n}^2$$

Thus, the tensor $\hat{\epsilon}_{ik}$ is sometimes replaced by $\hat{\epsilon}^{-1}_{ik}$:

$$E_i = \hat{\varepsilon}^{-1}_{ik} D_k, \quad \hat{\varepsilon}^{-1}_{ik} = \varepsilon^{-1}_{ik} + \beta_{iklm} s_l s_m \hat{n}^2. \quad (1.4)$$

The symmetry properties of this tensor are the same as those of ϵ_{ik}. The introduction of two tensors $\hat{\epsilon}_{ik}$ and $\hat{\epsilon}^{-1}_{ik}$ should not occasion surprise since the vectors **D** and **E** are of equal rank. In order of magnitude terms the coefficients α and β are generally the same. The choice of one or the other of the expansions (1.3) or (1.4) is dictated by the nature of the individual problem and will be clarified below.

The propagation of plane waves is determined by the field equations

$$\mathbf{H} = \hat{n}[\mathbf{s}\times\mathbf{E}], \quad \mathbf{D} = -\hat{n}[\mathbf{s}\times\mathbf{H}], \quad (1.5)$$

whence

$$\mathbf{D} = \hat{n}^2\{\mathbf{E} - \mathbf{s}(\mathbf{s}\cdot\mathbf{E})\}. \quad (1.6)$$

Here **H** is the magnetic field associated with the wave, the magnetic permeability μ is set equal to unity and the medium is assumed homogeneous (the same applies in (1.3), (1.4), and below).

Substituting in Eq. (1.6) the relation given in (1.1), we obtain the well-known equation for $\hat{n}^2$:

$$\begin{aligned}&(\varepsilon_x s_x^2 + \varepsilon_y s_y^2 + \varepsilon_z s_z^2)\hat{n}^4\\ &- [\varepsilon_x(\varepsilon_y + \varepsilon_z)s_x^2 + \varepsilon_y(\varepsilon_x + \varepsilon_z)s_y^2\\ &+ \varepsilon_z(\varepsilon_x + \varepsilon_y)s_z^2]\hat{n}^2 + \varepsilon_x\varepsilon_y\varepsilon_z = 0,\end{aligned} \quad (1.7)$$

where ϵ_x, ϵ_y and ϵ_z are the principal values of the tensor ϵ_{ik}. It is characteristic that Eq. (1.7) is quadratic in $\hat{n}^2$ whereas the system in (1.6) consists of three homogeneous equations and, in the general case, leads to a cubic equation in $\hat{n}^2$. The coefficient for $\hat{n}^6$ can be set equal to zero only when the local relation in (1.1) applies; if, on the other hand, (1.3) applies, the equation in $\hat{n}^2$ is of the third degree. This fact is responsible for the appearance of the additional "proper" wave. These considerations indicate the need for taking spatial dispersion into account under certain conditions.

2. ISOTROPIC MEDIUM

In an isotropic medium the tensors $\hat{\epsilon}_{ik}$, ϵ_{ik}, α_{iklm} and β_{iklm} become scalars and from (1.3)

we have*

$$\mathbf{D} = \hat{\varepsilon}\mathbf{E}, \quad \hat{\varepsilon} = \varepsilon - \alpha\hat{n}^2. \tag{2.1}$$

For transverse waves, in which $\mathbf{s}\cdot\mathbf{E} = 0$, substitution of (2.1) in (1.6) leads to the double root $\hat{n}^2_{1,2} = \epsilon/(1+\alpha)$ which, because α is so small, virtually coincides with the value $\hat{n}^2 = \epsilon$ which is obtained when spatial dispersion is neglected. For longitudinal waves, in which $\mathbf{s}(\mathbf{s}\cdot\mathbf{E}) = \mathbf{E}$, we have:

$$\hat{n}_3^2 = \varepsilon(\omega)/\alpha. \tag{2.2}$$

In a longitudinal wave $\mathbf{D} = 0$, as is clear from the condition $\operatorname{div}\mathbf{D} = -(i\omega/c)n\,\mathbf{s}\cdot\mathbf{D} = 0$ or, better still, from Eq. (1.6). However, the field $\mathbf{E}$ associated with this wave may be different from zero since the expression in (2.2) is equivalent to $\hat{\epsilon} = 0$, which, according to Eq. (2.1), is compatible with the conditions $\mathbf{D} = 0$ and $\mathbf{E} \neq 0$. If spatial dispersion is neglected, when $\hat{\epsilon} = \epsilon$ a longitudinal wave is possible only if

$$\varepsilon(\omega) = 0. \tag{2.3}$$

This condition is also clear from Eq. (2.2) since $\hat{n}_3^2$ remains finite as $\alpha \to 0$ only if $\epsilon \to 0$.

The existence condition for longitudinal waves in the form given in (2.3) was given a long time ago (cf. for example reference 4, §4) but has been a subject of discussion until very recently.[5,6]

If spatial dispersion is neglected the longitudinal waves are characterized by a vanishing group velocity $u = d\omega/dk$ and are associated only with discrete frequencies ω_l which satisfy (2.3). When $\alpha \neq 0$ the longitudinal waves assume the same importance as the proper waves in the medium. Longitudinal waves are well-known in plasmas: if collisions are neglected,

$$\varepsilon(\omega) = 1 - 4\pi e^2 N/m\omega^2 = 1 - \omega_0^2/\omega^2$$

and, if a Maxwellian velocity distribution obtains and the quasi-hydrodynamic approximation is used $\alpha = \kappa T/mc^2$. On the other hand, if the calculation is carried out using the kinetic equation, $\alpha = 3\kappa T/mc^2$ where κ is the Boltzmann constant and T is the temperature. In a plasma longitudinal waves are not strongly attenuated close to the frequency ω_0 only when the index n_3 is small (plasma waves are considered in detail in reference 1). In the general case, in a plasma we have $\alpha \sim (v_0/c)^2$ where v_0 is some characteristic velocity (in a degenerate gas v_0 is the order of the velocity at the Fermi limit). This result for α is found to be in agreement with an estimate made earlier $\alpha \sim (a/\lambda_0)^2 = (\omega a/2\pi c)^2$ since, for a gas in a high frequency field the characteristic length $a \sim 2\pi v_0/\omega$, that is, the path traversed by the particle during one oscillation period (in order of magnitude terms $2\pi v_0/\omega_0$ is the shielding radius or Debye radius).

In solids the longitudinal waves are similar to plasma waves and, as is well known, are described by "plasmons" when quantized.[6] Just as in the plasma case, the attenuation of these longitudinal waves can be small only in the neighborhood of frequencies ω_l, at which $\epsilon(\omega_l) = 0$. We may note that in principal α can also be negative, as in optical vibrations of a solid lattice. When $\alpha < 0$ obviously $\hat{n}_3^2 > 0$ for $\epsilon(\omega) < 0$.

For transverse waves, in the region $\hat{n}^2_{1,2} = \epsilon \to \infty$ the expansion in (2.1) is not affected although one would expect strong effects due to spatial dispersion (cf. Introduction). However, because the quantity ϵ^{-1} is so small it is necessary to use an expansion of form (1.4) which applies for an isotropic medium (it is assumed that $\mathbf{s}\cdot\mathbf{D} = 0$)

$$\mathbf{E} = \mathbf{D}/\hat{\varepsilon}, \quad 1/\hat{\varepsilon} = 1/\varepsilon + \beta\hat{n}^2. \tag{2.4}$$

In the case of longitudinal waves, substituting Eq. (2.4) in Eq. (1.6) we obtain the condition $\hat{\epsilon} = 0$, that is to say, when $\epsilon \neq 0$ we have $\hat{n}_3^2 = \infty$. In other words, in the resonance region, as well as at frequencies far from ω_l, it is impossible for longitudinal waves to exist in an isotropic medium (keeping in mind the fact that macroscopic waves exist only when $n \ll \lambda_0/a$; (cf. below). For transverse waves, from Eqs. (2.4) and (1.6) we obtain the equation $\beta\hat{n}^4 + \hat{n}^2/\epsilon - 1 = 0$, whence

$$\hat{n}^2 = -1/2\varepsilon\beta \pm \sqrt{(1/2\,\varepsilon\beta)^2 + 1/\beta}. \tag{2.5}$$

Having in mind the frequency region close to an absorption line we may use the following expression for ϵ:

$$\varepsilon(\omega) \equiv \varepsilon_1 - i\varepsilon_2 = \varepsilon_0 + \frac{4\pi e^2 N_{\text{eff}}/m}{\omega_j^2 - \omega^2 + i\omega\nu}$$

$$\approx \varepsilon_0 - \frac{A\xi}{\xi^2+\delta^2} - i\frac{A\delta}{\xi^2+\delta^2}, \tag{2.6}$$

$$\xi = (\omega - \omega_j)/\omega_j, \quad \delta = \nu/2\omega_j, \quad A = 2\pi e^2 N_{\text{eff}}/m\omega_j^2.$$

In the absence of absorption, in which case $\delta = 0$,

$$\varepsilon(\omega) = \varepsilon_1(\omega) = \hat{n}_0^2 = \varepsilon_0 - A/\xi, \tag{2.7}$$

*In an isotropic medium a tensor of the 4-th rank has two independent components which, in (1.3) correspond to the expansion

$$\mathbf{D} = \varepsilon\mathbf{E} + \delta_1\Delta\mathbf{E} + \delta_2\,\text{grad}\,\text{div}\,\mathbf{E} = (\varepsilon - \alpha_1\hat{n}^2)\,\mathbf{E} - \alpha_2\mathbf{s}\,(\mathbf{sE})\,\hat{n}^2.$$

Thus, for transverse waves, in Eq. (2.1) $\alpha = \alpha_1$; for longitudinal waves $\alpha = \alpha_1 + \alpha_2$. In (1.4), because of the condition $\operatorname{div}\mathbf{D} = 0$ in an isotropic medium, there is only one coefficient β, i.e., β_{iklm} can be replaced by a scalar unconditionally.

where $\hat{n}_0$ is the refractive index when both absorption and spatial dispersion are neglected. From Eq. (2.5) it is clear that when

$$\varepsilon^2|\beta| \ll 1, \tag{2.8}$$

$$\hat{n}_1^2 = \varepsilon(1 - \varepsilon^2\beta + \cdots), \quad \hat{n}_2^2 = -1/\varepsilon\beta - \varepsilon + \cdots. \tag{2.9}$$

With $\beta \sim 10^{-6}$, the condition given in (2.8) becomes $\hat{n}_0^2 \ll 10^3$, and when $\epsilon_0 \sim 1$ and $A \sim 1$ [cf. Eq. (2.7)] we find $|\xi| = |\omega - \omega_j|/\omega_j \gg 10^{-3}$; in the optical region, with $\lambda_j = 2\pi c/\omega_j \sim 5 \times 10^{-5}$ cm this means that the expressions in (2.9) apply at distances $\Delta\lambda \gg 10^{-3}\lambda_j \sim 5$ A from the center of the absorption line. In this region it is obvious that $\hat{n}_1^2 = \hat{n}_0^2$ since, if absorption is present, the root n_1^2 is approximately equal to $\hat{n}^2$ which corresponds to the case $\beta = 0$. However, the root $\hat{n}_2^2$ is very large and, when $\epsilon \sim 1$, as can be the case far from the line, $|\hat{n}_2^2| \sim 1/|\beta| \sim 10^6$. In this case $\lambda = \lambda_0/n_2 \sim 5 \times 10^{-8}$ and Eqs. (1.3), (1.4), (2.1), and (2.4) no longer apply, so that macroscopic analysis of the problem is no longer meaningful. The new root of the dispersion equation n_2 is real only close to the line, in the region where $\lambda = \lambda_0/n_2 \sim \sqrt{|\beta|}\lambda_0 \gg a \sim 3 \times 10^{-8}$, i.e., as long as $n_2 \ll \lambda_0/a$. It will be assumed below that this condition is satisfied.

As is clear from Figs. 1 and 2, close to the absorption line spatial dispersion has a qualitative effect on the $\hat{n}^2(\omega)$ curves. Both of the curves refer to the case $A = 1$ and $\delta = 0$ but in Fig. 1 the value $\beta = 10^{-5}$ has been taken while in Fig. 2 $\beta = -10^{-5}$. The dashed curves in both cases represent the limiting curve (2.7), also for $A = 1$ (generally $\epsilon_0 \sim 1$ and since we are interested in the region $|\epsilon| \gg 1$ we may set $\epsilon_0 = 0$ everywhere). We may note that if there is no absorption and if $\hat{n}^2$ is real with $\hat{n}^2 > 0$ it is obvious that $\hat{n}^2 = n^2$; for $\hat{n}^2 < 0$ we have $\hat{n}^2 = -\kappa^2$, i.e., there is total internal reflection from the medium. For $\beta = 0$ and $\beta > 0$ we are dealing with cases of this kind since $\hat{n}^2$ is real. If, however $\beta < 0$ in the region $|\epsilon| > 1/2\sqrt{|\beta|}$ the values $(\hat{n}^2 = n - i\kappa)^2$ are complex (in this region of Fig. 2 there are no solid curves).

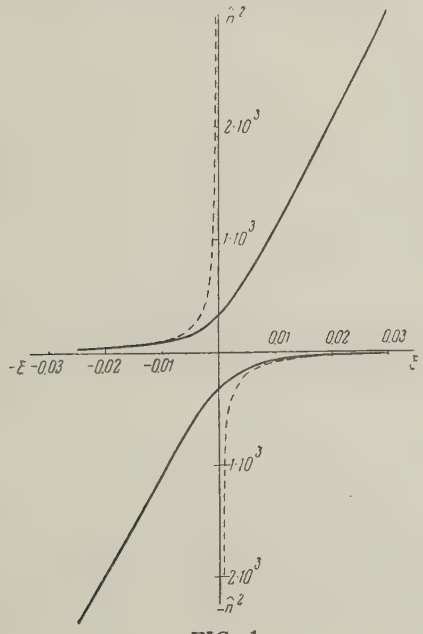

FIG. 1

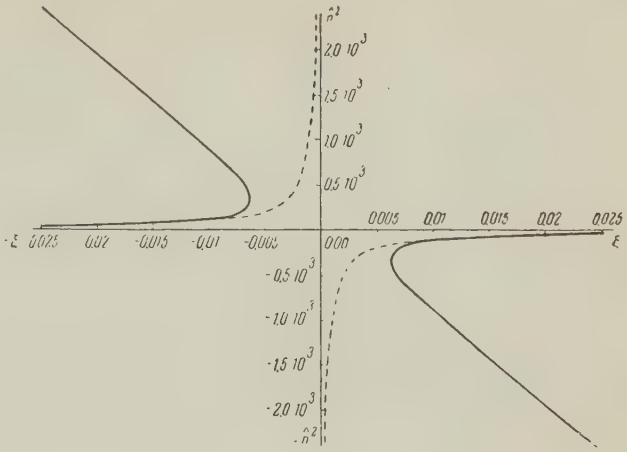

FIG. 2

Thus, when spatial dispersion is taken into account, near a resonance (absorption line), for a given value of ω we find a new root for $\hat{n}^2$ (more precisely double roots, because of the two independent directions of polarization). The peculiar behavior of the $\hat{n}^2$-curves close to resonance, shown in Figs. 1 and 2, was known earlier from work on magneto-active plasmas;[1] in the crystal case an expression such as (2.5) has been obtained recently by Pekar[2] starting from a concrete model.*

To a considerable degree the possibility of observing the new wave close to resonance depends on the amount of absorption. In the absence of absorption the effect of spatial dispersion is large in the region in which $4\epsilon_1^2|\beta| \sim 1$, i.e., when $|\xi| \sim \xi_k = 2A\sqrt{|\beta|}$. Furthermore, if

$$\delta \ll \xi_k = 2A\sqrt{|\beta|}, \tag{2.10}$$

at a frequency such that $|\xi| = |\omega - \omega_j|/\omega_j \geq \xi_k$ the absorption has only a small effect on the quantity $\epsilon_1 = \mathrm{Re}\,\epsilon$ while $\epsilon_2 = \mathrm{Im}\,\epsilon \ll |\epsilon_1|$. Similarly the curves $n^2(\omega)$ and $\kappa^2(\omega)$ are not changed if we neglect the effect of attenuation in the region which is completely transparent for $\delta = 0$. Suppose, for example, the condition in (2.10) is satisfied, $\beta > 0$, and we consider a frequency for which $4\epsilon_1^2|\beta| = 1$. Then, with $\xi < 0$ we have $n \approx 0.6\beta^{-1/4}$

*The fact that the results obtained by Pekar[2] correspond to an expansion such as that given in (2.4) was noted still earlier by L. D. Landau in conversation with the author.

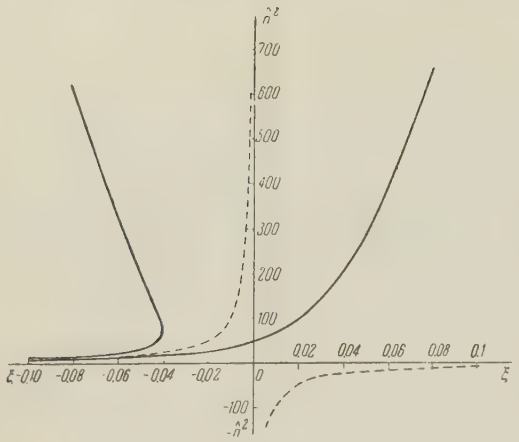

FIG. 3

and $\kappa \approx 0.2(\delta/\xi_k)\beta^{-1/4}$, which, for $\xi_k \sim 10^{-3}$, $\beta \sim 10^{-6}$ and $\delta \sim 10^{-7}$ yields $n \sim 20$ and $\kappa \sim 6 \times 10^{-4}$. Since the radiation intensity falls off in accordance with the relation $I = I_0 e^{-2\omega\kappa z/c} = I_0 e^{-\mu z}$, this means that $\mu = (2\omega/c)n \sim 150\ \text{cm}^{-1}$ (for $\lambda_0 \sim 5 \times 10^{-5}$ cm). For the same values but with $\beta < 0$:

$$n = 1/\sqrt{2\varepsilon_1 |\beta|} = |\beta|^{-1/4} \approx 30, \quad \kappa = \sqrt{\varepsilon_2/\varepsilon_1}/2(2\varepsilon_1|\beta|)^{1/4} = \sqrt{\delta/\xi_k}/2|\beta|^{1/4} \approx 0.15,$$

i.e., $\mu \sim 3 \times 10^4\ \text{cm}^{-1}$. Thus the intensity is reduced by a factor of e in a distance $\lambda_0/1.8 = 3 \times 10^{-5}$ cm whereas $\lambda = \lambda_0/n \approx 2 \times 10^{-6}$ cm. Hence, even in the second case, the attenuation in one wavelength in the medium is relatively small although it is enormous in terms of macroscopic distances. With $\beta < 0$ and $4\epsilon_1^2|\beta| < 1$ the absorption is less and in order of magnitude terms is approximately the same as that for $\beta > 0$. On the other hand, in actual crystals it is probably always true that $\delta \gg 10^{-7}$. From these examples it is clear that the observation of spatial dispersion close to absorption lines is very much complicated by absorption effects and would require very special and favorable conditions (assuming ordinary optical methods of observation).

Because of the small spatial dispersion in a non-gyrotropic medium, it is of special interest to consider the resonance region in naturally active materials in which case the effect of interest is of order a/λ. For optically active isotropic solids and cubic crystals far from resonance (cf. reference 3, §83)

$$\mathbf{D} = \varepsilon\mathbf{E} - if[\mathbf{s}\times\mathbf{E}]\hat{n}. \tag{2.11}$$

Assuming large values of ϵ it is necessary to use the related expression

$$\mathbf{E} = \mathbf{D}/\varepsilon + ig[\mathbf{s}\times\mathbf{D}]n. \tag{2.12}$$

Substituting this expression in (1.6), for transverse waves we have:

$$g^2\hat{n}^6 - (\hat{n}^2/\varepsilon - 1)^2 = 0. \tag{2.13}$$

With $gn_0^3 \ll 1$, $n_0^2 = \epsilon$ it is easily shown that

$$\hat{n}_{1,2}^2 = n_0^2(1 \pm gn_0^3), \quad \hat{n}_3^2 = 1/\varepsilon^2 g^2. \tag{2.14}$$

The curves for real values of $\hat{n}_{1,2,3}^2$ are shown in Fig. 3 for $\epsilon = -1/\xi$, $g^2 = 10^{-5}$. We may note that the multiple root corresponds to the values

$$\varepsilon_m = 2^{2/3}/3g^{2/3}, \quad \hat{n}_m^2 = (2/g)^{2/3}, \quad \hat{n}^2 = \tfrac{1}{4}(2/g)^{2/3}$$

whence, with $g \sim 3 \times 10^{-3}$ we have: $\epsilon_m = -1/\xi_m \sim 25$ and $\xi_m = |\Delta\omega|/\omega_j \sim 4 \times 10^{-2}$ or, in the optical region, $\Delta\lambda \sim 100$ to 200 A. It is also apparent that in the case of a gyrotropic medium the absorption will not be as effective in masking the effect of spatial dispersion simply because the latter effect is so much stronger.

3. CRYSTALLINE MEDIUM

In rhombic, tetragonal, and cubic crystals the principle axes of the tensor ϵ_{ik} coincide with the symmetry axes (these will also be used as the coordinate axes x, y and z below). Under these conditions the tensor α_{iklm} is simplified and in rhombic, tetragonal, and cubic crystals has 12, 7 and 3 independent components respectively. Thus, in the tetragonal case the nonvanishing components are

$$\alpha_{xxxx} = \alpha_{yyyy}, \quad \alpha_{zzzz}, \quad \alpha_{xxyy} = \alpha_{yyxx}, \quad \alpha_{xxzz} = \alpha_{yyzz}, \quad \alpha_{zzxx} = \alpha_{zzyy}, \quad \alpha_{xzxz} = \alpha_{yzyz} \text{ and } \alpha_{xyxy},$$

where the z axis is the axis of 4-th order symmetry. In a cubic crystal the non-vanishing components are

$$\alpha_1 = \alpha_{xxxx} = \alpha_{yyyy} = \alpha_{zzzz}, \quad \alpha_2 = \alpha_{xxyy} = \alpha_{yyxx} = \alpha_{xxzz} = \alpha_{zzxx} = \alpha_{yyzz} = \alpha_{zzyy} \text{ and } \alpha_3 = \alpha_{xyxy} = \alpha_{xzxz} = \alpha_{yzyz}.$$

Whence it is clear that a weak optical anisotropy should be observed in cubic crystals where $\epsilon_{ik} = \epsilon\delta_{ik}$. Far from frequencies at which ϵ is zero or infinite, to a first approximation $\hat{n}^2 = n_0^2 = \epsilon$ (it is assumed that $\epsilon > 0$ and that absorption can be neglected). To take account of the weak anisotropy is obviously necessary to substitute this value $\hat{n}^2 = n_0^2$ for $\hat{\epsilon}_{ik}$ in (1.3). The resulting tensor $\hat{\epsilon}_{ik}$ is of the form:

$$\begin{aligned}
\hat{\varepsilon}_{xx} &= \varepsilon[1 + \alpha_1 s_x^2 + \alpha_2(s_x^2 + s_z^2)], \\
\hat{\varepsilon}_{yy} &= \varepsilon[1 + \alpha_1 s_y^2 + \alpha_2(s_x^2 + s_z^2)], \\
\hat{\varepsilon}_{zz} &= \varepsilon[1 + \alpha_1 s_z^2 + \alpha_2(s_x^2 + s_y^2)], \quad \hat{\varepsilon}_{xy} = 2\varepsilon\alpha_3 s_x s_y, \\
\hat{\varepsilon}_{xz} &= 2\varepsilon\alpha_3 s_x s_z, \quad \hat{\varepsilon}_{yz} = 2\varepsilon\alpha_3 s_y s_z.
\end{aligned} \tag{3.1}$$

The principle axes of the tensor $\hat{\epsilon}_{ik}$ depend on the direction of the normal and in the general case will not coincide with the axes of 4-th order symmetry x, y and z. To detect the weak birefringence it is probably easiest to observe the ellipticity of the light transmitted through the crystal. The ellipticity is defined by the difference in the refractive indices for waves with different polarization $\Delta n \sim n_0\alpha$, where α is a suitable combination of the coefficients α_i and s_i. With $n_0 \sim 1$ and $\alpha \sim 10^{-6}$ the phase shift $\Delta\varphi = (2\pi/\lambda_0)\Delta n l \sim 0.1 l$ where l is the path in cm traversed by the light in the crystal. An effect of this order of magnitude is detectable. On the other hand it should be kept in mind that the values of α may be somewhat smaller than those which have been assumed and that the observation may be complicated by possible directional effects and other factors.

When the light propagates along a cubic axis, there is no birefringence and when $\epsilon \to 0$ or $\epsilon \to \infty$, one should observe the features discussed above for the isotropic case. For other directions of $\mathbf{s}$ and $\epsilon = 0$ all the roots $\hat{n}^2_{1,2,3} = 0$ and in this region one of the waves is like a plasma wave while the others are like transverse waves. In other words, the picture is similar to that which obtains for the isotropic case, being only slightly complicated by the weak anisotropy. The same considerations apply to the region $\epsilon \to \infty$ in which it is necessary to make use of the expansion in (1.4).

In non-cubic crystals, in which the tensor ϵ_{ik} is not completely degenerate, in the general case the situation is entirely different. For a uniaxial crystal, to which we shall limit ourselves for simplicity, with $\alpha_{iklm} = 0$:

$$\hat{n}_1^2 = \varepsilon_\perp, \quad 1/\hat{n}_2^2 = \sin^2\theta/\varepsilon_\parallel + \cos^2\theta/\varepsilon_\perp, \qquad (3.2)$$

where

$$\sin\theta = s_z, \quad \cos\theta = s_x, \quad s_y = 0, \quad \varepsilon_\parallel = \varepsilon_z, \quad \varepsilon_\perp = \varepsilon_x = \varepsilon_y.$$

Suppose that

$$\theta \neq 0, \quad \theta \neq \pi/2, \quad \varepsilon_\parallel \neq \varepsilon_\perp. \qquad (3.3)$$

In this case the refractive index for the extraordinary wave n_2 does not approach infinity as either $\epsilon_\parallel$ or $\epsilon_\perp$ approach infinity. If, however, the values of $\epsilon_\parallel$ and $\epsilon_\perp$ are finite but of different sign, $\hat{n}_2^2 = \infty$ when

$$\varepsilon_\perp \sin^2\theta + \varepsilon_\parallel \cos^2\theta = 0. \qquad (3.4)$$

If either $\epsilon_\parallel$ or $\epsilon_\perp$ is zero, $\hat{n}_2^2 = 0$. The cases $\theta = 0$ and $\theta = \pi/2$ are degenerate; wave 2 becomes transverse and there is a longitudinal wave whose frequency, for $\alpha = 0$, is determined by the conditions $\epsilon_\parallel(\omega) = 0$ or $\epsilon_\perp(\omega) = 0$. Another special case, which is not realizable, occurs if $\epsilon_\parallel = \epsilon_\perp = 0$ or $\epsilon_\parallel = \epsilon_\perp = \infty$ at the same frequency (in a biaxial crystal this refers to all three principal values ϵ_x, ϵ_y and ϵ_z). In essence, at this frequency the crystal degenerates into a cubic crystal, with all the features characteristic of the latter. In particular, only with $\epsilon_x = \epsilon_y = \epsilon_z$ for any direction will there be a wave (longitudinal) characterized by $\mathbf{D} = 0$. In the case indicated by (3.3) $\mathbf{D} \neq 0$, but if (3.4) is satisfied wave 2 becomes longitudinal. This is due to the fact that as $\hat{n}^2$ increases, for a given $\mathbf{D}$ the angle between $\mathbf{s}$ and $\mathbf{E}$ is reduced and when $n^2 \to \infty$, $\mathbf{s}\cdot\mathbf{E} \to 0$ [cf. Eq. (1.6)]. Hence, in non-cubic crystals, with $\alpha_{iklm} = 0$ in general there is no new wave analogous to the longitudinal wave 3 in an isotropic medium. The limiting transiton to a cubic crystal is not trivial. If $\epsilon_\parallel \to 0$ and $\epsilon_\perp > 0$ the tensor ellipsoid

$$(x^2 + y^2)/\varepsilon_\perp + z^2/\varepsilon_\parallel = 1$$

degenerates into a plane disc; if $\epsilon_\perp \to 0$ and $\epsilon_\parallel > 0$, it becomes a line. In other words, as one of the principal values ϵ_i approaches zero the crystal becomes anisotropic in the limit even if the other principal values are small. Different signs for $\epsilon_\parallel$ and $\epsilon_\perp$ means that we do not have a tensor ellipsoid but a tensor hyperboloid, with (3.4) as the asymptote. As one of the principle values approaches zero in the limit the anisotropy is also large in this case. If $\epsilon_x = \epsilon_y = \epsilon_z = 0$ the tensor ellipsoid or hyperboloid degenerates to a point.

In the case given by (3.3), which we also consider, if spatial dispersion is taken into account and the condition in (3.4) is not satisfied there is a non-real third wave with a very high value of $\hat{n}_3^2$. Only in the region of angles and frequencies for which the quantity $\epsilon_\perp \sin^2\theta + \epsilon_\parallel \cos^2\theta$ is very small does spatial dispersion lead to an interesting result.* If the condition in (3.4) is observed the values of $\epsilon_\parallel$ and $\epsilon_\perp$ are different from zero and finite. In this case the expansions in (1.3) and (1.4) are equivalent. In the general case the expressions which are obtained are extremely complicated. In order to illustrate the qualitative aspects of the problem we make a further far-reaching assumption: namely,

$$\hat{\varepsilon}_\parallel = \varepsilon_\parallel - \alpha\hat{n}^2, \quad \hat{\varepsilon}_\perp = \varepsilon_\perp - \alpha\hat{n}^2. \qquad (3.5)$$

The equation for $\hat{n}^2$ assumes the form:

*The fact that in general the third wave in an anisotropic medium has a real value only in the region where $n_2 \to \infty$ was noted by the author earlier in the case of a magneto-active plasma (cf. reference 7, § 75).

$$(\varepsilon_\perp - \hat{n}^2)\{\alpha\hat{n}^4 - [\varepsilon_\perp \sin^2\theta + \varepsilon_\parallel \cos^2\theta + (\varepsilon_\perp + \varepsilon_\parallel)\alpha]\hat{n}^2 + \varepsilon_\parallel\varepsilon_\perp\} = 0, \quad (3.6)$$

where small terms have been neglected.

With $\alpha = 0$ Eq. (3.6) becomes Eq. (1.7) with $\epsilon_x = \epsilon_y = \epsilon_\perp$ and $\epsilon_z = \epsilon_\parallel$ and its solution is given by (3.2). When

$$\hat{n}_1^2 = \varepsilon_\perp, \quad \hat{n}_{2,3}^2 = \mu/2\alpha \pm \sqrt{(\mu/2\alpha)^2 - \varepsilon_\perp\varepsilon_\parallel/\alpha},$$
$$\mu = \varepsilon_\perp \sin^2\theta + \varepsilon_\parallel \cos^2\theta + (\varepsilon_\parallel + \varepsilon_\perp)\alpha. \quad (3.7)$$

The dependence of $\hat{n}_{2,3}^2$ on angle θ or frequency ω close to the point $\mu = 0$ is completely analogous to the dependence on ω in (2.5) close to the point $\epsilon = \infty$ (cf. Figs. 1 and 2). With $\mu^2 \gg |4\alpha\epsilon_\perp\epsilon_\parallel|$, it is apparent that $\hat{n}_2^2$ is determined by (3.2) and $\hat{n}_3^2 \approx \mu/\alpha$. When $\theta \to 0$ and $\epsilon_\perp \to 0$: $\hat{n}_2^2 = \epsilon_\perp$, $\hat{n}_3^2 = \epsilon_\parallel$ as is to be expected. When $\theta \to \pi/2$ and $\epsilon_\perp \to 0$, similarly $\hat{n}_2^2 = \epsilon_\parallel$ and $n_3^2 = \epsilon_\perp/\alpha$. Moreover, when $\theta = 0$ and $\theta = \pi/2$, $\hat{n}_2^2 \to \infty$ correspondingly for $\epsilon_\perp \to \infty$ and $\epsilon_\parallel \to \infty$ ($\hat{n}_1^2 \to \infty$ for $\epsilon_\perp \to \infty$ at all angles for wave 1). In these cases spatial dispersion is taken into account through the use of an expansion such as that given in (2.4).

As in an isotropic medium and cubic crystals in non-cubic crystals, spatial dispersion is considerably stronger when the medium is gyrotropic (cf. Sec. 2). However, we shall not stop here to consider this problem nor a number of other problems which require special investigation (the behavior of the rays and the group velocity, gyrotropic effects under the influence of an external magnetic field, magnetic media such as ferrites, biaxial crystals, conical refraction, axial dispersion, dispersion relations, artificial anisotropy induced by electric fields, in which case it is possible to realize the limiting transition to isotropy, a more detailed analysis of absorption, etc.).

We have considered above only waves in an unbounded medium. Any observation of these effects would always require an examination of the boundary situation (for example, a first step would be to solve the problem of transmission of light through a plane slab). Thus boundary conditions must be considered. The ordinary conditions

$$D_{2n} = D_{1n}, \; H_{2n} = H_{1n}, \; E_{2t} = E_{1t}, \; H_{1t} = H_{2t},$$

are valid but not adequate if one is to take account of the new waves. Within the framework of the phenomenological approach employed here, additional boundary conditions can be obtained only by introducing certain assumptions.

For example, we may consider the boundary between a medium and vacuum and write the vector $\mathbf{D}$ in the form

$$D_i = \varepsilon_{ik}E_k + D_i' = E_i + (\varepsilon_{ik} - \delta_{ik})E_k + D_i' = E_i + D_i''. \quad (3.8)$$

In vacuum $\mathbf{D}'' = 0$ and if the boundary is not sharp $\mathbf{D}''$ approaches zero smoothly in the transition layer. On this basis, one would write at a sharp boundary:

$$\mathbf{D}'' = \mathbf{D} - \mathbf{E} = 4\pi\mathbf{P} = 0. \quad (3.9)$$

On the other hand, if spatial dispersion is neglected completely, and $\mathbf{D}' = 0$, (3.9) is no longer correct (in this case, from the condition $D_{2n} = D_{1n} = E_{1n}$ it is clear that only $P_n = 0$). Hence, a more reasonable boundary condition is

$$\mathbf{D}' = 0. \quad (3.10)$$

In his paper Pekar[2] used a boundary condition which was an "average" of (3.9) and (3.10) while the vector $\mathbf{P}$ was specifically set equal to zero except for an indefinite part of local origin. Since the new waves generally appear only under very special circumstances, further refinement of the analysis of boundary conditions will probably result from the solution of specific problems.

One might also be interested in finding the electromagnetic field and radiated energy for sources located in a medium with spatial dispersion. In the isotropic case this problem can be solved by an extension of classical methods; in crystals, however, it is more feasible to use the Hamiltonian method. This approach was used in reference 8, in which spatial dispersion was not taken into account.

4. REMARKS ON COLLECTIVE ENERGY LOSSES AND THE CERENKOV EFFECT

The discrete energy losses of fast electrons or other charged particles which move in a medium are related to the excitation of longitudinal waves (plasmons).[6]

If spatial dispersion is not taken into account, the longitudinal oscillations take place at frequencies ω_l such that $\epsilon(\omega_l) = 0$ and the corresponding energy losses are associated with the so-called polarization or Bohr energy loss in the medium (cf. reference 9). In the presence of spatial dispersion the polarization loss becomes the Cerenkov effect and is associated with the emission of a longitudinal wave 3 for which $n_3^2 = \epsilon(\omega)/\alpha$ [cf. Eq. (2.2)], assuming an isotropic medium. In this case it is apparent that the following condition must be satisfied:

$$\cos\theta = c/vn(\omega), \quad (4.1)$$

where θ is the angle between the normal $\mathbf{s}$ and the particle velocity $\mathbf{v}$, $n = n_3$ and the variation

in particle energy is neglected (this last condition assumes that $v \gg v_0$ – the velocity at the Fermi limit).

Since $\alpha \sim (v_0/c)^2 \sim 10^{-5}$, even with $\Delta\omega/\omega_l = (\omega - \omega_l)/\omega_l \sim 0.03$ to 0.1 a macroscopic analysis becomes unfeasible because $n_3 \sim 10^2$, $\epsilon \sim 0.1$ and $\lambda = \lambda_0/n_3 \sim 10^{-7}$. As a result the intensity of the Cerenkov radiation falls off sharply and the absorption increases. Hence the radiated longitudinal waves (plasmons) are characterized by a relatively narrow spectrum with $\Delta\omega \leq 0.1\,\omega_l$. Transverse Cerenkov radiation occurs if the condition

$$\varepsilon = n_{1,2}^2 > (c/v)^2 \qquad (4.2)$$

is satisfied but usually the radiation is characterized by a wide spectrum, i.e., non-discrete losses. An exception might be a medium with weak absorption in which the condition in (4.2) would be satisfied only over a relatively narrow frequency range, for example close to an absorption line.

In cubic crystals, in the first approximation the discrete (collective) losses are of the same nature as those in an isotropic medium. The only distinction is due to the spatial dispersion which leads to the weak optical anisotropy for cubic crystals (cf. Sec. 3). This anisotropy is especially marked in metals because for a cubic structure the Fermi surface is not a sphere and the corresponding velocity v_0 depends on direction. Inasmuch as the width of the longitudinal Cerenkov radiation in an isotropic medium is not small in absolute magnitude the weak anisotropy which is indicated in the discrete losses is not of great importance.*

The situation in non-cubic crystals is different because in the general case there is no specific individual branch for the longitudinal waves. Even if spatial dispersion is neglected, there are no polarization losses. Hence, all the collective losses are to be associated with the Cerenkov effect (cf. also reference 9). On the other hand, in non-cubic crystals even when $\epsilon_i < 1$ there are frequencies for which the refractive index becomes rather large. This is the case particularly in a region which corresponds to the condition in (3.4) or, for an arbitrary crystal, to the condition

$$\varepsilon_x(\omega_{ls})\, s_x^2 + \varepsilon_y(\omega_{ls})\, s_y^2 + \varepsilon_z(\omega_{ls})\, s_z^2 = 0. \qquad (4.3)$$

Under these conditions, as has already been pointed out, wave 1 or 2 is longitudinal and it is important to take account of spatial dispersion. In solids, particularly in metals, at frequencies of the order of 10^{16} (energies of approximately 10 ev) the Cerenkov condition (4.1) may be satisfied only for $\omega = \omega_{ls}$ [cf. Eq. (4.3)]. As a result the collective losses are again of discrete nature although, in addition to spatial dispersion there is one other effect which tends to broaden the spectrum. This effect is a result of the fact that the frequency ω_{ls}, as is clear from Eq. (4.3), depends on the direction of wave propagation in the crystal. If the vector associated with the normal $\mathbf{s}$ approaches the direction of the principal axis i Eq. (4.3) assumes the form $\epsilon_i(\omega_{li}) = 0$, which is the same as the existence condition for longitudinal waves along the i axis. The additional broadening of the discrete line is then due simply to the fact that $\omega_{lx} \neq \omega_{ly} \neq \omega_{lz}$, or, in a uniaxial crystal the fact that $\omega_{l\perp} \neq \omega_{l\parallel}$.

In conclusion we may note that the use of the Cerenkov effect would seem to offer the best approach to the problem of exciting "spatial dispersion" waves although problems such as those mentioned at the end of Sec. 3 would arise.

*In this connection the anisotropy in the optical properties of cubic crystals, which results from spatial dispersion, may be important in analyzing the interaction of plasmons with an external transverse electromagnetic field and may lead, for example, to the excitation of quasi-longitudinal plasmons when light is incident on the crystal boundary. It is likely that taking account of spatial dispersion in the macroscopic behavior is, in some degree, equivalent to the quasi-microscopic analysis of plasmons as waves in a degenerate electron gas of inhomogeneous density.[10]

[1] Gershman, Ginzburg and Denisov, Usp. Fiz. Nauk **61**, 561 (1957); see also J. Exptl. Theoret. Phys. (U.S.S.R.) **31**, 707 (1956); Soviet Phys. JETP **4**, 582 (1957).

[2] S. I. Pekar, J. Exptl. Theoret. Phys. (U.S.S.R.) **33**, 1022 (1957); Soviet Phys. JETP **6**, 785 (1958).

[3] Landau and Lifshitz, Электродинамика сплошных сред (Electrodynamics of Continuous Media) Moscow, 1957.

[4] V. L. Ginzburg, Теория распространения радиоволн в ионосфере (Propagation of Radio Waves in the Ionosphere) Gostekhizdat, 1949.

[5] H. Frolich and H. Pelzer, Proc. Phys. Soc. (London) **68A**, 525 (1955).

[6] D. Pines, Revs. Modern Phys. **28**, 184 (1956); Usp. Fiz. Nauk **62**, 399 (1957).

[7] Al'pert, Ginzburg, and Feinberg, Распространение радиоволн (Propagation of Radio Waves) Gostekhizdat 1953.

[8] V. L. Ginzburg, J. Exptl. Theoret. Phys. (U.S.S.R.) **10**, 601 (1940).

[9] B. M. Bolotovskii, Usp. Fiz. Nauk **62**, 201 (1957).

[10] E. L. Feinberg, J. Exptl. Theoret. Phys. (U.S.S.R.) **34**, 1125 (1958), Soviet Phys. JETP **7**, 780 (1958).

Translated by H. Lashinsky
311

OBLIQUE SHOCK WAVES IN A PLASMA WITH FINITE CONDUCTIVITY

M. I. KISELEV and V. I. TSEPLIAEV

Moscow State University

Submitted to JETP editor January 20, 1958

J. Exptl. Theoret. Phys. (U.S.S.R.) **34**, 1605-1607 (June, 1958)

The structure of an oblique shock wave in a plasma with finite conductivity is considered neglecting its viscosity and thermal conductivity. The conditions of applicability of the approximation are obtained. An estimate of the width of the wave front is given. The limiting angle for the propagation of an oblique shock wave is obtained in a plasma of infinite conductivity.

1. BOUNDARY CONDITIONS

THE structure of the front of a normal shock wave in a plasma of finite conductivity has been investigated neglecting viscosity and thermal conductivity in the paper by Golitsyn and Staniukovich.[1] In this paper we consider the problem of the structure of the front of an oblique shock wave for an arbitrary orientation of the field ahead of the front in the same kind of plasma.

We consider a plasma with a constant and isotropic conductivity sufficiently large not to have to take displacement current into account. Let us determine the conditions for neglecting the kinematic viscosity ν and the electronic thermal conductivity κ in comparison with the magnetic viscosity ν_m in the system of equations of magneto-hydrodynamics (cf., for example, Syrovatskii[2]).

As is well known (cf. Chapman and Cowling[3]),

$$\nu_m = c^2/4\pi\sigma = c^2/4\pi e^2 n_e \tau_{ei} = c^2/\omega_0^2 \tau_{ei}; \quad (1)$$

$$\nu = 3a^2\tau_{ii}/2\gamma, \quad (2)$$

where $\omega_0^2 = 4\pi n_e e^2/m_e$ is the characteristic plasma frequency, $\gamma = c_p/c_v$ is the ratio of specific heats, a is the velocity of sound, τ_{ei} and τ_{ii} are the times between electron-ion and ion-ion collisions respectively

$$\tau_{ei} = m_e^{1/2}(3kT)^{3/2}/0.7\cdot 4\pi n_e e^4 \ln\lambda_e,$$
$$\tau_{ii} = m_i^{1/2}(3kT)^{3/2}/0.7\cdot 8\pi n_i e^4 \ln\lambda_i. \quad (3)$$

Here

$$\lambda = (3/2e^3)(k^3T^3/\pi n)^{1/2} = h/p_0,$$

where h is the Debye screening radius, p_0 is the impact parameter for which an electron on colliding with an ion is deflected by 90° (for details see Spitzer[4]); n_e and n_i are the electron and ion densities respectively. We assume everywhere in the following that $n_e = n_i = n$.

If the kinetic and magnetic energies satisfy the inequality $\rho v^2 \leq H^2/4\pi$, then the condition $\nu_m \gg \nu$ assumes the form:

$$\frac{S^2}{r_0 v_{av}}\left(\frac{m_i}{m_e}\right)^{1/2} \gg 1, \qquad S = \frac{1}{\pi}\left(\frac{e^2}{kT}\right)^4 \ln\lambda. \quad (4)$$

Here S is the electron-ion collision cross-section; $r_0 = e^2/m_e c^2$ is the classical electron radius, $1/n = v_{av}$ is the average volume per particle. For $n = 10^{16}\,cm^{-3}$, $T = 10^4\,°K$, $m_i = 3.2\times 10^{-24}\,gm$ the left-hand side of the inequality is $\sim 10^4$.

A similar condition for neglecting the electronic thermal conductivity $\kappa = 20(2/\pi)^{3/2} kT/m^{1/2} e^4 \ln\lambda$ (cf. Spitzer[4]) can be written in the case $nkT \leq H^2/4\pi$ in the form:

$$S^2/22.5 r_0 v_{av} \gg 1. \quad (5)$$

The system of equations of magneto-hydrodynamics has the following particular integrals of the motion if all the quantities depend on only one coordinate x:

$$[\mathbf{v}\times\mathbf{H}]_{y,z} - \nu_m \mathbf{curl}_{y,z}\mathbf{H} = cE_{y,z} = \text{const}, \quad H_x = \text{const}.$$
$$\rho v_x = \text{const} = m, \quad g_x = \text{const} = \varepsilon, \quad \pi_{ix} = \text{const} = I_i, \quad (6)$$

where g_x is the energy flux density, while π_{ix} is the momentum flux density.

2. THE STRUCTURE OF AN OBLIQUE SHOCK WAVE

We consider an oblique shock wave in a plasma of finite conductivity. The parameters of the medium ahead of the front we shall denote by the subscript 1, while those for the medium inside the transition layer and behind the front we shall denote by 2. If $v_{iz} = 0$, $H_{iz} = 0$ then the system (6) assumes the form:

$$\rho_1 v_{1x} = \rho_2 v_{2x} = m, \qquad H_{1x} = H_{2x} = H_x,$$

$$v_{1x}H_{1y} - v_{1y}H_{1x} = v_{2x}H_{2y} - v_{2y}H_{2x} - \nu_m \frac{dH_{2y}}{dx} = cE_z,$$

$$\rho_1 v_{1x}v_{1y} - H_{1x}H_{1y}/4\pi = \rho_2 v_{2x}v_{2y} - H_{2x}H_{2y}/4\pi = \alpha,$$

$$\rho_1 v_{1x}\left(\frac{v_1^2}{2} + \frac{\gamma}{\gamma-1}\frac{p_1}{\rho_1}\right) + \frac{cE_{z1}}{4\pi} H_{1y} = \tag{7}$$

$$= \rho_2 v_{2x}\left(\frac{v_2^2}{2} + \frac{\gamma}{\gamma-1}\frac{p_2}{\rho_2}\right) + \frac{cE_{z2}}{4\pi} H_{2y} = \varepsilon,$$

$$p_1 + H_1^2/8\pi + \rho_1 v_{1x}^2 = p_2 + H_2^2/8\pi + \rho_2 v_{2x}^2 = I.$$

By solving the system for dH_{2y}/dx, and by eliminating all the variables except for H_{2y}, we obtain the following equation:

$$\nu_m \frac{dH_{2y}}{dx} = \frac{\gamma}{\gamma-1}\frac{H_{2y}}{m}\left(I - \frac{H_{2y}^2}{8\pi}\right) - \frac{H_x}{m}\left(\alpha + \frac{H_x}{4\pi} H_{2y}\right) - cE_z$$

$$+ H_{2y}\left\{\frac{\gamma^2}{(\gamma-1)^2 m^2}\left(I - \frac{H_{2y}^2}{8\pi}\right)^2\right. \tag{8}$$

$$\left. + 2\frac{\gamma-1}{\gamma+1}\left[\frac{1}{2m^2}\left(\alpha + \frac{H_x H_{2y}}{4\pi}\right)^2 - \frac{\varepsilon}{m} + \frac{cE_z}{4\pi m} H_{2y}\right]\right\}^{1/2} = f(H_{2y}).$$

Hence

$$x - x_0 = \nu_m \int_{H_{2y_0}}^{H_{2y}} dH_{2y}/f(H_{2y}). \tag{9}$$

The integral (9) is obtained by numerical methods.

Let the wave be propagated in monatomic deuterium whose initial parameters are given by:

$$\begin{aligned} &T_1 = 2\cdot 10^4\,^\circ\mathrm{K}, && p_1 = 2\cdot 10^4\ \mathrm{g/cm\text{-}sec^2}, \\ &v_{1x} = 2.36\cdot 10^6\ \mathrm{cm/sec}, && H_{1y} = 700\ \text{oersted}, \\ &v_{1y} = v_{1x}\tan\chi, && H_{1y} = H_{1x}\tan\varphi, \end{aligned} \tag{10}$$

and let $\varphi = \chi = 45°$ to simplify the calculations. The results are given in graphical form (Fig. 1), where the dimensionless quantity $\xi = xa/\nu_m$ is plotted along the horizontal axis.

The width of the front may be defined by

$$\Delta x = \Delta H_y / (dH_y/dx)_{\max}. \tag{11}$$

In the present case the width of the front is given in dimensionless units by $\Delta\xi = 6$. On calculating the number $k = \Delta x/l$ of mean free paths $l = \tau_{ii}/a$ contained in the width of the wave front we obtain

$$\Delta x = \nu_m \Delta\xi/a = c^2\Delta\xi/a\omega_0^2\tau_{ei}. \tag{12}$$

Finally

$$k = c^2\Delta\xi/\omega_0^2 a^2 \tau_{ei}\tau_{ii} \gg 1 \tag{13}$$

according to the inequality (6). In the case considered above $k \sim 10^4$.

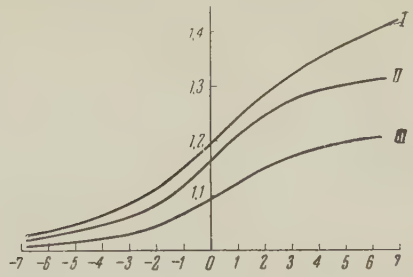

FIG. 1. Curve I shows the dependence of p/p_1, on ξ, curve II shows H_y/H_{1y}, curve III shows ρ/ρ_1. $p_2\infty/p_1 = 1.45$, $H_{2y\infty}/H_{1y} = 1.32$; $\rho_{2\infty}/\rho_1 = 1.22$, where the subscript ∞ refers to the limiting values of the quantities behind the wave front.

3. THE LIMITING ANGLE FOR THE PROPAGATION OF AN OBLIQUE SHOCK WAVE IN A PLASMA OF INFINITE CONDUCTIVITY

The following system is equivalent to an equation of the type which holds for a shock wave in an ideally conducting plasma with $H_{iz} = 0$:

$$v_{2x} = \frac{4\pi(mcE_z + \alpha H_x) + H_{2y}H_x^2}{4\pi m H_{2y}}, \qquad v_{2y} = \frac{(\alpha + H_x H_{2y}/4\pi)}{m}, \tag{14}$$

where the parameter H_{2y} is the first root of the equation

$$\frac{\gamma}{\gamma-1}\left(I - \frac{y^2}{8\pi}\right)\frac{y}{m} + y\left\{\frac{\gamma^2}{(\gamma-1)^2}\left(I - \frac{y^2}{8\pi}\right)^2\right.$$

$$\left. + 2\frac{\gamma-1}{\gamma+1}\left[\frac{1}{2m^2}\left(\alpha + \frac{H_x}{4\pi}y\right) - \frac{\varepsilon}{m} + \frac{cE_z}{4\pi m}y\right]\right\}^{1/2}$$

$$- \frac{H_x}{m}\left(\alpha + \frac{H_x}{4\pi}y\right) - \frac{cE_z}{m} = 0,$$

which satisfies the condition $y \geq H_{iy}$.

In order to find $v_{2y}\,\varphi\,(v_{2x})$ it is necessary to vary $\mathbf{v}_1$ keeping v_1 constant. Variation of the magnitude of H_1 and of the angle at which H_1 is inclined with respect to the front will yield a two-parametric family of shock waves.

It is possible to obtain an expression for the limiting angle of tilt of an oblique shock wave in a certain special case when $\mathbf{H}_1(0, H_{1y}, H_{1z})$, $\mathbf{v}_1(v_{1x}, 0, 0)$, i.e. when the coordinate system is so chosen that the wave front is at rest in it, and makes a certain angle χ with the YZ plane (cf. Fig. 2).

In order to obtain boundary conditions for this problem we rotate the original system of coordinates by an angle χ about the Z axis. Then

$$\rho_1 v_{1x} = \rho_2 (v_{2x} - v_{2y}\tan\chi); \tag{15}$$

$$H_{2x} = H_{2y}\tan\chi; \tag{16}$$

$$v_{1x}H_{1z} = H_{2z}(v_{2x} - v_{2y}\tan\chi), \quad v_{1x}H_{1y} = H_{2y}(v_{2x} - v_{2y}\tan\chi); \tag{17}$$

$$\frac{v_1^2}{2} + \frac{\gamma}{\gamma-1}\frac{p_1}{\rho_1} + \frac{H_{1y}^2}{4\pi\rho_1\cos^2\chi} - \frac{H_{1z}^2}{4\pi}$$

$$= \frac{v_2^2}{2} + \frac{\gamma}{\gamma-1}\frac{p_2}{\rho_2} + \frac{H_{1y}H_{2y}}{4\pi\rho_1\cos^2\chi} + \frac{H_{1z}H_{2z}}{4\pi\rho_1}; \tag{18}$$

$$p_1 + \rho_1 v_{1x}^2\cos^2\chi + \frac{H_{1y}^2}{8\pi\cos^2\chi} + \frac{H_{1z}^2}{8\pi}$$

$$= p_2 + \rho_1 v_{1x}\cos^2\chi(v_{2x} - v_{2y}\tan\chi) + \frac{H_{2y}^2}{8\pi\cos^2\chi} + \frac{H_{2z}^2}{8\pi}; \tag{19}$$

$$v_{1x}\tan\chi = v_{2x}\tan\chi + v_{2y}, \quad v_{2z} = 0. \tag{20}$$

For $v_{2X} \to v_{1X}$, $v_{2y} \to 0$ we have $H_{2y} \to H_{1y}$, $H_{2Z} \to H_{1Z}$, $\rho_2 \to \rho_1$, $p_2 \to p_1$ and from (20):

$$(dv_{2y}/dv_{2x})_{v_{2x}\to v_{1x}} \to -\tan\chi_0,$$

where χ_0 is the limiting angle for the propagation of an oblique shock wave. From (15), (17) and (19) we obtain ρ_2, H_{2y}, H_{2Z} and p_2 as functions of v_{2y} and v_{2X}. On substituting these values into (18) we obtain the implicit relation $f(v_{2X}, v_{2y}) = 0$. On differentiating it with respect to v_{2X}, and then after setting $v_{2X} \to v_{1X}$, $v_{2y} \to 0$ we obtain

$$\cos^2\chi_0 = \frac{1}{2}\left(\frac{a_1^2}{v_1^2} - \frac{H_{1z}^2}{4\pi\rho_1 v_1^2}\right)$$

$$\pm\frac{1}{2}\left\{\left(\frac{a_1^2}{v_1^2} - \frac{H_{1z}^2}{4\pi\rho_1 v_1^2}\right)^2 - \frac{2\gamma-1}{\pi\rho_1 v_1^2}H_{1y}^2\right\}^{1/2}, \tag{21}$$

where $a_1^2 = \gamma p_1/\rho_1$ is the velocity of sound in the medium ahead of the front. It is necessary to retain the plus sign in formula (21) as is evident from a transition to ordinary hydrodynamics ($H = 0$) where $\cos^2\chi_0 = a_1^2/v_1^2$.

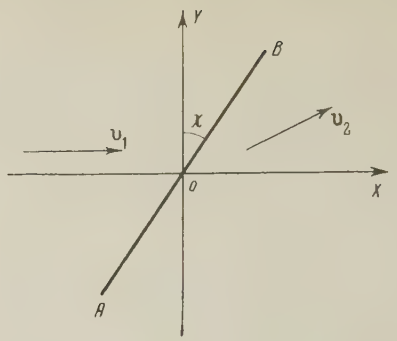

FIG. 2. AB is the front of an oblique shock wave, v_1 is the velocity ahead of the front, v_2 is the velocity behind the front.

It is clear from formula (21) that the limiting angle for the propagation of oblique shock waves in the presence of a magnetic field is greater than in the field-free case.

In conclusion we consider it to be our pleasant duty to express our gratitude to K. P. Staniukovich for suggesting the problem and for constant interest in the work.

[1] G. S. Golitsyn and K. P. Staniukovich, J. Exptl. Theoret. Phys. (U.S.S.R.) **33**, 1417 (1957). Soviet Phys. JETP **6**, 1090 (1958).

[2] S. I. Syrovatskii, Usp. Fiz. Nauk **62**, 247 (1957).

[3] S. Chapman and T. G. Cowling, The Mathematical Theory of Nonuniform Gases, Cambridge, 1939.

[4] L. Spitzer, The Physics of Fully Ionized Gases, New York, 1955 (Russian translation, Moscow, 1957).

Translated by G. Volkoff
312

PHENOMENOLOGICAL THEORY OF KINETIC PROCESSES IN FERROMAGNETIC DIELECTRICS

M. I. KAGANOV and V. M. TSUKERNIK

Physico-Technical Institute, Academy of Sciences, Ukrainian S.S.R.

Submitted to JETP editor March 22, 1958

J. Exptl. Theoret. Phys. (U.S.S.R.) **34**, 1610-1618 (June, 1958)

The relaxation time resulting from the interaction of spin waves with each other, in ferromagnetic dielectrics, is calculated.

THE present paper is concerned with those relaxation processes, in ferromagnets, that result from the interaction of spin waves with each other. In contrast to the work of Akhiezer,[1] the treatment is carried through without any assumption about the nominal magnetization of the ferromagnetic in its ground state.

Relaxation processes in a ferromagnetic are not limited to interactions within the spin system; spin waves also interact with lattice vibrations. However, as will be shown below, there are a number of cases in which interactions between spin waves play the fundamental role in the establishment of equilibrium.

1. THE ENERGY SPECTRUM OF A FERROMAGNET

As was shown by Herring and Kittel,[2] the energy spectrum of a ferromagnet in the neighborhood of the ground state can be obtained without assuming a model for the spin structure of the ground state. Instead, purely phenomenological assumptions are made in regard to the existence of exchange interaction with a positive exchange integral and, consequently, the presence of a spontaneous magnetic moment at $T = 0$.

In order to study kinetic processes in ferromagnetics, it is necessary to know not only the energy spectrum, which determines all the thermodynamic quantities[3] but also the wave functions of the spin waves; it is by means of these that the probabilities of transition between different states of the system are calculated. Therefore we shall here use a systematic quantum-mechanical method to find the energy levels related to the motion of the magnetic moment in a ferromagnetic. We shall take account both of the large exchange interaction and of the small relativistic contribution (the anisotropy energy and the magnetic interaction). At very low temperatures, as was shown in reference 3, the magnetic interaction plays an essential role in the spectrum.

We shall start with the Hamiltonian

$$\mathcal{H} = \int dv \left\{ -\mathbf{H}_0\mathbf{M} + \frac{1}{2}\beta M_\perp^2 + \frac{1}{2}\alpha_{ik}\frac{\partial M_l}{\partial x_i}\frac{\partial M_l}{\partial x_k} \right\} + \iint \frac{dvdv'}{2R^5}\left[\mathbf{M}(\mathbf{r})\,\mathbf{M}(\mathbf{r}')\,R^2 - 3\,(\mathbf{RM}(\mathbf{r}))\,(\mathbf{RM}(\mathbf{r}'))\right], \quad (1)$$

where the first term in curly brackets describes the interaction of the magnetic moment of unit volume, $\mathbf{M} = \mathbf{M}(\mathbf{r})$,* with a constant magnetic field $\mathbf{H}_0$; $\mathbf{H}_0$ coincides with the external magnetic field if the demagnetizing factor is negligible. The second term is the anisotropy energy; $M_\perp$ is the projection of the magnetic moment on a plane perpendicular to the axis of easiest magnetization, and β is the magnetic anisotropy constant at $T = 0$.† The third term describes an isotropic exchange interaction; the quantities α_{ik} are the constants of this interaction, and in order of magnitude they are equal to $\Theta_C a^2/\mu M_0$, where a is the lattice constant and μ the Bohr magneton.[5]

The second term in (1) (the double integral) describes the magnetic interaction; $\mathbf{R} = \mathbf{r} - \mathbf{r}'$.

The integration extends over all space (the ferromagnet is assumed to be infinite).

Let the magnetic field $\mathbf{H}_0$ be directed at angle φ to the axis of easiest magnetization. Then the magnetic moment in the ground state, $\mathbf{M}_0$, makes some angle ψ with the axis of easiest magnetization. The angle ψ is determined by the condition

*$\mathbf{M}(\mathbf{r})$ is the magnetic moment density. The total magnetic moment of the ferromagnetic is $\mathfrak{M} = \int \mathbf{M}(\mathbf{r})dv$.

†The form of the anisotropy energy that we have chosen is correct for small angles of inclination of the magnetic moment to the axis of easiest magnetization.[4] In the general case the anisotropy energy is a complicated function of M_x, M_y, and M_z. As will be clear from what follows, spin waves can always be introduced in the manner described here.

that the magnetic energy in the ground state be a minimum:

$$\sin(\varphi - \psi) = (\beta M_0 / 2H_0)\sin 2\psi. \quad (2)$$

We note that in the ground state ($\mathbf{M}$ = const.) the magnetic interaction energy is equal to zero.*

We choose a system of coordinates in the following manner: with the z axis along the direction of the magnetic moment $\mathbf{M}_0$, and with the x axis in the plane of the vectors $\mathbf{M}_0$ and $\mathbf{H}_0$. Then the anisotropy energy $\mathcal{H}_A$ has the form

$$\mathcal{H}_A = \int dv\,\{M_x\cos\psi + M_z\sin\psi)^2 + M_y^2\}. \quad (3)$$

As regards the other terms in the Hamiltonian (1), their form, by virtue of invariance, is independent of the choice of the coordinate system.

In quantum theory, the projections of the magnetic moment must be treated as operators with the commutation rules

$$M^-(\mathbf{r})M^+(\mathbf{r}') - M^+(\mathbf{r}')M^-(\mathbf{r}) = 2g\hbar M_z\delta(\mathbf{r}-\mathbf{r}'), \quad (4)$$

where

$$M^\pm = M_x \pm iM_y, \quad (5)$$

and where g is the gyromagnetic ratio ($g > 0$). The commutation rule for the components of $\mathbf{M}(\mathbf{r})$ follows from the commutation rule for the components of the total moment,

$$\mathfrak{M}_x\mathfrak{M}_y - \mathfrak{M}_y\mathfrak{M}_x = -ig\hbar\mathfrak{M}_z.$$

Following Holstein and Primakoff,[6] we introduce operators $a(\mathbf{r})$ and $a^*(\mathbf{r})$ that satisfy the commutation rule

$$a(\mathbf{r})a^*(\mathbf{r}') - a^*(\mathbf{r}')a(\mathbf{r}) = \delta(\mathbf{r}-\mathbf{r}'), \quad (6)$$

and we express in terms of them the operators M^+, M^-, and M_Z:

$$\begin{aligned} M^+ &= (2g\hbar M_0)^{1/2}a^*(1 - g\hbar a^*a/2M_0)^{1/2},\\ M^- &= (2g\hbar M_0)^{1/2}(1 - g\hbar a^*a/2M_0)^{1/2}a,\\ M_z &= M_0 - g\hbar a^*a. \end{aligned} \quad (7)$$

In the neighborhood of the ground state, $M_Z \approx M_0$, and M_X and M_Y are much smaller than M_0. We may therefore treat the operators a and a* as small and expand the integrand in the Hamiltonian (1) in powers of a and a*. For finding the spectrum, we may limit ourselves to terms of the second order in a and a* (the first-order terms drop out by virtue of the choice of the ground state).

After simple transformations we get $\mathcal{H} = \mathcal{H}_0 + \mathcal{H}'$, where $\mathcal{H}'$ contains the terms of third and higher orders in a and a*, and where

$$\mathcal{H}_0 = (a^*\hat{A}a) + {}^1/_2(a\hat{B}a) + {}^1/_2(a^*\hat{B}^*a^*). \quad (8)$$

In the expression (8), the parentheses denote integration over the volume of the ferromagnetic, and the operators $\hat{A}$ and $\hat{B}$ are defined by the equations.

$$\begin{aligned} \hat{A}a(\mathbf{r}) &= \left[g\hbar H_0\cos(\varphi-\psi) + \tfrac{1}{2}\beta g\hbar M_0(\cos 2\psi + \cos^2\psi)\right]a(\mathbf{r})\\ &- g\hbar M_0\alpha_{ik}\frac{\partial^2 a(\mathbf{r})}{\partial x_i\partial x_k} - g\hbar M_0\int\frac{dv'}{R^5}\left(\frac{3}{2}R^+R^- - R^2\right)a(\mathbf{r}'). \end{aligned}$$

$$\hat{B}a(\mathbf{r}) = -\frac{1}{2}\beta g\hbar M_0(\cos^2\psi - 1)a(\mathbf{r}) - \frac{3}{2}g\hbar M_0\int\frac{dv'}{R^5}(R^+)^2 a(\mathbf{r}'). \quad (9)$$

$$R^\pm = R_x \pm iR_y.$$

The finding of the spectrum is related, as is well known, to the diagonalization of the Hamiltonian (8). For this purpose it is convenient to go over to the equations of motion of the operators a:[7,8]

$$\dot{a} = (i/\hbar)(\mathcal{H}_0 a - a\mathcal{H}_0). \quad (10)$$

By use of (8) and (6), we get from (10)

$$\dot{a} = -(i/\hbar)(\hat{A}a + \hat{B}^*a^*). \quad (11)$$

Since Eqs. (11) are linear, and since the operators $\hat{A}$ and $\hat{B}$ have difference-dependent kernels, we may seek a solution of (11) in the form of a Fourier series

$$a(\mathbf{r}, t) = \sum_\lambda\{u_\lambda(\mathbf{r})a_\lambda(t) + v_\lambda^*(\mathbf{r})a_\lambda^*(t)\}, \quad (12)$$

where

$$u_\lambda(\mathbf{r}) = u_\lambda e^{i\mathbf{k}_\lambda\mathbf{r}};\quad v_\lambda(\mathbf{r}) = v_\lambda e^{i\mathbf{k}_\lambda\mathbf{r}},$$

$$a_\lambda(t) = a_\lambda\exp\{-i\varepsilon_\lambda t/\hbar\}, \quad (13)$$

and the operators a_λ and a_λ^* satisfy the commutation rules

$$a_\lambda a_\mu^* - a_\mu^* a_\lambda = \delta_{\lambda\mu}. \quad (14)$$

On substituting (12) in (11) and comparing coefficients of a_λ and a_λ^*, we get

$$\varepsilon_\lambda u_\lambda = A_\lambda u_\lambda + B_\lambda^* v_\lambda,\quad -\varepsilon_\lambda v_\lambda = A_\lambda v_\lambda + B_\lambda u_\lambda. \quad (15)$$

Here

$$\begin{aligned} A_\lambda &= g\hbar H_0\cos(\varphi-\psi) + {}^1/_2\beta g\hbar M_0(\cos 2\psi + \cos^2\psi)\\ &+ g\hbar M_0\alpha_{ij}k_{\lambda i}k_{\lambda j} + 2\pi g\hbar M_0(k_{\lambda x}^2 + k_{\lambda y}^2)/k_\lambda^2; \end{aligned} \quad (16)$$

$$B_\lambda = -{}^1/_2\beta g\hbar M_0\sin^2\psi + 2\pi g\hbar M_0(k_{\lambda x} + ik_{\lambda y})^2/k_\lambda^2.$$

*The Hamiltonian (1) takes no account of the dependence of the magnitude of the magnetic moment in the ground state upon the magnetic field. This is legitimate up to fields of order $\varepsilon_a/\mu \sim 10^8$, where ε_a is the energy of an electron in the atom ($\varepsilon_a \sim 10^{-12}$ erg).

From Eqs. (15) we find

$$\varepsilon_\lambda = \sqrt{A_\lambda^2 - |B_\lambda|^2}. \tag{17}$$

The homogeneous equations (15) determine the values of u_λ and v_λ except for an arbitrary factor, whose value may be obtained from the normalization condition

$$|u_\lambda|^2 - |v_\lambda|^2 = 1/V, \tag{18}$$

where V is the volume of the ferromagnet. Condition (18) guarantees conformity to the commutation rules (14) and (6); it can be obtained by using the orthogonality relation for the solutions of the system (15):

$$\int \{u_\lambda(\mathbf{r})\, u_\mu^*(\mathbf{r}) - v_\lambda(\mathbf{r})\, v_\mu^*(\mathbf{r})\}\, dv = 0, \quad (\lambda \neq \mu),$$
$$\int \{u_\lambda(\mathbf{r})\, u_\mu(\mathbf{r}) - u_\lambda(\mathbf{r})\, v_\mu(\mathbf{r})\}\, dv = 0. \tag{19}$$

From (15) and (18) we have, except for a phase factor,

$$u_\lambda = \frac{1}{V 2V}\left(\frac{A_\lambda + \varepsilon_\lambda}{\varepsilon_\lambda}\right)^{1/2}, \quad v_\lambda = \frac{1}{V 2V}\frac{B_\lambda}{|B_\lambda|}\left(\frac{A_\lambda - \varepsilon_\lambda}{\varepsilon_\lambda}\right)^{1/2}. \tag{20}$$

By use of the equations of motion (11), the Hamiltonian $\mathcal{H}_0$ can be put into the following form:

$$\mathcal{H}_0 = (i\hbar/2)\{(a^*, \dot{a}) - (\dot{a}^*, a)\}. \tag{21}$$

On substituting a and a* from the Fourier series (12), we get

$$\mathcal{H}_0 = \sum_\lambda \varepsilon_\lambda (a_\lambda^* a_\lambda + 1/2) + G; \quad G = -1/2 \sum_\lambda A_\lambda; \tag{22}$$

G is a constant, which may always be omitted in the Hamiltonian.

The quantities $a_\lambda^* a_\lambda$, as is evident from (14) and (22), have the meaning of occupancy numbers (n_λ) for spin waves. Thus

$$\mathcal{H}_0 = \sum_\lambda \varepsilon_\lambda (n_\lambda + 1/2), \tag{23}$$

where ϵ_λ is determined by formulas (17) and (16).

We consider the limiting cases:

(1) Magnetic field H_0 parallel to the axis of easiest magnetization. In this case $\varphi = \psi = 0$;

$$A_\lambda = g\hbar(H_0 + \beta M_0) + g\hbar M_0 \alpha_{ij} k_{\lambda i} k_{\lambda j} + 2\pi g\hbar M_0 \sin^2\theta_\lambda,$$
$$B_\lambda = 2\pi g\hbar M_0 \sin^2\theta_\lambda e^{2i\varphi_\lambda} \tag{24}$$

(θ_λ and φ_λ are the polar angles of the vector $\mathbf{k}_\lambda$): If we treat α_{ij} as an isotropic tensor, $\alpha_{ij} = \alpha\delta_{ij}$, we arrive at the well known spectrum.[2] Here the quantity βM_0 plays the role of a magnetic anisotropy field. However, in the general case (H_0 not parallel to the axis of easiest magnetization), the magnetic anisotropy density cannot be expressed in the form $-\mathbf{MH}_A$, since the constant β enters in a different way in the expression for A_λ and B [cf. (16)].

(2) For large k_λ ($\alpha_{ij} k_{\lambda i} k_{\lambda j} \gg 1$),* $A_\lambda \gg |B_\lambda|$, and

$$\varepsilon_\lambda \approx A_\lambda \approx g\hbar H_0 + g\hbar M_0 \alpha_{ij} k_{\lambda i} k_{\lambda j}. \tag{25}$$

(We recall that $\beta \sim 1$.)

(3) For small k_λ ($\alpha_{ij} k_{\lambda i} k_{\lambda j} \ll 1$), A_λ and B_λ are of the same order of magnitude. In this case the expressions for A_λ and B_λ do not simplify.

2. INTERACTION OF SPIN WAVES WITH EACH OTHER

In the processes of interaction of spin waves with each other, a fundamental role is played by the terms of third and fourth order with respect to the operators a and a*. The third-order terms arise from expansion of the anisotropic relativistic terms in the Hamiltonian (1) (anisotropy energy and magnetic interaction energy):

$$\mathcal{H}_a' = -\frac{1}{4}(2g\hbar M_0)^{1/2} \beta g\hbar \sin 2\psi \int (a^* + a)\, a^* a\, dv$$
$$-\frac{3}{2}(2g\hbar M_0)^{1/2} g\hbar \iint \frac{R_z R^+}{R^5}\, a^*(\mathbf{r})\, a(\mathbf{r})\, a(\mathbf{r}')\, dv\, dv' + \text{c.c.} \tag{26}$$

(c.c. denotes the complex conjugate terms).

The fourth-order terms arise from expansion of the exchange interaction energy

$$\mathcal{H}_{\text{exch}}' = \frac{(g\hbar)^2 \alpha}{4} \int \{2[\nabla(a^* a)]^2 - \nabla a^* \nabla(a^* a a)$$
$$- \nabla(a^* a^* a)\nabla a\}\, dv. \tag{26'}$$

(a) We consider first the terms of third order.

Henceforth we shall suppose that the magnetic field is applied in the direction of the axis of easiest magnetization.† Therefore $\psi = 0$, and

$$\mathcal{H}_a' = -\frac{3}{2}(2g\hbar M_0)^{1/2} g\hbar \iint \frac{R_z R^+}{R^5}\, a^*(\mathbf{r})\, a(\mathbf{r})\, a(\mathbf{r}')\, dv\, dv'$$
$$+ \text{c.c.} \tag{27}$$

On substituting in (27) the expansion (12) of the operators a and a*, we get

*This corresponds to a temperature $T \gg 2\pi\mu M_0 \sim 1°K$.

†In the general case ($\psi \neq 0$), the terms related to the anisotropic energy do not change the magnitude of the relaxation time to any essential degree, since the structure of the first term in (26) is similar to that of the second and since the coefficient $\beta \sim 1$.

$$\mathcal{H}'_a = \sum_{\lambda\mu\nu} \Phi_{\lambda\mu\nu} a_\lambda a_\mu a_\nu^* + \text{c.c.}, \tag{28}$$

where

$$\Phi_{\lambda\mu\nu} = -2\pi g\hbar\,(2g\hbar M_0)^{1/2} V \left\{ \frac{k_\nu^z}{k_\nu^2} v_\lambda u_\mu\,(v_\nu^* k_\nu^+ + u_\nu^* k_\nu^-) + \frac{k_\lambda^z}{k_\lambda^2}\,(u_\lambda k_\lambda^+ + v_\lambda k_\lambda^-)(u_\mu u_\nu^* + v_\mu v_\nu^*) \right\}, \tag{29}$$

and where the sum extends over all wave vectors $\mathbf{k}_\lambda$, $\mathbf{k}_\mu$, and $\mathbf{k}_\nu$ satisfying the law of conservation of quasi-momentum

$$\mathbf{k}_\lambda + \mathbf{k}_\mu = \mathbf{k}_\nu. \tag{30}$$

We do not consider transfer processes, since they play no role in the problems being solved here.

We may consider the Hamiltonian (28) as a perturbation that causes transitions between stationary states of the system of spin waves.

The probability of transition (per second) is, as is well known,

$$W_{if} = (2\pi/\hbar)\,|\,\mathcal{H}'^{i}_{af}|^2\,\delta(E_i - E_f),$$

where $\mathcal{H}'^{i}_{af}$ is the matrix element for a transition from the initial state (i) to the final state (f), and E_i (E_f) is the energy of the initial (final) state.

According to the commutation rule (14), the nonvanishing matrix elements of the operators a_λ and a_λ^* are

$$(a_\lambda)^{n_\lambda}_{n_\lambda+1} = \sqrt{n_\lambda + 1}\; e^{-i\varepsilon_\lambda t/\hbar}.$$
$$(a_\lambda^*)^{n_\lambda}_{n_\lambda-1} = \sqrt{n_\lambda}\; e^{i\varepsilon_\lambda t/\hbar}. \tag{31}$$

Therefore, according to (28), the nonvanishing matrix elements of the operator $\mathcal{H}'$ are the following:

$$(\mathcal{H}')^{n_\lambda,\, n_\mu,\, n_\nu}_{n_\lambda-1,\, n_\mu-1,\, n_\nu+1}, \quad (\mathcal{H}')^{n_\lambda,\, n_\mu,\, n_\nu}_{n_\lambda+1,\, n_\mu-1,\, n_\nu+1},$$

$$(\mathcal{H}')^{n_\lambda,\, n_\mu,\, n_\nu}_{n_\lambda-1,\, n_\mu+1,\, n_\nu+1}$$

together with the matrix elements of the opposite transitions.

The corresponding transition probabilities have the form:

$$W^{n_\lambda,\, n_\mu,\, n_\nu}_{n_\lambda-1,\, n_\mu-1,\, n_\nu+1} = \frac{2\pi}{\hbar} A_{\lambda\mu\nu} n_\lambda n_\mu (n_\nu + 1)\,\delta(\varepsilon_\lambda + \varepsilon_\mu - \varepsilon_\nu);$$
$$W^{n_\lambda,\, n_\mu,\, n_\nu}_{n_\lambda+1,\, n_\mu-1,\, n_\nu+1} = \frac{2\pi}{\hbar} A_{\lambda\nu\mu}\,(n_\lambda + 1)\, n_\mu\,(n_\nu + 1) \times \delta(\varepsilon_\lambda - \varepsilon_\mu + \varepsilon_\nu); \tag{32}$$
$$W^{n_\lambda,\, n_\mu,\, n_\nu}_{n_\lambda-1,\, n_\mu+1,\, n_\nu+1} = \frac{2\pi}{\hbar} A_{\nu\mu\lambda} n_\lambda\,(n_\mu + 1)\,(n_\nu + 1) \times \delta(\varepsilon_\lambda - \varepsilon_\mu - \varepsilon_\nu).$$

Here

$$A_{\lambda\mu\nu} = |\,\Phi_{\lambda\mu\nu} + \Phi_{\mu\lambda\nu}\,|^2. \tag{33}$$

Using the expressions obtained for the transition probabilities, we write the collision integral for n_ν:

$$(\dot{n}_\nu)^a_{\text{coll}} = \frac{2\pi}{\hbar} \sum_{\lambda\mu} \{ A_{\lambda\mu\nu} [n_\lambda n_\mu (n_\nu + 1) - (n_\lambda + 1)(n_\mu + 1) n_\nu]\,\delta(\varepsilon_\lambda + \varepsilon_\mu - \varepsilon_\nu) \tag{34}$$
$$+ A_{\lambda\nu\mu} [(n_\lambda + 1) n_\mu (n_\nu + 1) - n_\lambda (n_\mu + 1) n_\nu]\,\delta(\varepsilon_\lambda - \varepsilon_\mu + \varepsilon_\nu)$$
$$+ A_{\nu\mu\lambda} [n_\lambda (n_\mu + 1)(n_\nu + 1) - (n_\lambda + 1) n_\mu n_\nu]\,\delta(\varepsilon_\lambda - \varepsilon_\mu - \varepsilon_\nu)\}.$$

We shall calculate the mean relaxation time of a gas of spin waves with the processes under consideration taken into account.

For small deviations of the system from the state of statistical equilibrium, the mean occupancy numbers n_ν can be expressed in the form

$$n_\nu = n_\nu^0 + \Delta n_\nu, \quad n_\nu^0 = 1/(e^{\varepsilon_\nu/T} - 1), \tag{35}$$

where Δn_ν is a small correction to the Bose equilibrium distribution

Upon substituting (35) in (34), we shall limit ourselves to linear terms in the expansion with respect to the correction to the equilibrium distribution function.

The coefficient of Δn_ν in the linearized collision integral, averaged over all the equilibrium states, may be regarded as the reciprocal of the mean relaxation time.[1] After simple transformations we get

$$\frac{1}{\tau_a} = \frac{2\pi}{\hbar} \sum_{\lambda\mu\nu} (n_\nu^0 + 2n_\lambda^0 n_\mu^0)\,\delta(\varepsilon_\lambda + \varepsilon_\mu - \varepsilon_\nu)\, A_{\lambda\mu\nu} \Big/ \sum_\nu n_\nu^0, \tag{36}$$

where $A_{\lambda\mu\nu}$ is determined by formulas (33), (29), (20), (16), and (17).

We consider first the case of high temperatures, $T \gg 2\pi\mu M_0$. As was pointed out in Sec. 1, under these conditions the spectrum is considerably simplified. If we suppose that $\alpha_{ik} = \alpha\delta_{ik} = (\Theta_c a^2/\mu M_0) \times \delta_{ik}$, then

$$\varepsilon_\lambda = \mu H_{\text{eff}} + \Theta_c (a k_\lambda)^2. \tag{37}$$

Here $H_{\text{eff}} = H_0 + \beta M_0$. In this approximation

$$u_\lambda = 1/\sqrt{V}; \quad v_\lambda = 0. \tag{38}$$

From (33), (29), and (38), we get

$$A_{\lambda\mu\nu} = \frac{(2\pi\mu)^2\, 2\mu M_0}{V} \left| \frac{k_\lambda^z k_\lambda^+}{k_\lambda^2} + \frac{k_\mu^z k_\mu^+}{k_\mu^2} \right|^2. \tag{39}$$

In expression (36) we go over from summation to integration; after integrating over angles and

changing to dimensionless variables, we get

$$\frac{1}{\tau_a} = \frac{\pi}{5} gM_0 \frac{\mu^2}{a^3\Theta_c}\left(\frac{T}{\Theta_c}\right)^{1/2} F(\eta), \tag{40}$$

where

$$F(\eta) = \iint\limits_{(xy>\eta^2)} \left\{\frac{1}{e^{x+y}-1} + \frac{2}{(e^x-1)(e^y-1)}\right\} \times \left\{\frac{1}{3} + \frac{\eta^2}{xy}\right\} dx\,dy \Big/ \int_0^\infty \frac{x^2\,dx}{e^{x+2\eta}-1}, \tag{41}$$

$$\eta = \mu H_{\text{eff}} / 2T. \tag{42}$$

On calculating the asymptotic behavior of the function $F(\eta)$, we get

$$F(\eta) \approx \begin{cases} (2/3\zeta(3))\ln^2\eta, & (\eta \ll 1) \\ 2\sqrt{\pi\eta}. & (\eta \gg 1). \end{cases} \tag{43}$$

Thus for $\Theta_C \gg T \gg 2\pi\mu M_0$:

$$\frac{1}{\tau_a} = \begin{cases} \dfrac{2\pi}{15\zeta(3)} gM_0 \dfrac{\mu^2}{a^3\Theta_c}\left(\dfrac{T}{\Theta_c}\right)^{1/2} \ln^2 \dfrac{\mu H_{\text{eff}}}{2T}, & (\mu H_{\text{eff}} \ll T) \\ \dfrac{\sqrt{2}\,\pi^{3/2}}{5} gM_0 \dfrac{\mu^2}{a^3\Theta_c}\left(\dfrac{\mu H_{\text{eff}}}{\Theta_c}\right)^{1/2}, & (\mu H_{\text{eff}} \gg T). \end{cases} \tag{44}$$

It should be noticed that at strong magnetic fields, the relaxation time slowly decreases with increase of the field ($\tau_a \sim H^{-1/2}$) but is independent of temperature. The relaxation time at small fields agrees in order of magnitude with the result obtained by Akhiezer,[1] if we suppose that $M_0 \approx \mu/a^3$ and if we set μH_{eff} equal to μ^2/a^3.

In the case of low temperatures ($T \ll 2\pi\mu M_0$), the fundamental role in the expression (16) is played by the term related to the magnetic interaction of the spins.* Therefore for small k_λ, A_λ and $|B_\lambda| \gg \epsilon_\lambda$. On taking account of this, we get from (33), (29), and (20)

$$A_{\lambda\mu\nu} = \frac{\pi^2\mu^3 M_0}{V\varepsilon_\lambda\varepsilon_\mu\varepsilon_\nu}\left\{\varepsilon_\lambda\sqrt{\frac{A_\mu A_\nu}{A_\lambda}}\sin 2\theta_\lambda \cos(\varphi_\mu - \varphi_\nu) + \varepsilon_\mu\sqrt{\frac{A_\lambda A_\nu}{A_\mu}}\sin 2\theta_\mu \cos(\varphi_\lambda - \varphi_\nu) - \varepsilon_\nu\sqrt{\frac{A_\lambda A_\mu}{A_\nu}}\sin 2\theta_\nu \cos(\varphi_\lambda - \varphi_\mu)\right\}^2. \tag{45}$$

If in the dispersion law we limit ourselves to the lowest power of k_λ, then

$$\varepsilon_\lambda = \sqrt{4\pi\mu M_0\Theta_c}\, ak_\lambda \sin\theta_\lambda.$$

Under these conditions, however, simultaneous fulfilment of the laws of conservation of energy and of momentum leads to a divergence of the integral in the expression for $1/\tau_a$ to the extent of a delta function. On the other hand, $A_{\lambda\mu\nu}$ approaches zero. Therefore in the calculation of the relaxation time, it is necessary to take account, in the spectrum, of further terms in the expansion with respect to k_λ ($\sim k_\lambda^3$).

After rather tedious calculations we get, except for a numerical factor:

$$1/\tau_a \sim gM_0 (T/\Theta_c)^{2/3} (T/\mu M_0)^3, \quad (T \ll 2\pi\mu M_0). \tag{46}$$

Thus, according to (44) and (46),

$$\tau_a \sim \begin{cases} T^{-3/2} & (T \ll 2\pi\mu M_0) \\ T^{-1/2}\ln^{-2} T & (2\pi\mu M_0 \ll T \ll \Theta_c). \end{cases} \tag{47}$$

(b) We now calculate the relaxation time with the exchange interaction taken into account.

From (26′) we have, for $T \gg 2\pi\mu M_0$ (for $T \ll 2\pi\mu M_0$, the exchange interaction is quite unimportant for kinetic processes),

$$\mathcal{H}'_{\text{exch}} = \sum_{\varkappa\lambda\mu\nu} \Phi_{\varkappa\lambda\mu\nu} a_\varkappa^* a_\lambda^* a_\mu a_\nu, \quad (\mathbf{k}_\varkappa + \mathbf{k}_\lambda = \mathbf{k}_\mu + \mathbf{k}_\nu), \tag{48}$$

where

$$\Phi_{\varkappa\lambda\mu\nu} = (\mu^2\alpha/4V)[2\mathbf{k}_\lambda\mathbf{k}_\mu - (\mathbf{k}_\mu + \mathbf{k}_\lambda)(\mathbf{k}_\varkappa + \mathbf{k}_\nu)]. \tag{49}$$

Hence the transition probabilities, which correspond to nonvanishing matrix elements of $\mathcal{H}'_{\text{exch}}$, have the form

$$\begin{aligned} W^{n_\varkappa n_\lambda n_\mu n_\nu}_{n_\varkappa-1\, n_\lambda-1\, n_\mu+1\, n_\nu+1} &= \frac{2\pi}{\hbar}\{A_{\varkappa\lambda\mu\nu} + A_{\varkappa\lambda\nu\mu}\} n_\varkappa n_\lambda (n_\mu+1) \times (n_\nu+1)\,\delta(\varepsilon_\varkappa + \varepsilon_\lambda - \varepsilon_\mu - \varepsilon_\nu), \\ W^{n_\varkappa n_\lambda n_\mu n_\nu}_{n_\varkappa-1\, n_\lambda+1\, n_\mu-1\, n_\nu+1} &= \frac{2\pi}{\hbar} A_{\varkappa\nu\mu\lambda} n_\varkappa (n_\lambda+1) n_\mu \times (n_\nu+1)\,\delta(\varepsilon_\varkappa - \varepsilon_\lambda + \varepsilon_\mu - \varepsilon_\nu), \\ W^{n_\varkappa n_\lambda n_\mu n_\nu}_{n_\varkappa+1\, n_\lambda-1\, n_\mu-1\, n_\nu+1} &= \frac{2\pi}{\hbar} A_{\nu\lambda\mu\varkappa} (n_\varkappa+1) n_\lambda n_\mu \times (n_\nu+1)\,\delta(\varepsilon_\varkappa - \varepsilon_\lambda - \varepsilon_\mu + \varepsilon_\nu). \end{aligned} \tag{50}$$

Here

$$A_{\varkappa\lambda\mu\nu} = |\Phi_{\varkappa\lambda\mu\nu} + \Phi_{\lambda\varkappa\mu\nu}|^2. \tag{51}$$

With the aid of the collision integral corresponding to these transition probabilities, we find the relaxation time in the same manner as before:

$$\frac{1}{\tau_{\text{exch}}} = \frac{2\pi}{\hbar}\sum_{\varkappa\lambda\mu\nu} A_{\varkappa\lambda\mu\nu}\{n_\varkappa^0 n_\lambda^0 (n_\mu^0 + n_\nu^0 + 2) + n_\mu^0 n_\nu^0 (n_\varkappa^0 + n_\lambda^0 + 2)\}\,\delta(\varepsilon_\varkappa + \varepsilon_\lambda - \varepsilon_\mu - \varepsilon_\nu) / \sum_\nu n_\nu^0. \tag{52}$$

On substituting the value of $A_{\kappa\lambda\mu\nu}$ and going over

*At low temperatures the whole treatment is carried out in the absence of a magnetic field. Furthermore it is assumed that $\beta \ll 2\pi$. This permits neglect of the anisotropy energy in (16).

from summation to integration, we get except for a numerical factor

$$1/\tau_{exch} \sim (\Theta_c/\hbar)(T/\Theta_c)^4. \quad (53)$$

By comparison of this expression for $1/\tau_{exch}$ with $1/\tau_a \sim gM_0(\mu M_0/\Theta_C)(T/\Theta_C)^{1/2}$ [cf. formula (44)], we conclude that for

$$T \gg \mu M_0 (\Theta_c/\mu M_0)^{3/7}, \quad \tau_{exch} \ll \tau_a,$$

and that for

$$T \ll \mu M_0 (\Theta_c/\mu M_0)^{3/7}, \quad \tau_{exch} \gg \tau_a.$$

This means that for $T \gg \mu M_0 (\Theta_C/\mu M_0)^{3/7} \sim 10$ to 30°K, the relaxation of a spin-wave gas occurs in the following manner: in a time $t = \tau_{exch}$, the spin waves reach a quasiequilibrium state with a nonequilibrium value of the magnetic moment;* thereafter, the magnetic moment "slowly" (in a time τ_a) relaxes to its equilibrium value. For $T \ll \mu M_0 \times (\Theta_C/\mu M_0)^{3/7}$, the nonequilibrium state of the spin system cannot be described as having a definite value of the moment.

It must further be remembered that for $T \gg \Theta^2/\Theta_C$ (Θ = Debye temperature), a fundamental role is played by processes of interaction of the spin waves with phonons.[1] These processes will be treated from the phenomenological point of view in a separate article.

*This is a consequence of the fact that the exchange interaction does not change the magnetic moment of the system.

The authors take this opportunity to thank A. I. Akhiezer, L. D. Landau, and I. M. Lifshitz for valuable suggestions, and also V. G. Bar'iakhtar and S. V. Peletminskii for helpful discussions.

[1] A. I. Akhiezer, J. Phys. (U.S.S.R.) **10**, 217 (1946).

[2] C. Herring and C. Kittel, Phys. Rev. **81**, 869 (1951).

[3] M. I. Kaganov and V. M. Tsukernik, Физика металлов и металловедение (Physics of Metals and Metal Research) (in press).

[4] S. V. Vonsovskii and Ia. S. Shur, Ферромагнетизм (Ferromagnetism), Gostekhizdat, Moscow — Leningrad, 1948.

[5] L. D. Landau and E. M. Lifshitz, Physik. Z. Sowjetunion **8**, 153 (1935).

[6] T. Holstein and H. Primakoff, Phys. Rev. **58**, 1098 (1940).

[7] N. N. Bogoliubov, Лекції з квантової статистики (Lectures on Quantum Statistics). Kiev, 1951.

[8] V. M. Tsukernik, Dissertation, Kharkov State University, 1957.

[9] L. D. Landau and E. M. Lifshitz, Квантовая механика (Quantum Mechanics), Gostekhizdat, Moscow — Leningrad, 1948.

Translated by W. F. Brown, Jr.
313

COLLECTIVE EXCITATION OF ODD NONSPEHERICAL NUCLEI

A. S. DAVYDOV and B. M. MURASHKIN

Moscow State University

Submitted to JETP editor January 24, 1958

J. Exptl. Theoret. Phys. (U.S.S.R.) **34**, 1619-1624 (June, 1958)

A theory is developed for the energy states of odd nuclei corresponding to collective nucleon motion in which the axial symmetry of the nucleus is preserved. It is shown that the energy spectrum of the nucleus can be determined by only two parameters. Conditions under which the energy spectrum splits up into a system of rotational-vibrational bands are determined.

In the articles of Davydov and Filippov[1] and Davydov and Chaban[2] a theory of collective excitations of states of even-even axially-symmetric nuclei was developed without assuming that the rotational energy is small in comparison with the energy of the surface vibrations. It was shown that the energy of excited states in which the axial symmetry of the nucleus is not destroyed, can be represented by a function which depends on only two parameters; conditions under which collective excitations split up into a system of rotational-vibrational bands were found. In the present work the theory is extended to the case of axially-symmetric odd nuclei, having a spin equal to or larger than $3/2$ in the ground state.

1. COLLECTIVE EXCITATIONS OF ODD NUCLEI WHICH PRESERVE THE AXIAL SYMMETRY OF THE NUCLEUS

According to the unified model of the nucleus,[3] in the case of strong coupling the classical energy of collective motion of the nucleus is obtained after averaging the energies of the interaction of external nucleons with the nuclear surface over the states of motion of the external nucleons. In the case that interests us — motion which preserves the axial symmetry of the nucleus ($\gamma = 0$, j_{i3} are good quantum numbers) – this energy can be written in the form

$$E = T + V(\beta), \tag{1.1}$$

$$T = {}^1/_2 B\dot{\beta}^2 + \hbar^2 \{J(J+1) - K^2\}/6B\beta^2, \tag{1.2}$$

$$V(\beta) = {}^1/_2 C\beta^2 + A\beta + \hbar^2 D/6B\beta^2, \tag{1.3}$$

where C and B characterize the properties of the nucleus, A and D depend on the number of external nucleons and on the state of their motion, $K = J_3 = \sum j_{i3}$ is the spin of the nucleus in the ground state, J is the total angular momentum of the nucleus, $\beta \geq 0$ determines the deviation of the nucleus from spherical symmetry.

Equation (1.1) corresponds to the Schrödinger equation

$$\{\hat{T} + V(\beta) - E\}\Psi = 0, \tag{1.4}$$

$$\hat{T} = -\frac{\hbar^2}{2B\beta^2}\left\{\frac{\partial}{\partial\beta}\left(\beta^2\frac{\partial}{\partial\beta}\right) + \frac{1}{3\sin\theta}\frac{\partial}{\partial\theta}\left(\sin\theta\frac{\partial}{\partial\theta}\right) + \frac{1}{3\sin^2\theta}\left[\frac{\partial^2}{\partial\varphi^2} + 2\cos\theta\frac{\partial^2}{\partial\varphi\,\partial\psi} + \frac{\partial^2}{\partial\psi^2}\right] - \frac{1}{3}\frac{\partial^2}{\partial\psi^2}\right\}. \tag{1.5}$$

The solution of Eq. (1.4) can be obtained in the form

$$\Psi = \sum_J \frac{1}{\beta} u_{JK}(\beta) D^J_{MK}(\varphi, \theta, \psi), \tag{1.6}$$

where $J = K, K+1, \ldots$; D^J_{MK} are the generalized spherical functions which are the irreducible representations of the rotation group.

Substituting Eq. (1.6) into (1.4) we see that the functions u_{JK} should satisfy the boundary condition

$$u_{JK}(0) = 0 \tag{1.7}$$

and the equation

$$\left\{-\frac{\hbar^2}{2B}\frac{d^2}{d\beta^2} + V_K(\beta) + \frac{\hbar^2[J(J+1) - K(K+1)]}{6B\beta^2} - E\right\} u_{JK} = 0, \tag{1.8}$$

where

$$V_K = {}^1/_2 C\beta^2 + A\beta + \hbar^2(D+K)/6B\beta^2 \approx V_K(\beta_K) + {}^1/_2 C_K(\beta - \beta_K)^2 \tag{1.9}$$

The quantities β_K and C_K which enter into Eq. (1.9) can be expressed in terms of A, B, C, D and K by means of the equations

$$\beta_K = -A/C + \hbar^2(D+K)/3B\beta_K^3,$$
$$C_K = C + \hbar^2(D+K)/B.$$

However, it is more convenient to consider them as some parameters characterizing the nucleus

in the ground state (J = K). Then Eq. (1.8) can be put in the form

$$\left[-\frac{\hbar^2}{2B}\frac{d^2}{d\beta^2}+W_{JK}(\beta)-\varepsilon\right]u_{JK}=0, \qquad (1.8a)$$

where $\epsilon = E - V_K(\beta_K)$,

$$W_{JK}(\beta)=\frac{C_K}{2}(\beta-\beta_K)^2+\frac{\hbar^2[J(J+1)-K(K+1)]}{6B\beta^2} \qquad (1.10)$$
$$\approx W_{JK}(\beta_{JK})+\frac{1}{2}C_{JK}(\beta-\beta_{JK})^2.$$

Here

$$\beta_{JK}=\beta_K+\hbar^2[J(J+1)-K(K+1)]/3BC_K\beta_{JK}^3, \qquad (1.11)$$

$$C_{JK}=C_K+(\hbar^2/B\beta_{JK}^4)[J(J+1)-K(K+1)], \qquad (1.12)$$

$$W_{JK}(\beta_{JK}) \qquad (1.13)$$
$$=\tfrac{1}{2}C_K(\beta_{JK}-\beta_K)^2+\hbar^2[J(J+1)-K(K+1)]/6B\beta_{JK}^2.$$

After introduction of the dimensionless parameters*

$$\delta=\beta_K(BC_K/\hbar^2)^{1/4},\quad \xi=\beta_{JK}/\beta_K\geqslant 1,\quad \omega_0=\sqrt{C_K/B},$$

Equations (1.11) to (1.13), respectively, take the form

$$\xi^3(\xi-1)=[J(J+1)-K(K+1)]/3\delta^4, \qquad (1.11a)$$

$$C_{JK}=C_K(1+[J(J+1)-K(K+1)]/\delta^4\xi^4), \qquad (1.12a)$$

$$W_{JK}(\beta_{JK})/\hbar\omega_0 \qquad (1.13a)$$
$$=\tfrac{1}{2}\delta^2(\xi-1)^2+[J(J+1)-K(K+1)]/6\delta^2\xi^2.$$

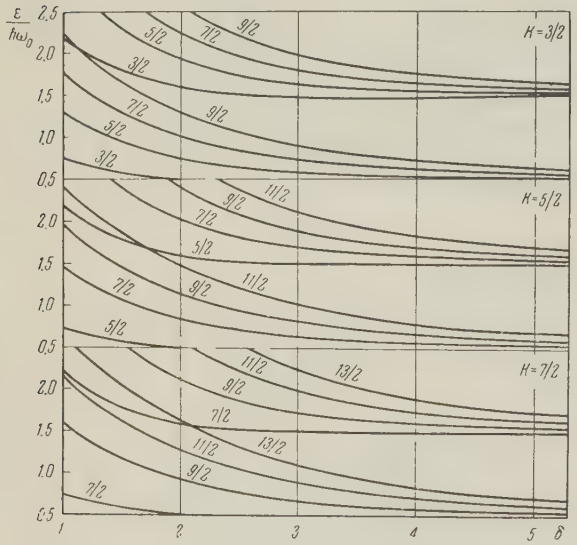

Substituting Eq. (1.10) into (1.8a) we find

$$\left\{-\frac{\hbar^2}{2B}\frac{d^2}{d\beta^2}+\frac{1}{2}C_{JK}(\beta-\beta_{JK})^2-[\varepsilon-W_{JK}(\beta_{JK})]\right\}u_{JK}=0. \qquad (1.14)$$

In order to determine the eigenfunctions and eigenvalues of Eq. (1.14) we introduce the new variable

$$\zeta=\xi\delta_1(\beta-\beta_{JK})/\beta_{JK},\quad \delta_1^4=\delta^4C_{JK}/C_K,$$

which varies in the interval $\xi\delta_1 \leq \zeta > \infty$, and the new function $v(\zeta)$ using the relation

$$u_{JK}(\beta)=v(\zeta)\exp(-\zeta^2/2).$$

Then the function $v(\zeta)$ will satisfy the equation

$$v''(\zeta)-2\zeta v'(\zeta)+2\nu v(\zeta)=0,$$
$$\nu=\frac{\varepsilon-W_{JK}(\beta_{JK})}{\hbar\omega_{JK}}-\frac{1}{2}, \qquad (1.15)$$
$$\omega_{JK}=\left(\frac{C_{JK}}{B}\right)^{1/2}=\omega_0\left[1+\frac{J(J+1)-K(K+1)}{\delta^4\xi^4}\right]^{1/2}$$

and the boundary condition

$$v(-\xi\delta_1)=0,\quad \exp(-\zeta^2/2)\,v(\zeta)\to 0 \quad \text{for } \zeta\to\infty. \qquad (1.16)$$

The solution of Eq. (1.15) satisfying Eq. (1.16) can be put in the form

$$v_\nu(\zeta)=aH_\nu(\zeta), \qquad (1.17)$$

where

$$H_\nu(\zeta)\equiv[2\Gamma(-\nu)]^{-1}\sum_{K=0}^{\infty}\frac{(-1)^K}{K!}\Gamma\left(\frac{K-\nu}{2}\right)(2\zeta)^K$$

are Hermitian functions of the first kind. Here the energy of collective motion of the nucleus will be determined by the formula

$$\frac{\varepsilon}{\hbar\omega_0}=(\nu+1/2)\left[1+\frac{J(J+1)-K(K+1)}{\delta^4\xi^4}\right]^{1/2}+\frac{\delta^2(\xi-1)^2}{2}+\frac{J(J+1)-K(K+1)}{6\delta^2\xi^2}. \qquad (1.18)$$

The quantum number ν (which is, in the general case, not integral) is the kernel of the transcendental equation

$$H_\nu(-\delta_1\xi)=0. \qquad (1.19)$$

The quantities ξ and δ_1, for given J and K, are determined using Eqs. (1.11a) and (1.12a) through the parameter δ. For $\delta > 2$, $\delta_1 \approx \delta$.

2. SPECTRUM OF COLLECTIVE EXCITATIONS OF ODD NONSPHERICAL NUCLEI

In the preceding section it was shown that the energies of collective excitations (for which the axial symmetry is preserved) of odd nonspherical

*From Eq. (1.8a) follows that for J = K the square of the amplitude of zero-point vibrations $\overline{\beta_{00}^2}=\hbar/2\sqrt{BC_K}$. Thus, the parameter $\delta=\beta_K(2\overline{\beta_{00}^2})^{-1/2}$ is proportional to the ratio of the value of β_K, which defines the equilibrium form of the nucleus in the ground state, to the amplitude of zero-point vibrations of the nuclear surface.

Nucleus	J		Energy level, kev		$\hbar\omega_0$, kev	δ
	Theoret.	Exptl.	Theoret.	Exptl.		
Tb^{159} [4]	3/2	3/2	0	0		
	5/2	5/2	57.6	57		
	7/2	7/2	130	136	353	2.43
	3/2	3/2	364	364		
	5/2	—	440	—		
Gd^{157} [5]	3/2	3/2	0	0		
	5/2	5/2	55	55	732	3.5
	7/2	7/2	130	131		
	3/2	—	732	—		
Eu^{153} [4,5]	5/2	5/2	0	0		
	7/2	7/2	84	84		
	9/2	9/2	184	194	700	3.31
	11/2	—	300	—		
	5/2	5/2	700	700		
	7/2	—	805	—		
Re^{187} [4,5]	5/2	5/2	0	0		
	7/2	7/2	134.6	134.6		
	9/2	9/2	294	300		
	11/2	—	473	—	910	2.99
	5/2	—	910	910		
	7/2	—	1075	—		
U^{233} [4]	5/2	5/2	0	0		
	7/2	7/2	40.1	40.1		
	9/2	9/2	92	92.8	476	3.988
	11/2	—	151	—		
	5/2	—	476	476		
	7/2	—	528	—		
Np^{237} [4,6,7]	5/2(−)	5/2(—)	0	0		
	7/2(−)	7/2(—)	33.1	33.1		
	9/2(−)	9/2(—)	78	76.1	433	3.99
	5/2(−)	—	433	433		
	7/2(−)	—	476	—		
	5/2(+)	5/2(+)	59.8	59.8		
	7/2(+)	7/2(+)	103.2	103.2		
	9/2(+)	9/2(+)	157.6	157.2		
	11/2(+)	11/2(+)	220.2	224	433	3.60
	13/2(+)	13/2(+)	289	303		
	5/2(+)	—	492.8	—		
Th^{229} [4,6]	5/2	5/2	0	0		
	7/2	7/2	43.2	43.2		
	9/2	9/2	98.2	100		
	11/2	11/2	163.2	164	555	4.0
	5/2	—	555	—		
Ho^{165} [4]	7/2	7/2	0	0		
	9/2	9/2	94	94		
	11/2	11/2	217	216		
	13/2	—	356	360	989	4.06
	7/2	—	989	989		
	9/2	—	1108	1100		
U^{235} [4]	7/2	7/2	0	0		
	9/2	9/2	46.5	46.5		
	11/2	11/2	105	104.3		
	13/2	—	168	172	379	3.63
	7/2	—	379	379		
	9/2	—	436	430		
Lu^{175} [4,5,8]	7/2	7/2	0	0		
	9/2	9/2	113	113		
	11/2	11/2	248	250		
	7/2	—	990	—	990	3.80
	5/2	5/2	342	342		
	7/2	(5/2, 7/2)	431	431		
	9/2	—	540	—		
	5/2	—	1332	—		

nuclei can be represented by the formula (1.18) depending only on the two parameters ω_0 and δ. The values $\epsilon/\hbar\omega_0$ are given on the figure as a function of the parameter δ for $K = 3/2$, $5/2$ and $7/2$, respectively. From the figure it follows that for some values of δ the spectrum of collective excitations of the nucleus splits up into a system of rotational-vibrational bands.

In the table a comparison is given between the theoretical values of the excitation energies of the first and second rotational-vibrational bands of excited states of odd nuclei and experimental data. There the values of the parameters $\hbar\omega_0$ and δ, used in the calculation of theoretical values, are also given.

Comparing the spectrum of collective excitations of odd nuclei with the spectrum of collective excitation of even-even nuclei, it is possible to draw the following conclusions: (1) The break-up of collective excitations into a system of rotational-vibrational bands in odd nuclei sets in for lower values of δ than in even-even nuclei; (2) The values of the parameter ω_0, which can be called the frequency of vibration of the nuclear surface, in the ground state is smaller in odd nuclei than in even-even nuclei having the same value of the parameter δ.

For $\delta > 3$ the quantity ν takes on values near to integral ones 0, 1, 2, . . .; further, according to Eq. (1.11a) one can approximately set

$$\xi = 1 + g\,[J(J+1) - K(K+1)]\,/\,3\delta^4.$$

Then Eq. (1.18) can be replaced by the approximate equality

$$\varepsilon/\hbar\omega_0 = (\nu + 1/2) + [J(J+1) - K(K+1)]\,/\,6\delta^2 - a\,[J(J+1) - K(K+1)]^2\,/\,\delta^6. \quad (2.1)$$

[1] A. S. Davydov and G. F. Filippov, J. Exptl. Theoret. Phys. (U.S.S.R.) **33**, 723 (1957), Soviet Phys. JETP **6**, 555 (1958).

[2] A. S. Davydov and A. A. Chaban, J. Exptl. Theoret. Phys. (U.S.S.R.) **33**, 547 (1957), Soviet Phys. JETP **6**, 428 (1958).

[3] A. B. Bohr, Phys. Rev. **81**, 134 (1951); Danske Mat.-Fys. Medd. **26**, No. 14 (1952); K. Ford, Phys. Rev. **90**, 29 (1953).

[4] B. S. Dzhelepov and L. K. Peker, Схемы распада радиоактивных изотопов (Decay schemes of Radioactive Isotopes) Acad. Sci. Press, 1957.

[5] Alder, Bohr, Huus, Mottelson and Winther, Rev. Mod. Phys. **28**, 432 (1956).

[6] Goldin, Novikova and Tretyakov, Phys. Rev. **103**, 1004 (1956).

[7] Rasmussen, Canavan and Hollander, Phys. Rev. **107**, 141 (1957).

[8] Mize, Bunker and Starner, Phys. Rev. **100**, 1390 (1955).

Translated by G. E. Brown
314

SOVIET PHYSICS JETP VOLUME 34 (7), NUMBER 6 DECEMBER, 1958

BEHAVIOR OF THE DISTRIBUTION FUNCTION OF A MANY-PARTICLE SYSTEM NEAR THE FERMI SURFACE

D. A. KIRZHNITS

P. N. Lebedev Physics Institute, Academy of Sciences, U.S.S.R.

Submitted to JETP editor January 30, 1958

J. Exptl. Theoret. Phys. (U.S.S.R.) **34**, 1625-1628 (June, 1958)

The form of the distribution function of a system of electrons is studied in the Hartree approximation near the Fermi surface, for the case of a weakly inhomogeneous distribution. It is shown that in this region the inhomogeneity has a particularly strong effect, so that the correct expression for the distribution function, as given in this paper, is decidedly different in this region from the expression usually employed (that calculated from the Thomas-Fermi model). It is pointed out that the latter expression is completely unsuitable for use in problems in which the neighborhood of the Fermi surface plays an important part.

As is well known, the distribution function (the density matrix in a mixed representation) is the most important quantity characterizing a many-particle system. By means of it one can calculate without difficulty quite a number of physical quantities for the system in question.

In the present note we study in the Hartree approximation the form of the distribution function in the region of phase space near the Fermi surface. Our specific problem is that of a system of nonrelativistic electrons in a stationary state at temperature zero, and we confine ourselves to the case in which the occupation numbers of the levels depend only on the energy.

If our system is characterized by a sufficiently smooth distribution of the density and potential energy, namely if the condition for quasi-classical behavior,

$$\xi \equiv |\nabla(p_0^2)|/p_0^3 \ll 1, \tag{1}$$

is satisfied, then it is common practice to use for the distribution function the following expression, which corresponds to the Thomas-Fermi model:*

$$f(\mathbf{r}, \mathbf{p}) = 2(2\pi)^{-3}\theta(p^2 - p_0^2(\mathbf{r})), \tag{2}$$

$$\theta(x) = {}^1/_2(1 - x/|x|).$$

Here p_0 is the Fermi limiting momentum, related to the sum $\Phi(\mathbf{r})$ of the potentials of the external and self-consistent fields and the limiting energy E_0 by the equation $p_0^2(\mathbf{r}) = 2(E_0 - \Phi(\mathbf{r}))$. We use throughout atomic units with $e = \hbar = M = 1$.

It will be shown below (cf. also reference 1) that near the Fermi surface, namely for

$$|p - p_0| \sim \sqrt{\xi}\, p_0, \tag{3}$$

the expression (2) is not a useful one even when Eq. (1) holds, since in this region effects of the inhomogeneity of p_0^2 become very pronounced. It turns out to be possible to find an expression for f which is acceptable also in the region (3).

It is convenient to start from the operator expression for f in the Hartree approximation[1,2]

$$f(\mathbf{r}, \mathbf{p}) = (2\pi)^{-3} 2 \langle \theta(\hat{p}^2 - p_0^2(\mathbf{r})) \rangle_{\mathbf{p}}, \tag{4}$$

where for an arbitrary operator $\hat{a}$

$$\langle \hat{a} \rangle_{\mathbf{p}} \equiv \exp(-i\mathbf{pr})\, \hat{a} \exp(i\mathbf{pr}).$$

Apart from an unimportant factor the argument of the function θ is equal to the quantity $\hat{H} - E_0$, where $\hat{H} = \hat{p}^2/2 + \Phi(\mathbf{r})$ is the Hamiltonian. Expression (4) thus corresponds to a step-function distribution in the energy space; it is clear, however, that in the phase space this distribution must inevitably be smeared out because of the fact that the coordinates and momentum do not commute with the Hamiltonian. This fact is displayed formally in the failure to commute of the operators $\hat{p}$ and p_0^2 in the argument of the θ function in Eq. (4). If we denote by $\hat{K}_n$ the corresponding n-th order commutator, then we have for small ξ, in order of magnitude*

$$\langle \hat{K}_n \rangle_{\mathbf{p}} \sim p_0^{2n+2} \xi^n.$$

On the other hand, the quasi-classical value of the argument of the θ function, corresponding to complete neglect of the commutators, is given by $p^2 - p_0^2$. From this it follows that the ratios

$$\varkappa_n \equiv \langle \hat{K}_n \rangle_{\mathbf{p}} / |p^2 - p_0^2|^{n+1}. \tag{5}$$

are dimensionless parameters that determine the part played by the commutators of various orders, and thus also determine the importance of the inhomogeneity.

If the phase point lies far enough from the Fermi surface so that $|p^2 - p_0^2| \sim p_0^2$, then for small ξ we have $\kappa_n \sim \xi^n$, and we actually arrive at Eq. (2). Near the Fermi surface, however, κ_n increases because of the decrease of the denominator, and the inhomogeneities begin to play a decisive role.

To find the region of phase space in which the commutators must not be neglected, it suffices to equate κ_n to a quantity of the order unity. Then the difference $p^2 - p_0^2$ defining the size of this region will be equal to the largest of the quantities

$$|\langle \hat{K}_n \rangle_{\mathbf{p}}|^{1/(n+1)} \sim p_0^2 \xi^{n/(n+1)}, \quad n = 1 \div \infty.$$

For small ξ we must take $n = 1$, which at once leads to the estimate (3).

The next question is to find out the relative importance of commutators of different orders. The answer is provided by the values of the ratios

$$\varkappa_n/\varkappa_1 \sim [p_0^2 \xi/|p^2 - p_0^2|]^{n-1}. \tag{6}$$

In the region (3) in which we are interested these ratios are of the order $\xi^{(n-1)/2}$ and vanish for $\xi \to 0$, which shows that only the first commutator needs to be taken into account. The region in which other commutators also become important is considerably narrower:

$$|p - p_0| \sim \xi p_0. \tag{7}$$

The contribution of this region is usually small because of its small width.

It must be noted that the behavior of the distribution function just at the Fermi surface has been studied by Migdal.[3] There, moreover, the interactions between the particles were taken into account exactly, but only an isolated system was considered, without any external field.

*The factor 2 in this formula corresponds to the two orientations of the spin.

*A characteristic value of the momentum is a quantity of the order of p_0.

Proceeding to a quantitative study of the situation in the region (3), we note that the function of noncommuting arguments appearing in Eq. (4),

$$\theta(\hat{p}^2 - p_0^2) = \frac{i}{2\pi}\int_{-\infty}^{\infty}\frac{dt}{t+i\varepsilon}\exp[it(\hat{p}^2 - p_0^2)] \qquad (8)$$

can be given a meaning by means of the relations[1,2]

$$\langle \exp[it(\hat{p}^2 - p_0^2)]\rangle_p \qquad (9)$$
$$= \exp[it(p^2 - p_0^2)]\,\langle F(t^2\hat{K}_1, \ldots t^{n+1}\hat{K}_n \ldots)\rangle_p,$$

where F is a certain function of the commutators of the operators $t\hat{p}^2$ and tp_0^2, which reduces to unity when the latter commute. According to the estimates given above, which are immediately confirmed if one makes the replacement $t \to t|p^2 - p_0^2|^{-1}$ in Eqs. (8) and (9), in the region (3) we can neglect all the commutators except the first. This makes it possible to use a well known formula of Glauber[4] which takes account of the first commutator and all its powers*

$$\langle F\rangle_p = \langle \exp(t^2\hat{K}_1/2)\rangle_p \approx \exp\{-it^2 \mathbf{p}\nabla(p_0^2)\}. \qquad (10)$$

Here we neglect quantities of higher order in ξ. Substituting Eqs. (8) to (10) into Eq. (4), we get

$$f(\mathbf{r}, \mathbf{p}) = (2\pi)^{-3}\{1 - (1 - is)(C(x) + is\,S(x))\},$$
$$s \equiv \mathbf{p}\nabla(p_0^2)/|\mathbf{p}\nabla(p_0^2)|, \quad x \equiv (p^2 - p_0^2)/2|\mathbf{p}\nabla(p_0^2)|^{1/2}. \qquad (11)$$

C and S are the Fresnel integrals.

For reference we present the general formula, which may be useful in the nondegenerate case:

$$\langle \varphi(\hat{p}^2 - p_0^2)\rangle_p = \frac{1-is}{\sqrt{2\pi}}\int_{-\infty}^{\infty} e^{ist^2}\varphi[(p^2 - p_0^2)(1 + t/x)]\,dt, \qquad (12)$$

where φ is an arbitrary function.

We also give the expression (11) in a form averaged over the directions of p

$$f(\mathbf{r}, \mathbf{p}) = (2\pi)^{-3}\,2\left[\theta(p^2 - p_0^2)\,\chi + \frac{1-\chi}{2}\right],$$
$$\chi = (1 + 2y^2)\,S(y) + (1 - 2y^2)\,C(y) \qquad (13)$$
$$+ \sqrt{\frac{2}{\pi}}\,y(\cos y^2 + \sin y^2),$$
$$y \equiv |p^2 - p_0^2|/2(p|\nabla(p_0^2)|)^{1/2}.$$

For $y \gg 1$ we get the required value $\chi = 1$, but for $y \sim 1$,, i.e., in the region 3, the expressions (11) and (13) are decidedly different from Eq. (2). In particular, for small y we have $\chi = 2(2/\pi)^{1/2}y$. The distribution obtained is qualitatively similar to the curve corresponding to the nondegenerate case with the effective temperature

$$kT_{\text{eff}} \sim \sqrt{\xi}\,p_0^2.$$

From this it follows in particular that in the nondegenerate case the effect in question is unimportant for $T \gg T_{\text{eff}}$. We emphasize once again that Eqs. (11) to (13) apply only in the region in which $|p - p_0|/\xi \to \infty$ for $\xi \to 0$.

From what has been said above it follows that if a quantity with which we are concerned and which relates to a system of particles is expressed in terms of an integral of the function f over a sufficiently wide region of the phase space, $|p - p_0| \sim p_0$, then it is permissible to use Eq. (2) if the condition (1) holds.

In a number of problems of many-body theory, however, the decisive part is played by the neighborhood of the Fermi surface, with the width of this region determined by the distribution smeared out by the inhomogeneity, as discussed above. In this region, where $|p - p_0| \sim \xi^{1/2}p_0$, it is necessary to use Eqs. (11) to (13). This is the case, for example, in the problem of calculating exchange and correlation effects, which will be dealt with in special papers.

Finally, if for any reason the decisive role is played by a still narrower neighborhood of the Fermi surface, with $|p - p_0| \sim \xi p_0$, the problem becomes much more complicated, and it is evidently impossible to give a closed expression for f in this case.

In conclusion I thank V. L. Ginzburg for a number of helpful remarks, and A. B. Migdal, who kindly made the results of his work available to me before their publication.

*At points where the first commutator vanishes, the main role will be played by commutators of higher order. Nevertheless this fact is unimportant, since ordinarily we are interested in integral expressions, to which these points contribute very little.

[1] D. A. Kirzhnits, Dissertation (in Russian), Physics Institute of the Academy of Sciences, 1956.

[2] D. A. Kirzhnits, J. Exptl. Theoret. Phys. (U.S.S.R.) **32**, 115 (1957), Soviet Phys. JETP **5**, 64 (1957).

[3] A. B. Migdal, J. Exptl. Theoret. Phys. (U.S.S.R.) **32**, 399 (1957), Soviet Phys. JETP **5**, 333 (1957).

[4] R. J. Glauber, Phys. Rev. **84**, 395 (1951).

Translated by W. H. Furry
315

REFLECTION FROM A BARRIER IN THE QUASI-CLASSICAL APPROXIMATION. II

V. L. POKROVSKII, F. R. ULINICH, and S. K. SAVVINYKH

Institute of Radiophysics and Electronics, Siberian Branch, Academy of Sciences, U.S.S.R.

Submitted to JETP editor January 31, 1958

J. Exptl. Theoret. Phys. (U.S.S.R.) **34**, 1629-1631 (June, 1958)

An asymptotic expression for the coefficient of reflection from a barrier, valid for the whole range of the parameters U_0/E and k_0a, has been obtained using the condition for the quasi-classical approximation $k_0a \gg 1$ and the condition $k_0a(E-U_0)/U_0 \gg 1$.

IT was shown in a previous paper[1] that the amplitude of reflection R from a one-dimensional potential barrier has the following form in the quasi-classical approximation:

$$R = -i\exp\left\{\frac{2i}{\alpha}\int^{\xi_0} k\,d\xi\right\}. \tag{1}$$

We follow the notation of reference 1. It was shown that formula (1) is applicable in that region of the parameters $\kappa = U_0/E$ and $\alpha = 1/k_0a$ where perturbation theory is inapplicable. For example, if the potential U has only poles of first order, formula (1) is valid for $\kappa/\alpha \gg 1$, whereas perturbation theory is applicable for $\kappa/\alpha \ll 1$. Here the intermediate region $\kappa/\alpha \sim 1$ is not included in the investigation. The aim of the present paper is to present an asymptotic formula for the reflection amplitude which is valid in the whole range of the parameters κ, α, $(1-\kappa \gg \alpha)$. The form of this formula depends essentially on the type of singularity of the potential.

We restrict our discussion to the two most important cases: poles of first and of second order.

As in reference 1, we seek the reflection amplitude in the form of the expansion

$$R = -\frac{1}{2i}\left\{V_{-1,1} + \frac{1}{2\pi}\int \frac{V_{-1,k}V_{k,1}}{1-k^2}\,dk + \frac{1}{(2\pi)^2} \times \iint \frac{V_{-1,k_1}V_{k_1,k_2}V_{k_2,1}}{(1-k_1^2)(1-k_2^2)}\,dk_1\,dk_2 \ldots\right\}, \tag{2}$$

$$V_{k,k'} = -\alpha\int_{-\infty}^{\infty} \exp\left\{\frac{i}{\alpha}(k'-k)\tau\right\} q(\tau)\,d\tau.$$

We write the function q in the form

$$q = 5[(k^2)']^2/16k^6 - (k^2)''/4k^4. \tag{3}$$

For small κ the root ξ_0 of the function $k^2 = 1 - U/E$ lies close to the singularity ξ_1 of the potential $U(\xi)$. Let this singularity be a pole of first order. Close to ξ_1 we have then

$$\frac{U}{E} = \varkappa\frac{A}{\xi-\xi_1}; \quad k^2 = \frac{\xi-\xi_0}{\xi-\xi_1}, \tag{4}$$

where $\xi_0 = \xi_1 + A\kappa$ and the quantity A is of order unity. By formula (3) we obtain the approximate expression

$$q = \frac{\mu}{16}\frac{8(\xi-\xi_0)+5\mu}{(\xi-\xi_1)(\xi-\xi_0)^3}, \quad \mu = A\varkappa. \tag{5}$$

For $\tau = \int^{\xi} k\,d\xi$ we get

$$\frac{\tau-\tau_0}{\mu} = \sqrt{\frac{\xi-\xi_0}{\mu}\frac{\xi-\xi_1}{\mu}} - \frac{1}{4}\ln\left(\sqrt{\frac{\xi-\xi_0}{\mu}} + \sqrt{\frac{\xi-\xi_1}{\mu}}\right). \tag{6}$$

With the notations

$$(\tau-\tau_0)/\mu = t, \quad (\xi-\xi_0)/\mu = \eta,$$

we obtain:

$$t = f(\eta), \tag{7}$$

$$f(\eta) = \sqrt{\eta(1+\eta)} - \frac{1}{4}\ln(\sqrt{\eta} + \sqrt{1+\eta}). \tag{8}$$

We denote by g the inverse function of f. We have

$$\eta = g(t); \quad q = (8g(t)+5)/16\mu^2[1+g(t)]\,g^3(t). \tag{9}$$

Computing the leading term of the matrix element, we obtain

$$V_{k,k'} = -\frac{\alpha}{16\mu}\exp\left\{\frac{i\rho(k'-k)}{\alpha} - \frac{\sigma|k'-k|}{\alpha}\right\} \times \int_C \frac{8g(t)+5}{[1+g(t)]\,g^3(t)}\exp\left\{\frac{i(k'-k)\mu}{\alpha}t\right\}dt \tag{10}$$

$$(\tau_0 = \rho + i\sigma),$$

where the integral is taken along a contour C which encloses the singular points of the expression under the integral sign. We use the notation

$$F_1(x) = -\frac{1}{16x}\int_C \frac{8g(t)+5}{[1+g(t)]\,g^3(t)}\,e^{ixt}\,dt. \qquad (11)$$

Then formula (10) takes the form:

$$V_{k,k'} = (k'-k)\,F_1\left((k'-k)\frac{\mu}{\alpha}\right) \times \exp\left\{\frac{i\rho(k'-k)}{\alpha} - \frac{\sigma|k'-k|}{\alpha}\right\}. \qquad (10')$$

In computing the reflection amplitude (2) we restrict the integration to the interior of the region $-1 \le k_1 \le k_2 \le \ldots \le k_n \le 1$. The function $F_1(x)$ is small x proportional to x. Therefore all integrals converge, and the sum of the series (2) is represented in the form

$$R = F\left(\frac{\mu}{\alpha}\right)\exp\left\{\frac{2i}{\alpha}\int^{\xi_0} k\,d\xi\right\}, \qquad (12)$$

where $F(x)$ is a universal function independent of the form of the potential $U(\xi)$. We find the function $F(x)$ with the help of the known exact solution of the Schroedinger equation with the potential $U = U_0/(1+e^{-\xi})$ (reference 2):

$$F(x) = -\frac{2\pi i \exp\{ix\ln(x/2e) - \pi x/2\}}{\Gamma(ix/2)\,\Gamma(1+ix/2)}. \qquad (13)$$

The absolute value of this function is equal to

$$|F(x)| = 2\sinh\frac{\pi x}{2}\,e^{-\pi x/2}. \qquad (14)$$

It is easily seen that for small values $x = A\kappa/\alpha$, the function $|F(x)| \approx \pi x$, and for large x, $|F(x)| \approx 1$.

In the case of a pole of second order, analogous considerations lead to the formula

$$R = G\left(\frac{\sqrt{\mu}}{\alpha}\right)\exp\left\{\frac{2i}{\alpha}\int^{\xi_0} k\,d\xi\right\}, \qquad (15)$$

where $G(x)$ is the universal function

$$|G(x)| = 2\cosh\left(\pi\sqrt{x^2-\frac{1}{4}}\right)e^{-\pi x}. \qquad (16)$$

(Here we made use of the known exact solution of the Schroedinger equation with the potential $U = U_0/\cosh^2\xi$ (reference 2).)

Schiff and Saxon[3,4] investigated the potential scattering of particles with high energies in three dimensions under the assumption $\kappa/\alpha \sim 1$, $\alpha \ll 1$. The results of the present paper show that the methods of these authors cannot be applied to the scattering into large angles, when the cross sections are exponentially small. In the one-dimensional case it can indeed be easily shown that their method leads to the following expression for the reflection amplitude R (the potential is assumed to have a pole of first order):

$$|R| = \frac{\pi\mu}{\alpha}\left|\exp\left\{\frac{2i}{\alpha}\int^{\xi_0} k\,d\xi\right\}\right|.$$

Comparing this expression with (12) and (14), we see that the results agree only for small κ/α, i.e., in the region where perturbation theory is applicable. The error arises from the fact that in their calculations Schiff and Saxon neglect integrals along the real axis over small quantities of order κ^2/α and higher multiplied by strongly oscillating functions. However, these integrals give a contribution comparable to the included terms.

[1] Pokrovskii, Ulinich, and Savvinykh, J. Exptl. Theoret. Phys. (U.S.S.R.) **34**, 1272 (1958), Soviet Phys. JETP **7**, 879 (1958).

[2] L. D. Landau and E. M. Lifshitz, Квантовая механика (Quantum Mechanics), GITTL, 1948.

[3] L. I. Schiff, Phys. Rev. **103**, 443 (1956).

[4] D. S. Saxon and L. I. Schiff, Nuovo cimento **6**, 614 (1957).

Translated by R. Lipperheide
316

Letters to the Editor

EXACT NONLINEAR GRAVITATIONAL EQUATIONS FOR A SPECIAL CASE ON THE BASIS OF BIRKOFF'S THEORY

A. A. BORGARDT

Dnepropetrovsk State University

Submitted to JETP editor December 16, 1957

J. Exptl. Theoret. Phys. (U.S.S.R.) **34**, 1632-1633 (June, 1958)

BIRKHOFF's linear theory of gravitation,[1-4] unlike the general theory of relativity, is based on the general premises of modern field theory. This theory, like the general theory of relativity, predicts a number of observable effects (the deflection of light rays in a gravitational field, the red shift, and the advance of the perihelion) in good agreement with experiment.* We select as initial equations

$$\partial h_{\mu[\nu\lambda]}/\partial x_\lambda = -\alpha T_{\mu\nu}, \quad (\alpha = G/c^4); \tag{1}$$

$$\partial h_{\lambda[\nu\rho]}/\partial x_\mu + \partial h_{\lambda[\rho\mu]}/\partial x_\nu + \partial h_{\lambda[\mu\nu]}/\partial x_\rho = 0, \tag{2}$$

where $T_{\mu\nu}$ is the symmetrized momentum-energy tensor of gravitating matter.

Equation (2) can be replaced by the equivalent definitions of $h_{\mu[\nu\rho]}$ in terms of the potentials $h_{\mu\nu}$:

$$h_{\mu[\nu\rho]} = \partial h_{\mu\rho}/\partial x_\nu - \partial h_{\mu\nu}/\partial x_\rho. \tag{3}$$

Equations (1) and (3) lead to the potential equation

$$\Box^2 h_{\mu\nu} = \alpha T_{\mu\nu}, \tag{4}$$

if we take into account the additional Lorentz-type condition that follows from conservation of $T_{\mu\nu}$:

$$\partial h_{\mu\lambda}/\partial x_\lambda = 0. \tag{5}$$

This theory is a good approximation under ordinary conditions because of the smallness of α, but it is still only an approximation because the field $h_{\mu\nu}$ itself possesses energy and momentum that produce a gravitational effect. This inherent nonlinearity of the gravitational field can be taken into account only by perturbation theory, since the exact nonlinear equations are unknown. We shall not attempt here to treat Birkhoff's theory as a limiting form of the general theory of relativity for slightly curved space (which is shown to be justified by subsequent calculation). We shall show that in the special case of static fields of masses the infinite expansions of perturbation theory can be put into closed form. This procedure results in exact nonlinear equations of the generalized Birkhoff theory.

In the absence of an external $T_{\mu\nu}$, Eq. (4) is obtained from the linear Lagrangian

$$\mathscr{L}_L = -\tfrac{1}{4}\delta_{\lambda\sigma}(\partial h_{\rho\tau}/\partial x_\lambda)(\partial h_{\rho\tau}/\partial x_\sigma). \tag{6}$$

The Lagrangian of the nonlinear field, with the self-force taken into account, must be

$$\mathscr{L}_{NL} = \mathscr{L}_L + (\alpha/2) h_{\lambda\sigma} T^{(NL)}_{\lambda\sigma}, \tag{7}$$

where $T^{(NL)}_{\mu\nu}$ is the unknown momentum-energy tensor of the nonlinear gravitational field. This can be defined in terms of the Lagrangian $\mathscr{L}_{NL}$, which is also unknown, in the usual form

$$T^{(NL)}_{\mu\nu} = (\partial h_{\rho\tau}/\partial x_\mu)(\partial \mathscr{L}_{NL}/\partial(\partial h_{\rho\tau}/\partial x_\nu)) - \delta_{\mu\nu}\mathscr{L}_{NL}, \tag{8}$$

thus giving an equation for $\mathscr{L}_{NL}$:

$$\mathscr{L}_{NL} = \mathscr{L}_L + (\alpha/2) h_{\lambda\sigma}((\partial h_{\rho\tau}/\partial x_\lambda)\partial \mathscr{L}_{NL}/\partial(\partial h_{\rho\tau}/\partial x_\sigma) - \delta_{\lambda\sigma}\mathscr{L}_{NL}). \tag{9}$$

This equation can be solved by representing $\mathscr{L}_{NL}$ as a power series in $\alpha/2$:

$$\mathscr{L}_{NL} = \mathscr{L}_L + (\alpha/2)\mathscr{L}_1 + (\alpha/2)^2\mathscr{L}_2 + \cdots, \tag{10}$$

from which we obtain for $\mathscr{L}_k$:

$$\mathscr{L}_k = -\tfrac{1}{4}a^{(k)}_{\lambda\sigma}(\partial h_{\rho\tau}/\partial x_\lambda)(\partial h_{\rho\tau}/\partial x_\sigma), \tag{11}$$

$$a^{(k)}_{\mu\nu} = h_{\mu\lambda}a^{(k-1)}_{\lambda\nu} + a^{(k-1)}_{\mu\lambda}h_{\lambda\nu} - h_{\lambda\lambda}a^{(k-1)}_{\mu\nu}. \tag{12}$$

Thus

$$\mathscr{L}_{NL} = -\tfrac{1}{4}a_{\lambda\sigma}(h_{\mu\nu})(\partial h_{\rho\tau}/\partial x_\lambda)(\partial h_{\rho\tau}/\partial x_\sigma), \tag{13}$$

where $a_{\mu\nu}$ is a series like (10), with the coefficients $a^{(k)}_{\mu\nu}$ ($a^{(0)}_{\mu\nu} \equiv \delta_{\mu\nu}$).

For fields produced by masses

$$h_{\mu\nu} = h\delta_{\mu\nu}, \quad h_{\mu[\nu\rho]} = (\delta_{\mu\rho}\delta_{\nu\lambda} - \delta_{\mu\nu}\delta_{\rho\lambda})\partial h/\partial x_\lambda \tag{14}$$

and all the series can be summed. For a static gravitational field that takes account of the nonlinear self-force we obtain

$$\nabla^2 h(\mathbf{x}) + (\alpha/2)(\nabla h(\mathbf{x}))^2/(1 - \alpha h(\mathbf{x})) = 0. \tag{15}$$

The solution will always be a function of the linear solution $h_L(\mathbf{x}) = MG/c^2|\mathbf{x}|$ in the form

$$h(\mathbf{x}) = (c^4/G)(1 - (MG^2/2c^6|\mathbf{x}| - 1)^2). \tag{16}$$

For $|\mathbf{x}| \to \infty$, $\mathbf{h} \to h_L$ with $x_0' = MG^2/2c^6$ the potential is at its maximum and equal to c^4/G; $h = 0$ when $x_0'' = MG^2/4c^6$ and $h \to -\infty$ when $|\mathbf{x}| \to 0$. The phase plane of Eq. (15) contains no

solutions of another kind. It is easily seen that the solution (16) cannot be reduced to Schwarzschild's solution, which follows from the general theory of relativity.

*There is an evident illusoriness in the currently widely discussed "test" of the general theory of relativity through measurement of the perihelion shifts of artificial satellites.[5] Such a test can provide no basis for a choice between the general theory of relativity and Birkhoff's theory.

[1] G. Birkhoff, Proc. Nat. Acad. Sci. **29**, 231 (1943); **30**, 324 (1944).

[2] Barajas, Birkhoff, Graef and Vallarta, Phys. Rev. **66**, 138 (1944).

[3] A. Barajas, Proc. Nat. Acad. Sci. **30**, 54 (1944).

[4] G. Birkhoff, Bull, Soc. Mat. Mexicana **1**, 1 (1944).

[5] V. Ginzburg, Usp. Fiz. Nauk **63**, 119 (1957).

Translated by I. Emin
317

ON THE THEORY OF THE POSITIVE COLUMN IN AN ELECTRONEGATIVE GAS

M. V. KONIUKOV

Tula Pedagogical Institute

Submitted to JETP editor March 17, 1958

J. Exptl. Theoret. Phys. (U.S.S.R.) **34**, 1634-1635 (June, 1958)

1. In a positive column where negative ions are produced spatially and disappear at the wall, their relative concentration, which was obtained in reference 1, satisfies the condition $\kappa > D_e/2D_p - 1$,* where D_e and D_p are the diffusion coefficients of electrons and positive ions. This condition is required for the flow of negative ions to the wall, where they recombine. The wall is a surface sink for the negative ions produced within the volume.

2. When decay of the negative ions through collisions with neutral atoms[2] is included, the situation becomes somewhat more complicated, but we still have a linear problem which can be completely solved. For ambipolar diffusion, subject to the assumptions $D_e \gg D_p$, $D_p \approx D_n$, $b_e \gg b_p$ and $b_p \approx b_n$, we obtain an equation† for the concentration of negative ions in the column:

$$\frac{2\varkappa(1+\varkappa)D_p/D_e - \varkappa}{1+2\varkappa} = \frac{\beta - \gamma\varkappa}{Z - (\beta - \gamma\varkappa)},$$

where γ is the rate of decay of negative ions per ion and the rest of the notation is that used in reference 1. This is a cubic equation in κ which can be solved as follows:

(a) $\kappa > D_e/2D_p - 1$. With this concentration more negative ions are created per unit volume than decay, so that the column is a spatial source of negative ions. The negative ions produced in the column diffuse to the wall, which serves as a surface sink.

(b) $\kappa = D_e/2D_p - 1$. In this case the negative ions created by electrons adhering to neutral atoms equals those vanishing through decay. There is no effective resulting creation or disappearance of negative ions in the column. Their radial flow is zero and the total number of negative ions in the column is determined only by processes in the space.

(c) $\kappa < D_e/2D_p - 1$. Here the number of negative ions disappearing from the column exceeds the number produced, so that the column is a spatial sink for negative ions. Their radial flow is directed toward the axis and a stationary state is possible only in the presence of a surface source at the wall.‡

Thus in a positive column, where the disappearance of negative ions obeys a linear law, small values of κ are possible when there is near the surface of the wall** a layer that produces a flow of negative ions into the column, where they disappear through decay as a result of collisions with neutral particles. Our conclusion that a surface source exists agrees with Günterschulze's hypothesis[4] of a layer of negative ions at the wall.

3. When we take into account the spatial recombination of positive and negative ions, we can in general distinguish two regions of the column, an inner region where recombination predominates over creation, and an outer region where creation is stronger than recombination. We are here concerned with effective spatial sources and sinks.†† Since the equations of balance are nonlinear the problem can be solved more or less simply only for regions close to the axis of the discharge.[1]

*In reference 3 it was assumed that $\varkappa \ll 1$ in the absence of spatial disappearance of negative ions. This is unacceptable to us, since $\varkappa$ is a solution of the system and is fully determined by the kinetics of the column. The analysis carried out in reference 1 and in the present note shows that $\varkappa$ can be small only when a spatial loss occurs.

†The solution is obtained as in reference 1.

‡The strength of the surface source per unit length of the column is given by the integral $2\pi \int_0^R (\beta - \gamma\varkappa) N_e r dr$, where N_e is the electron density.

**Reference 3 considers negative ion concentrations which fulfill the condition $b_p\varkappa/b_e \ll 1$. Then, as is easily seen from the expression for the flow given in reference 2, there must be a source of negative ions at the wall. We therefore consider the boundary condition $N_n(R) = 0$ not to be stringent enough.

††The inclusion of surface sources of negative ions will only shift the boundary between the regions toward the wall.

[1] M. V. Koniukov, J. Exptl. Theoret. Phys. (U.S.S.R.) **34**, 908 (1958), Soviet Phys. JETP **7**, 629 (1958).

[2] R. Seeliger, Ann. Physik **6**, 93 (1949).

[3] L. Holm, Z. Physik **75**, 171 (1932).

[4] A. Günterschulze, Z. Physik **91**, 724 (1934).

Translated by I. Emin
318

SURFACE WAVES ON THE BOUNDARY OF A GYROTROPIC MEDIUM

M. A. GINTSBURG

Submitted to JETP editor January 31, 1958

J. Exptl. Theoret. Phys. (U.S.S.R.) **34**, 1635-1637 (June, 1958)

1. We consider the surface waves (s.w.) $\exp[i(hz - \omega t) + \gamma x]$ propagating along the interface $x = 0$ of two semi-infinite media. Medium 1 ($x > 0$) is isotropic ($\epsilon = \epsilon_0$, $\mu = \mu_0$). Medium 2 ($x < 0$) is gyrotropic with a dielectric constant ϵ and magnetic permeability μ_{ik}:

$$\mu_{xx} = \mu_{zz} = \mu_1; \quad \mu_{yy} = \mu_3; \quad \mu_{xz} = -\mu_{zx} = i\mu_2, \tag{1}$$

that is, the direction of the external magnetizing field is such that $H_0 \parallel OY$. We shall consider H-mode surface waves ($H_Z \neq 0$) in a medium with tensor μ_{ik} (ferrites). All of our results will also be valid for media with tensor ϵ_{ik} (plasma, Hall effect etc.) when E, H, ϵ, μ_{ik}, ω are replaced by H, E, μ, ϵ_{ik}, $-\omega$.

2. From the continuity of E_y and H_Z at $x = 0$ (H_Z is given in terms of E_y in reference 2) we obtain an equation for $u = -hc/\omega$, the retardation coefficient of the wave ($u = c/v_\phi$, where v_ϕ is the phase velocity):

$$\mu_0(u^2 - \varepsilon\mu_\perp)^{1/2} + \mu_\perp(u^2 - \varepsilon_0\mu_0)^{1/2} = \mu_0\Gamma u, \tag{2}$$

$$\Gamma = \mu_2/\mu_1.$$

Equation 2 was analyzed graphically. Some of the results follow. For $\Gamma > 0$ and $\mu_\perp > 0$, Eq. (2) has a real root if

$$\text{for } \varepsilon\mu_\perp > \varepsilon_0\mu_0\text{: } \mu_\perp + \mu_0 > \mu_0\Gamma > \mu_0(1 - \varepsilon_0\mu_0/\varepsilon\mu_\perp)^{1/2},$$
$$\text{for } \varepsilon\mu_\perp < \varepsilon_0\mu_0\text{: } \mu_\perp + \mu_0 > \mu_0\Gamma > \mu_0(1 - \varepsilon_0\mu_\perp/\varepsilon\mu_0)^{1/2}. \tag{3}$$

This is the only root; the wave thus propagates in only one direction ($h < 0$). For $\epsilon_0\mu_0 \neq \epsilon\mu_\perp$ slight gyrotropy ($\Gamma \ll 1$) cannot invalidate the law for an isotropic boundary. Just as in the isotropic case,[1] a s.w. does not propagate for $\epsilon > 0$, $\mu > 0$. But with $\epsilon\mu_\perp$ close to $\epsilon_0\mu_0$ a unidirectional wave (only in the z direction) is possible even for slight gyrotropy (theoretically also for paramagnetics).

For $\mu_\perp < 0$, $\Gamma > 0$, and $|\mu_\perp| > \mu_0$ the condition for propagation of the direct wave ($h > 0$) is $\mu_0\Gamma < |\mu_0 + \mu_\perp|$, while for the reverse wave ($h < 0$), $\Gamma < (1 + |\epsilon\mu_\perp|/\epsilon_0\mu_0)^{1/2}$. Thus, depending on the values of ϵ and μ_{ik}, both waves are propagated or one alone, or, finally, s.w. are impossible.

3. We now consider the more complicated case of s.w. in a gyrotropic plate 3 ($0 < x < d$, $\mu = \mu_{ik}$) between isotropic media 1 ($\epsilon = \epsilon_0$; $\mu = \mu_0$) and 2 ($\epsilon = \tilde{\epsilon}$; $\mu = \tilde{\mu}$). Let d be large; for the boundary $x = d$ we set up an equation similar to (2), different from (2) only in the sign of the right-hand side, i.e., the boundary $x = d$ guides s.w. in a direction opposite to that on the boundary $x = 0$. Accordingly the field of the direct wave is concentrated at one boundary and the field of the reverse wave at the opposite boundary: for $\epsilon_0 = \tilde{\epsilon}$ and $\mu_0 = \tilde{\mu}$:

$$E_y = A_1 e^{\gamma_3 x} + A_2 e^{-\gamma_3 x}, \quad A_{1,2} = \gamma_3\mu_0 \pm \gamma_1\mu_\perp \mp \mu_0\Gamma h.$$

When the boundary which conducts energy in the undesired direction is covered with an absorbing film we obtain a unidirectional system.

For $\gamma_3 d \leq 1$ we must take into account the interaction of the boundaries and investigate the characteristic equation. In the general case ($\epsilon_0 \neq \tilde{\epsilon}$, $\mu_0 \neq \tilde{\mu}$) this equation is

$$h^2\Gamma^2 + h\Gamma(\gamma_1 P_1 - \gamma_2 P_2) - \gamma_1\gamma_2 P_1 P_2 - \gamma_3^2 = \gamma_3(\gamma_1 P_1 + \gamma_2 P_2)\coth\gamma_3 d, \tag{4}$$

$$P_1 = \frac{\mu_\perp}{\mu_0}; \quad P_2 = \frac{\mu_\perp}{\tilde{\mu}}; \quad \gamma_1^2 = h^2 - \frac{\omega^2}{c^2}\varepsilon_0\mu_0;$$

$$\gamma_2^2 = h^2 - \frac{\omega^2}{c^2}\tilde{\varepsilon}\tilde{\mu}; \quad \gamma_3^2 = h^2 - \frac{\omega^2}{c^2}\varepsilon\mu_\perp.$$

This equation contains a term which is linear in h, so that the direct and reverse waves differ not only with respect to the field distribution but also with respect to the phase velocity and critical velocity. For $\epsilon\mu_\perp > \epsilon_0\mu_0 > \tilde{\epsilon}\tilde{\mu}$

$$\omega_{cr} = \frac{c}{d}\frac{\alpha P_1 + \beta P_2}{(\alpha P_1 + \Gamma)(\beta P_2 - \Gamma)}, \tag{5}$$

$$\alpha = \left(1 - \frac{\varepsilon_0\mu_0}{\varepsilon\mu_\perp}\right)^{1/2}; \quad \beta = \left(1 - \frac{\tilde{\varepsilon}\tilde{\mu}}{\varepsilon\mu_\perp}\right)^{1/2}.$$

When $\omega > \omega_{cr}$, a sufficient condition for the propagation of s.w. is $M < 0$, where $M = (\Gamma + P_1 + 1)(\Gamma - P_2 - 1)$. When $\omega < \omega_{cr}$, the sufficient condition is $M > 0$. Equation (5) applies to the direct wave; for the reverse wave the sign of Γ must be reversed, giving different conditions for propagation of the two different waves.

4. Analogous conflicting properties are characteristic of a channel 3 ($0 < x < d$; $\epsilon = \epsilon_0$; $\mu = \mu_0$) between two gyrotropic media 1 ($x < 0$; $\mu = \mu_{ik}$) and 2 ($x > d$; $\mu = \tilde{\mu}_{ik}$). With $\mu_\perp < 0$ and $\tilde{\mu}_\perp < 0$, the gyrotropic plates 1 and 2 insulate channel 3 from the surrounding medium like the walls of a metal waveguide. The characteristic equation which corresponds to (4) is

$$h^2\Gamma\tilde{\Gamma} + h(\gamma_1\tilde{\Gamma} - \gamma_2\Gamma) - \gamma_1\gamma_2 - \gamma_3^2 Q\tilde{Q} = \gamma_3 [h(\Gamma\tilde{Q} - \tilde{\Gamma}Q) + \gamma_2 Q + \gamma_1\tilde{Q}] \coth\gamma_3 d, \quad (6)$$

where $Q = \mu_\perp/\mu_0$; $\tilde{Q} = \tilde{\mu}_\perp/\mu_0$. The critical frequency is

$$\omega_{cr} = \frac{c}{d}\left(\frac{\tilde{Q}}{\tilde{\Gamma} - \beta} - \frac{Q}{\Gamma + \alpha}\right),$$

$$\alpha = \left(1 - \frac{\varepsilon\mu_\perp}{\varepsilon_0\mu_0}\right)^{1/2}, \quad \beta = \left(1 - \frac{\tilde{\varepsilon}\tilde{\mu}_\perp}{\varepsilon_0\mu_0}\right)^{1/2}.$$

Sufficient conditions for the propagation of the direct s.w. are $N < 0$ for $\omega > \omega_{cr}$ and $N > 0$ for $\omega < \omega_{cr}$, where $N = (\Gamma + Q + 1)(\tilde{\Gamma} - \tilde{Q} - 1)$. By interchanging the signs of Γ and $\tilde{\Gamma}$ we obtain the conditions for the propagation of the reverse wave.

Waves of the waveguide type (by which we mean waves for which $\gamma_3^2 < 0$) can also propagate in this channel. In such waves the energy maximum is not at the walls as in s.w. but in the middle of the channel, so that we can expect smaller loss.

5. The boundary of a gyrotropic medium and the plate and channel discussed in Secs. 3 and 4 are of considerable interest as retarding systems. Their advantages are the possibility of modifying (and specifically, modulating) the retardation coefficient in time (by changing H_0) and in space, and the absence of distortions.

[1] L. D. Landau and E. M. Lifshitz, Электродинамика сплошных сред (The Electrodynamics of Continuous Media), GTTI, 1957, p. 364.

[2] M. A. Gintsburg, Izv. Akad. Nauk SSSR, Ser. Fiz., **18**, 444 (1954).

Translated by I. Emin
319

ENERGY SPECTRUM OF NUCLEAR-ACTIVE PARTICLES IN EXTENSIVE AIR SHOWERS

O. I. DOVZHENKO, O. A. KOZHEVNIKOV, S. I. NIKOL'SKII, and I. V. RAKOBOL' SKAIA

P. N. Lebedev Physics Institute, Academy of Sciences, U.S.S.R.

Submitted to JETP editor February 26, 1958

J. Exptl. Theoret. Phys. (U.S.S.R.) **34**, 1637-1638 (June, 1958)

As a continuation of our earlier work,[1] we studied the energy spectrum of nuclear-active particles in extensive air showers (EAS) of cosmic radiation at 3860 m above sea level. Nuclear-active particles of the shower were identified by production of electron-nuclear showers in lead plates of a large rectangular cloud chamber.* Total thickness of the lead plates amounted to ~ 100 g/cm^2. As a criterion of the nature of secondary showers we used the presence of penetrating or heavily ionizing particles in electron-nuclear showers, which corresponds to that used in reference 3.

The experiment was carried out in two variants, one with no absorber above the chamber, and another with an absorber of ~ 100 g/cm^2 Al. A diagram of the arrangement is shown in Fig. 1.

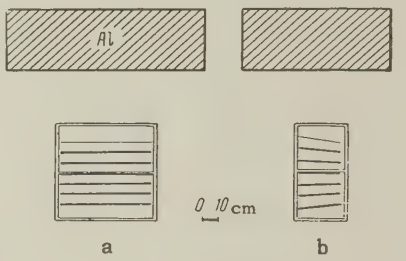

FIG. 1. Diagram of the array, a – front view, b – side view.

EAS with total number of particles N between 10^4 to 10^6 were recorded. The average shower size was $N \sim 10^5$ in the first variant of the experiment, $N \sim 2 \times 10^5$ in the second. A hodoscope consisting of a large number of self-quenching counters made it possible to select EAS, the axes of which fell within 9 m from the cloud chamber, and to determine the total number of particles in a shower.[4] The error in the axis location amounted to ~ 1 m. The energy of nuclear-active particles was determined from the energy of the electron-photon component produced by these particles.[3]

Integral energy spectra of nuclear-active particles for the energy region 2 to 50 Bev at dis-

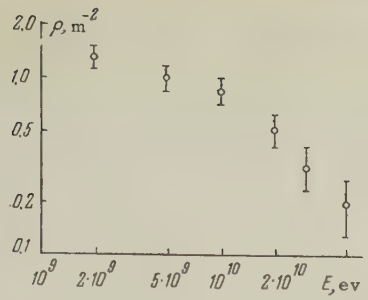

FIG. 2. Integral energy spectrum of nuclear-active particles in the energy region 2 to 50 Bev. The x axis represents the energy of nuclear-active particles in ev, and the y axis the absolute flux density of nuclear-active particles.

tances 0 to 9 m from the shower axis were constructed from 52 nuclear interaction events. Since the spectra obtained in the two variants of the experiments were identical, we averaged the results of both series of measurements.

The observed integral energy spectrum of nuclear-active particles in the 10 to 50 Bev energy region can be approximated by a power law E^{-k}, where $k = 0.95 \pm 0.25$ (cf. Fig. 2). This result is not surprising, since a spectrum of this shape can be expected from the integral energy spectrum of μ mesons in EAS, measured at the same altitude.[5] Furthermore, the same value of the spectrum exponent has been obtained for 10^{11} to 10^{12} ev nuclear-active particles.[1]

We estimated the fraction of nuclear-active particles of > 2 Bev, at a distance of 0 to 9 m from the axis, by comparing the observed number of nuclear-active particles with the electron flux density in showers detected by our array. We have obtained a value $(1.3 \pm 0.3)\%$ which, within the limits of experimental error, is in a good agreement with the value $(1 \pm 0.1)\%$ obtained earlier[6] by means of a hodoscope. It should be noted that the fraction of nuclear-active particles measured in the present experiment may be underestimated, in view of the difficulties in identifying nuclear-active particles when the number of electrons in the shower produced in the chamber is large.

*For details of the cloud chamber, cf. reference 2.

[1] Zatsepin, Krugovykh, Murzina, and Nikol'skii, J. Exptl. Theoret. Phys. (U.S.S.R.) **34**, 298 (1958), Soviet Phys. JETP **7**, 207 (1958).

[2] Danilova, Dovzhenko, Nikol'skii, and Rakobol'skaia, J. Exptl. Theoret. Phys. (U.S.S.R.) **34**, 541 (1958), Soviet Phys. JETP **7**, 374 (1958).

[3] Ivanovskaia, Sarycheva, and Chikin, J. Exptl. Theoret. Phys. (U.S.S.R.) **34**, 45 (1958), Soviet Phys. JETP **7**, 30 (1958).

[4] Dovzhenko, Zatsepin, Murzina, Nikol'skii, Rakobol'skaia, and Tukish, Dokl. Akad. Nauk SSSR **118**, 5 (1958).

[5] Dovzhenko, Nelepo, and Nikol'skii, J. Exptl. Theoret. Phys. (U.S.S.R.) **32**, 463 (1957), Soviet Phys. JETP **5**, 391 (1957).

[6] Nikol'skii, Vavilov, and Batov, Dokl. Akad. Nauk SSSR **111**, 71 (1956), Soviet Phys. "Doklady" **1**, 625 (1956).

Translated by H. Kasha
320

CALCULATION OF THE LIFETIMES OF EXCITED STATES OF Hf^{178} *AND* Hf^{180}

V. V. ANISOVICH

Leningrad Physico-Technical Institute

Submitted to JETP editor February 6, 1958

J. Exptl. Theoret. Phys. (U.S.S.R.) **34**, 1639-1641 (June, 1958)

THE nuclides Hf^{178} and Hf^{180} have excited states from which transitions occur to a level of the rotational band with total angular momentum $I = 8$, with emission of E1 radiation. The γ-ray energies are 88.8 and 56.6 kev, respectively. The lifetimes of these long-lived states are 3 seconds and 5.5 hours.[1,2] The standard theoretical estimates of the lifetimes of these excited states according to the independent particle model (examples of which can be found in reference 3) give values approximately 10^{16} times smaller. However, in highly deformed nuclei (such as Hf^{178} and Hf^{180}) a new quantum number K appears — the magnitude of the projection of the total angular momentum on the symmetry axis of the nucleus. For γ transitions in such nuclei there is therefore a new selection rule on K: $\Delta K \leq L$, where L is the angular momentum of the emitted radiation. The selection rule on K is not strict, since the rotational motion of the nucleus somewhat perturbs the nucleon configuration and distorts its shape. Transitions with $\Delta K > L$ are said to be K-forbidden, and their degree of forbiddenness is characterized by the number $\nu = \Delta K - L$. The occurrence of K-forbiddenness can explain the long lifetimes of the Hf nuclides.

The possibility of K-forbiddenness has been treated by A. Bohr in the uniform nuclear model which he proposed.[4] For a numerical estimate of

the transition probability when K-forbiddenness occurs, we still have to make assumptions about the nature of the interaction of the nucleons in the nucleus. We shall use Nilsson's scheme,[5] which gives the correct order of levels for an unpaired nucleon. However, the nuclides Hf^{178} and Hf^{180} are even-even. We must therefore, in treating the nucleon, also take into account its interaction with its paired partner. We shall assume that the pairing energy is zero when the nucleons are in different single particle levels as given by the Nilsson scheme, while the pairing energy of nucleons which are in the same single particle level (so that they have equal and opposite projections of their total angular momenta on the symmetry axis) is equal to the difference between the excitation energy as calculated from the uniform model and the experimental value. The pairing energies for Hf^{178} and Hf^{180} are then 1100 and 1300 kev, respectively. According to the Nilsson scheme, in the ground state of the nucleus the nucleons successively fill all the single particle levels, and there can be no more than two nucleons in each of the levels. The long-lived states are the first excited states which involve a change in the nucleon configuration, since rotational excitations are associated with slow rotation of the nucleus, which does not affect its internal structure. It is therefore natural to assume that these long-lived states are formed as a result of the shift of a nucleon which is in the last filled level to the next higher level. According to the collective model, the lowest excitations with change of internal structure will be those in which $I = K = \Sigma\Omega_i$, where Ω_i is the projection of the total angular momentum of the i-th nucleon on the axis of symmetry. From the fact that an E1 transition was observed to a rotational level with $I = 8$, it follows that the total angular momentum I of the long-lived excited states is 7, 8, or 9. From the positions of the single particle levels in the Nilsson scheme, we see that, for the Hf^{178} and Hf^{180} nuclei, the only one of these three values which is possible is $\Sigma\Omega_i = 8$ (when a neutron is excited). However, there are experimental data which apparently favor $K = 9$ for the case of Hf^{180}.[2] This may occur, for example, as a result of a poor estimate of the pairing energy. If it happens that the difference between the pairing energies when the nucleons are in levels 49 and 40* (so that the projections of their angular momenta on the symmetry axis are $9/2$ and $9/2$) and when they are in levels 49 and 48 (with projections of their total angular momenta on the symmetry axis equal to $9/2$ and $7/2$) is less than or approximately equal to 200 kev, then the energy of the state with $K = 9$ will be lower than that of the state with $K = 8$. In this case it is difficult to say anything definite about the lifetimes of the excited states. However, if the pairing energy of nucleons which are in different levels is small, the lifetime of the excited state will be approximately one order of magnitude greater than that calculated here (because the degree of K-forbiddenness is increased by unity). The E1 transition to the rotational level with $K = 0$ is possible because K is not a strict quantum number.

We have treated the perturbations

$$u_1 = -(\hbar^2/J_1)\, I_1 j_1 - (\hbar^2/J_2)\, I_2 j_2,$$
$$u_2 = -\beta \sin\gamma M\omega_0^2 r^2 (Y_{22}(\vartheta, \varphi) + Y_{2-2}(\vartheta, \varphi))/\sqrt{2},$$
$$u_3 = (\hbar^2/4J_1 - \hbar^2/4J_2)(I_1^2 - I_2^2),$$

where I_κ, j_κ are the projections on the κ axis of the total angular momentum of the nucleus and the total angular momentum of the particular nucleon; r, ϑ, φ are the coordinates of the nucleon, and M its mass. ω_0 is determined by the number of nucleons in the nucleus, and $I_\kappa = 4B\beta^2 \sin^2(\gamma - 2\pi\kappa/3)$.

The matrix elements of u_2 and u_3 are different from zero only between states with different values of the quantum number n_γ which characterizes the nuclear surface oscillations. In the calculations we included corrections only from intermediate states with $n_\gamma = 1$, since the contribution from intermediate states with $n_\gamma > 1$ will be much smaller. The corrections from u_2 and u_3 are smaller, but are still significant in the cases we are considering, since they affect the order of magnitude of the lifetime.

It was assumed that the long-lived state of Hf^{180} results from the ground state through the shift of a neutron from level 49 ($\Omega = -9/2$) to level 48 (having $\Omega = 7/2$), so that $I = K = \Sigma\Omega_i = 8$. The single particle energies and nucleon wave functions were taken for $\beta = 0.2$. The lifetime of the long-lived excited state was found to be $\tau = 175$ hours (while the experimental value is $\tau = 5.5$ hours).

For Hf^{178} it was assumed that the long-lived state is formed by the transition of a neutron from level 41, with $\Omega = -7/2$, to level 49, with $\Omega = -9/2$, so that $I = K = \Sigma\Omega_i = 8$, and that $\beta = 0.25$. The calculated lifetime was $\tau = 130$ sec (while the experimental value is $\tau = 3$ sec).

The values of the deformation parameter β were chosen to be close to the experimental values (as determined from the nuclear quadrupole moment), and to give the smallest possible values of the lifetimes. We should remark that the result

changes very slightly for small changes in the size of β.

The cases we are considering are of interest because the magnitudes of the lifetimes are determined by corrections in the 7-th order of perturbation theory, since the degree of K-forbiddenness is 7. Therefore any deficiencies of the scheme will strongly affect the result. The calculated values were found to be 30 to 40 times those observed in experiment. It should be remarked that, in addition to the perturbations considered here, there may also be perturbations due to the presence of the paired nucleon. Even though we cannot, because of possible deficiencies of the scheme, definitely assert that these perturbations give a contribution amounting to approximately $\frac{1}{4}$ of the contribution of the perturbations considered here (as would follow from our result), it is clear that these perturbations will be small. The main contribution will come from the perturbations which we have considered.

I am deeply grateful to L. A. Sliv for his interest in this work, and also to K. A. Aristova for carrying out the numerical computations.

*The levels are designated according to reference 5.

[1] F. F. Felber, Nucl. Sci. Abstracts **11**, No. 1126 (1957).

[2] L. I. Rusinov and V. S. Gvozdev, Программа и тезисы совещания по ядерной спектроскопии (Program and Abstracts of the Conference on Nuclear Spectroscopy) Acad. Sci. Press (1958).

[3] J. M. Blatt and V. F. Weisskopf, Theoretical Nuclear Physics, Wiley, 1952.

[4] A. Bohr, Kgl. Danske Videnskab. Selskab Mat.-fys. Medd. **26**, No. 14 (1952); A. Bohr and B. Mottelson, Kgl. Danske Videnskab. Selskab Mat.-fys. Medd. **27**, No. 16 (1953).

[5] S. G. Nilsson, Kgl. Danske Videnskab. Selskab Mat.-fys. Medd. **29**, No. 16 (1955).

Translated by M. Hamermesh
321

PHONON INTERACTIONS OF ELECTRONS IN POLAR CRYSTALS

A. V. TULUB

Leningrad State University

Submitted to JETP editor February 28, 1958

J. Exptl. Theoret. Phys. (U.S.S.R.) **34**, 1641-1643 (June, 1958)

THE interaction energy of two electrons in polar crystals can be split into parts. The first part is the direct Coulomb interaction of the electrons, including the polarization of the electron shells of the atoms. This polarization is evaluated by introducing the dielectric constant $\epsilon_\infty = n^2$, where n is the index of refraction of light. The second part is the interaction through the phonon field. An evaluation of the phonon interaction is also important for a system consisting of an electron and a hole, for instance, an exciton. This problem was considered by a number of authors: in the strong coupling approximation by Dykman and Pekar,[1] and in the intermediate-coupling approximation by Meyer,[2] Haken,[3] and others. The authors of the cited papers used different variational principles to find the energy spectrum of the exciton.

In the present communication the phonon interaction potential of the electrons is derived in the intermediate-coupling approximation, with allowance for their relative momentum.

The operator of the interaction energy of an electron with the phonon field can be written in the form[4,5] (we put henceforth $\hbar = 1$):

$$\sum_k V_k a_k e^{i\mathbf{kr}} + V_k^* a_k^+ e^{-i\mathbf{kr}}, \tag{1}$$

$$V_k = -(i\omega/k)\,(1/2\, m\omega)^{1/4}\,(4\pi\alpha/V)^{1/2},$$

$$\alpha = \frac{e^2}{2}\left(\frac{2m}{\omega}\right)^{1/2}\left(\frac{1}{n^2} - \frac{1}{\varepsilon}\right). \tag{2}$$

The quantity α plays the role of the coupling constant, m is the effective mass of the electron, ω the limiting frequency of the longitudinal optical vibrations, and the a_k are the second-quantization operators. In the center-of-mass system, the energy operator of the two-electron system under consideration is of the form

$$\hat{H} = -\frac{1}{2M}\nabla_R^2 - \frac{1}{2\mu}\nabla_r^2 + \frac{e^2}{n^2 r} + \sum_k \omega a_k^+ a_k + \sum_k 2\cos\frac{\mathbf{kr}}{2}\,(V_k a_k e^{i\mathbf{kR}} + \text{c.c.}), \tag{3}$$

where

$$\mathbf{R} = {}^1/_2(\mathbf{r}_1 + \mathbf{r}_2), \quad \mathbf{r} = \mathbf{r}_1 - \mathbf{r}_2, \quad M = 2m.$$

The center-of-mass coordinates can be eliminated from (3) by means of the canonical transformation S;

$$S = \exp\left\{i\left(\mathbf{P} - \sum_k \mathbf{k} a_k^+ a_k\right)\right\} \mathbf{R}; \tag{4}$$

$\mathbf{P}$ is the total momentum of the system. After the transformation we have

$$S^{-1}HS = -\frac{1}{2\mu}\nabla_r^2 + \frac{e^2}{n^2 r} + \frac{\mathbf{P}^2}{2M} + \sum_k \left(\omega + \frac{k^2}{2M} - \frac{(\mathbf{pk})}{M}\right) a_k^+ a_k$$

$$+ \sum_k 2\cos\frac{\mathbf{kr}}{2}\cdot(V_k a_k + V_k^* a_k^+) + \frac{1}{2M}\sum_{kk'}(\mathbf{kk}')\, a_k^+ a_{k'}^+ a_k a_{k'}. \tag{5}$$

In the following we consider, for the sake of simplicity, the case of zero total momentum. We single out in the energy operator (5) the following three terms:

$$H_0 = -\frac{1}{2\mu}\nabla_r^2 + \sum_k \left(\omega + \frac{k^2}{2M}\right) a_k^+ a_k$$

$$+ \sum_k V_k a_k e^{i\mathbf{kr}/2} + V_k^* a_k^+ e^{-i\mathbf{kr}/2}. \tag{6}$$

The operator H_0 describes the "free" motion of a polaron of effective mass μ in the center-of-mass system of the two particles. The remaining terms in (5) distort the motion of the free polaron and describe the influence of the second particle on the motion of the first one, thus playing the part of a potential energy operator. If we denote these terms by H_1, we can find the correction to the energy approximately from the relation $\varphi_q(r) = \langle \Omega_q, H_1 \Omega_q \rangle$ where Ω_q is the eigenfunctional of the operator H_0, the approximate form of which was found in the paper by Lee, Low, and Pines.[5] Using the explicit form of these functionals we get, apart from an additive term which does not depend on r, the following expression for $\varphi_q(r)$:

$$\varphi_q(r) = -\frac{e^2}{r}\left(\frac{1}{r^2} - \frac{1}{\varepsilon}\right)\frac{a^2 - 2b^2}{a^2}$$

$$+ \frac{e^2}{r}\left(\frac{1}{n^2} - \frac{1}{\varepsilon}\right)\exp\{-(a^2 - b^2)^{1/2} r\} \tag{7}$$

$$\times a^{-2}[(a^2 - 2b^2)\cos br - 2(a^2 - b^2)^{1/2} b \sin br],$$

where η is a parameter defined in reference 5, $a^2 = M\omega$, and $2b = q(1 - \eta)$.

One must note that if the total relative momentum q is zero the expression for $\varphi_q(r)$ in the limits of applicability of the intermediate coupling approximation is not approximate, but exact. The phonon interaction itself goes leads to the attraction of two electrons, but the magnitude of the attraction is insufficient for the formation of a "bipolaron," since the sum of the Coulomb potential $e^2/n^2 r$ and the phonon potential $\varphi_q(r)$ is always positive. As $r \to 0$ the potential $\varphi_q(r)$ stays finite, and as $r \to \infty$ it has a Coulomb character. If $r \to \infty$, the interaction of the two electrons is described by the usual Coulomb law, $e^2/\epsilon r$.

The source of the deviation of the phonon interaction from the Coulomb interaction consists in taking into account the recoil during the emission of phonons. Owing to recoil, the electrons experience fluctuating displacements, which leads to an additional interaction energy.

In a similar manner one can show that the interaction of an electron with a hole in an exciton is described by the potential[3]

$$-(e^2/\varepsilon r) - e^2(1/n^2 - 1/\varepsilon)\, e^{-ar}/r.$$

The deviation of the potential from the Coulomb potential is important at distances of the order $(M\omega)^{-1/2}$ which amounts to 10 to 15 A for Cu_2O. The ground state and partly the next energy levels of the exciton are shifted downwards.

[1] I. M. Dykman and S. I. Pekar, Trans. Phys. Inst. Acad. Sci. Ukr. S.S.R. **92**, No. 3 (1952).

[2] H. J. G. Meyer, Physica **22**, 109 (1956).

[3] H. Haken, Z. Physik **146**, 527 (1956).

[4] S. I. Pekar, Исследования по электронной теории кристаллов (Investigations on the Electron Theory of Crystals) Gostekhizdat 1951; German translation: Untersuchungen über die Elektronentheorie der Kristalle, Berlin, Akademie Verlag, 1954.

[5] T. D. Lee and D. Pines, Phys. Rev. **92**, 883 (1953); Lee, Low and Pines, Phys. Rev. **90**, 297 (1953).

Translated by D. ter Haar
322

THE QUESTION OF THE SYMMETRY OF THE MANY-ELECTRON SCHRÖDINGER WAVE FUNCTION

E. D. TRIFONOV

Leningrad State University

Submitted to JETP editor March 4, 1958

J. Exptl. Theoret. Phys. (U.S.S.R.) **34**, 1643-1644 (June, 1958)

We consider the Schrödinger equation for a many-electron system. We assume that the Hamiltonian in this equation does not contain spin operators. Because of the equivalence of the electrons, the Hamiltonian is invariant under the symmetric group of interchanges of the spatial coordinates of the electrons. According to Wigner's theorem, the eigenfunctions belonging to each eigenvalue of the energy will then form the basis for one of the irreducible representations of the symmetric group. If we assume that the system is in a state with definite spin S, then the only allowed energy eigenvalues are those which correspond to the definite irreducible representation given by a Young scheme of two columns containing respectively λ_1 and λ_2 cells,[1] where

$$\lambda_1 \geqslant \lambda_2,\ \lambda_1 + \lambda_2 = n,\ \lambda_1 - \lambda_2 = 2S. \qquad (1)$$

This gives the connection between the energy values and the value of the spin, although, as we mentioned, the Hamiltonian of our system does not contain spin operators.

The symmetry properties of the many-electron coordinate function necessary and sufficient to make this function an element of the subspace transforming according to a definite irreducible representation $\{\lambda_1\lambda_2\}$ are conveniently illustrated with the help of the corresponding Young scheme. We write into the cells of the Young scheme the position numbers of the arguments, e.g., in their natural order (cf. figure).

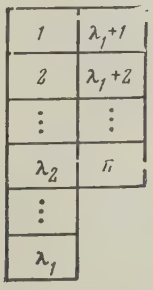

Then one can so choose the basis functions of the subspace transforming according to the irreducible representation $\{\lambda_1\lambda_2\}$, that each of them is antisymmetric with respect to the interchange of the arguments whose numbers lie in either of the columns of the Young scheme; one can also choose them such that each of the functions is symmetric with respect to the interchange of the arguments whose numbers lie in each of the rows of the Young scheme. These properties we shall call properties A.

There exists, however, another set of conditions, the three Fock conditions,[2] which are equivalent to the conditions A, as we shall show. The Fock conditions, which we shall call conditions B for brevity, consist in the requirement that the function be antisymmetric with respect to two groups of k and n − k arguments (two conditions), and in the requirement of cyclic symmetry. Moreover,

$$n - k \geqslant k,\ (n-k) - k = 2S. \qquad (2)$$

Comparing (1) and (2), we see that $\lambda_1 = n - k$, $\lambda_2 = k$, and that, of course, the first two of the conditions B coincide with the first half of condition A. The requirement of cyclic symmetry may be interpreted as the impossibility of antisymmetrizing the function in more than n − k arguments.

We proceed to the systematic proof of the equivalence of conditions A and B. We shall make use of a group-theoretical method based on the material of chapters IV and V of Murnaghan's book.[3]

We consider the space of the functions subject to the first two of conditions B. We denote it by the symbol $(\lambda_1\lambda_2)$. This space is subdivided into several subspaces transforming according to the irreducible representations of the symmetric group. Among these will certainly be the irreducible representation $\{\lambda_1\lambda_2\}$, as well as some representations $\{\lambda_1'\lambda_2'\}$ with $\lambda_1' > \lambda_1$, but there will be no representation $\{\lambda_1''\lambda_2''\}$ with $\lambda_1'' < \lambda_1$.

We now impose the requirement of cyclic symmetry on the functions of space $(\lambda_1\lambda_2)$. Evidently, the functions of the subspace transforming according to $\{\lambda_1'\lambda_2'\}$ do not satisfy this requirement, since they can, according to property A, be antisymmetrized in more than λ_1 arguments. Of the whole space $(\lambda_1\lambda_2)$ there remains only one subspace, transforming according to $\{\lambda_1\lambda_2\}$, whose functions satisfy the requirement of spherical symmetry.[4] Indeed, the subspace transforming according to $\{\lambda_1\lambda_2\}$ is not contained in the spaces $(\lambda_1'\lambda_2')$, and hence cannot, according to the reciprocity theorem of Frobenius, be antisymmetric in more than λ_1 arguments.

Thus the three Fock conditions are necessary and sufficient for the functions satisfying these conditions to belong to the subspace transforming according to the irreducible representation of the symmetric group of interchanges of their arguments.

In closing I want to express my sincere gratitude to M. I. Petrashen' for a discussion of this paper.

[1] H. Weyl, Gruppentheorie und Quantenmechanik, 1931.

[2] V. A. Fock, J. Exptl. Theoret. Phys. (U.S.S.R.) **10**, 961 (1940).

[3] F. Murnaghan, The Theory of Group Representations, Baltimore, 1938.

[4] Iu. N. Demkov, J. Exptl. Theoret. Phys. JETP **35** (1958), Soviet Phys. JETP **8** (1959) (in press).

Translated by R. Lipperheide
323

THE HEAVY NEUTRAL MESON: DECAY MODES AND METHOD OF OBSERVATION

Ia. B. ZEL'DOVICH

Institute of Chemical Physics, Academy of Sciences, U.S.S.R.

Submitted to JETP editor March 9, 1958

J. Exptl. Theoret. Phys. (U.S.S.R.) **34**, 1644-1646 (June, 1958)

THE classification of the elementary particles admits the existence of a meson with strangeness 0 and isotopic spin 0 (see, e.g., the review by Okun'[1]). Such an hypothesis has been advanced repeatedly.[2,3] Evidently such a meson (let us call it ρ) must be neutral and interact strongly with nuclei; in particular, it may be produced singly in collisions of two nucleons.

We assume that the ρ meson differs from the neutral pion only in mass and isotopic spin, but that the space spin and parity of the ρ meson are the same as for the neutral pion (pseudoscalar). Let the ρ meson be equivalent to a nucleon-antinucleon pair in the state $0^S\,{}^1S_0$, whereas the neutral pion is equivalent to a pair in the state $1^S\,{}^1S_0$, $T_Z = 0$ according to the classification of Bethe and Hamilton[4] (see also reference 5). These two pair states differ by the relative phase $\overline{PP}$ and $\overline{NN}$.

In this letter we consider the possible decay modes of the ρ meson and the method of observing it in an experiment. It is obvious that the mass of the ρ meson is greater than that of the neutral pion; otherwise the ρ meson would have been discovered in experiments on neutral pion production. The transformations $\rho \to 2\pi^0$ and $\rho \to \pi^+ + \pi^-$ are not possible as they would not conserve parity: two pions in a state with $L = 0$ are an even system, whereas the ρ meson is odd.

By applying the operator CT (C is charge conjugation, i.e., conversion of particles into antiparticles; T is charge symmetry, i.e., conversion of protons into neutrons). Bethe and Hamilton have shown that three-pion annihilation cannot occur in a 0^S state. Hence the decay modes $\rho \to 3\pi^0$ and $\rho \to \pi^+ + \pi^- + \pi^0$ are forbidden. This applies to any odd number of pions.

To treat the decay into four pions, we separate them into two pairs and denote the isotopic spin of the first pair by t_1, its orbital angular momentum by l_1, the corresponding quantities of the second pair by t_2 and l_2 and the angular momentum of the center of mass of the first pair relative to the other by L. From the assumption that the ρ meson is pseudoscalar and has $T = 0$, it follows that $t_1 = t_2$, $|L| = |l_1 + l_2|$, and that $L + l_1 + l_2$ is odd. If t_1 is even, then l_1 and l_2 are even; if t_1 is odd, then l_1 and l_2 are also odd.

If $l_1 = l_2$, then both pairs can be regarded as identical bosons, and the wave function must be symmetric with respect to their exchange.

The lowest values of the momenta that satisfy all these conditions are $l_1 = l_2 = 2$, $L = 1$, $t_1 = t_2 = 0$, or $t_1 = t_2 = 2$.

For $l_1 \neq l_2$, such a state is $l_1 = 1$, $l_2 = 3$, $L = 3$, and $t_1 = t_2 = 1$. The need for large orbital momenta can reduce substantially the probability of the $\rho \to 4\pi$ decay.

The decay $\rho \to \pi^0 + \gamma$ is forbidden, since radiative $0 - 0$ transitions are forbidden. The decay $\rho \to \pi^+ + \pi^- + \gamma$ is allowed, if the pion pair is in a state with $L = 1$. Also allowed is the decay $\rho \to 2\gamma$, which is analogous to the decay $\pi^0 \to 2\gamma$. If $m_\rho > 2m_\pi$, one can expect the single photon decay to be more probable.

The expected time of decay is 10^{-18} to 10^{-20} sec.

It will be extremely difficult to identify the decay $\rho \to \pi^+ + \pi^- + \gamma$ in the presence of photon background from the $\pi^0 \to 2\gamma$ decay.

We propose below a method for detecting events of single production of ρ mesons in interactions of charged particles by energy-momentum balance. Consider the reaction $p_1 + p_2 \to p_3 + p_4 + \rho$, where

p_1 is a proton from the accelerator, p_2 is a proton at rest, and p_3 and p_4 are also protons.

This process is followed by the decay of the ρ meson, but we do not record the decay products. The energies and momenta of the protons p_1, p_3, and p_4 must be measured with great accuracy. Let us form the expression

$$A = [(E_1 + Mc^2 - E_3 - E_4)^2 - c^2(\mathbf{p}_1 - \mathbf{p}_3 - \mathbf{p}_4)^2].$$

For single production of ρ mesons we have $A = m_\rho^2 c^4$. In the case of an arbitrary process with production of two or more pions, we have a continuous spectrum of A values.

If it is observed in an experiment that there is a sufficiently narrow line (whose width must correspond to the accuracy of measurement of the magnitudes and directions of p_3 and p_4) in the distribution of A, the existence of a neutral meson with a strong nuclear interaction will have been demonstrated and its mass will have been determined.

I am grateful to V. B. Berestetskii and L. B. Okun' for their valuable advice.

[1] L. B. Okun', Usp. Fiz. Nauk **61**, 535 (1957).
[2] E. Teller, Science News Letter **71**, 195 (1957).
[3] L. B. Okun', J. Exptl. Theoret. Phys. (U.S.S.R.) **34**, 469 (1958), Soviet Phys. JETP **7**, 322 (1958).
[4] H. A. Bethe and J. Hamilton, Nuovo cimento **4**, 1 (1956).
[5] T. D. Lee and C. N. Yang, Nuovo cimento **3**, 749 (1956).

Translated by J. Heberle
324

INTERACTION OF A MEDIUM WITH A CURRENT INCIDENT ON IT

V. N. TSYTOVICH

Moscow State University

Submitted to JETP editor March 10, 1958

J. Exptl. Theoret. Phys. (U.S.S.R.) **34**, 1646-1648 (June, 1958)

In the present note we analyze the interaction of a constant, straight current of strength I with a medium occupying the half-space $x \leq 0$ and described by arbitrary μ $\epsilon(\omega)$. The current is parallel to the dividing boundary and moves onto the medium with a velocity v which is perpendicular to the dividing boundary. Morozov[1] considered the interaction for the motion along a metal.

The force acting upon a unit current length is of the form

$$F_x = \frac{2I^2}{c^2\sqrt{1-\beta^2}} \int_0^\infty e^{-2kr} \frac{\zeta(-ikv)-\mu}{\zeta(-ikv)+\mu} dk, \tag{1}$$

$$r = -vt, \quad \zeta(-ikv) = \zeta(\omega)|_{\omega=-ikv};$$

$$\mathrm{Re}\,\zeta > 0, \quad \mathrm{Im}\,\zeta(-i\omega) = 0, \tag{2}$$

$$\zeta = \sqrt{1+\beta^2(\varepsilon(\omega)\mu - 1)}.$$

Expression (1) can be obtained, for instance, by applying the image method to the separate terms of a plane-wave expansion of the potential, taking it into account that the only singularities of the expressions under the integral sign are the poles ϵ and $1/\epsilon$ which lie in the upper half-plane of complex ω (see references 2 and 3; the time factor here is $e^{i\omega t}$).

For a dispersionless medium we get

$$F_x = -\frac{I^2}{c^2\sqrt{1-\beta^2}} \frac{\mu - \sqrt{1+(\varepsilon\mu-1)\beta^2}}{\mu + \sqrt{1+(\varepsilon\mu-1)\beta^2}} \frac{1}{r}. \tag{3}$$

For $\beta^2 > (\mu^2 - 1)/(\epsilon\mu - 1)$ the attraction changes into repulsion. For sufficiently small r, expression (3) is, of course, inapplicable since dispersion becomes important (from dimensional considerations, the order of magnitude of the excited frequencies is $\omega \sim v/r$).

If ζ is expanded in terms of $(\epsilon - 1)\beta^2$, and if we put $(\mu = 1, \ \beta^2 \ll 1)$

$$\varepsilon = 1 + \frac{4\pi n e^2}{m} \sum_k \frac{f_k}{\omega_k^2 - \omega^2 + i\gamma_k\omega}, \tag{4}$$

we find

$$F_x^k = \frac{\pi n e^2 \beta}{mc^3 i\omega_k'} \{e^{-\alpha\eta_k + i\alpha}\,\mathrm{Ei}(-\alpha\eta_k - i\alpha)$$

$$- e^{-\alpha\eta_k - i\alpha}\,\mathrm{Ei}(-\alpha\eta_k + i\alpha)\}, \tag{5}$$

where Ei is the exponential integral, and

$$F_x = \sum_k f_k F_x^k; \quad \omega_k' = \sqrt{\omega_k^2 - \gamma_k^2/4};$$

$$\eta_k = \gamma_k/2\omega_k'; \quad \alpha = 2\omega_k' r/v. \tag{6}$$

For $r \gg v/\omega_k$, from (5), in particular, we get in accordance with (3)

$$F_x = \frac{\varepsilon(0)-1}{4} \beta^2 \frac{I^2}{c^2} \frac{1}{r}, \tag{7}$$

and for $r \ll v/\omega_k$ we have

$$F_x^k = \pi^2 I^2 n e^2 \beta / mc^3 \omega_k'. \quad (8)$$

If a current moves onto a plasma or a metal, such an expansion is impossible, since we must assume

$$\varepsilon = 1 - \omega_0^2/(\omega^2 - i\gamma\omega); \quad \gamma = \omega_0^2/4\pi\sigma;$$

$$\omega_0^2 = 4\pi n e^2/m; \quad \mu = 1, \quad (9)$$

where σ is the electrical conductivity for $\omega = 0$. In that case it is necessary to evaluate expression (3) more accurately, retaining the radical under the integral sign. We shall give the results for particular cases. If $r \gg c/\omega_0$ and $\beta \gg (\gamma/\omega_0) \times (c/\omega_0 r)$, we have*

$$F_x = I^2/c^2 r\sqrt{1-\beta^2}. \quad (10)$$

If the conditions $r \gg c/\omega_0$ and $\beta \ll (\gamma/\omega_0) \times (c/\omega_0 r')$ are satisfied, we get

$$F_x = \frac{2\pi I^2 \beta}{c^3\sqrt{1-\beta^2}}\,\sigma \ln \frac{1.356\,c}{8\pi\sigma\beta r}. \quad (11)$$

For $r \ll c/\omega_0$ and $\beta \geq \gamma/2\omega_0$ the evaluation of the integral (3) gives

$$F_x = \frac{I^2\omega_0}{3c^3\sqrt{1-\beta^2}}\{\eta^2 K(\sqrt{1-\eta^2/4}) + 2(2-\eta^2)E(\sqrt{1-\eta^2/4}) + \eta(\eta^2-3)\}, \quad (12)$$

where K and E are the complete elliptic integrals. In the particular case $\beta \gg \gamma/2\omega_0$, we expand (12) in powers of $\eta = \gamma/\omega_0\beta$,

$$F_x = (4I^2/3c^2\sqrt{1-\beta^2})\,\omega_0/c. \quad (13)$$

If $r \ll c/\omega_0$ and $\beta \leq \gamma/2\omega_0$, we get the following result

$$F_x = \frac{2I^2\omega_0}{c^3\sqrt{1-\beta^2}}\left\{-\frac{1}{6}\eta + \frac{2}{3\sqrt{|z_1|}}F(\varphi, k) - \frac{1}{3}\frac{(2-\eta^2)|z_2|}{\sqrt{|z_1|}}\left[\frac{\sqrt{k'^2+|z_2|}\,k'^{-2}}{\sqrt{|z_2|(1+|z_2|)}} - k'^{-2}E(\varphi, k)\right]\right\}, \quad (14)$$

where $E(\varphi, k)$ and $F(\varphi, k)$ are incomplete elliptic integrals, and

$$k^2 = (z_1 - z_2)/z_1; \quad k'^2 = 1 - k^2;$$

$$\tan^2\varphi = 1/|z_2|; \quad \eta = \gamma/\omega_0\beta; \quad (15)$$

$$z_1 = 1 - \frac{\eta^2}{2} - \frac{\eta^2}{2}\sqrt{1-4/\eta^2};$$

$$z_2 = 1 - \frac{\eta^2}{2} + \frac{\eta^2}{2}\sqrt{1-4/\eta^2}. \quad (16)$$

The expansion of (14) for $\beta \ll \gamma/\omega_0$ gives

$$F_x = \frac{20\pi I^2\beta\sigma}{3c^3\sqrt{1-\beta^2}} \ln \frac{1.492\,\omega_0}{2\pi\sigma\beta}. \quad (17)$$

I express my sincere gratitude to M. S. Rabinovich, M. L. Levin, and L. M. Kovrizhnyi for discussing the results of this paper.

*The second condition is in fact equivalent to $r \gg \delta$, where δ is the skin depth for a frequency v/r.

[1] A. I. Morozov, J. Exptl. Theoret. Phys. (U.S.S.R.) **31**, 1079 (1956), Soviet Phys. JETP **4**, 920 (1957).

[2] N. Bohr, The Passage of Atomic Particles Through Matter (Russ. Transl.) IIL, 1950, p. 145. Note from the editor of the translation.

[3] L. D. Landau add E. M. Lifshitz, Электродинамика сплошных сред (Electrodynamics of Continuous Media), M., Gostekhizdat, 1957.

Translated by D. ter Haar
325

ENERGY DEPENDENCE OF THE REACTION CROSS SECTIONS FOR SLOW NEUTRONS

F. L. SHAPIRO

P. N. Lebedev Physics Institute, Academy of Sciences, U.S.S.R.

Submitted to JETP editor March 12, 1958

J. Exptl. Theoret. Phys. (U.S.S.R.) **34**, 1648-1649 (June, 1958)

IT follows from very general assumptions that the reaction cross section for low-energy neutrons is proportional to $E^{-1/2}$ (cf., e.g., reference 1):

$$\sigma_r = (\sigma_r E^{1/2})_0 E^{-1/2}, \quad (1)$$

where the index 0 denotes evaluation at the neutron energy $E = 0$. Expression (1) is essentially the first term in the series

$$\sigma_r = (\sigma_r E^{1/2})_0 (E^{-1/2} - \alpha + \gamma E^{1/2} + \cdots). \quad (2)$$

The aim of the present paper is to show that the assumptions leading to the 1/v law also determine the quantity α in (2). The effective reaction cross section can be expressed through the logarithmic derivative of the wave function of the incoming particle at the nuclear boundary (f_0). In the notations of Blatt and Weisskopf[1] the reaction cross section for s neutrons incident on a nucleus with spin zero is equal to

$$\sigma_r = \frac{-4\pi R \operatorname{Im} f_0}{(\operatorname{Re} f_0)^2 + (\operatorname{Im} f_0 - kR)^2} \frac{1}{k}. \quad (3)$$

Expanding f_0 in a power series in k, we obtain only even powers of k:

$$f_0 = (\operatorname{Re} f_0)_0 (1 + ak^2 + \cdots) + i (\operatorname{Im} f_0)_0 (1 + bk^2 + \cdots). \quad (4)$$

Qualitatively this follows from the fact that f_0 is determined by the neutron state inside the nucleus (for $r \leq R$), which can approximately be characterized by the wave number $K = (K_0^2 + k^2)^{1/2}$, where $K_0^2 \gg k^2$. If the effect of the nucleus on the neutron can be described by an operator V that satisfies the condition

$$\int_0^\infty [\psi(r) V\varphi(r) - \varphi(r) V\psi(r)]\, dr = 0$$

[e.g., a complex potential $V = U(r) + iW(r)$], then one can prove (4) rigorously, following, e.g., Bethe.[2] Substituting (4) into (3) and using

$$k^2 = 2mE\hbar^{-2}(A/(A+1))^2, \quad (5)$$

where E is the neutron energy in the laboratory system, m is the mass of the neutron, and A the mass number of the target nucleus, we obtain

$$(\sigma_r E^{1/2})_0 / \sigma_r E^{1/2} = 1 + \alpha E^{1/2} + \beta E + \cdots, \quad (6)$$

where

$$\alpha = \alpha_0 = \frac{m}{\pi\hbar^2}\left(\frac{A}{A+1}\right)^2 (\sigma_r E^{1/2})_0. \quad (7)$$

Expressions (6) and (2) are equivalent. For a nucleus with spin $i \neq 0$, the expansions (2) and (6) remain unchanged, but instead of (7) the relation between α and α_0 is

$$\alpha = \alpha_0 [x_-^2 / g_- + (1 - x_-)^2 / (1 - g_-)], \quad (8)$$

where $g_- = i/(2i+1)$ is the statistical weight of the reaction channel with spin $J = i - \frac{1}{2}$, and x_- is the relative contribution of this channel to the thermal cross section. The value of α goes through a minimum $\alpha_{min} = \alpha_0$ at $x_- = g_-$. Expressions (6) to (8) have been previously obtained[3] from the Breit-Wigner formula for an isolated level. Actually, as is clear from the foregoing considerations, the validity of these relations is not restricted to the range of applicability of the single-term Breit-Wigner formula, nor to the applicability of the concepts of the compound nucleus.

If the reaction induced by a slow neutron has only one open channel for a given channel spin then, using the reciprocity theorem, one can obtain from (6) an expression for the cross section of the reverse reaction close to its threshold:

$$(\sigma_{rev} E_n^{-1/2})_0 / \sigma_{rev} E_n^{-1/2} = 1 + \alpha \frac{A+1}{A} E_n^{1/2} + \beta_1 E_n + \cdots, \quad (9)$$

where E_n is the kinetic energy of the emitted neutron in the center-of-mass system, and α is given by (7) and (8) if the statistical weights of the entrance and exit channels are identical.

The term $\alpha E^{1/2}$ in (6) can be noticed in experiment if the thermal reaction cross section is very large, but the coefficient β is small. This last condition is fulfilled if there are no narrow resonance levels for small neutron energies. In reference 3 the α term appears in the expression for the energy dependence of the reaction cross sections for the processes $He^3(n,p)$ and $B^{10}(n,\alpha)$. A value $\alpha = 4.1 \times 10^{-2}$ kev$^{-1/2}$ was found for the first reaction. Comparing (7) and (8), it appears that for low energies the reaction goes essentially through the channel $J = 0$. The cross section for the reaction $Li^7(p,n)$, measured in reference 4, agrees near the threshold with (9) if $\alpha \approx 0.21$. From this and from the value for $(\sigma E^{1/2})_0$ there follow two possibilities for the spin of the channel: (1) $x_- = 0$, $x_+ = 1$ and (2) $x_- = 0.75$, $x_+ = 0.25$. The mere presence of the α term in the expression for the reaction cross section does not yet tell anything about the resonance levels of the compound nucleus. However, the fact that the reaction has a very large cross section and goes essentially through one of two possible channels, as in the reaction $He^3(n,p)$, supports the argument in favor of the presence of the level.

[1] J. Blatt and V. Weisskopf, Theoretical Nuclear Physics, Wiley, N. Y., 1952.

[2] H. A. Bethe, Phys. Rev. **76**, 38 (1949).

[3] Bergman, Isakov, Popov, and Shapiro, J. Exptl. Theoret. Phys. (U.S.S.R.) **33**, 9 (1957); Soviet Phys. JETP **6**, 6 (1958). Proc. of the Columbia Conference on Neutron Interactions, 1957 (in press). Proc. of the Moscow Conference on Nuclear Reactions, 1957 (in press).

[4] R. L. Macklin and J. H. Gibbons, Phys. Rev. **109**, 105 (1958).

Translated by R. Lipperheide
326

APPROXIMATIONS OF THE THOMAS-FERMI FUNCTION

F. G. SANNIKOV

P. N. Lebedev Physics Institute, Academy of Sciences, U.S.S.R.

Received by JETP editor March 13, 1958

J. Exptl. Theoret. Phys. (U.S.S.R.) **34**, 1650-1651 (June, 1958)

NUMEROUS articles have appeared recently (see reference 1, for example) concerning approximations to the solution of the Thomas-Fermi equation[2] for a free neutral atom:

$$\varphi'' = \varphi^{3/2}/\xi^{1/2}. \tag{1}$$

Here $\xi = r/\mu$, r is the distance from the center of the atom, $\mu = \nu a_0/Z^{1/3}$, a_0 is the Bohr radius, and $\nu = 0.8853$.

As a measure of the accuracy of an approximate solution, Umeda[3] has suggested using the numerical solution of an integral whose variation gives Eq. (1):

$$I(\varphi) = \int_0^\infty [\varphi'^2 + (1/5)\varphi^{3/2}\xi^{-1/2}]\, d\xi. \tag{2}$$

This functional has a minimum value[4] of 1.3612 when φ is an exact solution of (1). The deviation of I from the minimum value can serve as an estimate of the degree of accuracy of the approximate solution. Thus for Sommerfeld's approximation[5] $\varphi = [1 + (\xi/12^{2/3})^\lambda]^{-3/\lambda}$, I = 1.3670; for Kerner's form $\varphi = [1 + \lambda\xi]^{-1}$, I = 1.3679; for Tietz's solution $\varphi = [1 + \lambda\xi]^{-2}$, I = 1.3662; and for Rosenthal's solution[6] $\varphi = 0.7345e^{-0.562\xi} + 0.2655e^{-3.392\xi}$, I = 1.3636.

We can write φ in a new form for which I = 3.624, which is much closer to the minimum value:

$$\varphi(\xi) = e^{-x^{1/2}}(1 + {}^1/_2 x^{1/2})^2. \tag{3}$$

Here and hereinafter $x = \lambda\xi$, where λ is a parameter which can be determined in different ways. $\lambda = \lambda_{Um} = 6.119$ is determined by Umeda's method from the condition $\partial I/\partial\lambda = 0$.

Equation (3) can be derived by making the transition from the Lenz-Jensen approximate expression $\rho(r)$ for electron density in an atom to the function $\varphi(\xi)$. For this purpose let us consider the following relation between $\rho(r)$ and $\varphi(\xi)$:

$$\rho_I(r) = (Z/4\pi\mu^3)\varphi''/\xi, \tag{4}$$

$$\rho_{II}(r) = (Z/4\pi\mu^3)(\varphi/\xi)^{3/2}. \tag{4a}$$

When φ is an exact solution of (1), ρ_I and ρ_{II} will of course coincide. When φ is approximate, (4a) must be used because the function itself is a better approximation than its second derivative. But (4a) does not generally satisfy the normalization condition $\int_0^\infty \rho 4\pi r^2\, dr = Z$ for approximate φ and arbitrary λ. Therefore instead of ρ_{II} we must take

$$\rho = \rho_{II}(\lambda/\lambda_{Ma})^{3/2}, \tag{4b}$$

where λ_{Ma} is determined by the mean value method:

$$\int_0^\infty (\varphi'' - \varphi^{3/2}/\xi^{1/2})\,\xi d\xi = 0,$$

which has been proposed by March.[1,7] The transformation (4b) insures normalization of ρ for arbitrary λ as well as fulfillment of the virial theorem $2H_k + H_p = 0$. The advantage of (4a) and (4b) over (4) now also follows from energy considerations. Thus using Tietz's simple and convenient approximation of φ, (4) gives for the total energy of an atom by the Ritz method[2] $H = -0.660$ in the units $Z^{7/3}e^2/a_0$, whereas from (4a) and (4b) we obtain $H = -0.768$, which is much closer to the exact value $H = -0.769$. The value of ρ obtained from (4a) and (4b), with $\lambda = \lambda_{Ri}$ as determined by the Ritz method from $\partial H/\partial\lambda = 0$, may be regarded as the approximation that corresponds to a given approximate φ. For example, from Tietz's form ($\lambda_{Ma} = (\pi/8)^{2/3} = 0.536$), we obtain an expression which insures normalization and fulfillment of the virial theorem, and also gives a good value for the energy:

$$\rho_{TI} = \frac{Z}{4\pi\mu^3}\frac{8\lambda^3}{\pi}x^{-3/2}(1+x)^{-3}, \tag{5}$$

where $\lambda = \lambda_{Ri} = 0.527$.

On the other hand, let us start with the well-known Lenz-Jensen approximation[8] for ρ:

$$\rho_{LJ} = \frac{Z}{4\pi\mu^3}\frac{\lambda^3}{4P}x^{-3/2}\exp(-x^{1/2})(1 + Cx^{1/2})^3 \tag{6}$$

and pass in reverse to φ using (4a) and (4b) [$\lambda_{Ma} = (4P)^{2/3}$]. Letting $C = 1/3$, we then obtain (3), where λ differs from the λ of (6) by the factor $4/9$. The selection of $C = 1/3$, which differs somewhat from Jensen's value $C = 0.265$, is required to improve the form of φ at zero [$\varphi'(0) = -1.530$ instead of $\varphi'(0) = -\infty$ with the exact solution $\varphi'(0) = -1.588$]. When $C = 1/3$, $\lambda_{Ri} = 11.41$ and $H = -0.76$ [for comparison $\lambda_{Ma} = 11.87$ and $\lambda_{Um} = (9/4)6.12 = 13.77$]. The form (3) which has been obtained is quite simple and convenient. In the principal range of variation, $0 < \xi < 1$, the

value of φ obtained from (3) differs on the average from the exact solution obtained numerically in reference 9 by less than 0.5%, and never differs by more than 1%. In the same region, φ' differs by less than 2.5% on the average and by not more than 5% from the exact value of φ'.

In conclusion it should be noted that any attempt to derive an extremely accurate approximation of the Thomas-Fermi function at small and at large distances from the nucleus is devoid of meaning, for there Eq. (1) does not correctly indicate the potential in the atom.

I am indebted to D. A. Kirzhnits for suggestions and discussions.

[1] N. H. March, Proc. Cambridge Phil. Soc. **46**, 365 (1950); E. H. Kerner, Phys. Rev. **83**, 71 (1951); H. C. Brinkman, Physica **20**, 44 (1954); T. Tietz, Ann. Physik **15**, 186 (1955), Nuovo cimento 1, 955 (1955); H. A. Buchdahl, Ann. Physik **17**, 238 (1956).

[2] P. Gombas, Die statistische Theorie des Atoms und ihre Anwendungen, Springer-Wien, 1949.

[3] K. Umeda, J. Phys. Soc. Japan **9**, 290 (1954).

[4] K. Umeda and S. Kobayashi, J. Phys. Soc. Japan **10**, 749 (1955).

[5] A. Sommerfeld, Z. Physik **78**, 283 (1935).

[6] S. Rosenthal, Z. Physik **98**, 742 (1935).

[7] C. A. Coulson and N. H. March, Proc. Phys. Soc. (London) **A63**, 367 (1950).

[8] W. Lenz, Z. Physik **77**, 713 (1932); H. Jensen, Z. Physik **77**, 722 (1932).

[9] Kobayashi, Matsukuma, Nagai, and Umeda, J. Phys. Soc. Japan **10**, 759 (1955).

Translated by I. Emin
327

PRODUCTION OF A STAR AND A FAST PROTON OR ANTIPROTON

A. S. BUSHEV and Iu. A. VDOVIN

Moscow Institute of Engineering and Physics

Submitted to JETP editor March 27, 1958

J. Exptl. Theoret. Phys. (U.S.S.R.) **34**, 1652-1653 (June, 1958)

THE production of a star by a γ-quantum through an intermediate π-meson pair was investigated in reference 1. In the present work we consider an analogous process: a high-energy γ-quantum produces a proton-antiproton pair one particle of which is absorbed in the nucleus, producing a star. The other particle carries away energy of the order of the energy of the star. The study is carried out for the ultra-relativistic region where only small angles between the momentum of the γ-quantum and that of the emitted proton (or antiproton) are of importance. The strong interaction between the proton (and antiproton) and the nucleus is accounted for by using the optical model. The nucleus is regarded as an ideal black body of a given radius, as far as the proton and antiproton are concerned.

We shall assume that the behavior of nucleons is described by Dirac's equation. The anomalous magnetic moment of the nucleon is not of great importance for such high energies. Let us assume, for example, that the proton is absorbed and the antiproton is emitted to an infinite distance. Dirac's equation for such a process can be written as follows: ($\hbar = c = 1$)

$$(\gamma\nabla - \gamma_4 E_1 + m)\,\psi_{p_1}(\mathbf{r}) = \frac{ie}{\sqrt{2\omega}}(\gamma\mathbf{e})\,e^{i\mathbf{kr}}\psi^{(-)}_{p_2}(\mathbf{r}). \qquad (1)$$

where $\mathbf{p}, E_1(\mathbf{p}_2, E_2)$ are the momentum and energy of the proton (or antiproton). We shall denote the momentum of a γ-quantum of frequency ω by $\mathbf{k}$, and its polarization vector by $\mathbf{e}$. The wave function of the antiproton, which is a free particle in its final state, is a superposition of a plane wave and of a wave diffracted on the black nucleus.[2]

We find the wave function ψ_{p_1} of the proton by means of the Green's function[3] of Eq. (1), under the condition that the antiproton is at infinity. We obtain the cross section for the process by calculating the total flux of protons incident upon the nucleus:

$$d\sigma = \int j(\mathbf{s}_1)\,d\mathbf{s}_1\,|F|^2\,dp_2\,d\mathbf{k}_2/(2\pi)^3;$$
$$j(\mathbf{s}_1) = (\psi_{p_1}(\mathbf{s}_1)\,\frac{i\gamma\mathbf{p}_1}{p_1}\,\psi_{p_1}(\mathbf{s}_1)),$$

where $\mathbf{k}_2$ is the transverse momentum of the emitted antiproton and F is in the nature of a nucleon form-factor.[4] Integration over $\mathbf{s}_1(\mathbf{s}_2)$ is carried out along a circle with radius R, perpendicular to $\mathbf{p}_1(\mathbf{p}_2)$ and passing through the center of the nucleus.

We obtain the following expression for the differential cross-section of the process, averaged over possible polarization of the γ-quantum:

$$d\sigma(E_2, \boldsymbol{\eta}) = \frac{e^2}{\omega^3}\,\frac{|F|^2 R}{(2\pi)^3 m}\,\{[E_2^2 + (\omega - E_2)^2]\,K(\varepsilon) + E_2(\omega - E_2)\,E(\varepsilon)\}\,\frac{dE_2 d\eta}{(1+\eta^2)^{3/2}}; \qquad (2)$$

$$\boldsymbol{\eta} = \mathbf{k}_2/m, \quad \varepsilon^2 = \eta^2/(1+\eta^2), \quad d\boldsymbol{\eta} = \eta d\eta d\varphi_\eta,$$

where $K(\epsilon)$ and $E(\epsilon)$ are complete elliptic in-

tegrals of the first and second kind respectively. It can be seen from Eq. (2) that $\eta_{\text{eff}} \sim 1$, i.e. $\vartheta_{\text{eff}} \sim m/E_2$. The form-factor F can be determined from comparison with experiment. At high energies, the differential cross section for small angles attains large values.

Integration over E_2 and η can be carried out only for $F = 1$. We have then

$$\sigma = (e^2/24\pi^2)(R/m)\,\Phi(\eta_{\max}),$$

$$\Phi(\eta_{\max}) = \int_0^{\eta_{\max}} \left\{4K\left(\frac{\eta}{\sqrt{1+\eta^2}}\right) + E\left(\frac{\eta}{\sqrt{1+\eta^2}}\right)\right\} \frac{\eta d\eta}{(1+\eta^2)^{3/2}}. \quad (3)$$

If we put $\eta_{\max} = \infty$ (in general, $\eta_{\max}$ should be of the order of unity) we have $\Phi(\infty) = 9\pi^2/8$, $\sigma \sim 10^{-28}\,\text{cm}^2$. As in the scalar case,[1] the total cross section is independent of the γ-quantum energy and is proportional to R/m and not to R^2, since in the effective region for the process, that ahead of the nucleus, the ψ-function of the emitted particle has a shadow and the whole process is determined by the penumbra region.

Equation (2) has been obtained under the assumption that the nuclear radii (R_1 with respect to protons and R_2 with respect to antiprotons) are equal, $R_1 = R_2 = R$. The cross section for the process is then independent of which particle, the proton or the antiproton, is free in the final state. If $R_1 \neq R_2$, and $\Delta R \gg 1/m$, then the cross section for the process with emission of the more strongly interacting particle is, in the given approximation, exponentially small ($\sim \exp(-\alpha\Delta R)$, $\alpha \sim m$). The cross section for the process with emission of the less strongly interacting particle (the proton) can be obtained from Eq. (2) by replacing R with $2R_1$ for $R_1 > R_2$ (or with $2R_2$ for $R_2 < R_1$).

[1] Iu. A. Vdovin, J. Exptl. Theoret. Phys. (U.S.S.R.) **30**, 782 (1956), Soviet Phys. JETP **3**, 755 (1956).

[2] Iu. A. Vdovin, J. Exptl. Theoret. Phys. (U.S.S.R.) **32**, 542 (1957), Soviet Phys. JETP **5**, 452 (1957).

[3] A. I. Akhiezer, Dokl. Akad. Nauk SSSR **94**, 651 (1954).

[4] I. Ia. Pomeranchuk, Dokl. Akad. Nauk SSSR **96**, 265, 481 (1954).

Translated by H. Kasha
328

OVERHAUSER EFFECT IN NONMETALS

G. R. KHUTSISHVILI

Tbilisi State University

Submitted to JETP editor March 26, 1958

J. Exptl. Theoret. Phys. (U.S.S.R.) **34**, 1653-1654 (June, 1958)

RECENTLY a number of papers[1-4] have appeared in which different modifications of the Overhauser method are proposed to obtain nuclear polarization in nonmetals. In particular, these papers discuss the polarization of the nuclei of paramagnetic atoms in salts and of the nuclei of donor and acceptor impurities in silicon and germanium. The problem is mainly to obtain a nonequilibrium nuclear polarization thanks to the fast passage effect. In the present paper we shall be concerned with obtaining a stationary nuclear polarization.

Let us consider a system consisting of a nucleus of spin I and an electron located in a magnetic field of strength H. The system will have $2(2I+1)$ levels corresponding to two values of the electron spin component (M), and $2I+1$ values of the nuclear spin component (m). Assuming the external field to be sufficiently strong (Zeeman energy of the electron considerably larger than the spin-spin interaction energy of the electron with the nucleus) we get $2I+1$ transitions in the paramagnetic-resonance spectrum (selection rules: $\Delta M = \pm 1$, $\Delta m = 0$). To evaluate the population of the levels, we neglect the spin-spin interaction energy and the Zeeman energy of the nuclear spin, and we obtain $2I+1$ pairs of levels with an energy level difference in each pair equal to $2\beta H$ (see figure).

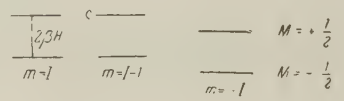

We consider the most important case, where we can neglect for the nuclear spin all interactions except the contact interaction, which is proportional to $(\mathbf{S}\cdot\mathbf{I})\delta(\mathbf{r})$. In that case we have, for the relaxation processes involving the nuclear spin, the selection rule $\Delta(M+m) = 0$.

Let complete saturation be reached (that is, let the saturation parameter be equal to unity) for all $2I+1$ paramagnetic resonance levels. We get then Overhauser's known result, i.e., the degree of polarization is equal to

$$f = B_I(2I\delta),\ \delta = \beta H/kT, \quad (1)$$

where B_I is the Brillouin function. In other words, we have the result that the effective nuclear gyromagnetic ratio is equal to the electronic gyromagnetic ratio.

In the case of nonmetals, however, we have a developed hyperfine structure of the paramagnetic resonance, and it is difficult to saturate all its components. Simple calculation shows that upon total saturation of the hyperfine structure components corresponding to a nuclear spin component equal to m, we get for the nuclear polarization

$$f = \frac{[I(I+1) - m^2](e^{2\delta} - e^{-2\delta}) - m(e^{\delta} - e^{-\delta})^2}{2I[2(I+1) + (I-m)e^{2\delta} + (I+m)e^{-2\delta}]}. \quad (2)$$

In particular, we have for $\delta \ll 1$

$$f = \frac{I(I+1) - m^2}{I(2I+1)}\delta, \quad (3)$$

and for $\delta \gg 1$

$$f = (I+1+m)/2I, \qquad \text{if } m \neq I,$$

$$f = 1/2(I+1), \qquad \text{if } m = I. \quad (4)$$

We see thus that for small δ it is more advantageous to saturate the lines with $m = 0$ or $m = \pm\frac{1}{2}$ (depending on whether I is integral or half-integral) to obtain the largest f. In the case of large δ it is advantageous to saturate the line with $m = I - 1$. In particular, in the latter case we get $f \approx 1$ for $\delta \gg 1$, as can easily be understood (practically only the level $M = -\frac{1}{2}$, $m = I$ will be occupied).

Experimentally the magnitude of the nuclear polarization can be measured from the intensity of the unsaturated paramagnetic resonance lines, from the intensity of the nuclear magnetic resonance lines (transitions $\Delta M = 0$, $\Delta m = \pm 1$), or, in the case of the polarization of radioactive nuclei, from the angular anisotropy of the γ-radiation.

[1] G. Feher, Phys. Rev. **103**, 500 (1956); G. Feher and E. A. Gere, Phys. Rev. **103**, 501 (1956).

[2] A. Abragam and J. Combrisson, Nuovo cimento Suppl. **6**, 1197 (1957).

[3] C. D. Jeffries, Phys. Rev. **106**, 164 (1957).

[4] Pines, Bardeen, and Slichter, Phys. Rev., **106**, 489 (1957).

Translated by D. ter Haar
329

MEAN FREE PATH OF ELECTRONS IN HIGH-PURITY TIN

B. N. ALEXANDROV and B. I. VERKIN

Physico-Technical Institute, Academy of Sciences, Ukrainian S.S.R.

Submitted to JETP editor March 26, 1958

J. Exptl. Theoret. Phys. (U.S.S.R.) **34**, 1655-1656 (June, 1958)

THE production of many pure metals has been made possible by to the development of the method of multiple zone crystallization ingots.[1] Thus, multiple zone crystallization of tin ingots[2] combined with prolonged high-temperature heating of this metal in high vacuum[3] has yielded tin of very high purity.

The purification of the tin was controlled by measuring the residual resistance $\delta = R_{4.2}/R_{room}$ of samples taken from different sections of the thoroughly heated and re-crystallized ingot. (Here $R_{4.2}$ is the resistance of the sample at 4.2°K and R_{room} — its resistance at room temperature.) While working with high-purity tin, $R_{4.2}$ was found to depend on the cylindrical-sample, wire diameter, owing to the fact that this diameter became commensurate with the electron mean free path.

Figure 1 A presents δ as a function of the cylindrical-wire diameter for tin with $\delta_\infty = 1.8 \times 10^{-5}$.

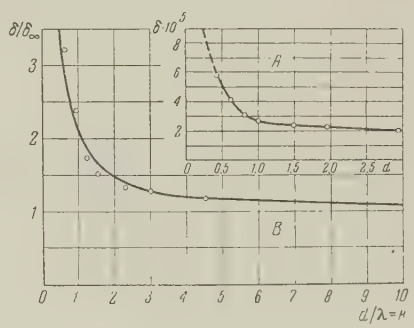

FIG. 1. A — Variation of residual resistance of tin with $\delta_\infty = 1.8 \cdot 10^{-5}$ with the diameter of the cylindrical wires. B — theoretical curve[4] of δ/δ_∞ as a function of $k = d/\lambda$ for $p = 0$; d — diameter of the cylindrical wires, λ — electron mean free path, o — experimental data for $\lambda = 0.65$ mm.

It is known that the investigation of the electric resistances of thin films and metal wires is the oldest method of determining the electron mean free path in these materials. This problem was theoretically investigated for cylindrical wires by Dingle.[4] His work contains a table of σ_∞/σ for arbitrary k, along with the formulas

$$\frac{\sigma_\infty}{\sigma} = 1 + \frac{3}{4}\frac{1-p}{k} \quad (k \gg 1),$$

$$\frac{\sigma_\infty}{\sigma} = \frac{1-p}{1+p}\frac{1}{k} \quad (k \ll 1) \qquad (1)$$

(where $k = d/\lambda$, d is the wire diameter σ_∞ the conductivity of the bulk metal, and p the probability that the electron scatters elastically). The curve of Fig. 1B displays this function graphically for $p = 0$. The dots represent the experimental values. They fit the theoretical curve best when $\lambda = 0.65$ mm.

It is known that

$$\sigma_\infty/\lambda = 1/\rho_\infty\lambda = (8\pi/3)^{1/3} e^2 (n_A n)^{2/3}/h$$

$$= 7.1 \cdot 10^7 (n_A n)^{2/3}, \qquad (2)$$

where n_A is the number of electrons per unit volume, and n their number for one atom of metal. For tin at room temperature, $\rho = 1.1 \times 10^{-5}$ ohm-cm, while $\rho_\infty^{4.2} = 1.98 \times 10^{-10}$ ohm-cm. Using this value we find, according to formula (2), that at 4.2°K

$$\lambda n^{2/3} = 5.7 \cdot 10^{-2}$$

or $n \approx 0.8$. This value agrees with Borovik's[5] data, obtained for tin by experimental investigations of galvano-magnetic phenomena at low temperatures. The results of the present work, as well as data of other authors who investigated the influence of size on the electric resistivity of tin are given in a table below.

	Purity of specimens	T° K	λ, cm	$\rho\lambda \cdot 10^{11}$ ($\Omega \cdot cm^2$)	n	State of specimen
Present work	$\frac{R_{4.2}}{R_{294}} = 1.8 \cdot 10^{-5}$	4.2	$6.5 \cdot 10^{-2}$	1.3	0.8	Crystal
Andrew[6]	$\frac{R_{3.8}}{R_{291}} = 1.8 \cdot 10^{-4}$	3.8	$9.5 \cdot 10^{-3}$	2.0	0.43	Polycrystalline film
Kunzler and Renton[7]	$\frac{R_{4.2}}{R_{273}} = 3.5 \cdot 10^{-5}$	4.2	$4.5 \cdot 10^{-2}$	2.3	0.35	Crystal

All these data are in full agreement with the results obtained when investigating the anomalous skin effect in tin. Really, Chambers[8] has obtained by similar investigations of tin $\rho\lambda = 1.0 \times 10^{-11}$ Ω cm^2 and $n \approx 1.1$.

[1] W. G. Pfann, J. Metals **4**, 747-753 (1952). Alexandrov, Verkin, Lifshitz, and Stepanova, **Физика металлов и металловедение** (Phys. of Metals and Met. Res.) **2**, 105 (1956).

[2] Alexandrov, Verkin and Lazarev, **Физика металлов и металловедение** (Phys. of Metals and Met. Res.) **2**, 93 (1956).

[3] Alexandrov, Verkin and Lazarev, **Физика металлов и металловедение** (Phys. of Metals and Met. Res.) **2**, 100 (1956).

[4] R. B. Dingle, Proc. Roy. Soc. **A201**, 546-560 (1950).

[5] E. S. Borovik, Izv. Akad. Nauk SSSR, Ser. Fiz. **19**, 429-443 (1955). [Columbia Tech. Transl. **19**, 383 (1955)].

[6] E. R. Andrew, Proc. Phys. Soc. **A62**, 77-87 (1949).

[7] J. E. Kunzler and C. A. Renton, Phys. Rev. **108**, 1397 (1957).

[8] R. G. Chambers, Nature **165**, 239-240 (1950). E. H. Sondheimer, Advances in Physics **1**, 1-42 (1952).

Translated by R. K. Even
330

SCATTERING BY A SCHWARZSCHILD FIELD IN QUANTUM MECHANICS

N. V. MITSKEVICH

Moscow State University

Submitted to JETP editor March 28, 1958

J. Exptl. Theoret. Phys. (U.S.S.R.) **34**, 1656-1658 (June, 1958)

WHEN dealing with a metric which is almost Galilean, we can write

$$\mathfrak{G}^{\mu\nu} = g^{\mu\nu}\sqrt{-g} = \delta^{\mu\nu} - k\gamma^{\mu\nu}; \quad k = \sqrt{16\pi\varkappa}/c;$$
$$\delta^{00} = -\delta^{11} = -\delta^{22} = -\delta^{33} = 1. \tag{1}$$

It is then possible to expand the Lagrangians of all the fields in powers of the constant k. For the scalar (or pseudoscalar), spinor (as developed by Rumer[1]), electromagnetic, and gravitational fields these expansions are, respectively

$$\mathscr{L}_{sc} = \frac{1}{2}(\delta^{\mu\nu}\varphi_{,\mu}\varphi_{,\nu} - m^2\varphi^2)$$
$$+ \frac{k}{2}\left(\frac{1}{2}\gamma^{\nu}{}_{\nu}m^2\varphi^2 - \gamma^{\mu\nu}\varphi_{,\mu}\varphi_{,\nu}\right) + O(k^2); \tag{2}$$

$$\mathscr{L}_{sp} = \frac{i}{2}(\bar{\psi}\gamma(\alpha)\psi_{,\mu} - \bar{\psi}_{,\mu}\gamma(\alpha)\psi)\delta^{\mu}(\alpha)$$
$$+ k\left[-\frac{i}{4}(\bar{\psi}\gamma(\alpha)\psi_{,\mu} - \psi_{,\mu}\gamma(\alpha)\psi)\right. \tag{3}$$
$$\left.\times\left(-\frac{1}{2}\delta_{\omega\varepsilon}\delta^{\mu}(\alpha) + \delta^{\mu}_{\varepsilon}\delta_{\omega}(\alpha)\right) + \frac{1}{2}m\bar{\psi}\psi\delta_{\omega\varepsilon}\right]\gamma^{\omega\varepsilon} + O(k^2);$$

$$\mathscr{L}_{em} = -\frac{1}{4}F_{\mu\nu}F_{\alpha\beta}\left[\delta^{\mu\alpha}\delta^{\nu\beta}\right.$$
$$\left. + k\left(\frac{1}{2}\gamma_{\lambda}\delta^{\mu\alpha}\delta^{\nu\beta} - 2\gamma^{\mu\alpha}\delta^{\nu\beta}\right)\right] + O(k^2); \tag{4}$$

$$\mathscr{L}_g \equiv \frac{\sqrt{-g}}{k^2}R = -\frac{1}{k}\left(\gamma^{\mu\nu}_{,\mu\nu} + \frac{1}{2}\gamma_{,\mu\nu}\delta^{\mu\nu}\right) + \left(\frac{1}{2}\gamma^{\mu\nu}\gamma_{,\mu\nu}\right.$$
$$-\frac{1}{2}\gamma^{\alpha\beta}\gamma_{\alpha\beta,\mu\nu}\delta^{\mu\nu} - \frac{1}{8}\gamma_{,\mu}\gamma_{,\nu}\delta^{\mu\nu} - \frac{1}{4}\gamma^{\alpha\beta}_{,\mu}\gamma_{\alpha\beta,\nu}\delta^{\mu\nu}$$
$$+\frac{1}{2}\gamma_{,\lambda}\gamma^{\lambda\nu}_{,\nu} - \frac{1}{2}\gamma^{\rho\nu}_{,\lambda}\gamma^{\lambda}_{\nu,\rho}\Big) + k\left(\frac{1}{2}\gamma^{\mu\nu}\gamma^{\alpha\beta}\gamma_{\alpha\beta,\mu\nu}\right.$$
$$-\frac{1}{2}\gamma^{\alpha\beta}\gamma_{\beta\varepsilon}\gamma^{\varepsilon}_{\alpha,\mu\nu}\delta^{\mu\nu} + \frac{1}{8}\gamma^{\mu\nu}\gamma_{,\mu}\gamma_{,\nu} + \frac{1}{4}\gamma^{\mu\nu}\gamma^{\rho\tau}_{,\mu}\gamma_{\rho\tau,\nu} \tag{5}$$
$$-\frac{1}{2}\gamma^{\mu\nu}\gamma^{\beta}_{\mu,\lambda}\gamma^{\lambda}_{\nu,\rho} - \frac{1}{2}\gamma^{\alpha\beta}\gamma^{\lambda}_{\alpha,\mu}\gamma_{\lambda\beta,\nu}\delta^{\mu\nu}$$
$$\left.-\frac{1}{4}\gamma^{\alpha\beta}\gamma_{\alpha\beta,\mu}\gamma^{\sigma}{}_{\sigma\nu}\delta^{\mu\nu} + \frac{1}{2}\gamma^{\alpha\beta}\gamma_{\alpha\beta,\lambda}\gamma^{\lambda\nu}_{,\nu}\right) + O(k^2);$$
$$\delta^0(0) = 1, \ \delta^1(1) = \delta^2(2) = \delta^3(3) = i$$

From these expressions, it is an easy matter to obtain the cross sections for scattering of the quanta associated with these fields by a static spherically-symmetric gravitational field given by

$$\gamma^{\mu\nu}_{st} = \gamma^{\lambda}_{st\,\lambda}\delta^{\mu}_{0}\delta^{\nu}_{0}; \ \gamma^{\lambda}_{st\,\lambda} = -Mk/4\pi r. \tag{6}$$

It is clear that one of these processes, namely the scattering of a graviton by a Schwarzschild field, is entirely nonlinear. We remark that this effect is similar to the well-known Delbrück scattering effect (scattering of a photon by the Coulomb field of the nucleus), which lies at the frontier of modern experimental techniques. Graviton scattering by a Schwarzschild field, however, takes place at a lower order of perturbation theory. We shall here make use of the usual expressions for the commutation relations for all the fields involved (see, for instance, Bogoliubov and Shirkov[2]) including the gravitational,[3] since we shall be using the interaction representation (which was first used for the gravitational field by Gupta[4]). The matrix elements for our processes are

$$F_{sc}(k, k')\delta(k_0 - k_0') = -\frac{k^2M}{32\pi^2}\,\frac{m^2 - 2k_0^2}{2k_0\mathbf{k}^2}\,\frac{\delta(k_0 - k_0')}{\sin^2(\theta/2)}; \tag{7}$$

$$F_{sp}(k, k') = -\frac{k^2M}{32\pi^2}\,\frac{k_0 v_{\tau}^{+}(\mathbf{k}')\gamma(0)\bar{v}_{\sigma}^{-}(\mathbf{k})}{\mathbf{k}^2\sin^2(\theta/2)}; \tag{8}$$

$$F_{em}(k, k') = \frac{ik^2M}{32\pi^2}\,\frac{1}{k_0\sin^2(\theta/2)}\left(e_k^{\tau'}e_k^{\tau}\cos^2\frac{\theta}{2} - \frac{k_i'k_k}{2k_0^2}e_k^{\tau'}e_i^{\tau}\right); \tag{9}$$

$$F_g(k, k') = \frac{ik^2M}{128\pi^2}\,\frac{1}{k_0\sin^2(\theta/2)}$$
$$\times\left[\left(1 - 2\sin^2\frac{\theta}{2}\right)\delta_{\mu\alpha}\delta_{\nu\beta} - \frac{1}{2}\delta_{\mu\nu}\delta_{\varkappa\beta}\right] \tag{10}$$
$$\times e_{\sigma}^{\alpha}e_{\tau}^{\beta}e_{\sigma'}^{\mu}e_{\tau'}^{\nu}\delta_{\omega\varepsilon,\sigma\tau}\delta_{\omega'\varepsilon',\sigma'\tau'}; \quad \delta_{\omega\varepsilon,\sigma\tau} = \delta_{\omega\varepsilon}\delta_{\sigma\tau} - \delta_{\omega\sigma}\delta_{\varepsilon\tau} - \delta_{\omega\tau}\delta_{\varepsilon\sigma},$$

and from these, after the usual summation and averaging over polarizations of the particles involved, we obtain the differential cross sections

$$d\sigma_{sc} = \frac{k^4M^2}{(16\pi)^2}\left(\frac{k_0^2 - m^2/2}{\mathbf{k}^2}\right)^2\frac{d\Omega}{\sin^4(\theta/2)};$$

$$d\sigma_{sp} = \frac{k^4M^2}{(16\pi)^2}\left(\frac{k_0^2}{\mathbf{k}^2}\right)^2\frac{d\Omega}{\sin^4(\theta/2)}; \tag{11}$$

$$d\sigma_{em} = \frac{k^4M^2}{(16\pi)^2}\cot^4(\theta/2)\,d\Omega; \quad d\sigma_g = \frac{k^4M^2}{(16\pi)^2}\,\frac{\cos^2\theta}{\sin^4(\theta/2)}\,d\Omega.$$

It is interesting that these cross sections all become the same at small angles for zero rest mass of the quanta, independent of the spin. For nonzero rest mass, however, as well as at large angles, the different dimensionalities of the tensors describing the fields lead to large differences in the cross sections. In general one can say that the mass causes the cross sections to increase.

Thus when the mass is included in the equations, it is found to have gravitational properties, from considerations of special relativity (energy considerations).

We note that one of the cross sections here obtained (that for photon scattering) was previously obtained by Pijr,[3] who clearly showed the analogy of this effect to the corresponding classical effect. Since, as we have seen, the scattering cross section of a particle with zero rest mass by a Schwarzschild field is

$$d\sigma_0 = (k^4M^2/8\pi)\,|d\vartheta/\vartheta^3|,$$

then, inserting the angle $\theta = k^2M/4\pi R$ (the angle through which light rays are bent according to the classical theory), we have $d\sigma_0 = 2\pi R dR$, which is the classical expression for the cross section for scattering by a sphere of radius R.

In conclusion I thank D. D. Ivanenko and M. M. Mirianashvili for their interest in the work.

[1] Iu. B. Rumer, Исследования по пятиоптике (Investigations in Five-Optics) GITTL, M., 1956.

[2] N. N. Bogoliubov and D. V. Shirkov, Введение в теорию квантованных полей (Introduction to the Theory of Quantized Fields) GITTL, M., 1957.

[3] I. Pijr, Тр. Ин-та физ. и астрон. АН Эстонск. ССР (Trans. Inst. Phys. and Astron. Eston. S.S.R.) **5**, 41 (1957).

[4] S. N. Gupta, Proc. Phys. Soc. (London) **A65**, 161 (1952).

Translated by E. J. Saletan
331

MOLECULAR AMPLIFIER AND GENERATOR FOR SUBMILLIMETER WAVES

A. M. PROKHOROV

P. N. Lebedev Physics Institute, Academy of Sciences, U.S.S.R.

Submitted to JETP editor April 1, 1958

J. Exptl. Theoret. Phys. (U.S.S.R.) **34**, 1658-1659 (June, 1958)

IN the present paper we consider the possibility of constructing a molecular amplifier and generator (MAG), for waves shorter than 1 mm, using ammonia molecules. The rotational transitions of the NH_3 molecules lie in the wavelength region below 1 mm. These transitions can be used to construct the MAG. The rotational transitions are sorted out at the same time as the inversion levels, viz.: molecules in the lower inversion level are sorted out by passing the molecular beam through a quadrupole condenser. The system of rotational-inversion levels after sorting is given in the figure for J = 3, 2, 1, and 0 and for K = 0. Levels which are not occupied by molecules are shown by dotted lines. The solid arrows show transitions increasing the energy of the incident radiation; dotted arrows show those absorbing energy.

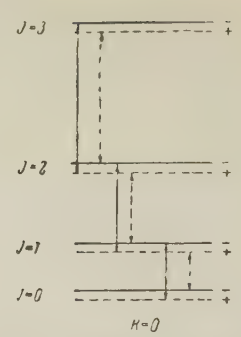

The rotational spectrum of NH_3 for J = 3, 2, 1, and 0, and for K = 0.

An amplifier can be constructed using a device in which the radiation coming from one horn crosses a number of molecular beams and falls on a second horn. If the average density of the number of active molecules is equal to N, the coefficient of negative absorption is determined by the equation

$$\alpha = 8\pi^2\nu\,|\mu_{mn}|^2 N/hc\Delta\nu, \qquad (1)$$

where ν is the frequency of the transition, μ_{mn} the dipole-moment matrix element, $\Delta\nu$ the line width, h Planck's constant, and c the velocity of light.

If the power of the radiation leaving horn 1 is equal to P_0, the power after passing a path l and entering horn 2 rises to $P_k = P_0 e^{\alpha l}$. Let $\nu = 6 \times 10^{11}$ cps ($\lambda = 0.5$ mm), $|\mu_{mn}|^2 = 2 \times 10^{-36}$, $\Delta\nu = 5 \times 10^3$ cps, and $N = 10^{10}$ cm^{-3}. Then $\alpha = 1$ cm^{-1}. If $l = 10$ cm, $P_k/P_0 = 2.2 \times 10^4$. The maximum power which such a beam can produce is about one microwatt. To construct a molecular generator one can use two plane-parallel mirrors as the resonator. If the distance between the mirrors is l, the reflection coefficient of the mirrors is k, and we assume that energy losses of the plane waves occur only upon reflection from the mirrors, the Q-factor of such a system is equal to

$$Q = (2\pi l/\lambda)/(1 - k). \qquad (2)$$

If $l = 1$ cm, $\lambda = 0.05$ cm, k = 0.95, then Q = 2400. However, energy losses occur also because the

wave is not plane but has an angular spread $2\theta \approx \lambda/D$, where D is the linear dimension of the mirror. Because of this effect, the energy P_n after n reflections will be

$$P_n = P_0/(1 + nl\lambda/D^2)^2. \quad (3)$$

The quantity nl is the path traversed by the wave during the n reflections. This time is equal to $\tau = nl/c$.

If we know the Q-factor of the system, the time in which the power decreases by a factor e is equal to $\tau = Q/2\pi\nu$. During this time the wave traverses a path $nl = c\tau$; if $Q = 2400$, and $\nu = 6 \times 10^{11}$ cps, $nl = 21$ cm.

If D = 3 cm, we get from (3) $P_n = 0.8P_0$, i.e., in our case the losses during reflection play the dominant part.

The condition for self-excitation can be written in the form

$$ke^{\alpha l} > 1. \quad (4)$$

If $\alpha = 1\ \text{cm}^{-1}$, $l = 1$ cm, k = 0.95, condition (4) is satisfied by a wide margin. If $e^{\alpha l} \gg 1$, self-excitation occurs for small k.

Translated by D. ter Haar
332

A CHROMIUM CORUNDUM PARAMAGNETIC AMPLIFIER AND GENERATOR

G. M. ZVEREV, L. S. KORNIENKO, A. A. MANENKOV, and A. M. PROKHOROV

P. N. Lebedev Physics Institute, Academy of Sciences, U.S.S.R.

Submitted to JETP editor April 1, 1958

J. Exptl. Theoret. Phys. (U.S.S.R.) **34**, 1660-1661 (June, 1958)

In reference 1 it was proposed to use a molecular system possessing three energy levels for the construction of molecular amplifiers and generators. Later this problem was considered in more detail as applied to paramagnetic crystals.[2] There are reports about the construction of three-level paramagnetic amplifiers using a single crystal of gadolinium ethylsulphate[3] and a single crystal of chromium cyanide.[4,5] We have investigated the possibility of constructing a paramagnetic amplifier and generator using a single crystal of chromium corundum ($Al_2O_3 \cdot Cr_2O_3$). The spectrum of Cr^{3+} in corundum was investigated in a number of papers.[6-9] The Cr^{3+} ion in corundum is in an axial electrical field which splits the spin quadruplet of the lower orbital singlet level into two doublets, the distance between which is equal to $2D = -0.3824\ \text{cm}^{-1}$. The spin-lattice relaxation time of Cr^{3+}, even at liquid nitrogen temperatures, is sufficiently long,[10] $\sim 10^{-4}$ sec.

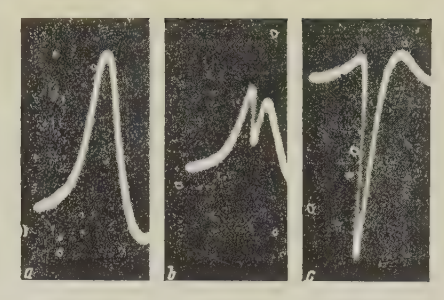

Photograph of the $M = 3/2 \rightarrow \frac{1}{2}$ absorption line at 3000 Mcs for different power levels of the auxiliary radiation P_{aux}. Fig. 1a corresponds to $P_{aux} = 0$. Fig. 1c corresponds to a value of P_{aux} for which saturation is reached. Fig. 1b corresponds to an intermediate case.

For a paramagnetic amplifier, we have used the levels that are characterized by the quantum numbers $M = \frac{3}{2}, \pm\frac{1}{2}$ when the crystalline axis is oriented parallel to the constant external magnetic field. If the axis of the crystal is turned, the states mix and transitions between all three levels become allowed. The levels $M = -\frac{1}{2}, \frac{1}{2}$ were used for amplification, and the auxiliary radiation excited transitions between the levels $M = \frac{1}{2}, -\frac{3}{2}$. The frequency at which emission (or generation) occurred was ~ 3000 Mcs and the frequency of the auxiliary radiation ~ 15000 Mcs.

In the figure we show photographs of the line corresponding to the $-\frac{1}{2} \longleftrightarrow +\frac{1}{2}$ transition at a frequency of 3000 Mcs, as a function of the power level of the auxiliary radiation. It is clear from the photographs how the absorption line (1a) goes over into an emission line (1c) when the power of the auxiliary radiation is increased. At $T \sim 2°K$, the system became self-excited and acted as a generator.

Detailed data on the operation of the constructed amplifier will be published later.

The authors express their gratitude to Professor A. I. Shal'nikov for his assistance with the performance of the experiments at low temperatures.

[1] N. G. Basov and A. M. Prokhorov, J. Exptl. Theoret. Phys. (U.S.S.R.) **28**, 249 (1955), Soviet Phys. JETP **1**, 184 (1955).

[2] N. Bloembergen, Phys. Rev. **104**, 324 (1956).

[3] Scovil, Feher, and Seidel, Phys. Rev. **105**, 762 (1957).

[4] W. H. Culver, Science **126**, 810 (1957).

[5] McWhorter, Meyer, and Strum, Phys. Rev. **108**, 1642 (1957).

[6] A. A. Manenkov and A. M. Prokhorov, J. Exptl. Theoret. Phys. (U.S.S.R.) **28**, 762 (1955), Soviet Phys. JETP **1**, 611 (1955).

[7] M. M. Zaripov and Iu. Ia. Shamonin, J. Exptl. Theoret. Phys. (U.S.S.R.) **30**, 291 (1956), Soviet Phys. JETP **3**, 171 (1956).

[8] A. A. Manenkov and A. M. Prokhorov, J. Exptl. Theoret. Phys. (U.S.S.R.) **31**, 346 (1956), Soviet Phys. **4**, 288 (1957).

[9] G. M. Zverev and A. M. Prokhorov, J. Exptl. Theoret. Phys. (U.S.S.R.) **34**, 1023 (1958), Soviet Phys. JETP **7**, 707 (1958).

[10] P. P. Pashinin and A. M. Prokhorov, J. Exptl. Theoret. Phys. (U.S.S.R.) **34**, 777 (1958), Soviet Phys. JETP **7**, 535 (1958).

Translated by D. ter Haar
333

ON THE ELECTROSTATIC THEORY OF IONIC CRYSTALS

A. V. STEPANOV

Leningrad Physico-Technical Institute, Academy of Sciences, U.S.S.R.

Submitted to JETP editor November 3, 1956; resubmitted April 4, 1958

J. Exptl. Theoret. Phys. (U.S.S.R.) **34**, 1661-1662 (June, 1958)

IT is impossible to define a sharp boundary between typical ionic crystals and typical molecular crystals.

1. It is well known, that ionic compounds evaporate in the form of molecules, which are quite stable. Their energy of dissociation (into ions) is in the range of 160 to 40 kcal/mole and exceeds the sublimation heat of the same crystals. Considering the formation of liquid and solid state as the result of condensation of molecular vapor, it is possible to expect the molecules to be conserved, to some degree, also in the crystalline state.

2. A considerable part of the molecules of ionic compounds have large dipole moments, and the interaction between them can supply binding energies on the order of the sublimation heat of these substances. For example, for the molecules of CsI, $\mu = 10 \times 10^{-18}$ CGS electrostatic units. Supposing that the intermolecular distances are equal to 5×10^{-8} cm, we find the work of the attraction forces between two molecules to be 11 kcal/mole. Hence the contribution of the dipole interaction to the energy in the molecular lattice of CsI is approximately equal to $11(l/2) = 66$ kcal/mole (assuming that the coordination number is $l = 12$ for a hypothetical lattice comprising two atomic molecules). In those cases, when the molecules of the ionic compounds have no dipole moments, as for example $HgCl_2$, the Van-der-Waals interaction between them can provide a binding energy on the order of their sublimation heat. Example:

The energy of the dispersion interaction between two $HgCl_2$ molecules is 3 kcal/mole (taking the ionization potential as 12 ev, the coefficient of polarization as 9×10^{-24} cm^{-3}, and the distances between molecules as 4.3×10^{-8} cm) and the lattice energy is approximately equal to $3(l/2) = 18$ kcal/mole (if $l = 12$). In practice the sublimation heat of $HgCl_2$ is 20 kcal/mole.

3. The principal feature of the molecular structure of crystals is the existence of differences in the interatomic distances between a given atom (ion) and its nearest neighbor. In these cases it is possible to distinguish the "molecules" in the structure. At the same time, the structure is characterized by the distances (radii) between the molecules and inside the molecules. The majority of studied heteropolar compounds exhibit this feature, although, with some exceptions, no attempt has yet been made to describe the structures of the ionic compounds as molecular ones. Things are different for a comparatively small number of heteropolar compounds with structures of the NaCl, CsCl, ZnS type. It is therefore possible to consider these structures not as the rule, but as an exception in the group of heteropolar substances.

4. In many compounds such as NaCl, $HgCl_2$ or HCl properties such as the temperature and the heat of melting and evaporation, as well as compressibility, change gradually from typical ionic to typical molecular structures, which indicates a gradual change in the degree of molecularity of the crystals, and the presence, to a certain degree, of bonds of molecular character in typical ion substances.

5. Based on the above, one might think that many properties of ionic crystals are determined by the energy U^S of "small" intermolecular interaction, which is less than the Born lattice energy E^B. In particular cases, $U^e = S$, the sublimation heat. The question of the dimensions and forms of the molecules in crystals of different substances should be resolved separately. In some cases one must consider the "molecules" that make

up the crystals as infinitely long unidimensional or two-dimensional atom complexes, bound together by "small" forces of one nature, whereas in the complex itself the atoms are bound by "big" forces of another nature.

6. The difference between the typical molecular crystals (e.g., the CH_4 or C_6H_6 crystals) and the heteropolar molecular crystals (such as the NaCl, $HgCl_2$ or PbS crystals) lies: (1) in the degree of molecularity β; (2) in the nature of the forces in the molecules; (3) in the nature of intermolecular forces. The quantity β is defined as the ratio of the intramolecular energy $U^a \cong D$ (D is the energy of dissociation of the diatomic molecule into ions) to the intermolecular energy U^e per bond. For the substances for which β is given below, it is possible to take $U^e \approx 2S/l$. Example:

$\beta = 300\,(CH_4)$, $200\,(HCl)$, $22\,(HgCl_2)$, $10\,(NaCl)$ taking $l = 12$ in all four cases.

Translated by I. Polidi
334

ERRATA

Volume 5

Page	Line	Reads	Should Read
1043	Eq. (4)		$W = y^2 a_{14}^2 \sin 2\phi/2\rho\,(a_{11}a_{44} - \alpha_{14}^2 \sin^2 3\phi)$ The coefficient k_2 equals $0.185 \times 10^{-3}\,cm^{-1}$.
1044	3 from bottom (l.h.)	$\Delta y = 2.87 \times 10^{-3}$ cm	$\Delta y = 3.18 \times 10^{-3}$ cm
	4 from top (r.h.)	$\Delta\vartheta_\Sigma = 7.2 \times 10^{-5}$ radians	$\Delta\vartheta_\Sigma = 5.9 \times 10^{-5}$ radians

Volume 6

1090	4 and 5 from top	2—(d, 3n); and of the I_{53}^{127} cross section, 3—(d, 2n); 4—(d, 3n)	2—(d, 3n) on I_{53}^{127} and 3—(d, 3n); 4—(d, 3n) on Bi_{83}^{209}
1091	6 from bottom expression for determinant C(y)	ρ, γp, h, $1/\rho$	ρy_2, $\gamma p y_2$, $h y_2$, y_2/ρ
1094	7 from bottom	For $\gamma = 5/3$, μ has . . .	Here μ has . . .

Volume 7

55	16 from bottom		Correct submittal date is April 5, 1957
169	17 from bottom		Delete "Joint Institute for Nuclear Research"
215	Table		Add: Note. Columns 2—9 give the number of counts per 10^6 monitor counts
215	Table, column headings	1, 2, 3, 4-7, 8	1, 2, 3, 4, 8-7
312	Eq. (8)	. . . $(1 \pm \mu/2M)^2$	. . . $(1 \mp \mu/2M)^2$
313	2, r.h. col.	$\alpha_{33} = 0.235$	$a_{33} = 0.235$
692	Eq. (5)	$m_B/M_B = \ldots \mp [1 + \ldots]$	$m_B/M_B = \mp [1 + \ldots]$
461	Title	. . . Elastically Conducting	. . . Electrically Conducting

Author Index to Volume 34 (7)

References with L are Letters to the Editor

Analytic Subject Index to Volume 34 (7)

References with L are Letters to the Editor. Items are listed under the following categories: